Thermodynamic Evaluation of Carbohydrate-Lectin Interactions

Inauguraldissertation

zur

Erlangung der Würde eines Doktors der Philosophie

vorgelegt der

Philosophisch-Naturwissenschaftlichen Fakultät

der Universität Basel

von

Katrin Lemme

von Magdeburg, Deutschland

Basel, 2013

Genehmigt von der Philosophisch-Naturwissenschaftlichen Fakultät
auf Antrag von

Referent: Prof. Dr. Beat Ernst
Ko-Referent: Prof. Dr. Gerhard Klebe

Basel, 15.11.2011

Prof. Dr. Martin Spiess
The Dean of the Faculty

Acknowledgment

Most of all, I would like to express my sincere gratitude and appreciation to Prof. Dr. Beat Ernst for the opportunity to perform my thesis in this outstanding interdisciplinary group and scientific environment. I am grateful for the scientific discussions and his support throughout the past almost 4 years.

I would like to thank Prof. Dr. Gerhard Klebe for accepting to be the co-referee of this thesis.

Special thanks go to Peggy Brunet-LeFeuvre and Dr. Francis Bitsch, Novartis, for allowing me to use their VP-ITC for almost one year as well as for advices regarding the experimental setup and analyzing the data.

Many thanks go to Dr. Said Rabbani for introducing me to cell culture, protein purification, and various protein assays and to Dr. Céline Weckerle for introducing me into the surface plasmon resonance technology.

I am very grateful to Dr. Roland Preston, Dr. Stefanie Mesch, Dr. Matthias Wittwer, Dr. Meike Scharenberg, Dr. Adam Zalewski, and PD Brian Cutting for the many scientific discussions and for their support.

Huge thanks go to the persons who directly contributed to my work: Dr. Florian Binder, Bea Wagner, Dr. Stefanie Mesch, Dr. Katharina Mayer, Lijuan Pang, and Dr. Xiaohua Jiang (provided analytes), Dr. Adam Zalewski (modeling), Dr. Said Rabbani, Dr. Roland Preston, Dr. Meike Scharenberg, and Dr. Hendrik Koliwer-Brandl (provided protein).

I would like to thank my master student Samantha Notaro for her support concerning the correct determination of protein concentrations.

Many thanks go to my lab members Matthias, Katja, Simon, Céline, Jacqueline, and Daniela for the wonderful atmosphere and the encouragement.

Thanks to all former and present members of the IMP for the unique time.

Finally, I am greatly indebted to my husband René and my family for all their support and encouragement.

Abbreviations

7A9	Monoclonal antibody against E-selectin
AAA	Amino acid analysis
ABTS	2,2'-azino-bis[3-ethylbenz-thiazoline-6-sulfonic acid]
Ac	Acetyl
AIBN	α,α'-Azodiisobutyronitrile
Aq.	Aqueous
bb	Backbone
BCA	Bicinchonic acid
BCR	B-cell receptor
BnBr	Benzyl bromide
Boc	*tert*-butyloxycarbonyl
BSA	Bovine serum albumin
CBB	Coomassie brilliant blue G-250 dye
CD	Cluster of differentiation
CD22	Siglec-2
CMC	Critical micelle concentration
CRD	Carbohydrate recognition domain
ΔC_P	Change in heat capacity
DC	Dentritic cell
DCE	1,2-Dichlorethane
DCM	Dichlormethane
DC-SIGN	DC-specific ICAM-3 grabbing nonintegrin
DMAc	Dimethylacetamide
DMAP	4-Dimethylamino-pyridine
DMF	*N*,*N*-Dimethylmethanamide
DMSO	Dimethyl sulfoxyde
EC_{50}	Effective concentration 50%
E. coli	*Escherichia coli*
EDC	3-(*N*,*N*-dimethylamino)propyl-*N*-ethylcarbodiimide
ESI	Electronspray-ionization
ESL-1	E-selectin ligand-1
Et	Ethyl
FAc	Fluoro-acetyl
FCS	Fetal calf serum
FID	Flame ionization detector
FPLC	Fast protein liquid chromatography
Fuc	Fucose
ΔG	Change in free energy
$\Delta G°$	Change in standard free energy
Gal	Galactose
Gal*N*Ac	*N*-Acetylglalactosamine
GC	Gas chromatography
Glc	Glucose
Glc*N*Ac	*N*-Acetylglucosamine
h	hours
$\Delta H°$	Change in enthalpy
$\Delta H°_{vH}$	Van't Hoff change in enthalpy
HBS-Ca	HEPES/NaCl/$CaCl_2$ buffer *pH* 7.4
HBS-E	HEPES/NaCl/EDTA buffer *pH* 7.4
HBS-EP	HEPES/NaCl/EDTA/P20 buffer *pH* 7.40
HEPES	2-[4-(2-Hydroxyethyl)piperazin-1-yl]ethanesulfonic acid
HIV	Human immunodeficiency virus
HPLC	High performance liquid chromatography
HRMS	High resolution mass spectrometry
IC_{50}	Inhibition concentration 50%
ICAM-3	Intracellular Adhesion Molecule-3
IgG	Immunoglobulin G
IgSF	Immunoglobulin superfamily
ITC	Isothermal titration calorimetry
K_A	Equilibrium association constant
K_D	Equilibrium dissociation constant
k_{on}	Association rate constant
k_{off}	Dissociation rate constant
L	Ligand
Le^a	$Lewis^a$
Le^x	$Lewis^x$
MD	Molecular dynamics
MAG	Myelin-associated glycoprotein, Siglec-4
Me	Methyl
MeCN	Acetonitril
MeOH	Methanol
min	minute(s)
MPLC	Medium pressure liquid chromatography
MS	Mass spectrometry
N	Stoichiometry
n.b.	not binding
n.d.	not determined
Neu5Ac	*N*-Acetylneuraminic acid
NgR	Nogo receptor
NHS	*N*-Hydroxysuccinimide
NIS	*N*-Iodosuccinimide
NMR	Nuclear magnetic resonance
Nosyl	2-Nitrobenzylsulfonyl
OD	Optical density
OH	Hydroxyl
P	Protein
PAA	Polyacrylamide polymer
Page	Polyacrylamide gel electophoresis

PAMPA	Parallel artificial membrane permeation assay
PL	Protein-ligand complex
PPB	Plasma protein binding
R	Universal gas constant (8.314 J mol^{-1} K^{-1})
rIC_{50}	Relative IC_{50}
RP	Reverse phase
r.t.	Room temperature
RU	Resonance units
RMSD	Root mean square deviation
s	seconds
$\Delta S°$	Change in entropy
SAR	Structure activity relationship
sat.	Saturated
sc	Side chain
SDS	Sodium dodecyl sulfate
Siglec	Sialic acid-binding immunoglobulin-like lectins
sLe^a	Sialyl Lewis^a
sLe^x	Sialyl Lewis^x
SPR	Surface plasmon resonance
STD	Saturation transfer difference
T	Temperature
TBS	*tert*-butyltrimethylsilyl
TFA	Trifluoracetic acid
TfOH	Trifluoracetic acid
THF	Tetrahydrofuran
TMS	Trimethylsilyl
trNOE	transfer Nuclear Overhauser effect
$T\Delta S°$	Change in entropy at 298.15 K
TsCl	*p*-Toluensolfonyl chloride
UPEC	Uropathogenic *E. coli*
UV	Ultraviolet

Table of Content

1 Introduction

Calor, the Latin word for 'heat', defines the science of measuring heat as calorimetry.[1] The start of calorimetry was the invention of the first thermometer to measure heat. Since modern calorimetric instruments are very sensitive and allow to detect temperature changes of just a few millionths of a degree,[2] they can be used to thermodynamically characterize the heat of biomolecular interactions.[3] The thermodynamic fingerprint of a series of compounds can give useful information of protein-ligand interactions for structure activity relationship and furthermore for decision making in lead discovery.[4]

1.1 Thermodynamics of Protein-Ligand Interactions

1.1.1 The Basics of Thermodynamics in Protein-Ligand Interactions

In a biomolecular interaction a protein in its native conformation (*P*) interacts with a ligand (*L*). In a closed thermodynamic system this interaction can be represented as:

$$P + L \rightleftharpoons PL \qquad (1.1.1.1)$$

This equilibrium can be characterized by following equation:

$$K_D = \frac{[P][L]}{[PL]} = \frac{1}{K_A} \qquad (1.1.1.2)$$

where K_D is the dissociation constant and K_A is the association constant. The change in free energy (ΔG), under arbitrary conditions, for complex formation (*PL*) is related to the standard free energy change ($\Delta G°$), under defined conditions (e.g. 1 M [*P*] and 1 M [*L*] at *pH* 7 and 25 °C), by the equation:

$$\Delta G = \Delta G° - RT \ln K_D \qquad (1.1.1.3)$$

At equilibrium, where $\Delta G = 0$ and equilibrium concentrations of [*L*], [*P*], and [*PL*] are reached:

$$\Delta G° = RT \ln K_D = -RT \ln K_A \qquad (1.1.1.4)$$

where *R* is the universal gas constant (8.314 J mol^{-1} K^{-1}) and *T* the absolute temperature in K. Thus, the standard free energy can be directly calculated from K_D.

K_D values can be determined using a variety of experimental techniques. Assuming that the change in enthalpy ($\Delta H°$) is not depending on temperature, the measurement of K_D at several temperatures (K_{DT1}, K_{DT2} at T_1, T_2, respectively), can

be used to calculate the van't Hoff enthalpy ($\Delta H°_{vH}$) and entropy ($\Delta S°_{vH}$) with the van't Hoff relationship:

$$\ln K_D = \frac{\Delta G°}{RT} = \frac{\Delta H°_{vH}}{RT} - \frac{T\Delta S°_{vH}}{RT} \qquad (1.1.1.5)$$

However, since the assumption that the enthalpy does not change with the temperature is usually incorrect, the non-linear van't Hoff equation is expected to give better results:

$$\ln \frac{K_{DT_1}}{K_{DT_2}} = \frac{\Delta H_{vH}° - T_1 \Delta C_p}{R}\left(\frac{1}{T_1} - \frac{1}{T_2}\right) + \frac{\Delta C_p}{R} \ln \frac{T_2}{T_1} \qquad (1.1.1.6)$$

where ΔC_p is the heat capacity change under constant pressure.[5] Nevertheless, discrepancies between van't Hoff and determination of the enthalpy with isothermal titration calorimetry (ITC) exist.[6]

ITC is a direct measurement that allows the values of enthalpy change ($\Delta H°$), K_D, and stoichiometry (N) to be measured in a single experiment. Once these parameters are measured, the size of $\Delta S°$ can be calculated using the relationship:

$$\Delta G° = RT \ln K_D = -RT \ln K_A = \Delta H° - T\Delta S° \qquad (1.1.1.7)$$

This relation is applicable when temperature and pressure are constant. Binding is favored if $\Delta G°$ is negative, therefore negative values of $\Delta H°$ and positive values of $\Delta S°$ promote complex formation.[5]

A further parameter that can be determined by ITC is the change in heat capacity (ΔC_p) since both, $\Delta H°$ and $\Delta S°$, are related with temperature by the heat capacity change:

$$\Delta C_p = \frac{\Delta H°_{T_2} - \Delta H°_{T_1}}{(T_2 - T_1)} = \frac{\Delta S°_{T_2} - \Delta S°_{T_1}}{\ln \frac{T_2}{T_1}} \qquad (1.1.1.8)$$

1.1.2 The Change in Enthalpy ($\Delta H°$)

The changes in enthalpy ($\Delta H°$) and entropy ($\Delta S°$) influence the change in free energy of binding ($\Delta G°$). Negative enthalpy and positive entropy are leading to a negative free energy of binding results.

$\Delta H°$ of binding is related to the net change in the number and/or strength of non-covalent bonds going from the free to the bound state. This includes solvent reorganization as well as the binding interface as well as other parts of the protein, *e.g.* undergoing conformational changes within the binding process. Before a ligand

can bind, the interacting surfaces have to be desolvated. Desolvation of polar groups that cannot establish polar non-covalent interaction in the complex will induce an enthalpic penalty.[4,7]

Non-covalent interactions that influence $\Delta H°$ are electrostatic interaction like salt bridge formation, van-der-Waals interaction, hydrogen bond formation, as well as π-π and cation-π stacking of aromatic interaction.

Electrostatic interactions are described with Coulomb's equation. The potential energy (U_{i-i}) between two point charges q_1 and q_2 decreases with increasing distance r:

$$U_{i-i} = \frac{q_1 q_2}{4\pi\varepsilon_o \varepsilon r} \qquad (1.1.2.1)$$

where ε_o is the permittivity of free space and ε is the relative dielectric constant of the medium.[8] Charge-charge (or ion-ion) interaction can provide large contribution to enthalpy although we have to keep in mind that the desolvation of a charged group can compensate the gain by charge-charge interactions. At physiological *pH* (ca. 7.40), interactions of the protonated side chain of arginine (pK_a = 12.5) and lysine (pK_a = 10.8), and the deprotonated carboxy groups of aspartic acid (pK_a = 3.9) and glutamic acid (pK_a = 4.1), form important salt bridges. We have, however, to keep in mind, that their exact protonation state depends on the local *pH*.[9]

When protein and ligand are in close proximity, attractive forces called van-der-Waals interactions occur. These forces depend on the distance with r^{-6}. Three types of van-der-Waals forces can be defined: (i) permanent dipole-dipole interactions, (ii) permanent dipole-induced dipole forces, and (iii) induced dipole-induced dipole interactions. The latter interaction is called London or dispersion forces[8] and are assumed to be the major source of stabilizing energy between two aromatic molecules, for example in π-π-stacking or cation-π interaction.[10] The overall van-der-Waals energy is a sum of the very short-range attraction and the extremely short-range steric repulsion between atoms. This relationship can be described with following equation:

$$U_{vdW} = \frac{A}{r^m} - \frac{B}{r^6} \qquad (1.1.2.2)$$

where A and B are constants that describe the magnitude of the repulsive and attractive terms, respectively, and m is the power of the repulsive term (usually between 5 and 12).[1]

The formation of hydrogen bonds is the most important interaction in biological system. Hydrogen bonds are composed of electrostatic, covalent, as well as resonance components, where the electrostatic component is probably dominant.[8] Hydrogen bonds consist of an interaction between a hydrogen bond donor (X-H) and an acceptor (Y). Generally, X and Y are more electronegative than carbon, *i.e*. heteroatoms as O and N. The bridging distance should be smaller than the van-der-Waals radii.[8] The length of an optimal hydrogen bond in water is 1.8 Å, whereas the interaction is negligible at a distance of 5 Å. Besides the bond length, bond angle, temperature, pressure, and environment (characterized by the local dielectric constant) influence the quality of a hydrogen bond.[11] The energy of a hydrogen bond is in the range of –15 and –30 kJ mol^{-1} and therefore between a covalent bond and a van-der-Waals interaction. When one of the interacting partner is charged, the interactional energy can be higher.[8] Accounting for desolvation and the reduction of residual motion, the general benefit of a neutral hydrogen bond is in the order of –5 kJ mol^{-1} in the free energy change.[12]

1.1.3 The Change in Entropy ($\Delta S°$)

As mentioned in chapter 1.1.2, negative enthalpy of interaction ($\Delta H°$) and positive entropy of interaction ($\Delta S°$) result in high binding affinities. $\Delta S°$ is influenced by the order of the system such as conformational changes, water molecules released upon desolvation of protein and ligand, the loss of rotational and translational degrees of freedom, the restriction of rotational bonds, and vibrational modes.[12-14] If the order increases, for example the protein gets structured upon binding, the influence on $\Delta S°$ is unfavorable and negative in sign.[15] In contrast, the release of structured water upon binding positively influences $\Delta S°$. The release of a structural water molecule – *i.e*. a water molecule forming three and more geometrically optimal hydrogen bonds – can cost up to 10 kJ mol^{-1} at 298.15 K.[16] Usually, in protein-ligand interactions not all motion of ligand, protein, and water are lost upon binding. Therefore, 10 kJ mol^{-1} is the upper limit that will be probably not reached in biomolecular interactions.[12,16] For the loss of translational and rigid body rotational degrees of freedom upon complex formation different $\Delta S°$ values exist, ranging from 5.4,[12] the cratic contribution 10,[17] 44,[18] up to 62 kJ mol^{-1}[18] (at 298.15 K), whereas the highest values might be attributed to a total loss of motion.[12] However, when different ligands binding to a target protein are compared, not the absolute but the relative

values ($\Delta\Delta S°$) are of importance.[18] Another source of entropic costs are rotatable bonds that become restricted upon binding. Again, since in protein-ligand complexes vibrational entropy remains, the restriction of one rotatable bond is in the range of 1.4 kJ mol^{-1} ($T\Delta S°$ at 298.15 K) instead of 5 kJ mol^{-1} for the complete restriction of rotations.[12] Therefore, it is an accepted practice in ligand design to introduce conformational constraints to pre-organize a ligand in its bioactive conformation to reduce entropy costs upon binding.[19] This holds to be true in some cases.[20] Whereas other data suggest that constraints can lead to less favorable $\Delta S°$ but a gain in $\Delta H°$ because of additional contacts,[19,21] since additional interactions reduce the residual motion.[12,22] On the other side, it was published that flexible ligands bind with high affinity because of reduced entropic penalties.[4,23] Overall, it is difficult to dissect $\Delta H°$ and $\Delta S°$, since they depend on each other.

1.1.4 The Change in Heat Capacity (ΔC_p)

Further information of protein-ligand interactions can be obtained from the change in heat capacity (ΔC_p) describing the temperature dependence of the change in enthalpy ($\Delta H°$) and entropy ($\Delta S°$) (see 1.1.1). ΔC_p is usually negative in value indicating that the complex exhibits a smaller heat capacity then the sum of the heat capacities of the two components.[24] ΔC_p effects mostly result from the change in hydration of interacting groups.[25] It is known that the desolvation of polar surface increases ΔC_p,[7,19,26] whereas non-polar surface desolvation leads to a reduction.[7] The inclusion of water molecules upon binding can largely reduce ΔC_p.[26] Other influences arise from low frequency vibrational modes.[7,24] Correlation between ΔC_p and the surface area that is buried upon complex formation exist for *e.g.* protein folding/unfolding[27] as well as carbohydrate-lectin interactions.[25] These correlations differ in their contribution from polar and non-polar surfaces what makes a correct extrapolation to other systems difficult. Additionally, discrepancies between calculated and experimentally determined ΔC_p values are probably due to other effects than the surface buried upon binding.[24]

1.1.5 The Hydrophobic Effect

Desolvation is a prerequisite for protein-ligand interactions and affects the change in enthalpy ($\Delta H°$), entropy ($\Delta S°$), and heat capacity (ΔC_p) of binding. It was previously proposed that from 25% up to 100% of the net measured $\Delta H°$ accounts for solvent

reorganization.[14] The desolvation of non-polar surfaces increases $\Delta S°$, since a hydrogen-bond network with high order (low entropy) is disturbed. This process is termed the classical hydrophobic effect. Additionally, hydrophobic interactions exhibit a small enthalpic contribution that is strongly temperature dependent, leading to a large negative change in heat capacity.[10,28] In contrast, the non-classical hydrophobic effect is accompanied by a favorable enthalpic term and is related to favorable changes in solvent cohesive interactions and to gain in electrostatic interaction between non-polar surfaces. In this case, water molecules can form stronger interactions to bulk water upon desolvation of non-polar surfaces.[10] This behavior is described for protein-ligand interaction dewetting a poorly hydrated non-polar cavity upon complex formation[28,29] and for ligands of increasing lipophilicity.[10,30]

1.1.6 Theory of Isothermal Titration Calorimetry

Several methods exist to determine heat changes for biomolecular interactions. One of the most common techniques is isothermal titration calorimetry (ITC). A scheme of a typical calorimetric instrument is shown in Figure 1.1.6.1.

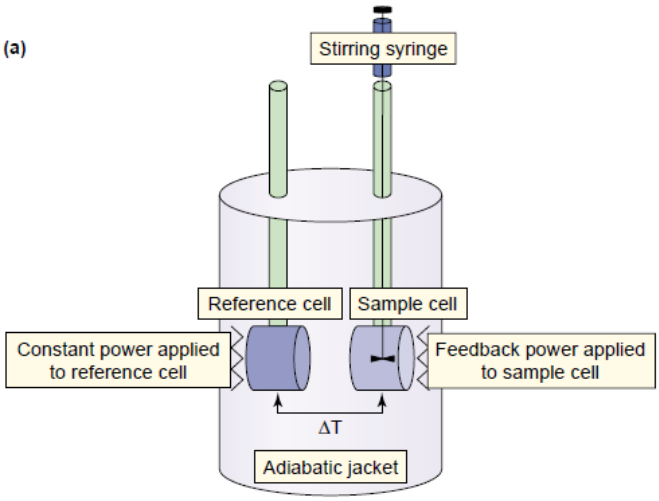

Figure 1.1.6.1. Schematic representation of the power compensation isothermal titration calorimeter. A constant power is applied to the reference cell. Over a feedback circuit, a variable power is applied to the sample cell. This allows monitoring of very small temperature differences between both cells. During an exothermic interaction, heat is generated and less power is applied to the sample cell, vice versa for an endothermic interaction. The syringe continuously rotates and a computer-controlled plunger injects precise volume of ligand solution. (Picture from Holdgate and Ward.[5])

In an ITC experiment a ligand solution (*L*) is gradually added to a protein solution (*P*) forming a simple binary complex (*PL*):

$$P + L \rightleftharpoons PL \qquad (1.1.6.1)$$

The amount of heat absorbed or released by this interaction is monitored. In case of an exothermic binding process, heat is released and less power is applied to the sample cell resulting in a negative peak. Overall, the amount of energy required to maintain constant temperatures of reference cell and sample cell is measured over time. The heat released or absorbed (q) for each injection at a given temperature ($\Delta H^\circ_{(T)}$) depends on the enthalpy the number of moles of complex formed, the reaction volume (V) of the sample cell, and the concentration of the complex [PL]:

$$q = V\Delta H^\circ_{(T)}\Delta[PL] \qquad (1.1.6.2)$$

Initially, the amount of free protein is sufficient to bind ligand according to the concentration of the free ligand and protein in solution. With ongoing titration, the concentration of unoccupied binding sites decreases, correspondingly, the heat released decreases over time as well, ending in dilution effects (Figure 1.1.6.2). The integral heat of reaction after the i^{th} addition, q_i, will be:

$$q_i = N[P_T]V\Delta H^\circ_{(T)}\Theta_i \qquad (1.1.6.3)$$

where [P_T] is the total protein concentration, N is the stoichiometry and Θ the fractional saturation.

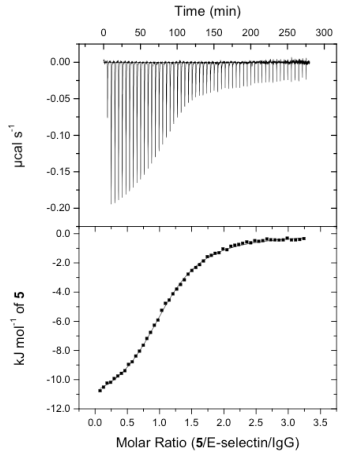

Figure 1.1.6.2. A typical result of an isothermal calorimetric titration of a selectin antagonist with E-selectin/IgG (Chapter 2.1.1.2). The top panel shows the recorded change in heat in units of µcal s^{-1} as a function of time for successive injections of antagonist (raw data). The bottom plot shows the integrals of the peaks (black squares) from the top plot plotted against the molar ratio of the binding process together with a line of best fit, used to estimate ΔH°, K_D, and N.

The differential heat (Q) of the i^{th} injection is:

$$Q = N[P_T]\Delta H^{\circ}_{(T)} V(\Theta_i - \Theta_{i-1}) \qquad (1.1.6.4)$$

A non-linear fit of this sigmoidal curve in the differential heat mode (q_i vs. $[L_T]$ or vs. $[L_T]/[P_T]$, where $[L_T]$ is the total ligand concentration) is then used to estimate the parameter K_A, $\Delta H°$, and N from a single experiment.[2]

1.1.7 Experimental Setup of an ITC Experiment

The success of an ITC experiment depends on the thermodynamic characteristics of the system (protein-ligand interaction, buffer, temperature, *pH*). Depending on the affinity, an appropriate concentration range can be estimated, where a sigmoidal curve reliably fits all three parameter, $\Delta H°$, K_D, and N. The dimensionless parameter c describes the shape of the curve:

$$c = \frac{N[P_T]}{K_D} \qquad (1.1.7.1)$$

The optimal c-values was recently proposed to be 40.[31] Experiments with c-values above 500 accurately determine $\Delta H°$ and N,[2] whereas K_D can only be measured correctly if a strong $\Delta H°$ contribution allows small injection volumes of the ligand solution. On the other side, for reliably determination of K_D and $\Delta H°$ in experiments with c-values below 1, accurate concentrations of protein and ligand solution, a big excess of ligand, and a two parameter fit, where N is fixed, are required.[32]

Another point to consider is the heat related to changes in the protonation state of protein and/or ligand upon binding. This heat contributes to the overall heat of binding and depends on the ionization enthalpy of the buffer system used ($\Delta H°_{Ion}$). With this dependency, the deprotonation n_{H+} ($n_{H+} > 1$) or protonation ($n_{H+} < 1$) can be determined:

$$\Delta H°_{Obs} = n_{H+}\Delta H°_{Ion} + \Delta H°_{Bind} \qquad (1.1.7.2)$$

where $\Delta H°_{Obs}$ is the measured enthalpy and $\Delta H°_{Bind}$ is the enthalpy corrected for protonation effects.[2]

1.2 Lectins

Lectins are defined as carbohydrate binding proteins, excluding enzymes or antibodies, and were first discovered in plants in 1888, when Stillmark found that an extract of castor bean seeds contained a protein capable of agglutinating animal red blood cells.[33] Lectins are widespread in most living organisms such as animals, plants, viruses, and bacteria. The first pure lectin was concanavalin A (Con A) from jack beans, used to elucidate the molecular basis for blood group specificity.[34] Lectins were shown to be involved in diverse biological processes in many species such as clearance of glycoproteins from the circulatory system, adhesion of infectious agents to host cells, recruitment of leukocytes to inflammatory sites, cell interactions in the immune system, in malignancy and metastasis.[34,35] The major types of animal lectins are galectins, C-type, P-type, and I-type lectins (Figure 1.2.1).

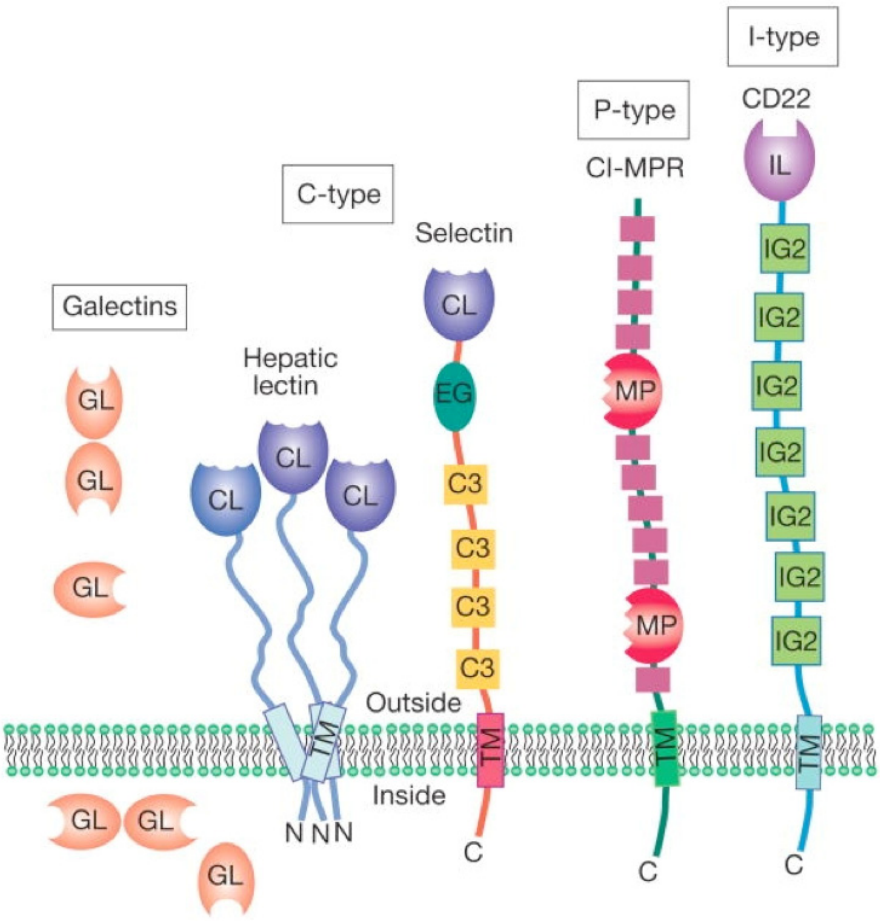

Figure 1.2.1. Schematic representation of major types of animal lectins with the carbohydrate-binding domains (CRD) of C-type lectin CRD (CL), S-type lectin CRD (GL), P-type lectin CRD (MP), I-type lectin CRD (IL), EGF-like domain (EG), immunoglobulin C2-set domain (IG2), transmembrane region (TM), and complement regulatory repeat (C3) (picture from Varki *et al.*[33]).

Galectins are soluble lectins, previously termed S-type lectins, that recognize β-galactose-containing glycoconjugates and contribute to cell-cell and cell-matrix interactions and can modulate cellular function.

C-type lectins interact with glycans in a Ca^{2+}-dependent manner and share homology in their carbohydrate recognition domain (CRD). Collectins, selectins, endocytic receptors, and proteoglycans belong to the C-type family which function as adhesion signaling receptor in many immune functions such as inflammation and immunity to tumor and virally infected cells. Among the C-type lectins, the selectins are perhaps the best characterized lectins (chapter 2.1.1).[33] Selectins are expressed on vascular endothelial cells, leukocytes, and platelets, and enable the adhesive interaction among theses cells. They play a crucial role in leukocyte trafficking and are the key players in the early stages of inflammation. Therefore, the selectins are promising targets for the development of anti-inflammatory drugs, as needed for the treatment of asthma, psoriasis, or rheumatoid arthritis.[36] Another C-type lectin, DC-SIGN (DC-specific intracellular adhesion molecule-3 (ICAM-3) grabbing nonintegrin, chapter 2.1.2), located on dentritic cells (DC), plays a crucial role in the defense mechanism against pathogens, however, some pathogens exploit this way to infect the host.[37]

P-type lectins contain a phosphate group and enable the lysosomal trafficking of soluble acid hydrolyses to the lysosome.

Lectins belonging to the immunoglobulin superfamily (IgSF), excluding antibodies and T-cell receptors, are called I-type lectins. The largest family within the I-type lectins are the sialic acid-binding immunoglobulin-like lectins (siglec), including CD22 (Siglec-2, chapter 2.2.1) and myelin-associated glycoprotein MAG (Siglec-4, chapter 2.2.2), both inhibitory proteins in the immune system and the central nervous system, respectively.[33]

Lectins other than plant and animal lectins are lectins that are expressed on viruses, bacteria, and protozoa. They exploit host cell-surface glycans as receptors for cell attachment and tissue colonization. Several pathogens infect their hosts using carbohydrate-lectin interaction, *e.g.* the influenza virus via hemagglutinin binding to sialic acid containing glycans derivatives on the upper respirator tract mucosa, *Escherichia coli* via fimbriae binding to glycans in the urinary tract (chapter 2.3.1) or intestinal cells, and Helicobacter pylori via BabA binding to $Lewis^b$ in the stomach.[33]

1.3 Thermodynamic of Carbohydrate-Lectin Interactions

Most of the calorimetric studies on lectins so far were made with plant lectins[34,35,38,39] although human lectin[34,35,38-41] and bacterial lectin[42,43] investigations have recently gained increasing interest. The majority of these studies describe carbohydrate-lectin interactions as enthalpically driven processes accompanied by an entropic penalty[34,35,38,39] yielding binding affinities in the millimolar range for monosaccharides.[34] It is argued that the entropic gain from desolvating polar[44] and apolar surfaces[4] is offset by unfavorable conformational entropy.[45] However, it is described that the bioactive conformation of carbohydrates is a low energy conformation and, moreover, the protein surface is well preorganized,[34,38,45] why other than conformational penalty must be the reason for the entropic loss. For the example of entropically driven binding processes, which are attributed to hydrophobic interactions,[41,46] to the release of structural water upon binding,[43,47] to a favorable conformational change of the protein,[48] or to a combination of desolvation and preorganization of protein and ligand as reported for E-selectin interaction to E-selectin ligand-1 (ESL-1).[49]

An often observed property of carbohydrate-lectin interactions is the enthalpy-entropy compensation behavior,[34,38] a common phenomenon for weak intermolecular interactions in aqueous solution.[22,50] Enthalpy-entropy compensation is a linear behavior in a $\Delta H°$ versus $-T\Delta S°$ plot with several ligands binding to a target protein (Figure 1.3.1). A slope of –1 denotes for ligands for which a favorable change in enthalpy is completely compensated by an entropic penalty.

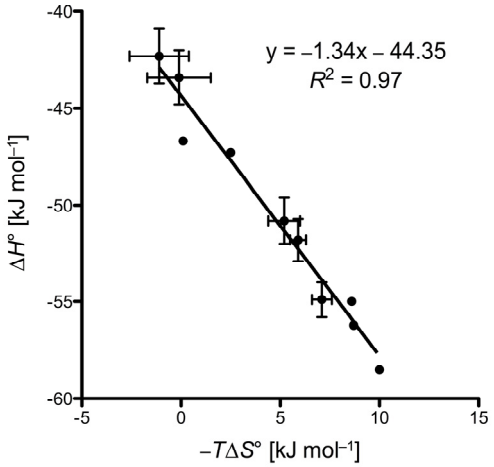

Figure 1.3.1. Correlation of the change in enthalpy ($\Delta H°$) versus the change in entropy ($-T\Delta S°$) of FimH antagonists interacting with FimH-CRD (enthalpy-entropy-compensation plot, chapter 2.3.1.2).

The change in heat capacity for carbohydrate-lectin interactions is usually small and negative[34,38] and might be attributed to a combination of the desolvation of a polar surface and the sequestering of water upon complex formation.[7,26] However, a hydrogen bond network with water-mediated hydrogen bonds is another property of carbohydrate-lectin interactions[34,39] as well as fast kinetics with half-life times of the complex typically below 1 second.[51]

References

[1] K. E. van Holde, W. C. Johnson, P. Ho, *Principles of physical biochemistry, Vol. 2nd*, Pearson Education, Inc., New Jersey, **2006**.

[2] R. Perozzo, G. Folkers, L. Scapozza, *J. Recept. Signal. Transduct. Res.* **2004**, *24*, 1-52.

[3] T. Wiseman, S. Williston, J. F. Brandts, L. N. Lin, *Anal. Biochem.* **1989**, *179*, 131-137.

[4] J. E. Ladbury, G. Klebe, E. Freire, *Nat. Rev. Drug Discov.* **2010**, *9*, 23-27.

[5] G. A. Holdgate, W. H. Ward, *Drug Discov. Today* **2005**, *10*, 1543-1550.

[6] a) H. Naghibi, A. Tamura, J. M. Sturtevant, *Proc. Natl. Acad. Sci. USA* **1995**, *92*, 5597-5599; b) Y. Liu, J. M. Sturtevant, *Biophys. Chem.* **1997**, *64*, 121-126; c) Y. Liu, J. M. Sturtevant, *Protein Sci.* **1995**, *4*, 2559-2561; d) L. S. Mizoue, J. Tellinghuisen, *Biophys. Chem.* **2004**, *110*, 15-24; e) B. W. Sigurskjold, D. R. Bundle, *J. Biol. Chem.* **1992**, *267*, 8371-8376.

[7] P. R. Connelly, *The Cost of Releasing Site-Specific, Bound Water Molecules from Proteins: Toward a Quantitative Guide for Structure-Based Drug Design*, Springer-Verlag, **1997**.

[8] P. R. Bergethon, *The physical basis of biochemistry*, Springer Science+Business Media, LLC, New York, **2010**.

[9] K. A. Sharp, B. Honig, *Annu. Rev. Biophys. Biophys. Chem.* **1990**, *19*, 301-332.

[10] E. A. Meyer, R. K. Castellano, F. Diederich, *Angew. Chem. Int. Edit.* **2003**, *42*, 1210-1250.

[11] C. L. Perrin, J. B. Nielson, *Annu. Rev. Phys. Chem.* **1997**, *48*, 511-544.

[12] D. H. Williams, E. Stephens, D. P. O'Brien, M. Zhou, *Angew. Chem. Int. Edit.* **2004**, *43*, 6596-6616.

[13] T. S. Olsson, M. A. Williams, W. R. Pitt, J. E. Ladbury, *J. Mol. Biol.* **2008**, *384*, 1002-1017.

[14] M. C. Chervenak, E. J. Toone, *J. Am. Chem. Soc.* **1994**, *116*, 10533-10539.

[15] E. Freire, *Chem. Biol. Drug Des.* **2009**, *74*, 468-472.

[16] J. D. Dunitz, *Science* **1994**, *264*, 670.

[17] K. W., *Adv. Protein Chem.* **1959**, *14*, 1-63.

[18] M. C. Chervenak, E. J. Toone, *Biochemistry* **1995**, *34*, 5685-5695.

[19] D. G. Udugamasooriya, M. R. Spaller, *Biopolymers* **2008**, *89*, 653-667.

[20] a) N. Navarre, N. Amiot, A. van Oijen, A. Imberty, A. Poveda, J. Jimenez-Barbero, A. Cooper, M. A. Nutley, G. J. Boons, *Chem-Eur. J.* **1999**, *5*, 2281-2294; b) B. W. Sigurskjold, C. R. Berland, B. Svensson, *Biochemistry* **1994**, *33*, 10191-10199; c) R. S. McGavin, R. A. Gagne, M. C. Chervenak, D. R. Bundle, *Org. Biomol. Chem.* **2005**, *3*, 2723-2732.

[21] J. E. DeLorbe, J. H. Clements, M. G. Teresk, A. P. Benfield, H. R. Plake, L. E. Millspaugh, S. F. Martin, *J. Am. Chem. Soc.* **2009**, *131*, 16758-16770.

[22] M. S. Searle, D. H. Williams, *J. Am. Chem. Soc.* **1992**, *114*, 10690-10697.

[23] A. A. Edwards, J. M. Mason, K. Clinch, P. C. Tyler, G. B. Evans, V. L. Schramm, *Biochemistry* **2009**, *48*, 5226-5238.

[24] F. Dullweber, M. T. Stubbs, D. Musil, J. Stürzebecher, G. Klebe, *J. Mol. Biol.* **2001**, *313*, 593-614.

[25] E. A. Chavelas, E. García-Hernández, *Biochem. J.* **2009**, *420*, 239-247.

[26] J. Gomez, E. Freire, *A Structure-Based Thermodynamic Approach to Molecular Design*, Springer Verlag, **1997**.

[27] a) G. I. Makhatadze, P. L. Privalov, *Adv. Protein Chem.* **1995**, *47*, 307-425; b) J. K. Myers, C. N. Pace, J. M. Scholtz, *Protein Sci.* **1995**, *4*, 2138-2148.

[28] S. W. Homans, *Drug Discov. Today* **2007**, *12*, 534-539.

[29] a) R. J. Bingham, J. B. Findlay, S. Y. Hsieh, A. P. Kalverda, A. Kjellberg, C. Perazzolo, S. E. Phillips, K. Seshadri, C. H. Trinh, W. B. Turnbull, G. Bodenhausen, S. W. Homans, *J. Am. Chem. Soc.* **2004**, *126*, 1675-1681; b) E. Barratt, A. Bronowska, J. Vondrásek, J. Cerný, R. Bingham, S. Phillips, S. W. Homans, *J. Mol. Bio.l* **2006**, *362*, 994-1003.

[30] a) L. Englert, A. Biela, M. Zayed, A. Heine, D. Hangauer, G. Klebe, *Biochim. Biophys. Acta* **2010**, *1800*, 1192-1202; b) T. Young, R. Abel, B. Kim, B. J. Berne, R. A. Friesner, *Proc. Natl. Acad. Sci. USA* **2007**, *104*, 808-813.
[31] J. Broecker, C. Vargas, S. Keller, *Anal. Biochem.* **2011**, *418*, 307-309.
[32] a) J. Tellinghuisen, *Anal. Biochem.* **2008**, *373*, 395-397; b) W. B. Turnbull, A. H. Daranas, *J. Am. Chem. Soc.* **2003**, *125*, 14859-14866.
[33] A. Varki, R. D. Cummings, J. D. Esko, H. H. Freeze, P. Stanley, C. R. Bertozzi, G. W. Hart, M. E. Etzler, *Essentials of Glycobiology*, Cold Spring Harbor Laboratory Press, New York, **2009**.
[34] M. Ambrosi, N. R. Cameron, B. G. Davis, *Org. Biomol. Chem.* **2005**, *3*, 1593-1608.
[35] T. K. Dam, C. F. Brewer, *Chem. Rev.* **2002**, *102*, 387-429.
[36] G. S. Kansas, *Blood* **1996**, *88*, 3259-3287; S. A. Mousa, D. A. Cheresh, *Drug Discov. Today* **1997**, *2*, 187-199.
[37] Y. van Kooyk, T. B. Geijtenbeek, *Nat. Rev. Immunol.* **2003**, *3*, 697-709.
[38] E. J. Toone, *Curr. Opin. Struc. Biol.* **1994**, *4*, 719-728.
[39] B. A. Williams, M. C. Chervenak, E. J. Toone, *J. Biol. Chem.* **1992**, *267*, 22907-22911.
[40] a) N. Ahmad, H. J. Gabius, S. Sabesan, S. Oscarson, C. F. Brewer, *Glycobiology* **2004**, *14*, 817-825; b) Y. Ito, S. Hagihara, M. A. Arai, I. Matsuo, M. Takatani, *Glycoconj. J.* **2004**, *21*, 257-266; c) M. A. Arai, I. Matsuo, S. Hagihara, K. Totani, J. Maruyama, K. Kitamoto, Y. Ito, *ChemBiochem* **2005**, *6*, 2281-2289; d) T. K. Dam, H. J. Gabius, S. André, H. Kaltner, M. Lensch, C. F. Brewer, *Biochemistry* **2005**, *44*, 12564-12571; e) C. F. Brewer, *Glycoconj. J.* **2004**, *19*, 459-465; f) M. S. Quesenberry, R. T. Lee, Y. C. Lee, *Biochemistry* **1997**, *36*, 2724-2732; g) P. Sörme, P. Arnoux, B. Kahl-Knutsson, H. Leffler, J. M. Rini, U. J. Nilsson, *J. Am. Chem. Soc.* **2005**, *127*, 1737-1743; h) K. Bachhawat-Sikder, C. J. Thomas, A. Surolia, *Febs Lett.* **2001**, *500*, 75-79; i) P. Szabo, T. K. Dam, K. Smetana, B. Dvoránková, D. Kübler, C. F. Brewer, H. J. Gabius, *Anat. Histol. Embryol.* **2009**, *38*, 68-75.
[41] a) C. O. Sallum, R. A. Kammerer, A. T. Alexandrescu, *Biochemistry* **2007**, *46*, 9541-9550; b) M. Kapoor, H. Srinivas, E. Kandiah, E. Gemma, L. Ellgaard, S. Oscarson, A. Helenius, A. Surolia, *J. Biol. Chem.* **2003**, *278*, 6194-6200.
[42] a) K. Marotte, C. Sabin, C. Préville, M. Moumé-Pymbock, M. Wimmerová, E. P. Mitchell, A. Imberty, R. Roy, *ChemMedChem* **2007**, *2*, 1328-1338; b) M. Durka, K. Buffet, J. Iehl, M. Holler, J. F. Nierengarten, J. Taganna, J. Bouckaert, S. P. Vincent, *Chem. Commun.* **2011**, *47*, 1321-1323; c) M. Almant, V. Moreau, J. Kovensky, J. Bouckaert, S. G. Gouin, *Chem. Eur. J.* **2011**, *17*, 10029-10038.
[43] M. Andreini, M. Anderluh, A. Audfray, A. Bernardi, A. Imberty, *Carbohydr. Res.* **2010**, *345*, 1400-1407.
[44] a) J. L. Dashnau, K. A. Sharp, J. M. Vanderkooi, *J. Phys. Chem. B* **2005**, *109*, 24152-24159; b) E. Garcia-Hernandez, R. A. Zubillaga, E. A. Chavelas-Adame, E. Vazquez-Contreras, A. Rojo-Dominguez, M. Costas, *Protein Sci.* **2003**, *12*, 135-142.
[45] V. Roldós, F. J. Cañada, J. Jiménez-Barbero, *Chembiochem* **2011**, *12*, 990-1005.
[46] a) V. R. Srinivas, G. Bhanuprakash Reddy, A. Surolia, *Febs Lett.* **1999**, *450*, 181-185; b) R. Ramkumar, A. Surolia, S. K. Podder, *Biochem. J.* **1995**, *308 (Pt 1)*, 237-241; c) B. N. Murthy, S. Sinha, A. Surolia, S. S. Indi, N. Jayaraman, *Glycoconj. J.* **2008**, *25*, 313-321; d) A. Surolia, N. Sharon, F. P. Schwarz, *J. Biol. Chem.* **1996**, *271*, 17697-17703.
[47] a) N. E. Ziółkowska, S. R. Shenoy, B. R. O'Keefe, J. B. McMahon, K. E. Palmer, R. A. Dwek, M. R. Wormald, A. Wlodawer, *Proteins* **2007**, *67*, 661-670; b) A. Imberty, E. P. Mitchell, M. Wimmerová, *Curr. Opin. Struct. Biol.* **2005**, *15*, 525-534.
[48] a) F. H. Cederkvist, S. F. Saua, V. Karlsen, S. Sakuda, V. G. Eijsink, M. Sørlie, *Biochemistry* **2007**, *46*, 12347-12354; b) C. Diehl, O. Engström, T. Delaine, M. Håkansson, S. Genheden, K. Modig, H. Leffler, U. Ryde, U. J. Nilsson, M. Akke, *J. Am. Chem. Soc.* **2010**, *132*, 14577-14589.
[49] M. K. Wild, M. C. Huang, U. Schulze-Horsel, P. A. van der Merwe, D. Vestweber, *J. Biol. Chem.* **2001**, *276*, 31602-31612.
[50] J. D. Dunitz, *Chem. Biol.* **1995**, *2*, 709-712.
[51] T. R. Bakker, C. Piperi, E. A. Davies, P. A. Merwe, *Eur. J. Immunol.* **2002**, *32*, 1924-1932.

2 Results and Discussion

2.1 Thermodynamics of Glycomimetics Binding to C-type Lectins

2.1.1 E-selectin

2.1.1.1 E-selectin Binding to sLe^x Derivatives

Sialyl Lewis^x – a Pre-organized Water Oligomer?

Florian P. C. Binder,[#] Katrin Lemme, [#] Roland C. Preston and Beat Ernst*

Institute of Molecular Pharmacy, University of Basel, Klingelbergstr. 50, 4056 Basel, Switzerland

[#]Authors contributed equally

**Corresponding author. Tel: 0041 267 15 51; Fax: 0041 267 15 52; e-mail: beat.ernst@unibas.ch*

Published in: *Angew. Chem. Int. Ed.* **2012**, *7*, 7327-7331.

Keywords: Carbohydrate, glycomimetics, isothermal titration calorimetry, lectin, selectin.

Contribution of Katrin Lemme: E-selectin/IgG expression and purification, determination of protein concentration, competitive binding assay, and ITC experiments.

Angewandte International Edition Chemie

DOI: 10.1002/anie.201202555

VIP Glycomimetics

Sialyl Lewis^x: A "Pre-Organized Water Oligomer"?**

*Florian P. C. Binder, Katrin Lemme, Roland C. Preston, and Beat Ernst**

In memory of Daniel Bellûs

In recent years, lectins, such as selectins,[1] galectins,[2] or siglecs[3] have received increasing attention as drug targets. Among them, selectins are the most extensively studied, since they are key players in the early stages of inflammation and therefore promising targets for the treatment of diseases with an inflammatory component, such as stroke, asthma, psoriasis, or rheumatoid arthritis.[4] The key role of selectins is to promote the initial step of the inflammatory cascade, by allowing leukocytes to roll along the vascular endothelial surface. This step is followed by the integrin-mediated firm adhesion and the final extravasation to the site of the inflammatory stimulus.[5]

The specific interaction between E-selectin and its physiological ligand ESL-1 (E-selectin ligand-1) is mediated by the tetrasaccharide sialyl Lewis^x (sLe^x, **1**).[6] Consequently, sLe^x (**1**) became the lead structure for the search of drug-like, high-affinity selectin antagonists.[1,7] Elucidation of the structure activity relationship (SAR),[8] mutation studies,[9] transferred nuclear overhauser enhancement NMR spectroscopy (trNOE-NMR),[10] saturation transfer difference NMR spectroscopy (STD-NMR),[11] molecular modeling,[12] and finally X-ray crystallography[13] yielded a precise picture of the interactions of sLe^x and E-selectin on an atomic level (Figure 1). Because docking studies[7] and STD-NMR experiments[11] revealed that the *N*-acetyl-D-glucosamine (D-Glc*N*Ac) and *N*-acetyl-D-neuraminic acid (D-Neu5Ac) moieties have only weak interactions with the protein,[12] they were replaced with structurally simplified mimics, resulting in E-selectin antagonists with significantly improved binding affinities. However, the affinity of these antagonists,

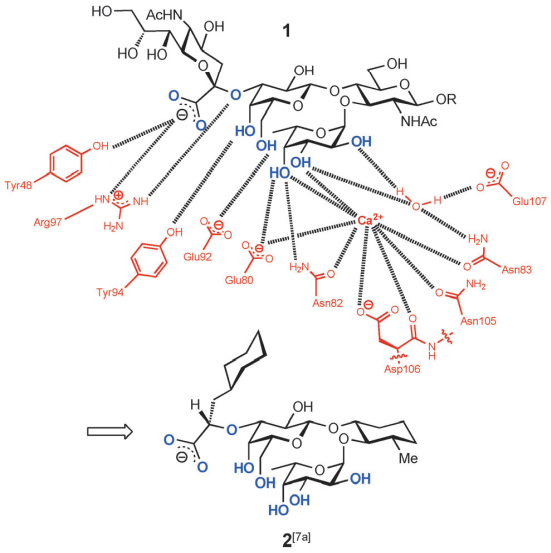

Figure 1. Top: Detailed representation of the interactions between sLe^x (**1**) and E-selectin as observed in the crystal structure;[13] the pharmacophores of **1** are highlighed in blue. Bottom: The glycomimetic **2** exhibits a 13 μM affinity in a cell-free ligand-based competitive binding assay.[7a]

for example, **2** in Figure 1,[7a] is still only in the low micromolar range.

Despite the progress made, the driving force of the interaction of E-selectin with its ligands has not been fully characterized to date, neither for sLe^x (**1**), nor for any low molecular weight selectin antagonist. However, Wild et al. estimated the enthaplic contribution of the E-selectin/ESL-1 interaction by van't Hoff analysis, which involves the correlation of the binding affinity measured at different temperatures. The results indicated that enthalpic changes contribute only 10 to 25% of the binding free energy ΔG and that the interaction is primarily driven by favorable entropy changes.[14]

Recently, the thermodynamic aspects of protein–ligand interactions have gained increasing interest in drug discovery.[15] Particularly enthalpy and entropy changes provide valuable information for lead optimization. Having access to these individual components of binding affinity rather than the overall value facilitates the successful design of high-affinity ligands. Herein, we report a comprehensive study on the thermodynamic fingerprint of a series of E-selectin antagonists.

[*] Dr. F. P. C. Binder,[+] Dr. K. Lemme,[+] R. C. Preston, Prof. Dr. B. Ernst
Institute of Molecular Pharmacy, University of Basel
Klingelbergstrasse 50, 4056 Basel (Switzerland)
E-mail: beat.ernst@unibas.ch

[+] These authors contributed equally to this work.

[**] We gratefully acknowledge the financial support by the Swiss National Science Foundation (grant no. 200020-103875/1) and by GlycoMimetics Inc., Gaithersburg, MD (USA). We are greatly indebted to Dr. Francis Bitsch and Peggy Brunet-LeFeuvre (Novartis, Basel, Switzerland) for giving us access to their VP-ITC as well as for their advice regarding experimental setup and data analysis. Finally, we are thankful to Dr. Martin Smiesko (Institute of Molecular Pharmacy, University of Basel) for preparing the sLe^x/E-selectin illustrations.

Supporting information for this article (details of the synthesis of antagonist **4**, the expression and purification of E-selectin/IgG, the competitive binding assay, and the isothermal calorimetry experiments) is available on the WWW under http://dx.doi.org/10.1002/anie.201202555.

The binding free energy (ΔG) associated with a protein–ligand interaction is composed of enthalpic (ΔH) and entropic ($-T\Delta S$) contributions ($\Delta G = \Delta H - T\Delta S$). The binding energy under standard conditions ($\Delta G°$), where all reactants and products are at a concentration of 1 mol L^{-1}, is calculated from the dissociation constant K_D using the equation $\Delta G = RT \ln K_D$. With isothermal titration calorimetry (ITC),[16] K_D and the enthalpy ΔH are measured directly if no changes in the protonation states occur during the interaction. The enthalpic term (ΔH) represents the contribution of non-covalent interactions upon binding,[15b] that is, hydrogen bonds, electrostatic, and dipole–dipole interactions between ligand and receptor.[17] The entropy term can be dissected into translational and rigid-body rotational entropy,[18] solvation entropy,[19] and conformational entropy.[20]

For our study, an E-selectin/IgG construct consisting of the lectin domain, the EGF-like domain, and six short consensus repeats fused to the Fc part of human IgG1 was used.[21] The 148 kDa protein was expressed in Chinese Hamster Ovarian cells and purified from the conditioned culture medium by affinity chromatography, first with protein A-Sepharose, followed by a second functional purification with the monoclonal anti-hE-selectin antibody 7A9 (see the Supporting Information). The high degree of purity and functionality of the protein is reflected by the stoichiometry (N) of the calorimetric experiments (Table 1). Batches of up to 50 mg E-selectin/IgG were necessary for ITC measurement to reach c values close to 1.

Our calorimetric investigation had two goals: first, the determination of K_D values of a series of E-selectin ligands and their comparison with data collected by a competitive binding assay (Table 1)[22] and second, the elucidation of the thermodynamic fingerprints of these ligands. The K_D value for sLe^x (**1**) binding to E-selectin determined by ITC is (878 ± 93) μM and is thereby in good agreement with previously reported data (e.g. 1.1 to 2.0 mM,[23] (0.7 ± 0.4) mM[10b]). In addition, the relative K_D values (rK_D) for the antagonists **2** to **6** also nicely correlate with their relative IC_{50} values (rIC_{50}). In analogy to earlier findings,[7a] replacement of D-Glc*N*Ac with carbocyclic mimics enhanced binding affinity up to 25-fold (**1**→**4**), whereas the replacement of D-Neu5Ac by (*S*)-cyclohexyllactic acid improved binding 2- to 5-fold (**1**→**5**; **3**→**6**; **4**→**2**).

Except for some isolated cases,[14,27] lectin–oligosaccharide interactions are typically enthalpy driven with mostly unfavorable entropies.[28] In contrast, the binding of sLe^x to E-selectin is driven by a large entropy term ($-T\Delta S = -23$ kJ mol^{-1}). Clearly, the entropy costs caused by the loss of translational and rotational degrees of freedom and conformational changes of ligand and protein upon binding are overcompensated by the beneficial entropy arising from the release of bound water molecules.[29] This argumentation is supported by two experimental observations. First, the bound conformation was identified as one of two low-energy solution conformations of sLe^x,[30] demanding only minor conformational adjustments upon binding. Second, the comparison of the crystal structure of apo-E-selectin and E-selectin bound to sLe^x revealed only minor conformational differences.[13]

The beneficial entropy term, however, is partially compensated by an unfavorable change in enthalpy. To enable the pharmacophoric groups of sLe^x (**1**) to interact with their target, a predominantly polar surface area of approximately 275 Å^2[13a] on both interacting moieties has to be desolvated. Because the newly formed polar interactions between the pharmacophores of sLe^x and E-selectin do not fully compensate for the desolvation penalty of the polar binding interface (Figure 2),[31] a net loss of enthalpy ($\Delta H° = +5.4$ kJ mol^{-1}) is observed. Thus, the directed polar interactions of the pharmacophores contribute to specificity rather than affinity.

Thus, sLe^x (**1**) represents a surrogate of clustered water molecules attached to a scaffold. As a "pre-organized water oligomer" it offers an array of directed hydrogen bonds for the highly specific binding to E-selectin. The clear entropic benefit of the release of water molecules from the large binding interface to bulk water and the high degree of pre-organization of sLe^x result in the observed large entropy gain which provides the impetus for the binding process.

The concept of conformational pre-organization was also exploited for the development of selectin antagonists (Figure 3). More precisely, in sLe^x (**1**), D-Glc*N*Ac acts as

Table 1: Affinity and thermodynamic parameters for the interaction of **1**–**6** with E-selectin.[a]

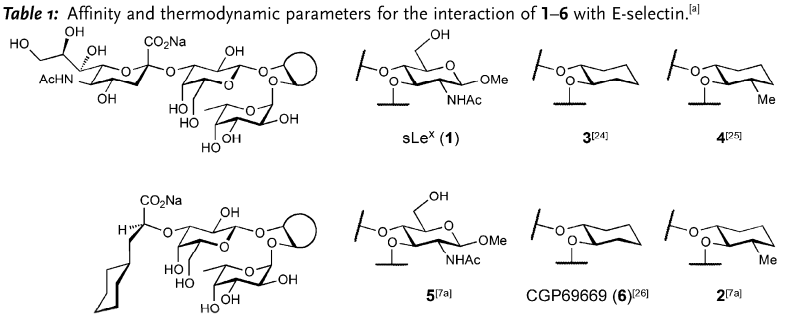

Ligand	rIC_{50}	rK_D	K_D [μM]	ΔG [kJ mol^{-1}]	ΔH [kJ mol^{-1}]	$-T\Delta S$ [kJ mol^{-1}]	N
1	1	1	878 ± 93	−17.5 ± 0.2	+5.4 ± 0.7	−23 ± 1	1
3	0.3	0.36	317	−20.0	−0.5	−19.5	1
4	0.05	0.04	38	−25.3	+0.9	−26.2	0.94
5	0.27	0.30	260	−20.5	−2.2	−18.3	1
6	0.08	0.07	59 ± 4	−24.2 ± 0.2	−5.3 ± 0.4	−18.9 ± 0.6	0.93 ± 0.08
2	0.014	0.02	19 ± 2	−27.1 ± 0.2	−5.8 ± 0.1	−21.3 ± 0.4	0.97 ± 0.01

[a] Relative IC_{50} values (rIC_{50}) and relative K_D values (rK_D) are reported relative to the reference compound sLe^x (**1**). IC_{50} values were determined in a competitive binding assay.[22] K_D and ΔH were measured in ITC experiments, ΔG, and $T\Delta S$ were calculated according the equations $\Delta G = \Delta H - T\Delta S$ and $\Delta G = RT \ln K_D$. N = stoichiometric ratio of ligand and protein.

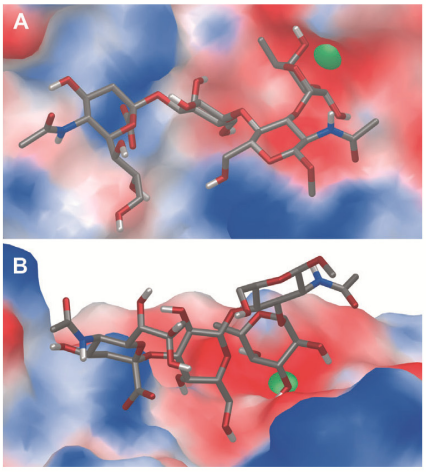

Figure 2. sLe^x (**1**) bound to E-selectin as observed in the crystal structure (protein data bank (PDB) code: 1G1T).[13a] A) top view: the binding epitope on E-selectin is dominated by polar residues [polar residues in red (positively charged) and blue (negatively charged), nonpolar in white]. The contact area is 275 Å^2. B) side view: Only a small part of sLe^x directly contributes to binding (graphics generated by Maestro[32]).

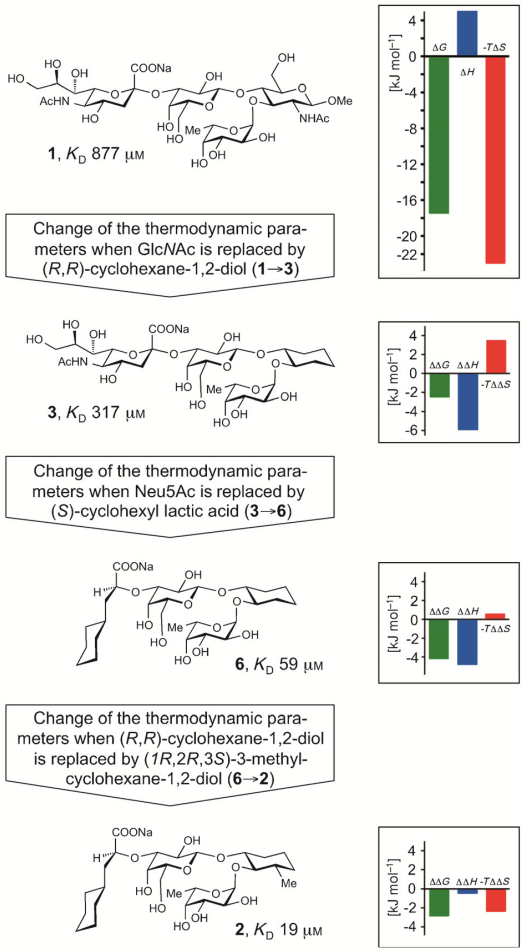

Figure 3. Thermodynamic signature (ΔG, ΔH, $-T\Delta S$) of sLe^x (**1**) (the corresponding data for the antagonists **2**–**6** are summarized in Table 1) and the changes of the thermodynamic parameters ($\Delta\Delta G$, $\Delta\Delta H$, and $-T\Delta\Delta S$) when D-GlcNAc in **1** is replaced by (*R*,*R*)-cyclohexane-1,2-diol (**1**→**3**), D-Neu5Ac in antagonist **3** by (*S*)-cyclohexyl lactic acid (**3**→**6**), and (*R*,*R*)-cyclohexane-1,2-diol in antagonist **6** by (1*R*,2*R*,3*S*)-3-methylcyclohexane-1,2-diol (**6**→**2**).

a scaffold to ensure the correct spatial orientation of L-Fuc and D-Gal in the bioactive conformation, that is, its role is to pre-organize the Le^x core. D-GlcNAc itself has only weak contacts with the target protein (Figure 2B).[13] A comparable role is attributed to D-Neu5Ac, which only contributes to binding through a salt bridge involving its carboxylate group.[13] Consequently, mimics of D-GlcNAc and D-Neu5Ac were designed to stabilize the bioactive conformation and to keep the entropic costs for binding low or virtually the same as for the highly pre-organized sLe^x (**1**). With (*R*,*R*)-cyclohexane-1,2-diol (**1**→**3**) which was demonstrated to be a moderate mimic of D-GlcNAc,[7a] substantial entropy costs arose ($-T\Delta\Delta S$: 3.5 kJ mol^{-1}, Figure 3). When D-Neu5Ac in **3** was replaced by (*S*)-cyclohexyl lactic acid (**3**→**6**, $-T\Delta\Delta S$: 0.6 kJ mol^{-1}), only a small entropy penalty emerged. Finally, (1*R*,2*R*,3*S*)-3-methylcyclohexane-1,2-diol (**6**→**2**) proved to be an optimal replacement of D-GlcNAc (Figure 3),[7a] resulting in an entropy term similar to that of sLe^x (**1**; Table 1). Compared to antagonist **6**, the improved pre-organization of the core conformation in **2** led to a substantial reduction of the entropy costs ($-T\Delta\Delta S$: −2.4 kJ mol^{-1}). Because the investigated mimics are significantly less polar than D-GlcNAc and D-Neu5Ac, an additional effect needs to be taken into account, namely a substantial alteration of the solvation properties. Although only partial desolvation is necessary, the desolvation of the carbocyclic mimics is enthalpically less unfavorable compared to that of the more polar D-GlcNAc or D-Neu5Ac moieties.[31]

Strikingly, the introduction of (*R*,*R*)-cyclohexane-1,2-diol (**1**→**3**) has the same relative effect on enthalpy and entropy as the exchange of D-Neu5Ac for (*S*)-cyclohexyllactic acid (**1**→**5**), which is reflected in the same slope in the entropy–enthalpy plot in Figure 4. In both cases, a significant gain in enthalpy is partially compensated by a loss in entropy. Furthermore, when both mimics are combined in one molecule (→**6**), the effect is not additive, that is, less entropy is lost but also less enthalpy is gained than expected (**6** vs **6**$_{expected}$, Figure 4). Clearly, the exchange of the carbohydrate moieties does not only change local conformational and solvation properties, but rather the properties of the entire ligand.

In summary, thermodynamic binding parameters for the interaction of E-selectin with sLe^x (**1**) and the glycomimetics **2**–**6** were investigated by ITC. The interaction of sLe^x with E-selectin is driven by a large favorable entropy term which is partially compensated by an unfavorable enthalpy contribution. The exchange of residues acting as scaffolds with less

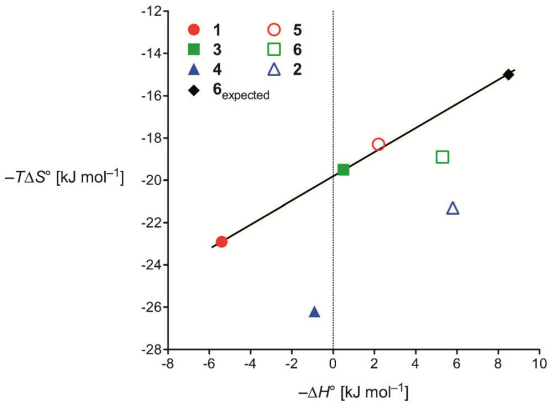

Figure 4. Entropy–enthalpy plot for ligands **1** to **6** and the values expected for **6** ($\mathbf{6}_{expected}$) in case the effects caused by the mimetic replacements of D-Glc*N*Ac by cyclohexane-1,2-diol and D-Neu5Ac by (*S*)-cyclohexyllactic acid were additive.

polar mimics, that is, D-Neu5Ac for (*S*)-cyclohexyllactic acid and D-Glc*N*Ac for (*R*,*R*)-cyclohexane-1,2-diol, resulted in improved binding enthalpy, however accompanied by a loss of binding entropy. Only for mimetic structures that maintain the pre-organization of sLe^x (**1**) in its bioactive conformation, as it is the case for the replacement of D-Glc*N*Ac by (1*R*,2*R*,3*S*)-3-methylcyclohexane-1,2-diol (**1**→**4** or **5**→**2**), a similar entropy term was found. Overall, the almost 50-fold improved affinity of **2** compared to **1** results from a gain in binding enthalpy, whereas the binding entropy is not significantly changed.

The development of glycomimetics with improved binding properties is intrinsically difficult because of the similarity of the ligand (carbohydrate) and the solvent (water). The results of this thermodynamic study suggest, that for a successful development of glycomimetics, carbohydrate moieties with predominantly structural tasks and no or only weak contacts with the target protein should be replaced by hydrophobic mimics, resulting in reduced desolvation penalties and therefore improved enthalpic contributions to binding. In addition, the mimetic replacement should contribute to an improved pre-organization of the binding conformation to optimize the entropy term as well. When the carbohydrate ligand is already almost optimally pre-organized in solution, as it is the case for sLe^x (**1**), the identification of such mimics is a most challenging task.[7a]

Received: April 2, 2012
Published online: July 2, 2012

Keywords: carbohydrates · E-selectin · glycomimetics · isothermal titration calorimetry · sialyl Lewis^x

[1] a) B. Ernst, J. L. Magnani, *Nat. Rev. Drug Discovery* **2009**, *8*, 661–677; b) N. Kaila, B. E. Thomas, *Med. Res. Rev.* **2002**, *22*, 566–601; c) E. E. Simanek, G. J. McGarvey, J. A. Jablonowski, C. H. Wong, *Chem. Rev.* **1998**, *98*, 833–862.

[2] a) C. T. Öberg, H. Leffler, U. J. Nilsson, *Chimia* **2011**, *65*, 18–23; b) L. Ingrassia, I. Camby, F. Lefranc, V. Mathieu, P. Nshimyumukiza, F. Darro, R. Kiss, *Curr. Med. Chem.* **2006**, *13*, 3513–3527.

[3] P. R. Crocker, J. C. Paulson, A. Varki, *Nat. Rev. Immunol.* **2007**, *7*, 255–266.

[4] S. A. Mousa, D. A. Cheresh, *Drug Discovery Today* **1997**, *2*, 187–199.

[5] a) G. S. Kansas, *Blood* **1996**, *88*, 3259–3287; b) D. B. Cines, E. S. Pollak, J. Loscalzo, C. A. Buck, G. A. Zimmerman, R. P. McEver, J. S. Pober, T. M. Wick, B. A. Konkle, B. S. Schwartz, E. S. Barnathan, K. R. McCrae, B. A. Hug, A.-M. Schmidt, D. M. Stern, *Blood* **1998**, *91*, 3527–3561.

[6] M. L. Phillips, E. Nudelman, F. C. A. Gaeta, M. Perez, A. K. Singhal, S. I. Hakomori, J. C. Paulson, *Science* **1990**, *250*, 1130–1132; G. Walz, A. Aruffo, W. Kolamus, M. Bevilacqua, B. Seed, *Science* **1990**, *250*, 1132–1134.

[7] a) D. Schwizer, J. Patton, B. Cutting, M. Smiesko, B. Wagner, A. Kato, C. Weckerle, F. P. C. Binder, S. Rabbani, O. Schwardt, J. L. Magnani, B. Ernst, *Chem. Eur. J.* **2012**, *18*, 1342–1351; b) P. W. Bedard, N. Kaila, *Expert Opin. Ther. Pat.* **2010**, *20*, 781–793; c) N. Kaila, B. E. Thomas, *Expert Opin. Ther. Pat.* **2003**, *13*, 305–317; d) G. Thoma, R. Bänteli, W. Jahnke, J. L. Magnani, J. T. Patton, *Angew. Chem.* **2001**, *113*, 3756–3759; *Angew. Chem. Int. Ed.* **2001**, *40*, 3644–3647; e) G. Thoma, J. L. Magnani, J. T. Patton, B. Ernst, W. Jahnke, *Angew. Chem.* **2001**, *113*, 1995–1999; *Angew. Chem. Int. Ed.* **2001**, *40*, 1941–1945; f) H. C. Kolb, B. Ernst, *Chem. Eur. J.* **1997**, *3*, 1571–1578.

[8] a) W. Stahl, U. Sprengard, G. Kretzschmar, H. Kunz, *Angew. Chem.* **1994**, *106*, 2186–2188; *Angew. Chem. Int. Ed. Engl.* **1994**, *33*, 2096–2098; b) J. Y. Ramphal, Z. L. Zheng, C. Perez, L. E. Walker, S. A. Defrees, F. C. A. Gaeta, *J. Med. Chem.* **1994**, *37*, 3459–3463; c) B. K. Brandley, M. Kiso, S. Abbas, P. Nikrad, O. Srivasatava, C. Foxall, Y. Oda, A. Hasegawa, *Glycobiology* **1993**, *3*, 633–641; d) D. Tyrrell, P. James, N. Rao, C. Foxall, S. Abbas, F. Dasgupta, M. Nashed, A. Hasegawa, M. Kiso, D. Asa, J. Kidd, B. K. Brandley, *Proc. Natl. Acad. Sci. USA* **1991**, *88*, 10372–10376.

[9] D. V. Erbe, B. A. Wolitzky, L. G. Presta, C. R. Norton, R. J. Ramos, D. K. Burns, J. M. Rumberger, B. N. N. Rao, C. Foxall, B. K. Brandley, L. A. Lasky, *J. Cell Biol.* **1992**, *119*, 215–227.

[10] a) R. Harris, G. R. Kiddle, R. A. Field, M. J. Milton, B. Ernst, J. L. Magnani, S. W. Homans, *J. Am. Chem. Soc.* **1999**, *121*, 2546–2551; b) L. Poppe, G. S. Brown, J. S. Philo, P. V. Nikrad, B. H. Shah, *J. Am. Chem. Soc.* **1997**, *119*, 1727–1736; c) K. Scheffler, J. R. Brisson, R. Weisemann, J. L. Magnani, W. T. Wong, B. Ernst, T. Peters, *J. Biomol. NMR* **1997**, *9*, 423–436; d) K. Scheffler, B. Ernst, A. Katopodis, J. L. Magnani, W. T. Wang, R. Weisemann, T. Peters, *Angew. Chem.* **1995**, *107*, 2034–2037; *Angew. Chem. Int. Ed. Engl.* **1995**, *34*, 1841–1844.

[11] M. Rinnbauer, B. Ernst, B. Wagner, J. Magnani, A. J. Benie, T. Peters, *Glycobiology* **2003**, *13*, 435–443.

[12] T. Ishida, *J. Phys. Chem. B* **2010**, *114*, 3950–3964.

[13] a) W. S. Somers, J. Tang, G. D. Shaw, R. T. Camphausen, *Cell* **2000**, *103*, 467–479; b) B. J. Graves, R. L. Crowther, C. Chandran, J. M. Rumberger, S. Li, K.-S. Huang, D. H. Presky, P. C. Familletti, B. A. Wolitzky, D. K. Burns, *Nature* **1994**, *367*, 532–538.

[14] M. K. Wild, M. C. Huang, U. Schulze-Horsel, P. A. van der Merwe, D. Vestweber, *J. Biol. Chem.* **2001**, *276*, 31602–31612.

[15] a) J. E. Ladbury, *Biochem. Soc. Trans.* **2010**, *38*, 888–893; b) J. E. Ladbury, G. Klebe, E. Freire, *Nat. Rev. Drug Discovery* **2010**, *9*, 23–27.

[16] G. A. Holdgate, W. H. Ward, *Drug Discovery Today* **2005**, *10*, 1543–1550.

[17] a) J. E. DeLorbe, J. H. Clements, M. G. Teresk, A. P. Benfield, H. R. Plake, L. E. Millspaugh, S. F. Martin, *J. Am. Chem. Soc.*

2009, *131*, 16758 – 16770; b) M. C. Chervenak, E. J. Toone, *J. Am. Chem. Soc.* **1994**, *116*, 10533 – 10539.
[18] A. V. Finkelstein, J. Janin, *Protein Eng.* **1989**, *3*, 1 – 3.
[19] a) K. P. Murphy, *Biophys. Chem.* **1994**, *51*, 311 – 326; b) R. L. Baldwin, *Proc. Natl. Acad. Sci. USA* **1986**, *83*, 8069 – 8072.
[20] K. K. Frederick, M. S. Marlow, K. G. Valentine, A. J. Wand, *Nature* **2007**, *448*, 325 – 330.
[21] W. Jahnke, H. C. Kolb, M. J. J. Blommers, J. L. Magnani, B. Ernst, *Angew. Chem.* **1997**, *109*, 2715 – 2719; *Angew. Chem. Int. Ed. Engl.* **1997**, *36*, 2603 – 2607.
[22] a) G. Weitz-Schmidt, G. Stokmaier, G. Scheel, N. E. Nifant'ev, B. Tuzikov, N. V. Bovin, *Anal. Biochem.* **1996**, *238*, 184 – 190; b) G. Thoma, J. L. Magnani, R. Oehrlein, B. Ernst, F. Schwarzenbach, R. O. Duthaler, *J. Am. Chem. Soc.* **1997**, *119*, 7414 – 7415.
[23] R. M. Cooke, R. S. Hale, S. G. Lister, G. Shah, M. P. Weir, *Biochemistry* **1994**, *33*, 10591 – 10596.
[24] A. Toepfer, G. Kretzschmar, E. Bartnik, *Tetrahedron Lett.* **1995**, *36*, 9161 – 9164.
[25] For the synthesis of **4**, see the Supporting Information.
[26] K. E. Norman, G. P. Anderson, H. C. Kolb, K. Ley, B. Ernst, *Blood* **1998**, *91*, 475 – 483.
[27] a) C. O. Sallum, R. A. Kammerer, A. T. Alexandrescu, *Biochemistry* **2007**, *46*, 9541 – 9550; b) M. Kapoor, H. Srinivas, E. Kandiah, E. Gemma, L. Ellgaard, S. Oscarson, A. Helenius, A. Surolia, *J. Biol. Chem.* **2003**, *278*, 6194 – 6200; c) P. G. Rani, K. Bachhawat, G. B. Reddy, S. Oscarson, A. Surolia, *Biochemistry* **2000**, *39*, 10755 – 10760.
[28] a) M. Ambrosi, N. R. Cameron, B. G. Davis, *Org. Biomol. Chem.* **2005**, *3*, 1593 – 1608; b) T. K. Dam, C. F. Brewer, *Chem. Rev.* **2002**, *102*, 387 – 429; c) T. K. Dam, B. S. Cavada, T. B. Grangeiro, C. F. Santos, V. M. Ceccatto, F. A. M. de Sousa, S. Oscarson, C. F. Brewer, *J. Biol. Chem.* **2000**, *275*, 16119 – 16126; d) E. J. Toone, *Curr. Opin. Struct. Biol.* **1994**, *4*, 719 – 728.
[29] a) P. R. Connelly in *Structure-Based Drug Design: Thermodynamics, Modeling, and Strategy* (Eds.: J. E. Ladbury, P. R. Connelly), Springer, Berlin, **1997**, pp. 143 – 157; b) J. D. Dunitz, *Science* **1994**, *264*, 670.
[30] a) T. J. Rutherford, D. G. Spackman, P. J. Simpson, S. W. Homans, *Glycobiology* **1994**, *4*, 59 – 68; b) Y. Ichikawa, Y. C. Lin, D. P. Dumas, G. J. Shen, E. Garciajunceda, M. A. Williams, R. Bayer, C. Ketcham, L. E. Walker, J. C. Paulson, C. H. Wong, *J. Am. Chem. Soc.* **1992**, *114*, 9283 – 9298; c) Y. C. Lin, C. W. Hummel, D. H. Huang, Y. Ichikawa, K. C. Nicolaou, C. H. Wong, *J. Am. Chem. Soc.* **1992**, *114*, 5452 – 5454.
[31] a) A. J. Ruben, Y. Kiso, E. Freire, *Chem. Biol. Drug Des.* **2006**, *67*, 2 – 4; b) P. R. Connelly, R. A. Aldape, F. J. Bruzzese, S. P. Chambers, M. J. Fitzgibbon, M. A. Fleming, S. Itoh, D. J. Livingston, M. A. Navia, J. A. Thomson, K. P. Wilson, *Proc. Natl. Acad. Sci. USA* **1994**, *91*, 1964 – 1968; c) S. Cabani, P. Gianni, V. Mollica, L. Lepori, *J. Solution Chem.* **1981**, *10*, 563 – 595.
[32] Maestro, Version 9.1, Schrödinger, LLC, New York, NY, **2010**.

Angewandte Chemie
Eine Zeitschrift der Gesellschaft Deutscher Chemiker

Supporting Information

69451 Weinheim, Germany

Sialyl Lewis^x: A "Pre-Organized Water Oligomer"?**

*Florian P. C. Binder, Katrin Lemme, Roland C. Preston, and Beat Ernst**

anie_201202555_sm_miscellaneous_information.pdf

Contents

1. Synthesis of ligand 4

General Information

NMR spectra were recorded on a Bruker Avance DMX-500 (500 MHz) spectrometer. Assignment of ^{1}H and ^{13}C NMR spectra was achieved using 2D methods (COSY, HSQC, HMQC, HMBC). Chemical shifts are given in ppm and were assigned in relation to the solvent signals on the d-scale[S1] or to tetramethylsilane (0 ppm) as internal standard. Coupling constants *J* are given in Hertz (Hz). Multiplicities were specified as follows: s (singlet), d (doublet), dd (doublet of a doublet), t (triplet), q (quartet), m (multiplet). For assignment of resonance signals to the appropriate nuclei the following abbreviations were used: Fuc (fucose), Gal (galactose), MeCy (3-methylcyclohexane-1,2-diol), Sia (sialic acid). Reactions were monitored by TLC using glass plates coated with silica gel 60 F_{254} (Merck) and visualized by using UV light and/or by charring with a molybdate solution (a 0.02 M solution of ammonium cerium sulfate dihydrate and ammonium molybdate tetrahydrate in aqueous 10% H_2SO_4. Column chromatography was performed using the RediSep Companion from Teledyne Isco with normal phase RediSep columns from the same manufacturer or reversed-phase columns containing LiChroprep RP-18 (40-63 µm) from Merck KGaA, Darmstadt, Germany. Size exclusion chromatography was performed with Bio-Gel® P-2 Gel (45-90 mm) from Bio-Rad. Solvents were purchased from Sigma-Aldrich. Dichloromethane (CH_2Cl_2) was dried by filtration over Al_2O_3 (Fluka, type 5016 A basic). Optical rotations were measured using a Perkin-Elmer Polarimeter 341. Electron spray ionization mass spectra (ESI-MS) were obtained on a Waters micromass ZQ. HRMS analysis were carried out using a Agilent 1100 LC equipped with a photodiode array detector and a Micromass QTOF I equipped with a 4 GHz digital-time converter. Microanalysis was performed at the Institute of Organic Chemistry at the University of Basel, Switzerland. Purity of final compounds was determined on an Agilent 1100 HPLC; detector: ELS, Waters 2420; column: Waters Atlantis dC18, 3 µm, 4.6 x 75 mm; eluents: A: water + 0.1% TFA; B: 90% acetonitrile + 10% water + 0.1% TFA; linear gradient: 0 - 1 min 5% B; 1 - 20 min 5 to 70% B; flow: 0.5 mL/min.

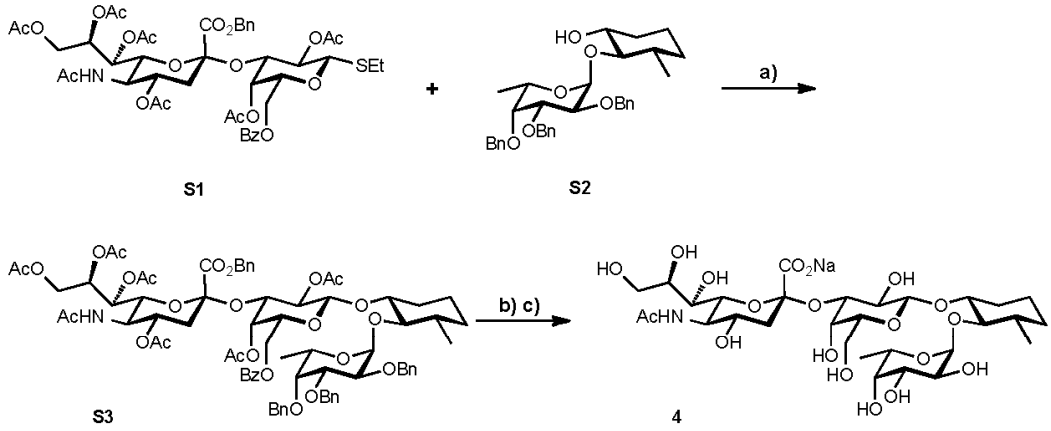

Scheme a) DMTST, CH_2Cl_2, MS 4 Å, RT, 3 d, 55%; b) H_2, $Pd(OH)_2/C$, dioxane, H_2O, RT, 12 h; c) aq. NaOH, MeOH, RT, 81% from **S3**.

Donor **S1**[S2] was coupled to pseudodisaccharide **S2**[S3] using dimethyl(methylthio)sulfonium triflate (DMTST)[S4] as promotor (Scheme). Hydrogenolytic debenzylation followed by saponification with sodium hydroxide afforded **4**.

(Benzyl 5-acetamido-4,7,8,9-tetra-*O*-acetyl-3,5-dideoxy-D-*glycero*-(-D-*galacto*-2-nonulopyranosynate)-(2? 3)-2,4-di-*O*-acetyl-6-*O*-benzoyl-®-D-galactopyranosyl-(1? 1)-[2,3,4-tri-*O*-benzyl-α-L-fucopyranosyl-(1? 2)]-(1*R*,2*R*,3*S*)-3-methyl-cyclohexane-1,2-diol (S3).

Compound **S1** (300 mg, 0.31 mmol) and **S2** (256 mg, 0.47 mmol) were dissolved in anhydrous CH_2Cl_2 (6.0 mL). Powdered activated molecular sieves 4 Å (0.6 g) were added and the mixture was stirred at RT under argon. After 3.5 h, a solution of DMTST (246 mg, 0.95 mmol) in anhydrous CH_2Cl_2 (1.9 mL) that had been stirred with molecular sieves 4 Å (0.19 g) for 3.5 h, was added. After stirring for 3 d, the solution was diluted with CH_2Cl_2 (40 mL), filtered, and successively washed with satd. aq. $NaHCO_3$ (50 mL) and brine (50 mL). The aqueous layers were extracted with CH_2Cl_2 (2 · 50 mL) and the combined organic layers were dried over Na_2SO_4 and concentrated under reduced pressure. Column chromatography on silica (PE/EtOAc/MeOH 8/5/0.5 to 8/5/0.7) afforded **S3** as white foam (248 mg, 0.17 mmol, 55%).

$[\alpha]_D^{20}$ -18.9° (*c* 1.01, $CHCl_3$); ^{1}H NMR (500.1 MHz, $CDCl_3$): δ 8.04-7.14 (m, 25H, Ar-H), 5.48 (ddd, ^3J = 2.6, 6.2, 9.1Hz, 1H, Sia-H8), 5.21 (A of AB, ^2J = 12.0Hz, 1H, PhCH_2), 5.20 (dd, ^3J = 2.8, 9.4Hz, 1H, Sia-H7), 5.01 (d, ^3J = 3.7Hz, 2H, Fuc-H1, Gal-H4), 4.90 (A' of A'B', J = 12.0Hz, 1H, PhCH_2), 4.88-4.64 (m, 10H, Fuc-H5, Gal-H2, SiaN*H*, Sia-H4, 3

PhCH_2), 4.56 (d, ^3J = 8.0Hz, 1H, Gal-H1), 4.48 (dd, ^3J = 3.3, 10.2Hz, 1H, Gal-H3), 4.25 (dd, ^3J = 2.6Hz, ^2J = 12.4Hz, 1H, Sia-H9a), 4.17 (dd, ^3J = 6.4Hz, ^2J = 10.8Hz, 1H, Gal-H6a), 4.05 (dd, ^3J = 3.7, 10.3Hz, 2H, Fuc-H2), 4.02-3.93 (m, 3H, Fuc-H3, Gal-H6b, Sia-H5), 3.90-3.83 (m, 2H, Gal-H5, Sia-H9b), 3.59 (m, 1H, Fuc-H4), 3.50 (m, 1H, MeCy-H1), 3.37 (dd, 1H, ^3J = 2.7, 10.8Hz, Sia-H6), 3.18 (t, ^3J = 9.2Hz, MeCy-H2), 2.50 (dd, ^3J = 4.6Hz, ^2J =12.7Hz, 1H, Sia-H3^{eq}), 2.09, 2.05 (2s, 6H, 2 COCH_3), 1.99 (m,1H, MeCy), 1.99, 1.94, 1.90, 1.74, 1.72 (5s, 15H, 5 COCH_3), 1.65-1.47 (m, 4H, Sia-H3^{ax}, MeCy) 1.21-1.11 (m, 5H, Fuc-H6, MeCy), 1.03 (d, ^3J = 6.4Hz, 3H, MeCy-CH_3), 0.98 (m, 1H, MeCy); ^{13}C NMR (125.8 MHz, $CDCl_3$): δ 170.8, 170.7, 170.6, 170.4, 169.9, 169.5 (7C, *C*OCH$_3$), 167.5 (Sia-C1), 165.8 (Ar*C*O), 139.3, 139.1, 138.7, 134.9, 133.3, 128.9, 128.7, 128.6, 128.5, 128.4, 128.3, 127.6, 127.4, 127.3 (30C, Ar-C), 99.4 (Gal-C1), 98.3 (Fuc-C1), 96.9 (Sia-C2), 82.2 (MeCy-C2), 80.6, 80.5 (Fuc-C3, MeCy-C1), 77.8 (Fuc-C4), 76.7 (Fuc-C2), 74.6, 74.3, 72.7 (3C, PhCH_2), 72.0, 71.9 (Gal-C3, Sia-C6), 70.0, 69.8 (Gal-C2, Gal-C5), 69.4 (Sia-C4), 68.4 (PhCH_2), 67.8 (2C, Gal-C4, Sia-C8), 67.1 (Sia C7), 66.3 (Fuc-C5), 62.8 (Sia-C9), 61.5 (Gal-C6), 49.0 (Sia-C5), 39.2 (MeCy-C3) 37.5 (Sia-C3), 33.6 (MeCy-C4), 30.9 (MeCy-C6), 23.3 (*C*H$_3$CO), 23.1 (MeCy-C5), 21.5, 21.0, 20.9, 20.8 (6C, CO*C*H$_3$), 18.9 (MeCy-*C*H$_3$), 17.1 (Fuc-C6); MS (ESI) *m/z*: calcd. for $C_{77}H_{91}NNaO_{26}$ $[M+Na]^+$: 1468.6; found: 1468.6; elemental analysis calcd (%) for $C_{77}H_{91}NO_{26}$ + 0.5 H_2O (1455.55): C 63.54, H 6.37, N 0.96; found: C 63.58, H 6.35, N 0.80.

(Sodium 5-acetamido-3,5-dideoxy-D-*glycero*-⟨-D-*galacto*-2-nonulopyranosynate)-(2? 3)-®-D-galactopyranosyl-(1? 1)-[α-L-fucopyranosyl-(1? 2)]-(1*R*,2*R*,3*S*)-3-methyl-cyclohexane-1,2-diol (4).

Compound **S3** (310 mg, 0.21 mmol) was dissolved in dioxane/water (4/1, 10 mL) under argon. $Pd(OH)_2$/C (40 mg, 10% $Pd(OH)_2$) was added and the resulting mixture was hydrogenated (4 bar H_2) at RT. After 24 h, the mixture was filtered and the solvent removed under reduced pressure yielding 220 mg of a white solid, which was directly used for saponification. The crude product (75 mg) was stirred in aqueous NaOH (1 N, 1.5 mL) for 24 h at RT, lyophilized, and purified *via* SEC and RP chromatography (H_2O/MeOH). Lyophilization from water afforded **4** as white fluffy solid (42 mg, 0.056 mmol, 81%).

$[\alpha]_D^{20}$ -47.4° (*c* 0.89, MeOH); ^{1}H NMR (500.1 MHz, D_2O): δ 5.07 (d, ^3J = 3.6Hz, 1H, Fuc-H1), 5.05-4.71 (m, Fuc-H5), 4.53 (d, ^3J = 7.8Hz, 1H, Gal-H1), 4.05 (dd, ^3J = 2.4, 9.6Hz, 1H, Gal-H3), 3.92 (m, Gal-H4), 3.90-3.50 (m, 15H, Fuc-H2, Fuc-H3, Fuc-H4, Gal-H2, Gal-H5, Gal-H6a, Gal-H6b, MeCy-H1, Sia-H4, Sia-H5, Sia-H6, Sia-H7, Sia-H8, Sia-H9a, Sia-H9b), 3.20 (t, ^3J = 9.6Hz, 1H, MeCy-H2), 2.73 (dd, ^3J = 4.4Hz, ^2J = 12.1Hz, 1H, Sia-H3^{eq}), 2.13

(m, 1H, MeCy-H6a), 2.00 (s, 3H, COCH_3), 1.78 (t, $^3J = ^2J$ = 12.1Hz, 1H, Sia-H3^{ax}) 1.69-1.52 (m, 3H, MeCy-H3, MeCy-H4a, MeCy-H5a), 1.33-1.17 (m, 2H, MeCy-H5b, MeCy-H6b), 1.15 (d, ^3J = 6.4Hz, 1H, Fuc-H6), 1.11-0.99 (m, 4H, MeCy-CH_3, MeCy-H4b); ^{13}C NMR (125.8 MHz, D_2O, CD_3OD_{ref}): δ 176.0 (*C*OCH$_3$), 175.0 (Sia-C1), 100.8 (Sia-C2), 100.5 (Gal-C1), 99.8 (Fuc-C1), 85.0 (MeCy-C2), 79.4 (MeCy-C1), 76.9 (Gal-C3), 75.5 (Gal-C5), 73.8 (Sia-C6), 73.0 (Fuc-C4), 72.7 (Sia-C8), 70.2 (Fuc-C3), 69.9 (Gal-C2), 69.4, 69.2, 69.1 (3C, Fuc-C2, Sia-C4, Sia-C7), 68.5 (Gal-C4), 67.5 (Fuc-C5), 63.6 (Sia-C9), 62.6 (Gal-C6), 52.7 (Sia-C5), 40.6 (Sia-C3), 39.8 (MeCy-C3), 34.2 (MeCy-C4), 31.1 (MeCy-C6), 23.6 (MeCy-C5), 23.0 (CO*C*H$_3$), 19.2 (MeCy-*C*H$_3$), 16.4 (Fuc-C6); HR-MS (ESI) *m/z*: calcd for $C_{30}H_{50}NNa_2O_{19}$ $[M+Na]^+$: 774.2767; found: 774.2768; HPLC-purity ≥ 99.5 %.

2. Materials and methods

Ham'sF-12 medium, RPMI 1640 medium, geneticin (G418) sulfate, αDMEM-medium, peroxidase ABTS (2,2'-azino-bis[3-ethylbenzthiazoline-6-sulfonic acid]) single solution, and FCS (fetal calf serum) were all purchased from Invitrogen (Paisley, UK). Sodium pyruvate, penicillin/streptomycin, HEPES, NaOH, $CaCl_2$ x 2 H_2O, Tween 20, amonium acetate, acetic acid, and cyanogen bromide-activated-Sepharose® 4B were purchased from Sigma-Aldrich Chemie GmbH (Steinheim, Germany). NaCl and HCl were purchased form Merck KGsA (Darmstadt, Germany). Tris was purchased from AppliChem GmbH (Darmstadt, Germany). Protein A-Sepharose® was purchased from BioVision (Mountain View, CA), sLe^a-PAA-biotin was purchased from GlycoTech Corporation (Gaithersburg). The streptavidin peroxidase conjugate was purchased from Roche Diagnostic (Rotkreuz, Switzerland). The BioLogic Duo Flow fast protein liquid chromatography (FPLC) system and the UNO™ Q ion exchange column were purchased from BioRad (Reinach. Switzerland). The Vivaspin® 20 centrifugal concentration tubes were purchased from Sartorius-Stedim (Göttingen, Germany). The SpectraMax 190 microplate reader was obtained from Molecular Devices (Sunnyvale, CA, USA). The VP-ITC apparatus was purchased from MicroCal Inc. (Uppsala, Sweden). Slide-A-Lyzer cassettes were obtained from Thermo Fisher Scientific (Rockford, IL, USA)

3. Generation of the 7A9 antibody column

For the purification of E-selectin/IgG, an affinity column with the functional monoclonal anti-hE-selectin antibody 7A9 was prepared. Mouse hybridoma cells expressing the 7A9 antibody (ATCC No. HB-10135™) were cultivated in suspension at 37 °C and 5% CO_2 with

RPMI 1640 culture medium supplemented with 10-15% FCS, 100 U/mL penicillin, and 100 µg/mL streptomycin. The cells were maintained at 10^5-10^6 cells/mL at all times. Culture medium was harvested once or twice weekly by centrifugation at 1000 rpm and 4 °C for 10 minutes. The 7A9 antibody was purified using fast protein liquid chromatography, first on a Protein A-sepharose® column with the buffers A (50 mM Tris, 150 mM NaCl, pH 7.4, 0.05% Tween 20) for loading, B (5 mM ammonium acetate, pH 5) for washing, C (500 mM acetate, pH 3.0) for elution, and D (2 M Tris) for neutralizing. Higher purity was achieved by subsequent anion exchange chromatography on a Uno™ Q column with buffers E (20 mM Tris, pH 8.0) and F (20 mM Tris, 1 M NaCl, pH 8.0). Approximately 5 mg of purified antibody was coupled to 1 mL of swollen cyanogen bromide-activated-Sepharose® 4B according to the manufacturer's protocol.

4. E-selectin/IgG expression and purification

CHO-K1 cells expressing the E-selectin/IgG construct, which includes the lectin domain, the EGF-like domain, and six complement repeat domains of human E-selectin fused to the Fc part of human IgG1 were generated as previously described.[S5] The cells were cultivated as monolayers at 37 °C, 5% CO_2, in F-12 culture medium supplemented with 10 mM sodium pyruvate, 10% FCS, 100 U/mL penicillin, 100 µg/mL streptomycin, and 0.4 mg/mL geneticin (G418) sulfate. For the expression, the cells were adapted to 5% FCS and αDMEM-medium with the same additives as for the F-12 culture medium. Conditioned culture medium was harvested once a week and stored at -20 °C.

E-selectin/IgG was purified from the conditioned culture medium by affinity chromatography, first with protein A-Sepharose®, followed by a second purification with the 7A9-Sepharose® column. In both cases, buffers A, B, C, and D were used (see above). Purified E-selectin/IgG was concentrated by ultrafiltration (1610 x g, Vivaspin 20, 50 kDa cut off) and dialysed over night against assay buffer (10 mM HEPES, 150 mM NaCl, 1 mM $CaCl_2$, pH 7.4) using Slide-A-Lyzer dialysis cassettes (cut off 10 kDa). The protein purity was confirmed by standard SDS-PAGE analysis and the concentration was determined by HPLC-UV against a BSA standard.[S6].

The binding activity was verified with a carbohydrate polymer-binding assay for the EC_{50} determination, similar to the protocols described in Ref[S7] Peroxidase coupled sLe^a-polymer was prepared as follows: 20 µL biotinylated sLe^a (sLe^a-PAA-biotin, 1 mg/mL), 80 µL streptavidin peroxidase conjugate (500 U/mL), 20 µL FCS, and 80 µL assay buffer were combined and incubated for 2 h at 37 °C. The complex is stable for several weeks at 4 °C.

Nunc MaxiSorp™ 96 well plates were coated with E-selectin/IgG (1 µg/ml, 100 µL/well) over night at 4 °C and were subsequently blocked with BSA (3% w/v in assay buffer, 200 µL/well) for 2 h at 4 °C, followed by incubation for 3 h at room temperature with a serial dilution of peroxidase coupled sLe^a-polymer. The excess of sLe^a-polymer was washed, ABTS solution (100 µL/well) was added, and the colorimetric reaction was stopped after 10 min with 100 µL/well oxalic acid (2% w/v). The OD was measured at 415 nm with a microplate reader .

5. Competitive binding assay

The competitive binding assay was adapted from Ref[S7] Most steps were performed according to the EC_{50} determination (see above). In the incubation step, a constant concentration of sLe^a-polymer (100 ng/mL, 50 µL/well), and a serial dilution of antagonist (50 µL/well) was applied.

6. Isothermal titration calorimetry

ITC experiments were performed with a VP-ITC instrument. Protein samples were dialyzed over night against assay buffer using Slide-A-Lyzer dialysis cassettes (10 kDa cut-off). Protein and ligand samples were degassed with vacuum prior to the assays. All measurements were performed at 25 °C. Injections of 5 to 15 µL ligand solutions (1.4 - 12 mM) were added from a computer controlled 300 µl microsyringe at an interval of 5 min into the sample cell solution containing E-selectin/IgG (45 to 200 µM, sample cell volume 1.4037 mL or 1.4523 mL) with stirring at 307 rpm. The quantity $c = Mt(0)\ K_D^{-1}$, where Mt(0) is the initial macromolecule concentration, is of importance in titration microcalorimetry and should be between 1 and 1000.[S8] The c-values for compound **2**, **4**, and **6** were between 1 and 5. The experiments with methyl sLe^X (**1**), **3**, and **5** were performed with c values below 1. In these cases, the stoichiometry N was fixed to 1 to allow for reliable determination of the dissociation constant K_D and the change in enthalpy $?H$.[S9] Control experiments, i.e. ligand injection into buffer (10 mM HEPES, 150 mM NaCl, 1 mM $CaCl_2$, pH 7.4) in absence of protein, showed that the heats of dilution were small and constant. The first injection was always excluded from data analysis as it usually suffers from sample loss during the mounting of the syringe and the equilibration preceding the actual titration. Raw data was collected and the area under each peak was integrated, followed by correction for heats of dilution and mixing by subtracting the final baseline consisting of small peaks of the same size to zero. The data were analyzed with ORIGIN Software (Microcal Inc.) by three-parameter data fitting of a single-site binding isotherm, which yields $?H$ (enthalpy of

binding), K_D (dissociation constant) and N (stoichiometry) for compounds **2**, **4** and **6**. A two-parameter data fitting of a single-site binding isotherm was used for methyl sLe^x (**1**), compound **3** and **5**, which yields ?H and K_D.

Thermodynamic parameters were calculated from equation S1.

$\Delta G = \Delta H - T\Delta S = RT\ln K_D$ (S1)

where ?G, ?H, and ?S are the changes in free energy, enthalpy, and entropy, respectively. T is the absolute temperature, and R is the gas constant (8.314 J/molK).

methyl sLe^x (1)

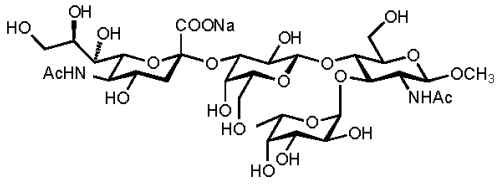

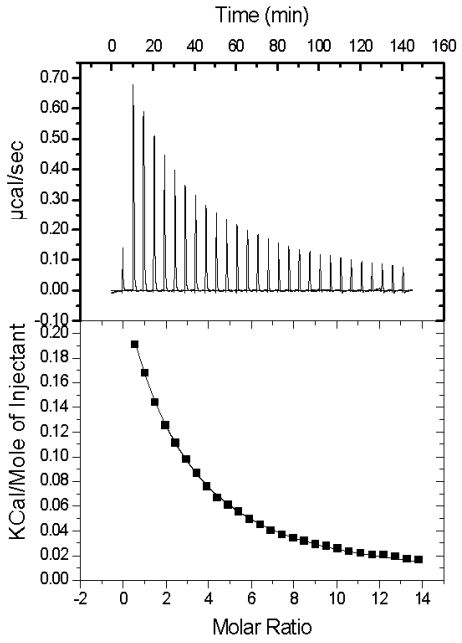

Compound 2

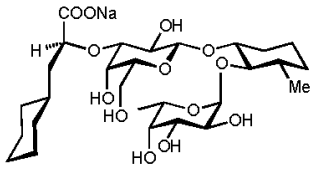

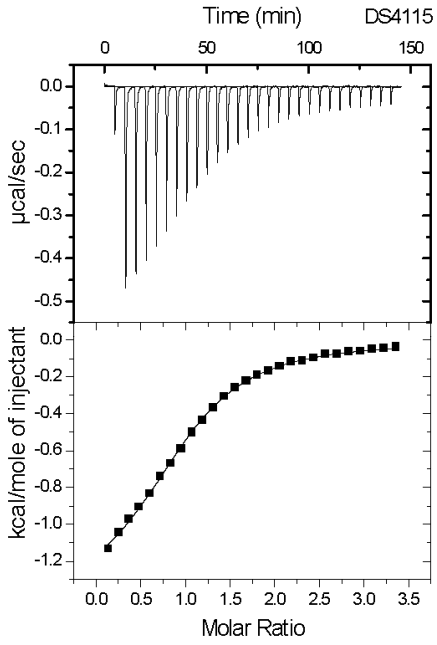

Compound 3

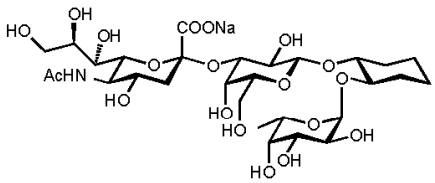

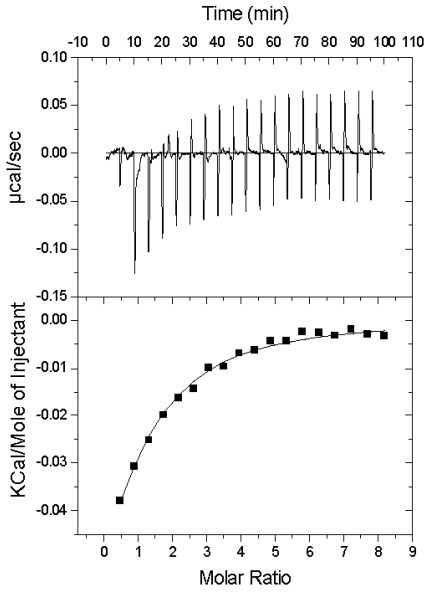

Compound 4

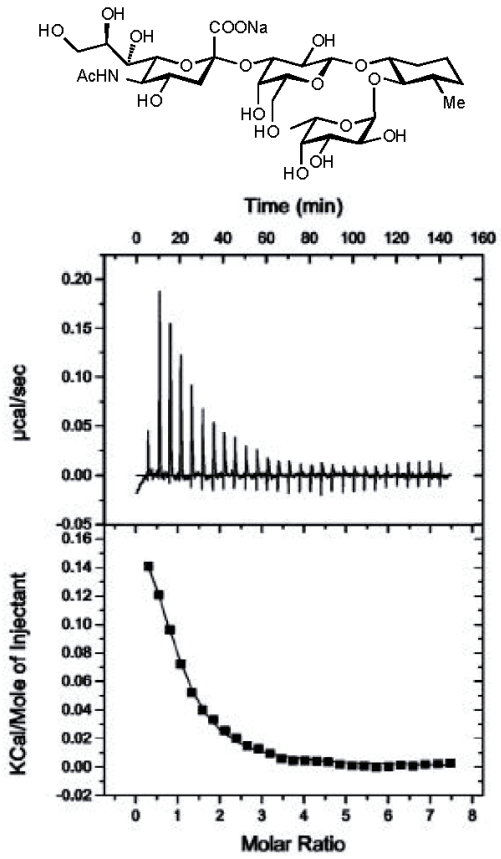

Compound 5

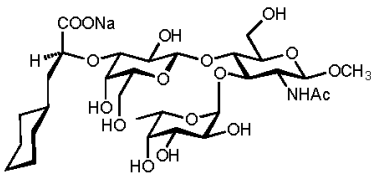

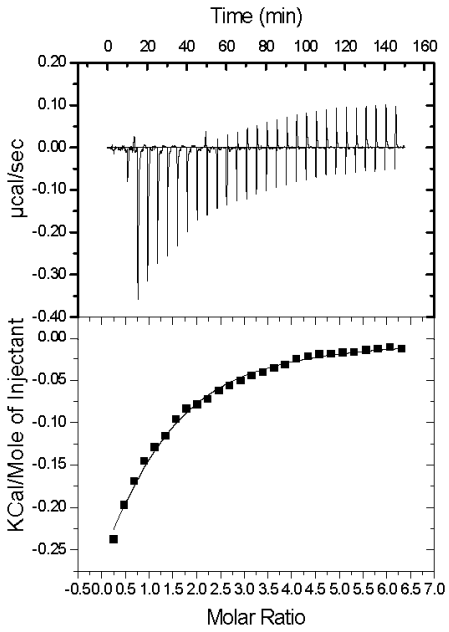
Time (min)
µcal/sec
KCal/Mole of Injectant
Molar Ratio

Compound 6

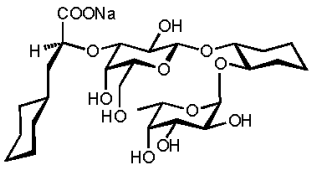
COONa
OH
H
O
HO
HO
OH
HO

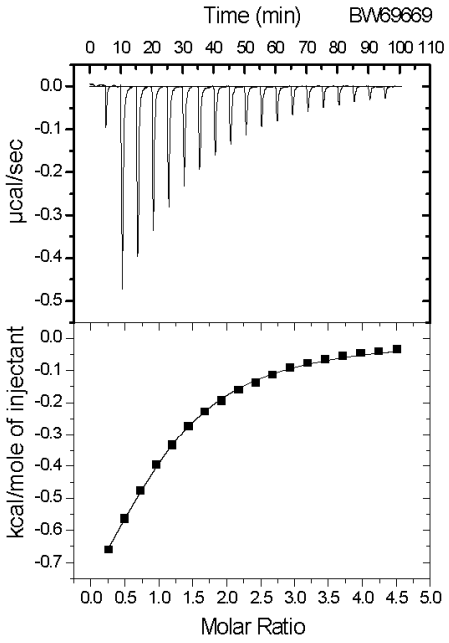
Time (min)
BW69669
µcal/sec
kcal/mole of injectant
Molar Ratio

7. Graphics

The graphical abstract and Figure 2 are based on the crystal structure of sLe^X in complex with E-selectin (pdb-code 1G1T)[S10] and illustrated with the software Maestro version 9.1, Schrödinger, LLC, New York, NY, 2010.

8. References

[S1] H. E. Gottlieb, V. Kotlyar, A. Nudelman, *J. Org. Chem.* **1997**, *62*, 7512-7515.

[S2] A. Bhunia, O. Schwardt, H. Gathje, G. P. Gao, S. Kelm, A. J. Benie, M. Hricovini, T. Peters, B. Ernst, *Chembiochem* **2008**, *9*, 2941-2945.

[S3] D. Schwizer; J. Patton; B. Cutting; M. Smiesko; B. Wagner; A. Kato; C. Weckerle, F.P.C. Binder, S. Rabbani, O. Schwardt, J.L. Magnani, B. Ernst, *Chem. Eur. J.* **2012**, *18*, 1342-1351.

[S4] P. Fugedi, P. J. Garegg, *Carbohydr. Res.* **1986**, *149*, C9-C12.

[S5] W. Jahnke, H. C. Kolb, M. J. J. Blommers, J. L. Magnani, B. Ernst, *Angew. Chem. Int. Ed. Engl.* **1997**, *36*, 2603-2607.

[S6] a) S. Mesch, K. Lemme, H. Koliwer-Brandl, D. S. Strasser, O. Schwardt, S. Kelm, B. Ernst, *Carbohydr. Res.* **2010**, *345*, 1348-1359; b) F. Bitsch, R. Aichholz, J. Kallen, S. Geisse, B. Fournier, J. M. Schlaeppi, *Anal. Biochem.* **2003**, *323*, 139-149.

[S7] a) G. Thoma, J. T. Patton, J. L. Magnani, B. Ernst, R. Oehrlein, R. O. Duthaler, *J. Am. Chem. Soc.* **1999**, *121*, 5919-5929; b) G. Weitz-Schmidt, K. W. Gong, C. H. Wong, *Analytical Biochemistry* **1999**, *273*, 81-88; c) G. Weitz-Schmidt, D. Stokmaier, G. Scheel, N. E. Nifant'ev, A. B. Tuzikov, N. V. Bovin, *Anal. Biochem.* **1996**, *238*, 184-190.

[S8] T. Wiseman, S. Williston, J. F. Brandts, L. N. Lin, *Anal. Biochem.* **1989**, *179*, 131-137.

[S9] a) J. Tellinghuisen, *Anal. Biochem.* **2008**, *373*, 395-397; b) W. B. Turnbull, A. H. Daranas, *J. Am. Chem. Soc.* **2003**, *125*, 14859-14866.

[S10] W. S. Somers, J. Tang, G. D. Shaw, R. T. Camphausen, *Cell* **2000**, *103*, 467-479.

9. Experimental data

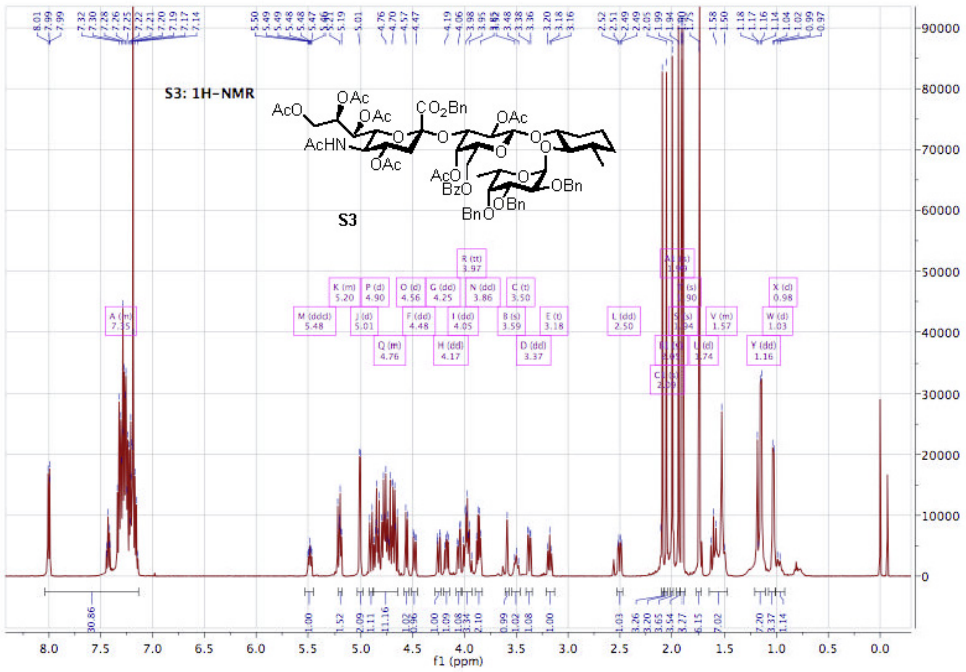

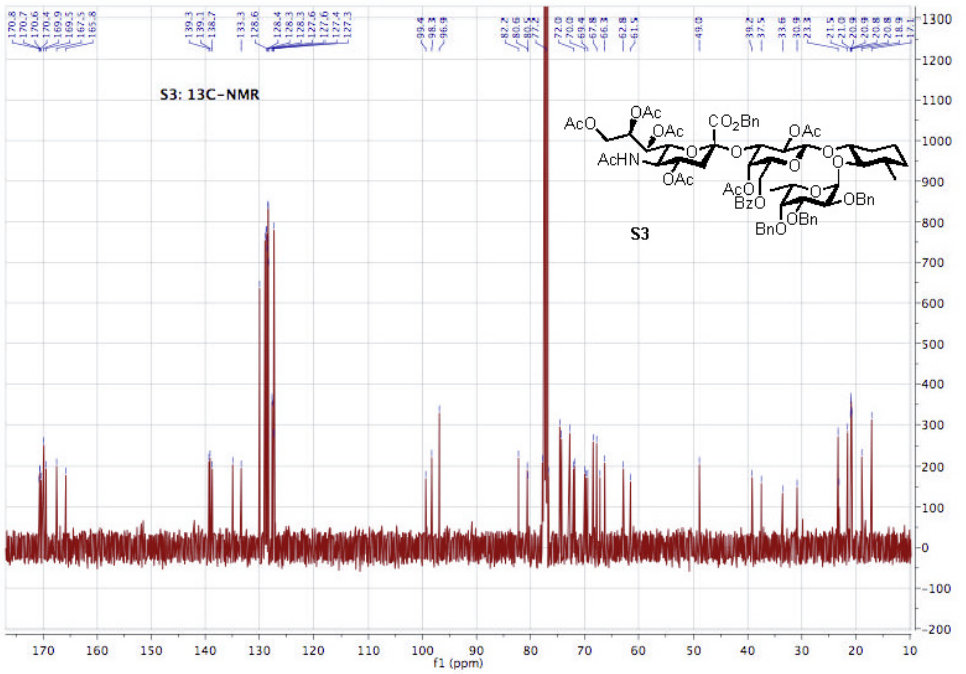

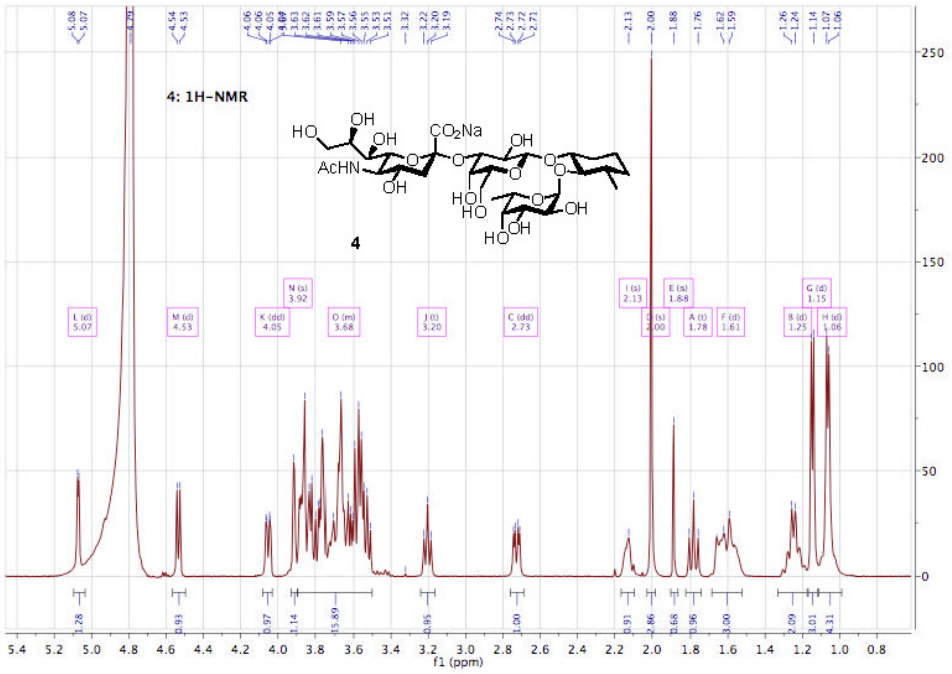
4: 1H-NMR
4
f1 (ppm)

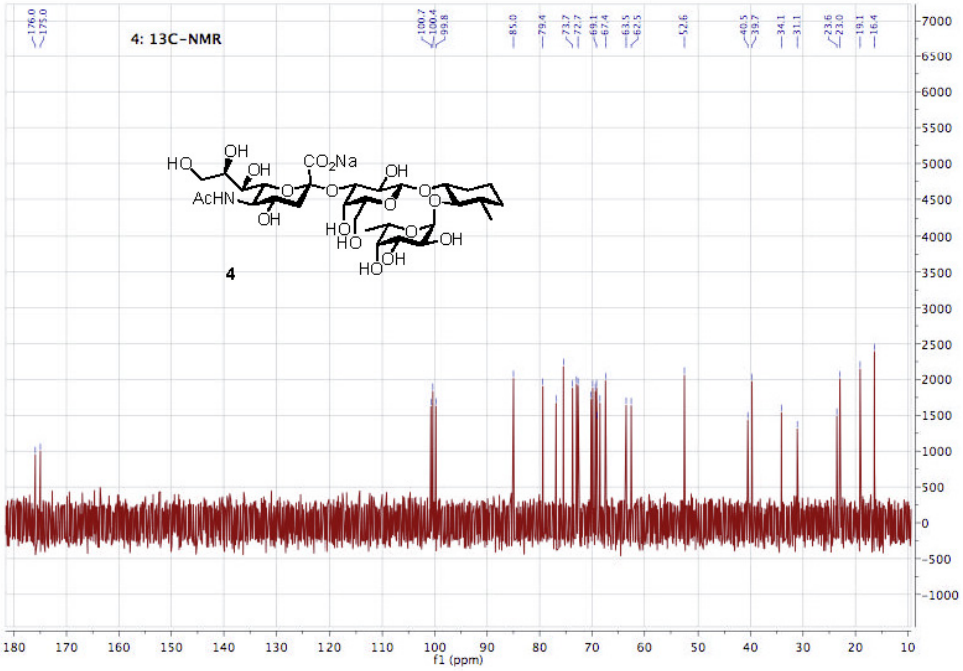
4: 13C-NMR
4
f1 (ppm)

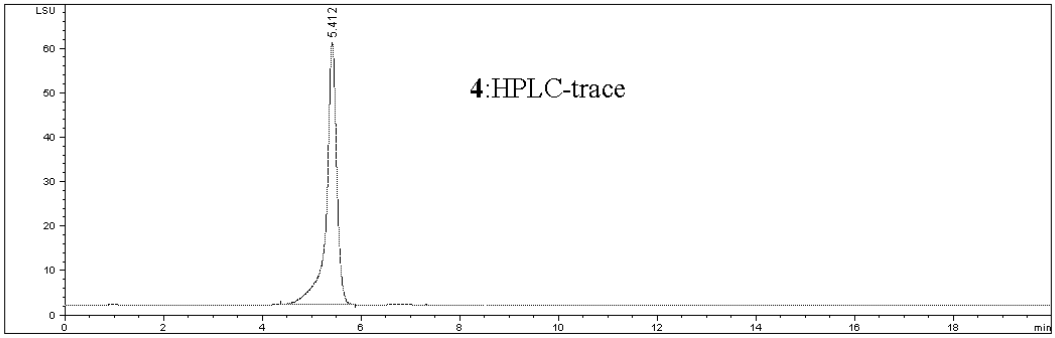

4:HPLC-trace

2.1.1.2 E-selectin Binding to Aromatic Glycomimetics

Enhanced Binding Affinity to E-selectin with Aromatic Antagonists

Katrin Lemme, Bea Wagner, Roland C. Preston, and Beat Ernst*

Institute of Molecular Pharmacy, University of Basel, Klingelbergstr. 50, 4056 Basel, Switzerland

**Corresponding author. Tel: 0041 267 15 51; Fax: 0041 267 15 52; e-mail: beat.ernst@unibas.ch*

Keywords: Lectin, selectin, glycomimetics, isothermal titration calorimetry, change in heat capacity.

Contribution of Katrin Lemme: Manuscript, E-selectin/IgG expression and purification, determination of protein concentration, competitive binding assay, and ITC experiments.

Draft version.

Introduction

Selectins are carbohydrate-binding proteins that belong to the family of C-type lectins, as they bind their ligands in a Ca^{2+}-dependent manner. They are key players in states of inflammation and metastasis.[1] Selectins are cell-adhesion molecules that mediate the earliest stage of leukocyte trafficking[2] which serves to initially slow down the leukocytes and allow activation of integrins, which then ensure firm adhesion to the endothelial layer. Finally, leukocytes transmigrate through the endothelial layer and migrate to the site of inflammation.[3] To date, three selectins have been identified, P-, E-, and L-selectin, that bind their natural ligands with fast kinetics[4] what is typical for carbohydrate-lectin interactions.[5] The tetrasaccharide sialyl Lewis^x (sLe^x, **1**) constitutes the minimum binding epitope of all three selectins.[6] In this communication we focus on E-selectin. The interactions of sLe^x (**1**) to E-selectin are depicted in Figure 1.[7] *N*-Acetylglucosamine (Glc*N*Ac) is not directly involved in binding, but serves as a spacer to ensure the correct spatial orientation between Fuc and Gal.[8]

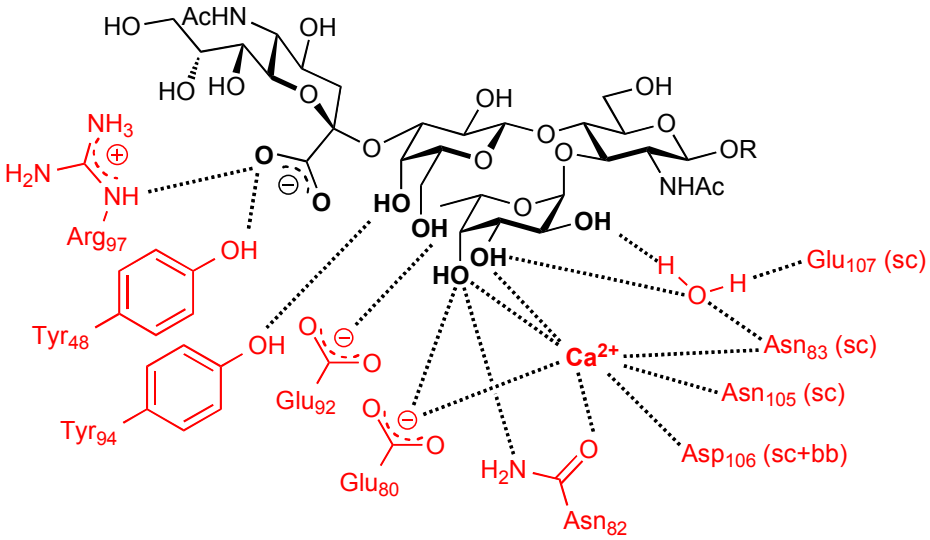

Figure 1. Schematic presentation of interactions between sLe^x (**1**) and E-selectin as observed in the crystal structure of Somers *et al.*[9] The 3- and 4-hydroxyl groups of Fuc directly coordinate to Ca^{2+} and are involved in further hydrogen bonding with protein side chains coordinating to Ca^{2+}. The 2-hydroxyl group of Fuc forms water mediated hydrogen bonds to the side chains of Asn83 and Glu107. The 4- and 6-hydroxyl groups of Gal bind to the side chains of Tyr94 and Glu92, respectively. The carboxylate of sialic acid forms a hydrogen bond to the side chain of Tyr48 and a salt bridge to the side chain of Arg97. The guanidine moiety of Arg97 furthermore binds to the oxygen of the glycosidic bond between Gal and Neu5Ac.

sc = side chain; bb = backbone; pharmacophoric groups in bold.[7]

The binding affinity and kinetics of E-selectin ligand-1 (ESL-1) have been described with a dissociation constant K_D of 56 μM and an off-rate k_{off} of 2.7 s^{-1} resulting in a calculated k_{on} of $4.8 \cdot 10^4$ $M^{-1}s^{-1}$. Additionally, the binding was characterized to be entropically driven with a weak enthalpic contribution ($\Delta G°$ = –24 kJ mol^{-1}, $\Delta H°$ = –4 ± 3 kJ mol^{-1}, $-T\Delta S°$ = –20 kJ mol^{-1}, at 25 °C). The thermodynamic parameters were determined indirectly with a van't Hoff plot. Vestweber *et al.* attributed the favorable entropy to the desolvation and/or unexpectedly low entropic costs of complex formation between E-selectin and ESL-1. The relatively low enthalpic contribution was explained by the small number of beneficial interactions and/or disruption of favorable interactions upon binding.[10] Such entropy driven binding has been reported for other lectins,[11] although carbohydrate-lectin interactions are typically enthalpy driven with unfavorable or only weakly favorable change in entropies.[12] Later, this entropically driven binding was confirmed for sLe^x (**1**) binding to E-selectin with isothermal titration calorimetry (ITC), where the enthalpy is measured directly. It was argued that the entropy costs caused by the loss of translational and rotational degrees of freedom and conformational changes of ligand and protein upon are overcompensated by the beneficial entropy arising from the release of bound water. However, the interaction exhibits an unfavorable enthalpic contribution related to the desolvation penalty that is not compensated by the polar interaction between the pharmacophores of sLe^x (**1**) and E-selectin.[7]

One successful strategy of optimizing E-selectin antagonists was the replacement of sialic acid by (*S*)-cyclohexyllactic acid and of Glc*N*Ac by (1*R*,2*R*)-cyclohexane-1,2-diol-3-methyl leading to compound **3** (Figure 2).[7] Here, very polar moieties, like sialic acid and Glc*N*Ac that exhibit minor contacts to the protein, were replaced with hydrophobic parts. The binding affinity increased from 878 μM to 19 μM, a factor of 49. Interestingly, only the change in enthalpy became more favorable, whereas the entropy remains almost the same, suggesting that the gain in affinity is caused by different desolvation penalties for the two compounds. Additionally, a perfect pre-organization of protein and ligand and/or the release of coordinated water molecules from solvation results in a large favorable entropic contribution.[7] To further improve pre-organization, parts of the antagonist that do not directly interact with E-selectin were modified and their influence on enthalpy and entropy of binding were studied by isothermal titration calorimetry.

Results and Discussion

After the successful replacement of sialic acid and Glc*N*Ac leading the E-selectin antagonist **3**,[7] exhibiting low micromolar affinity, further modifications that were expected to not affect the key interactions were introduced. The new antagonists (Figure 2) were tested in a competitive binding assay and ITC allowing the deconvolution of $\Delta G°$ into $\Delta H°$ and $T\Delta S°$ (Table 1). A typical ITC experiment is shown in Figure 3.

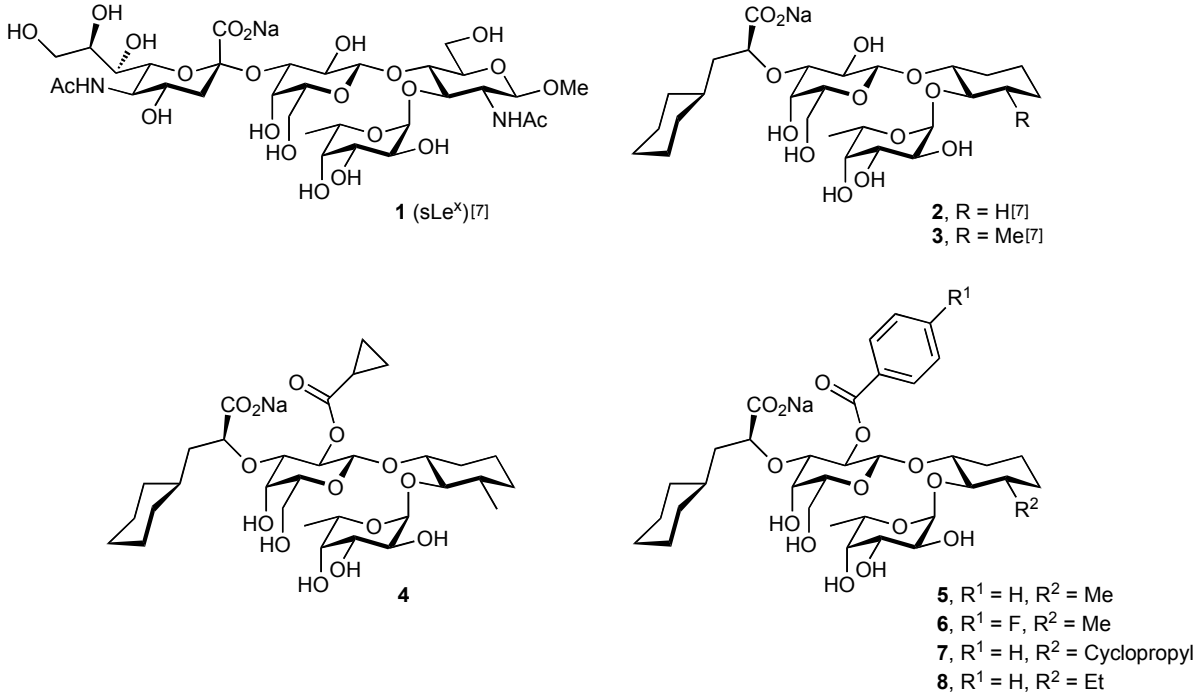

Figure 2. Schematic presentation of the compounds tested in ITC and competitive binding assay with E-selectin.

Table 1. IC_{50} values were determined in a competitive binding assay. K_D, $\Delta G°$, $\Delta H°$, and $-T\Delta S°$ values were obtained from ITC experiments.

Ligand	IC_{50} [µM]	K_D [µM]	$\Delta G°$ [kJ mol^{-1}]	$\Delta H°$ [kJ mol^{-1}]	$-T\Delta S°$ [kJ mol^{-1}]	*N*
sLe^x (**1**)[7]	875 ± 138	878 ± 93	–17.5 ± 0.2	+5.4 ± 0.7	–22.9 ± 1.1	1
2[7]	61.4 ± 13.6	59.0 ± 4.4	–24.2 ± 0.2	–5.3 ± 0.4	–18.9 ± 0.6	0.93 ± 0.08
3[7]	13.7 ± 3.3	18.5 ± 1.8	–27.1 ± 0.2	–5.8 ± 0.1	–21.3 ± 0.4	0.97 ± 0.01
4	8.7 ± 0.1	4.8	–30.4	–7.2	–23.2	1.17
5	6.7 ± 2.0	4.0 ± 0.3	–30.8 ± 0.2	–12.4 ± 0.6	–18.4 ± 0.8	1.00 ± 0.07
6	7.4 ± 1.5	3.6	–31.1	–11.3	–19.8	1.08
7	5.2 ± 1.0	8.6	–28.9	–11.6	–17.3	1.04
8	6.1 ± 1.7	2.1	–32.5	–12.7	–19.8	1.11

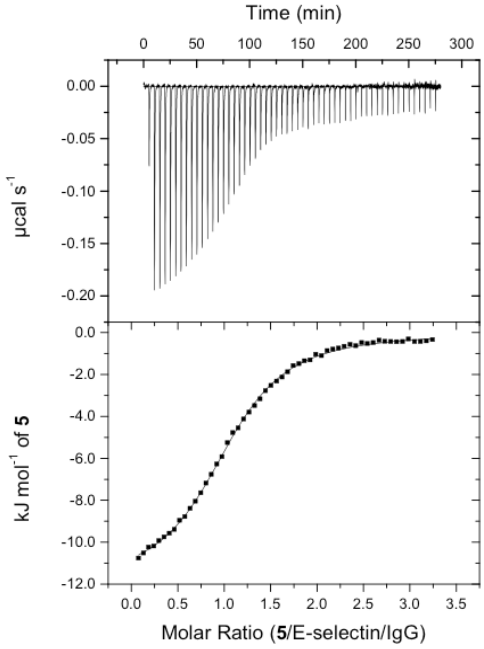

Figure 3. A typical result of an isothermal calorimetric titration with antagonist **5** and E-selectin. The top panel shows the recorded change in heat in units of µcal s^{-1} as a function of time for successive injections of inhibitor (raw data). The bottom plot shows the integrals of the peaks (black squares) from the top panel plotted against the molar ratio of the binding process together with a line of best fit, used to estimate $\Delta H°$, K_D, and N.

Both methods gave comparable results, except for compound **3** and **7** were ITC revealed 50% lower binding affinity, respectively. The binding affinities and thermodynamics of sLe^x (**1**), **2**, and **3** are already published and discussed by Binder *et al*.[7] In this communication we focus on modifications of the 3'-position (3-OH of galactose). Acylation with cyclopropanecarboxylic acid (→**4**) led to a four-fold improvement of **3**, resulting from both enthalpy and entropy change. Surprisingly, a benzoylation of the 3'-hydroxy group (→**5**) revealed similar binding affinity but significantly altered thermodynamics ($\Delta\Delta H°$ = –5.2 kJ mol^{-1}, $-T\Delta\Delta S°$ = +4.8 kJ mol^{-1}). A change in the electron density of the acyl group by a fluoro substituent in the *para*-position (→**6**) did not alter the thermodynamics. A hydrophobic interaction of the benzene ring is expected to be influenced by an electron-withdrawing group leading to changes in the thermodynamic fingerprint.[13] Unspecific binding can be excluded, since the binding isotherm revealed very good fits with a one-to-one binding model and the stoichiometry of all ligands was close to 1. In order to exclude an influence of the Fc-part of E-selectin/IgG, a construct without the Fc-part was

expressed.[14] This monomeric E-selectin exhibited identical thermodynamics for binding to antagonist **5** (Table 2).

Table 2. Results of ITC experiments with different protein construct interacting with antagonist **5**.

E-selectin construct	K_D [µM]	$\Delta G°$ [kJ mol^{-1}]	$\Delta H°$ [kJ mol^{-1}]	$-T\Delta S°$ [kJ mol^{-1}]	N	ΔC_p [kJ mol^{-1} K^{-1}]
IgG	4.0 ± 0.3	–30.8 ± 0.2	–12.4 ± 0.6	–18.4 ± 0.7	1.00 ± 0.07	–0.16
Monomer	3.4	–31.2	–11.8	–19.4	1.14	-

The increased enthalpic contribution of the benzoate compared to the hydroxyl could either result from an additional contact with the protein, different desolvation properties, and/or an influence on the pre-organization of the core. When identical polar interactions for both sLe^x (**1**) and the glycomimetics are assumed, the acyl group points to water making an interaction with E-selectin unlikely. The bioactive conformation and the binding epitope of **2** and sLe^x (**1**) determined by tr-NOE-NMR and STD-NMR, respectively, strongly suggest a conserved binding mode.[15] To account for changes in desolvation, the enthalpy of **1**, **2** and **5** interacting with E-selectin was measured at different temperatures to determine the heat capacity change (ΔC_p). The ΔC_p value of compound **5** was the lowest (–0.16 kJ mol^{-1} K^{-1}) compared to compound **2** and sLe^x (**1**) with –0.11 and –0.06 kJ mol^{-1} K^{-1}, respectively. Since, heat capacity changes are related to different surface area buried upon binding they are related to changes in solvation. Hydrophobic surfaces are expected to reduce ΔC_p, whereas polar surfaces increase ΔC_p.[16,17] Additionally, internal vibrational modes,[17,18] the inclusion of water upon complex formation,[16] as well as solvent rearrangements in peripheral solvent layers influences ΔC_p.[18] Therefore, the lower ΔC_p value for compound **5** can indicate differences of the solvent structure of the ligand, if we assume identical key interactions for all compounds. Otherwise, the lower ΔC_p value can indicate greater hydrophobic interaction which might be related to a different binding mode were the benzoate points toward the protein and not to bulk water.

Antagonist **5** was additionally tested in different buffer systems to determine protonation and deprotonation effects (Table 3).[19] The $\Delta H°$ values are almost identical in all three different buffer systems which makes protonation and deprotonation effects unlikely as far as they are not mutually compensating.

Table 3. Results of ITC experiment of antagonist **5** interacting with E-selectin in different buffer systems determined at 25 °C.

Buffer	$\Delta H°_{Ion}$ [kJ mol^{-1}]	K_D [µM]	$\Delta G°$ [kJ mol^{-1}]	$\Delta H°$ [kJ mol^{-1}]	$-T\Delta S°$ [kJ mol^{-1}]	N
TRIS HCL	46.9	3.8	–30.9	–11.6	–19.3	1.05
HBS-Ca	21.0	3.8	–31.0	–12.0	–19.0	1.08
PBS	5.1	3.9	–30.8	–12.0	–18.8	1.02

Other changes in the antagonist were made on the spacer moiety lining Gal and Fuc. A methyl group was introduced at the former *N*Ac position of Glc*N*Ac with the intention to enhance the pre-organization of the core *via* steric compression between the α-face of fucose and the β-face of galactose (**2**→**3**).[7] The binding affinity increasing by a factor of 3 can be attributed to the enhanced preorganization as has been already described for some examples related to more favorable entropic term,[20] whereas some other examples are related to an enthalpic gain.[21] Starting from **5** (R: Me), the exchange of the ring substituent by cyclopropyl (→**7**) and ethyl (→**8**) decreased and increased binding affinity, respectively.

An entropy-enthalpy compensation plot is shown in Figure 4. The slope is small and negative, indicating that most of the differences are related to changes in enthalpy and only marginally to changes in entropy. The correlation coefficient is very low and there are two clusters of antagonists and one single antagonist visible. One clusters of antagonists can be attributed to the benzoates (**5**-**8**), the other one to antagonists **2**-**4** were little changes in thermodynamics occurred. The single dot is sLe^x (**1**) that exhibits unique thermodynamics.

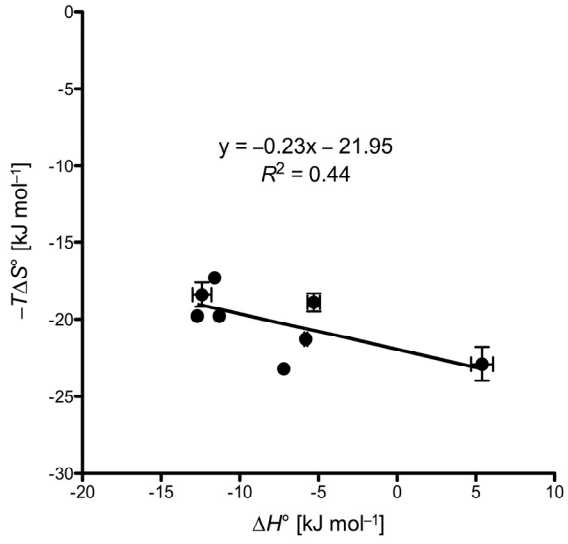

Figure 4. Entropy-enthalpy compensation plot of E-selectin antagonists.

Summary and Conclusion

New E-selectin antagonists that exhibiting modifications on the Glc*N*Ac replacement and the substituent on the 3'-hydroxy, both substitutions that are not expected to interact with the protein, were synthesized. The antagonists were investigated by ITC whereas the enthalpic part of binding was improved; additional entropy costs only partially compensated the gain in affinity.

Experimental Procedure

Synthesis of Compounds. Will be published elsewhere.

E-selectin/IgG Expression, Purification and Competitive Binding Assay. As described by Binder *et al*.[7]

E-selectin Monomer Expression and Purification. Will be published elsewhere.[14]

Isothermal Titration Calorimetry. ITC experiments were performed using a VP-ITC instrument from MicroCal, Inc. (GE Healthcare, Northampton) after vacuum degassing of the samples. The measurements were performed at 25 °C, and for ΔC_p determination additionally at 10 and 37 °C. Injections of 5 to 15 µL ligand solutions (0.5 – 1.8 mM) were added from a computer controlled 300 µL microsyringe at an interval of 5 min into the sample cell solution containing E-selectin/IgG (45 to 83 µM, sample cell volume 1.4037 mL or 1.4523 mL) with stirring at 307 rpm. Protein concentration was determined by HPLC-UV against a BSA standard.[22] The quantity $c = Mt(0)\ K_D^{-1}$ where $Mt(0)$ is the initial macromolecule concentration, is of importance in titration microcalorimetry. The *c*-values were between 1 and 36. Control experiments injecting ligand solution into buffer without protein showed that the heats of dilution were small and constant. The assay buffer was: 10 mM HEPES, 150 mM NaCl, and 1 mM $CaCl_2$, pH 7.4 (HBS-Ca). Ligand **5** was as well tested in TrisHCl and PBS buffer. The first injection was always excluded from data analysis because it usually suffers from sample loss during the mounting of the syringe and the equilibration preceding the actual titration. Data were evaluated using Origin 7 supplied with the instrument (OriginLab, Northampton). A three-parameter data fitting was performed to determine N, K_D, and $\Delta H°$, that are stoichiometry, dissociation constant, and change in enthalpy, respectively.

Thermodynamic parameters were calculated from the equation (1) and (2),

$$\Delta G° = \Delta H° - T\Delta S° = RT\ln K_D = -RT\ln K_A \qquad (1)$$

$$\Delta C_p = \frac{\Delta H°_{T2} - \Delta H°_{T1}}{(T_2 - T_1)} \qquad (2)$$

where $\Delta G°$, $\Delta H°$, $\Delta S°$, and ΔC_p are the changes in free energy, enthalpy, entropy, and heat capacity of binding, respectively, T is the absolute temperature, and R the universal gas constant (8.314 J mol^{-1} K^{-1}).[23]

Acknowledgement

The authors gratefully acknowledge the financial support by the Swiss National Science Foundation (grant no. 200020-103875/1) and by GlycoMimetics Inc., Gaithersburg, MD, USA. We are greatly indebted to Dr. Francis Bitsch and Peggy Brunet-LeFeuvre, Novartis, Basel, for allowing us to use their VP-ITC for thermodynamic evaluation as well as for advices regarding the experimental setup and analyzing the data.

References

[1] S. A. Mousa, D. A. Cheresh, *Drug Discov. Today* **1997**, *2*, 187-199.
[2] R. D. Cummings, R. P. McEver, *Essentials of Gycobiology*, Cold Spring Harbor, New York, **2009**.
[3] G. S. Kansas, *Blood* **1996**, *88*, 3259-3287.
[4] a) R. Alon, D. A. Hammer, T. A. Springer, *Nature* **1995**, *374*, 539-542; b) R. Alon, S. Chen, K. D. Puri, E. B. Finger, T. A. Springer, *J. Cell Biol.* **1997**, *138*, 1169-1180; c) S. Chen, R. Alon, R. C. Fuhlbrigge, T. A. Springer, *Proc. Natl. Acad. Sci. USA* **1997**, *94*, 3172-3177.
[5] H. M. Baker, I. Basu, M. C. Chung, T. Caradoc-Davies, J. D. Fraser, E. N. Baker, *J. Mol. Biol.* **2007**, *374*, 1298-1308.
[6] C. Foxall, S. R. Watson, D. Dowbenko, C. Fennie, L. A. Lasky, M. Kiso, A. Hasegawa, D. Asa, B. K. Brandley, *J. Cell Biol.* **1992**, *117*, 895-902.
[7] F. Binder, K. Lemme, B. Ernst, *Angew. Chem. Int Ed.* **2012***, 51,* 7327-7331.
[8] a) D. Tyrrell, P. James, N. Rao, C. Foxall, S. Abbas, F. Dasgupta, M. Nashed, A. Hasegawa, M. Kiso, D. Asa, *Proc. Natl. Acad. Sci. USA* **1991**, *88*, 10372-10376; b) S. A. DeFrees, F. C. A. Gaeta, Y. C. Lin, Y. Ichikawa, C. H. Wong, *J. Am. Chem. Soc.* **1993**, *115*, 7549-7550; c) Y. Wada, T. Saito, N. Matsuda, H. Ohmoto, K. Yoshino, M. Ohashi, H. Kondo, H. Ishida, M. Kiso, A. Hasegawa, *J. Med. Chem.* **1996**, *39*, 2055-2059; d) G. Thoma, J. L. Magnani, J. T. Patton, B. Ernst, W. Jahnke, *Angew. Chem. Int. Ed. Engl.* **2001**, *40*, 1941-1945.
[9] W. S. Somers, J. Tang, G. D. Shaw, R. T. Camphausen, *Cell* **2000**, *103*, 467-479.
[10] M. K. Wild, M. C. Huang, U. Schulze-Horsel, P. A. van der Merwe, D. Vestweber, *J. Biol. Chem.* **2001**, *276*, 31602-31612.
[11] a) F. H. Cederkvist, S. F. Saua, V. Karlsen, S. Sakuda, V. G. Eijsink, M. Sørlie, *Biochemistry* **2007**, *46*, 12347-12354; b) C. O. Sallum, R. A. Kammerer, A. T. Alexandrescu, *Biochemistry* **2007**, *46*, 9541-9550; S. Castro, M. Duff, N. L. Snyder, M. Morton, C. V. Kumar, M. W. Peczuh, *Org. Biomol. Chem.* **2005**, *3*, 3869-3872; c) J. B. Corbell, J. J. Lundquist, E. J. Toone, *Tetrahedron-Asymmetr.* **2000**, *11*, 95-111; d) N. E. Ziółkowska, S. R. Shenoy, B. R. O'Keefe, J. B. McMahon, K. E. Palmer, R. A. Dwek, M. R. Wormald, A. Wlodawer, *Proteins* **2007**, *67*, 661-670; e) A. Surolia, N. Sharon, F. P. Schwarz, *J. Biol. Chem.* **1996**, *271*, 17697-17703; f) D. Gupta, M. Cho, R. D. Cummings, C. F. Brewer, *Biochemistry* **1996**, *35*, 15236-15243; g) M. Kapoor, H. Srinivas, E. Kandiah, E. Gemma, L. Ellgaard, S. Oscarson, A. Helenius, A. Surolia, *J. Biol. Chem.* **2003**, *278*, 6194-6200; h) P. G. Rani, K. Bachhawat, G. B. Reddy, S. Oscarson, A. Surolia, *Biochemistry* **2000**, *39*, 14364; i) A. Arockia Jeyaprakash, G. Jayashree, S. K. Mahanta, C. P. Swaminathan, K. Sekar, A. Surolia, M. Vijayan, *J. Mol. Biol.* **2005**, *347*, 181-188.
[12] a) E. J. Toone, *Curr. Opin. Struc. Biol.* **1994**, *4*, 719-728; b) M. Ambrosi, N. R. Cameron, B. G. Davis, *Org. Biomol. Chem.* **2005**, *3*, 1593-1608; c) T. K. Dam, C. F. Brewer, *Chem. Rev.* **2002**, *102*, 387-429.
[13] E. A. Meyer, R. K. Castellano, F. Diederich, *Angew. Chem. Int. Edit.* **2003**, *42*, 1210-1250.
[14] R. C. Preston, *Dissertation,* **2012**.
[15] W. Jahnke, H. C. Kolb, M. J. J. Blommers, J. L. Magnani, B. Ernst, *Angew. Chem. Int. Ed. Engl.* **1997**, *36*, 2603-2607.

[16] J. Gomez, E. Freire, *A Structure-Based Thermodynamic Approach to Molecular Design*, Springer Verlag, **1997**.
[17] P. R. Connelly, *The Cost of Releasing Site-Specific, Bound Water Molecules from Proteins: Toward a Quantitative Guide for Structure-Based Drug Design*, Springer-Verlag, **1997**.
[18] F. Dullweber, M. T. Stubbs, D. Musil, J. Stürzebecher, G. Klebe, *J. Mol. Biol.* **2001**, *313*, 593-614.
[19] R. Perozzo, G. Folkers, L. Scapozza, *J. Recept. Signal. Transduct. Res.* **2004**, *24*, 1-52.
[20] a) B. W. Sigurskjold, D. R. Bundle, *J. Biol. Chem.* **1992**, *267*, 8371-8376; b) N. Navarre, N. Amiot, A. van Oijen, A. Imberty, A. Poveda, J. Jimenez-Barbero, A. Cooper, M. A. Nutley, G. J. Boons, *Chem-Eur. J.* **1999**, *5*, 2281-2294; c) G. Klebe, H. J. Böhm, *J. Recept. Signal Transduct. Res.* **1997**, *17*, 459-473.
[21] a) J. E. Ladbury, G. Klebe, E. Freire, *Nat. Rev. Drug Discov.* **2010**, *9*, 23-27; b) J. E. DeLorbe, J. H. Clements, M. G. Teresk, A. P. Benfield, H. R. Plake, L. E. Millspaugh, S. F. Martin, *J. Am. Chem. Soc.* **2009**, *131*, 16758-16770; c) D. R. Bundle, R. Alibes, S. Nilar, A. Otter, M. Warwas, P. Zhang, *J. Am. Chem. Soc.* **1998**, *120*, 5317-5318.
[22] a) S. Mesch, K. Lemme, H. Koliwer-Brandl, D. S. Strasser, O. Schwardt, S. Kelm, B. Ernst, *Carbohydr. Res.* **2010**, *345*, 1348-1359; b) F. Bitsch, R. Aichholz, J. Kallen, S. Geisse, B. Fournier, J. M. Schlaeppi, *Anal. Biochem.* **2003**, *323*, 139-149.
[23] T. Wiseman, S. Williston, J. F. Brandts, L. N. Lin, *Anal. Biochem.* **1989**, *179*, 131-137.

2.1.2 DC-SIGN

Thermodynamic Evaluation of DC-SIGN Antagonists

Katrin Lemme, Katharina Mayer, Meike Scharenberg, Sameh M. Eid, Arjan Odedra, and Beat Ernst*

Institute of Molecular Pharmacy, University of Basel, Klingelbergstr. 50, 4056 Basel, Switzerland

** Corresponding author. Tel: 0041 267 15 51; Fax: 0041 267 15 52; e-mail: beat.ernst@unibas.ch*

Keywords: DC-SIGN, lectin, antagonists, isothermal titration calorimetry.

Contribution of Katrin Lemme: Manuscript, ITC experiments, determination of protein concentration.

Draft version.

Introduction

Immature dentritic cells (DCs) are crucial for the defense against pathogens. They monitor pathogens, process, and present them to the immune system. Interestingly, some pathogens can escape dendritic cells and the immune surveillance.

Viruses (*e.g*. HIV, Ebola virus, cytomegalovirus, Dengue virus, hepatitis C virus), bacteria (*e.g. Mycobacterium tubercolosis*, *Helicobacter pylori*), and yeasts (*e.g. Candida albicans*) target the C-type lectin DC-SIGN (DC-specific intracellular adhesion molecule-3 (ICAM-3) grabbing nonintegrin) and either escape the degradation mechanism or alter TLR-mediated (Toll-like receptor) signaling which both result in an infection of the host.[1] Endogenous ligands of DC-SIGN are the glycoproteins ICAM-2 and ICAM-3 which are involved in DC migration[2] and DC-T-cell interaction,[3] respectively. The majority of pathogens bind with *N*-linked high mannose oligosaccharides.[1,4] Besides, the fucose-embodying blood group antigens Lewis^x (Le^x) and Lewis^a (Le^a) are as well common on pathogens and bind to DC-SIGN.[5] Binding affinities to DC-SIGN are in the low millimolar range for monosaccharides, such as mannose and L-Fuc,[6] and Lewis-type structures.[7] Multivalent ligands increase the binding affinity.[8] Being a C-type lectin, the binding to DC-SIGN is calcium dependent.[1]

A crystal structure of DC-SIGN complexed with lacto-*N*-fucopentaose III (LNFP III), containing a Le^x motif, suggests that 3- and 4-OH of Fuc coordinate the calcium ion, Gal contributes to binding via a hydrogen bond to Asp367 (6-OH) and a water-mediated hydrogen bond to Glu358 (4-OH) (Figure 1). Additionally, van-der-Waals contacts exist between the 2-OH of Fuc and Val351 and between 6-OH of Gal and Leu371.[9]

To gain further insights into the binding interaction of glycomimetics we report isothermal titration calorimetry experiments that allow the deconvolution of the change in free energy of binding ($\Delta G°$) into enthalpic ($\Delta H°$) and entropic ($\Delta S°$) contributions.[10,11] Hydrogen bond formation, electrostatic interaction, and dipole-dipole interaction influence the enthalpy term.[12-15] The entropy term describes the change of the order of the system, *e.g*. the change in the solvation entropy as well as translational, rotational, and vibrational entropy of the protein and ligand upon complex formation.[13,16]

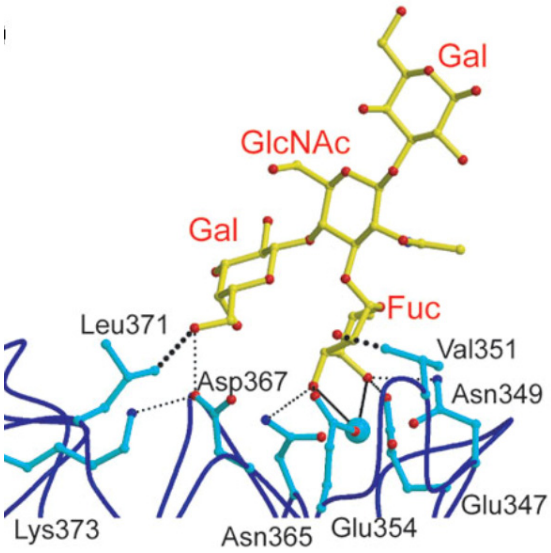

Figure 1. Resolved part of LNFP III and adjacent amino acids in the binding site of DC-SIGN (PDB 1SL5). The protein backbone is blue, bonds are cyan, and bonds in carbohydrate are yellow. Calcium coordination bonds are solid, hydrogen bonds are thin dotted lines, and van-der-Waals contacts are thick dotted lines (picture from Guo *et al*.).[9]

Results and Discussion

Antagonizing DC-SIGN already demonstrated that it prevents pathogen attachment to DCs and inhibits the infection of other immune cells at its earliest steps.[17] Although micromolar affinity glycomimetics exist,[6,7] the driving force of the interaction is not understood yet. Isothermal titration calorimetry experiments are useful to gain insight into the driving force of interaction.

Figure 3 shows a typical outcome of an ITC experiment. The investigated ligands are shown in Figure 2 and accompanying results are shown in Table 1. ITC results are in good agreement with those obtained from the competitive binding assay.[18] However, the differences in affinity are more pronounced in the competitive binding assay. The interactions between DC-SIGN and the antagonists are exothermic and partially compensated by unfavorable changes in entropy. This thermodynamic signature is a common property of carbohydrate-lectin interactions.[19]

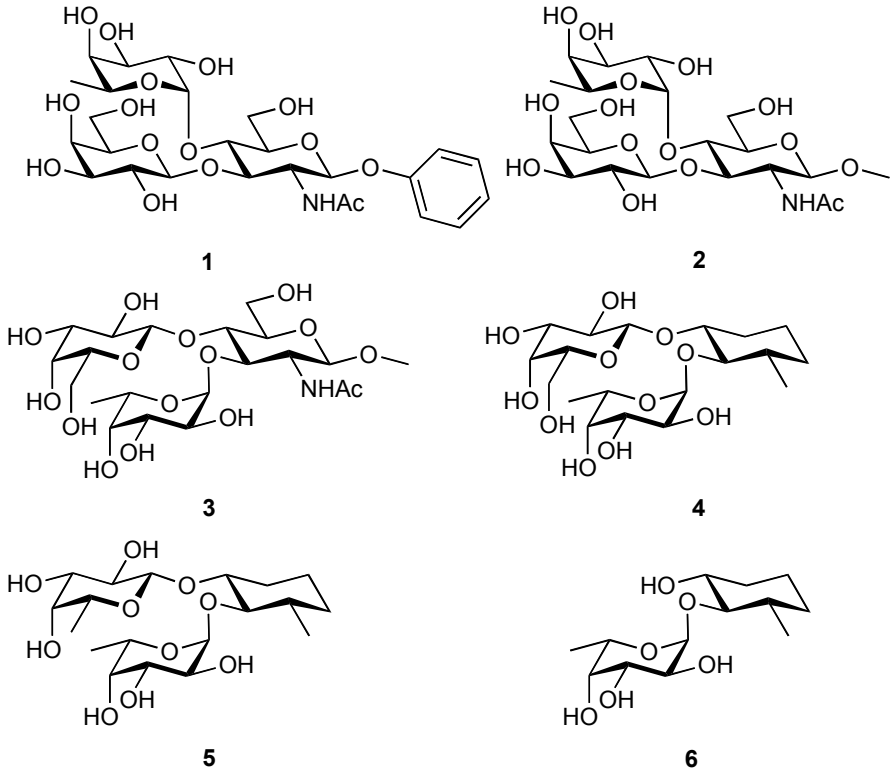

Figure 2. Structure of glycomimetics binding to DC-SIGN.

Table 1. Binding thermodynamics of DC-SIGN antagonists determined by ITC. rIC_{50}[18] values were calculated against **1** as reference compound. rK_D values were calculated relative to phenyl Le[a] (**1**). The stoichiometry *N* was set to 1 (see Experimental Procedure).

Compound	rIC_{50}	rK_D	K_D [µM]	$\Delta G°$ [kJ mol^{-1}]	$\Delta H°$ [kJ mol^{-1}]	$-T\Delta S°$ [kJ mol^{-1}]
1	1	1	583 ± 41	–18.5 ± 0.2	–28.0 ± 2.0	+9.5 ± 1.8
2	2.9 ± 0.5	1.3	735	–17.9	–27.9	+10.0
3	3.3 ± 0.2	n.d.	n.d.	n.d.	n.d.	n.d.
4	1.8 ± 0.5	1.1	645	–18.2	-31.4	+13.2
5	4.7 ± 1.0	2.2	1277	–16.5	–29.7	+13.2
6	n.d.	1.8	1073	–16.9	–34.7	+17.8

n.d. - not determined.

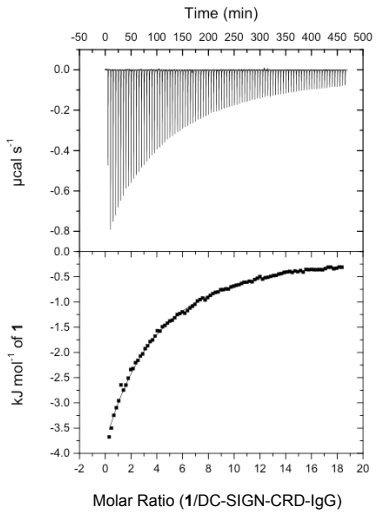

Figure 3. A typical result of an isothermal calorimetric titration with DC-SIGN antagonist **1** interacting and DC-SIGN-CRD-IgG. The top panel shows the recorded change in heat in units of µcal s^{-1} as a function of time for successive injections of inhibitor (raw data). The bottom panel shows the integrals of the peaks (black squares) from the top panel plotted against the molar ratio of the binding process together with a line of best fit, used to estimate $\Delta H°$ and K_D. The stoichiometry (N) was set to 1 (see Experimental Procedure).

Crystallographic data suggests that Glc*N*Ac has the function of a spacer only orienting Fuc and Gal moiety. Therefore, the phenyl moiety in phenyl Le^a (**1**) is as well expected to point into bulk water, making no additional contact with the protein. However, phenyl Le^a (**1**) exhibited the highest binding affinity towards DC-SIGN within this series. It is known that modifications far from binding site can influence binding affinity and thermodynamics because of structure rearrangement.[14,20,21] Additionally, another binding mode might be possible, where the phenyl moiety contacts the protein. Replacing the phenyl by a methyl moiety (**1**→**2**) reduces the affinity slightly whereas enthalpy and entropy values are similar to one another. Binding affinity of methyl Le^x (**3**) is slightly lower compared to methyl Le^a (**2**) as has been previously reported.[8] Since Glc*N*Ac serves as a spacer it was replaced with methyl cyclohexanediol. Interestingly, this substituent enhanced the binding affinity (**3**→**4**). A better preorganization[15,22] and/or different solvation properties[14] may explain this difference. Compound **5**, the 6-deoxy Le^x mimic, showed the lowest binding affinity. It suggests that the 6-OH of the galactose does contribute to binding but not essentially. This is in accordance with the published binding mode for Le^x from crystallography with LNFP III, which supposes hydrogen bond formation for 6-

OH.[4] However, a disaccharide mimic without galactose (**6**) is able to bind with similar binding affinity. Nevertheless, studies with deoxy-congeners are important to identify key hydroxyl groups. The amount of affinity loss and the change in thermodynamics give information about the importance of certain hydroxyl groups.[20,23]

Conclusion

To the best of our knowledge, this was the first thermodynamic characterization of DC-SIGN ligand interaction. The millimolar binding affinities are a result of an exothermic interaction opposed by an unfavorable entropic penalty.

Experimental Procedures

Protein Expression, Purification and Competitive Binding Assay and Synthesis of Compounds. Will be published elsewhere.[18]

Isothermal Titration Calorimetry (ITC). ITC experiments were performed using a VP-ITC instrument from MicroCal, Inc. (GE Healthcare, Northampton). The measurements were performed at 25 °C. Injections of 3 to 5 µL ligand solutions (5.5 - 25 mM) were added at an interval of 5 min into the sample cell solution containing DC-SIGN-CRD-IgG (DC-SIGN-CRD fused to the Fc part of human IgG; 30 to 110 µM, sample cell volume 1.4523 mL) with stirring at 307 rpm. Protein concentration was determined by HPLC-UV against a BSA standard.[24] Control experiments injecting ligand solution into buffer without protein showed that the heats of dilution were small and constant. The assay buffer was: 10 mM HEPES, 150 mM NaCl, 10 mM $CaCl_2$, *pH* 7.4 (HBS-Ca). The first injection was always excluded from data analysis because it usually suffers from sample loss during the mounting of the syringe and the equilibration preceding the actual titration. The experimental data were fitted to a theoretical titration curve (one site binding model) using Origin software (version 7, MicroCal). The quantity $c = Mt(0)\ K_D^{-1}$ where *Mt(0)* is the initial macromolecule concentration, is of importance in titration microcalorimetry.[10] The experiments were performed with *c*-values below 1. The stoichiometry was fixed to 1 to allow reliable determination of K_D and $\Delta H°$.[25] Thermodynamic parameters were calculated from the equation (1),

$$\Delta G° = \Delta H° - T\Delta S° = RT\ln K_D = -RT\ln K_A \qquad (1)$$

where $\Delta G°$, $\Delta H°$, and $\Delta S°$ are the changes in free energy, enthalpy, and entropy of binding, respectively, T is the absolute temperature, and R is the universal gas constant (8.314 J mol^{-1} K^{-1}).

References

[1] Y. van Kooyk, T. B. Geijtenbeek, *Nat. Rev. Immunol.* **2003**, *3*, 697-709.

[2] J. J. García-Vallejo, E. van Liempt, P. da Costa Martins, C. Beckers, B. van het Hof, S. I. Gringhuis, J. J. Zwaginga, W. van Dijk, T. B. Geijtenbeek, Y. van Kooyk, I. van Die, *Mol. Immunol.* **2008**, *45*, 2359-2369.

[3] T. B. Geijtenbeek, D. J. Krooshoop, D. A. Bleijs, S. J. van Vliet, G. C. van Duijnhoven, V. Grabovsky, R. Alon, C. G. Figdor, Y. van Kooyk, *Nat. Immunol.* **2000**, *1*, 353-357.

[4] A. A. Bashirova, L. Wu, J. Cheng, T. D. Martin, M. P. Martin, R. E. Benveniste, J. D. Lifson, V. N. KewalRamani, A. Hughes, M. Carrington, *J. Virol.* **2003**, *77*, 217-227.

[5] a) H. Feinberg, D. A. Mitchell, K. Drickamer, W. I. Weis, *Science* **2001**, *294*, 2163-2166; b) I. van Die, S. J. van Vliet, A. K. Nyame, R. D. Cummings, C. M. Bank, B. Appelmelk, T. B. Geijtenbeek, Y. van Kooyk, *Glycobiology* **2003**, *13*, 471-478; c) B. J. Appelmelk, I. van Die, S. J. van Vliet, C. M. Vandenbroucke-Grauls, T. B. Geijtenbeek, Y. van Kooyk, *J. Immunol.* **2003**, *170*, 1635-1639.

[6] D. A. Mitchell, A. J. Fadden, K. Drickamer, *J. Biol. Chem.* **2001**, *276*, 28939-28945.

[7] G. Timpano, G. Tabarani, M. Anderluh, D. Invernizzi, F. Vasile, D. Potenza, P. M. Nieto, J. Rojo, F. Fieschi, A. Bernardi, *Chembiochem* **2008**, *9*, 1921-1930.

[8] E. van Liempt, C. M. Bank, P. Mehta, J. J. Garciá-Vallejo, Z. S. Kawar, R. Geyer, R. A. Alvarez, R. D. Cummings, Y. Kooyk, I. van Die, *FEBS Lett.* **2006**, *580*, 6123-6131.

[9] Y. Guo, H. Feinberg, E. Conroy, D. A. Mitchell, R. Alvarez, O. Blixt, M. E. Taylor, W. I. Weis, K. Drickamer, *Nat. Struct. Mol. Biol.* **2004**, *11*, 591-598.

[10] T. Wiseman, S. Williston, J. F. Brandts, L. N. Lin, *Anal. Biochem.* **1989**, *179*, 131-137.

[11] J. E. Ladbury, *Thermochim. Acta* **2001**, *380*, 209-215.

[12] J. E. Ladbury, G. Klebe, E. Freire, *Nat. Rev. Drug Discov.* **2010**, *9*, 23-27.

[13] E. Freire, *Drug Discov. Today* **2008**, *13*, 869-874.

[14] M. C. Chervenak, E. J. Toone, *J. Am. Chem. Soc.* **1994**, *116*, 10533-10539.

[15] J. E. DeLorbe, J. H. Clements, M. G. Teresk, A. P. Benfield, H. R. Plake, L. E. Millspaugh, S. F. Martin, *J. Am. Chem. Soc.* **2009**, *131*, 16758-16770.

[16] T. S. Olsson, M. A. Williams, W. R. Pitt, J. E. Ladbury, *J. Mol. Biol.* **2008**, *384*, 1002-1017.

[17] a) N. Obermajer, S. Sattin, C. Colombo, M. Bruno, U. Svajger, M. Anderluh, A. Bernardi, *Mol. Divers.* **2011**, *15*, 347-360; b) M. J. Borrok, L. L. Kiessling, *J. Am. Chem. Soc.* **2007**, *129*, 12780-12785; c) J. J. Reina, S. Sattin, D. Invernizzi, S. Mari, L. Martínez-Prats, G. Tabarani, F. Fieschi, R. Delgado, P. M. Nieto, J. Rojo, A. Bernardi, *ChemMedChem* **2007**, *2*, 1030-1036; d) B. Ernst, J. L. Magnani, *Nat. Rev. Drug Discov.* **2009**, *8*, 661-677.

[18] a) M. Scharenberg *Dissertation* **2011**; b) K. Mayer *Dissertation* **2012**.

[19] a) B. A. Williams, M. C. Chervenak, E. J. Toone, *J. Biol. Chem.* **1992**, *267*, 22907-22911; b) E. J. Toone, *Curr. Opin. Struc. Biol.* **1994**, *4*, 719-728; c) T. K. Dam, C. F. Brewer, *Chem. Rev.* **2002**, *102*, 387-429; d) M. Ambrosi, N. R. Cameron, B. G. Davis, *Org. Biomol. Chem.* **2005**, *3*, 1593-1608.

[20] R. U. Lemieux, *Accounts Chem. Res.* **1996**, *29*, 373-380.

[21] R. U. Lemieux, M. H. Du, U. Spohr, *J. Am. Chem. Soc.* **1994**, *116*, 9803-9804.

[22] N. Navarre, N. Amiot, A. van Oijen, A. Imberty, A. Poveda, J. Jimenez-Barbero, A. Cooper, M. A. Nutley, G. J. Boons, *Chem-Eur. J.* **1999**, *5*, 2281-2294.

[23] a) T. K. Dam, S. Oscarson, C. F. Brewer, *J. Biol. Chem.* **1998**, *273*, 32812-32817; b) T. K. Dam, S. Oscarson, J. C. Sacchettini, C. F. Brewer, *J. Biol. Chem.* **1998**, *273*, 32826-32832; c) D. Gupta, T. K. Dam, S. Oscarson, C. F. Brewer, *J. Biol. Chem.* **1997**, *272*, 6388-6392.

[24] a) F. Bitsch, R. Aichholz, J. Kallen, S. Geisse, B. Fournier, J. M. Schlaeppi, *Anal. Biochem.* **2003**, *323*, 139-149; b) S. Mesch, K. Lemme, H. Koliwer-Brandl, D. S. Strasser, O. Schwardt, S. Kelm, B. Ernst, *Carbohydr. Res.* **2010**, *345*, 1348-1359.

[25] J. Tellinghuisen, *Anal. Biochem.* **2008**, *373*, 395-397.

2.2 Thermodynamics of Glycomimetics Binding to I-type Lectins

2.2.1 MAG – Siglec-4

2.2.1.1 High Affinity Binding of Glycomimetics to MAG

High Affinity Sialoside Ligands of Myelin Associated Glycoprotein

Ying Zeng,[a] Christoph Rademacher,[a] Corwin M. Nycholat,[a] Satoshi Futakawa,[a]

Katrin Lemme,[b] Beat Ernst,[b] James C. Paulson[a,*]

[a]*Department of Physiological Chemistry, The Scripps Research Institute, 10550 N. Torrey Pines Road, La Jolla, CA 92037, United States*

[b]*Institute of Molecular Pharmacy, University of Basel, Klingelbergstr. 50, 4056 Basel, Switzerland*

**Corresponding author; e-mail: jpaulson@scripps.eu*

Published in: *Bioorg. Med. Chem. Lett.* **2011**, *21*, 5045-5049.

Contribution of Katrin Lemme: ITC experiment, determination of protein concentration.

Bioorganic & Medicinal Chemistry Letters 21 (2011) 5045–5049

Contents lists available at ScienceDirect

Bioorganic & Medicinal Chemistry Letters

journal homepage: www.elsevier.com/locate/bmcl

High affinity sialoside ligands of myelin associated glycoprotein

Ying Zeng [a], Christoph Rademacher [a], Corwin M. Nycholat [a], Satoshi Futakawa [a], Katrin Lemme [b], Beat Ernst [b], James C. Paulson [a,*]

[a] Department of Physiological Chemistry, The Scripps Research Institute, 10550 N. Torrey Pines Road, La Jolla, CA 92037, United States
[b] Institute of Molecular Pharmacy, University of Basel, Klingelbergstrasse 50, 4056 Basel, Switzerland

ARTICLE INFO

Article history:
Received 8 March 2011
Revised 13 April 2011
Accepted 15 April 2011
Available online 23 April 2011

Keywords:
Myelin associated glycoprotein
MAG
Siglec
Sialic acid
Lectin

ABSTRACT

Myelin associated glycoprotein (Siglec-4) is a myelin adhesion receptor, that is, well established for its role as an inhibitor of axonal outgrowth in nerve injury, mediated by binding to sialic acid containing ligands on the axonal membrane. Because disruption of myelin–ligand interactions promotes axon outgrowth, we have sought to develop potent ligand based inhibitors using natural ligands as scaffolds. Although natural ligands of MAG are glycolipids terminating in the sequence NeuAcα2–3Galβ1–3(±NeuAcα2–6)GalNAcβ-R, we previously established that synthetic O-linked glycoprotein glycans with the same sequence α-linked to Thr exhibited ~1000-fold increased affinity (~1 μM). Attempts to increase potency by introducing a benzoylamide substituent at C-9 of the α2–3 sialic acid afforded only a two-fold increase, instead of increases of >100-fold observed for other sialoside ligands of MAG. Surprisingly, however, introduction of a 9-*N*-fluoro-benzoyl substituent on the α2–6 sialic acid increased affinity 80-fold, resulting in a potent inhibitor with a K_d of 15 nM. Docking this ligand to a model of MAG based on known crystal structures of other siglecs suggests that the Thr positions the glycan such that aryl substitution of the α2–3 sialic acid produces a steric clash with the GalNAc, while attaching an aryl substituent to the other sialic acid positions the substituent near a hydrophobic pocket that accounts to the increase in affinity.

Myelin associated glycoprotein (MAG, Siglec-4) is a member of the sialic acid immunoglobulin lectin (siglec) family, which bind sialic acid containing glycans as ligands.[8] While most of the 15 human siglecs described to date are expressed on various white blood cells of the immune system,[8] MAG is unique in that it is exclusively expression by glial cells that produce the myelin wrapped around the axons of neuronal cells. It's function is well established as a cell adhesion protein, which is, important in maintaining the integrity of the myelin–axon organization, mediated by the interaction of MAG expressed on the innermost leaflet on the myelin membrane, interacting with sialic acid containing gangliosides as ligands on the axon.[9] Gene knockout mice that are missing either MAG or its ganglioside ligands exhibit increased demyelination and axon degeneration in the central and peripheral nervous system, with resulting neuronal deficiencies.[9]

In addition to its role in stabilizing axon–myelin interactions, MAG is one of several glial receptors that contribute to inhibition of axon growth following nerve injury.[9–11] Others include neurite outgrowth inhibitor (Nogo) and oligodenrocyte myelin glycoprotein MOgp. These receptors mediate inhibition of the outgrowth of axons in injured nerve by interacting with their respective ligands on the axon. Although MAG is unique in its recognition of axonal gangliosides as ligands, Nogo, MAG and MOgp all interact with the Nogo receptors, NgR1 and NgR2, as ligands. Although there is not consensus on the mode of MAG interaction with NgRs,[9,12] several reports suggest that the interaction is sialic acid dependent.[13–15]

Numerous studies suggest that disruption of the interaction of MAG, Nogo and MOgp with their ligands can release the inhibition of axonal outgrowth and promote nerve regeneration following nerve injury.[9–11] This has been elegantly demonstrated for MAG in in vivo experiments that show improvement of nerve regeneration by administration of sialidase to destroy sialic acid dependent ligands.[16] Demonstration that sialoside ligands can reverse MAG dependent inhibition of axon outgrowth in vitro[17] has suggested the possibility that small molecules of sufficient potency could also promote nerve regeneration in vivo. This has stimulated our interest in the development of inhibitors of MAG based on its natural sialoside ligands.[1–4,6,7,18–23]

Early investigations into the natural axonal ligands of MAG documented that it binds preferentially to gangliosides that contain the terminal sequence NeuAcα2–3Galβ1–3GalNAcβ-R found in GD1a and GT1b, and the di-sialylated sequence NeuAcα2–3Galβ1–3(NeuAcα2–6)GalNAcβ-R found in rare gangliosides such as GQ1bα.[9,24] These same sequences are found as O-linked glycans

* Corresponding author.
E-mail address: jpaulson@scripps.edu (J.C. Paulson).

0960-894X/$ - see front matter © 2011 Elsevier Ltd. All rights reserved.
doi:10.1016/j.bmcl.2011.04.068

of glycoproteins in α-linkage to threonine. These structures β-linked to synthetic aglycons (**1** and **3**) exhibited K_d values for MAG of 820 μM and 180 μM, respectively,[2] affinities that are typical of glycan binding proteins that mediate cell-to-cell contact through multivalent binding of receptors on one cell and glycan ligands on the other.[25–28] However, in contrast to the β-glycosides, the same sialoside sequences α-linked to threonine exhibit potencies over 100-fold higher (Fig. 1).

Modifications of sialic acids with substituents at the C-9, C-5 and C-2 positions have also been documented to afford substantial increases in affinity (Fig. 1). Addition of an aromatic substituent at C-9 typically results in affinity increases of 60–250-fold, even for simple sialosides such as α-methyl-NeuAc, and other linear sialosides such as NeuAcα2–3Galβ1–4GlcNAc.[2–4,6,7,18–23,29–31] Systematic analysis of the additive gains in affinity with substituents added at the C-9, C-5 and C-2 positions of sialic acid have yielded sialic acid analogs with K_d values of 150–500 nM (e.g., **8**), representing affinity gains of over 1000-fold over most natural sialosides (e.g., **1**, **3**),[1,6,7,18,19,31] with the exception of the synthetic O-linked sialosides with an α-Thr aglycon, which already exhibited affinities in this range (**2**, **6**).[1]

Since the sialosides α-linked to Thr already exhibited low/sub μM potencies (**2** and **6**), we sought to achieve significant increased affinity by addition of an aromatic substituent at C-9 of the sialic acid linked α2–3 to Gal. To our surprise, only a modest two-fold increase in affinity was observed. Thus, the affinity increases afforded by the aromatic substituent at C-9 (**7**) and the α-Thr aglycons (**6**) were not additive, a seemingly counter intuitive finding since the substituents were at the non-reducing and reducing ends of the sialoside, respectively.

To explore this finding further, we evaluated the effect of adding single ring aromatic substituents selected from our previous studies[3,6,19,22] to each sialic acid of the disialyl-T-antigen (**2**). As shown in Scheme 1, T-antigen (**9**) was prepared chemically as previously described,[32] and was enzymatically sialylated with either NeuAc or C-9 substituted analogs of NeuAc using porcine ST3Gal I or chicken/human ST6GalNAc I. For C-9 substituted analogs of the NeuAcα2–3Gal sequence, 9-N substituted NeuAc analogs (**10b**–**d**) were activated to the corresponding CMP-NeuAc donor substrate and transferred directly to the acceptor glycan using the porcine ST3Gal I. For C-9 substituted analogs of the NeuAcα2–6GalNAc sequence, 9-azido-NeuAc was activated to CMP-9-azido-NeuAc and transferred to T-antigen (**9**) or sialyl-T-antigen (**11a**) using ST6GalNAc I. Once transferred, the 9-azide was reduced to the 9-amine, which was then acylated with the corresponding benzoyl chloride. The strategy of introducing the 9-azido-NeuAc followed by reduction and acylation was used because the chicken ST6GalNAc I did not efficiently transfer the 9-amino or 9-N-substituted sialic acids.

Each of the sialylated products was assessed for their ability to compete the binding of a MAG-Fc chimera to NeuAcα2–3Galβ1–4GlcNAc-R coupled to biotinylated polyacrylamide, which is adsorbed to streptavidin coated 96 well plates (Fig. 2). To insure that day-to-day variation in the assay was not a factor in for comparing their potency, each compound was analyzed three times on separate days, with at least one other compound to insure that there was no significant 'drift' in the assay. The IC_{50} values in Table 1 represent the mean and standard deviation of the values obtained for the three separate assays. The standard error ranged from 5% to 15%, demonstrating the reproducibility of the results over course of the analysis of all compounds.

Although the earlier results of ours and others that aryl substituents at C-9 of sialic acid afford ~100-fold increased affinity, 9-*N*-benzoyl (**11b**) or 9-*N*-*p*-chloro-benzoyl (**11c**) substituents in the NeuAcα2–3 linked sialic acid of the 3′-sialyl-T-antigen revealed affinity increases of only two-fold. The one exception in this series was **11d** with the *p*-fluoro-benzoyl substituent, which gave a 14-fold increase in affinity with an IC_{50} of 80 nM. However, with the same substituent on the NeuAcα2–3 linked sialic acid of the disialyl-T-antigen (**13b**) increased affinity by only two-fold. In contrast, the *p*-fluoro-benzoyl substituent on the NeuAcα2–6 sialic acid (**13c**) resulted in an 80-fold increase in potency, with an IC_{50} of 9 nM. This represents a potency at least 10-fold higher than any other synthetic ligand of MAG reported to date.

In order to more directly compare the affinities of these synthetic ligands with others reported by us and other groups using various related assays, we determined the K_d of the disialyl-T-antigen (**13a**) by isothermal titration calorimetry. This gave a K_d value of 1.2 μM, in good agreement with the IC_{50} of 0.75 ± 0.17 μM (see Supplementary data). Using this as a reference, we have calculated

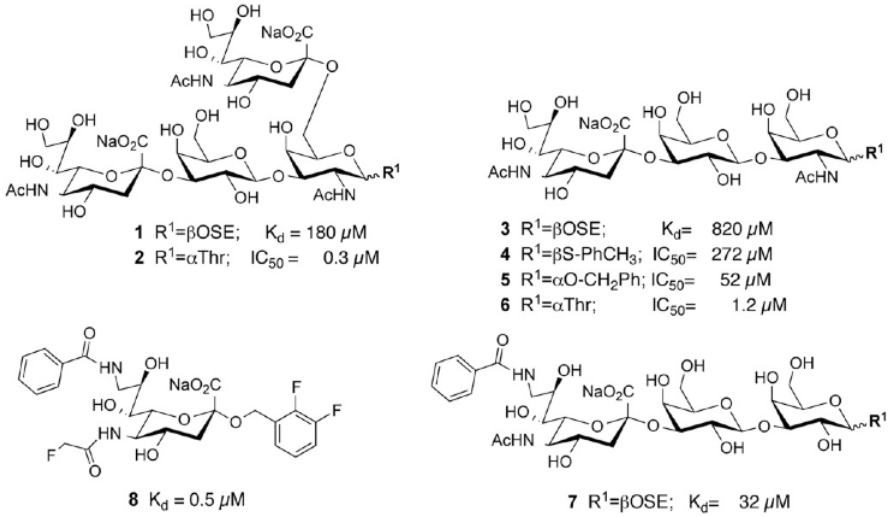

Figure 1. Relative potencies of representative sialoside ligands of MAG. Natural sialoside sequences (**1**–**6**) β-linked (**1**, **3**, **4**)[1,2] or α-linked (**2**, **5**, **6**)[1] to synthetic aglycons correspond to MAG ligands found in some gangliosides (e.g., GQ1bα) and O-linked glycans of glycoproteins, respectively. Modification of sialic acid with aryl substituents at C-9 and/or C-2 afford significant gains in affinity (**7**, **8**)[3–7,19].

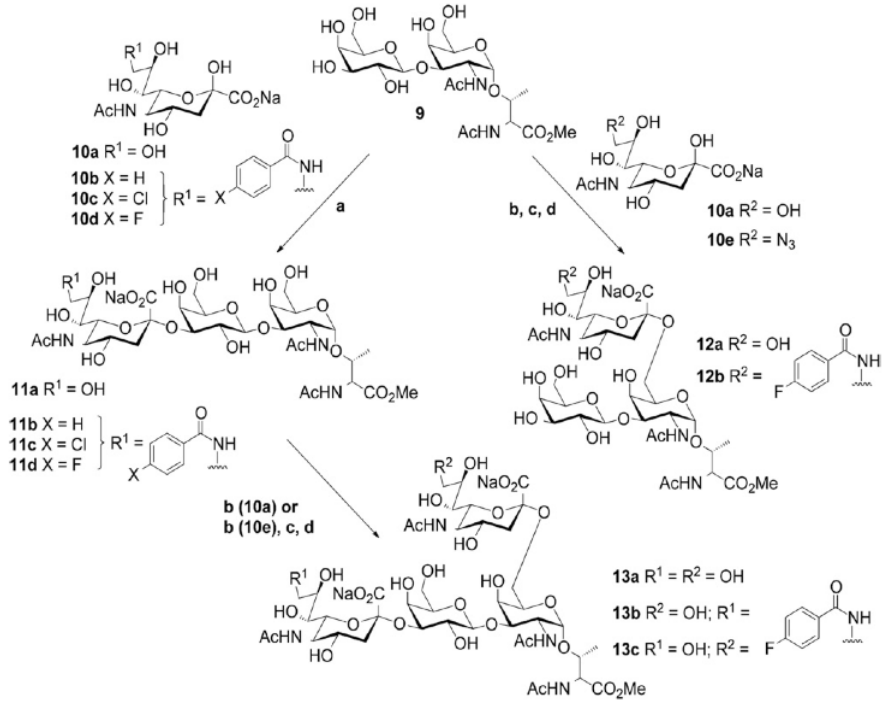

Scheme 1. Synthesis of the sialosides (a) pST3Gal I, buffer, yields 83–94%; (b) ChST6GalNAc I, 92%; (c) PMe_3, $CH_3OH/THF/H_2O$, 87%; (d), RCOCl, DMF, Et_3N, 78–89%.

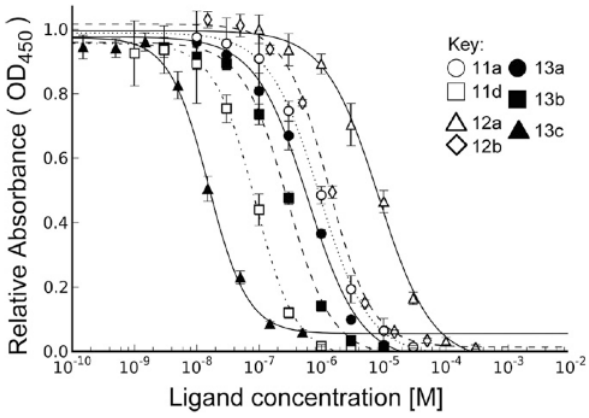

Figure 2. Analysis of the inhibitory potency of sialoside analogs in MAG binding assay. Each compound is analyzed in triplicate for inhibition of the binding of MAG-Fc chimera to polymeric ligand adsorbed to the wells of 96 well plates as described in Supplementary data.

the K_d apparent for each of the compounds assuming that the IC_{50} values are proportional (Table 1).

The apparent K_d of the most potent compound **13c** is 15 nM, representing at least 10,000-fold higher than the native structure **1**. This is remarkable since **13c** is identical except for αThr as the aglycon, and the 9-*N*-*p*-fluoro-benzoyl substituent on the sialic acid linked α2–6 to GalNAc. To better understand the basis for these dramatic affinity increases, we investigated the docking of this ligand to a homology model of MAG, which is based on existing crystal structures of several siglecs.

A homology model of the carbohydrate binding domain of MAG was constructed based on the available crystal structures determined for sialoadhesin in complex with a 9-*N*-biphenyl-carbonyl-NeuAcαCH$_3$, Siglec-5 in complex with α2,3-sialylated lactose and Siglec-7 in complex with an α2,8 linked ganglioside (See Fig. S3). Distinct structural features were picked based on careful analysis of the X-ray data in combination with structural sequence alignment and homology modeling tools to enable the interpretation of the binding data. A modular approach was used, considering the unique features of MAG relative to the other siglecs. Although the backbone structure surrounding the conserved sialoside binding site is assumed to be the same for MAG as for the available template structures, we considered the CC′-loop and the GG′-linker as critical variable elements of the homology model.[33] Accordingly, we used the sialoadhesion structure as the basis for the backbone and essential parts of the sialic acid recognition site. This included the position of the essential arginine for the salt bridge with the carboxyl of the Neu5Ac, the 5′ site for the *N*-acetyl group, Trp29 stabilizing the glycerol side chain and the positioning of the C-9 aryl substituents. Sialoadhesin was also used as a template for the GG′-linker, a crucial determinant of the hydrophobic pocket at the C-9 position. This represents a conservative assumption since 9-aryl analogs of α-methyl-NeuAc are documented to dramatically increase affinity for both sialoadhesin and MAG.[29] The second determinant of the carbohydrate recognition is the CC′-loop, which is known to vary in siglecs, and influence receptor specificity.[33,34] Siglec-5 and -7 have the same number of amino acids in the CC′-loop as MAG and were therefore served as templates.

Homology models using these criteria were further subjected to an automated docking of known 9′substituted trisaccharide inhibitors of MAG (see Supplementary data). When bound ligands violated the conserved features of sialic acid recognition at the C-5 *N*-acetyl, C7-C9 polyhydroxy side chain or C-1 carboxylic acid sites, the model was excluded from further consideration. The final model comprises all features of siglec/sialic acid recognition

Table 1
Inhibitory potencies of C-9 substituted analogs of sialylated Core 1 O-linked glycans for MAG

Compound[a]	R^1 (NeuAcα2–3)	R^2 (NeuAcα2–6)	IC_{50}[b] (nM)	rIP[c]	Apparent K_d[d] (μM)
11a	HO–	–	1200 ± 110	1.0	1.9
11b	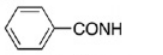	–	650 ± 73	1.8	1.0
11c	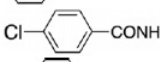	–	610 ± 61	1.9	1.0
11d	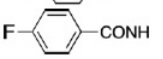	–	79 ± 12	14	0.13
12a	–	HO–	7900 ± 420	0.15	13
12b	–	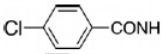	640 ± 54	1.9	1.0
12c	–	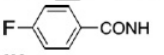	1100 ± 230	1.1	1.760
13a	HO–	HO–	750 ± 170	1.6	1.2
13b	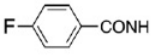	HO–	300 ± 53	4	0.48
13c	HO–	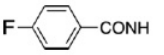	9 ± 1	129	0.015

[a] See structures in Scheme 1.
[b] IC_{50} values were determined by competition assays as described in Methods.
[c] Relative inhibitory potency (rIP) is based on the IC_{50} values relative to **11a**.
[d] Apparent K_d values are calculated from the IC_{50} values with reference to the K_d determined for **13a** by isothermal titration (Fig. 2).

conserved in available structures of sialoadhesion, Siglec-5 and -7 (Fig. 3).

The model accommodated sialosides with α2,3 or α2,6 linked sialic acids (e.g., 3′- or 6′- sialyllactose), consistent with the binding of both linkage types to MAG.[1,6] Di-sialylated ligands such as disialyl-T-antigen (**2**) invoked the question whether the α2,3 or α2,6 linked sialic acid occupied the conserved site. Taking into account the significant gain in affinity when substituting the reducing end with αThr, we assumed there would be an interaction of this group with the protein. Accordingly, we performed docking of the corresponding monosialylated derivatives **11a** and **12a** to investigate the position of the αThr with the sialic acid bound to the conserved site. With the α2,6-linked Neu5Ac of **12a** fixed to the conserved site, there was no interaction of αThr with the protein. In contrast, positioning the α2,3-linked sialic acid of **11a** in the conserved site allows the αThr to interact favorably with the protein. In the model, the αThr is harbored in a shallow grove formed by the CC′-loop and the G′-strand. This pose anchors the reducing end GalNAc with the *N*-acetyl group pointing towards the GG′-linker (Fig. 3). This directs the *N*-acetyl methyl group into the strongly favored hydrophobic site accessed by C-9 substituents, a site well described for other siglecs.[30] The placement of the *N*-acetyl group in this hydrophobic site then imposes steric restrictions for the substitution of the α2–3 sialic acid glycerol chain in the C-9 position which would occupy the same site (Fig. 3c). This model is entirely consistent with the observation that introducing an aryl substituent at C-9 enhances affinity of α-methyl-NeuAc, but does not enhance the affinity of the sialyl-T-antigens (**11a** and **13a**), which are anchored by the αThr. The 14-fold increase in affinity observed for the 9-*N*-*para*-flurobenzyl substituent of the α2,3-linked Neu5Ac (**11d**) can be accommodated by the successful competition with the GalNAc and αThr *N*-acetyl groups pointing into the same space.

With the glycan anchored by the α2–3 linked sialic acid at one end, and the αThr at the other, the α2–6 linked sialic acid has a minimal interaction with the protein. Although alternative positioning of the CC′ loop might provide such interactions, in the absence of evidence that such interactions exist, they were not further explored. However, the 9-*N*-*p*-fluorobenzyl substituent that affords 80-fold increase in affinity (**13c**) is in position to engage in protein contacts. In this model, the gain of affinity is

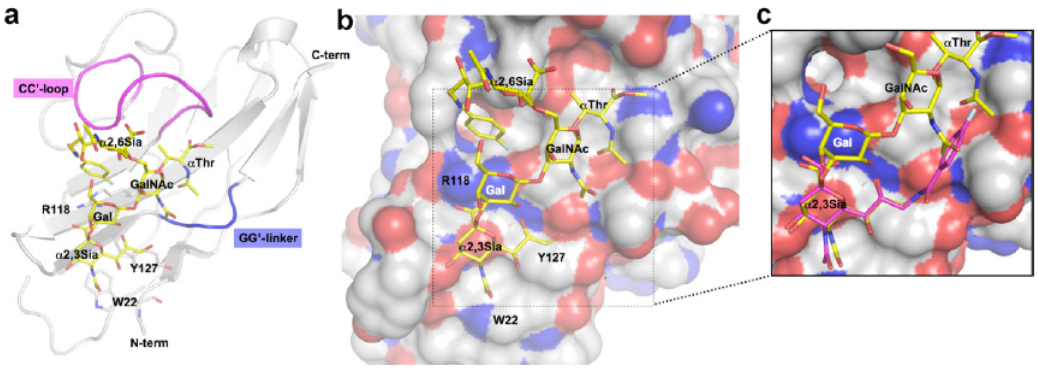

Figure 3. Proposed binding of sialyl-T-antigen analogs to MAG. (a) Homology model of MAG constructed from the solved structures siglecs-1, -5 and -7 depicting the binding of an analog of disialyl-T-antigen (**13c**). (b) Model highlighting the spatial relationship of the α2–3 sialic acid bound to the conserved arginine (R118), the αThr and the 9-*N*-fluoro-benzolamide on the α2–6 sialic acid (see Supplementary data for analysis of glycan torsion angles; Fig. S1). (c) Inset showing the steric clash of the 9-*N*-fluoro-benzolamide on the α2–3 sialic acid with the *N*-acetyl groups of the GalNAc and αThr.

attributed to a stacking interaction of the *para*-fluorobenzyl moiety with the conserved arginine (R118) (Fig. 3a,b; and Fig. S2). This is a known mode of interaction of fluoro-aryl inhibitors to proteins as described for the binding of type 2 statins to HMG CoA reductase (see also Fig. S2).[35] As an alternative, the fluorobenzyl moiety could interact with a hydrophobic pocket seen in Figure 3 below the phenyl ring, previously suggested to account for the increased affinity of aryl substituents attached at C-6 of the GalNAc in place of sialic acid.[4] However, we believe that stacking interaction of the fluorobenzyl with R118 better accounts for the high affinity observed.

We previously reported that the disialyl-T-antigen (**11a**) exhibited activity for reversing MAG inhibition of neurite outgrowth in an in vitro cell culture model.[17] However, it is not optimal for in vivo studies due to its relatively low (μM) potency, and the rapid clearance of small oligosaccharides from the blood. Since **13c** exhibits significantly higher potency (K_d = 15 nM), and has increased hydrophobicity due to the 9-aryl substituent, it will be of interest to determine if it has suitable phamacokinetic properties to evaluate its ability to promote axonal outgrowth in animal models of nerve injury.[16] This would provide an important proof of concept for the use of small molecule inhibitors of MAG for treatment of nerve injury. Longer term, however, we believe that the approach of minimizing the structural complexity of such inhibitors is ultimately the best route to obtaining pharmaceutically acceptable inhibitors. The detailed understanding of the basis for the potent inhibitory potency of **13c** may aid in the rational design of such sialoside mimic inhibitors.

Acknowledgments

The authors thank Ola Blixt, Tasneem Islam, and Karin Norgard Sumnicht for discussions and preliminary experiments on the nature of O-linked glycans as inhibitors of MAG, and Anna Crie with help in preparation of the manuscript and Figures. These studies were supported by NIH grant GM60928 (J.C.P.), EMBO fellowship (C.R.) and Swiss National Science Foundation (project 200020-120628 (B.E.).

Supplementary data

Supplementary data associated with this article can be found, in the online version, at doi:10.1016/j.bmcl.2011.04.068.

References and notes

1. Blixt, O.; Collins, B. E.; van den Nieuwenhof, I. M.; Crocker, P. R.; Paulson, J. C. *J. Biol. Chem.* **2003**, *278*, 31007.
2. Shin, S. Y.; Gathje, H.; Schwardt, O.; Gao, G. P.; Ernst, B.; Kelm, S.; Meyer, B. *ChemBioChem* **2008**, *9*, 2946.
3. Mesch, S.; Lemme, K.; Koliwer-Brandl, H.; Strasser, D. S.; Schwardt, O.; Kelm, S.; Ernst, B. *Carbohydr. Res.* **2010**, *345*, 1348.
4. Schwardt, O.; Gathje, H.; Vedani, A.; Mesch, S.; Gao, G. P.; Spreafico, M.; von Orelli, J.; Kelm, S.; Ernst, B. *J. Med. Chem.* **2009**, *52*, 989.
5. Kelm, S.; Brossmer, R.; Isecke, R.; Gross, H. J.; Strenge, K.; Schauer, R. *Eur. J. Biochem.* **1998**, *255*, 663.
6. Blixt, O.; Han, S.; Liao, L.; Zeng, Y.; Hoffmann, J.; Futakawa, S.; Paulson, J. C. *J. Am. Chem. Soc.* **2008**, *130*, 6680.
7. Schwardt, O.; Koliwer-Brandl, H.; Zimmerli, R.; Mesch, S.; Rossato, G.; Spreafico, M.; Vedani, A.; Kelm, S.; Ernst, B. *Bioorg. Med. Chem.* **2010**, *18*, 7239.
8. Crocker, P. R.; Paulson, J. C.; Varki, A. *Nat. Rev. Immunol.* **2007**, *7*, 255.
9. Schnaar, R. L.; Lopez, P. H. *J. Neurosci. Res.* **2009**, *87*, 3267.
10. Zorner, B.; Schwab, M. E. *Ann. N. Y. Acad. Sci.* **2010**, *1198 Suppl 1*, E22.
11. Cao, Z.; Gao, Y.; Deng, K.; Williams, G.; Doherty, P.; Walsh, F. S. *Mol. Cell. Neurosci.* **2010**, *43*, 1.
12. Worter, V.; Schweigreiter, R.; Kinzel, B.; Mueller, M.; Barske, C.; Bock, G.; Frentzel, S.; Bandtlow, C. E. *PLoS ONE* **2009**, *4*, e5218.
13. Robak, L. A.; Venkatesh, K.; Lee, H.; Raiker, S. J.; Duan, Y.; Lee-Osbourne, J.; Hofer, T.; Mage, R. G.; Rader, C.; Giger, R. J. *J. Neurosci.* **2009**, *29*, 5768.
14. Venkatesh, K.; Chivatakarn, O.; Lee, H.; Joshi, P. S.; Kantor, D. B.; Newman, B. A.; Mage, R.; Rader, C.; Giger, R. J. *J. Neurosci.* **2005**, *25*, 808.
15. Strenge, K.; Schauer, R.; Kelm, S. *FEBS Lett.* **1999**, *444*, 59.
16. Mountney, A.; Zahner, M. R.; Lorenzini, I.; Oudega, M.; Schramm, L. P.; Schnaar, R. L. *Proc. Natl. Acad. Sci. U.S.A.* **2010**, *107*, 11561.
17. Vyas, A. A.; Blixt, O.; Paulson, J. C.; Schnaar, R. L. *J. Biol. Chem.* **2005**, *280*, 16305.
18. Shelke, S. V.; Cutting, B.; Jiang, X.; Koliwer-Brandl, H.; Strasser, D. S.; Schwardt, O.; Kelm, S.; Ernst, B. *Angew. Chem., Int. Ed. Engl.* **2010**, *49*, 5721.
19. Mesch, S.; Moser, D.; Strasser, D. S.; Kelm, A.; Cutting, B.; Rossato, G.; Vedani, A.; Koliwer-Brandl, H.; Wittwer, M.; Rabbani, S.; Schwardt, O.; Kelm, S.; Ernst, B. *J. Med. Chem.* **2010**, *53*, 1597.
20. Bhunia, A.; Schwardt, O.; Gathje, H.; Gao, G. P.; Kelm, S.; Benie, A. J.; Hricovini, M.; Peters, T.; Ernst, B. *ChemBioChem* **2008**, *9*, 2941.
21. Shelke, S. V.; Gao, G. P.; Mesch, S.; Gathje, H.; Kelm, S.; Schwardt, O.; Ernst, B. *Bioorg. Med. Chem.* **2007**, *15*, 4951.
22. Gao, G.; Smiesko, M.; Schwardt, O.; Gathje, H.; Kelm, S.; Vedani, A.; Ernst, B. *Bioorg. Med. Chem.* **2007**, *15*, 7459.
23. Schwizer, D.; Gathje, H.; Kelm, S.; Porro, M.; Schwardt, O.; Ernst, B. *Bioorg. Med. Chem.* **2006**, *14*, 4944.
24. Collins, B. E.; Yang, L. J.; Mukhopadhyay, G.; Filbin, M. T.; Kiso, M.; Hasegawa, A.; Schnaar, R. L. *J. Biol. Chem.* **1997**, *272*, 1248.
25. Cairo, C. W.; Gestwicki, J. E.; Kanai, M.; Kiessling, L. L. *J. Am. Chem. Soc.* **2002**, *124*, 1615.
26. Gestwicki, J. E.; Cairo, C. W.; Strong, L. E.; Oetjen, K. A.; Kiessling, L. L. *J. Am. Chem. Soc.* **2002**, *124*, 14922.
27. Collins, B. E.; Paulson, J. C. *Curr. Opin. Chem. Biol.* **2004**, *8*, 617.
28. Lee, R. T.; Ichikawa, Y.; Kawasaki, T.; Drickamer, K.; Lee, Y. C. *Arch. Biochem. Biophys.* **1992**, *299*, 129.
29. Zaccai, N. R.; Maenaka, K.; Maenaka, T.; Crocker, P. R.; Brossmer, R.; Kelm, S.; Jones, E. Y. *Structure* **2003**, *11*, 557.
30. Zaccai, N. R.; May, A. P.; Robinson, R. C.; Burtnick, L. D.; Crocker, P. R.; Brossmer, R.; Kelm, S.; Jones, E. Y. *J. Mol. Biol.* **2007**, *365*, 1469.
31. Abdu-Allah, H. H.; Watanabe, K.; Completo, G. C.; Sadagopan, M.; Hayashizaki, K.; Takaku, C.; Tamanaka, T.; Takematsu, H.; Kozutsumi, Y.; Paulson, J. C.; Tsubata, T.; Ando, H.; Ishida, H.; Kiso, M. *Bioorg. Med. Chem.* **2011**, *19*, 1966.
32. Blixt, O.; Allin, K.; Pereira, L.; Datta, A.; Paulson, J. C. *J. Am. Chem. Soc.* **2002**, *124*, 5739.
33. Zhuravleva, M. A.; Trandem, K.; Sun, P. D. *J. Mol. Biol.* **2008**, *375*, 437.
34. Yamaji, T.; Teranishi, T.; Alphey, M. S.; Crocker, P. R.; Hashimoto, Y. *J. Biol. Chem.* **2002**, *277*, 6324.
35. Istvan, E. S.; Deisenhofer, J. *Science* **2001**, *292*, 1160.

Supporting Information

High affinity sialoside ligands of myelin associated glycoprotein

Ying Zeng, Christoph Rademacher, Corwin M. Nycholat, Satoshi Futakawa, Katrin Lemme, Beat Ernst and James C. Paulson

secondary antibody (HRP-labeled anti-goat IgG 1.9 ng/well) at RT for 40 min. The antibody complex was then added to the neuraminidase treated MAG-Fc and further incubated at RT for 30min. Solutions of the inhibitor in H_2O (50 µl/well) and MAG-Fc/antibody complex (50 µl/well) were combined in the wells and incubated at 37 °C for 30 min. The wells were developed using the TMB substrate system (100 µl/well, Pierce Cat# 34021). Absorbance at 450 nm was measured using a Spectrocount plate reader (Packard Instruments, Meriden, CT). Wells without MAG-Fc or inhibitor were used as negative controls. For each set of competitive inhibition experiments, a reference compound was included as a positive control. Assays were performed in triplicate throughout and each inhibitor was tested in three independent experiments. From the inhibition curves IC_{50} values were determined by non-linear regression analysis (PRISM, GraphPad Software, Inc., San Diego, CA).

Homology modeling of murine MAG

Three crystal structures were chosen to resemble specific features as a template for the homology model of the sialic acid binding domain of murine MAG (UniProt: P20917). First, sialoadhesin in complex with a biphenyl substituted 9' position of a α2,3 linked sialic acid (pdb: 1ODA) was used for the entire backbone structure. It was also important to chose sialoadhesin as a template for the GG'-linker as it shares the same number of amino acids with MAG. On the other hand the CC'-loop was modeled using siglec-5 (pdb: 2ZG3) and siglec-7 (pdb: 2HRL), both in complex with a sialic acid bearing ligand. The CC'-loop has been described as a flexible portion of the sialic acid recognition site and has two amino acids less in sialoadhesin compared to MAG. Moreover, the low sequence identity (<10%) with the available templates in combination with the unusual feature of two prolines in the MAG CC'-loop raised the necessity of this modular approach building the loop. This strategy is based on the careful analysis of a multiple sequence alignment [4] and structural sequence alignment using Espresso (version 8.06) and STRAP. [5] The final model was built iteratively in MOE (Chemical Computing Group, 2008.10). Mutations were introduced using the default amino acid rotamer library and followed by a final energy

minimization employing AMBER99 force field with implicit solvent. Modeling of the loops was performed using the MODLOOP server for the GG'-linker and the CC'-loop in presence of inhibitor. [6] Here, a short stretch of either eight or four amino acids was defined for the CC'-loop or GG'-linker, respectively. The quality of the final protein model was validated using MolProbity. [7] Ligands were built using the Glycam webserver [8] and MOE. In cases where automated docking was applied, AUTODOCK Vina (version 1.0) [9] was used with a 60 x 54 x 50 point-sized box and flexibility being limited to the glycan torsions with exhaustiveness feature ranging from 32 to 128. The full-size ligand **13c** (38 rotateable bonds) was manually docked in MOE based on the resulting AUTODOCK Vina data of ligand **11a**. Final models for bound glycan structures were checked for glycan torsion violations using the available Glycomaps (GlycoMapsDB, DKFZ, Heidelberg) (Figure S1).

Figure S1: Glycotorsions of the model of ligand **13c** in complex with MAG

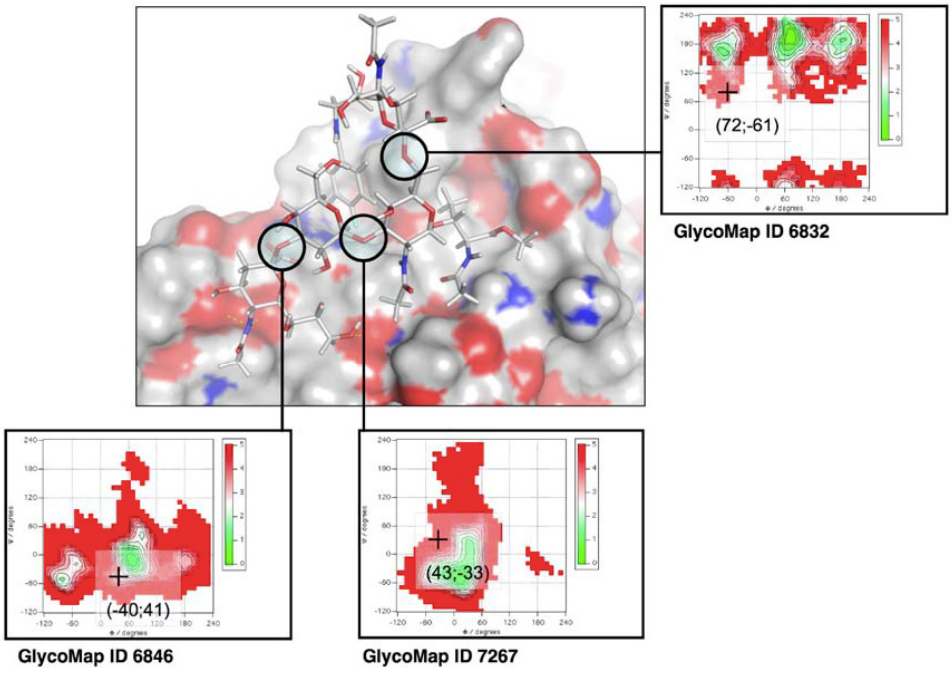

S4

Figure S2: Positioning of para-benzyl fluorine towards the guanidinium group of the essential arginine (R118). Stick and CPK representation highlight the full-length R118 side chain as found in our MAG homology model. To compare the distance and orientation of the fluorobenzyl group in **13c** with other structures in the PDB database a self-made script from the PDB module in BioPython [10] was used. Briefly, all fluorinated benzol substituents of bound ligands close to guanidinium groups of arginines in the PDB database were identified. The C-F bond vectors were isolated from the ligands and aligned according to their orientation towards the respective guanidinium group (carbon in white, fluorine in light blue). Due to the two-fold symmetry of the guanidinium group, vectors were randomly chosen to be on either side. For clarity, only the C-F bonds are shown. The majority of these C-F bond vectors locate the fluorine in close proximity to the guanidinium carbon with an angle between the C-F and the guanidinium group being almost parallel. For comparison between the C-F bond orientation of representative from the PDB database, the carbon and the fluorine of ligand **13c** are shown in red and dark blue, respectively. It is found that the distance and the orientation of the fluorobenzyl group towards the guanidinium group of R118 are in line with the C-F bonds of comparable aromatic substituents found the in database.

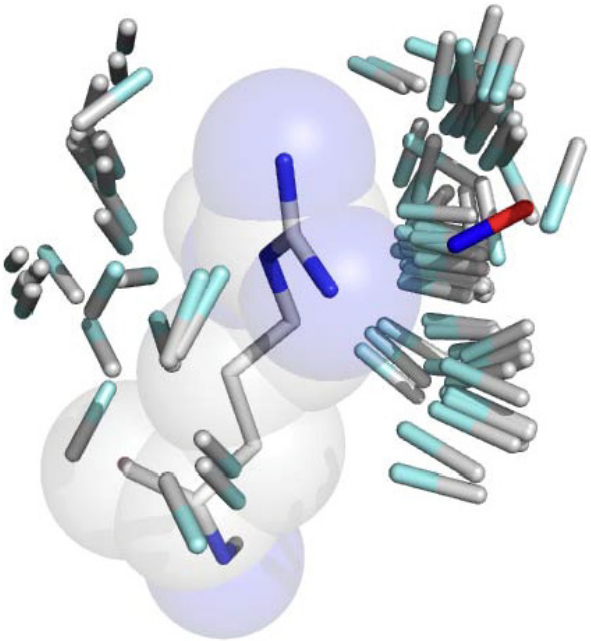

Isothermal titration calorimetry

ITC experiments of **13a** with freshly prepared MAG-wt were performed using a VP-ITC instrument from MicroCal, Inc. (Northampton, MA). Measurements were performed at 25 °C. The assay buffer was HBS-E (10 mM Hepes, 150 mM NaCl, 3mM EDTA, pH 7.4). The concentration of MAG was 14.8 μM, determined by HPLC. [11] Injections of 3 μl ligand solution were added from a computer controlled 300 μl microsyringe at an interval of 5 min into the sample cell (Figure S3). The experimental data was fitted to a theoretical titration curve (one site binding model) using Origin version 7 software (MicroCal) [11] with ΔH (enthalpy change in kJ/mol), K_D (dissociation constant in μM), and N (number of binding sites) as adjustable parameters (Table 1). [12]

Figure S3. Ligand **13a** (400 μM) titrated into MAG-wt (14.8 μM binding site). Assay buffer: 10 mM HEPES, 150 mM NaCl, 3 mM EDTA, pH 7.4, 25°C.

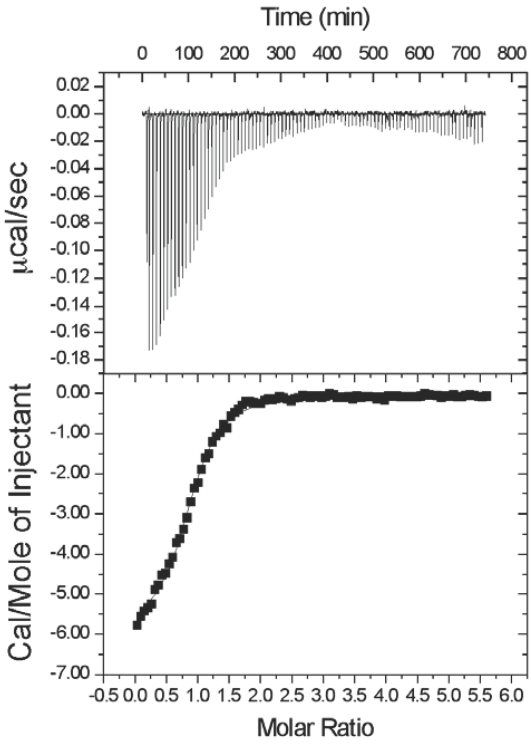

Table S1. Thermodynamic data of the ITC measurement with **13a** titrated into MAG-wt

	Value	Unit
N	0.894	-
K_D	1.2	**μM**
ΔG°	-33.8	**kJ/mol**
ΔH°	-24.9	**kJ/mol**
ΔS°	30.0	**J/mol/K**
TΔS°	8.9	**kJ/mol**

Synthesis of compounds 13b and 13c

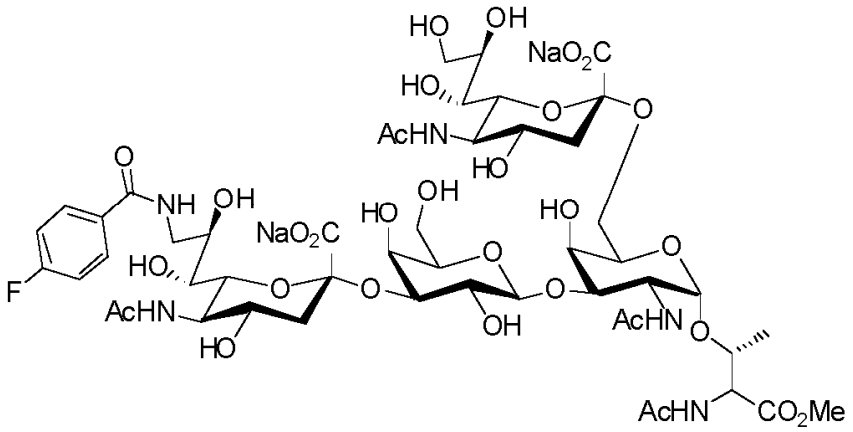

O^3-[(5-acetamido-9-*p*-fluoro-benzoylamido-3,5,9-trideoxy-D-*glycero*-α-D-*galacto*-2-nonulo-pyranosylonic acid)-(2→3)-β-D-galactopyranosyl-(1→3)-[5-acetamido-3,5-dideoxy-D-*glycero*-α-D-*galacto*-2-nonulo-pyranosylonic acid-(2→6)]-2-acetamido-2-deoxy-α-D-galactopyranosyl]-*N*-acetamido-L-threonine methyl ester **13b.**

Compound **11d** (20 mg, 0.24 mmol) was mixed with CMP-Neu5Ac (1.2 eq) in sodium cacodylate buffer ($MnCl_2$ (20 mM), pH 7.0). chST6GalNAc-I (0.2 U) was added then the mixture was incubated at 37 °C for 72 h. When TLC (EtOAc-MeOH-AcOH-H_2O 6:3:3:2) showed consumption of the starting material the mixture was loaded onto a gel filtration column (Sephadex G15 1.5x100 cm) and eluted with H_2O containing 5% BuOH. Appropriate fractions were combined and lyophilized to provide a white amorphous solid **13b** (yield 78%). ^{1}H NMR (600 MHz, D_2O) δ 7.90-7.83 (m, 2H), 7.26 (dd, 1H, *J* = 8.8 Hz), 4.63 (d, 1H, *J* = 1.7 Hz), 4.51 (d, 1H, *J* = 7.8 Hz), 4.47-4.42 (m, 1H), 4.27-4.19 (m, 2H), 4.12 (dd, 1H, *J* = 8.0, 3.9 Hz), 4.07 (dd, 1H, *J* = 9.8, 3.1 Hz), 4.04 (dd, 1H, *J* = 8.4, 3.0 Hz), 3.99 (dd, 1H, *J* = 11.2, 2.7 Hz), 3.96-3.80 (m, 7H), 3.78-3.49 (m, 17H), 2.77 (dd, 1H, *J* = 12.4, 4.5 Hz), 2.71 (dd, 1H, *J* = 12.5, 4.6 Hz), 2.05 (s, 3H), 2.04 (s, 3H), 2.01 (s, 3H), 1.99 (s, 3H), 1.80 (dd, 1H, *J* = 12.2 Hz), 1.67 (dd, 1H, *J* = 12.2 Hz), 1.28 (d, 3H, *J* = 6.4 Hz); ^{13}C NMR (150 MHz, D_2O) δ 175.8, 175.7, 175.59, 175.0, 174.7, 174.1, 172.7, 170.9, 166.4, 164.7, 130.7, 130.6, 130.5, 116.6, 116.4, 105.2, 101.09, 100.5, 99.8,

77.5, 76.8, 76.5, 75.6, 73.5, 73.3, 72.5, 71.1, 70.7, 70.4, 69.8, 69.3, 69.1, 69.0, 68.1, 64.6, 63.4, 62.3, 61.8, 58.0, 53.6, 52.7, 52.5, 49.4, 43.7, 40.9, 40.7, 34.2, 23.0, 22.8, 22.8, 22.4, 19.2, 18.8, 13.8; ESI HRMS exact mass calculated for $[M+H]^+$ ($C_{50}H_{75}FN_5O_{30}$) requires *m/z* 1244.4475, found 1244.4473.

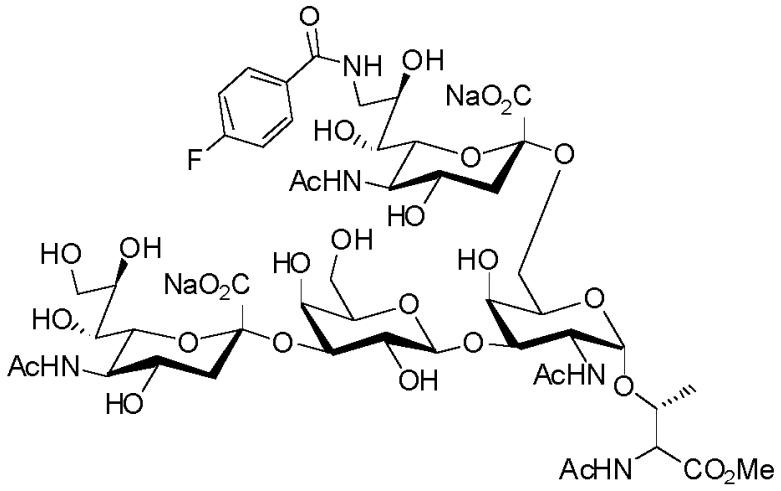

O^3-[(5-acetamido-3,5-dideoxy-D-*glycero*-α-D-*galacto*-2-nonulo-pyranosylonic acid)-(2→3)-β-D-galactopyranosyl-(1→3)-[5-acetamido-9-*p*-fluoro-benzoylamido-3,5,9-trideoxy-D-*glycero*-α-D-*galacto*-2-nonulo-pyranosylonic acid-(2→6)]-2-acetamido-2-deoxy-α-D-galactopyranosyl]-*N*-acetamido-L-threonine methyl ester **13c**.

Compound **11a** (40 mg, 0.48 mmol) was mixed with crude CMP-9-azido-9-deoxy Neu5Ac (1.2 eq). chST6GalNAc-I (0.4 U) was added, and the mixture was incubated at 37 °C for 72 h. When TLC (EtOAc-MeOH-AcOH-H_2O 6:3:3:2) showed complete consumption of starting material the mixture was loaded onto a gel filtration column (Sephadex G15 1.5x100 cm) and eluted with H_2O containing 5% BuOH. Appropriate fractions were combined and lyophilized. Typical yields ranged from 82-88%. The tetrasaccharide was then dissolved in methanol-water (5 mL, 9:1) and treated with a solution of PMe_3 (2 eq) in THF (5.0 mL). The mixture was stirred at RT for 2 h then concentrated under reduced pressure and lyophilized. The product was then taken up in dry

DMF containing Et_3N (2 eq). *p*-Flurobenzoyl chloride (1.5 eq) was added and the reaction stirred until starting material was consumed as monitored by TLC (EtOAc-MeOH-AcOH-H_2O 8:3:3:2). The reaction mixture was concentrated under reduced pressure and the product purified by chromatography using Iatrobeads (EtOAc-MeOH-AcOH-H_2O 8:3:3:2) to provide **13c** as a white amorphous solid (yield 60-70% 2 steps). ^{1}H NMR (600 MHz, D_2O) δ 7.94-7.73 (m, 2H), 7.24 (dd, 2H, *J* = 8.8 Hz), 4.56 (d, 1H, *J* = 1.9 Hz), 4.51 (d, 1H, *J* = 7.9 Hz), 4.43-4.40 (m, 1H), 4.22 (s, 1H), 4.20 (dd, 1H, *J* = 11.2, 3.9 Hz), 4.10 (dd, 1H, *J* = 7.8, 4.2 Hz), 4.06 (dd, 1H, *J* = 9.8, 3.0 Hz), 4.04-4.00 (m, 2H), 3.98 (dd, 2H, *J* = 11.2, 2.8 Hz), 3.92-3.47 (m, 30H), 2.75 (dd, 1H, *J* = 12.4, 4.5 Hz), 2.69 (dd, 1H, *J* = 12.4, 4.5 Hz), 2.12 (s, 3H), 2.02 (s, 3H), 1.99 (s, 3H), 1.91 (s, 3H), 1.77 (dd, 1H, *J* = 12.2 Hz), 1.66 (dd, 1H, *J* = 12.2 Hz), 1.26 (d, 3H, *J* = 7.2 Hz); ^{13}C NMR (150 MHz, D_2O) δ 174.9, 172.1, 163.9, 129.7, 129.6, 115.7, 115.5, 104.6, 99.5, 98.8, 76.8, 75.6, 75.5, 74.8, 72.7, 72.4, 71.9, 70.2, 69.9, 69.6, 68.8, 68.4, 68.3, 68.1, 68.1, 67.3, 63.6, 62.5, 60.9, 57.2, 52.8, 51.8, 51.6, 48.5, 46.6, 42.7, 39.8, 22.2, 22.0, 21.9, 21.6, 18.0, 8.2; ESI HRMS exact mass calculated for $[M+H]^+$ ($C_{50}H_{75}FN_5O_{30}$) requires *m/z* 1244.4475, found 1244.4484.

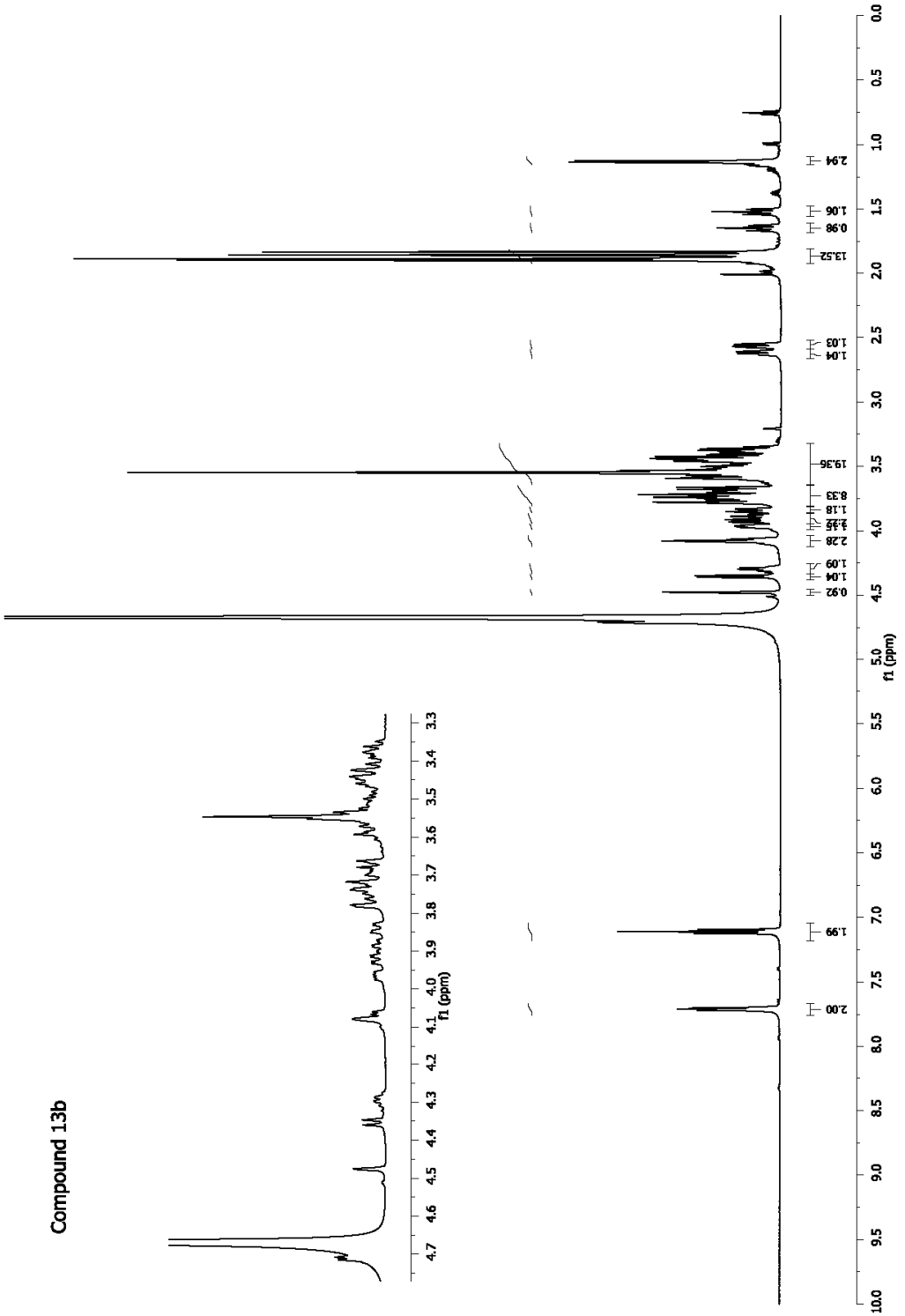
Compound 13b
f1 (ppm)
0.92
1.04
1.09
2.28
3.35
1.18
8.33
19.36
1.04
1.03
13.52
0.98
1.06
2.94
1.99
2.00

S10

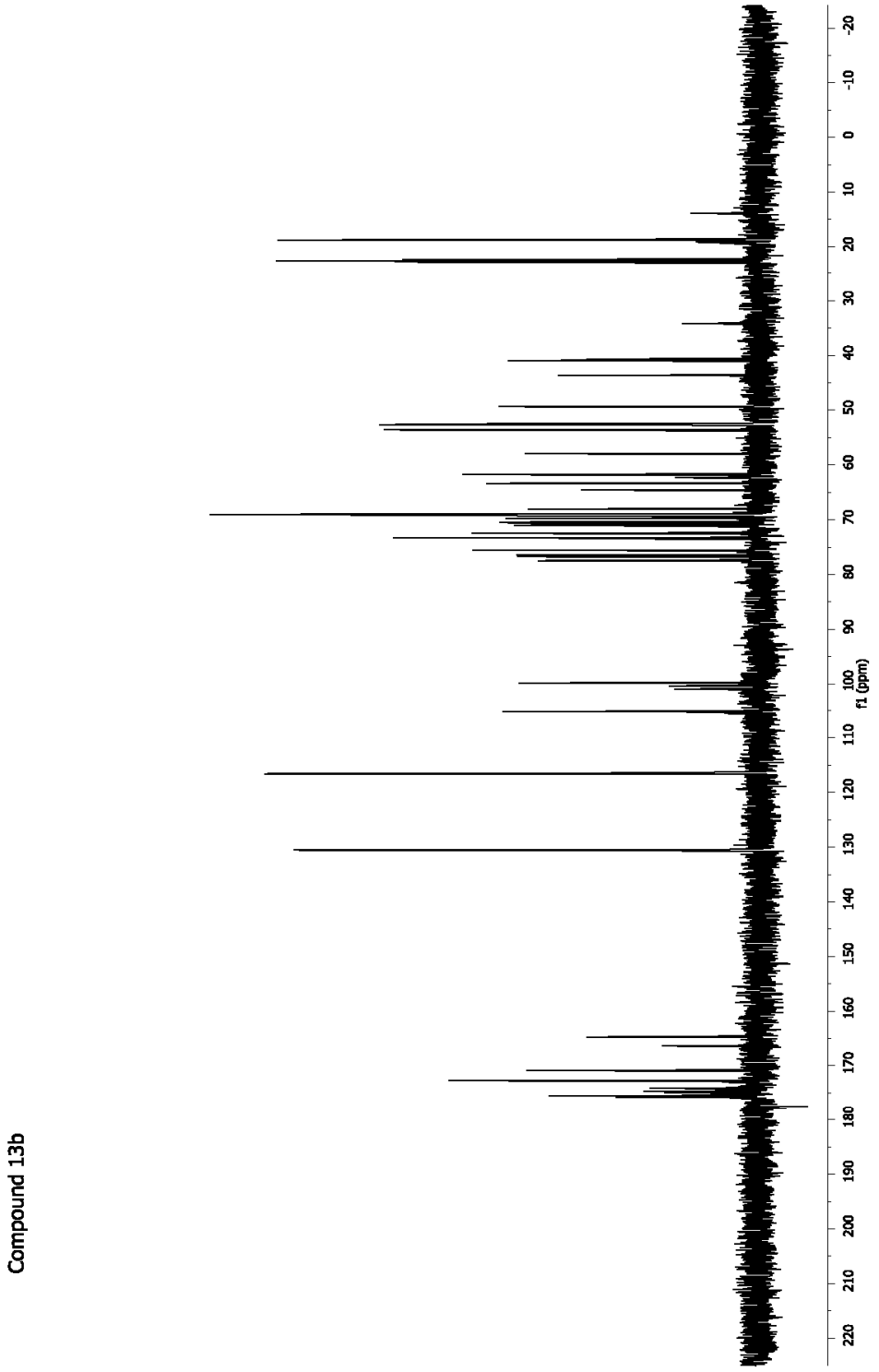

S11

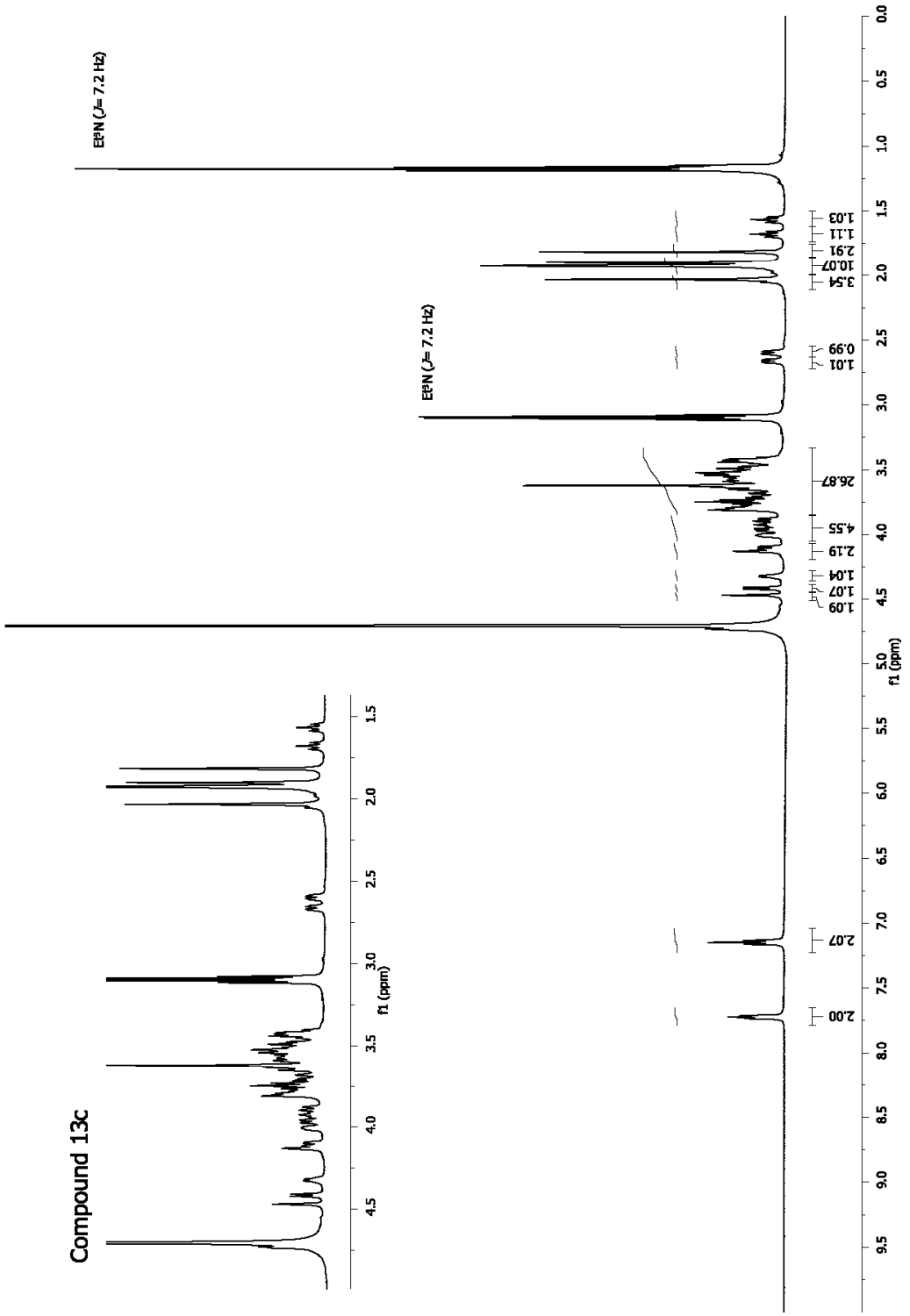
Compound 13c
Et3N (J= 7.2 Hz)
Et3N (J= 7.2 Hz)
f1 (ppm)
f1 (ppm)
2.00
2.07
1.09
1.07
1.04
2.19
4.55
26.87
1.01
0.99
3.54
10.07
2.91
1.11
1.03

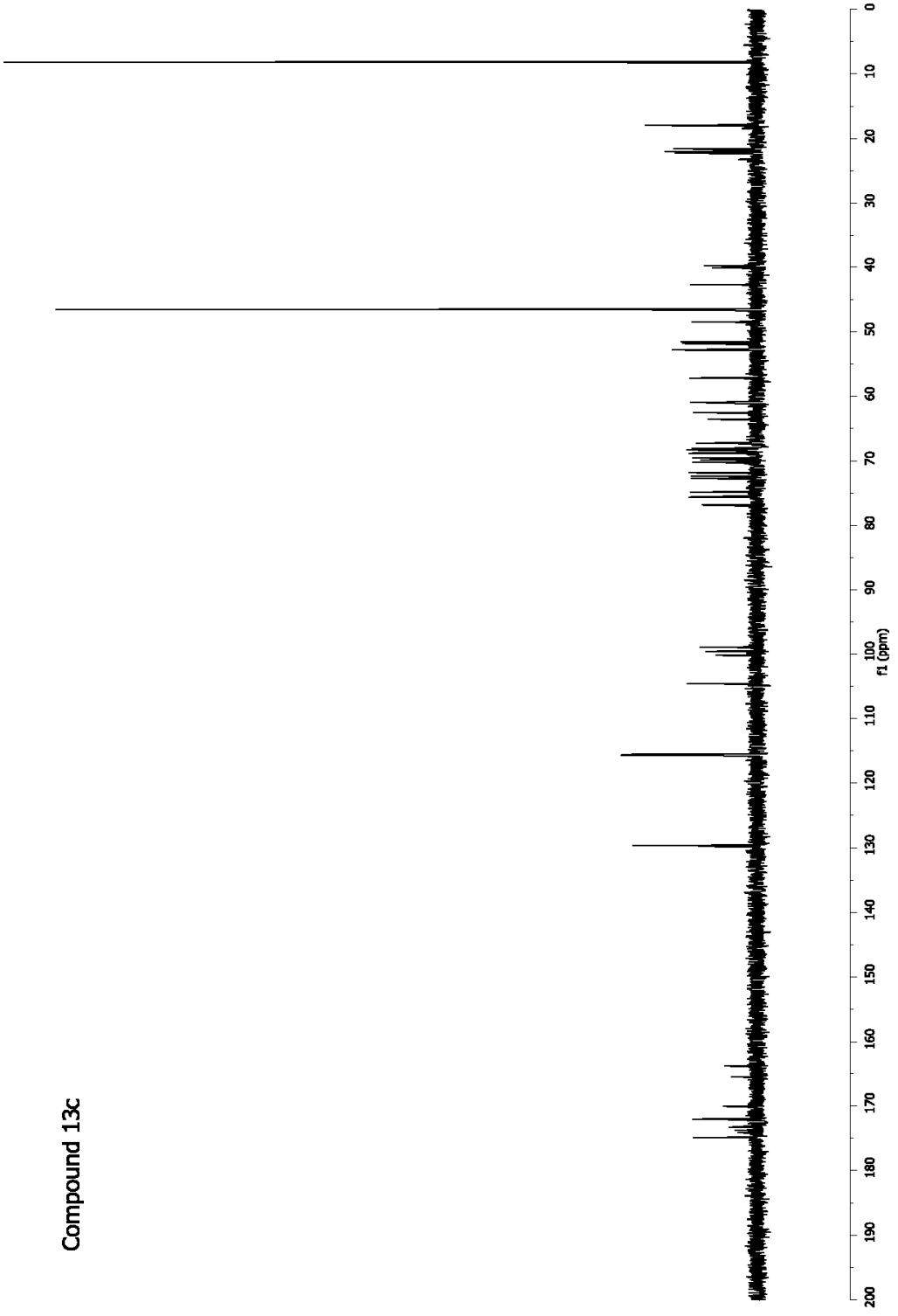
Compound 13c
f1 (ppm)
0
10
20
30
40
50
60
70
80
90
100
110
120
130
140
150
160
170
180
190
200

S13

References

1. Blixt, O.; Allin, K.; Pereira, L.; Datta, A.; Paulson, J. C. *Journal of the American Chemical Society* **2002,** *124*, 5739.
2. Blixt, O.; Han, S. F.; Liao, L.; Zeng, Y.; Hoffmann, J.; Futakawa, S.; Paulson, J. C. *Journal of the American Chemical Society* **2008,** *130*, 6680.
3. Blixt, O.; Collins, B. E.; van den Nieuwenhof, I. M.; Crocker, P. R.; Paulson, J. C. *Journal of Biological Chemistry* **2003,** *278*, 31007.
4. Alphey, M. S.; Attrill, H.; Crocker, P. R.; van Aalten, D. M. *J Biol Chem* **2003,** *278*, 3372.
5. Gille, C.; Frommel, C. *Bioinformatics* **2001,** *17*, 377.
6. Fiser, A.; Sali, A. *Bioinformatics* **2003,** *19*, 2500.
7. Davis, I. W.; Murray, L. W.; Richardson, J. S.; Richardson, D. C. *Nucleic Acids Res* **2004,** *32*, W615.
8. WoodsGroup. *Complex Carbohydrate Research Center, University of Georgia, Athens, GA. (http://www.glycam.com)* **2005-2011**.
9. Trott, O.; Olson, A. J. *J Comput Chem* **2009**.
10. Hamelryck, T.; Manderick, B. *Bioinformatics* **2003,** *19*, 2308.
11. MeschA, S.; Lemme, K.; Koliwer-Brandl, H.; Strasser, D. S.; Schwardt, O.; Kelm, S.; Ernst, B. *Carbohydrate Research* **2010,** *345*, 1348.
12. Wiseman, T.; Williston, S.; Brandts, J. F.; Lin, L. N. *Anal Biochem* **1989,** *179*, 131.

Kinetic and Thermodynamic Properties of MAG Antagonists

Stefanie Mesch,[a] Katrin Lemme,[a] Hendrik Koliwer-Brandl,[b] Daniel Strasser,[a] Oliver Schwardt,[a] Soerge Kelm,[b] Beat Ernst[a,*]

[a]*Institute of Molecular Pharmacy, University of Basel, Klingelbergstr. 50, 4056 Basel, Switzerland*

[b]*Center for Biomolecular Interactions Bremen, Glycobiochemistry, University of Bremen, P.O.B. 330440, D- 28334 Bremen, Germany*

**Corresponding author. Tel: 0041 267 15 51; Fax: 0041 267 15 52; e-mail: beat.ernst@unibas.ch*

Published in: *Carbohydr. Res.* **2010**, *345*, 1348-1359.

Contribution of Katrin Lemme: ITC experiment, determination of protein concentration.

Carbohydrate Research 345 (2010) 1348–1359

Contents lists available at ScienceDirect

Carbohydrate Research

journal homepage: www.elsevier.com/locate/carres

Kinetic and thermodynamic properties of MAG antagonists

Stefanie Mesch [a], Katrin Lemme [a], Hendrik Koliwer-Brandl [b], Daniel S. Strasser [a], Oliver Schwardt [a], Soerge Kelm [b], Beat Ernst [a,*]

[a] Institute of Molecular Pharmacy, Pharmacenter, University of Basel, Klingelbergstr. 50, 4056 Basel, Switzerland
[b] Center for Biomolecular Interactions Bremen, Glycobiochemistry, University of Bremen, POB 330440, D-28334 Bremen, Germany

ARTICLE INFO

Article history:
Received 21 January 2010
Received in revised form 4 March 2010
Accepted 9 March 2010
Available online 16 March 2010

Keywords:
Carbohydrate mimetics
Siglecs
Myelin-associated glycoprotein (MAG)
Thermodynamics of carbohydrate–protein interactions
Kinetics of carbohydrate–lectin interactions

ABSTRACT

Paraplegia is caused by injuries of the central nervous system (CNS) and especially young people suffer from these severe consequences as, for example, the loss of motor functions. The lack of repair of the injured nerve strands originates from the inhibitory environment for axon regeneration in the CNS. Specific inhibitory proteins block the regrowth of nerve roots. One of these neurite outgrowth inhibitors is the myelin-associated glycoprotein (MAG), which is a member of the Siglec family (sialic acid-binding immunoglobulin-like lectin). In previous studies, we identified potent small molecule MAG antagonists. In this communication, we report new neuraminic acid derivatives modified in the 4- and 5-position, and the influence of various structural modifications on their kinetic and thermodynamic binding properties.

1. Introduction

Paraplegia is caused by injuries of the central nervous system (CNS). A therapy for full regeneration of injured nerve strands is not yet available. The lack of regeneration originates from the inhibitory environment in the CNS,[1,2] that is, specific inhibitors on residual myelin and on astrocytes, which are recruited to the site of injury.[3–5] In the last decade, several inhibitor proteins have been identified, one of them being the myelin-associated glycoprotein (MAG).[6] MAG is a transmembrane glycoprotein, belonging to the Siglec family (sialic acid-binding immunoglobulin-like lectin).[7,8] On the surface of neurons, MAG interacts with two classes of targets: proteins of the Nogo receptor family[9,10] and gangliosides, primarily the gangliosides GD1a and GT1b.[11–14] Although the relative role of Nogo receptors and gangliosides as MAG ligands has yet to be resolved, in some systems, neurite outgrowth can be initiated by sialidase treatment, suggesting that the sialic acid-mediated interactions of MAG predominantly contribute to the inhibitory process.[15] Therefore, blocking MAG with potent glycomimetic antagonists may be a valuable therapeutic approach to enhance axon regeneration. Based on the best known natural ligand of MAG identified to date, the ganglioside GQ1ba (Fig. 1), different series of antagonists have been developed.[16–21]

With neuraminic acid derivatives such as **1**,[16] Kelm et al. reported a remarkable simplification of the relevant tetrasaccharide binding epitope of GQ1ba. Further reported modifications are related to lipophilic interactions. Thus, antagonists with a lipophilic core, for example, the biphenyl derivatives **2**[18] or a lipophilic replacement of the a-(2→6)-linked Neu5Ac, for example, **3**[19] were synthesized (Fig. 1).

The concept of drug discovery is based upon selectively addressing particular biological targets preferably by low molecular weight compounds. In vitro determined drug–target interactions are classically rated in terms of binding parameters such as IC_{50}'s and K_D's. An alternative perspective on drug optimization is the residence time of the drug–target binary complex,[22] as quantified by the dissociation half-life ($t_{1/2}$). Potential advantages of a long residence time are extended duration of the pharmacological effect and target selectivity.[22,23] Especially in the field of carbohydrate–lectin interactions, this is a crucial point to address. As a result of the shallow and water accessible binding sites of lectins, carbohydrates bind with only low affinity and show very fast dissociation off-rates, leading to $t_{1/2}$ in the range of seconds. Examples

Abbreviations: AIBN, a,a′-azodiisobutyronitrile; aq, aqueous; BnBr, benzyl bromide; DCM, dichloromethane; DMAP, 4-dimethylaminopyridine; DMF, *N*,*N*-dimethylformamide; FAc, fluoro-acetyl; HBS-E, HEPES/NaCl/EDTA buffer; HBS-EP, HEPES–NaCl–EDTA–P20 buffer; ITC, isothermal titration calorimetry; K_D, dissociation constant; MS, mass spectrometry; Neu5Ac, *N*-acetylneuraminic acid; NgR, Nogo receptor; NMR, nuclear magnetic resonance; PDC, pyridinium dichromate; PPTS, pyridinium *p*-toluenesulfonate; RP, reversed phase; SPR, surface plasmon resonance; STD-NMR, saturation transfer difference nuclear magnetic resonance spectroscopy; THF, tetrahydrofuran.

* Corresponding author. Tel.: +41 267 15 51; fax: +41 267 15 52.
E-mail address: beat.ernst@unibas.ch (B. Ernst).

0008-6215/$ - see front matter © 2010 Elsevier Ltd. All rights reserved.
doi:10.1016/j.carres.2010.03.010

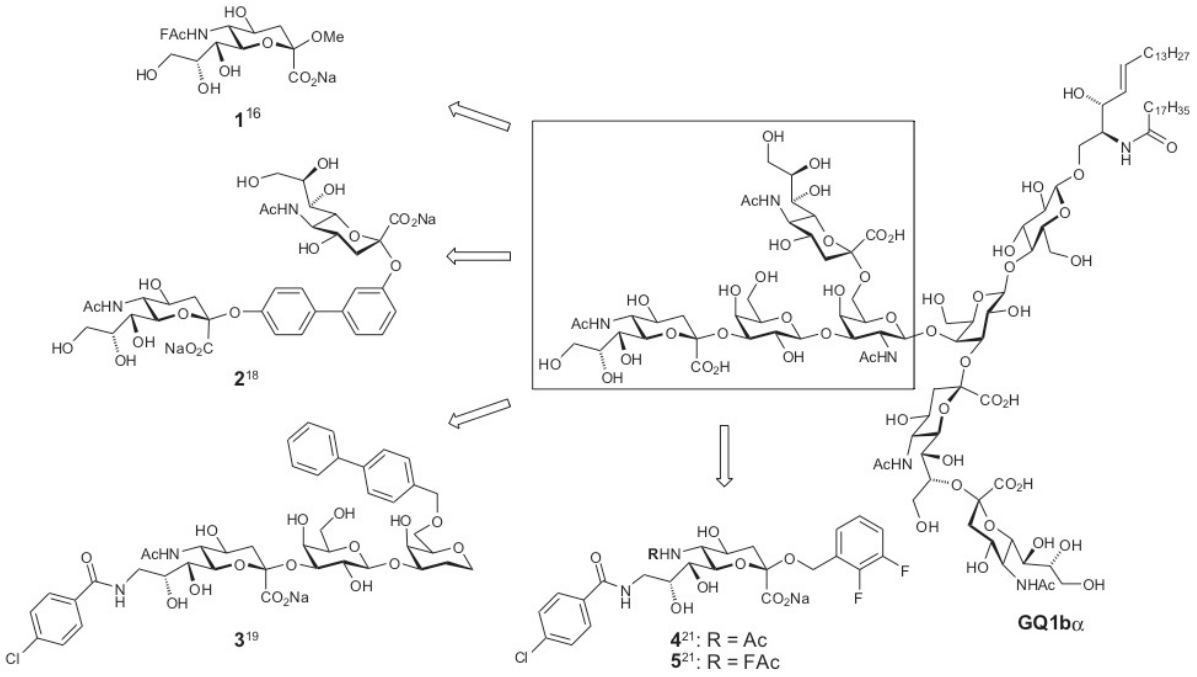

Figure 1. MAG antagonists **1**[16], **2**[18], **3**[19] and **4**, **5**[21]derived from the tetrasaccharide core structure (highlighted in box) of GQ1bα.

Table 1
Carbohydrate–protein interactions: thermodynamic and kinetic binding parameters

Protein	Ligand	K_D (μM)	k_{on} (M^{-1} s^{-1})	k_{off} (s^{-1})	$t_{1/2}$ (s)
P-Selectin[24]	PSGL-1	0.3	$4{\cdot}10^6$	1.4	0.5
E-Selectin[25]	ESL-1	62	$4{\cdot}10^4$	3.0	0.2
GSLA-2 mAb[26]	Sialyl Lewis^a	4.3	$1.1{\cdot}10^5$	0.48	1.5
MAG[19]	Neu5Ac derivative **3**[19]	2.8	$3.5{\cdot}10^5$	0.8	0.9

of thermodynamic and kinetic parameters for carbohydrate–protein interactions are summarized in Table 1.

For medical applications, an improved $t_{1/2}$ of the drug–protein complex is beneficial, because the therapeutic effect can be reached with a lower dose. Zanamivir is one of the prominent examples, where a carbohydrate-based lead was optimized to yield a drug with a dramatically improved kinetic behavior, showing a half-life of 33 min of its complex with the B/Memphis/3/89 (H3N2) influenza virus.[27] In this communication, we present various MAG antagonists modified at the 4- and 5-position with the aim to modulate their kinetic properties. In general, lead optimization is often achieved by additional lipophilic contacts and thereby improving the binding entropy. As a result of the increased lipophilicity, the dissociation half-life ($t_{1/2}$) of the drug–target complex is extended.[28,29] The starting point for our investigation was MAG antagonist **5**,[21] a result of an extended optimization program focusing exclusively on the improvement of its thermodynamic binding properties.[17–19,21]

2. Results and discussion

Recently, we reported the synthesis and biological evaluation of a series of MAG antagonists with affinities in the low micromolar range.[21] Furthermore, pharmacokinetic parameters such as stability and membrane penetration indicated that the antagonists **4** and **5** (Fig. 1) fulfill the basic requirements for lead compounds. As halogenated acetates at the 5-position led to a drastic improvement of the binding affinity,[16,21] we investigated the impact of this position on the thermodynamic properties and also examined its influence on the dissociation half-life time. Molecular modeling studies with a homology model of MAG[30] suggested that the hydroxy group in the 4-position is not directly involved in the binding process[19] and therefore provides a possibility for derivatization. Because additional hydrophobic contacts based on the 4-position and an inverted configuration at C-4 are expected to alter the thermodynamic and kinetic behavior, we synthesized a small library of antagonists and analyzed their binding properties by surface plasmon resonance.

2.1. A MAG antagonist modified in the 5-position of the Neu5Ac scaffold

With isothermal titration calorimetry, we determined the thermodynamic parameters ΔH, ΔS, and ΔG[31] of antagonist **5** interacting with a recombinant protein consisting of the three N-terminal domains of MAG and the Fc part of human IgG (MAG_{d1-3}-Fc).[32] For the ITC experiment, a solution of **5** (500 μM, HBS-E buffer) was injected into a solution of MAG_{d1-3}-Fc (48.35 μM, HBS-E buffer) at 25 °C (Fig. 2).

The experimental data were fitted to a theoretical titration curve (one site binding model) using *Origin version 7* software (MicroCal) and the thermodynamic parameters calculated according to the equation shown in Table 2. The ITC experiment confirmed the high potency of **5**, having a K_D in the nanomolar

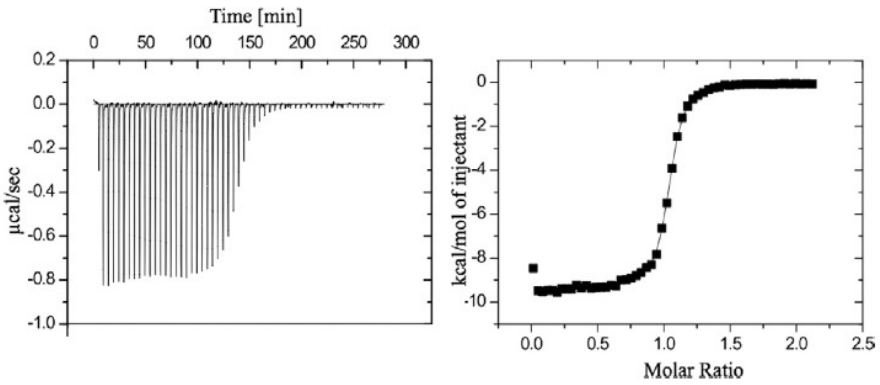

Figure 2. Enthalpogram (left) and corresponding fit (right) of the titration of MAG_{d1-3}-Fc with antagonist **5**. For the fit, the first injection was not taken into account.

Table 2
Thermodynamic parameters of antagonist **5**

Ligand	N	K_D (nM)	DG (kJ/mol)*	DH (kJ/mol)*	TDS (kJ/mol)*
5	1.03	142	−39.1	−39.2	−0.14

DH, DS, and DG were calculated according to the equation $DG = DH - TDS = RT\ln K_A = -RT\ln K_D$; N represents the stoichiometry, * values' accuracy ±5%.

range.[21] Interestingly, the interaction is exclusively enthalpy driven.[33,34]

In a next step, the kinetic binding properties of **5** were determined by surface plasmon resonance (SPR) (Fig. 3). Because the off-rate at 25 C turned out to be very fast, the Biacore experiment was repeated at lower temperature. At 5 C, a clear slowdown of k_{off} for **5** (R: FAc) compared to that for **4** (R: Ac) was observed.

2.2. MAG antagonists modified in the 4-position of the Neu5Ac scaffold

As an increased lipophilicity often leads to prolonged residence times,[35] hydrophobic substituents were introduced in the 4-position. Furthermore, we planned to investigate the influence of the configuration at this position on the kinetic binding behavior.

Starting from the Neu5Ac donor **6**,[36] compound **8** was obtained according to published procedures (Scheme 1).[21] After deacetylation under Zemplén conditions (→**9**), the acetonide[37] **10** was formed with the two hydroxy groups in the 7- and 8-position, permitting selective modifications of the 4-position. To obtain the 4-deoxy compound **14**, the 4-hydroxy group in **10** was transformed into the corresponding thiocarbonate **12**, a precursor for a Barton deoxygenation using tributyltin hydride.[38] Cleavage of the aceto-

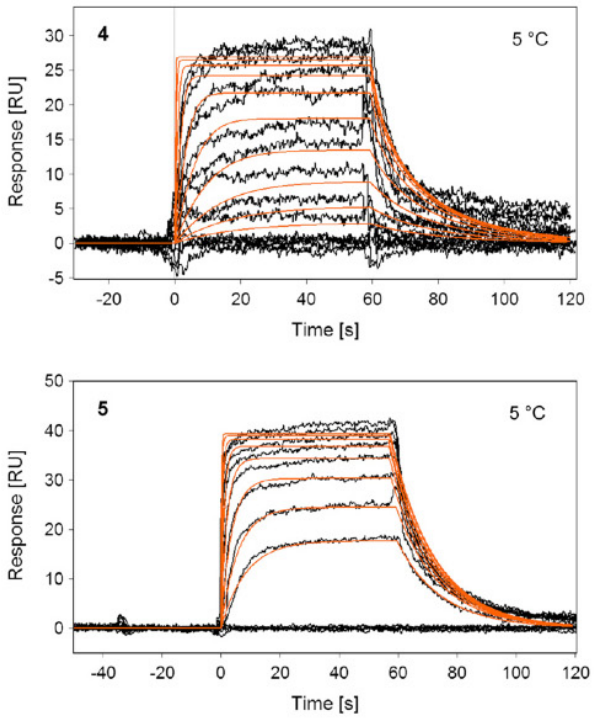

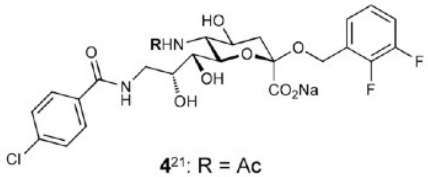

4[21]: R = Ac
5[21]: R = FAc

Compound	k_{on} [$M^{-1}s^{-1}$]	k_{off} [s^{-1}]	$t_{1/2}$ [s]
4 5 °C	$9.4 \cdot 10^4$	0.153	4.5
5 5 °C	$2.75 \cdot 10^5$	0.07	9.9
5 25 °C	$2.8 \cdot 10^5$	0.154	4.5

Figure 3. Kinetic fits of compounds **4** and **5** at 5 C. In the case of **5**, an increase of the dissociation half-life ($t_{1/2}$) by a factor of 2 was observed. For the fitting of the sensorgrams Scrubber 2.0c was applied.

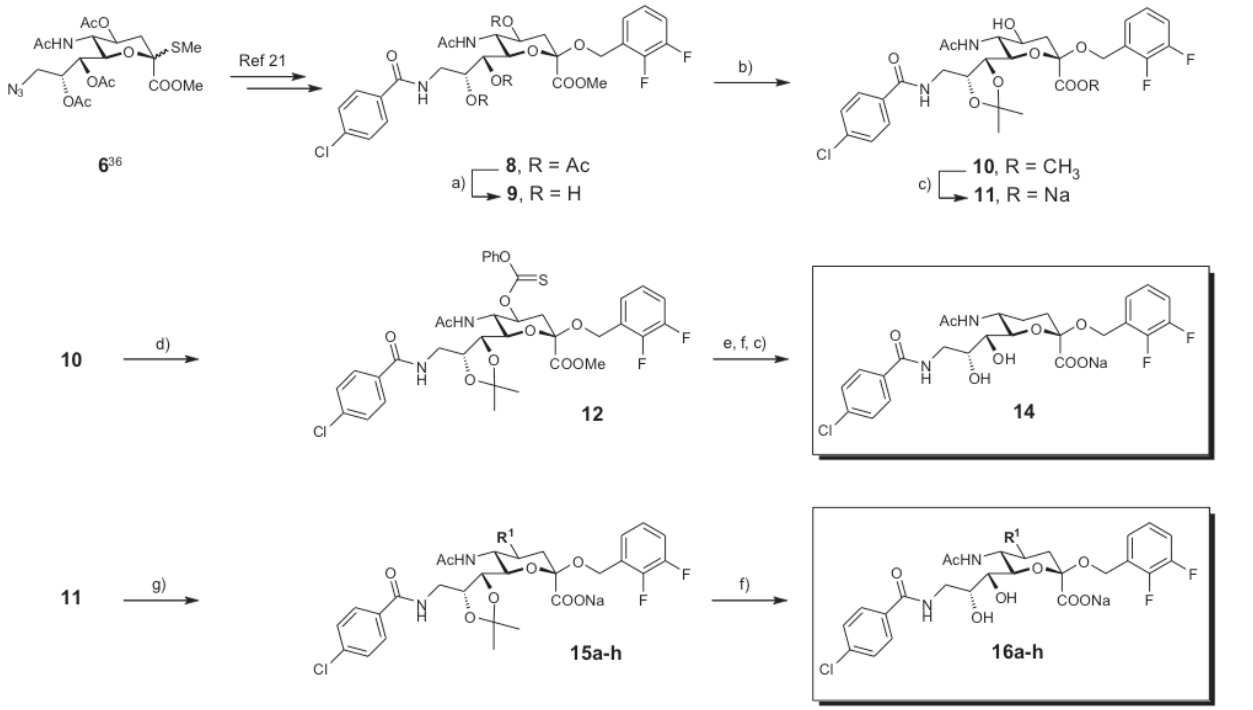

Scheme 1. Reagents and conditions: (a) NaOMe, MeOH (61%); (b) $MeO_2C(CH_3)_2$, PPTS, MeCN (60%); (c) 10% NaOH (aq), MeOH (42%); (d) $C_7H_5ClO_2S$, DCM, pyridine (83%); (e) *n*-Bu_3SnH, AIBN, toluene, 100 °C (→**13**, 20%); (f) 80% AcOH (aq), 60 °C (→**16a–h**, 10–80%); (g) (i) $(R^1O)_2C@O$, DMAP, pyridine (→**15a**, 80%, **15b**, 61%); or (ii) BnBr, KOH (aq, 50%), 18-crown-6, DCM, 60 °C (→**15c**, 60%); or (iii) R^1NCO, DMAP, pyridine (→**15d–h**, 20–37%).

nide under acidic conditions followed by hydrolysis of the methyl ester yielded test compound **14** in excellent overall yield.

Starting from **11**, the hydroxy group in the 4-position was either acylated with the corresponding anhydrides (→**15a**,**b**), the corresponding isocyanides (→**15d–h**), or reacted with benzyl bromide under phase-transfer catalysis conditions (→**15c**). Finally, the acetonide was cleaved under acidic conditions to yield the test compounds **16a–h** (Scheme 1, Table 3).

The 4-disubstituted antagonist **19** was obtained in a two-step procedure (Scheme 2). Oxidation of **10** with pyridinium dichromate under acidic conditions[39] yielded **17**; however, due to the instability of the acetonide only in moderate 30% yield. Various other conditions, for example, using molecular sieves instead of acetic anhydride[40] did not lead to notably improved yields. Then, **17** was reacted with the tetramethylzirconium complex[41] followed by the cleavage of the acetonide to yield **18** with an acceptable stereoselectivity (11% of the *S*-stereoisomer was formed). The zirconium complex was chosen in order to avoid undesired side reactions (e.g., enolization) as reported earlier by Hartmann et al.[42] Final deprotection gave compound **19**.

Test compound **22** was obtained by reduction of **17** with $BH_3{\cdot}NH_3$, yielding the 4-hydroxy compound **20** [(*R*)-stereoisomer] with the inverted configuration at C-4 compared to Neu5Ac.[43] Finally, removal of the acetonide and hydrolysis of the methyl ester gave compound **22**.

2.3. Biological evaluation and kinetic studies

First, the affinity of the test compounds **14**, **16a–h**, **19**, and **22** toward MAG was determined by a surface plasmon resonance based biosensor (Biacore) experiment.[21] Fc-$MAG_{d1\text{-}3}$-Fc[32] was immobilized on a dextran chip containing a surface of covalently bound protein A. A reference cell providing only protein A was used to compensate unspecific binding to the matrix.

Dilution series of the compounds were prepared either in pure HEPES-buffer or in buffer containing 3% DMSO and passed over the flow cells. As reported earlier,[21] negative sensorgrams were obtained (after subtraction of the reference cell). After their mirroring, they could be fitted to a one-to-one binding model using Scrubber 2.0c (Table 4). The kinetic parameters k_{on} and k_{off} were obtained by applying a global fit (Scrubber 2.0c).

Table 3
Substituents R^1 in antagonist **16**

16a	16b	16c	16d	16e	16f	16g	16h
	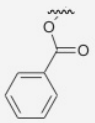	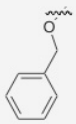	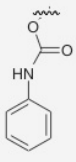	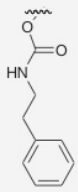	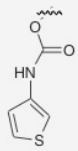	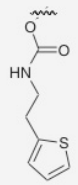	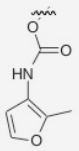

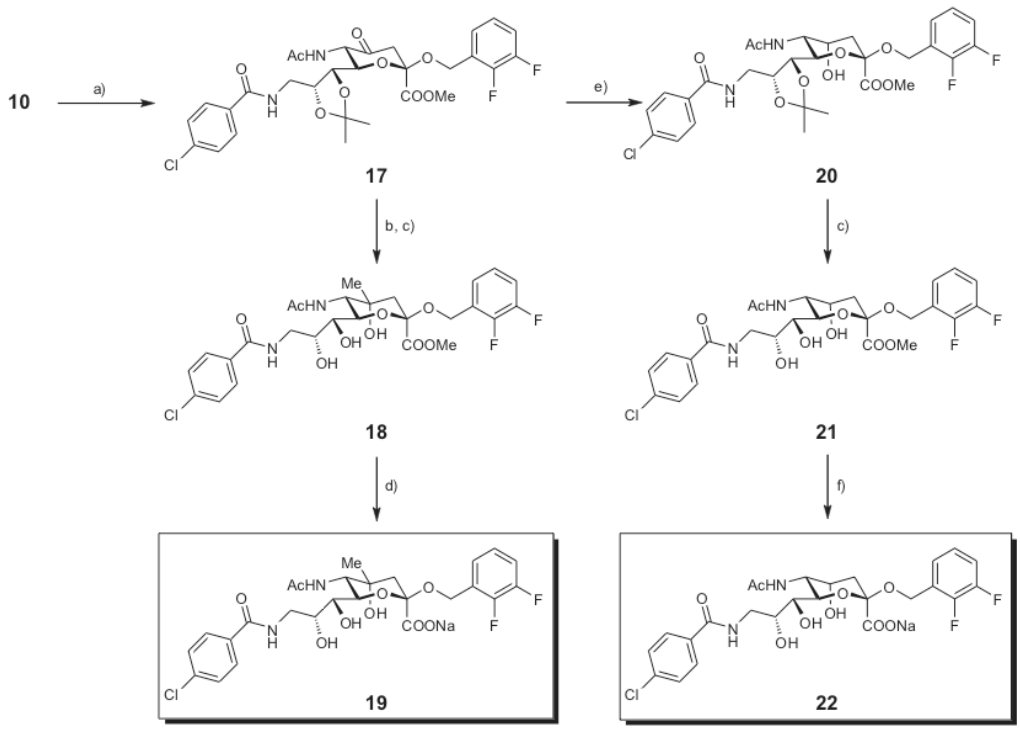

Scheme 2. Reagents and conditions: (a) PDC, Ac_2O, DCM, rt (30%); (b) Me_4Zr, THF, −78 °C, 50% NH_4Cl (aq); (c) 80% AcOH (aq), 60 °C (→**18**, 32 + 11% (*S*)-stereoisomer, two steps; →**21**, 90%); (d) LiOH (aq), THF (34%); (e) $BH_3{\cdot}NH_3$, MeOH, 0 °C (36%); (f) 10% NaOH (aq) (34%).

Table 4
Affinities and kinetic parameters of Neu5Ac derivatives modified in the 4-position

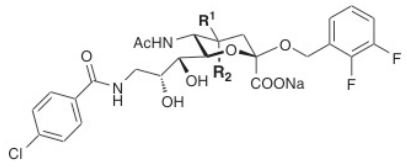

Compd	R^1	R^2	K_D (1M)	k_{on} ($M^{-1}\,s^{-1}$)	k_{off} (s^{-1})	$t_{1/2}$ (s)
4[21]	OH	H	2.0	1.5×10^5	0.54	1.2
14	H	H	11.4	2.8×10^4	0.28	2.5
16a	OAc	H	11.5	4.6×10^4	0.52	1.3
16b	OBz	H	26.0	1.6×10^4	0.41	1.7
16c	OBn	H	2.1	1.6×10^4	0.33	2.1
16d	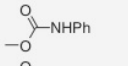	H	257	2.7×10^4	7.00	0.1
16e	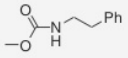	H	114	5.3×10^6	>100	<0.01
16f	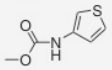	H	15.6	n.d.	n.d.	n.d.
16g	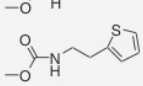	H	n.b.	n.d.	n.d.	n.d.
16h	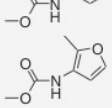	H	49.4	2.2×10^4	1.10	0.6
19	Me	OH	30.0	2.4×10^{-4}	0.53	1.3
22	H	OH	9.0	3.6×10^{-4}	0.33	2.1

n.d., not determined; n.b., not binding.

The deoxy compound **14** showed a decrease in affinity by a factor of six. The inversion of the configuration at the 4-position (→**22**) or the introduction of a methyl group in equatorial position (→**19**) led also to a drop in binding affinity (factor of 4 and 15, respectively). Originally, we assumed based on docking studies to a homology model of MAG[30] that the hydroxy group in the 4-position is not directed toward the protein and can therefore be modified. Our results, however, suggest that the equatorial 4-hydroxy contributes to binding, maybe by hydrogen bonding, as the change of the configuration at C-4 also leads to a decreased affinity. Furthermore, a steric clash of the methyl group in **19** could be responsible for a further reduction of affinity.

In case of antagonists **16a**,**b** and **16d**–**h**, a pronounced drop in the binding affinity or even a complete abolishment of binding was observed. In contrast, **16c** showed the same binding affinity as reference compound **4**. The loss in potency for **16a**,**b** and **16d**–**h** is probably the consequence of the rigid geometry of ester and carbamate substituents, leading to a steric clash with the protein, whereas the benzyl ether in **16c** seems to adapt a favorable spatial arrangement compensating the impact of the 4-hydroxy to binding affinity.

Beside the decreased binding affinity, no substantial improvement of the kinetic properties could be achieved. All compounds showed fast dissociation rate constants, leading to residence times in the range of seconds (Table 4). Despite the increased lipophilicity, even **16c** does not show an extended dissociation half-life.

3. Conclusion

A small library of MAG antagonists modified in the 4-position of the Neu5Ac scaffold was synthesized with the goal to improve the half-life of the antagonist-MAG complex. Although all modifica-

tions in the 4-position were not successful, the investigation of modifications in the 5-position led to a reduction of the dissociation rate constant k_{off}, although only by a factor of 2. In conclusion, the prolongation of the residence time remains a challenge and will be a critical issue in further studies on the kinetic properties of glycomimetics.

4. Experimental

4.1. General methods

NMR spectra were recorded on a Bruker Avance DMX-500 (500 MHz) spectrometer. Assignment of ^{1}H and ^{13}C NMR spectra was achieved using 2D methods (COSY, HSQC, TOCSY, ROESY, and NOESY). Chemical shifts are expressed in ppm using residual $CHCl_3$, CHD_2OD, CHD_2CN, and HDO as references. Optical rotations were measured using Perkin–Elmer Polarimeters 241 and 341. MS analyses were carried out using a Waters Micromass ZQ Detector system. The spectra were recorded in positive or negative ESI mode. Reactions were monitored by TLC using glass plates coated with Silica Gel 60 F_{254} (Merck) and visualized by using UV light and/or by charring with a molybdate solution (a 0.02 M solution of ammonium cerium sulfate dihydrate and ammonium molybdate tetrahydrate in aq 10% H_2SO_4). Column chromatography was performed on silica gel (Fluka, 40–60 mesh). MeOH was dried by heating at reflux with sodium methoxide and distilled immediately before use. Pyridine was freshly distilled under argon over CaH_2. Dichloromethane (DCM), dichloroethane (DCE), acetonitrile (MeCN), toluene, and benzene were dried by filtration over Al_2O_3 (Fluka, type 5016 A basic). Molecular sieves (3 or 4 Å) were activated in vacuo at 500 °C for 2 h immediately before use. Compounds **6**–**8** were prepared according to a published procedure.[21,36]

4.2. Synthesis and characterization of compounds 9–22

4.2.1. Methyl [(2,3-difluorobenzyl) 5-acetamido-9-(4-chlorobenzamido)-3,5,9-trideoxy-D-*glycero*-α-D-*galacto*-2-nonulopyranosid]onate (9)

Compound **8**[21] (217 mg, 42.0 mmol) was dissolved in dry MeOH (8.0 mL) and treated with methanolic NaOMe (1 M, 1.0 mL) for 2 h. The reaction mixture was neutralized with Amberlyst 15, filtered over a pad of Celite, and the Celite was washed thoroughly with MeOH. The solvent was evaporated under reduced pressure and the crude product was purified by chromatography on silica gel (1% gradient of MeOH in DCM) to yield **9** (90.0 mg, 61%) as a white foam. ^{1}H NMR (500 MHz, CD_3OD) δ 1.80 (t, J = 12.3 Hz, 1H, H-3a), 1.97 (s, 3H, NHAc), 2.72 (dd, J = 4.5, 12.8 Hz, 1H, H-3b), 3.45 (d, J = 8.8 Hz, 1H, H-7), 3.55 (dd, J = 7.3, 13.8 Hz, 1H, H-9a), 3.61–3.74 (m, 2H, H-4, H-6), 3.75–3.90 (m, 5H, OMe, H-5, H-9), 4.04 (td, J = 3.2, 8.8 Hz, 1H, H-8), 4.68, 4.86 (A, B of AB, J = 12.1 Hz, 2H, CH_2Ar), 7.06–7.24 (m, 3H, CH_{ar}), 7.46, 7.82 (AA′, BB′ of AA′BB′, J = 8.4 Hz, 4H, CH_{ar}); ^{13}C NMR (126 MHz, CD_3OD): δ 22.7 (NHAc), 41.6 (C-3), 45.1 (C-9), 53.4 (OMe), 53.8 (C-5), 68.5 (C-4), 70.8 (C-8), 72.1 (C-7), 74.9 (C-6), 117.8, 125.4, 126.4, 128.0, 129.7, 130.1, 131.3, 133.0, 134.4, 138 (12C, C-Ar), 169.6, 170.6, 175.0 (3CO). ESI-MS calcd for $C_{26}H_{29}ClF_2N_2O_9$ $[M+Na]^+$: 609.14; found m/z 609.19.

4.2.2. Methyl [(2,3-difluorobenzyl) 5-acetamido-9-(4-chlorobenzamido)-3,5,9-trideoxy-7,8-*O*-isopropylidene-D-*glycero*-α-D-*galacto*-2-nonulopyranosid]onate (10)

Compound **9** (20.0 mg, 30 μmol) was dissolved in dry MeCN (250 μL) and 2,2-dimethoxypropane (17 μL, 0.12 mmol) was added. After cooling to 0 °C PPTS (3.0 mg, 10 μmol) was added. The reaction mixture was stirred at rt overnight. After completion of the reaction, IRA-93 was added and stirring was continued for 30 min. After filtration, the solvent was evaporated and the pure product **10** (13 mg, 60%) was obtained by chromatography on silica gel (1% gradient of MeOH in DCM). ^{1}H NMR (500 MHz, CD_3OD): δ 1.33, 1.51 (2s, 6H, 2 C(CH_3)$_2$), 1.75 (t, J = 12.4 Hz, 1H, H-3a), 1.99 (s, 3H, NHAc), 2.67 (dd, J = 4.3, 12.6 Hz, 1H, H-3b), 3.56–3.65 (m, 1H, H-4), 3.83 (s, 3H, OMe), 3.86–4.00 (m, 3H, H-5, H-6, H-9a), 4.03 (dd, J = 3.1, 14.1 Hz, 1H, H-9b), 4.26 (d, J = 6.8 Hz, 1H, H-7), 4.48 (ddd, J = 3.3, 7.1, 8.7 Hz, 1H, H-8), 4.56–4.69 (m, 1H, CH_2Ar), 4.96 (B of AB, J = 11.6 Hz, 1H, CH_2Ar), 7.09–7.27 (m, 4H, NH, CH_{ar}), 7.46, 7.83 (AA′, BB′ of AA′BB′, J = 8.6 Hz, 4H, CH_{ar}); ^{13}C NMR (126 MHz, CD_3OD): δ 23.0 (NHAc), 25.8, 27.1 (C(CH_3)$_2$), 41.6, 41.8 (2C, C-3, C-9), 53.2 (OMe), 54.3 (C-5), 61.0 (CH_2Ar), 68.4 (C-4), 74.3 (C-6), 75.8 (C-7), 77.7 (C-8), 100.5 (C-2), 110.2 (C(CH_3)$_2$), 117.9, 118.0, 125.4, 126.7, 129.7, 130.1, 130.2, 134.3, 138.7 (12C, C-Ar), 169.3, 170.4, 173.9 (3CO). ESI-MS calcd for $C_{29}H_{33}ClF_2N_2O_9$ $[M+Na]^+$: 649.18; found m/z 649.15.

4.2.3. Sodium [(2,3-difluorobenzyl) 5-acetamido-9-(4-chlorobenzamido)-3,5,9-trideoxy-7,8-*O*-isopropylidene-D-*glycero*-α-D-*galacto*-2-nonulopyranosid]onate (11)

Compound **10** (20.0 mg, 30 μmol) was dissolved in MeOH (2 mL) and 10% aq NaOH (0.1 mL) was added. After 2 h, the solution was neutralized with 7% aq HCl. Then the solvent was evaporated and the pure product **11** (13 mg, 42%) was obtained by chromatography on RP-8 (10% of MeOH in water). $[\alpha]_D^{20}$ −33.4 (c 0.37, MeOH); ^{1}H NMR (500 MHz, CD_3OD): δ 1.27, 1.41 (2s, 6H, 2 (CH_3)$_2$), 1.65 (t, J = 12.0 Hz, 1H, H-3a), 1.92 (s, 3H, NHAc), 2.75 (dd, J = 4.3, 12.0 Hz, 1H, H-3b), 3.57 (ddd, J = 4.3, 10.3, 12.0 Hz, 1H, H-4), 3.82–3.99 (m, 3H, H-5, H-9a, H-9b), 4.11 (d, J = 10.3 Hz, 1H, H-6), 4.18 (d, J = 6.8 Hz, 1H, H-7), 4.35 (dd, J = 7.1, 12.5 Hz, 1H, H-8), 4.61, 4.89 (A, B of AB, J = 10.6 Hz, 2H, CH_2Ar), 7.00–7.16 (m, 2H, CH_{ar}), 7.30 (t, J = 6.8 Hz, 1H, CH_{ar}), 7.40, 7.91 (AA′, BB′ of AA′BB′, J = 8.6 Hz, 4H, CH_{ar}); ^{13}C NMR (126 MHz, CD_3OD): δ 22.9 (NHAc), 25.4, 27.4 (C(CH_3)$_2$), 41.9, 42.1 (2C, C-3, C-9), 54.7 (C-5), 60.3 (CH_2Ar), 69.75 (C-4), 73.1 (C-6), 75.8 (C-7), 76.5 (C-8), 102.8 (C-2), 109.3 (C(CH_3)$_2$), 117.0, 117.1, 125.2, 126.5, 129.6, 130.6, 134.1, 138.6 (12C, C-Ar), 169.5, 173.9, 174.4 (3CO). ESI-MS calcd for $C_{28}H_{30}ClF_2N_2NaO_9$ $[M+H]^+$: 634.15; found m/z 635.16.

4.2.4. Methyl [(2,3-difluorobenzyl) 5-acetamido-9-(4-chlorobenzamido)-3,5,9-trideoxy-7,8-*O*-isopropylidene-4-*O*-(phenoxycarbonothioyl)-D-*glycero*-α-D-*galacto*-2-nonulopyranosid]onate (12)

Compound **10** (96 mg, 0.15 mmol) was dissolved in dry pyridine/DCM (2/1; 1.5 mL). After cooling to 0 °C phenyl chlorothioformate (162 μL, 1.20 mmol) was added dropwise. Stirring was continued for 2 h at rt and then MeOH (2 mL) was added. After evaporation of the solvents, the residue was dissolved in DCM (5 mL) and washed with 0.5 M aq $CuSO_4$ (1 mL) and water (1 mL). The organic layer was dried over Na_2SO_4, filtered, and concentrated. The crude product was purified by chromatography on silica gel (1% gradient of MeOH in DCM) to yield **12** (14 mg, 83%). ^{1}H NMR (500 MHz, CD_3OD): δ 1.37, 1.54 (2s, 6H, C(CH_3)$_2$), 1.97–2.00 (m, 4H, NHAc, H-3a), 3.01 (dd, J = 4.6, 12.3 Hz, 1H, H-3b), 3.87 (s, 3H, OMe), 3.96–4.02 (m, 1H, H-9a), 4.05 (dd, J = 3.2, 14.2 Hz, 1H, H-9b), 4.15 (d, J = 10.3 Hz, 1H, H-6), 4.27–4.37 (m, 2H, H-5, H-7), 4.53 (td, J = 3.4, 8.6 Hz, 1H, H-8), 4.66, 5.02 (A, B of AB, J = 11.5 Hz, 2H, CH_2Ar), 5.59 (td, J = 4.6, 12.0 Hz, 1H, H-4), 7.07 (d, J = 8.3 Hz, 2H, CH_{ar}), 7.13–7.18 (m, 1H, CH_{ar}), 7.21–7.27 (m, 2H, CH_{ar}), 7.30 (t, J = 7.4 Hz, 1H, CH_{ar}), 7.43 (t, J = 7.9 Hz, 2H, CH_{ar}), 7.48, 7.84 (AA′, BB′ of AA′BB′, J = 8.6 Hz, 4H, CH_{ar}); ^{13}C NMR (126 MHz, CD_3OD): δ 23.0 (NHAc), 25.8, 27.0 (C(CH_3)$_2$), 37.9 (C-3), 41.7 (C-9), 51.3 (C-5), 53.4 (OMe), 61.3 (CH_2Ar), 73.9 (C-6), 75.5 (C-7), 77.7 (C-8), 80.1 (C-4), 100.1 (C-2), 110.4 (C(CH_3)$_2$), 118.0, 122.1, 122.9, 125.5, 126.8, 126.9, 127.3, 127.7, 129.7,

130.1, 130.6, 134.2, 138.8, 152.6, 154.6, 154.9 (18C, C-Ar), 169.3, 169.8, 173.5 (3CO), 196.0 (CS). ESI-MS calcd for $C_{36}H_{37}ClF_2N_2O_{10}S$ $[M+Na]^+$: 785.17; found *m*/*z* 785.27.

4.2.5. Methyl [(2,3-difluorobenzyl) 5-acetamido-9-(4-chlorobenzamido)-3,4,5,9-tetradeoxy-7,8-*O*-isopropylidene-D-*glycero*-α-D-*galacto*-2-nonulopyranosid]onate (13)

Compound **12** (96 mg, 0.13 mmol) was dissolved in dry toluene (4 mL). After the sequential addition of freshly distilled *n*-Bu_3SnH (340 μL, 1.3 mmol) and AIBN (29 mg, 0.18 mmol), the reaction mixture was stirred at 100 °C for 1 h. After evaporation of the solvent, the crude product was purified by chromatography on silica gel (1% gradient MeOH in DCM) to yield **13** (15.3 mg, 20%) as a white foam. ^{1}H NMR (500 MHz, CD_3OD): δ 1.33 (s, 3H, CH_3), 1.35–1.42 (m, 1H, H-4a), 1.51 (s, 3H, CH_3), 1.81 (td, J = 4.0, 13.8 Hz, 1H, H-3a), 1.94 (s, 3H, NHAc), 2.00–2.07 (m, 1H, H-4b), 2.37 (dt, J = 3.4, 13.1 Hz, 1H, H-3b), 3.81 (s, 3H, OMe), 3.92–4.02 (m, 2H, H-9a, H-9b), 4.02–4.08 (m, 2H, H-5, H-6), 4.26 (d, J = 7.6 Hz, 1H, H-7), 4.48 (ddd, J = 3.3, 7.0, 8.6 Hz, 1H, H-8), 4.56, 4.96 (A, B of AB, J = 11.6 Hz, 2H, CH_2Ar), 7.10–7.20 (m, 3H, CH_{ar}), 7.46, 7.83 (AA′, BB′ of AA′BB′, J = 8.7 Hz, 4H, CH_{ar}); ^{13}C NMR (126 MHz, CD_3OD): δ 22.8 (NHAc), 25.8, 27.1 (C(CH_3)$_2$), 27.5 (C-4), 32.8 (C-3), 41.7 (C-9), 46.2 (C-5), 53.0 (OMe), 61.0 (CH_2Ar), 75.9, 76.4, 77.7 (C-6, C-7, C-8), 100.9 (C-2), 110.2 (C(CH_3)$_2$), 117.8, 125.4, 126.7, 129.7, 130.1, 134.3, 138.7 (12C, C-Ar), 169.3, 170.8, 172.9 (3CO). ESI-MS calcd for $C_{29}H_{33}ClF_2N_2O_8$ $[M+Na]^+$: 633.18; found *m*/*z* 633.12.

4.2.6. Sodium [(2,3-difluorobenzyl) 5-acetamido-9-(4-chlorobenzamido)-3,4,5,9-tetradeoxy-D-*glycero*-α-D-*galacto*-2-nonulopyranosid]onate (14)

Compound **13** (15.0 mg, 20 μmol) was dissolved in 80% aq AcOH (2.5 mL) and heated for 3 h at 60 °C. After TLC showed completion of the reaction, the reaction mixture was cooled to rt. The pH was set to 10 by addition of 10% aq NaOH. Stirring was continued for 4 h and then the reaction mixture was neutralized with 7% aq HCl. After evaporation of the solvents, the crude product was purified by chromatography on RP-8 (5% gradient of MeOH in water) to yield **14** (4.5 mg, 34%) as a white solid. $[\alpha]_D^{20}$ −29.7 (*c* 0.13, MeOH); ^{1}H NMR (500 MHz, D_2O): δ 1.47 (q, J = 11.2 Hz, 1H, H-4a), 1.68 (td, J = 3.7, 13.3 Hz, 1H, H-3a), 1.94 (s, 3H, NHAc), 2.00–2.09 (m, 1H, H-4b), 2.35–2.47 (m, 1H, H-3b), 3.40–3.58 (m, 2H, H-7, H-9a), 3.70–3.81 (m, 3H, H-6, H-8, H-9b), 3.87 (td, J = 4.0, 11.1 Hz, 1H, H-5), 4.61, 4.79 (A, B of AB, J = 11.8 Hz, 2H, CH_2Ar), 7.00–7.27 (m, 3H, CH_{ar}), 7.53, 7.75 (AA′, BB′ of AA′BB′, J = 8.5 Hz, 4H, CH_{ar}); ^{13}C NMR (126 MHz, D_2O): δ 21.8 (C-4), 26.9 (NHAc), 31.7 (C-3), 44.5 (C-9), 51.7 (C-5), 60.5 (CH_2Ar), 68.2, 70.1 (C-7, C-8), 75.8 (C-6), 99.3 (C-2), 117.0, 124.3, 125.8, 126.5, 128.7, 128.8, 132.1, 137.5 (12C, C-Ar), 174.2, 186.3 (3C, 3CO). HRMS calcd for $C_{25}H_{26}ClF_2N_2NaO_{11}$ $[M]^+$: 601.1141; found *m*/*z* 601.1154.

4.2.7. Sodium [(2,3-difluorobenzyl) 5-acetamido-4-*O*-acetyl-9-(4-chlorobenzamido)-3,5,9-trideoxy-7,8-*O*-isopropylidene-D-*glycero*-α-D-*galacto*-2-nonulopyranosid]onate (15a)

Compound **11** (13.2 mg, 20 μmol) was dissolved in dry pyridine (0.5 mL). After cooling to 0 °C, acetic anhydride (0.25 mL, 2.64 mmol) and DMAP (1.0 mg, 8.0 μmol) were added. The reaction mixture was allowed to reach rt and stirring was continued for 24 h. After completion of the reaction, the solvent was removed by co-evaporation with toluene. Then DCM (5 mL) was added and the organic layer was washed with 0.5 M aq $CuSO_4$ (2 mL), satd aq $NaHCO_3$ (3 × 2 mL), and H_2O (2 mL). Finally, the crude product was purified by chromatography on silica gel (10% gradient MeOH in DCM) to yield **15a** (11.2 mg, 80%). ^{1}H NMR (500 MHz, CD_3OD): δ 1.29, 1.43 (2s, 6H, C(CH_3)$_2$), 1.70 (t, J = 11.5 Hz, 1H, H-3a), 1.86 (s, 3H, NHAc), 1.93 (s, 3H, OAc), 2.75 (dd, J = 4.5, 11.5 Hz, 1H, H-3b), 3.86–4.07 (m, 2H, H-5, H-9a), 4.15 (dd, J = 4.0, 14.5 Hz, 1H, H-9b), 4.20–4.28 (m, 2H, H-6, H-7), 4.39–4.46 (m, 1H, H-8), 4.63, 4.93 (A, B of AB, J = 11.9 Hz, 2H, CH_2Ar), 5.05–5.17 (m, 1H, H-4), 7.00–7.14 (m, 2H, CH_{ar}), 7.16–7.27 (m, 1H, CH_{ar}), 7.37, 7.84 (AA′, BB′ of AA′BB′, J = 7.9 Hz, 4H, CH_{ar}); ^{13}C NMR (126 MHz, CD_3OD): δ 20.9 (OAc), 22.9 (NHAc), 25.8, 27.2 (C(CH_3)$_2$), 39.2, 40.2 (C-3, C-9), 52.4 (C-5), 60.4 (CH_2Ar), 71.5, 72.7, 75.8, 76.9 (C-4, C-6, C-7, C-8), 101.3 (C-2), 110.1 (C(CH_3)$_2$), 117.2, 117.3, 125.3, 126.4, 129.6, 130.5, 138.9, 140.1 (12C, C-Ar), 170.6, 172.3, 173.5, 177.9 (4CO). ESI-MS calcd for $C_{30}H_{32}ClF_2N_2NaO_{10}$ $[M+H]^+$: 677.16; found *m*/*z* 677.21.

4.2.8. Sodium [(2,3-difluorobenzyl) 5-acetamido-4-*O*-benzoyl-9-(4-chlorobenzamido)-3,5,9-trideoxy-7,8-*O*-isopropylidene-D-*glycero*-α-D-*galacto*-2-nonulopyranosid]onate (15b)

Compound **11** (10.0 mg, 20 μmol) was dissolved in dry pyridine (0.5 mL) at rt. After cooling to 0 °C, benzoic anhydride (100 mg, 0.44 mmol) and DMAP (1.0 mg, 8.0 μmol) were added. The reaction mixture was allowed to reach rt and stirring was continued for 24 h. After completion of the reaction, the solvent was removed by co-evaporation with toluene. Then DCM (5 mL) was added and the organic layer was washed with 0.5 M aq $CuSO_4$ (2 mL), satd aq $NaHCO_3$ (3 × 2 mL), and H_2O (2 mL). Finally, the crude product was purified by chromatography on silica gel (10% gradient of MeOH in DCM) to yield **15b** (7.1 mg, 61%). ^{1}H NMR (500 MHz, CD_3OD): δ 1.31, 1.47 (2s, 6H, C(CH_3)$_2$), 1.76 (s, 3H, NHAc), 1.82–1.96 (m, 1H, H-3a), 2.93 (dd, J = 4.2, 11.8 Hz, 1H, H-3b), 3.97 (dd, J = 6.0, 13.4 Hz, 1H, H-9a), 4.10–4.20 (m, 1H, H-9b), 4.25 (d, J = 6.5 Hz, 1H, H-7), 4.27–4.37 (m, 2H, H-5, H-6), 4.46 (dd, J = 6.1, 12.4 Hz, 1H, H-8), 4.67, 4.98 (A, B of AB, J = 11.7 Hz, 2H, CH_2Ar), 5.23–5.40 (m, 1H, H-4), 6.98–7.15 (m, 2H, CH_{ar}), 7.27 (t, J = 6.5 Hz, 1H, CH_{ar}), 7.42 (d, J = 7.9 Hz, 2H, CH_{ar}), 7.48 (t, J = 7.4 Hz, 2H, CH_{ar}), 7.55 (t, J = 7.5 Hz, 1H, CH_{ar}), 7.88 (d, J = 8.3 Hz, 2H, CH_{ar}), 7.92 (d, J = 7.5 Hz, 2H, CH_{ar}); ^{13}C NMR (126 MHz, CD_3OD): δ 22.8 (NHAc), 25.7, 27.3 (C(CH_3)$_2$), 30.8 (C-3), 39.3 (C-9), 42.3 (C-5), 52.0 (CH_2Ar), 72.6, 72.9, 75.9, 76.8 (C-4, C-6, C-7, C-8), 110.0 (C-2), 111.4 (C(CH_3)$_2$), 117.3, 129.1, 129.5, 129.6, 130.5, 130.6, 130.7, 131.2, 133.0, 134.3, 135.1 (18C, C-Ar), 172.0 (4C, 4CO). ESI-MS calcd for $C_{35}H_{34}ClF_2N_2NaO_{10}$ $[M+Na]^+$: 739.18; found *m*/*z* 739.27.

4.2.9. Sodium [(2,3-difluorobenzyl) 5-acetamido-4-*O*-benzyl-9-(4-chlorobenzamido)-3,5,9-trideoxy-7,8-*O*-isopropylidene-D-*glycero*-α-D-*galacto*-2-nonulopyranosid]onate (15c)

Compound **11** (10 mg, 20 μmol) was dissolved in DCM/50% aq KOH (1/3, 0.5/1.5 mL). After adding 18-crown-6 (1.0 mg) and benzyl bromide (60 μL, 0.5 mmol), the reaction mixture was heated to 60 °C and stirring was continued for 18 h. The solvents were removed under reduced pressure and the crude product was purified by chromatography on silica gel (10% gradient of MeOH in DCM) to yield **15c** (6.8 mg, 60%). ^{1}H NMR (500 MHz, CD_3OD): δ 1.32, 1.47 (2s, 6H, C(CH_3)$_2$), 1.64–1.78 (m, 1H, H-3a), 1.94 (s, 3H, NHAc), 3.02 (dd, J = 4.0, 12.0 Hz, 1H, H-3b), 3.56–3.64 (m, 1H, H-4), 3.97 (dd, J = 6.1, 13.3 Hz, 1H, H-9a), 4.00–4.11 (m, 2H, H-5, H-9b), 4.22 (d, J = 10.5 Hz, 1H, H-6), 4.27 (d, J = 6.7 Hz, 1H, H-7), 4.44 (dd, J = 6.4, 12.8 Hz, 1H, H-8), 4.49 (A of AB, J = 12.0 Hz, 1H, CH_2Ar), 4.69 (A′, B′ of A′B′, J = 11.9 Hz, 2H, CH_2Ar), 4.99 (B of AB, J = 11.8 Hz, 1H, CH_2Ar), 7.08–7.19 (m, 3H, CH_{ar}), 7.22–7.28 (m, 5H, CH_{ar}), 7.46, 7.92 (AA′, BB′ of AA′BB′, J = 8.4 Hz, 4H, CH_{ar}); ^{13}C NMR (126 MHz, CD_3OD): δ 21.5 (NHAc), 24.1, 25.8 (C(CH_3)$_2$), 37.8 (C-3), 40.5 (C-9), 51.7 (C-5), 58.8 (CH_2Ar), 70.2 (C-6), 71.7 (CH_2Ar), 74.4 (C-4), 75.3, 75.4 (C-7, C-8), 100.7 (C-2), 108.1 (C(CH_3)$_2$), 115.6, 115.7, 123.8, 124.9, 127.0, 127.1, 127.8, 128.1, 128.9, 129.0, 132.6, 137.1, 138.6 (18C, C-Ar), 167.8, 171.9, 173.4 (3CO). ESI-MS calcd for $C_{35}H_{36}ClF_2N_2NaO_9$ $[M-H]^-$: 701.21; found *m*/*z* 701.52.

4.2.10. Sodium [(2,3-difluorobenzyl) 5-acetamido-9-(4-chlorobenzamido)-3,5,9-trideoxy-7,8-*O*-isopropylidene-4-*O*-phenylcarbamoyl-D-*glycero*-α-D-*galacto*-2-nonulopyranosid]onate (15d)

Compound **11** (30.0 mg, 50 μmol) was dissolved in dry pyridine (1.0 mL). Phenyl isocyanate (24 μL, 0.24 mmol) and DMAP (1.0 mg, 8.0 μmol) were added. The reaction mixture was stirred for 24 h and then water (0.1 mL) was added. After removal of the solvents under reduced pressure, the crude product was purified by chromatography on silica gel (10% gradient of MeOH in DCM) to yield **15d** (10 mg, 29%). ^{1}H NMR (500 MHz, CD_3OD): δ 1.25, 1.38 (2s, 6H, C(CH_3)$_2$), 1.85–1.92 (m, 4H, NHAc, H-3a), 2.76 (dd, J = 4.8, 13.0 Hz, 1H, H-3b), 3.50–3.64 (m, 1H, H-9a), 3.79–3.94 (m, 1H, H-9b), 4.10 (d, J = 10.4 Hz, 1H, H-7), 4.28–4.35 (m, 3H, H-5, H-6, H-8), 4.58, 4.70 (A, B of AB, J = 11.9 Hz, 2H, CH_2Ar), 5.21 (td, J = 4.7, 11.0 Hz, 1H, H-4), 6.96 (t, J = 7.3 Hz, 1H, CH_{ar}), 7.00–7.13 (m, 2H, CH_{ar}), 7.21 (dd, J = 7.7, 8.3 Hz, 2H, CH_{ar}), 7.23–7.28 (m, 1H, CH_{ar}), 7.31 (AA′ of AA′BB′, J = 8.6 Hz, 2H, CH_{ar}), 7.35 (d, J = 8.0 Hz, 2H, CH_{ar}), 7.84 (BB′ of AA′BB′, J = 8.6 Hz, 2H, CH_{ar}); ^{13}C NMR (126 MHz, CD_3OD): δ 22.9 (NHAc), 25.5, 27.6 (C(CH_3)$_2$), 38.3 (C-3), 42.5 (C-9), 52.1 (C-5), 60.7 (CH_2Ar), 70.9, 71.6 (C-4, C-7), 76.1, 76.8 (C-6, C-8), 101.8 (C-2), 109.3 (C(CH_3)$_2$), 117.5, 119.7, 124.0, 125.6, 126.0, 128.6, 128.7, 129.4, 129.5, 129.8, 130.6, 134.0, 138.6, 140.1, 150.4, 150.5, 152.4 (18C, C-Ar), 155.1 (NC(O)O), 169.4, 173.7, 173.9 (3CO). ESI-MS calcd for $C_{35}H_{35}ClF_2N_3O_{10}$ [M−H]$^-$: 730.20; found m/z 730.33.

4.2.11. Sodium [(2,3-difluorobenzyl) 5-acetamido-9-(4-chlorobenzamido)-3,5,9-trideoxy-7,8-*O*-isopropylidene-4-*O*-phenylethylcarbamoyl-D-*glycero*-α-D-*galacto*-2-nonulopyranosid]onate (15e)

Compound **11** (30.0 mg, 50 μmol) was dissolved in dry pyridine (1.5 mL). Phenylethyl isocyanate (50 μL, 0.42 mmol), DMAP (3.0 mg, 24.0 μmol), and NEt_3 (20 μL) were added. The reaction mixture was stirred at 60 °C for 24 h and then water (0.2 mL) was added. After removal of the solvents under reduced pressure, the crude product was purified by chromatography on silica gel (10% gradient of MeOH in DCM) to yield **15e** (7.3 mg, 20%). ^{1}H NMR (500 MHz, CD_3OD): δ 1.30, 1.35 (2s, 6H, $(CH_3)_2$), 1.79 (t, J = 12.3 Hz, 1H, H-3a), 1.88 (s, 3H, NHAc), 2.61–2.78 (m, 3H, H-3b, CH_2), 3.18–3.26 (m, 2H, CH_2), 3.53–3.70 (m, 1H, H-9a), 3.87 (d, J = 12.1 Hz, 1H, H-9b), 4.07 (d, J = 10.6 Hz, 1H, H-7), 4.18–4.26 (m, 2H, H-5, H-6), 4.27–4.36 (m, 1H, H-8), 4.56, 4.69 (A, B of AB, J = 11.6 Hz, 2H, CH_2Ar), 5.08 (td, J = 4.8, 11.0 Hz, 1H, H-4), 7.01–7.09 (m, 2H, CH_{ar}), 7.14 (d, J = 7.5 Hz, 4H, CH_{ar}), 7.19–7.27 (m, 2H, CH_{ar}), 7.31, 7.83 (AA′, BB′ of AA′BB′, J = 8.5 Hz, 4H, CH_{ar}); ^{13}C NMR (CD_3OD) δ 23.1 (NHAc), 25.8, 27.7 (C(CH_3)$_2$), 36.8 (CH_2), 38.4 (C-3), 42.6 (C-9), 43.4 (CH_2), 52.1 (C-5), 60.7 (CH_2Ar), 70.9 (C-7), 71.5 (C-4), 75.7 (C-6), 76.8 (C-8), 101.7 (C-2), 109.2 (C(CH_3)$_2$), 117.4, 125.5, 125.2, 126.0, 127.4, 128.7, 129.5, 129.9, 130.0, 130.4, 130.6, 134.1, 140.5, 150.5 (18C, C-Ar), 158.2 (COONH), 169.4, 173.5, 173.6 (3CO). ESI-MS calcd for $C_{37}H_{39}ClF_2N_3O_{10}$ [M−H]$^-$: 758.23; found m/z 758.37.

4.2.12. Sodium [(2,3-difluorobenzyl) 5-acetamido-9-(4-chlorobenzamido)-3,5,9-trideoxy-7,8-*O*-isopropylidene-4-*O*-(3-thienylcarbamoyl)-D-*glycero*-α-D-*galacto*-2-nonulopyranosid]onate (15f)

Compound **11** (20.0 mg, 30 μmol) was dissolved in dry pyridine (0.5 mL). 3-Thienyl isocyanate (12 μL, 0.1 mmol) and DMAP (1.0 mg, 8.0 μmol) were added. The reaction mixture was stirred for 24 h and then water (0.1 mL) was added. After removal of the solvents under reduced pressure, the crude product was purified by chromatography on silica gel (10% gradient of MeOH in DCM) to yield **15f** (8.0 mg, 35%). ^{1}H NMR (500 MHz, CD_3OD): δ 1.25, 1.38 (2s, 6H, C(CH_3)$_2$), 1.87–1.90 (m, 4H, H-3a, NHAc), 2.76 (dd, J = 4.3, 12.8 Hz, 1H, H-3b), 3.48–3.63 (m, 1H, H-9a), 3.81–3.94 (m, 1H, H-9b), 4.10 (d, J = 10.4 Hz, 1H, H-7), 4.27–4.36 (m, 3H, H-5, H-6, H-8), 4.58, 4.70 (A, B of AB, J = 11.6 Hz, 2H, CH_2Ar), 5.15–5.29 (m, 1H, H-4), 6.93 (d, J = 5.4 Hz, 1H, CH_{ar}), 7.02–7.08 (m, 1H, CH_{ar}), 7.09–7.19 (m, 2H, CH_{ar}), 7.20–7.25 (m, 2H, CH_{ar}), 7.31 (AA′, BB′ of AA′BB′, J = 8.5 Hz, 4H, CH_{ar}); ^{13}C NMR (126 MHz, CD_3OD): δ 22.8 (NHAc), 25.5, 27.7 (C(CH_3)$_2$), 38.3 (C-3), 42.5 (C-9), 52.1 (C-5), 60.7 (CH_2Ar), 70.9, 71.8 (C-4, C-7), 76.1, 76.8 (C-6, C-8), 101.8 (C-2), 108.1 (C(CH_3)$_2$), 109.3, 117.5, 117.6, 121.8, 125.3, 125.4, 125.6, 126.0, 129.5, 130.6, 134.1, 138.0, 138.6, 150.5, 152.5 (16C, C-Ar), 155.2 (NC(O)O), 169.4, 173.6, 173.9 (3CO). ESI-MS calcd for $C_{33}H_{33}ClF_2N_3O_{10}S$ [M−H]$^-$: 736.15; found m/z 736.26.

4.2.13. Sodium [(2,3-difluorobenzyl) 5-acetamido-9-(4-chlorobenzamido)-3,5,9-trideoxy-7,8-*O*-isopropylidene-4-*O*-(2-(2-thienyl)ethylcarbamoyl)-D-*glycero*-α-D-*galacto*-2-nonulopyranosid]onate (15g)

Compound **11** (28.0 mg, 40 μmol) was dissolved in dry pyridine (0.5 mL). 2-(2-Thienyl)ethyl isocyanate (27.5 mg, 0.18 mmol) and DMAP (1.0 mg, 8.0 μmol) were added. The reaction mixture was stirred for 24 h at 45 °C, then cooled to rt, and treated with water (0.1 mL). After removal of the solvents under reduced pressure, the crude product was purified by chromatography on silica gel (10% gradient of MeOH in DCM) to yield **15g** (16 mg, 37%). ^{1}H NMR (500 MHz, CD_3OD): δ 1.20, 1.27 (2s, 6H, C(CH_3)$_2$), 1.71 (t, J = 12.3 Hz, 1H, H-3a), 1.81 (s, 3H, NHAc), 2.62 (d, J = 4.8, 12.3 Hz, 1H, H-3b), 2.81–2.91 (m, 2H, CH_2), 3.15–3.22 (m, 2H, CH_2), 3.95–4.04 (m, 3H, H-7, H-9a, H-9b), 4.16–4.25 (m, 2H, H-5, H-8), 4.46–4.55 (m, 1H, H-6), 4.64, 4.88 (A, B of AB, J = 12.8 Hz, 2H, CH_2Ar), 4.98–5.08 (m, 1H, H-4), 6.64–6.74 (m, 1H, CH_{ar}), 6.75–6.81 (m, 1H, CH_{ar}), 6.84–6.93 (m, 1H, CH_{ar}), 6.94–7.00 (m, 1H, CH_{ar}), 7.07 (d, J = 4.9 Hz, 1H, CH_{ar}), 7.10–7.20 (m, 1H, CH_{ar}), 7.23, 7.74 (AA′, BB′ of AA′BB′, J = 8.3 Hz, 4H, CH_{ar}); ^{13}C NMR (126 MHz, CD_3OD): δ 23.0 (NHAc), 25.9, 27.7 (C(CH_3)$_2$), 31.0 (CH_2), 38.6 (C-3), 43.5 (C-9), 49.9 (CH_2), 52.1 (C-5), 60.8 (CH_2Ar), 71.0 (C-7), 75.8 (C-4), 76.1 (C-8), 76.9 (C-6), 101.6 (C-2), 109.4 (C(CH_3)$_2$), 117.7, 124.7, 126.3, 127.9, 129.5, 130.4, 130.6, 134.0, 138.7, 139.0, 140.0, 142.4, 142.5, 148.6, 150.5, 152.4 (16 C-Ar), 158.4 (NC(O)O), 169.4, 173.5, 173.6 (3CO). ESI-MS calcd for $C_{35}H_{38}ClF_2N_3O_{10}S$ [M+Na]$^+$: 788.19; found m/z 788.42.

4.2.14. Sodium [(2,3-difluorobenzyl) 5-acetamido-9-(4-chlorobenzamido)-3,5,9-trideoxy-7,8-*O*-isopropylidene-4-*O*-((2-methylfuran-3-yl)carbamoyl)-D-*glycero*-α-D-*galacto*-2-nonulopyranosid]onate (15h)

Compound **11** (37.0 mg, 50 μmol) was dissolved in dry pyridine (0.5 mL). 2-Methylfuran-3-yl isocyanate (22.0 mg, 0.18 mmol) and DMAP (1.0 mg, 8.0 μmol) were added. The reaction mixture was stirred for 24 h and then water was added. After removal of the solvents under reduced pressure, the crude product was purified by chromatography on silica gel (10% gradient of MeOH in DCM) to yield **15h** (11.0 mg, 28%). ^{1}H NMR (500 MHz, CD_3OD): δ 1.20, 1.33 (2s, 6H, C(CH_3)$_2$), 1.72–1.82 (m, 1H, H-3a), 1.85 (s, 3H, NHAc), 2.08 (s, 3H, CH_3), 2.68 (dd, J = 4.4, 12.8 Hz, 1H, H-3b), 3.40–3.53 (m, 1H, H-9a), 3.84 (d, J = 12.8 Hz, 1H, H-9b), 4.04 (d, J = 10.2 Hz, 1H, H-7), 4.20–4.29 (m, 3H, H-5, H-6, H-8), 4.51, 4.63 (A, B of AB, J = 11.7 Hz, 2H, CH_2Ar), 5.11 (td, J = 4.2, 10.7, 11.1 Hz, 1H, H-4), 6.36 (s, 1H, CH_{ar}), 6.97–7.20 (m, 4H, CH_{ar}), 7.27, 7.78 (AA′, BB′ of AA′BB′, J = 8.4 Hz, 4H, CH_{ar}); ^{13}C NMR (126 MHz, CD_3OD): δ 11.2 (CH_3), 22.9 (NHAc), 25.6, 27.6 (C(CH_3)$_2$), 38.3 (C-3), 42.5 (C-9), 52.2 (C-5), 60.7 (CH_2Ar), 70.9 (C-7), 71.9 (C-4), 76.1 (C-8), 76.9 (C-6), 101.8 (C-2), 109.3 (C(CH_3)$_2$), 111.4, 117.5, 117.6, 120.4, 125.5, 126.0, 126.4, 129.5, 130.6, 134.2, 138.6, 138.9, 140.8, 150.5 (16C, C-Ar), 156.4 (NC(O)O), 169.4, 173.6 (3C, 3CO). ESI-MS calcd for $C_{34}H_{36}ClF_2N_3O_{11}$ [M+Na]$^+$: 758.18; found m/z 758.42.

4.2.15. Sodium [(2,3-difluorobenzyl) 5-acetamido-4-*O*-acetyl-9-(4-chlorobenzamido)-3,5,9-trideoxy-D-*glycero*-α-D-*galacto*-2-nonulopyranosid]onate (16a)

Compound **15a** (11.0 mg, 20 μmol) was dissolved in 80% aq AcOH (1.5 mL) and stirred for 3 h at 60 °C. Then the reaction mixture was cooled to rt and neutralized with 10% aq NaOH. After removal of the solvents under reduced pressure the crude product was purified on RP-18 (10% gradient of MeOH in water) to yield **16a** (8.5 mg, 80%). $[\alpha]_D^{20}$ −32.8 (*c* 0.24, MeOH); ^{1}H NMR (500 MHz, D_2O): δ 1.79 (t, *J* = 12.1 Hz, 1H, H-3a), 1.91 (s, 3H, NHAc), 2.03 (s, 3H, OAc), 2.75 (dd, *J* = 4.8, 12.4 Hz, 1H, H-3b), 3.42 (dd, *J* = 7.9, 14.2 Hz, 1H, H-9a), 3.52 (d, *J* = 10.0 Hz, 1H, H-7), 3.69–3.80 (m, 2H, H-8, H-9b), 3.91 (d, *J* = 11.7 Hz, 1H, H-6), 4.04 (t, *J* = 10.3 Hz, 1H, H-5), 4.62, 4.87 (A, B of AB, *J* = 11.8 Hz, 2H, C*H*$_2$Ar), 4.91 (td, *J* = 4.9, 11.5 Hz, 1H, H-4), 7.08 (dt, *J* = 8.4, 13.1 Hz, 2H, CH_{ar}), 7.17 (t, *J* = 6.7 Hz, 1H, CH_{ar}), 7.49, 7.72 (AA′, BB′ of AA′BB′, *J* = 8.5 Hz, 4H, CH_{ar}); ^{13}C NMR (126 MHz, D_2O): δ 20.2 (OAc), 21.8 (NHAc), 37.3 (C-3), 42.6 (C-9), 49.3 (C-5), 60.6 (*C*H$_2$Ar), 69.6, 70.2, 70.8, 72.1 (C-4, C-6, C-7, C-8), 101.1 (C-2), 117.0, 124.3, 125.8, 126.5, 128.6, 128.8, 132.1, 137.5, 138.0, 147.5, 149.0, 149.5 (12 C-Ar), 167.0, 172.8, 173.1, 174.5 (4CO). HRMS calcd for $C_{27}H_{29}ClF_2N_2O_9$ [M+Na]$^+$: 637.1379; found *m*/*z* 637.1362.

4.2.16. Sodium [(2,3-difluorobenzyl) 5-acetamido-4-*O*-benzoyl-9-(4-chlorobenzamido)-3,5,9-trideoxy-D-*glycero*-α-D-*galacto*-2-nonulopyranosid]onate (16b)

Prepared from **15b** (7.1 mg, 10 μmol) according to the procedure described for **16a**. Purification on RP-18 (10% gradient of MeOH in water) yielded **16b** (4.1 mg, 60%). $[\alpha]_D^{20}$ −7.4 (*c* 0.28, MeOH); ^{1}H NMR (500 MHz, D_2O): δ 1.80 (s, 3H, NHAc), 1.96 (t, *J* = 12.0 Hz, 1H, H-3a), 2.90 (dd, *J* = 4.9, 12.4 Hz, 1H, H-3b), 3.43 (dd, *J* = 8.0, 14.3 Hz, 1H, H-9a), 3.56 (d, *J* = 8.7 Hz, 1H, H-7), 3.73–3.83 (m, 2H, H-8, H-9b), 4.00 (dd, *J* = 1.8, 10.6 Hz, 1H, H-6), 4.24 (t, *J* = 10.3 Hz, 1H, H-5), 4.66, 4.81 (A, B of AB, *J* = 11.9 Hz, 2H, C*H*$_2$Ar), 5.13 (ddd, *J* = 4.8, 10.2, 11.6 Hz, 1H, H-4), 7.01–7.17 (m, 2H, CH_{ar}), 7.20 (t, *J* = 6.9 Hz, 1H, CH_{ar}), 7.46–7.56 (m, 4H, CH_{ar}), 7.65 (t, *J* = 7.5 Hz, 1H, CH_{ar}), 7.74, 7.96 (AA′, BB′ of AA′BB′, *J* = 8.6 Hz, 4H, CH_{ar}); ^{13}C NMR (126 MHz, D_2O): δ 21.7 (NHAc), 37.4 (C-3), 42.6 (C-9), 49.4 (C-5), 60.7 (*C*H$_2$Ar), 69.6 (C-7), 70.2 (C-8), 71.7 (C-4), 72.2 (C-6), 100.0 (C-2), 117.0, 117.2, 125.8, 128.7, 128.8, 128.9, 129.4, 132.1, 133.9, 137.5 (18C, C-Ar), 172.9, 174.3 (4C, 4CO). HRMS calcd for $C_{32}H_{30}ClF_2N_2NaO_{10}$ [M+Na]$^+$: 721.1345; found *m*/*z* 721.1353.

4.2.17. Sodium [(2,3-difluorobenzyl) 5-acetamido-4-*O*-benzyl-9-(4-chlorobenzamido)-3,5,9-trideoxy-D-*glycero*-α-D-*galacto*-2-nonulopyranosid]onate (16c)

Prepared from **15c** (6.8 mg, 10 μmol) according to the procedure described for **16a**. Purification on RP-18 (10% gradient of MeOH in water) yielded **16c** (2.0 mg, 36%). $[\alpha]_D^{20}$ −8.4 (*c* 0.16, MeOH); ^{1}H NMR (500 MHz, D_2O): δ 1.55 (t, *J* = 12.0 Hz, 1H, H-3a), 1.77 (s, 3H, NHAc), 2.86 (dd, *J* = 4.6, 12.4 Hz, 1H, H-3b), 3.27–3.39 (m, 2H, H-7, H-9a), 3.42–3.51 (m, 1H, H-4), 3.60–3.69 (m, 3H, H-6, H-8, H-9b), 3.79 (t, *J* = 10.2 Hz, 1H, H-5), 4.39, 4.55 (A, B of AB, *J* = 11.8 Hz, 2H, C*H*$_2$Ar), 4.61, 4.70 (A′, B′ of A′B′, *J* = 11.6 Hz, 2H, C*H*$_2$Ar), 7.00–7.12 (m, 3H, CH_{ar}), 7.20–7.35 (m, 5H, CH_{ar}), 7.41, 7.62 (AA′, BB′ of AA′BB′, *J* = 8.6 Hz, 4H, CH_{ar}); ^{13}C NMR (126 MHz, D_2O): δ 21.9 (NHAc), 37.8 (C-3), 49.5 (C-9), 50.0 (C-5), 69.7, 70.2, 71.2 (C-7, C-8, *C*H$_2$Ar), 72.6 (C-6), 75.6 (C-4), 101.4 (C-2), 126.0, 128.3, 128.6, 128.7, 128.8, 132.1, 136.7 (18C, C-Ar), 170.0, 172.9, 174.5 (3CO). HRMS calcd for $C_{32}H_{32}ClF_2N_2NaO_9$ [M+H]$^+$: 685.1741; found *m*/*z* 685.1745.

4.2.18. Sodium [(2,3-difluorobenzyl) 5-acetamido-9-(4-chlorobenzamido)-3,5,9-trideoxy-4-*O*-phenylcarbamoyl-D-*glycero*-α-D-*galacto*-2-nonulopyranosid]onate (16d)

Prepared from **15d** (10 mg, 10 μmol) according to the procedure described for **16a**. Purification on RP-18 (10% gradient of MeOH in water) yielded **16d** (1.5 mg, 15%). $[\alpha]_D^{20}$ −1.0 (*c* 0.1, MeOH); ^{1}H NMR (500 MHz, CD_3OD): δ 1.78 (s, 3H, NHAc), 1.88–1.99 (m, 1H, H-3a), 2.68 (d, *J* = 9.1 Hz, 1H, H-3b), 3.33–3.49 (m, 1H, H-9a), 3.60 (d, *J* = 10.7 Hz, 1H, H-9b), 3.74 (d, *J* = 5.4 Hz, 1H, H-7), 4.14 (d, *J* = 2.6 Hz, 1H, H-8), 4.19–4.46 (m, 2H, H-5, H-6), 4.57, 4.79 (A, B of AB, *J* = 11.2 Hz, 2H, C*H*$_2$Ar), 5.26 (td, *J* = 4.9, 10.7 Hz, 1H, H-4), 6.95 (t, *J* = 7.2 Hz, 1H, CH_{ar}), 7.13 (d, *J* = 6.0 Hz, 2H, CH_{ar}), 7.19 (t, *J* = 7.7 Hz, 3H, CH_{ar}), 7.28–7.35 (m, 2H, CH_{ar}), 7.41, 7.82 (AA′, BB′ of AA′BB′, *J* = 8.3 Hz, 4H, CH_{ar}); ^{13}C NMR (126 MHz, CD_3OD): δ 22.8 (NHAc), 38.9 (C-3), 44.2 (C-9), 51.2 (C-5), 60.4 (*C*H$_2$Ar), 69.4 (C-7), 70.8 (C-4), 72.5 (C-8), 73.3 (C-6), 103.0 (C-2), 117.6, 117.7, 119.8, 124.2, 125.6, 126.3, 128.1, 129.4, 129.8, 130.3, 133.4, 139.1, 139.9, 150.6 (18C, C-Ar), 154.9 (NC(O)O), 169.9, 174.3, 177.6 (3CO). ESI-MS calcd for $C_{32}H_{32}ClF_2N_3O_{10}$ [M+Na]$^+$: 714.16; found *m*/*z* 714.30.

4.2.19. Sodium [(2,3-difluorobenzyl) 5-acetamido-9-(4-chlorobenzamido)-3,5,9-trideoxy-4-*O*-phenylethylcarbamoyl-D-*glycero*-α-D-*galacto*-2-nonulopyranosid]onate (16e)

Prepared from **15e** (7.3 mg, 10 μmol) according to the procedure described for **16a**. Purification on RP-18 (10% gradient of MeOH in water) yielded **16e** (1.5 mg, 20%). $[\alpha]_D^{20}$ −5.6 (*c* 0.11, MeOH); ^{1}H NMR (500 MHz, CD_3OD): δ 1.71–1.83 (m, 1H, H-3a), 1.87 (s, 3H, NHAc), 2.38–2.51 (m, 1H, H-3b), 2.53–2.68 (m, 2H, CH_2), 3.05–3.18 (m, 2H, CH_2), 3.31–3.47 (m, 2H, H-8, H-9a), 3.48–3.65 (m, 2H, H-7, H-9b), 4.05–4.29 (m, 2H, H-5, H-6), 4.46 (A, B of AB, *J* = 11.4 Hz, 2H, C*H*$_2$Ar), 5.04 (dt, *J* = 5.3, 10.5, 11.0 Hz, 1H, H-4), 6.93–7.19 (m, 8H, CH_{ar}), 7.32, 7.72 (AA′, BB′ of AA′BB′, *J* = 8.2 Hz, 4H, CH_{ar}); ^{13}C NMR (126 MHz, CD_3OD): δ 22.8 (NHAc), 37.0 (C-3), 39.0, 43.4 (2 CH_2), 44.6 (C-9), 51.2 (C-5), 60.4 (*C*H$_2$Ar), 70.0 (C-4), 70.9, 72.1 (C-7, C-8), 72.3 (C-6), 102.8 (C-2), 117.6, 125.3, 126.3, 126.6, 127.2, 127.3, 129.5, 129.8, 130.2, 130.3, 133.7, 134.2, 138.7, 139.0, 140.4, 152.5 (18C, C-Ar), 158.0 (NC(O)O), 169.9, 174.0, 175.9 (3CO). HRMS calcd for $C_{34}H_{36}ClF_2N_3O_{10}$ [M+Na]$^+$: 764.1774; found *m*/*z* 764.1791.

4.2.20. Sodium [(2,3-difluorobenzyl) 5-acetamido-9-(4-chlorobenzamido)-3,5,9-trideoxy-4-*O*-(3-thienylcarbamoyl)-D-*glycero*-α-D-*galacto*-2-nonulopyranosid]onate (16f)

Prepared from **15f** (8.0 mg, 10 μmol) according to the procedure described for **16a**. Purification on RP-18 (10% gradient of MeOH in water) yielded **16f** (2.1 mg, 31%). $[\alpha]_D^{20}$ −17.8 (*c* 0.5, MeOH); ^{1}H NMR (500 MHz, CD_3OD): δ 1.76 (t, *J* = 11.9 Hz, 1H, H-3a), 1.88 (s, 3H, NHAc), 3.02 (dd, *J* = 5.0, 12.1 Hz, 1H, H-3b), 3.44 (dd, *J* = 1.7, 9.0 Hz, 1H, H-7), 3.48 (dd, *J* = 7.7, 13.7 Hz, 1H, H-9a), 3.76 (dd, *J* = 3.1, 13.7 Hz, 1H, H-9b), 3.84 (dd, *J* = 1.3, 10.5 Hz, 1H, H-6), 3.97–4.08 (m, 2H, H-5, H-8), 4.66, 4.92 (A, B of AB, *J* = 12.2 Hz, 2H, C*H*$_2$Ar), 4.98 (td, *J* = 5.0, 11.0 Hz, 1H, H-4), 6.94 (d, *J* = 4.9 Hz, 1H, CH_{ar}), 7.04–7.11 (m, 2H, CH_{ar}), 7.17 (s, 1H, CH_{ar}), 7.23 (dd, *J* = 3.2, 5.1 Hz, 1H, CH_{ar}), 7.25–7.32 (m, 1H, CH_{ar}), 7.43, 7.80 (AA′, BB′ of AA′BB′, *J* = 8.6 Hz, 4H, CH_{ar}); ^{13}C NMR (126 MHz, CD_3OD): δ 22.6 (NHAc), 39.7 (C-3), 44.4 (C-9), 51.7 (C-5), 60.3 (*C*H$_2$Ar), 71.4 (C-8), 72.2 (C-7), 72.5 (C-4), 74.0 (C-6), 108.0 (C-2), 108.1, 117.0, 121.8, 122.4, 125.2, 125.4, 126.3, 129.7, 130.1, 134.4, 138.6 (16C, C-Ar), 152.4 (NC(O)O), 174.9 (3C, 3CO). HRMS calcd for $C_{30}H_{30}ClF_2N_3O_{10}S$ [M−H]$^-$: 720.1206; found *m*/*z* 720.1209.

4.2.21. Sodium [(2,3-difluorobenzyl) 5-acetamido-9-(4-chlorobenzamido)-3,5,9-trideoxy-4-*O*-(2-(2-thienyl)ethylcarbamoyl)-D-*glycero*-α-D-*galacto*-2-nonulopyranosid]onate (16g)

Prepared from **15g** (16.0 mg, 20 μmol) according to the procedure described for **16a**. Purification on RP-18 (10% gradient of MeOH in water) yielded **16g** (1.5 mg, 10%). $[\alpha]_D^{20}$ −5.9 (*c* 0.18, MeOH); ^{1}H NMR (500 MHz, CD_3OD): δ 1.73–1.83 (m, 4H, H-3a, NHAc), 2.54 (dd, *J* = 5.0, 13.0 Hz, 1H, H-3b), 2.85 (t, *J* = 7.0 Hz, 2H, CH_2), 3.16–3.22 (m, 2H, CH_2), 3.28 (dd, *J* = 6.4, 14.0 Hz, 1H, H-9a),

3.45 (dd, J = 5.0, 14.0 Hz, 1H, H-9b), 3.66 (d, J = 5.6 Hz, 1H, H-7), 4.00–4.13 (m, 2H, H-5, H-8), 4.20 (d, J = 10.6 Hz, 1H, H-6), 4.50, 4.69 (A, B of AB, J = 11.7 Hz, 2H, CH_2Ar), 5.07 (td, J = 4.9, 10.9 Hz, 1H, H-4), 6.71 (d, J = 3.0 Hz, 1H, CH_{ar}), 6.79–6.85 (m, 1H, CH_{ar}), 7.05–7.19 (m, 4H, CH_{ar}), 7.36, 7.78 (AA′, BB′ of AA′BB′, J = 8.6 Hz, 4H, CH_{ar}); ^{13}C NMR (126 MHz, CD_3OD): δ 22.9 (NHAc), 30.9 (CH_2), 43.5 (C-3), 44.0 (C-9), 46.7 (CH_2), 51.2 (C-5), 60.5 (CH_2Ar), 69.2, 70.6, 72.3 (C-4, C-7, C-8), 73.9 (C-6), 103.0 (C-2), 117.6, 117.7, 124.7, 125.7, 126.1, 126.3, 127.9, 129.8, 130.4, 133.3, 139.2, 142.4 (16C, C-Ar), 157.9 (NC(O)O), 169.8, 174.2, 174.6 (3CO). ESI-MS calcd for $C_{32}H_{34}ClF_2N_3O_{10}S$ [M+Na]$^+$: 748.14; found m/z 748.29.

4.2.22. Sodium [(2,3-difluorobenzyl) 5-acetamido-9-(4-chlorobenzamido)-3,5,9-trideoxy-4-*O*-((2-methylfuran-3-yl)carbamoyl)-D-*glycero*-α-D-*galacto*-2-nonulopyranosid]onate (16h)

Prepared from **15h** (11.0 mg, 10 μmol) according to the procedure described for **16a**. Purification on RP-18 (10% gradient of MeOH in water) yielded **16h** (2.4 mg, 25%). $[\alpha]_D^{20}$ −2.4 (c 0.37, MeOH); ^{1}H NMR (500 MHz, CD_3OD): δ 1.71 (dd, J = 7.9, 11.6 Hz, 1H, H-3a), 1.82 (s, 3H, NHAc), 2.07 (s, 3H, CH_3), 2.50 (dd, J = 5.1, 12.3 Hz, 1H, H-3b), 3.31 (d, J = 9.4 Hz, 1H, H-7), 3.44 (dd, J = 6.5, 13.8 Hz, 1H, H-9a), 3.71 (dd, J = 2.6, 13.6 Hz, 1H, H-9b), 3.84–3.97 (m, 1H, H-8), 4.06 (t, J = 11.5 Hz, 1H, H-6), 4.18 (t, J = 10.6 Hz, 1H, H-5), 4.45, 4.69 (A, B of AB, J = 11.2 Hz, 2H, CH_2Ar), 5.11–5.21 (m, 1H, H-4), 6.35 (s, 1H, CH_{ar}), 7.00–7.06 (m, 2H, CH_{ar}), 7.11 (s, 1H, CH_{ar}), 7.18 (s, 1H, CH_{ar}), 7.37, 7.74 (AA′, BB′ of AA′BB′, J = 8.4 Hz, 4H, CH_{ar}); ^{13}C NMR (126 MHz, CD_3OD): δ 11.3 (CH_3), 22.9 (NHAc), 39.3 (C-3), 44.1 (C-9), 60.4 (CH_2Ar), 67.5, 70.2, 71.0 (C-4, C-7, C-8), 72.0 (C-6), 101.9 (C-2), 111.4, 112.2, 117.2, 125.4, 126.7, 129.7, 130.2, 130.3, 134.1, 138.6, 138.8, 140.8, 143.5 (16C, C-Ar), 156.4 (NC(O)O), 169.8, 176.7, 180.5 (3CO). HRMS calcd for $C_{31}H_{32}ClF_2N_3O_{11}$ [M+Na]$^+$: 718.1592; found m/z 718.1584.

4.2.23. Methyl [(2,3-difluorobenzyl) 5-acetamido-9-(4-chlorobenzamido)-3,5,9-trideoxy-7,8-*O*-isopropylidene-α-D-*manno*-2,4-nonudiulopyranosid]onate (17)

Compound **10** (63.0 mg, 10 μmol) was dissolved in dry DCM (2.5 mL). Pyridinium dichromate (26.0 mg, 70 μmol) was added followed by the addition of acetic anhydride (28 μL, 0.3 mmol). The reaction mixture was stirred at rt for 4 h. After addition of 2-propanol (1 mL) the mixture was co-evaporated three times with toluene. Purification by chromatography on silica gel (EtOAc) yielded **17** (20 mg, 30%) as a white foam. ^{1}H NMR (500 MHz, $CDCl_3$): δ 1.37, 1.52 (2s, 6H, C(CH_3)$_2$), 2.17 (s, 3H, NHAc), 2.94 (d, J = 15.2 Hz, 1H, H-3a), 3.29 (d, J = 15.0 Hz, 1H, H-3b), 3.82 (s, 3H, OMe), 3.85–3.96 (m, 1H, H-9a), 4.02 (dt, J = 6.4, 13.0 Hz, 1H, H-9b), 4.27 (d, J = 6.4 Hz, 1H, H-7), 4.38–4.52 (m, 2H, H-5, H-6), 4.53–4.59 (m, 1H, H-8), 4.64, 5.07 (A, B of AB, J = 11.5 Hz, 2H, CH_2Ar), 6.06 (d, J = 6.9 Hz, 1H, NH), 6.97–7.21 (m, 4H, NH, CH_{ar}), 7.40, 7.76 (AA′, BB′ of AA′BB′, J = 8.5 Hz, 4H, CH_{ar}); ^{13}C NMR (126 MHz, $CDCl_3$): δ 23.1 (NHAc), 25.4, 26.9 (C(CH_3)$_2$), 44.3 (C-3), 47.6 (C-9), 53.7 (C-5), 56.3 (OMe), 60.4 (CH_2Ar), 73.2 (C-7), 74.6 (C-8), 75.3 (C-6), 99.8 (C-2), 109.1 (C(CH$_3$)$_2$), 117.2, 124.1, 124.2, 125.2, 125.9, 126.0, 128.5, 128.6, 128.8, 132.7, 137.8 (12C, C-Ar), 167.2, 170.7, 173.0, 200.1 (4CO). ESI-MS calcd for $C_{29}H_{31}ClF_2N_2O_9$ [M+Na]$^+$: 647.16; found m/z 647.13.

4.2.24. Methyl [(2,3-difluorobenzyl) 5-acetamido-9-(4-chlorobenzamido)-3,5,9-trideoxy-4-methyl-D-*glycero*-α-D-*talo*-nonulopyranosid]onate (18)

$ZrCl_4$ (50.0 mg, 0.13 mmol, 4.0 equiv) was dried for 30 min at 30 °C under high vacuum. After addition of dry THF (1.7 mL), the suspension was heated up to 50 °C for 20 min. Afterwards the colorless solution was cooled to −54 °C. MeLi (1 M in hexane, 0.5 mL) was added dropwise and the pale yellow solution was warmed up to 0 °C and stirring was continued for 30 min. After cooling to −78 °C, a solution of **17** (20.0 mg, 30 μmol) in THF (0.5 mL) was added. The reaction mixture was stirred for 3 h and then allowed to warm to 0 °C. After addition of semi-satd aq NH_4Cl (0.5 mL), the reaction mixture was extracted with DCM (5 mL). The combined organic layers were dried over Na_2SO_4, filtered, and the solvents were evaporated. Afterwards the crude mixture was dissolved in 80% aq AcOH (1 mL) and stirred for 3 h at 60 °C. After removal of the solvents under reduced pressure, the pure product **18** was obtained by chromatography on silica gel (1% gradient of MeOH in DCM) (6.0 mg, 32% + 2.0 mg, 11% (*S*)-stereoisomer). ^{1}H NMR (500 MHz, $CDCl_3$): δ 1.24 (s, 3H, CH_3), 2.07 (s, 3H, NHAc), 2.96 (d, J = 15.0 Hz, 1H, H-3a), 3.35 (d, J = 15.0 Hz, 1H, H-3b), 3.48 (d, J = 8.9 Hz, 1H, H-7), 3.73 (dd, J = 6.9, 13.1 Hz, 1H, H-9a), 3.79 (s, 3H, OMe), 3.82–3.90 (m, 2H, H-6, H-9b), 4.09–4.18 (m, 1H, H-8), 4.68–4.80 (m, 2H, H-5, CH_2Ar), 4.95 (B of AB, J = 11.7 Hz, 1H, CH_2Ar), 6.55 (d, J = 6.6 Hz, 1H, NHAc), 7.00–7.18 (m, 4H, NH, CH_{ar}), 7.39, 7.74 (AA′, BB′ of AA′BB′, J = 8.5 Hz, 4H, CH_{ar}); ^{13}C NMR (126 MHz, $CDCl_3$): δ 23.0 (NHAc), 29.0 (CH_3), 45.2 (C-9), 47.5 (C-3), 52.8 (C-5), 53.6 (OMe), 69.7 (C-8), 70.5 (C-7), 71.5 (C-6), 98.1 (C-2), 122.8, 128.5, 128.6, 129.0, 129.2 (12C, C-Ar), 178.1 (3C, 3CO). ESI-MS calcd for $C_{30}H_{35}ClF_2N_2O_9$ [M+Na]$^+$: 663.19; found m/z 663.05.

4.2.25. Sodium [(2,3-difluorobenzyl) 5-acetamido-9-(4-chlorobenzamido)-3,5,9-trideoxy-4-methyl-D-*glycero*-α-D-*talo*-nonulopyranosid]onate (19)

Compound **18** (6.0 mg, 10 μmol) was dissolved in THF (1.0 mL) and LiOH (9.0 mg, 0.4 mmol) in water (1.0 mL) was added. The mixture was stirred at rt for 4 h and neutralized with 7% aq HCl. After removal of the solvents under reduced pressure, the pure product **19** (2.0 mg, 34%) was obtained by chromatography on RP-8 (5% gradient of MeOH in water) followed by Dowex 50X8 ion-exchange and P2 size exclusion chromatography. $[\alpha]_D^{20}$ −6.3 (c 0.26, MeOH); ^{1}H NMR (500 MHz, D_2O): δ 1.19 (s, 3H, CH_3), 1.79 (d, J = 14.1 Hz, 1H, H-3a), 2.02 (s, 3H, NHAc), 2.60 (d, J = 14.1 Hz, 1H, H-3b), 3.45 (dd, J = 7.3, 13.6 Hz, 1H, H-9a), 3.50 (dd, J = 1.9, 8.6 Hz, 1H, H-7), 3.65–3.83 (m, 2H, H-8, H-9b), 3.88 (d, J = 10.6 Hz, 1H, H-5), 4.31 (dd, J = 2.0, 10.6 Hz, 1H, H-6), 4.56, 4.76 (A, B of AB, J = 12.0 Hz, 2H, CH_2Ar), 7.03–7.23 (m, 3H, CH_{ar}), 7.53, 7.76 (AA′, BB′ of AA′BB′, J = 8.6 Hz, 4H, CH_{ar}); ^{13}C NMR (126 MHz, D_2O): δ 21.8 (NHAc), 26.0 (CH_3), 42.6 (C-9), 44.8 (C-3), 52.1 (C-5), 60.1 (CH_2Ar), 70.3, 70.5, 70.6, 71.4 (C-4, C-6, C-7, C-8), 100.4 (C-2), 117.0, 124.3, 125.9, 126.7, 128.7, 128.8, 132.2, 137.5 (12C, C-Ar), 170.0, 174.4, 174.6 (3CO). HRMS calcd for $C_{26}H_{30}ClF_2N_2O_9$ [M+Na]$^+$: 585.1427; found m/z 585.1439.

4.2.26. Methyl [(2,3-difluorobenzyl) 5-acetamido-9-(4-chlorobenzamido)-3,5,9-trideoxy-7,8-*O*-isopropylidene-D-*glycero*-α-D-*talo*-nonulopyranosid]onate (20)

$BH_3{\cdot}NH_3$ (7.0 mg, 0.22 mmol) was dissolved in MeOH (0.5 mL) at 0 °C followed by the addition of **17** (30.0 mg, 50 μmol) in MeOH (0.5 mL). After stirring for 2 h at 0 °C, the solvent was evaporated under reduced pressure and the crude product was purified by chromatography on silica gel (2% gradient of 2-PrOH in DCM/MeOH 10:1) to yield **20** (11.0 mg, 36%) as a white solid. ^{1}H NMR (500 MHz, CD_3OD): δ 1.30, 1.48 (2s, 6H, C(CH_3)$_2$), 1.88 (dd, J = 2.0, 13.7 Hz, 1H, H-3a), 1.95 (s, 3H, NHAc), 2.62 (dd, J = 3.9, 13.7 Hz, 1H, H-3b), 4.02 (d, J = 3.8 Hz, 1H, H-4), 4.07 (t, J = 6.2 Hz, 2H, H-9a, H-9b), 4.13 (dd, J = 2.6, 10.7 Hz, 1H, H-5), 4.20 (d, J = 6.9 Hz, 1H, H-7), 4.37 (d, J = 10.7 Hz, 1H, H-6), 4.43 (A of AB, J = 11.4 Hz, 1H, CH_2Ar), 4.47 (tt, J = 4.5, 8.8 Hz, 1H, H-8), 4.90 (B of AB, J = 11.4 Hz, 1H, CH_2Ar), 7.04–7.13 (m, 1H, CH_{ar}), 7.13–7.22 (m, 2H, CH_{ar}), 7.44, 7.82 (AA′, BB′ of AA′BB′, J = 8.6 Hz, 4H, CH_{ar}); ^{13}C NMR (126 MHz, CD_3OD): δ 22.7 (NHAc), 25.8, 27.1 (C(CH_3)$_2$), 40.8

(C-3), 41.9 (C-9), 50.1 (C-5), 52.7 (OMe), 60.5 (CH_2Ar), 66.3 (C-4), 71.5 (C-7), 76.3 (C-6), 77.7 (C-8), 98.9 (C-2), 110.1 ($C(CH_3)_2$), 117.8, 125.4, 126.8, 128.3, 129.7, 130.1, 130.2, 134.3, 138.7 (12C, C-Ar), 169.3, 171.4, 173.1 (3CO). ESI-MS calcd for $C_{29}H_{33}Cl_2F_2N_2O_9$ $[M+Na]^+$: 649.18; found *m*/*z* 649.22.

4.2.27. Methyl [(2,3-difluorobenzyl) 5-acetamido-9-(4-chlorobenzamido)-3,5,9-trideoxy-D-*glycero*-α-D-*talo*-nonulopyranosid]onate (21)

Compound **20** (20.0 mg, 30 μmol) was dissolved in 80% aq AcOH (1.5 mL) and stirred for 3 h at 60 °C. Then, the reaction mixture was cooled to rt and neutralized with 10% aq NaOH. After evaporation of the solvents, the crude product was purified by chromatography on silica gel (10% gradient of MeOH in DCM) to yield **21** (17 mg, 90%) as a colorless oil. ^{1}H NMR (500 MHz, CD_3OD): δ 1.89–1.97 (m, 4H, H-3a, NHAc), 2.62 (dd, *J* = 3.4, 13.9 Hz, 1H, H-3b), 3.42 (dd, *J* = 5.1, 13.8 Hz, 1H, H-6), 3.52 (dd, *J* = 7.6, 13.8 Hz, 1H, H-9a), 3.70 (s, 3H, OMe), 3.78 (dd, *J* = 3.3, 13.9 Hz, 1H, H-9b), 4.01–4.11 (m, 3H, H-4, H-5, H-8), 4.35 (d, *J* = 11.4 Hz, 1H, H-7), 4.45, 4.76 (A, B of AB, *J* = 11.8 Hz, 2H, CH_2Ar), 7.00–7.21 (m, 3H, CH_{ar}), 7.41, 7.78 (AA′, BB′ of AA′BB′, *J* = 8.6 Hz, 4H, CH_{ar}); ^{13}C NMR (126 MHz, CD_3OD): δ 22.7 (NHAc), 41.1 (C-3), 44.9 (C-9), 49.8 (C-5), 53.2 (OMe), 60.3 (CH_2Ar), 67.0 (C-4), 71.3 (C-8), 71.8 (C-7), 72.5 (C-6), 99.0 (C-2), 117.9, 118.0, 125.5, 125.6, 126.7, 128.5, 128.6, 129.8, 130.2, 134.6, 138.8 (12C, C-Ar), 169.6, 172.0, 174.3 (3CO). ESI-MS calcd for $C_{26}H_{29}ClF_2N_2O_9$ $[M+Na]^+$: 587.25; found *m*/*z* 587.25.

4.2.28. Sodium [(2,3-difluorobenzyl) 5-acetamido-9-(4-chlorobenzamido)-3,5,9-trideoxy-D-*glycero*-α-D-*talo*-nonulopyranosid]onate (22)

Compound **21** (17.0 mg, 30 μmol) was dissolved in MeOH (3 mL) and 10% aq NaOH (0.1 mL) was added. After 2 h the reaction was neutralized with 7% aq HCl. The solvents were evaporated and the residue was purified by chromatography on RP-8 (10% gradient of MeOH in water) to yield **22** (2.0 mg, 34%). $[\alpha]_D^{20}$ −41.6 (*c* 0.37, MeOH); ^{1}H NMR (500 MHz, D_2O): δ 1.85 (dd, *J* = 2.9, 14.2 Hz, 1H, H-3a), 1.96 (s, 3H, NHAc), 2.62 (dd, *J* = 3.4, 14.2 Hz, 1H, H-3b), 3.44 (dd, *J* = 7.9, 14.2 Hz, 1H, H-9a), 3.49 (dd, *J* = 1.8, 8.9 Hz, 1H, H-7), 3.67–3.79 (m, 2H, H-8, H-9b), 4.00 (dd, *J* = 2.8, 10.7 Hz, 1H, H-5), 4.13 (q, *J* = 2.9 Hz, 1H, H-4), 4.37 (dd, *J* = 1.8, 10.7 Hz, 1H, H-6), 4.53, 4.73 (A, B of AB, *J* = 11.7 Hz, 2H, CH_2Ar), 6.97–7.25 (m, 3H, CH_{ar}), 7.49, 7.73 (AA′, BB′ of AA′BB′, *J* = 8.5 Hz, 4H, CH_{ar}); ^{13}C NMR (126 MHz, CD_3OD) δ 21.8 (NHAc), 39.2 (C-3), 42.6 (C-9), 48.2 (C-5), 60.1 (CH_2Ar), 65.8 (C-4), 69.4 (C-6), 70.2, 70.3 (C-7, C-8), 100.0 (C-2), 117.0, 125.9, 128.7, 128.8, 132.1, 137.5 (12C, C-Ar), 170.0, 174.5 (3C, 3CO). HRMS calcd for $C_{25}H_{27}ClF_2N_2O_9$ $[M+Na]^+$: 595.1273; found *m*/*z* 595.1276.

4.3. Surface plasmon resonance (SPR) analysis

The SPR measurements were performed on a Biacore 3000 surface plasmon resonance-based optical biosensor (Biacore AB, Sweden). Sensor chips (CM5), immobilization kits, maintenance supply, and HBS-EP (10 mM HEPES pH 7.4, 150 mM NaCl, 3 mM EDTA, 0.005% v/v surfactant P20) were purchased from Biacore AB (HBS-EP ready-to-use; degassed and filtered). CM5 chips were preconditioned prior to usage by injecting a series of conditioning solutions. A flow rate of 50 μL/min was used and 2 × 20 μL of 50 mM NaOH, 10 mM HCl, 0.1% SDS, and 100 mM H_3PO_4 were injected. The carboxy groups on the CM5 chip were activated for 10 min with a 1:1 mixture of 0.1 M *N*-hydroxysuccinimide (NHS) and 0.1 M 3-(*N*,*N*-dimethylamino)propyl-*N*-ethylcarbodiimide (EDC) at a flow rate of 10 μL/min. Protein A (P6031) was purchased from Sigma. A sample and a reference surface were prepared sequentially or in parallel. For immobilizing protein A, a stock solution (1 mg/mL in 50 mM phosphate buffer, pH 7.0) was diluted in 10 mM sodium acetate, pH 5.0, to obtain a concentration of 30 μg/mL. This solution was then injected over the activated surface for 10 min at a flow rate of 10 μL/min. Protein A densities around 4'000 to 5'000 RU were achieved. Flow cells were blocked with a 10-min injection of 1 M ethanolamine, pH 8.0. For capturing, $MAG_{d1\text{-}3}$-Fc solution (expressed and purified as described[32]) was diluted to a 30–40 μg/mL concentration using HBS-EP. Afterwards, $MAG_{d1\text{-}3}$-Fc was injected at a flow rate of 1 μL/min for 10 min. Using HBS-EP, the surface was equilibrated overnight at a flow rate of 5 μL/min, achieving densities around 2000 RU. Tenfold dilution series were freshly prepared in eluent buffer immediately before use (→**14**, **16a**–**c**, **19**, and **22**). All binding experiments were conducted at 25 °C at a flow rate of 20 μL/min. The samples were injected over 1 min followed by 1 min dissociation. Each sample was measured with a duplicate of one concentration, using a randomized concentration order. Several buffer samples were injected before the first concentration, and one blank between each concentration, which was used for the double blank referencing during data processing. Double referencing was applied to correct for bulk effects and other systematic artifacts. Data processing and equilibrium binding constant determinations were accomplished with Scrubber (BioLogic Software, Version 1.1 g or 2.0c). Kinetic data were simultaneously fit using Scrubber 2.0c. For the DMSO assay, DMSO (for molecular biology, >99.9%) was purchased from Fluka. The stock solution of the test compounds (→**16d**–**h**) was prepared in DMSO and was kept in glass vials to eliminate contaminations by, for example, softeners. The running buffer was 3% DMSO in HBS-EP. The surface was equilibrated at a flow of 5 μL/min until the baseline was stable. In order to eliminate the influence of DMSO on the signals, a calibration curve was done. Therefore, two solutions were prepared (A = 1 mL running buffer + 50 μL HBS-EP; B = 1 mL running buffer + 1 μL DMSO). Solutions A and B were mixed as indicated in Table 5 and used for calibration. DMSO calibration solutions were injected after five blank injections and before the sample solutions. The test compounds were diluted before measuring with HBS-EP to achieve a content of 3% DMSO. The DMSO calibration was accomplished directly in Scrubber© (version 2.0c).

4.4. Isothermal titration calorimetry

ITC experiments were performed using a VP-ITC instrument from MicroCal, Inc. (Northampton, MA). The measurements were performed at 25 °C. Injections of 5 μL ligand solutions were added from a computer controlled 300 μL microsyringe at an interval of 5 min into the sample cell solution of $MAG_{d1\text{-}3}$-Fc (cell volume 1.4512 mL) with stirring at 307 rpm. A control experiment was performed, where the identical ligand solutions were injected into buffer without protein. The enthalpogram showed negligible heat development, resulting from dilution effects. The assay buffer was HBS-E (10 mM HEPES, 150 mM NaCl, 3 mM EDTA, pH 7.4). The concentration of $MAG_{d1\text{-}3}$-Fc was 48.4 μM, and 500 μM antagonist was injected. The experimental data were fitted to a theoretical titration curve (one site binding model) using *Origin version 7* software (MicroCal), with ΔH (enthalpy change in kcal/mol), K_A (association constant in M^{-1}), and *N* (number of binding sites) as adjustable parameters. The quantity $c = K_A \cdot Mt(0)$, where Mt(0) is the initial macromolecule concentration, is of importance in titra-

Table 5
Calibration solutions

Calibration	1	2	3	4	5
A (μL)	400	300	200	100	0
B (μL)	0	100	200	300	400

tion microcalorimetry.[31] The experiment was performed with a *c* value of 340. Thermodynamic parameters were calculated from Eq. (1),

$$\Delta G = \Delta H - T\Delta S = RT \ln K_A = -RT \ln K_D \quad (1)$$

where ΔG, ΔH, and ΔS are the changes in free energy, enthalpy, and entropy of binding, respectively, T is the absolute temperature, and R = 1.98 cal/mol/K. For reasons of consistency the values were converted to kJ (1 cal = 4.1868 J).

4.5. HPLC

The concentration of $MAG_{d1\text{-}3}$-Fc was determined via HPLC against a standard curve of BSA at 210 nm using a Beckmann Gold system, with UV detection (210 nm). The column used was Poros R1/10 10 μm (100 × 2 mm, Dr. Maisch HPLC Markensäulen, po10.r1.s1002, Morvay Analytik GmbH). The running buffers were A: H_2O + 0.1% TFA and B: 90% MeCN + 0.09% TFA. All measurements were performed at 75 °C, applying a gradient of 20–90% running buffer B within 20 min at a flow rate of 0.2 mL/min.[44]

Acknowledgments

We are greatly indebted to Dr. Francis Bitsch and Peggy Brunet Lefeuvre, Novartis, for providing a HPLC method for protein concentration determination and for providing the VP-ITC instrument as well as for advices regarding the experimental setup and analyzing the data. In addition, we would like to thank the Swiss National Science Foundation (project 200020-120628), the German Ministry for Education and Research ((BMBF, project 031632A), and the Tönjes-Vogt Foundation (project XXI) for their support of this work.

References

1. Schwab, M. E.; Bandtlow, C. E. *Nature* **1994**, *371*, 658–659.
2. Cajal, R. Y. S. *Degeneration and Regeneration of the Nervous System*; Oxford Univ. Press: London, 1928.
3. Schwab, M. E.; Caroni, P. *J. Neurosci.* **1988**, *8*, 2381–2393.
4. Sandvig, A.; Berry, M.; Barrett, L. B.; Butt, A.; Logan, A. *GLIA* **2004**, *46*, 225–251.
5. Filbin, M. T. *Nature Rev. Neurosci.* **2003**, *4*, 703–713.
6. Quarles, R. H. *Neurochem. Res.* **2009**, *34*, 79–86.
7. Kelm, S.; Schauer, R.; Crocker, P. R. *J. Glycoconj.* **1996**, *13*, 913–926.
8. Crocker, P. R.; Kelm, S. *The Siglec Family of I-type Lectins*; Wiley-VCH Verlag GmBH: Weinheim, Germany, 2000. pp 579–595.
9. Lauren, J.; Hu, F.; Chin, J.; Liao, J.; Airaksinen, M. S.; Strittmatter, S. M. *J. Biol. Chem.* **2007**, *282*, 5715–5725.
10. Robak, L. A.; Venkatesh, K.; Lee, H.; Raiker, S. J.; Duan, Y.; Lee-Osbourne, J.; Hofer, T.; Mage, R. G.; Rader, C.; Giger, R. J. *J. Neurosci.* **2009**, *29*, 5768–5783.
11. Kelm, S.; Pelz, A.; Schauer, R.; Filbin, M. T.; Tang, S.; de Bellard, M. E.; Schnaar, R. L.; Mahoney, J. A.; Hartnell, A.; Bradfield, P. *Curr. Biol.* **1994**, *4*, 965–972.
12. Yang, L. J. S.; Zeller, C. B.; Shaper, N. L.; Kiso; Hasegawa, A.; Shapiro, R. E.; Schnaar, R. L. *PNAS* **1996**, *93*, 814–818.
13. Tang, S.; Shen, Y. J.; DeBellard, M. E.; Mukhopadhyay, G.; Salzer, J. L.; Crocker, P. R.; Filbin, M. T. *J. Cell Biol.* **1997**, *138*, 1355–1366.
14. Vinson, M.; Strijbos, P. J. L. M.; Rowles, A.; Facci, L.; Moore, S. E.; Simmons, D. L.; Walsh, F. S. *J. Biol. Chem.* **2001**, *276*, 20280–20285.
15. Yang, L. J. S.; Lorenzini, I.; Vajn, K.; Mountney, A.; Schramm, L. P.; Schnaar, R. L. *Proc. Natl. Acad. Sci. U.S.A.* **2006**, *103*, 11057–11062.
16. Kelm, S.; Brossmer, R.; Isecke, R.; Gross, H. J.; Strenge, K.; Schauer, R. *Eur. J. Biochem.* **1998**, *255*, 663–672.
17. Shelke, S. V.; Gao, G. P.; Mesch, S.; Gäthje, H.; Kelm, S.; Schwardt, O.; Ernst, B. *Bioorg. Med. Chem.* **2007**, *15*, 4951–4965.
18. Schwizer, D.; Gäthje, H.; Kelm, S.; Porro, M.; Schwardt, O.; Ernst, B. *Bioorg. Med. Chem.* **2006**, *14*, 4944–4957.
19. Schwardt, O.; Gaethje, H.; Vedani, A.; Mesch, S.; Gao, G.; Spreafico, M.; von Orelli, J.; Kelm, S.; Ernst, B. *J. Med. Chem.* **2009**, *52*, 989–1004.
20. Ernst, B.; Magnani, J. L. *Nat. Rev. Drug Disc.* **2009**, *8*, 661–677.
21. Mesch, S.; Moser, D.; Strasser, D. S.; Kelm, A.; Cutting, B.; Rossato, G.; Vedani, A.; Koliwer-Brandl, H.; Wittwer, M.; Rabbani, S.; Schwardt, O.; Kelm, S.; Ernst, B. *J. Med. Chem.* **2010**, *53*, 1597–1615.
22. Swinney, D. *J. PharmMed* **2008**, *22*, 23–34.
23. Copeland, R. A.; Pompliano, D. L.; Meek, T. D. *Nat. Rev. Drug Disc.* **2006**, *5*, 730–739.
24. Mehta, P.; Cummings, R. D.; McEver, R. P. *J. Biol. Chem.* **1998**, *273*, 32506–32513.
25. Wild, M. K.; Huang, M. C.; Schulze-Horsel, U.; van der Merwe, P. A.; Vestweber, D. *J. Biol. Chem.* **2001**, *276*, 31602–31612.
26. Herfurth, L.; Ernst, B.; Öhrlein, R.; Wagner, B.; Magnani, J. L.; Benie, A. J.; Peters, T. *J. Med. Chem.* **2005**, *48*, 6879–6886.
27. Kati, W. M.; Montgomery, D.; Carrick, R.; Gubareva, L.; Maring, C.; McDaniel, K.; Steffy, K.; Molla, A.; Hayden, F.; Kempf, D.; Kohlbrenner, W. *Antimicrob. Agents Chemother.* **2002**, *46*, 1014–1021.
28. Markgren, P. O.; Hamalainen, M.; Danielson, U. H. *Anal. Biochem.* **2000**, *279*, 71–78.
29. Markgren, P. O.; Lindgren, M. T.; Gertow, K.; Karlsson, R.; Hamalainen, M.; Danielson, U. H. *Anal. Biochem.* **2001**, *291*, 207–218.
30. Bhunia, A.; Schwardt, O.; Gaethje, H.; Gao, G.; Kelm, S.; Benie, A. J.; Hricovini, M.; Peters, T.; Ernst, B. *ChemBioChem* **2008**, *9*, 2941–2945.
31. Wiseman, T.; Williston, S.; Brandts, J. F.; Lin, L. N. *Anal. Biochem.* **1989**, *179*, 131–137.
32. Bock, N.; Kelm, S. Binding and Inhibition Assay for Siglecs. In *Methods in Molecular Biology*; Brockhausen, I., Ed.; Humana Press: Totowa NJ, 2006; Vol. 347, pp 359–376.
33. Schwarz, F. P.; Ahmed, H.; Bianchet, M. A.; Amzel, L. M.; Vasta, G. R. *Biochemistry* **1998**, *37*, 5867–5877.
34. Ladbury, J. E.; Klebe, G.; Feire, E. *Nat. Rev. Drug Disc.* **2010**, *9*, 23–27.
35. Regan, J.; Pargellis, C. A.; Cirillo, P. F.; Gilmore, T.; Hickey, E. R.; Peet, G. W.; Proto, A.; Swinamer, A.; Moss, N. *Bioorg. Med. Chem. Lett.* **2003**, *13*, 3101–3104.
36. Hasegawa, A.; Ohki, H.; Nagahama, T.; Ishida, H.; Kiso, M. *Carbohydr. Res.* **1991**, *212*, 277–281.
37. Kitamura, M.; Isobe, M.; Ichikawa, Y.; Goto, T. *J. Am. Chem. Soc.* **1984**, *106*, 3252–3257.
38. Yoshida, M.; Ishida, H.; Kiso, M.; Hasegawa, A. *Carbohydr. Res.* **1996**, *280*, 331–338.
39. Groves, D. R.; von Itzstein, M. *J. Chem. Soc., Perkin Trans. 1* **1996**, 2817–2821.
40. Hartmann, M.; Christian, M.; Zbiral, E. *Liebigs Ann. Chem.* **1990**, *1*, 83–91.
41. Hartmann, M.; Zbiral, E. *Liebigs Ann. Chem.* **1991**, 795–801.
42. Hartmann, M.; Zbiral, E. *Monatsh. Chem.* **1991**, *122*, 111–125.
43. Hartmann, M.; Zbiral, E. *Monatsh. Chem.* **1989**, *120*, 899–906.
44. Bitsch, F.; Aichholz, R.; Kallen, J.; Geisse, S.; Fournier, B.; Schlaeppi, J. M. *Anal. Biochem.* **2003**, *323*, 139–149.

2.2.1 MAG – Siglec-4

2.2.1.2 Discovering a Second Binding Site of MAG

MAG-antagonists - high-affinity ligands by fragment-based approach

Stefanie Mesch[a,#], Beatrice Wagner[a,#], Xiaohua Jiang[a,#], Gianluca Rossato[a], Heiko Gäthje,[b] Hendrik Koliwer-Brandl[b], Katrin Lemme[a], Angelo Vedani[a], Matthias Wittwer[a], Oliver Schwardt[a], Soerge Kelm[b], Beat Ernst[a*]

Dedicated to the memory of Robert. E. Ireland

[a]Institute of Molecular Pharmacy, Pharmacenter, University of Basel, Klingelbergstr. 50, 4056 Basel, Switzerland

[b]Center for Biomolecular Interactions Bremen, Glycobiochemistry, University of Bremen, P.O.B. 330440, D-28334 Bremen, Germany

[#]Authors Contributed equally

**Corresponding author, tel: 0041 267 15 51; fax: 0041 267 15 52; e-mail: beat.ernst@unibas.ch*

Keywords: Carbohydrate-mimetics, Myelin-associated glycoprotein (MAG), MAG antagonists, Surface plasmon resonance, Thermodynamics of carbohydrate-protein interactions.

Contribution of Katrin Lemme: ITC experiment, determination of protein concentration.

Introduction

The central nervous system (CNS) is an inhibitory environment for axon regeneration.[1,2] After injury, nerve strands lack the ability for regeneration due to the presence of several inhibitory proteins.[3] In the last decade, three inhibitor proteins have been identified, one of them being the myelin-associated glycoprotein (MAG).[4] MAG interacts with several neuronal receptors, such as proteins of the Nogo receptor family and gangliosides, primarily GD1a, GT1b and GQ1bα.[5] Although the relative role of Nogo receptors and gangliosides as MAG ligands has yet to be resolved, it is supposed that their binding to MAG leads to the activation of RhoA kinase and finally to growth cone collapse.[6]

Our focus is on the inhibitory cascade mediated by gangliosides, because it was shown that sialidase treatment results in enhanced neural outgrowth.[7] Therefore, blocking MAG with sialic acid derivatives offers a valuable therapeutic approach to enhance axon regeneration. Extensive SAR studies resulted in sialic acid derivatives with - compared to gangliosides, which are the physiological players in the inhibitory cascade - almost 1000-fold improved potencies.[8-11] To further enhance affinity for MAG (Siglec-4) and selectivity versus other Siglecs, a fragment-based approach was applied.[12] Thus, Shelke *et al.*[13] identified fragments binding to MAG in the close proximity of sialic acid binding site.[14] When these fragments were linked with a micromolar sialic acid derivative the lead structure **1** was identified.[13] (Figure 1). In this report, we present the optimization of lead **1** and the biological evaluation of the newly obtained MAG antagonists.

Results and Discussion

Second-site NMR screening with a spin-labeled first-site ligand allows detecting ligands that bind to the target protein simultaneously with and in the vicinity of the first-site ligand. The paramagnetic relaxation enhancement on protons by the unpaired electron of the spin label is depending on the distance between spin label and the proton of interest and therefore reveals precious information for the design of the spacer to link the two ligands.[15] In the case of MAG, Shelke *et al.* identified 5-nitroindole as second-site ligand.[13] The optimal spacer length was evaluated by *in situ* click chemistry,[16] leading to antagonist **1** with an affinity of 190 nM (Figure 1, Table 1).[13]

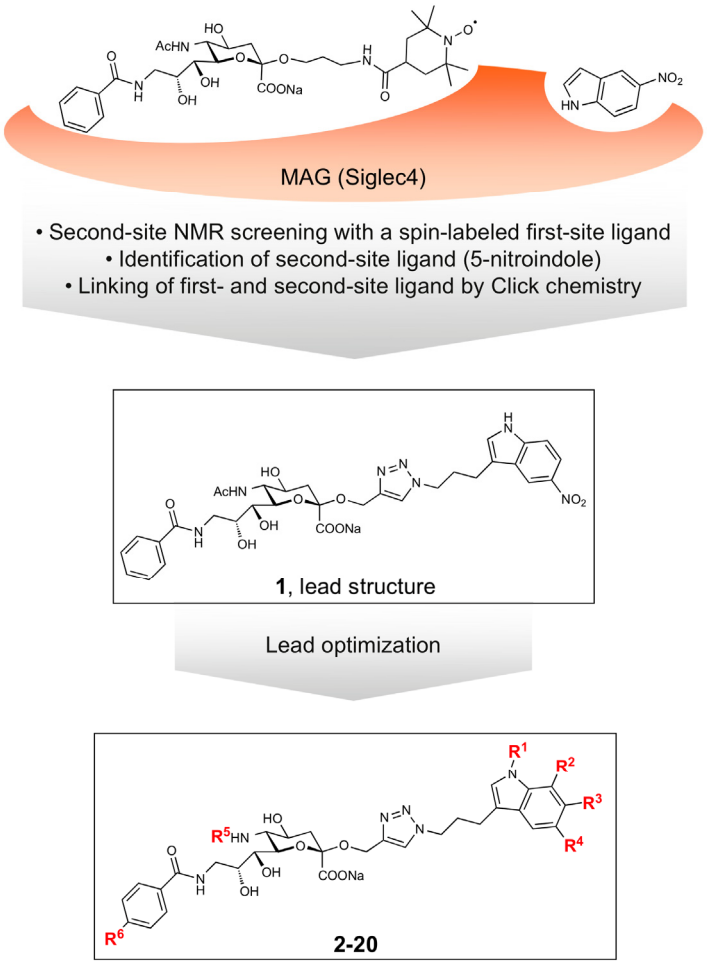

Figure 1. Lead identification by NMR-based screening followed by lead optimization.

In this communication, we modified substituents of the indole moiety (R^1 to R^4), the 5-position of sialic acid (R^5) and the *para*-position of the terminal benzamide (R^6). For the indole moiety, the effect of electron density as well as the enlargement of the hydrophobic surface was studied. The 5-position of sialic acid was modified to optimize the hydrophobic contact with tryptophane. Finally, *para*-substituted benzamides in the terminal position of the gycerol side chain of sialic acid have previously been shown to enhance the affinity of MAG antagonists.[11,17] The binding affinities of antagonists **2**-**20** were determined by surface plasmon resonance experiments. Furthermore, molecular mechanic studies were conducted to rationalize the binding process and the effect of indole substituents was scrutinized by testing the ligands with a MAG mutant with a hapten binding assay.[9-11] Finally, the thermodynamic profile of the most potent antagonists was investigated by isothermal titration calorimetry (ITC).

Synthesis

For the linking of the first- (sialosides **21** and **22**) and the second-site ligands (indoles **26a**-**o**, **33** & **34**) a copper(I)-catalyzed Huisgen 1,3-dipolar cycloaddition was applied (Schemes 4 & 5).[18] Sialoside **21**[13] was synthesized according to a reported procedure. The synthesis of sialosides **22a** & **22b** is summarized in Scheme 5. The synthesis of the various indoles was accomplished by following three different approaches (Schemes 1-3).

Synthesis of indoles 25a-o, 33 and 34. In more detail, 3- and 3,5-substituted indoles were synthesized by reacting hydrazine derivatives **23a**-**e** with 3,4-dihydro-2*H*-pyran under modified Fisher indolization conditions (→ **24a**-**e**) as earlier described by Campos *et al*.[19] Applying similar conditions yielded the indoles **24f**-**k**. Afterwards, the primary alcohols were converted into the corresponding azides **26a**-**k** by using the Appel reaction (Scheme 1).[20,21]

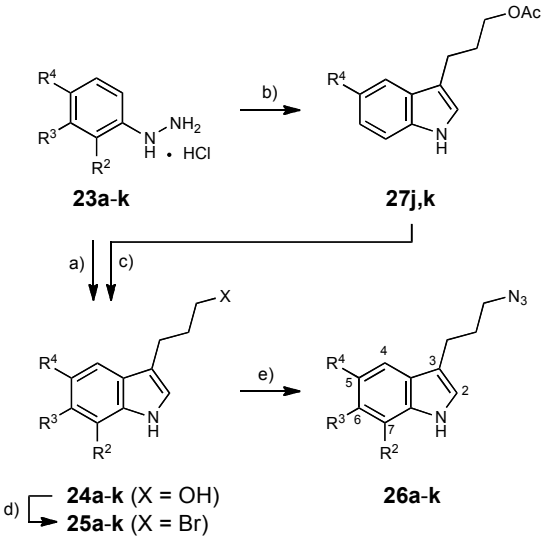

26	a	b	c	d	e	F	g	h	i	j	k
R^2	H	H	H	H	Me	H	H	H	Cl	H	H
R^3	H	H	H	H	H	Cl	H	H_2C —	H	H	H
R^4	H	OMe	Cl	F	H	H	^{i}Pr	H_2C — H_2C —	H	CN	SO_2Me

Scheme 1. a) 3,4-Dihydro-2*H*-pyran, DMAc, 4% aq. H_2SO_4, 100 °C (11-90%); b) 3,4-dihydro-2*H*-pyran, AcOH, conc. aq. HCl; c) NaOMe/MeOH (**24j**: 27%; **24k**: 42%); d) PPh_3, CBr_4, CH_3CN; e) NaN_3, DMF (16-85%, 2 steps).

Starting from intermediate **24a**, 3,6-disubstituted indoles were obtained after protection of the free alcohol (→ **28**[22]) and the indole-amine (→ **29**) by performing Friedel-Crafts acylation. Subsequent deprotection (→ **24l**, **m**) and conversion of the primary alcohol into the azide yielded the desired indole derivatives (→ **26l**, **m**) for click chemistry (Scheme 2).

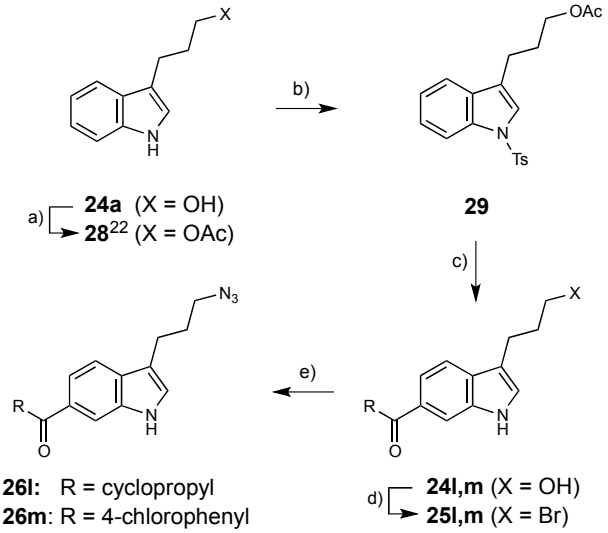

Scheme 2. a) Ac_2O, DMAP, pyridine (92%); b) TsCl, NaH, THF (70%); c) (i) RCOCl, $AlCl_3$, CH_3NO_2, (ii) 6 M NaOH, MeOH (**24l**: 61%; **24m**: 47%, yields refer to inseparable mixtures of 5- and 6-substituted indoles); d) PPh_3, CBr_4, DMF, 50 °C; e) DMF, NaN_3, 50 °C (**26l**: 36%; **26m**: 37%, two steps).

In the case of 1,3,5- and 3,5-substituted indoles, having electron-withdrawing substituents in 5'-position (Scheme 3), azide **26n** was synthesized by reacting 2-iodo-aniline derivative **30n** with **31** under Larock indole conditions[21,23] (→ **32n**). After removal of the silyl protecting group, the alcohol (→ **24n**) was converted into the desired azide (→ **26n**). Starting from **26o**[13] *N*-alkylation was performed using the corresponding alkyl iodides and potassium hydroxide as base to obtain **33** and **34**.

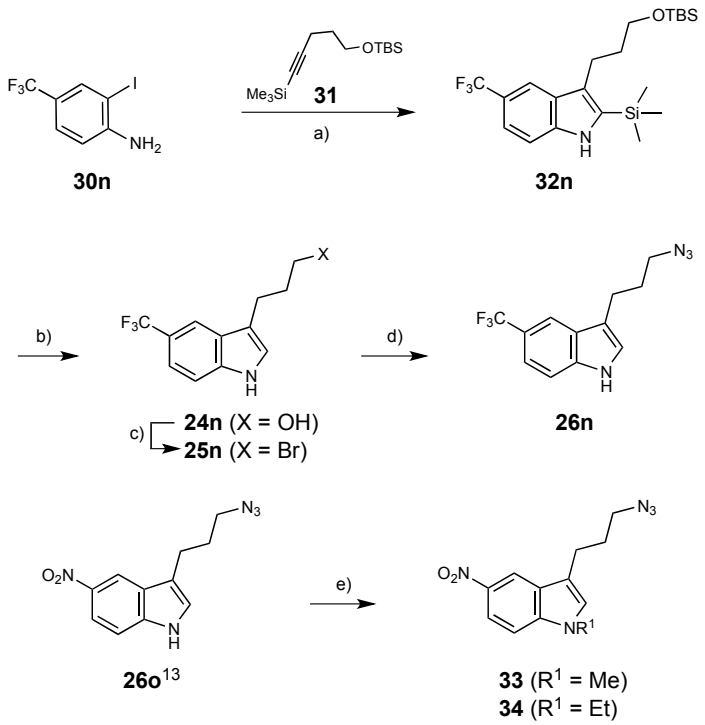

Scheme 3. a) $Pd(OAc)_2$, LiCl, KOAc, DMF, 70 °C; b) 48% HF, CH_3CN, rt (69%, 2 steps); c) PPh_3, CBr_4, CH_3CN; d) DMF, NaN_3, rt (80%, 2 steps); e) R^2I, KOH, DMF (**33**: 94%; **34**: 92%).

Copper(I)-catalyzed Huisgen 1,3-dipolar cycloaddition. Finally, with sialoside **21**[13] and the various substituted indole derivatives in hand, the final compounds **2**-**8** were synthesized applying Cu(I)-catalyzed click-conditions as shown in Scheme 4.

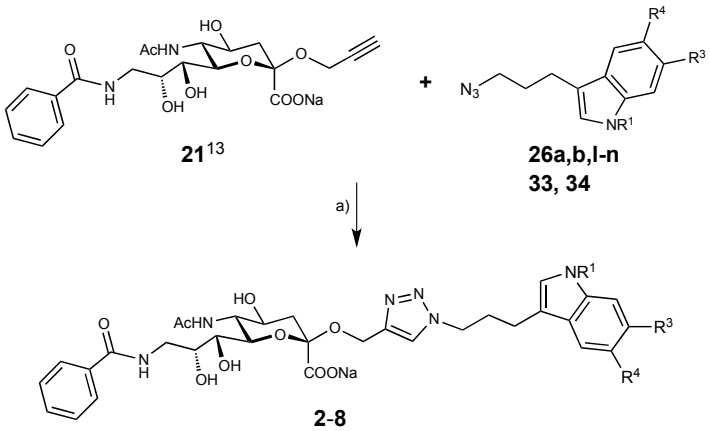

Triazole	2	3	4	5	6	7	8
Indole	26a	26b	26l	26m	26n	33	34
R^1	H	H	H	H	H	Me	Et
R^3	H	H		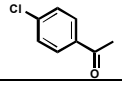	H	H	H
R^4	H	OMe	H	H	CF_3	NO_2	NO_2

Scheme 4. a) $CuSO_4 \cdot 5H_2O$, sodium ascorbate, H_2O/*t*-BuOH 1:1, rt (47-80%).

Earlier SAR studies showed that introduction of fluoroacetamide in 5-position leads to a distinct improvement of the binding affinity[5e,11,17] and therefore we decided to incorporate this modification into compound **1** (Scheme 5). Intermediate **36** was obtained from **35**[13] by cleavage of the *N*-acetate in 5-position followed by Boc-protection. After deprotection (→ **37**), selective fluoroacetylation was performed to give **38**. Afterwards, the azide was transformed into benzylamide or *p*-chlorobenzylamide, respectively, under modified Staudinger conditions (→ **39a**, **b**). After deprotection (→ **22a**, **b**) the test compounds **9**-**20** were obtained by click reaction with indole derivatives **26b**-**k**, **o**.

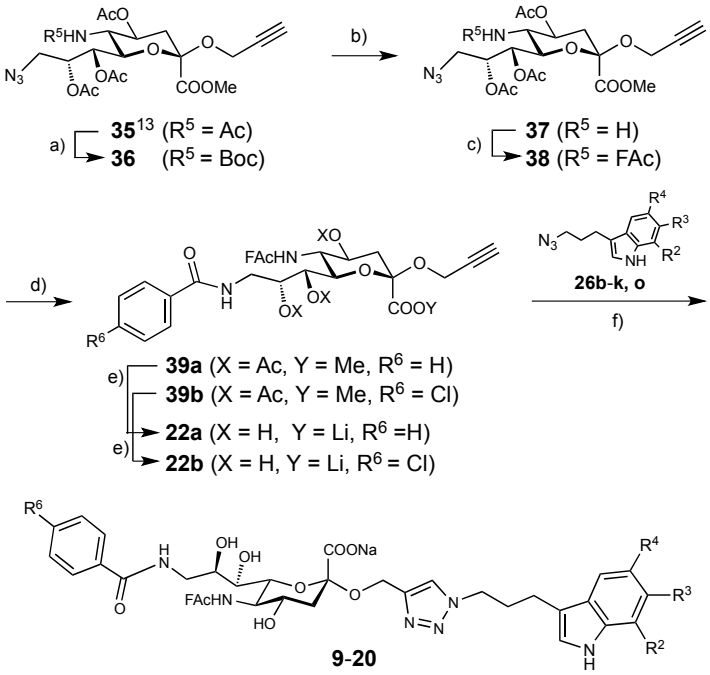

Triazole	9	10	11	12	13	14	15	16	17	18	19	20
Indole	26b	26c	26d	26e	26f	26g	26h	26i	26j	26k	26o	26o
R^2	H	H	H	Me	H	H	H	Cl	H	H	H	H
R^3	H	H	H	H	Cl	H	H_2C — H_2C H_2C —	H	H	H	H	H
R^4	OMe	Cl	F	H	H	^{i}Pr		H	CN	SO_2Me	NO_2	NO_2
R^6	Cl	Cl	Cl	Cl	Cl	Cl	Cl	Cl	Cl	Cl	H	Cl

Scheme 5. a) i. Boc_2O, DMAP, THF; ii. $N_2H_4{\cdot}H_2O$, MeOH; iii. Ac_2O, DMAP, pyridine (50%); b) PhOH, TMSCl, DCM, rt (70%); c) FCH_2COCl, NEt_3, DMAP, THF (43%); d) PPh_3, RCOCl, DCE, rt (**39a**: 52%; **39b**: 65%); e) 10% aq. LiOH, THF/H_2O (**22a**: 80%); **22b**: 50%); f) i. (**26b-k**, **o)**, $CuSO_4{\cdot}5H_2O$, sodium ascorbate, $H_2O/^t$BuOH 1:1, rt; ii. Dowex 50X8 (Na^+ form) (**9-20**: 16-80%).

Biological evaluation of antagonists 1-20. To evaluate the binding properties of the MAG antagonists surface plasmon resonance (SPR) experiments[11]

and a hapten inhibition assay[24] were used. For SPR experiments, recombinant protein, consisting of the three *N*-terminal domains of MAG and the Fc part of human IgG (MAG_{d1-3}-Fc)[24] was immobilized on polyclonal anti-Fc antibody, which was covalently bound to the chip surface. A reference cell, providing only antibody was used for compensation of unspecific binding to the matrix. The test compounds were dissolved in running buffer and injected over the surface. The obtained sensorgrams were fitted according to a 1:1 binding model.

Critical micelle concentration (CMC). Concerns that our test compounds might form micelles in aqueous solution or show surface activity were addressed by determining the critical micelle concentration (CMC) with surface tension measurements using a wire probe tensiometer on a series of different analyte concentrations. The expended energy to pull the wire probes out of a solution corresponds to the surface pressure (mN/m), which is inversely proportional to the surface tension. Due to the fact that the surface tension changes strongly with raising concentrations of a surface-active analyte and remains relatively constant as soon as micelles are being formed, the CMC can be obtained with a dilution series. In the case of our MAG antagonists no activity up to 1 mM was observed, thus excluding a possible influence of micelles formed by the test compounds on the affinity measurements.

The affinities (Table 1) revealed that *N*-alkylation of 5'-nitroindole with methyl ($\rightarrow$ **7**, entry 2) or ethyl ($\rightarrow$ **8**, entry 3) led to a slight decrease in affinity, whereas substituents in the 6- and 7-position of the indole moiety (entries 18-20) improved affinity by a factor of 2.

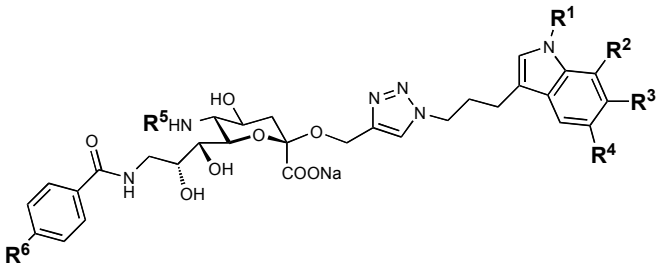

Table 1. Overview on affinities of antagonists **1**-**20**, determined by surface plasmon resonance.

Entry	Compound	R^1	R^2	R^3	R^4	R^5	R^6	K_D [nM]
1	**1**	H	H	H	NO_2	Ac	H	190
2	**7**	Me	H	H	NO_2	Ac	H	445
3	**8**	Et	H	H	NO_2	Ac	H	333
4	**2**	H	H	H	H	Ac	H	267
5	**3**	H	H	H	OMe	Ac	H	322
6	**6**	H	H	H	CF_3	Ac	H	354
7	**4**	H	H		H	Ac	H	300
8	**5**	H	H	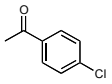	H	Ac	H	75
9	**19**	H	H	H	NO_2	FAc	H	50
10	**20**	H	H	H	NO_2	FAc	Cl	53
11	**10**	H	H	H	Cl	FAc	Cl	48
12	**11**	H	H	H	F	FAc	Cl	67
13	**17**	H	H	H	CN	FAc	Cl	66
14	**18**	H	H	H	SO_2Me	FAc	Cl	33
15	**9**	H	H	H	OCH_3	FAc	Cl	79
16	**14**	H	H	H	$CH(CH_3)_2$	FAc	Cl	101
17	**15**	H	H	$-CH_2CH_2CH_2-$		FAc	Cl	98
18	**13**	H	H	Cl	H	FAc	Cl	57
19	**16**	H	Cl	H	H	FAc	Cl	92
20	**12**	H	CH_3	H	H	FAc	Cl	96

The replacement of the nitro group by hydrogen (→ **3**, entry 5), trifluoromethyl (→ **6**, entry 6) or by the electron-donating methoxy-group decreased the affinity. These observations suggest that the nitro group's contribution to affinity is not related to its electron withdrawing capacity but rather a beneficial polar interaction with the protein. Next, substituents with increased lipophilic surfaces were introduced at the 6'-position of the indole moiety. No beneficial effect was observed for

cyclopropanecarbonyl (→ **4**, entry 7), however a gain in affinity by a factor of 3 resulted for 4-chlorobenzoyl (→ **5**, entry 8). However, due to the low solubility of antagonist **4** and **5**, modifications in the 6'-position were discontinued.

Earlier studies have shown an improvement in binding affinity upon insertion of fluoroacetamide in the 5-position of sialic acid derivatives.[11,17] This modification turned out to be successful when applied to lead compound **1**, leading to a three-fold improved affinity (→ **19**, entry 9). However, the reported beneficial effect for the replacement of the benzamide in the 9-position of the Neu5Ac moiety by *para*-chlorobenzamide[9] (→ **20**, entry 10) could not be observed. Based on antagonist **20**, we revisited our search for the replacement of the nitro group exhibiting a toxic potential[25] and substituents in the 6- and 7-position of the indole moiety. From the many explored substituents (see entries 11 to 20) methyl sulfone yielded the most active MAG antagonist with a K_D of 33 nM.

Isothermal titration calorimetry (**ITC**). We performed ITC measurements of lead **1** and two of the most active compounds **5** and **19** in order to gain further insight into the thermodynamic parameters $\Delta H°$, $\Delta S°$, and $\Delta G°$ of the binding event (Table 2). A solution of the ligands (**1**, **5**, and **19**) in HBS-E buffer was injected into a solution of MAG_{d1-3}-Fc[24] (HBS-E buffer) at 25 °C. The experimental data were fitted to a theoretical titration curve (one site binding model) using *Origin version 7* software (MicroCal). $\Delta H°$ and K_D are measured and $\Delta S°$ and $\Delta G°$ calculated according to equation (1)

$$\Delta G° = \Delta H° - T\Delta S° = RT \ln K_D = -RT \ln K_A \qquad (1)$$

With ITC, the high affinity of the antagonists could be reproduced, however, compared to SPR, the affinities were consistently weaker. As in most cases of carbohydrate-lectin interactions, the binding is enthalpy driven.[26]

Table 2. The thermodynamic parameters of **1**, **5**, and **19** are shown. $\Delta G°$ and $-T\Delta S°$ were calculated according to equation 1. *N* represents the stoichiometry.

Compound	N	K_D [nM]	$\Delta G°$ [kJ mol^{-1}]	$\Delta H°$ [kJ mol^{-1}]	$-T\Delta S°$ [kJ mol^{-1}]
1	0.91 ± 0.07	589 ± 30	–35.6 ± 0.2	–34.0 ± 0.9	–1.6 ± 0.7
5	0.91 ± 0.04	132 ± 20	–39.3 ± 0.4	–51.9 ± 0.1	+12.6 ± 0.2
19	1.05 ± 0.11	171 ± 50	–38.7 ± 0.7	–32.5 ± 0.6	–6.2 ± 1.3

When comparing compound **1** and **5**, the difference $\Delta G°$ results from $\Delta S°$, whereas the $\Delta H°$ values are almost equal. This could be the result, at least partially, of a more favorable desolvation entropy as **5** is more lipophilic than **1**. In contrast, the enhanced affinity of compound **19** compared to compound **1** is related to a more favorable enthalpy that is partially compensated by an unfavorable entropy term. Since 4-chlorbenzylacyl in 6'-position of the indole forms additional interactions, enthalpy is increased but partially compensated because of the reduced conformational freedom of the ligand.[27]

Molecular modeling studies. For an improved understanding of the biological data, compounds **2** and **19** and were docked to a homology model of MAG[10,11] and a molecular-dynamics simulation in aqueous solution was performed (4 ns at 300 K) using *Desmond*.[28] In both antagonist-protein complexes, the sialic acid core established the crucial interactions responsible for recognition and binding, *i.e.* a salt bridge of the carboxylate with Arg118[17] and a hydrophobic contact of the *N*-acetate/*N*-fluoroaceate in the 5-position with Trp22.[17] In addition, hydrogen bonds between 5-NH and the carbonyl of Gln126, 8-OH and Thr128 and 9-NH and Tyr125 are present in both antagonist-protein complexes. These interactions are in full agreement with those observed by X-ray crystallography of synthetic sialosides complexed with Siglec-1[29] and Siglec-7.[30]

In the case of **19**, the 5'-nitroindole is embedded in a hydrophobic pocket lined by the residues Tyr60, Tyr69 and Tyr116. The indole-moiety is sandwiched by Tyr69 and Tyr116, displaying an angle to Tyr69 of 17° and to Tyr116 an angle of 39° (Figure 2). It is noteworthy, that the π-π interactions are maintained during the whole simulation. Furthermore, the nitro substituent interacts with Lys67 by dipolar interactions and seems to stabilize the position of the indole. The nitro group is in a distance range of 2.6 to 5.0 Å, a value also found in other protein-ligand complexes.[31] In the case of the unsubstituted indole **2** no π-π interactions were observed (Figure 2B). The angles of both tyrosines are around 70-90° and the dispersion is clearly higher. Furthermore, the mobility of the linker was strikingly increased during the dynamic simulation. The nevertheless good binding affinity might be explained that no constraints raise from the linker positioning and that the core interactions might be slightly better established.

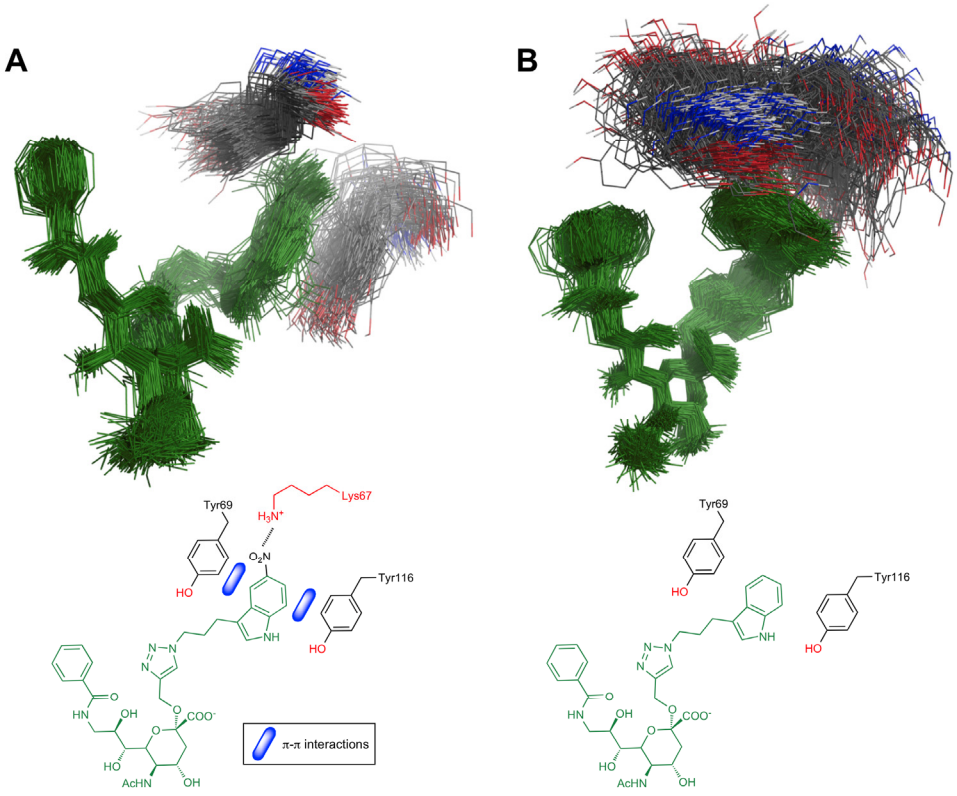

Figure 2. Conformations of the antagonists **2** and **19** and the position of Tyr69 and Tyr116 during the dynamic simulation were clustered. **A**) 5'-Nitroindole interacts via π-π interactions with Tyr69 and Tyr116 resulting in a locked conformation of the linker. In addition, a dipolar interactions with Lys67 can be established. **B**) Antagonist **2**, lacking the 5'-nitro substituent, is not sandwiched and consequently shows increased mobility of the linker.

In summary, these findings are in agreement with the observation that replacement of the 5'-nitro group by other substituents decreases the affinity (e.g. → **6**, entry 6), as the polar interaction with Lys67 is no longer possible. Furthermore, modifications in the 6'-position could be aligned into the hydrophobic cleft and additional hydrophobic interactions (→ **5**, entry 8) contribute to the binding affinity.

MAG mutant K67A. In order to elucidate the role of the nitro group experimentally, compounds **1** and **2** were tested with the MAG mutant where Lys67 is replaced by alanine (K67A) in a hapten inhibition assay.[24] The molecular docking experiments of sialoside **19** suggested an interaction of the nitro group of 5'-nitroindole with Lys67. To elucidate this interaction, affinities of the sialosides **1** and **2** for MAG_{d1-3}-Fc wt and the MAG mutant K67A were compared in hapten inhibition assays. The concentration of **1** and **2** required for 50 % inhibition (IC_{50}) was determined in microtiter plates coated with fetuin as the binding target for MAG_{d1-3}

Fc-chimeras.[24] Relative inhibitory potencies (rIP) were calculated as ratio of the IC_{50} of the compound of interest, *i.e.* **1** and **2** and the IC_{50} of **2** used as reference compound. For each compound at least three independent titrations were performed with seven or eight concentrations in triplicates (Figure 3 & Table 3). Both substances exhibit IC_{50} values in the low nanomolar range. The presence of the nitro group in sialoside **1** leads to a 4.25-fold stronger inhibition compared to **2** for MAG_{d1-3}-Fc wt, whereas for MAG_{d1-3}-Fc K67A this increase is only 2.14-fold. This supports the hypothesis that Lys67 contributes to binding via a polar interaction with the nitro group of compound **1**, as suggested in Figure 2A. However, additional parameters are likely to support binding, since the introduction of the nitro group also enhances affinity of the K67A mutant.

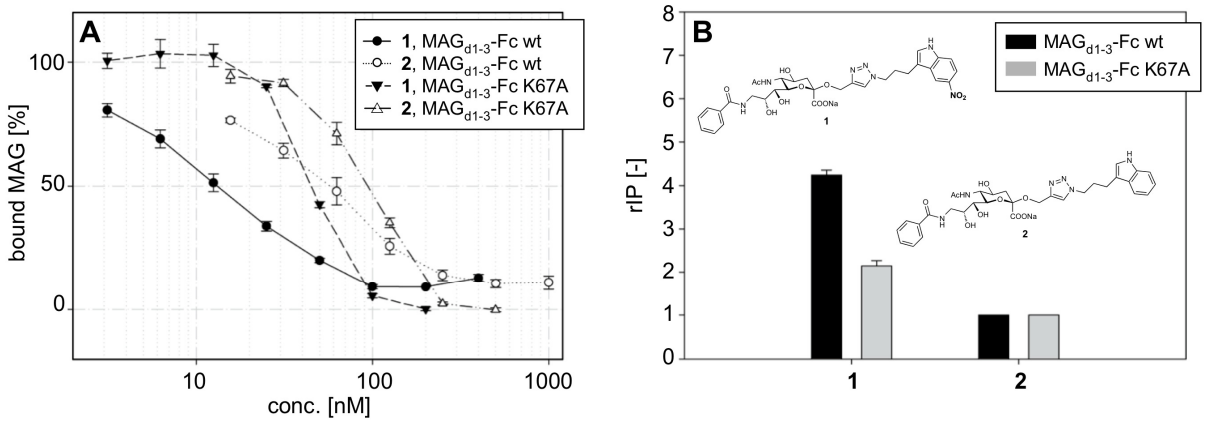

Figure 3. A) Inhibition curves of MAG_{d1-3}-Fc wild type (wt) and mutant K67A for the determination of IC_{50}-values by hapten inhibition assay. **B**) rIP of sialosides **1** and **2** for both Fc-chimeras MAG wt and K67A. Sialoside **2** (without nitro residue) was used as reference compound (rIP = 1) to obtain a factor of enhanced affinity related to the introduction of the nitro group.

Table 3. Comparison of the half maximal inhibitory concentrations (IC_{50}) and relative inhibitory potencies (rIP) for MAG_{d1-3}-Fc wild type (wt) and mutant K67A inhibited by sialosides **1** and **2** determined by hapten inhibition assay.[24]

Compound	**MAG_{d1-3}-Fc wt**		**MAG_{d1-3}-Fc K67A**	
	IC_{50} [nM]	rIP	IC_{50} [nM]	rIP
1	13 ± 2	4.25 ± 0.19	41 ± 5	2.14 ± 0.21
2	53 ± 9	1.00 ± 0.00	88 ± 4	1.00 ± 0.00

Summary and Conclusions

The lead compound **1** of our study showed nanomolar binding affinity (Table 1, entry 1), however, suffers from two metabolic soft spots, *i.e.* the unsubstituted benzamide prone to oxidation and the nitro group exhibiting a toxic potential.[27] We therefore replaced the benzamide by *p*-chlorobenzamide, which showed a comparable binding affinity as indicated by the antagonists **19** and **20** (entries 9 &10). Furthermore, we examined a series of ligands (entries 11-20) where the nitro group in the 5'-position of the nitroindole moiety was replaced by either halogen-, cynano-, methoxy-, alkyl- and methylsulfonyl-substituents. In agreement with our findings with the MAG-mutant K67A, *i.e.* that the nitro group establishes a polar interaction with Lys67, the methylsulfonyl substituent ($\rightarrow$ **18**) yielded the most active antagonist. Surprisingly, antagonists **10**, **11** and **17** (entries 11-13) showed comparable binding affinities (48-67 nM), probably also related to polar interactions with Lys67. Finally, introduction of substituents in the 7'-position (entries 19 & 20) or lipophilic substituents in the 5'-position (entries 16 & 17) led to a decreased binding affinity. Overall, we have identified with compound **18** a low nanomolar MAG antagonist ready for extended cellular and in vivo evaluation.

Experimental Procedure

Chemistry. NMR spectra were recorded on a Bruker Avance DMX-500 (500 MHz) spectrometer. Assignment of ^{1}H and ^{13}C NMR spectra was achieved using 2D methods (COSY, HSQC, TOCSY). Chemical shifts are expressed in ppm using residual $CHCl_3$, CHD_2OD and HDO as references. Optical rotations were measured using Perkin-Elmer Polarimeters 241 and 341. MS analyses were carried out using a Waters Micromass ZQ Detector system. The spectra were recorded in positive or negative ESI mode. The HPLC/HRMS analyses were carried out using an Agilent 1100 equipped with a photodiode array detector and a Micromass QTOF I equipped with a 4 GHz digital-time converter. All target compounds exhibit a purity of $\geq$ 95%. Reactions were monitored by TLC using glass plates coated with silica gel 60 F_{254} (Merck) and visualized by using UV light and/or by charring with a molybdate solution (a 0.02 M solution of ammonium cerium sulfate dihydrate and ammonium molybdate tetrahydrate in aqueous 10% H_2SO_4). Column chromatography was performed on silica gel (Uetikon, 40-60 mesh). Methanol was dried by refluxing with sodium methoxide and distilled immediately before use. Pyridine was freshly distilled under argon over CaH_2. Dichloromethane (DCM), dichloroethane (DCE), acetonitrile (MeCN), nitromethane, toluene, and benzene were dried by filtration over Al_2O_3 (Fluka, type 5016 A

basic). Molecular sieves (3 Å) were activated under vacuum at 500 °C for 2 h immediately before use. If not stated otherwise, all starting materials were commercially available.

*General procedure A: Synthesis of indoles (**24f-i**).* To a solution of hydrazine-HCl **23f**-**i** (2.50 mmol) and *N*,*N*-dimethylacetamide (DMAc, 10 mL) in aq. 4% H_2SO_4 (4 mL), 3,4 dihydro-2*H*-pyran (2.50 mmol) was added dropwise. The reaction was stirred for 2 h, then cooled to rt, extracted with EtOAc (20 mL) and washed with water (3 × 20 mL). The combined aqueous layers were extracted with EtOAc (20 mL) and the combined organic layers were dried over Na_2SO_4, filtered and evaporated. The crude product was purified by chromatography on silica (petroleum ether/EtOAc).

*General procedure B: Appel reaction (**26a-n**).* The alcohol **24a**-**n** (1.0 eq) was dissolved in dry MeCN and cooled to 0 °C. Afterwards, triphenylphosphine (1.2-1.5 eq) was added, followed by successive addition of CBr_4 (1.2-1.5 eq). The mixture was stirred at rt for 2 h and then diluted with EtOAc, washed with H_2O and brine, and dried over Na_2SO_4. The solvents were removed *in vacuo* and the residue was purified by chromatography on silica (petroleum ether/EtOAc) to yield the corresponding bromide **25a**-**n**. Afterwards, to a solution of bromide (1.0 eq) in dry DMF, NaN_3 (2.0-5.0 eq) was added at rt and stirring was continued overnight. The solvent was removed under reduced pressure and the residue was purified by chromatography on silica (petroleum ether/EtOAc) to afford azides **26a**-**n**.

*General procedure C: Triazole formation by click reaction (**2-20**).* To a solution of acetylene **21** or **22a**, **b** (1.0 eq) in degassed ^{t}BuOH:H_2O (v/v, 1:1), azide **26a**-**o**, **33** or **34** (1.2-1.5 eq), $CuSO_4 \cdot 5H_2O$ (0.25 eq) and sodium ascorbate (0.5 eq) were added. The reaction mixture was stirred at rt overnight. Then, the solvents were removed under reduced pressure and the residue was purified by reversed phase chromatography (Merck LiChroprep RP-18, 5% gradient of MeOH in water), Dowex 50X8 (Na^+ type) ion-exchange chromatography and P2 size-exclusion chromatography to afford the pure test compounds **2**-**20** after a final lyophilization from water.

The indoles **24f**-**k** were synthesized according to the procedure published by Campos *et al*. [19]

*3-(6-Chloro-1H-indol-3-yl)-propan-1-ol (**24f**).* Prepared from **23f** (400 mg, 2.23 mmol) according to general procedure A. Yield: 53 mg, 11%. ^{1}H NMR (500 MHz, $CDCl_3$): δ = 1.94-2.03 (m, 2H, CH_2), 3.01-3.09 (m, 2H, CH_2), 3.73 (t, J = 6.5 Hz, 2H, CH_2), 6.95 (s, 1H, CH_{ar}), 7.00-7.08 (m, 2H, CH_{ar}), 7.16-7.23 (m, 1H, CH_{ar}), 8.27 (s, 1H, NH); ^{13}C NMR (126 MHz, $CDCl_3$): δ = 22.7, 34.6, 62.7 (3 CH_2), 110.1, 116.5, 120.5, 122.6, 123.1, 124.3, 126.6, 138.1 (C-Ar); ESI-MS: *m/z* calcd for $C_{11}H_{13}ClNO$ $[M+H]^+$: 210.1, found: 209.9.

*3-(5-Isopropyl-1H-indol-3-yl)-propan-1-ol (**24g**).* Prepared from **23g** (300 mg, 1.61 mmol) according to general procedure A. Yield: 152 mg, 43%. ^{1}H NMR (500 MHz, $CDCl_3$): δ

= 1.34 (d, *J* = 6.9 Hz, 6H, 2 CH_3), 1.94-2.07 (m, 2H, CH_2), 2.88 (t, *J* = 7.5 Hz, 2H, CH_2), 3.05 (hept, *J* = 6.9 Hz, 1H, CH), 3.77 (t, *J* = 6.4 Hz, 2H, CH_2), 6.98 (s, 1H, CH_{ar}), 7.12 (dd, *J* = 1.4, 8.4 Hz, 1H, CH_{ar}), 7.30 (d, *J* = 8.4 Hz, 1H, CH_{ar}), 7.46 (s, 1H, CH_{ar}); ^{13}C NMR (126 MHz, $CDCl_3$): *δ* = 21.6 (CH_2), 24.9 (2C, 2 CH_3), 33.1 (CH_2), 34.5 (CH), 63.0 (CH_2), 111.1, 115.9, 116.0, 121.4, 121.6, 127.7, 135.2, 140.2 (C-Ar); ESI-MS: *m/z* calcd for $C_{14}H_{20}NO$ $[M+H]^+$: 218.2, found: 218.0.

*3-(1,5,6,7-Tetrahydrocyclopenta[f]indol-3-yl)-propan-1-ol (**24h**).* Prepared from **23h** (200 mg, 1.08 mmol) according to general procedure A. Yield: 140 mg, 60%. ^{1}H NMR (500 MHz, $CDCl_3$): *δ* = 1.86-1.94 (m, 2H, CH_2), 2.04 (p, *J* = 7.3 Hz, 2H, Cyc-CH_2), 2.74 (t, *J* = 7.4 Hz, 2H, CH_2), 2.90 (t, *J* = 7.3 Hz, 4H, 2 Cyc-CH_2), 3.64 (t, *J* = 6.4 Hz, 2H, CH_2), 6.82 (d, *J* = 2.0 Hz, 1H, CH_{ar}), 7.09 (s, 1H, CH_{ar}), 7.34 (s, 1H, CH_{ar}), 7.70 (s, 1H, NH); ^{13}C NMR (126 MHz, $CDCl_3$): *δ* = 22.7 (CH_2), 26.9, 32.6, 32.7 (3 Cyc-CH_2), 33.1 (CH_2), 63.0 (CH_2), 106.7, 113.9, 118.9, 121.0, 126.8, 136.1, 136.1, 139.4 (C-Ar); ESI-MS: *m/z* calcd for $C_{14}H_{18}NO$ $[M+H]^+$: 216.1, found: 215.9.

*3-(7-Chloro-1H-indol-3-yl)-propan-1-ol (**24i**).* Prepared from **23i** (300 mg, 1.68 mmol) according to general procedure A. Yield: 80 mg, 22%. ^{1}H NMR (500 MHz, $CDCl_3$): *δ* = 1.91-2.02 (m, 2H, CH_2), 2.84 (t, *J* = 7.4 Hz, 2H, CH_2), 3.71 (t, *J* = 6.4 Hz, 2H, CH_2), 6.92-7.13 (m, 2H, CH_{ar}), 7.17 (d, *J* = 7.3 Hz, 1H, CH_{ar}), 7.50 (d, *J* = 7.9 Hz, 1H, CH_{ar}), 8.16 (s, 1H, NH); ^{13}C NMR (126 MHz, $CDCl_3$): *δ* = 21.6, 33.1, 62.7 (3 CH_2), 116.8, 117.4, 117.8, 120.2, 121.6, 122.1, 129.2, 133.8 (C-Ar); ESI-MS: *m/z* calcd for $C_{11}H_{13}ClNO$ $[M+H]^+$: 210.1, found: 209.9.

*3-(3-Azidopropyl)-1H-indole (**26a**).* Prepared from **24a** (494 mg, 2.82 mmol) according to general procedure B. Yield: 277 mg, 50% (two steps), yellow oil. ^{1}H NMR ($CDCl_3$, 500 MHz): *δ* = 2.02 (m, 2H, CH_2), 2.88 (t, *J* = 7.5 Hz, 2H, CH_2), 3.34 (t, *J* = 7.0 Hz, 2H, CH_2), 7.01 (s, 1H, CH_{ar}), 7.15 (t, *J* = 7.0 Hz, 1H, CH_{ar}), 7.22 (t, *J* = 7.0 Hz, 1H, CH_{ar}), 7.37 (d, *J* = 8.0 Hz, 1H, CH_{ar}), 7.61 (d, *J* = 7.5 Hz, 1H, CH_{ar}), 7.99 (s, 1H, NH); ^{13}C NMR ($CDCl_3$, 126 MHz): *δ* = 22.1, 29.2, 50.9 (3 CH_2), 111.1, 115.0, 118.8, 119.3, 121.5, 122.1, 127.3, 136.3 (C-Ar); IR (film): *ν* = 3415, 2929, 2097, 1456, 742 cm^{-1}.

*3-(3-Azidopropyl)-5-methoxy-1H-indole (**26b**).* Prepared from **24b** (523 mg, 2.55 mmol) according to general procedure B. Yield: 396 mg, 68% (two steps), yellow oil. ^{1}H NMR ($CDCl_3$, 500 MHz): *δ* = 2.01 (m, 2H, CH_2), 2.85 (t, *J* = 7.0 Hz, 2H, CH_2), 3.36 (t, *J* = 7.0 Hz, 2H, CH_2), 3.89 (s, 3H, OMe), 6.88 (dd, *J* = 9.0, 2.5 Hz, 1H, CH_{ar}), 7.00 (d, *J* = 2.5 Hz, 1H, CH_{ar}), 7.05 (d, *J* = 2.0 Hz, 1H, CH_{ar}), 7.27 (d, *J* = 3.5 Hz, 1H, CH_{ar}), 7.87 (s, 1H, NH); ^{13}C NMR ($CDCl_3$, 126 MHz): *δ* = 22.1, 29.1, 50.8 (3 CH_2), 55.9 (OMe), 100.6, 111.8, 112.2, 114.7, 122.3, 127.7, 131.5, 153.9 (C-Ar); IR (film): *ν* = 3415, 2938, 2097, 1485, 1214 cm^{-1}.

*3-(3-Azidopropyl)-5-chloro-1H-indole (**26c**).* Prepared from **24c** (99.4 mg, 0.474 mmol) according to general procedure B. Yield: 86 mg, 77% (two steps). ^{1}H NMR (500 MHz,

$CDCl_3$): δ = 1.94 (p, J = 7.0 Hz, 2H, CH_2), 2.78 (t, J = 7.4 Hz, 2H, CH_2), 3.28 (t, J = 6.7 Hz, 2H, CH_2), 6.99 (d, J = 1.9 Hz, 1H, CH_{ar}), 7.12 (m, 1H, CH_{ar}), 7.22 (d, J = 3.8 Hz, 1H, CH_{ar}), 7.51 (d, J = 1.6 Hz, 1H, CH_{ar}), 7.95 (s, 1H, NH); ^{13}C NMR (126 MHz, $CDCl_3$): δ = 22.2, 29.4, 51.0 (3 CH_2), 112.4, 115.1, 118.6, 122.6, 123.2, 125.4, 128.7, 134.9 (C-Ar); IR (film): ν = 3435, 2929, 2098, 1463 cm^{-1}; ESI-MS: *m/z* calcd for $C_{11}H_{12}ClN_4$ $[M+H]^+$: 235.1, found: 234.8.

*3-(3-Azidopropyl)-5-fluoro-1H-indole (**26d**).* Prepared from **24d** (65.7 mg, 0.340 mmol) according to general procedure B. Yield: 54 mg, 73% (two steps). ^{1}H NMR (500 MHz, $CDCl_3$): δ = 1.83-1.94 (m, 2H, CH_2), 2.70 (t, J = 7.4 Hz, 2H, CH_2), 3.21 (t, J = 6.7 Hz, 2H, CH_2), 6.85 (td, $^3J_{1,2}$ = 2.5 Hz, $^3J_{H,F}$ = 9.0 Hz, 1H, CH_{ar}), 6.92 (s, 1H, CH_{ar}), 7.14 (m, 2H, CH_{ar}), 7.85 (s, 1H, NH); ^{13}C NMR (126 MHz, $CDCl_3$): δ = 22.2, 29.2, 51.0 (3 CH_2), 103.9 (d, $^2J_{C,F}$ = 23.3 Hz, C-4), 110.6 (d, $^2J_{C,F}$ = 26.4 Hz, C-6), 112.0 (d, $^3J_{C,F}$ = 9.7 Hz, C-7), 115.4 (d, $^4J_{C,F}$ = 4.8 Hz, C-8), 123.6 (C-Ar), 127.9 (d, $^3J_{C,F}$ = 9.5 Hz, C-3), 133.0 (C-Ar), 157.9 (d, $^1J_{C,F}$ = 234 Hz, C-5); IR (film): ν = 3429, 2927, 2098, 1485 cm^{-1}; ESI-MS: *m/z* calcd for $C_{11}H_{12}FN_4$ $[M+H]^+$: 219.1, found: 218.9.

*3-(3-Azidopropyl)-7-methyl-1H-indole (**26e**).* Prepared from **24e** (82.0 mg, 0.433 mmol) according to general procedure B. Yield: 64 mg, 70% (two steps). ^{1}H NMR (500 MHz, $CDCl_3$): δ = 1.96-2.08 (m, 2H, CH_2), 2.49 (s, 3H, CH_3), 2.88 (t, J = 7.3 Hz, 2H, CH_2), 3.33 (t, J = 6.7 Hz, 2H, CH_2), 6.97-7.05 (m, 2H, CH_{ar}), 7.08 (td, J = 2.0, 7.4 Hz, 1H, CH_{ar}), 7.47 (d, J = 7.8 Hz, 1H, CH_{ar}), 7.86 (s, 1H, NH); ^{13}C NMR (126 MHz, $CDCl_3$): δ = 16.7 (CH_3), 22.4, 29.5, 51.1 (3 CH_2), 115.7, 116.7, 119.8, 120.5, 121.5, 122.8, 127.0, 136.2 (C-Ar); IR (film): ν = 3418, 2930, 2097 cm^{-1}; ESI-MS: *m/z* calcd for $C_{12}H_{15}N_4$ $[M+H]^+$: 215.1, found: 214.9.

*3-(3-Azidopropyl)-6-chloro-1H-indole (**26f**).* Prepared from **24f** (43.0 mg, 0.205 mmol) according to general procedure B. Yield: 35 mg, 75% (two steps). ^{1}H NMR (500 MHz, $CDCl_3$): δ = 2.00-2.14 (m, 2H, CH_2), 3.10 (t, J = 7.5 Hz, 2H, CH_2), 3.37 (t, J = 6.8 Hz, 2H, CH_2), 7.03 (d, J = 1.9 Hz, 1H, CH_{ar}), 7.09-7.15 (m, 2H, CH_{ar}), 7.24-7.31 (m, 1H, CH_{ar}), 8.07 (s, 1H, NH); ^{13}C NMR (126 MHz, $CDCl_3$): δ = 23.5, 30.9, 51.1 (3 CH_2), 110.1, 115.8, 120.7, 122.8, 123.3, 124.3, 126.6, 138.1 (C-Ar); IR (film): ν = 3429, 2929, 2097, 1437 cm^{-1}; ESI-MS: *m/z* calcd for $C_{11}H_{12}ClN_4$ $[M+H]^+$: 235.1, found: 234.8.

*3-(3-Azidopropyl)-5-isopropyl-1H-indole (**26g**).* Prepared from **24g** (152 mg, 0.700 mmol) according to general procedure B. Yield: 144 mg, 85% (two steps). ^{1}H NMR (500 MHz, $CDCl_3$): δ = 1.32 (d, J = 6.9 Hz, 6H, 2 CH_3), 2.01 (p, J = 6.9 Hz, 2H, CH_2), 2.86 (t, J = 7.3 Hz, 2H, CH_2), 3.03 (hept, J = 6.9 Hz, 1H, CH), 3.34 (t, J = 6.8 Hz, 2H, CH_2), 6.95 (s, 1H, CH_{ar}), 7.11 (dd, J = 1.5, 8.4 Hz, 1H, CH_{ar}), 7.28 (d, J = 8.4 Hz, 1H, CH_{ar}), 7.42 (s, 1H, CH_{ar}), 7.83 (s, 1H, NH); ^{13}C NMR (126 MHz, $CDCl_3$): δ = 22.3 (CH_2), 24.9 (2C, 2 CH_3), 29.4 (CH_2),

34.5 (CH), 51.1 (CH_2), 111.1, 115.0, 115.9, 121.5, 121.9, 127.6, 135.2, 140.3 (C-Ar); IR (film): ν = 3412, 2957, 2096 cm^{-1}; ESI-MS: *m/z* calcd for $C_{14}H_{18}N_4$ $[M]^+$: 242.2, found: 242.1.

*3-(3-Azidopropyl)-1,5,6,7-tetrahydrocyclopenta[f]indole (**26h**).* Prepared from **24h** (36.0 mg, 0.167 mmol) according to general procedure B. Yield: 10 mg, 25% (two steps). ^1H NMR (500 MHz, $CDCl_3$): δ = 1.98 (p, *J* = 7.0 Hz, 2H, CH_2), 2.12 (dq, *J* = 7.3, 14.6 Hz, 2H, Cyc-CH_2), 2.82 (t, *J* = 7.3 Hz, 2H, CH_2), 2.98 (td, *J* = 2.1, 7.2 Hz, 4H, 2 Cyc-CH_2), 3.31 (t, *J* = 6.8 Hz, 2H, CH_2), 6.90 (d, *J* = 2.1 Hz, 1H, CH_{ar}), 7.18 (s, 1H, CH_{ar}), 7.40 (s, 1H, CH_{ar}), 7.75 (s, 1H, NH); ^{13}C NMR (126 MHz, $CDCl_3$): δ = 22.4 (CH_2), 26.9 (Cyc-CH_2), 29.4 (CH_2), 32.7, 33.1 (2 Cyc-CH_2), 51.1 (CH_2), 106.7, 113.8, 114.7, 121.3, 126.7, 136.2, 136.3, 139.5 (C-Ar); IR (film): ν = 3401, 2934, 2094, 1646 cm^{-1}; ESI-MS: *m/z* calcd for $C_{14}H_{17}N_4$ $[M+H]^+$: 241.1, found: 241.0.

*3-(3-Azidopropyl)-7-chloro-1H-indole (**26i**).* Prepared from **24i** (80.0 mg, 0.382 mmol) according to general procedure B. Yield: 10 mg, 16% (two steps). ^1H NMR (500 MHz, $CDCl_3$): δ = 1.91-2.02 (m, 2H, CH_2), 2.84 (t, *J* = 7.4 Hz, 2H, CH_2), 3.31 (t, *J* = 6.7 Hz, 2H, CH_2), 7.04 (t, *J* = 7.8 Hz, 2H, CH_{ar}), 7.18 (d, *J* = 7.6 Hz, 1H, CH_{ar}), 7.48 (d, *J* = 7.9 Hz, 1H, CH_{ar}), 8.17 (s, 1H, NH); ^{13}C NMR (126 MHz, $CDCl_3$): δ = 22.4, 29.4, 51.0 (3 CH_2), 116.5, 116.9, 117.7, 120.4, 121.7, 122.4, 129.0, 133.9 (C-Ar); IR (film): ν = 3427, 2925, 2098, 1437 cm^{-1}; ESI-MS: *m/z* calcd for $C_{11}H_{12}ClN_4$ $[M+H]^+$: 235.1, found: 235.8.

*3-(5-Cyano-1H-indol-3-yl)-propyl acetate (**27j**).* To a mixture of 3,4-dihydro-2*H*-pyran (242 µL, 2.65 mmol) in AcOH (6 mL) and conc. aq. HCl (2 mL) was added **23j** (150 mg, 0.883 mmol) at rt, and the reaction mixture was stirred for 3 h at 100°C. After cooling to rt the reaction mixture was diluted with EtOAc (50 mL) and washed with water (40 mL) and brine (40 mL). The aqueous layers were extracted with EtOAc (40 mL) and the combined organic layers were dried over Na_2SO_4, filtered and evaporated to dryness. Chromatography (petroleum ether/EtOAc, 2:1) of the residue gave **27j** (66 mg, 32%). ^1H NMR (500 MHz, $CDCl_3$): δ = 1.97-2.10 (m, 2H, CH_2), 2.06 (s, 3H, CH_3), 2.82 (t, *J* = 7.4 Hz, 2H, CH_2), 4.11 (t, *J* = 6.5 Hz, 2H, CH_2), 7.11 (m, 1H, CH_{ar}), 7.39 (s, 2H, CH_{ar}), 7.92 (s, 1H, CH_{ar}), 8.40 (s, 1H, NH); ^{13}C NMR (126 MHz, $CDCl_3$): δ = 21.1, 21.2 (CH_2, CH_3), 44.3 (CH_2), 63.9 (CH_2), 102.5, 112.2, 116.6, 121.0, 123.7, 124.7, 125.1, 127.5, 138.2 (C-Ar, CN), 171.4 (CO); IR (film): ν = 3343, 2924, 2219, 1734, 1246 cm^{-1}; ESI-MS: *m/z* calcd for $C_{14}H_{14}NaN_2O_2$ $[M+Na]^+$: 265.1, found: 264.9.

*3-(5-Cyano-1H-indol-3-yl)-propan-1-ol (**24j**).* A solution of **27j** (80.0 mg, 0.330 mmol) in MeOH (2 mL) was treated with freshly prepared NaOMe/MeOH (1.0 eq) for 2 h. Then, the reaction mixture was neutralized with AcOH and evaporated to dryness. Chromatography (petroleum ether/EtOAc, 3:2) of the residue gave **24j** (18 mg, 27%). ^1H NMR (500 MHz, $CDCl_3$): δ = 1.92-1.99 (m, 2H, CH_2), 2.84 (t, *J* = 7.5 Hz, 2H, CH_2), 3.71 (t, *J* = 6.3 Hz, 2H,

CH_2), 7.10 (s, 1H, CH_{ar}), 7.38 (d, *J* = 0.8 Hz, 2H, CH_{ar}), 7.93 (s, 1H, CH_{ar}), 8.49 (s, 1H, NH); ^{13}C NMR (126 MHz, $CDCl_3$): *δ* = 21.2, 33.0, 62.5 (3 CH_2), 102.4, 112.2, 117.2, 121.1, 123.6, 124.9, 125.1, 127.6, 138.2 (CN, C-Ar); IR (film): ν = 3339, 2932, 2220, 1472, 1056 cm^{-1}; ESI-MS: *m/z* calcd for $C_{12}H_{12}NaN_2O$ $[M+Na]^+$: 223.1, found: 222.8.

*3-(3-Azidopropyl)-5-cyano-1H-indole (**26j**).* Prepared from **24j** (30.0 mg, 0.150 mmol) according to general procedure B. Yield: 25 mg, 70% (two steps). ^{1}H NMR (500 MHz, $CDCl_3$): *δ* = 1.90-2.01 (m, 2H, CH_2), 2.84 (t, *J* = 7.4 Hz, 2H, CH_2), 3.32 (t, *J* = 6.7 Hz, 2H, CH_2), 7.12 (d, *J* = 2.0 Hz, 1H, CH_{ar}), 7.33-7.56 (m, 2H, CH_{ar}), 7.92 (s, 1H, CH_{ar}), 8.47 (s, 1H, NH); ^{13}C NMR (126 MHz, $CDCl_3$): *δ* = 22.0, 29.3, 50.9 (3 CH_2), 102.5, 112.3, 116.2, 121.0, 123.9, 124.7, 125.2, 127.4, 138.2 (CN, C-Ar); IR (film): ν = 3333, 2926, 2217, 2093 cm^{-1}; ESI-MS: *m/z* calcd for $C_{12}H_{11}NaN_5$ $[M+Na]^+$: 248.1, found: 247.9.

*3-(5-Methylsulfonyl-1H-indol-3-yl)-propyl acetate (**27k**).* Prepared from **23k** (150 mg, 0.593 mmol) according to the procedure described for **27j**. Yield: 65 mg, 37%. ^{1}H NMR (500 MHz, CD_3OD): *δ* = 2.00-2.09 (m, 2H, CH_2), 2.05 (s, 3H, CH_3), 2.90 (t, *J* = 7.4 Hz, 2H, CH_2), 3.11 (s, 3H, CH_3), 4.10 (t, *J* = 6.4 Hz, 2H, CH_2), 7.27 (s, 1H, CH_{ar}), 7.54 (d, *J* = 8.5 Hz, 1H, CH_{ar}), 7.65 (dd, *J* = 1.8, 8.6 Hz, 1H, CH_{ar}), 8.17 (d, *J* = 1.5 Hz, 1H, CH_{ar}); ^{13}C NMR (126 MHz, CD_3OD): *δ* = 21.0 (CH_3), 22.1, 30.7 (2 CH_2), 45.5 (CH_3), 65.2 (CH_2), 113.2, 117.6, 120.4, 120.8, 126.3, 128.6, 131.8, 140.6 (C-Ar), 173.3 (CO); ESI-MS: *m/z* calcd for $C_{14}H_{17}NaNO_4S$ $[M+Na]^+$: 318.1, found: 318.0.

3-(5-Methylsulfonyl-1*H*-indol-3-yl)-propan-1-ol (**24k**). Prepared from **27k** (102 mg, 0.3454 mmol) according to the procedure described for **24j**. Yield: 37 mg, 42%. ^{1}H NMR (500 MHz, $CDCl_3$): *δ* = 1.90-2.01 (m, 2H, CH_2), 2.88 (t, *J* = 7.5 Hz, 2H, CH_2), 3.07 (s, 3H, CH_3), 3.72 (t, *J* = 6.3 Hz, 2H, CH_2), 7.15 (s, 1H, CH_{ar}), 7.46 (d, *J* = 8.5 Hz, 1H, CH_{ar}), 7.70 (dd, *J* = 1.7, 8.5 Hz, 1H, CH_{ar}), 8.24 (d, *J* = 1.6 Hz, 1H, CH_{ar}), 8.35 (s, 1H, NH); ^{13}C NMR (126 MHz, $CDCl_3$): *δ* = 21.1, 32.9 (2 CH_2), 45.2 (CH_3), 61.8 (CH_2), 112.1, 117.3, 119.6, 119.7, 124.5, 127.2, 130.1, 139.0 (C-Ar); ESI-MS: *m/z* calcd for $C_{12}H_{15}NaNO_3S$ $[M+Na]^+$: 276.1, found: 275.9.

*3-(3-Azidopropyl)-5-methylsulfonyl-1H-indole (**26k**).* Prepared from **24k** (37.0 mg, 0.146 mmol) according to general procedure B. Yield: 22 mg, 55% (two steps). ^{1}H NMR (500 MHz, $CDCl_3$): *δ* = 1.91-2.02 (m, 2H, CH_2), 2.85 (t, *J* = 7.4 Hz, 2H, CH_2), 3.08 (s, 3H, CH_3), 3.30 (t, *J* = 6.7 Hz, 2H, CH_2), 7.14 (d, *J* = 2.1 Hz, 1H, Indole), 7.46 (d, *J* = 8.6 Hz, 1H, CH_{ar}), 7.68 (dd, *J* = 1.7, 8.6 Hz, 1H, CH_{ar}), 8.20 (d, *J* = 1.5 Hz, 1H, CH_{ar}), 8.68 (s, 1H, NH); ^{13}C NMR (126 MHz, $CDCl_3$): *δ* = 22.0, 29.4 (2 CH_2), 45.5 (CH_3), 50.9 (CH_2), 112.2, 116.9, 119.8, 120.6, 124.4, 127.3, 131.3, 138.9 (C-Ar); IR (film): ν = 3351, 2925, 2098, 1293, 1142 cm^{-1}; ESI-MS: *m/z* calcd for $C_{12}H_{14}NaN_4O_2S$ $[M+Na]^+$: 301.1, found: 301.0.

*3-(1H-Indol-3-yl)-propyl acetate (**28**).* To a solution of **24a** (3.90 g, 22.3 mmol) and DMAP (133 mg, 1.1 mmol) in pyridine (30 mL), Ac_2O (20 mL) was added and the reaction mixture was stirred at rt overnight. The solvents were co-evaporated with toluene and the residue purified by chromatography on silica (petroleum ether/EtOAc, 6:1 to 4:1) to yield **28** (4.44 g, 92%) as a colourless solid. The analytic data were in accordance with published data.[22]

*3-(1-Tosyl-1H-indol-3-yl)-propyl acetate (**29**).* A solution of **28** (2.34 g, 10.8 mmol) in THF (15 mL) was added to an ice-cold slurry of NaH (60% in oil, 1.31 g, 32.7 mmol) in THF (5 mL). After stirring for 1 h at 0 °C, tosyl chloride (6.15 g, 32.3 mmol) was added over a period of 1 h in three portions and the reaction mixture was stirred for another 2 h at 0 °C. After quenching with sat. aq. NH_4Cl (10 mL) the mixture was transferred into a separation funnel, diluted with EtOAc (100 mL) and washed with sat. aq. NH_4Cl (100 mL) and water (100 mL). The aqueous layers were extracted with EtOAc (100 mL). The combined organic layers were dried over Na_2SO_4, filtered and concentrated in vacuo. The residue was purified by chromatography on silica (toluene/EtOAc, 1:0 to 2:1) to yield **29** (2.81 g, 70%) as colorless oil. ^{1}H NMR ($CDCl_3$, 500 MHz): δ = 2.01 (m, 2H, CH_2), 2.05 (s, 3H, OAc), 2.33 (s, 3H, CH_3), 2.74 (t, J = 7.5 Hz, 2H, CH_2), 4.10 (t, J = 6.4 Hz, 2H, CH_2), 7.20-7.26 (m, 3H, CH_{ar}), 7.29-7.34 (m, 2H, CH_{ar}), 7.46 (m, 1H, CH_{ar}), 7.74 (m, 1H, CH_{ar}), 7.98 (m, 1H, CH_{ar}); ^{13}C-NMR ($CDCl_3$, 125 MHz): δ = 20.9 (OAc), 21.4 (CH_2), 21.5 (CH_3), 27.9, 63.7 (2 CH_2), 113.8, 119.3, 122.0, 122.9, 123.0, 124.6, 126.7, 129.8, 130.8, 135.3, 135.4, 144.7 (C-Ar), 171.1 (CO); ESI-MS: *m/z* calcd for $C_{20}H_{21}NaNO_4S$ $[M+Na]^+$: 394.1, found: 394.0.

*3-(6-Cyclopropanecarbonyl-1H-indol-3-yl)-propan-1-ol (**24l**).* To an ice-cold solution of **29** (302 mg, 0.80 mmol) in nitromethane (6 mL), cyclopropanecarbonyl chloride (340 µL, 3.7 mmol) and $AlCl_3$ (545 mg, 4.1 mmol) were added. After stirring for 1.5 h at 0 °C, the reaction mixture was quenched with water (10 mL). The mixture was transferred into a separation funnel, diluted with EtOAc (40 mL) and subsequently washed with water (40 mL) and brine (40 mL). The aqueous layers were extracted with EtOAc (40 mL). The combined organic layers were dried over Na_2SO_4, filtered and concentrated under reduced pressure. The residue was dissolved in MeOH (5 mL) and treated with aq. NaOH (6 M, 5 mL). After refluxing for 1 h, the mixture was transferred into a separation funnel with DCM (40 mL), neutralized with aq. HCl and washed with water (2 × 40 mL). The organic layers were extracted with DCM (2 × 40 mL). The combined organic layers were dried over Na_2SO_4, filtered and evaporated to dryness. The residue was purified by chromatography on silica (toluene/EtOAc, 2:1 to 1:2) to yield a inseparable mixture of **24l** and the 5-regioisomer (121 mg, 61%) as a white solid. The mixture was directly used in the next step.

*3-(3-Azidopropyl)-6-cyclopropanecarbonyl-1H-indole (**26l**).* A mixture of **24l** and its 5-regioisomer (112 mg, 0.460 mmol), CBr_4 (231 mg, 0.70 mmol) and triphenylphosphine (145 mg, 0.55 mmol) in dry DMF (1 mL) was shaken in an Eppendorf tube (2 mL) at 50 °C and 900 rpm for 30 min to give the intermediate bromide **25l**. NaN_3 (60.0 mg, 0.923 mmol) was added and the reaction mixture was shaken overnight at 50 °C. The reaction was quenched by addition of a few drops of water and directly purified by preparative LCMS to yield **26l** (44.4 mg, 36%, two steps) and the 5-regioisomer (15 mg, 12%, two steps) as colorless solids. ^{1}H NMR (500 MHz, $CDCl_3$): δ = 0.93-1.10 (m, 2H, CH_2) 1.21-1.32 (m, 2H, CH_2), 2.01 (p, *J* = 7.0 Hz, 2H, CH_2), 2.72-2.80 (m, 1H, CH), 2.89 (t, *J* = 7.4 Hz, 2H, CH_2), 3.34 (t, *J* = 6.7 Hz, 2H, CH_2), 7.20 (d, *J* = 1.9 Hz, 1H, CH_{ar}), 7.65 (d, *J* = 8.4 Hz, 1H CH_{ar}), 7.75-7.90 (m, 1H CH_{ar}), 8.10 (s, 1H, CH_{ar}), 8.25 (s, 1H, NH); ^{13}C NMR (126 MHz, $CDCl_3$): δ = 11.3 (CH_2), 17.1 (CH), 22.0, 29.3, 50.8 (3 CH_2), 111.9, 115.5, 118.4, 119.5, 125.3, 130.8, 132.4, 135.9 (C-Ar), 200.6 (CO); IR (film): ν = 3312, 2924, 2097, 1651, 1387 cm^{-1}; ESI-MS: *m/z* calcd for $C_{15}H_{17}N_4O$ $[M+H]^+$: 269.2, found: 268.9.

*3-(6-(4-Chlorobenzoyl)-1H-indol-3-yl)-propan-1-ol (**24m**).* To an ice-cold solution of **29** (408 mg, 1.10 mmol) in nitromethane (12 mL), 4-chlorobenzoyl chloride (560 µL, 4.40 mmol) and $AlCl_3$ (732 mg, 5.50 mmol) were added. After stirring for 2 h at 0 °C, the reaction mixture was quenched with water (10 mL). The mixture was transferred into a separation funnel, diluted with EtOAc (40 mL) and subsequently washed with water (40 mL) and brine (40 mL). The aqueous layers were extracted with EtOAc (40 mL). The combined organic layers were dried over Na_2SO_4, filtered and concentrated under reduced pressure. The residue was dissolved in methanol (8 mL) and treated with aq. NaOH (6 M, 8 mL). After stirring for 1.5 h at rt, the mixture was neutralized with aq. HCl, transferred into a separation funnel with DCM (40 mL), and washed with water (2 × 40 mL). The organic layers were extracted with DCM (40 mL). The combined organic layers were dried over Na_2SO_4, filtered and evaporated to dryness. The residue was purified by chromatography on silica (toluene/DCM/^{i}PrOH, 25:5:1 to 4:5:1) to yield a inseparable mixture of **24m** and the 5-regioisomer (163 mg, 47%). The mixture was directly used in the next step.

*3-(3-Azidopropyl)-6-(4-chlorobenzoyl)-1H-indole (**26m**).* A mixture of **24m** and its 5-regioisomer (104 mg, 0.33 mmol), CBr_4 (165 mg, 0.50 mmol) and triphenylphosphine (106 mg, 0.40 mmol) in dry DMF (1 mL) was shaken in an Eppendorf tube (2 mL) at 50 °C and 900 rpm for 15 min to give the intermediate bromide **25m**. NaN_3 (44 mg, 0.68 mmol) was added and the reaction mixture was shaken overnight at 50 °C. The reaction was quenched by addition of a few drops of water and directly purified by LCMS to yield **26m** (42 mg, 37%, two steps) and the 5-regioisomer (4.5 mg, 4%, two steps) as yellow solids. ^{1}H NMR (500 MHz, $CDCl_3$): δ = 2.02 (p, *J* = 7.0 Hz, 2H, CH_2), 2.90 (t, *J* = 7.4 Hz, 2H, CH_2), 3.35 (t, *J* = 6.7

Hz, 2H, CH_2), 7.22 (d, *J* = 2.0 Hz, 1H, CH_{ar}), 7.45 (d, *J* = 8.4 Hz, 2H, CH_{ar}), 7.58 (dd, *J* = 0.9, 8.3 Hz, 1H, CH_{ar}), 7.65 (d, *J* = 8.3 Hz, 1H, CH_{ar}), 7.76 (d, *J* = 8.4 Hz, 2H, CH_{ar}), 7.88 (s, 1H, CH_{ar}), 8.42 (s, 1H, NH); ^{13}C NMR (126 MHz, $CDCl_3$): δ = 22.1 (CH_2), 29.4 (CH_2), 50.9 (CH_2), 114.5, 115.9, 118.6, 121.7, 125.8, 128.6, 131.1, 131.3, 131.5, 135.7, 137.2, 138.3 (14 C-Ar), 196.1 (CO); IR (film): ν = 3271, 2918, 2096, 1611, 1334 cm^{-1}.

*3-(3-(tert-Butyldimethylsilyl)oxy)propyl-5-trifluoromethyl-2-trimethylsilyl-1H-indole (**32n**).* A mixture of **30n** (1.20 g, 4.20 mmol), **31**[13] (2.30 g, 8.40 mmol), potassium acetate (2.10 g, 21.0 mmol), lithium chloride (178 mg, 4.20 mmol) and palladium(II) acetate (77 mg, 0.42 mmol) in dry DMF (10 mL) was heated at 70-75 °C under argon for 2.5 h. After cooling to rt, the reaction mixture was diluted with ether and ice-water, the aqueous layer was separated and extracted with EtOAc (50 mL). The combined organic layers were washed with water (50 mL) and brine (50 mL), dried over Na_2SO_4 and evaporated. The residue was purified by chromatography on silica (petroleum ether/EtOAc, 8:1) to give **32n** (1.70 g, 89%) as yellow oil.[1] H NMR ($CDCl_3$, 500 MHz): δ = 0.12 (s, 6H, 2 CH_3), 0.43 (s, 9H, $C(CH_3)_3$), 0.97 (s, 9H, $C(CH_3)_3$), 1.89 (m, 2H, CH_2), 2.95 (m, 2H, CH_2), 3.77 (t, *J* = 6.0 Hz, 2H, CH_2), 7.42 (m, 2H, CH_{ar}), 7.92 (s, 1H, CH_{ar}), 8.06 (s, 1H, NH); ^{13}C NMR ($CDCl_3$, 126 MHz): δ = -5.3 (CH_3), -0.7 (CH_3), 18.4 ($C(CH_3)_3$), 22.4 (CH_2), 35.2 ($C(CH_3)_3$), 62.9 (CH_2), 107.1, 111.0, 116.7 (q, *J* = 4.3 Hz), 118.9 (q, *J* = 3.3 Hz), 126.4, 128.2, 135.1, 139.4 (C-Ar, CF_3).

*3-(5-Trifluoromethyl-1H-indol-3-yl)-propan-1-ol (**24n**).* To a solution of **32n** (1.70 g, 4.00 mmol) in MeCN (20 mL) was added in portions 48% aq. HF (2 mL). The mixture was stirred at rt for 48 h. Then, the reaction mixture was cautiously basified with sat. aq. Na_2CO_3 and extracted with EtOAc. The organic extract was washed with brine, dried over Na_2SO_4 and evaporated to give a viscous solid. Purification by chromatography on silica (petroleum ether/EtOAc, 1:1) gave **24n** (671 mg, 65%) as yellow oil. ^{1}H NMR ($CDCl_3$, 500 MHz): δ = 2.01 (m, 2H, CH_2), 2.89 (t, *J* = 7.5 Hz, 2H, CH_2), 3.75 (t, *J* = 6.5 Hz, 2H, CH_2), 7.11 (t, *J* = 1.0 Hz, 1H, CH_{ar}), 7.42 (d, *J* = 1.5 Hz, 2H, CH_{ar}), 7.90 (s, 1H, CH_{ar}), 8.17 (s, 1H, NH); ^{13}C NMR ($CDCl_3$, 125 MHz): δ = 21.1, 32.8, 62.4 (3 CH_2), 111.3, 116.6 (q, *J* = 4.3 Hz), 117.1, 118.8 (q, *J* = 3.5 Hz), 121.7 (q, *J* = 31.8 Hz), 122.9, 126.5, 126.9, 137.6 (C-Ar, CF_3); ESI-MS: *m/z* calcd for $C_{12}H_{13}F_3NO$ $[M+H]^+$: 244.1, found: 243.9.

*3-(3-Azidopropyl)-5-trifluoromethyl-1H-indole (**26n**).* Prepared from **24n** (607 mg, 2.50 mmol) according to general procedure B. Yield: 533 mg, 80% (two steps), yellow oil. ^{1}H NMR ($CDCl_3$, 500 MHz): δ = 2.02 (m, 2H, CH_2), 2.90 (t, *J* = 7.5 Hz, 2H, CH_2), 3.36 (t, *J* = 6.5 Hz, 2H, CH_2), 7.12 (d, *J* = 2.0 Hz, 1H, CH_{ar}), 7.44 (m, 2H, CH_{ar}), 7.89 (s, 1H, CH_{ar}), 8.17 (s, 1H, NH); ^{13}C NMR ($CDCl_3$, 125 MHz): δ = 21.9, 29.1, 50.8 (3 CH_2), 111.4, 116.1, 116.5 (q, *J* = 4.3 Hz), 118.9 (q, *J* = 3.5 Hz), 121.9 (q, *J* = 31.5 Hz), 123.1, 124.3, 126.7, 137.6 (C-Ar, CF_3); IR (film): ν = 3440, 2940, 2101, 1432, 1329, 1111 cm^{-1}.

*3-(3-Azidopropyl)-1-methyl-5-nitro-1H-indole (**33**).* To a stirred solution of **26o**[13] (48.5 mg, 0.198 mmol) in DMF (2 mL), powdered KOH (112 mg, 2.00 mmol) was added. Iodomethane (125 µL, 2.00 mmol) was added drop-wise and the reaction was stirred at rt for 2 h. The reaction mixture was quenched by addition of water (2 mL), transferred into a separation funnel with DCM (20 mL) and extracted with water (2 × 20 mL). The aqueous layers were extracted with DCM (20 mL). The combined organic layers were dried over Na_2SO_4, filtered and co-evaporated with toluene to dryness. The residue was purified by chromatography on silica (petroleum ether/EtOAc, 9:1 to 1:1) to yield **33** (48 mg, 94%) as yellow oil. ^{1}H NMR (500 MHz, $CDCl_3$): δ = 1.87-2.08 (m, 2H, CH_2), 2.88 (t, *J* = 7.4 Hz, 2H, CH_2), 3.35 (t, *J* = 6.7 Hz, 2H, CH_2), 3.81 (s, 3H, CH_3), 7.01 (s, 1H, CH_{ar}), 7.31 (t, *J* = 9.5 Hz, 1H, CH_{ar}), 8.13 (dd, *J* = 2.2, 9.0 Hz, 1H, CH_{ar}), 8.55 (d, *J* = 2.1 Hz, 1H, CH_{ar}); ^{13}C NMR (126 MHz, $CDCl_3$): δ = 21.8, 29.4 (2 CH_2), 33.2 (CH_3), 50.7 (CH_2), 109.2, 116.4, 117.5, 129.5 (C-Ar). IR (film): ν = 2941, 2098, 1515, 1334 cm^{-1}.

*3-(3-Azidopropyl)-1-ethyl-5-nitro-1H-indole (**34**).* According to the procedure described for **33**, compound **26o** (56.0 mg, 0.230 mmol) was treated with KOH (129 mg, 2.30 mmol) and iodoethane (185 µL, 2.30 mmol) in DMF (2 mL) at rt for 2 h. After work-up, the residue was purified by chromatography on silica (petroleum ether/EtOAc, 1:0 to 3:1) to yield **34** (57 mg, 92%) as yellow oil. ^{1}H NMR (500 MHz, $CDCl_3$): δ = 1.48 (t, *J* = 7.3 Hz, 3H, CH_3), 1.96-2.04 (m, 2H, CH_2), 2.88 (t, *J* = 7.5 Hz, 2H, CH_2), 3.35 (t, *J* = 6.7 Hz, 2H, CH_2), 4.18 (q, *J* = 7.3 Hz, 2H, CH_2), 7.07 (s, 1H, CH_{ar}), 7.32 (d, *J* = 9.1 Hz, 1H, CH_{ar}), 8.11 (dd, *J* = 2.2, 9.1 Hz, 1H, CH_{ar}), 8.54 (d, *J* = 2.1 Hz, 1H, CH_{ar}); ^{13}C NMR (126 MHz, $CDCl_3$): δ = 15.4 (CH_3), 21.9, 29.4, 41.4, 50.8 (4 CH_2), 109.1, 116.5, 117.3, 127.7 (C-Ar); IR (film): ν = 2937, 2097, 1514, 1332 cm^{-1}.

Methyl [2-propynyl 4,7,8-tri-*O*-acetyl-9-azido-5-(*tert*-butoxycarbonylamino)-3,5,9-trideoxy-D-*glycero*-α-D-*galacto*-2-nonulopyranosid]onate (**36**). Compound **35**[13] (39.0 mg, 80 µmol) was reacted with Boc_2O (33 mg, 0.15 mmol) and DMAP (2.5 mg, 20 µmol) at 50 °C for 5 h. After addition of $N_2H_4 \cdot H_2O$ (24 µL, 0.49 mmol), stirring was continued for 16 h. The mixture was diluted with $CHCl_3$ (20 mL) and washed successively with 1 M aq. HCl (5.0 mL), 0.5 M aq. $CuSO_4$ (5.0 mL) and sat. aq. $NaHCO_3$ (3 × 10 mL). The organic layer was dried over Na_2SO_4, filtered and concentrated under reduced pressure to give an yellow oil. The crude product was dissolved in dry pyridine (1.0 mL) and treated with acetic anhydride (0.5 mL) for 3 h at rt. The reaction mixture was diluted with $CHCl_3$ (10 mL) and washed with 0.5 M aq $CuSO_4$ (3 × 3 mL) and sat. aq. $NaHCO_3$ (3 × 5 mL). The organic layer was dried over Na_2SO_4, filtered and concentrated. The residue was purified by chromatography on silica (petroleum ether/EtOAc, 1:1) to yield **36** (14 mg, 34%) as white foam. $[\alpha]_D^{20}$ +7.6 (*c* 0.90, DCM); ^{1}H NMR (500 MHz, CD_3OD): δ = 1.40 (s, 9H, $C(CH_3)_3$), 1.77 (t, *J* = 12.4 Hz, 1H, H-

3a), 2.00, 2.13, 2.16 (3s, 9H, 3 OAc), 2.67 (dd, *J* = 4.7, 12.6 Hz, 1H, H-3b), 2.86 (t, *J* = 2.4 Hz, 1H, C≡CH), 3.35 (dd, *J* = 6.0, 13.5 Hz, 1H, H-9a), 3.56-3.70 (m, 2H, H-5, H-9b), 3.83 (s, 3H, OMe), 4.03 (dd, *J* = 2.0, 10.7 Hz, 1H, H-6), 4.19, 4.35 (A, B of ABX, *J* = 2.5, 15.8 Hz, 2H, H-1'), 4.79 (ddd, *J* = 4.7, 10.4, 12.0 Hz, 1H, H-4), 5.30-5.41 (m, 2H, H-7, H-8); ^{13}C NMR (CD_3OD, 126 MHz): δ = 20.8, 20.9, 21.2 (3 OAc), 28.7 (C(*C*H_3)$_3$), 39.0 (C-3), 51.4 (C-5), 52.2 (C-9), 53.4 (OMe), 53.5 (C-1'), 69.5 (C-7), 70.8 (2C, C-4, C-8), 73.8 (C-6), 75.8 (C≡*C*H), 80.1 (*C*≡CH), 80.6 (*C*(CH$_3$)$_3$), 99.4 (C-2), 157.7 (CONH), 169.1, 171.5, 171.7, 171.8 (4 CO); ESI-MS: *m/z* calcd for $C_{29}H_{33}Cl_2F_2N_2NaO_9$ $[M+Na]^+$: 593.2, found: 593.3.

*Methyl [2-propynyl 4,7,8-tri-O-acetyl-5-amino-9-azido-3,5,9-trideoxy-D-glycero-α-D-galacto-2-nonulopyranosid]onate (**37**).* Compound **36** (177 mg, 0.31 mmol) was dissolved in 4 M PhOH (5 mL, in dry DCM). After addition of 4 M TMSCl (5 mL, in dry DCM), the reaction mixture was stirred at rt for 2 h. $CHCl_3$ was added and the organic layer was washed with sat. aq. $NaHCO_3$ (3 × 10 mL) and water (10 mL). The organic layer was dried over Na_2SO_4, filtered and concentrated under reduced pressure. The crude product was purified by chromatography on silica (EtOAc/petroleum ether, 1:2; then EtOAc/acetone, 9:1) to yield **37** (98 mg, 67%) as colorless oil. $[\alpha]_D^{20}$ +8.2 (*c* 1.00, DCM); ^{1}H NMR (500 MHz, CD_2Cl_2): δ = 1.63 (t, *J* = 12.2 Hz, 1H, H-3a), 1.97, 2.08, 2.10 (3s, 9H, 3 OAc), 2.42 (t, *J* = 2.4 Hz, 1H, C≡CH), 2.49 (dd, *J* = 8.3, 10.9 Hz, 1H, H-5), 2.58 (dd, *J* = 4.5, 12.6 Hz, 1H, H-3b), 3.26 (dd, *J* = 5.0, 13.6 Hz, 1H, H-9a), 3.57 (dd, *J* = 2.8, 13.6 Hz, 1H, H-9b), 3.63 (dd, *J* = 1.0, 10.1 Hz, 1H, H-6), 4.04, 4.27 (A, B of ABX, *J* = 2.5, 15.5 Hz, 1H, H-1'), 4.53 (ddd, *J* = 4.6, 10.0, 11.9 Hz, 1H, H-4), 5.29 (m, 1H, H-8), 5.42 (dd, *J* = 1.1, 8.5 Hz, 1H, H-7); ^{13}C NMR (CD_2Cl_2, 126 MHz): δ = 21.1, 21.3, 21.4 (3 OAc), 37.2 (C-3), 52.3 (C-9), 52.9 (C-1'), 53.2 (C-5), 53.4 (OMe), 69.6 (2C, C-7, C-8), 71.8 (C-4), 72.1 (C≡*C*H), 74.8 (*C*≡CH), 75.9 (C-6), 117.2 (C-2), 170.4, 170.8, 170.9, 171.0 (4 CO); ESI-MS: *m/z* calcd for $C_{19}H_{26}N_4NaO_{10}$ $[M+Na]^+$: 493.2, found: 493.2.

*Methyl [2-propynyl 4,7,8-tri-O-acetyl-9-azido-3,5,9-trideoxy-5-fluoroacetamido-D-glycero-α-D-galacto-2-nonulopyranosid]onate (**38**).* Compound **37** (130 mg, 0.27 mmol) was dissolved in dry THF (3 mL) and cooled to 0 °C. Fluoroacetyl chloride (60 µL, 0.83 mmol) was added, followed by the addition of NEt_3 (190 µL, 1.35 mmol). The reaction mixture was allowed to reach rt and stirring was continued for 24 h. DCM (10 mL) was added and the organic layer was washed with sat. aq. $NaHCO_3$ (3 × 2 mL) and water (2 mL). The organic layer was dried over Na_2SO_4, filtered and the solvent removed under reduced pressure. The crude product was purified by chromatography on silica (petroleum ether/EtOAc, 1:1) to yield **38** (63 mg, 43%). $[\alpha]_D^{20}$ +8.0 (*c* = 0.40, DCM); ^{1}H NMR (500 MHz, $CDCl_3$): δ = 1.98 (t, *J* = 12.5 Hz, 1H, H-3a), 2.03, 2.15, 2.19 (3s, 9H, 3 OAc), 2.46 (t, *J* = 2.1 Hz, 1H, C≡CH), 2.69 (dd, *J* = 4.5, 12.8 Hz, 1H, H-3b), 3.26 (dd, *J* = 5.4, 13.5 Hz, 1H, H-9a), 3.56 (dd, *J* = 2.6, 13.5

Hz, 1H, H-9b), 3.83 (s, 3H, OMe), 4.08-4.20 (m, 3H, H-5, H-6, H-1'a), 4.40 (dd, *J* = 2.3, 15.6 Hz, 1H, H-1'b), 4.57-4.86 (m, 2H, CH_2F), 4.93 (m, 1H, H-4), 5.25-5.40 (m, 2H, H-7, H-8), 6.19 (d, *J* = 8.6 Hz, 1H, NH); ^{13}C NMR ($CDCl_3$, 126 MHz): δ = 21.0, 21.1, 21.2 (3 OAc), 38.1 (C-3), 48.7 (C-5), 51.1 (C-9), 53.3 (2C, OMe, C-1'), 67.9 (C-4), 68.7 (C-7), 69.4 (C-8), 72.7 (C-6), 74.8 (C≡*C*H), 79.0 (*C*≡CH), 79.5, 81.0 (d, *J* = 186 Hz, *C*H_2F), 98.3 (C-2), 168.3, 168.4, 170.3, 170.4, 170.9 (5 CO); ESI-MS: *m/z* calcd for $C_{21}H_{27}FNaN_4O_{11}$ $[M+Na]^+$: 553.2, found: 553.1.

*Methyl [2-propynyl 4,7,8-tri-O-acetyl-9-benzamido-3,5,9-trideoxy-5-fluoroacetamido-D-glycero-α-D-galacto-2-nonulopyranosid]onate (**39a**).* Compound **38** (63 mg, 0.12 mmol) was dissolved in dry DCE (2 mL). Benzoyl chloride (55 µL, 0.47 mmol) and triphenylphosphine (70 mg, 0.26 mmol) were added successively with stirring. After 24 h DCM (5 mL) was added and the organic layer was washed with sat. aq. $NaHCO_3$ (3 × 2 mL) and water (2 mL). The organic layer was dried over Na_2SO_4, filtered and the solvent removed under reduced pressure. The crude product was purified by chromatography on silica (0.5% gradient of MeOH in DCM) to yield **39a** (37 mg, 52%). $[\alpha]_D^{20}$ +12.8 (*c* 1.00, DCM); ^1H NMR (500 MHz, CD_2Cl_2): δ = 1.97 (m, 1H, H-3a) 2.08, 2.15, 2.21 (3s, 9H, 3 OAc), 2.53 (t, *J* = 2.4 Hz, 1H, C≡C*H*), 2.75 (dd, *J* = 4.7, 12.7 Hz, 1H, H-3b), 3.08 (td, *J* = 4.3, 15.2 Hz, 1H, H-9a), 3.79 (s, 3H, OMe), 4.14-4.33 (m, 4H, H-5, H-6, H-9b, H-1'a), 4.43 (dd, *J* = 2.5, 15.6 Hz, 1H, H-1'b), 4.75 (m, 2H, CH_2F), 4.99 (ddd, *J* = 4.7, 10.4, 12.1 Hz, 1H, H-4), 5.24 (d, *J* = 9.5 Hz, 1H, H-7), 5.33 (m, 1H, H-8), 6.64 (d, *J* = 9.9 Hz, 1H, 5-NH), 7.04 (dd, *J* = 4.4, 7.4 Hz, 1H, 9-NH), 7.48 (m, 2H, CH_{ar}), 7.58 (m, 1H, CH_{ar}), 7.69 (m, 2H, CH_{ar}); ^{13}C NMR (CD_2Cl_2, 126 MHz): δ = 21.0, 21.3, 21.4 (3 OAc), 38.2 (C-3), 38.5 (C-9), 48.9 (C-5), 53.1 (OMe), 53.3 (C-1'), 68.3 (C-7), 68.9 (C-8), 69.1 (C-4), 72.4 (C-6), 72.8 (C≡*C*H), 74.8 (*C*≡CH), 79.9 (CH_2F), 98.5 (C-2), 128.9, 129.0, 132.4, 134.8 (C-Ar), 167.9, 168.4, 168.6, 168.9, 170.8, 172.3 (6 CO); ESI-MS: *m/z* calcd for $C_{28}H_{33}FNaN_2O_{12}$ $[M+Na]^+$: 631.2, found: 631.2.

*Methyl [2-propynyl 4,7,8-tri-O-acetyl-9-(4-chlorobenzamido)-3,5,9-trideoxy-5-fluoroacetamido-D-glycero-α-D-galacto-2-nonulopyranosid]onate (**39b**).* Prepared from **38** (400 mg, 0.753 mmol) and 4-chlorobenzoyl chloride (385 µL, 3.01 mmol) according to the procedure described for **39a**. Yield: 313 mg, 65%. $[\alpha]_D^{20}$ -11.5 (*c* 1.41, DCM); ^1H NMR (500 MHz, $CDCl_3$): δ = 1.96 (m, 1H, H-3a), 2.01, 2.11, 2.21 (3s, 9H, 3 OAc), 2.42 (t, *J* = 2.4 Hz, 1H, C≡C*H*), 2.68 (dd, *J* = 4.6, 12.8 Hz, 1H, H-3b), 2.97 (dt, *J* = 4.0, 15.1 Hz, 1H, H-9a), 3.78 (s, 3H, OMe), 4.08 (m, 1H, H-6), 4.14 (dd, *J* = 2.4, 15.6 Hz, 1H, H-1'a), 4.17-4.30 (m, 2H, H-9b, H-5), 4.39 (dd, *J* = 2.5, 15.6 Hz, 1H, H-1'b), 4.58-4.79 (m, 2H, CH_2F), 4.86 (m, 1H, H-4), 5.13 (dd, *J* = 2.2, 9.8 Hz, 1H, H-7), 5.29 (m, 1H, H-8), 6.12 (dd, *J* = 3.2, 10.2 Hz, 1H, 5-NH), 6.89 (dd, *J* = 4.4, 8.0 Hz, 1H, 9-NH), 7.38 (d, *J* = 8.5 Hz, 2H, C_6H_4), 7.71 (d, *J* = 8.5 Hz, 2H, C_6H_4); ^{13}C NMR (126 MHz, $CDCl_3$): δ = 21.0, 21.3, 21.3 (3 OAc), 38.1 (C-3), 38.9 (C-9), 48.9

(C-5), 53.13, 53.14 (C-1', OMe), 67.9 (C-7), 68.4 (C-8), 68.8 (C-4), 72.3 (C-6), 74.8 (C≡*C*H), 79.0 (*C*≡CH), 80.2 (d, *J* = 186 Hz, CH_2F), 98.2 (C-2), 128.6, 129.0, 132.9, 138.0 (6C, C_6H_4), 166.6, 167.7, 170.6, 170.9, 172.5 (6C, 6 CO); ESI-MS: *m/z* calcd for $C_{28}H_{32}ClFN_2NaO_{12}$ $[M+Na]^+$: 665.1, found: 665.2.

*Lithium [2-propynyl 9-benzamido-3,5,9-trideoxy-5-fluoroacetamido-D-glycero-α-D-galacto-2-nonulopyranosid]onate (**22a**).* Compound **39a** (25 mg, 41 µmol) was dissolved in THF (4.5 mL) and LiOH (6.0 mg, 0.25 mmol in 0.5 mL water) was added. The reaction mixture was stirred at rt for 7 h. After neutralization with 7% aq. HCl the solvents were removed under reduced pressure and the crude product was purified by chromatography (1% gradient of water in DCM/MeOH, 5:1) to yield **22a** (15 mg, 80%). $[\alpha]_D^{20}$ -19.8 (*c* 1.34, MeOH); ^{1}H NMR (500 MHz, CD_3OD): δ = 1.59 (t, *J* = 11.6 Hz, 1H, H-3a), 2.70 (s, 1H, C≡CH), 2.80 (dd, *J* = 3.6, 11.9 Hz, 1H, H-3b), 3.42 (d, *J* = 8.7 Hz, 1H, H-7), 3.65 (m, 1H, H-9a), 3.68-3.85 (m, 4H, H-4, H-5, H-6, H-9b), 4.00 (m, 1H, H-8), 4.13, 4.40 (A, B of AB, *J* = 14.1 Hz, 2H, H-1'), 4.78 (m, 2H, CH_2F), 7.41 (t, *J* = 7.3 Hz, 2H, CH_{ar}), 7.48 (t, *J* = 7.1 Hz, 1H, CH_{ar}), 7.80 (d, *J* = 7.6 Hz, 2H, CH_{ar}); ^{13}C NMR (CD_3OD, 126 MHz): δ = 42.2 (C-3), 44.3 (C-9), 53.2 (C-1'), 53.7 (C-5), 69.2 (C-4), 71.6 (C-8), 72.1 (C-7), 73.8 (C-6), 75.0 (C≡*C*H), 80.9 (d, *J* = 181 Hz, CH_2F), 81.0 (*C*≡CH), 101.7 (C-2), 128.4, 129.6, 132.7, 135.6 (C-Ar), 172.0, 178.5 (2 CO); ESI-MS: *m/z* calcd for $C_{21}H_{24}FN_2O_9$ $[M-H]^-$: 467.2, found: 467.2.

Lithium [2-propynyl 9-(4-chlorobenzamido)-3,5,9-trideoxy-5-fluoroacetamido-D-*glycero*-α-D-*galacto*-2-nonulopyranosid]onate (**22b**). Prepared from **39b** (313 mg, 0.487 mmol) according to the procedure described for **22a**. Yield: 123 mg, 50%, white solid. $[\alpha]_D^{20}$ -17.4 (*c* 1.10, MeOH); ^{1}H NMR (500 MHz, CD_3OD): δ = 1.64 (t, *J* = 11.8 Hz, 1H, H-3a), 2.72 (t, *J* = 2.4 Hz, 1H, C≡CH), 2.85 (dd, *J* = 4.5, 12.3 Hz, 1H, H-3b), 3.45 (dd, *J* = 1.4, 8.9 Hz, 1H, H-7), 3.52 (m, 1H, H-9a), 3.73-3.92 (m, 4H, H-9b, H-4, H-5, H-6), 4.04 (td, *J* = 3.0, 8.4 Hz, 1H, H-8), 4.18 (dd, *J* = 2.3, 15.0 Hz, 1H, H-1'a), 4.44 (dd, *J* = 2.4, 15.0 Hz, 1H, H-1'b), 4.83 (d, *J* = 46.9 Hz, 2H, CH_2F), 7.46 (d, *J* = 8.5 Hz, 2H, C_6H_4), 7.82 (d, *J* = 8.5 Hz, 2H, C_6H_4), 8.35 (d, *J* = 5.1 Hz, 1H, NH); ^{13}C NMR (126 MHz, CD_3OD): δ = 42.4 (C-3), 44.6 (C-9), 53.3 (C-1'), 53.7 (C-5), 69.5 (C-4), 71.6 (C-8), 72.3 (C-7), 74.0 (C-6), 75.1 (C≡*C*H), 81.1 (d, *J* = 183 Hz, CH_2F), 81.1 (*C*≡CH), 129.8, 130.2, 134.6, 138.8 (6C, C_6H_4), 169.5, 172.2, 172.3 (3 CO); ESI-MS: *m/z* calcd for $C_{21}H_{24}ClFN_2NaO_9$ $[M+Na]^+$: 525.1, found: 525.0.

*Sodium [3-(1H-indol-3-yl)-propyl-[1,2,3]triazole-4-yl-methyl 5-acetamido-9-benzamido-3,5,9-trideoxy-D-glycero-α-D-galacto-2-nonulopyranosid]onate (**2**).* Prepared from **21**[13] (8.0 mg, 20 µmol) and **26a** (4.1 mg, 20 µmol) according to general procedure C. Yield: 7.7 mg, 68%, white solid. $[\alpha]_D^{20}$ -15.9 (*c* 0.20, MeOH); ^{1}H NMR (CD_3OD, 500 MHz): δ = 1.62 (t, *J* = 11.5 Hz, 1H, H-3a), 1.99 (s, 3H, NHAc), 2.28 (m, 2H, H-2''), 2.75 (t, *J* = 7.0 Hz,

2H, H-3"), 2.88 (dd, *J* = 4.5, 12.5 Hz, 1H, H-3b), 3.44 (d, *J* = 9.0 Hz, 1H, H-7), 3.51 (dd, 1H, *J* = 8.0, 13.5 Hz, H-9a), 3.67 (d, *J* = 9.0 Hz, 1H, H-6), 3.69-3.75 (m, 2H, H-4, H-5), 3.79 (dd, *J* = 3.0, 13.5 Hz, 1H, H-9b), 4.05 (dt, *J* = 3.0, 8.0 Hz, 1H, H-8), 4.38 (t, *J* = 7.0 Hz, 2H, H-1"), 4.68, 4.95 (A, B of AB, *J* = 12.5 Hz, 2H, H-1'), 6.98 (t, *J* = 7.5 Hz, 1H, CH_{ar}), 7.04-7.08 (m, 2H, CH_{ar}), 7.32 (d, *J* = 8.0 Hz, 1H, CH_{ar}), 7.41-7.49 (m, 4H, CH_{ar}), 7.81 (d, *J* = 7.5 Hz, 2H, CH_{ar}), 7.94 (s, 1H, triazole-H); ^{13}C NMR (CD_3OD, 125 MHz): *δ* = 22.6 (NHAc), 22.9 (C-3"), 31.8 (C-2"), 42.6 (C-3), 44.6 (C-9), 50.9 (C-1"), 54.1 (C-5), 58.9 (C-1'), 69.7 (C-4), 71.2 (C-8), 72.6 (C-7), 74.4 (C-6), 102.0 (C-2), 112.2, 112.8, 114.6, 119.2, 119.5, 122.3, 123.3, 125.3, 128.3, 129.5, 132.5, 135.9, 146.7 (C-Ar), 170.3, 174.1, 175.4 (3 CO); HRMS: *m/z* calcd for $C_{32}H_{37}N_6Na_2O_9$ $[M+Na]^+$: 695.2412, found: 695.2413.

*Sodium [3-(5-methoxy-1H-indol-3-yl)-propyl-[1,2,3]triazole-4-yl-methyl 5-acetamido-9-benzamido-3,5,9-trideoxy-D-glycero-α-D-galacto-2-nonulopyranosid]onate (**3**).* Prepared from **21** (10 mg, 20 µmol) and **26b** (5.8 mg, 30 µmol) according to general procedure C. Yield: 8.2 mg, 70%, white solid. $[\alpha]_D^{20}$ -24.3 (*c* 0.23, MeOH); ^{1}H NMR (CD_3OD, 500 MHz): *δ* = 1.63 (t, *J* = 11.5 Hz, 1H, H-3a), 2.0 (s, 3H, NHAc), 2.27 (m, 2H, H-2"), 2.72 (t, *J* = 7.0 Hz, 2H, H-3"), 2.88 (dd, *J* = 4.0, 13.5 Hz, 1H, H-3b), 3.44 (d, *J* = 9.0 Hz, 1H, H-7), 3.52 (dd, 1H, *J* = 8.0, 13.5 Hz, H-9a), 3.66 (d, *J* = 9.0 Hz, 1H, H-6), 3.80 (s, 3H, OMe), 3.73-3.80 (m, 3H, H-4, H-5, H-9b), 4.05 (m, 1H, H-8), 4.39 (t, *J* = 7.0 Hz, 2H, H-1"), 4.68, 4.95 (A, B of AB, *J* = 12.5 Hz, 2H, H-1'), 6.73 (d, *J* = 8.5 Hz, 1H, CH_{ar}), 6.95 (s, 1H, CH_{ar}), 7.02 (s, 1H, CH_{ar}), 7.20 (d, *J* = 8.5 Hz, 1H, CH_{ar}), 7.42-7.50 (m, 3H, CH_{ar}), 7.81 (d, *J* = 7.5 Hz, 2H, CH_{ar}), 7.95 (s, 1H, triazole-H); ^{13}C NMR (CD_3OD, 125 MHz): *δ* = 22.6 (NHAc), 22.9 (C-2"), 31.7 (C-3"), 42.6 (C-3), 44.5 (C-9), 50.9 (C-1"), 54.0 (C-5), 56.3 (OCH_3), 58.9 (C-1'), 69.7 (C-4), 71.2 (C-8), 72.5 (C-7), 74.4 (C-6), 101.1 (C-Ar), 102.0 (C-2), 111.4, 112.6, 112.9, 114.3, 124.1, 125.4, 128.3, 128.8, 129.5, 132.5, 133.4, 135.8, 146.7, 154.9 (C-Ar), 170.3, 174.1, 175.4 (3 CO); HRMS: *m/z* calcd for $C_{33}H_{39}N_6Na_2O_{10}$ $[M+Na]^+$: 725.2518, found: 725.2522.

*Sodium [3-(6-cyclopropanecarbonyl-1H-indol-3-yl)-propyl-[1,2,3]triazole-4-yl-methyl 5-acetamido-9-benzamido-3,5,9-trideoxy-D-glycero-α-D-galacto-2-nonulopyranosid]onate (**4**).* Prepared from **21** (6 mg, 10 µmol) and **26l** (4 mg, 20 µmol) according to general procedure C. Yield: 6.1 mg, 65%, white solid. $[\alpha]_D^{20}$ -15.3 (*c* 0.17, MeOH); ^{1}H NMR (CD_3OD, 500 MHz): *δ* = 1.07-1.15 (m, 4H, $CH(CH_2)_2$), 1.63 (t, *J* = 11.5 Hz, 1H, H-3a), 2.09 (s, 3H, NHAc), 2.30 (m, 2H, H-2"), 2.79 (t, *J* = 7.0 Hz, 2H, H-3"), 2.88-2.94 (m, 2H, $CH(CH_2)_2$, H-3b), 3.44 (dd, *J* = 1.5, 9.0 Hz, 1H, H-7), 3.51 (dd, 1H, *J* = 8.0, 14.0 Hz, H-9a), 3.68 (m, 1H, H-6), 3.72-3.78 (m, 2H, H-4, H-5), 3.80 (dd, *J* = 3.5, 13.5 Hz, 1H, H-9b), 4.05 (td, *J* = 3.0, 8.0 Hz, 1H, H-8), 4.42 (t, *J* = 7.0 Hz, 2H, H-1"), 4.69, 4.96 (A, B of AB, *J* = 12.5 Hz, 2H, H-1'), 7.32 (s, 1H, CH_{ar}), 7.42 (t, *J* = 7.5 Hz, 1H, CH_{ar}), 7.50 (t, *J* = 7.5 Hz, 2H, CH_{ar}), 7.60 (d, *J* = 8.5 Hz, 1H, CH_{ar}), 7.75 (dd, *J* = 1.5, 8.5 Hz, 1H, CH_{ar}), 7.82 (m, 2H, CH_{ar}), 7.98 (s, 1H, CH_{ar}),

8.12 (s, 1H, triazole-H); ^{13}C NMR (CD_3OD, 126 MHz): δ = 11.9 ($CH(\mathit{C}H_2)_2$), 17.8 ($\mathit{C}H(CH_2)_2$), 22.6 (NHAc), 22.7 (C-3"), 31.8 (C-2"), 42.6 (C-3), 44.6 (C-9), 50.8 (C-1"), 54.1 (C-4), 59.0 (C-1'), 69.7 (C-5), 71.2 (C-8), 72.5 (C-7), 74.4 (C-6), 102.0 (C-2), 113.5, 115.3, 119.2, 119.7, 125.4, 128.1, 128.3, 129.5, 132.4, 132.5, 135.8, 137.6, 146.9 (C-Ar), 170.3, 174.2, 175.4, 203.5 (4 CO); HRMS: *m/z* calcd for $C_{36}H_{41}N_6Na_2O_{10}$ $[M+Na]^+$: 763.2674, found: 763.2673.

*Sodium [3-(4-chlorobenzoyl)-1H-indol-3-yl)-propyl-[1,2,3]triazole-4-yl-methyl 5-acetamido-9-benzamido-3,5,9-trideoxy-D-glycero-α-D-galacto-2-nonulopyranosid]onate (**5**).* Prepared from **21** (6 mg, 15 μmol) and **26m** (6.8 mg, 20 μmol) according to general procedure C. Yield: 4.8 mg, 47%, pale yellow solid. $[\alpha]_D^{20}$ -12.0 (*c* 0.21, MeOH); ^{1}H NMR (CD_3OD, 500 MHz): δ = 1.62 (t, *J* = 11.5 Hz, 1H, H-3a), 2.07 (s, 3H, NHAc), 2.31 (m, 2H, H-2"), 2.80 (t, *J* = 7.0 Hz, 2H, H-3"), 2.89 (dd, *J* = 4.0, 12.0 Hz, 1H, H-3b), 3.42 (dd, *J* = 2.0, 9.0 Hz, 1H, H-7), 3.51 (dd, 1H, *J* = 8.0, 13.5 Hz, H-9a), 3.66 (m, 1H, H-6), 3.71-3.75 (m, 2H, H-4, H-5), 3.79 (dd, *J* = 3.0, 13.5 Hz, 1H, H-9b), 4.04 (td, *J* = 3.0, 8.0 Hz, 1H, H-8), 4.42 (t, *J* = 7.0 Hz, 2H, H-1"), 4.69, 4.96 (A, B of AB, *J* = 12.5 Hz, 2H, H-1'), 7.35 (s, 1H, CH_{ar}), 7.41 (m, 2H, CH_{ar}), 7.48-7.51 (m, 2H, CH_{ar}), 7.56 (d, *J* = 8.5 Hz, 2H, CH_{ar}), 7.64 (d, *J* = 8.5 Hz, 1H, CH_{ar}), 7.75-7.84 (m, 5H, CH_{ar}), 7.98 (s, 1H, triazole-H); ^{13}C NMR (CD_3OD, 125 MHz): δ = 22.6 (NHAc), 22.7 (C-3"), 31.7 (C-2"), 42.6 (C-3), 44.6 (C-9), 50.8 (C-1"), 54.1 (C-5), 59.0 (C-1'), 69.7 (C-4), 71.2 (C-8), 72.6 (C-7), 74.4 (C-6), 102.1 (C-2), 115.5, 116.1, 119.3, 121.6, 125.4, 128.3, 129.5, 131.0, 135.6, 137.2, 138.7, 139.1, 147.0 (C-Ar), 170.4, 174.1, 175.4, 198.2 (4 CO); HRMS: *m/z* calcd for $C_{39}H_{40}ClN_6Na_2O_{10}$ $[M+Na]^+$: 833.2284, found: 833.2284.

*Sodium [3-(5-trifluoromethyl-1H-indol-3-yl)-propyl-[1,2,3]triazole-4-yl-methyl 5-acetamido-9-benzamido-3,5,9-trideoxy-D-glycero-α-D-galacto-2-nonulopyranosid]onate (**6**).* Prepared from **21** (10 mg, 20 μmol) and **26n** (7 mg, 30 μmol) according to general procedure C. Yield: 7.7 mg, 67%, white solid. $[\alpha]_D^{20}$ -21.4 (*c* 0.14, MeOH); ^{1}H NMR (CD_3OD, 500 MHz): δ = 1.62 (t, *J* = 11.5 Hz, 1H, H-3a), 2.08 (s, 3H, NHAc), 2.29 (m, 2H, H-2"), 2.79 (t, *J* = 7.0 Hz, 2H, H-3"), 2.87 (dd, *J* = 3.5, 11.5 Hz, 1H, H-3b), 3.44 (dd, *J* = 2.0, 9.0 Hz, 1H, H-7), 3.50 (dd, 1H, *J* = 8.0, 13.5 Hz, H-9a), 3.66 (m, 1H, H-6), 3.68-3.77 (m, 2H, H-4, H-5), 3.80 (dd, *J* = 3.5, 13.5 Hz, 1H, H-9b), 4.05 (td, *J* = 3.0, 8.5 Hz, 1H, H-8), 4.41 (t, *J* = 7.0 Hz, 2H, H-1"), 4.69, 4.95 (A, B of AB, *J* = 12.0 Hz, 2H, H-1'), 7.21 (s, 1H, CH_{ar}), 7.33 (m, 1H, CH_{ar}), 7.41-7.50 (m, 4H, CH_{ar}), 7.81 (m, 3H, CH_{ar}), 7.97 (s, 1H, triazole-H); ^{13}C NMR (CD_3OD, 125 MHz): δ = 22.6 (C-2"), 22.6 (NHAc) 31.6 (C-3"), 42.6 (C-3), 44.5 (C-9), 50.8 (C-1"), 54.1 (C-5), 58.9 (C-1'), 69.7 (C-4), 71.2 (C-8), 72.6 (C-7), 74.4 (C-6), 102.0 (C-2), 112.7, 115.8, 116.9 (q, *J* = 4.3 Hz), 118.8 (q, *J* = 3.5 Hz), 121.9 (q, *J* = 31.3 Hz), 125.4, 125.6, 127.9, 128.2, 129.5, 132.5, 135.8, 139.6, 146.8 (C-Ar), 170.3, 174.2, 175.4 (3 CO); HRMS: *m/z* calcd for $C_{33}H_{36}F_3N_6Na_2O_9$ $[M+Na]^+$: 763.2286, found: 763.2295.

*Sodium [3-(1-methyl-5-nitro-1H-indol-3-yl)-propyl-[1,2,3]triazole-4-yl-methyl 5-acetamido-9-benzamido-3,5,9-trideoxy-D-glycero-α-D-galacto-2-nonulopyranosid]onate (**7**).* Prepared from **21** (10 mg, 20 µmol) and **33** (6.5 mg, 30 µmol) according to general procedure C. Yield: 12.3 mg, 80%, yellow solid. $[\alpha]_D^{20}$ -19.8 (*c* 0.30, MeOH); ^{1}H NMR (CD_3OD, 500 MHz): *δ* = 1.62 (t, *J* = 11.5 Hz, 1H, H-3a), 2.0 (s, 3H, NHAc), 2.30 (m, 2H, H-2"), 2.80 (t, *J* = 7.0 Hz, 2H, H-3"), 2.88 (dd, *J* = 3.0, 11.5 Hz, 1H, H-3b), 3.43 (d, *J* = 9.0 Hz, 1H, H-7), 3.48 (dd, 1H, *J* = 8.0, 13.5 Hz, H-9a), 3.66 (d, *J* = 9.0 Hz, 1H, H-6), 3.82 (s, 3H, NCH_3), 3.71-3.81 (m, 3H, H-4, H-5, H-9b), 4.03 (dt, *J* = 2.5, 8.5 Hz, 1H, H-8), 4.43 (t, *J* = 7.0 Hz, 2H, H-1"), 4.67, 4.94 (A, B of AB, *J* = 12.5 Hz, 2H, H-1'), 7.20 (s, 1H, CH_{ar}), 7.40-7.50 (m, 4H, CH_{ar}), 7.80 (d, *J* = 8.0 Hz, 2H, CH_{ar}), 7.96 (s, 1H, triazole-H), 8.06 (dd, *J* = 4.0, 1.5 Hz, 1H, CH_{ar}), 8.48 (d, *J* = 1.5 Hz, 1H, CH_{ar}); ^{13}C NMR (CD_3OD, 125 MHz): *δ* = 22.5 (NHAc), 22.6 (C-3"), 31.6 (C-2"), 33.2 (NCH_3), 42.6 (C-3), 44.6 (C-9), 50.8 (C-1"), 54.0 (C-5), 59.0 (C-1'), 69.6 (C-4), 71.3 (C-8), 72.5 (C-7), 74.4 (C-6), 102.0 (C-2), 110.6, 116.8, 117.3, 117.9, 125.4, 128.3, 131.6, 132.1, 135.8, 141.3, 142.2, 146.9 (C-Ar), 170.3, 174.1, 175.4 (3 CO); HRMS: *m/z* calcd for $C_{33}H_{38}N_7Na_2O_{11}$ $[M+Na]^+$: 754.2419, found: 754.2419.

*Sodium [3-(1-ethyl-5-nitro-1H-indol-3-yl)-propyl-[1,2,3]triazole-4-yl-methyl 5-acetamido-9-benzamido-3,5,9-trideoxy-D-glycero-α-D-galacto-2-nonulopyranosid]onate (**8**).* Prepared from **21** (10 mg, 20 µmol) and **34** (6.8 mg, 30 µmol) according to general procedure C. Yield: 11 mg, 71%, yellow solid. $[\alpha]_D^{20}$ -18.9 (*c* 0.27, MeOH); ^{1}H NMR (CD_3OD, 500 MHz): *δ* = 1.43 (t, *J* = 7.5 Hz, 3H, NCH_2CH_3), 1.62 (t, *J* = 11.5 Hz, 1H, H-3a), 2.0 (s, 3H, NHAc), 2.32 (m, 2H, H-2"), 2.81 (t, *J* = 7.5 Hz, 2H, H-3"), 2.88 (dd, *J* = 4.0, 12.5 Hz, 1H, H-3b), 3.43 (d, *J* = 9.0 Hz, 1H, H-7), 3.48 (dd, 1H, *J* = 8.0, 13.5 Hz, H-9a), 3.66 (m, 1H, H-6), 3.71-3.74 (m, 2H, H-5, H-4), 3.81 (dd, *J* = 3.0, 13.5 Hz, 1H, H-9b), 4.04 (td, *J* = 3.0, 8.0 Hz, 1H, H-8), 4.23 (q, *J* = 7.0 Hz, 2H, NCH_2), 4.44 (t, *J* = 7.0 Hz, 2H, H-1"), 4.67, 4.94 (A, B of AB, *J* = 12.5 Hz, 2H, H-1'), 7.28 (s, 1H, CH_{ar}), 7.40-7.49 (m, 4H, CH_{ar}), 7.81 (d, *J* = 7.5 Hz, 2H, CH_{ar}), 7.96 (s, 1H, triazole-H), 8.06 (dd, *J* = 2.0, 9.0 Hz, 1H, CH_{ar}), 8.49 (d, *J* = 1.5 Hz, 1H, CH_{ar}); ^{13}C NMR (CD_3OD, 126 MHz): *δ* = 15.8 (NCH_2CH_3), 22.6 (C-3"), 22.6 (NHAc), 31.6 (C-2"), 42.2 (NCH_2), 42.6 (C-3), 44.6 (C-9), 50.8 (C-1"), 54.1 (C-5), 59.0 (C-1'), 69.6 (C-4), 71.2 (C-8), 72.6 (C-7), 74.4 (C-6), 102.0 (C-2), 110.6, 116.9, 117.5, 117.8, 125.3, 128.3, 128.4, 129.5, 129.9, 132.5, 135.8, 140.4, 142.2, 146.9 (C-Ar), 170.3, 174.1, 175.4 (3 CO); HRMS: *m/z* calcd for $C_{34}H_{40}N_7Na_2O_{11}$ $[M+Na]^+$: 768.2576, found: 768.2580.

*Sodium [3-(5-methoxy-1H-indol-3-yl)-propyl-[1,2,3]triazole-4-yl-methyl 9-(4-chloro-benzamido)-3,5,9-trideoxy-5-fluoroacetamido-D-glycero-α-D-galacto-2-nonulopyranosid]onate (**9**).* Prepared from **22b** (10 mg, 20.0 µmol) and **26b** (6.9 mg, 30.0 µmol) according to general procedure C. Yield: 8.6 mg, 61%. $[\alpha]_D^{20}$ -20.5 (*c* 0.67, MeOH); ^{1}H NMR (500 MHz, CD_3OD): *δ* = 1.64 (t, *J* = 11.9 Hz, 1H, H-3a), 2.27 (p, *J* = 7.1 Hz, 2H, H-2"),

2.72 (t, *J* = 7.3 Hz, 2H, H-3"), 2.88 (dd, *J* = 4.7, 12.2 Hz, 1H, H-3b), 3.43-3.53 (m, 2H, H-7, H-9a), 3.81 (s, 3H, OCH_3), 3.77-3.87 (m, 3H, H-4, H-6, H-9b), 3.91 (m, 1H, H-5), 4.04 (td, *J* = 3.1, 8.4 Hz, 1H, H-8), 4.40 (t, *J* = 6.9 Hz, 2H, H-1"), 4.68 (A of AB, *J* = 12.2 Hz, 1H, H-1'a), 4.84 (d, *J* = 47.0 Hz, 2H, CH_2F), 4.96 (B of AB, *J* = 12.2 Hz, 1H, H-1'b), 6.73 (dd, *J* = 2.4, 8.8 Hz, 1H, CH_{ar}), 6.95 (d, *J* = 2.3 Hz, 1H, CH_{ar}), 7.02 (s, 1H, CH_{ar}), 7.21 (d, J = 8.8 Hz, 1H, CH_{ar}), 7.42 (d, *J* = 8.5 Hz, 2H, CH_{ar}), 7.80 (t, *J* = 7.1 Hz, 2H, CH_{ar}), 7.94 (s, 1H, CH_{ar}); ^{13}C NMR (126 MHz, CD_3OD): *δ* = 23.0 (C-3"), 31.9 (C-2"), 42.7 (C-3), 44.7 (C-9), 51.0 (C-1"), 53.7 (C-5), 56.5 (OCH_3), 59.1 (C-1'), 69.7 (C-4), 71.7 (C-8), 72.5 (C-7), 74.0 (C-6), 81.1 (d, *J* = 183 Hz, CH_2F), 101.3 (C-2), 112.8, 113.1, 114.4, 124.3, 125.5, 129.0, 129.8, 130.2, 133.6, 134.6, 138.7, 155.1 (C-Ar), 169.4, 172.2, 172.3 (3 CO); HRMS: *m/z* calcd for $C_{33}H_{37}ClFN_6Na_2O_{10}$ $[M+Na]^+$: 777.2039, found: 777.2039.

*Sodium [3-(5-chloro-1H-indol-3-yl)-propyl-[1,2,3]triazole-4-yl-methyl 9-(4-chloro-benzamido)-3,5,9-trideoxy-5-fluoroacetamido-D-glycero-α-D-galacto-2-nonulopyranosid]onate (**10**).* Prepared from **22b** (30.0 mg, 59.1 µmol) and **26c** (20.8 mg, 88.6 µmol) according to general procedure C. Yield: 27 mg, 60%. $[\alpha]_D^{20}$ -21.0 (*c* 1.08, MeOH); ^{1}H NMR (500 MHz, CD_3OD): *δ* = 1.61 (m, 1H, H-3a), 2.23 (p, *J* = 7.1 Hz, 2H, H-2"), 2.69 (t, *J* = 7.3 Hz, 2H, H-3"), 2.88 (dd, *J* = 4.6, 12.2 Hz, 1H, H-3b), 3.39-3.59 (m, 2H, H-7, H-9a), 3.74-3.97 (m, 4H, H-4, H-5, H-6, H-9b), 4.03 (td, *J* = 3.0, 8.5 Hz, 1H, H-8), 4.37 (t, *J* = 7.0 Hz, 2H, H-1"), 4.68 (A of AB, *J* = 12.2 Hz, 1H, H-1'a), 4.84 (d, *J* = 46.7 Hz, 2H, CH_2F), 4.95 (B of AB, *J* = 12.2 Hz, 1H, H-1'b), 7.02 (dd, *J* = 2.0, 8.6 Hz, 1H, CH_{ar}), 7.09 (s, 1H, CH_{ar}), 7.28 (d, *J* = 8.6 Hz, 1H, CH_{ar}), 7.40 (d, *J* = 8.6 Hz, 2H, CH_{ar}), 7.44 (d, *J* = 1.9 Hz, 1H, CH_{ar}), 7.79 (d, *J* = 8.6 Hz, 2H, CH_{ar}), 7.91 (s, 1H, CH_{ar}); ^{13}C NMR (126 MHz, CD_3OD): *δ* = 22.9 (C-3"), 31.8 (C-2"), 42.6 (C-3), 44.6 (C-9), 51.0 (C-1"), 53.7 (C-5), 59.0 (C-1'), 69.6 (C-4), 71.8 (C-8), 72.4 (C-7), 74.0 (C-6), 81.1 (d, *J* = 183 Hz, CH_2F), 102.2 (C-2), 113.6, 114.5, 118.8, 122.6, 125.3, 125.4, 125.5, 129.8, 130.2, 134.5, 136.7, 138.7, 146.8 (C-Ar), 169.4, 172.1, 172.3 (3 CO); HRMS: *m/z* calcd for $C_{32}H_{35}Cl_2FN_6NaO_9$ $[M+Na]^+$: 781.1544, found: 781.1547.

*Sodium [3-(5-fluoro-1H-indol-3-yl)-propyl-[1,2,3]triazole-4-yl-methyl 9-(4-chloro-benzamido)-3,5,9-trideoxy-5-fluoroacetamido-D-glycero-α-D-galacto-2-nonulopyranosid]onate (**11**).* Prepared from **22b** (13 mg, 25.7 µmol) and **26d** (8.4 mg, 38.5 µmol) according to general procedure C. Yield: 10 mg, 50%. $[\alpha]_D^{20}$ -17.6 (*c* 0.68, MeOH); ^{1}H NMR (500 MHz, CD_3OD): *δ* = 1.65 (t, *J* = 12.0 Hz, 1H, H-3a), 2.26 (p, *J* = 7.2 Hz, 2H, H-2"), 2.71 (t, *J* = 7.3 Hz, 2H, H-3"), 2.88 (dd, *J* = 4.8, 12.3 Hz, 1H, H-3b), 3.42-3.54 (m, 2H, H-7, H-9a), 3.75-3.87 (m, 3H, H-4, H-6, H-9b), 3.91 (m, 1H, H-5), 4.04 (td, *J* = 3.1, 8.1 Hz, 1H, H-8), 4.39 (t, *J* = 7.0 Hz, 2H, H-1"), 4.68 (A of AB, *J* = 12.2 Hz, 1H, H-1'a), 4.84 (d, *J* = 47.0 Hz, 2H, CH_2F), 4.95 (B of AB, *J* = 12.2 Hz, 1H, H-1'b), 6.83 (td, *J* = 2.5, 9.1 Hz, 1H, CH_{ar}), 7.11

(s, 1H, CH_{ar}), 7.14 (dd, *J* = 2.5, 9.9 Hz, 1H, CH_{ar}), 7.27 (dd, *J* = 4.4, 8.8 Hz, 1H, CH_{ar}), 7.39-7.46 (m, 2H, CH_{ar}), 7.76-7.84 (m, 2H, CH_{ar}), 7.94 (s, 1H, CH_{ar}); ^{13}C NMR (126 MHz, CD_3OD): *δ* = 23.0 (C-3"), 31.8 (C-2"), 42.8 (C-3), 44.7 (C-9), 51.0 (C-1"), 53.8 (C-5), 59.1 (C-1'), 69.7 (C-4), 71.7 (C-8), 72.5 (C-7), 74.0 (C-4), 81.1 (d, *J* = 183 Hz, CH_2F), 102.2 (C-2), 104.0 (d, *J* = 23.4 Hz, Ind-C4), 110.5 (d, *J* = 26.5, Ind-C6), 113.2 (d, *J* = 9.7 Hz, Ind-C7), 114.9 (d, *J* = 4.8 Hz, Ind-C8), 125.5, 125.6 (C-Ar), 129.0 (d, *J* = 9.6 Hz, Ind-C3), 129.8, 130.2, 134.7, 135.0, 138.8, 146.9 (C-Ar), 159.0 (d, *J* = 232 Hz, Ind-C5), 169.5, 172.2, 172.3 (3 CO); HRMS: *m/z* calcd for $C_{32}H_{34}ClF_2N_6Na_2O_9$ $[M+Na]^+$: 765.1839, found: 765.1842.

*Sodium [3-(7-methyl-1H-indol-3-yl)-propyl-[1,2,3]triazole-4-yl-methyl 9-(4-chloro-benzamido)-3,5,9-trideoxy-5-fluoroacetamido-D-glycero-α-D-galacto-2-nonulopyranosid]onate (**12**).* Prepared from **22b** (16.0 mg, 32.7 µmol) and **26e** (10.6 mg, 49.0 µmol) according to general procedure C. Yield: 18 mg, 75%. $[\alpha]_D^{20}$ -23.2 (*c* 1.00, MeOH); ^{1}H NMR (500 MHz, CD_3OD): *δ* = 1.65 (t, *J* = 11.9 Hz, 1H, H-3a), 2.25-2.29 (m, 2H, H-2"), 2.46 (s, 3H, CH_3), 2.74 (t, *J* = 7.3 Hz, 2H, H-3"), 2.88 (dd, *J* = 4.7, 12.3 Hz, 1H, H-3b), 3.44-3.53 (m, 2H, H-7, H-9a), 3.76-3.87 (m, 3H, H-4, H-6, H-9b), 3.95 (m, 1H, H-5), 4.03 (td, *J* = 2.9, 8.5 Hz, 1H, H-8), 4.37 (t, *J* = 7.0 Hz, 2H, H-1"), 4.67 (A of AB, *J* = 12.2 Hz, 1H, H-1'a), 4.84 (d, *J* = 46.9 Hz, 2H, CH_2F), 4.95 (B of AB, *J* = 12.2 Hz, 1H, H-1'b), 6.83-6.94 (m, 2H, CH_{ar}), 7.05 (s, 1H, CH_{ar}), 7.31 (d, *J* = 7.5 Hz, 1H, CH_{ar}), 7.41 (d, *J* = 8.5 Hz, 2H, CH_{ar}), 7.79 (d, *J* = 8.5 Hz, 2H, CH_{ar}), 7.92 (s, 1H, CH_{ar}); ^{13}C NMR (126 MHz, CD_3OD): *δ* = 17.0 (CH_3), 23.2 (C-3"), 32.0 (C-2"), 42.7 (C-3), 44.7 (C-9), 51.0 (C-1"), 53.7 (C-5), 59.0 (C-1'), 69.6 (C-4), 71.7 (C-8), 72.4 (C-7), 74.0 (C-6), 81.1 (d, *J* = 183 Hz, CH_2F), 102.1 (C-2), 115.0, 117.1, 120.0, 121.8, 123.0, 123.3, 125.5, 128.3, 129.8, 130.2, 134.6, 137.8, 138.7 (C-Ar), 169.4, 172.2, 172.3 (3 CO); HRMS: *m/z* calcd for $C_{33}H_{37}ClFN_6Na_2O_9$ $[M+Na]^+$: 761.2090, found: 761.2091.

*Sodium [3-(6-chloro-1H-indol-3-yl)-propyl-[1,2,3]triazole-4-yl-methyl 9-(4-chloro-benzamido)-3,5,9-trideoxy-5-fluoroacetamido-D-glycero-α-D-galacto-2-nonulopyranosid]onate (**13**).* Prepared from **22b** (16.0 mg, 32.7 µmol) and **26f** (11.3 mg, 48.2 µmol) according to general procedure C. Yield: 19 mg, 79%). $[\alpha]_D^{20}$ -24.3 (*c* 1.07, MeOH); ^{1}H NMR (500 MHz, CD_3OD): *δ* = 1.65 (t, *J* = 12.0 Hz, 1H, H-3a), 2.28 (p, *J* = 7.1 Hz, 2H, H-2"), 2.88 (dd, *J* = 4.7, 12.3 Hz, 1H, H-3b), 2.95 (t, *J* = 7.4 Hz, 2H, H-3"), 3.40-3.57 (m, 2H, H-7, H-9a), 3.77-3.87 (m, 3H, H-4, H-6, H-9b), 3.92 (m, 1H, H-5), 4.04 (td, *J* = 3.1, 8.4 Hz, 1H, H-8), 4.41 (t, *J* = 6.9 Hz, 2H, H-1"), 4.67 (A of AB, *J* = 12.2 Hz, 1H, H-1'a), 4.84 (d, *J* = 47.0 Hz, 2H, CH_2F), 4.95 (B of AB, *J* = 12.2 Hz, 1H, H-1'b), 6.92 (d, *J* = 7.5 Hz, 1H, CH_{ar}), 6.98 (t, *J* = 7.8 Hz, 1H, CH_{ar}), 7.08 (s, 1H, CH_{ar}), 7.25 (d, *J* = 8.0 Hz, 1H, CH_{ar}), 7.41 (d, *J* = 8.5 Hz, 2H, CH_{ar}), 7.79 (d, *J* = 8.5 Hz, 2H, CH_{ar}), 7.95 (s, 1H, CH_{ar}); ^{13}C NMR (126 MHz, CD_3OD): *δ* = 24.3 (C-3"), 33.7 (C-2"), 42.7 (C-3), 44.7 (C-9), 51.0 (C-1"), 53.7 (C-5), 59.0 (C-

1'), 69.7 (C-4), 71.7 (C-8), 72.5 (C-7), 74.0 (C-6) 81.1 (d, *J* = 183 Hz, CH_2F), 102.2 (C-2), 111.5, 115.1, 120.7, 123.0, 125.2, 125.5, 125.6, 126.9, 129.8, 130.2, 134.6, 138.7, 140.0, 146.9 (C-Ar), 169.4, 172.2, 172.3 (3 CO); HRMS: *m/z* calcd for $C_{32}H_{34}Cl_2FN_6Na_2O_9$ $[M+Na]^+$: 781.1544, found: 781.1548.

*Sodium [3-(5-isopropyl-1H-indol-3-yl)-propyl-[1,2,3]triazole-4-yl-methyl 9-(4-chloro-benzamido)-3,5,9-trideoxy-5-fluoroacetamido-D-glycero-α-D-galacto-2-nonulopyranosid]onate (**14**).* Prepared from **22b** (17.5 mg, 34.9 µmol) and **26g** (12.7 mg, 52.4 µmol) according to general procedure C. Yield: 13 mg, 50%. $[\alpha]_D^{20}$ -18.5 (*c* 0.97, MeOH); ^{1}H NMR (500 MHz, CH_3OD): *δ* = 1.28 (d, *J* = 6.9 Hz, 6H, 2 CH_3), 1.65 (t, *J* = 11.8 Hz, 1H, H-3a), 2.28 (p, *J* = 7.1 Hz, 2H, H-2"), 2.74 (t, *J* = 7.3 Hz, 2H, H-3"), 2.89 (dd, *J* = 3.3, 11.8 Hz, 1H, H-3b), 2.95 (m, 1H, CH), 3.43-3.52 (m, 2H, H-7, H-9a), 3.77-3.87 (m, 3H, H-4, H-6, H-9b), 3.91 (m, 1H, H-5), 4.04 (td, *J* = 2.3, 8.3 Hz, 1H, H-8), 4.39 (t, *J* = 6.9 Hz, 2H, H-1"), 4.68 (A of AB, *J* = 11.9 Hz, 1H, H-1'a), 4.84 (d, *J* = 47.0 Hz, 2H, CH_2F), 4.95 (B of AB, *J* = 11.9 Hz, 1H, H-1'b), 6.98 (dd, *J* = 1.3, 8.4 Hz, 1H, CH_{ar}), 7.01 (s, 1H, CH_{ar}), 7.24 (d, *J* = 8.4 Hz, 1H, CH_{ar}), 7.29 (s, 1H, CH_{ar}), 7.41 (d, *J* = 8.5 Hz, 2H, CH_{ar}), 7.79 (d, *J* = 8.5 Hz, 2H, C_6H_4), 7.95 (s, 1H, CH_{ar}); ^{13}C NMR (126 MHz, CD_3OD): *δ* = 23.1 (C-3"), 25.4 (2C, 2 CH_3), 31.9 (C-2"), 35.7 (CH), 42.7 (C-3), 44.7 (C-9), 51.1 (C-1"), 53.7 (C-5), 59.1 (C-1'), 69.7 (C-4), 71.7 (C-8), 72.5 (C-7), 74.0 (C-6), 81.1 (d, *J* = 183 Hz, CH_2F), 102.1 (C-2), 112.2, 114.4, 116.2, 121.6, 123.6, 128.8, 129.8, 130.2, 134.6, 137.0, 138.7, 140.4 (C-Ar), 169.4, 172.2, 172.3 (3 CO); HRMS: *m/z* calcd for $C_{35}H_{41}ClFN_6Na_2O_9$ $[M+Na]^+$: 789.2403, found: 789.2406.

*Sodium [3-(1,5,6,7-tetrahydrocyclopenta[f]indole-3-yl)-propyl-[1,2,3]triazole-4-yl-methyl 9-(4-chlorobenzamido)-3,5,9-trideoxy-5-fluoroacetamido-D-glycero-α-D-galacto-2-nonulopyranosid]onate (**15**).* Prepared from **22b** (10 mg, 19.1 µmol) and **26h** (6.9 mg, 28.7 µmol) according to general procedure C. Yield: 9 mg, 64%. $[\alpha]_D^{20}$ -24.5 (*c* 0.57, MeOH); ^{1}H NMR (500 MHz, CD_3OD): *δ* = 1.65 (t, *J* = 11.9 Hz, 1H, H-3a), 2.07 (p, *J* = 7.2 Hz, 2H, Cyc-CH_2), 2.26 (p, *J* = 6.9 Hz, 2H, H-2"), 2.71 (t, *J* = 7.2 Hz, 2H, H-3"), 2.89 (dd, *J* = 4.7, 12.3 Hz, 1H, H-3b), 2.93 (t, *J* = 7.2 Hz, 4H, 2 Cyc-CH_2), 3.43-3.53 (m, 2H, H-7, H-9a), 3.76-3.86 (m, 3H, H-4, H-6, H-9b), 3.91 (m, 1H, H-5), 4.03 (td, *J* = 3.0, 8.4 Hz, 1H, H-8), 4.38 (t, *J* = 7.0 Hz, 2H, H-1"), 4.68 (A of AB, *J* = 12.2 Hz, 1H, H-1'a), 4.84 (d, *J* = 47.0 Hz, 2H, CH_2F), 4.96 (B of AB, *J* = 12.2 Hz, 1H, H-1'b), 6.94 (s, 1H, CH_{ar}), 7.14 (s, 1H, CH_{ar}), 7.26 (s, 1H, CH_{ar}), 7.41 (d, *J* = 8.5 Hz, 2H, CH_{ar}), 7.79 (d, *J* = 8.5 Hz, 2H, CH_{ar}), 7.93 (s, 1H, CH_{ar}); ^{13}C NMR (126 MHz, CD_3OD): *δ* = 23.2 (C-3"), 27.9 (Cyc-CH_2), 31.9 (C-2"), 33.6, 33.9 (2 Cyc-CH_2), 42.7 (C-3), 44.7 (C-9), 51.1 (C-1"), 53.7 (C-5), 59.0 (C-1'), 69.7 (C-4), 71.7 (C-8), 72.5 (C-7), 74.0 (C-6), 81.1 (d, *J* = 183 Hz, CH_2F), 101.9 (C-2), 107.6, 114.1, 114.1, 122.9, 125.5, 128.0, 129.8, 130.2, 134.6, 136.2, 138.1, 138.7, 139.5 (C-Ar), 169.4, 172.2, 172.3 (3 CO); HRMS: *m/z* calcd for $C_{35}H_{39}ClFN_6Na_2O_9$ $[M+Na]^+$: 787.2246, found: 787.2248.

*Sodium [3-(7-chloro-1H-indol-3-yl)-propyl-[1,2,3]triazole-4-yl-methyl 9-(4-chlorobenzamido)-3,5,9-trideoxy-5-fluoroacetamido-D-glycero-α-D-galacto-2-nonulopyranosid]onate (**16**).* Prepared from **22b** (12.0 mg, 24.1 µmol) and **26i** (8.5 mg, 30.2 µmol) according to general procedure C. Yield: 15 mg, 83%. $[\alpha]_D^{20}$ -22.6 (*c* 1.00, MeOH); ^{1}H NMR (500 MHz, CD_3OD): *δ* = 1.65 (t, *J* = 11.9 Hz, 1H, H-3a), 2.28 (p, *J* = 7.2 Hz, 2H, H-2"), 2.74 (t, *J* = 7.4 Hz, 2H, H-3"), 2.88 (dd, *J* = 4.7, 12.3 Hz, 1H, H-3b), 3.43-3.53 (m, 2H, H-7, H-9a), 3.74-3.88 (m, 3H, H-4, H-6, H-9b), 3.92 (m, 1H, H-5), 4.03 (td, *J* = 3.1, 8.4 Hz, 1H, H-8), 4.40 (t, *J* = 7.0 Hz, 2H, H-1"), 4.69 (A of AB, *J* = 12.3 Hz, 1H, H-1'a), 4.84 (d, *J* = 47.0 Hz, 2H, CH_2F), 4.96 (B of AB, *J* = 12.2 Hz, 1H, H-1'b), 6.97 (t, *J* = 7.7 Hz, 1H, CH_{ar}), 7.09 (d, *J* = 7.5 Hz, 1H, CH_{ar}), 7.14 (s, 1H), 7.38-7.47 (m, 3H, CH_{ar}), 7.76-7.83 (m, 2H, CH_{ar}), 7.96 (s, 1H, CH_{ar}); ^{13}C NMR (126 MHz, CD_3OD): *δ* = 23.0 (C-3"), 31.9 (C-2"), 42.7 (C-3), 44.7 (C-9), 51.0 (C-1"), 53.7 (C-5), 59.1 (C-1'), 69.7 (C-4), 71.7 (C-8), 72.5 (C-7), 74.0 (C-6), 81.1 (d, *J* = 183 Hz, CH_2F), 102.0 (C-2), 116.0, 117.8, 118.4, 120.6, 121.9, 124.7, 125.5, 129.8, 130.2, 130.6, 134.6, 135.2, 138.7 (C-Ar), 169.4, 172.2, 172.3 (3 CO); HRMS: *m/z* calcd for $C_{32}H_{34}Cl_2FN_6Na_2O_9$ $[M+Na]^+$: 781.1544, found: 781.1544.

*Sodium [3-(5-cyano-1H-indol-3-yl)-propyl-[1,2,3]triazole-4-yl-methyl 9-(4-chlorobenzamido)-3,5,9-trideoxy-5-fluoroacetamido-D-glycero-α-D-galacto-2-nonulopyranosid]onate (**17**).* Prepared from **22b** (15.3 mg, 30.5 µmol) and **26j** (10.3 mg, 45.7 µmol) according to general procedure C: Yield: 16 mg, 72%. $[\alpha]_D^{20}$ -22.1 (*c* 1.07, MeOH); ^{1}H NMR (500 MHz, CD_3OD): *δ* = 1.65 (t, *J* = 11.9 Hz, 1H, H-3a), 2.28 (p, *J* = 7.1 Hz, 2H, H-2"), 2.73-2.83 (m, 2H, H-3"), 2.88 (dd, *J* = 4.8, 12.3 Hz, 1H, H-3b), 3.48 (dd, *J* = 8.1, 13.9 Hz, 2H, H-7, H-9a), 3.76-3.88 (m, 3H, H-4, H-6, H-9b), 3.91 (m, 1H, H-5), 4.03 (td, *J* = 3.1, 8.3 Hz, 1H, H-8), 4.41 (t, *J* = 6.9 Hz, 2H, H-1"), 4.68 (A of AB, *J* = 12.3 Hz, 1H, H-1'a), 4.84 (d, *J* = 47.0 Hz, 2H, CH_2F), 4.95 (B of AB, *J* = 12.3 Hz, 1H, H-1'b), 7.23 (s, 1H, CH_{ar}), 7.35 (dd, *J* = 1.4, 8.4 Hz, 1H, CH_{ar}), 7.42 (d, *J* = 8.6 Hz, 2H, CH_{ar}), 7.46 (d, *J* = 8.4 Hz, 1H, CH_{ar}), 7.79 (d, *J* = 8.6 Hz, 2H, CH_{ar}), 7.95 (s, 2H, CH_{ar}); ^{13}C NMR (126 MHz, CD_3OD): *δ* = 22.7 (C-3"), 31.7 (C-2"), 42.7 (C-3), 44.7 (C-9), 50.9 (C-1"), 53.7 (C-5), 59.0 (C-1'), 69.7 (C-4), 71.7 (C-8), 72.5 (C-7), 74.0 (C-6), 81.1 (d, *J* = 183 Hz, CH_2F), 102.2, 102.3 (C-2, C-Ar), 113.6, 116.1, 122.2, 125.3, 125.4, 125.5, 126.3, 128.6, 129.8, 130.2, 134.6, 138.7, 140.1, 146.9 (CN, C-Ar), 169.4, 172.2, 172.3 (3 CO); HRMS: *m/z* calcd for $C_{33}H_{34}ClFN_7Na_2O_9$ $[M+Na]^+$: 772.1886, found: 772.1891.

*Sodium [3-(5-methylsulfonyl-1H-indol-3-yl)-propyl-[1,2,3]triazole-4-yl-methyl 9-(4-chlorobenzamido)-3,5,9-trideoxy-5-fluoroacetamido-D-glycero-α-D-galacto-2-nonulopyranosid]onate (**18**).* Prepared from **22b** (9.6 mg, 19.2 µmol) and **26k** (8.0 mg, 28.7 µmol) according to general procedure C. Yield: 15 mg, 66%. $[\alpha]_D^{20}$ -20.4 (*c* 0.60, MeOH); ^{1}H NMR (500 MHz, CD_3OD): *δ* = 1.64 (t, *J* = 12.0 Hz, 1H, H-3a), 2.32 (p, *J* = 7.1 Hz, 2H, H-2"),

2.82 (t, *J* = 7.4 Hz, 2H, H-3"), 2.88 (dd, *J* = 4.8, 12.3 Hz, 1H, H-3b), 3.12 (s, 3H, CH_3), 3.43-3.50 (m, 2H, H-7, H-9a), 3.77-3.86 (m, 3H, H-4, H-6, H-9b), 3.90 (m, 1H, H-5), 4.04 (td, *J* = 3.1, 8.3 Hz, 1H, H-8), 4.42 (t, *J* = 6.9 Hz, 2H, H-1"), 4.67 (A of AB, *J* = 12.3 Hz, 1H, H-1'a), 4.84 (d, *J* = 46.9 Hz, 2H, CH_2F), 4.94 (B of AB, *J* = 12.3 Hz, 1H, H-1'b), 7.28 (s, 1H, CH_{ar}), 7.42 (d, *J* = 8.5 Hz, 2H, CH_{ar}), 7.53 (d, *J* = 8.6 Hz, 1H, CH_{ar}), 7.64 (dd, *J* = 1.7, 8.6 Hz, 1H, CH_{ar}), 7.80 (d, *J* = 8.5 Hz, 2H, CH_{ar}), 7.94 (s, 1H, CH_{ar}), 8.14 (d, *J* = 1.4 Hz, 1H, CH_{ar}); ^{13}C NMR (126 MHz, CD_3OD): *δ* = 22.8 (C-3"), 31.7 (C-2"), 42.7 (C-3), 44.7 (C-9), 45.5 (CH_3), 50.9 (C-1"), 53.7 (C-5), 59.1 (C-1'), 69.7 (C-4), 71.7 (C-8), 72.5 (C-7), 74.0 (C-6), 81.1 (d, *J* = 183 Hz, CH_2F), 102.2 (C-2), 113.2, 116.8, 120.4, 120.9, 125.5, 126.7, 128.3, 129.8, 130.2, 131.8, 134.6, 138.7, 140.7, 147.0 (C-Ar), 169.4, 172.2, 172.3 (3 CO); HRMS: *m/z* calcd for $C_{33}H_{37}ClFN_6Na_2O_{11}S$ $[M+Na]^+$: 825.1709, found: 825.1709.

*Sodium [3-(5-nitro-1H-indol-3-yl)-propyl-[1,2,3]triazole-4-yl-methyl 9-benzamido-3,5,9-trideoxy-5-fluoroacetamido-D-glycero-α-D-galacto-2-nonulopyranosid]onate (**19**).* Prepared from **22a** (15 mg, 30 µmol) and **26o** (12 mg, 45 µmol) according to general procedure C. Yield: 3.7 mg, 16%, yellow solid. $[\alpha]_D^{20}$ -20.6 (*c* 1.00, MeOH); ^{1}H NMR (500 MHz, D_2O): *δ* = 1.64 (t, *J* = 12.1 Hz, 1H, H-3a), 2.16-2.23 (m, 2H, H-2"), 2.61 (dd, *J* = 6.5, 11.9 Hz, 2H, H-3"), 2.69 (dd, *J* = 4.8, 12.5 Hz, 1H, H-3b), 3.34 (dd, *J* = 8.3, 14.0 Hz, 1H, H-9a), 3.52 (dd, *J* = 1.3, 8.6 Hz, 1H, H-7), 3.73 (m, 1H, H-4), 3.77-3.91 (m, 3H, H-6, H-8, H-9b), 3.95 (t, *J* = 10.1 Hz, 1H, H-5), 4.25-4.36 (m, 3H, H-1'a, H-1"), 4.55 (B of AB, *J* = 12.2 Hz, 1H, H-1'b), 4.92 (m, 1H, CH_2F), 7.04 (s, 1H, CH_{ar}), 7.23 (d, *J* = 9.0 Hz, 1H, CH_{ar}), 7.33 (t, *J* = 7.7 Hz, 2H, CH_{ar}), 7.43 (t, *J* = 7.4 Hz, 1H, CH_{ar}), 7.58 (s, 1H, CH_{ar}), 7.61 (d, *J* = 7.4 Hz, 2H, CH_{ar}), 7.78 (dd, *J* = 1.9, 8.9 Hz, 1H, CH_{ar}), 8.06 (d, *J* = 1.8 Hz, 1H, CH_{ar}); ^{13}C NMR (D_2O, 126 MHz): *δ* = 28.9 (C-3"), 40.2 (C-2"), 42.5 (C-9), 50.0 (C-1"), 51.1 (C-5), 57.0 (C-1'), 67.8 (C-4), 69.8 (C-7), 70.0 (C-8), 72.0 (C-6), 79.6 (d, *J* = 190 Hz, CH_2F), 101.9 (C-2), 111.0, 116.8, 125.0, 126.0, 126.7, 128.4, 131.9, 133.3 (C-Ar); HRMS: *m/z* calcd for $C_{32}H_{35}FN_7Na_2O_{11}$ $[M+Na]^+$: 758.2174, found: 758.2176.

*Sodium [3-(5-nitro-1H-indol-3-yl)-propyl-[1,2,3]triazole-4-yl-methyl 9-(4-chloro-benzamido)-3,5,9-trideoxy-5-fluoroacetamido-D-glycero-α-D-galacto-2-nonulopyranosid]onate (**20**).* Prepared from **22b** (18.3 mg, 36.4 µmol) and **26o** (13.3 mg, 54.6 µmol) according to general procedure C. Yield: 19 mg, 70%. $[\alpha]_D^{20}$ -21.6 (*c* 1.00, MeOH); ^{1}H NMR (500 MHz, CD_3OD): *δ* = 1.65 (t, *J* = 11.9 Hz, 1H, H-3a), 2.30 (p, *J* = 7.1 Hz, 2H, H-2"), 2.80 (t, *J* = 7.4 Hz, 2H, H-3"), 2.87 (dd, *J* = 3.9, 12.1 Hz, 1H, H-3b), 3.44-3.52 (m, 2H, H-7, H-9a), 3.78-3.95 (m, 4H, H-4, H-5, H-6, H-9b), 4.03 (m, 1H, H-8), 4.43 (t, *J* = 6.8 Hz, 2H, H-1"), 4.68 (A of AB, *J* = 12.2 Hz, 1H, H-1'a), 4.80 (m, 1H, CH_2F), 4.94 (B of AB, *J* = 12.2 Hz, 1H, H-1'b), 7.27 (s, 1H, CH_{ar}), 7.42 (dd, *J* = 8.8, 11.0 Hz, 3H, CH_{ar}), 7.79 (d, *J* = 8.5 Hz, 2H, CH_{ar}), 7.97 (s, 1H, CH_{ar}), 8.01 (dd, *J* = 2.1, 9.0 Hz, 1H, CH_{ar}), 8.48 (d, *J* = 2.1 Hz,

1H, CH_{ar}); ^{13}C NMR (126 MHz, CD_3OD): δ = 22.7 (C-3"), 31.7 (C-2"), 42.6 (C-3), 44.7 (C-9), 51.0 (C-1"), 53.8 (C-5), 59.0 (C-1'), 69.6 (C-4), 71.7 (C-8), 72.4 (C-7), 74.0 (C-6), 81.1 (d, *J* = 183 Hz, CH_2F), 102.0 (C-2), 112.6, 116.8, 117.7, 118.0, 127.3, 128.0, 129.8, 130.2, 134.5, 138.8, 141.4, 142.4 (C-Ar) 169.4, 172.2, 172.3 (3 CO); HRMS: *m/z* calcd for $C_{32}H_{34}ClFN_7Na_2O_{11}$ $[M+Na]^+$: 792.1784, found: 792.1787.

Surface Plasmon Resonance. The SPR measurements were performed on a Biacore 3000 surface plasmon resonance based optical biosensor (Biacore AB, Sweden). Sensor chips (CM5), immobilization kits, maintenance supply and HBS-EP (10 mM HEPES pH 7.4, 150 mM NaCl, 3 mM EDTA, 0.005% v/v surfactant P20) were purchased from Biacore AB. CM5 chips were preconditioned prior to usage by injecting a series of conditioning solutions. A flow rate of 50 µL/min was used and 2 × 20 µL of 50 mM NaOH, 10 mM HCl, 0.1% SDS and 100 mM H_3PO_4 were injected. The carboxyl groups on the CM5 chip were activated for 10 min with a 1:1 mixture of 0.1 M *N*-hydroxysuccinimide (NHS) and 0.1 M 3-(*N*,*N*-dimethylamino)propyl-*N*-ethylcarbodiimide (EDC) at a flow rate of 10 µL/min. Polyclonal goat anti-human IgG (Fc specific) was purchased from Sigma (I2136, Sigma-Aldrich Chemie GmbH, Buchs, Switzerland). A sample and a reference surface were prepared sequentially or in parallel. For immobilizing, a 30 µg/mL solution of the polyclonal antibody diluted in acetate buffer (10 mM sodium acetate, pH 5.0) was then injected over the activated surface for 10 min at a flow rate of 10 µL/min. Densities around 13,000 to 14,000 RU were achieved. Flow cells were blocked with a 10 min injection of 1 M ethanolamine, pH 8.0. For capturing, $MAG_{d1\text{-}3}$-Fc solution (expressed and purified as described[24]) was diluted to a 30-40 µg/mL concentration using HBS-EP. $MAG_{d1\text{-}3}$-Fc was injected at a flow rate of 1 µL/min for 10 min. The surface was equilibrated overnight at a flow rate of 5 µL/min, achieving densities around 3,500 to 4,000 RU. Tenfold dilution series were freshly prepared in eluent buffer immediately before use. All binding experiments were conducted at 25 °C at a flow rate of 20 µL/min. The samples were injected over 1 min followed by 1 min dissociation. Each sample was measured in duplicates for each concentration, using a randomized concentration order. Several buffer samples were injected before the first concentration, and one blank between each concentration, which were used for the double blank referencing during data processing. Double referencing was applied to correct for bulk effects and other systematic artifacts. Data processing and equilibrium binding constant determinations were accomplished with Scrubber (BioLogic Software, Version 1.1g or 2.0c). Kinetic data were simultaneously fit using the non-linear regression program Clamp or Scrubber 2.0c.

CMC determination. 10 mM stock solutions of the samples were prepared in DMSO. Then, a dilution series in DMSO was prepared by a Hamilton Microlab Star robot (Hamilton AG, Bonaduz, Switzerland) and 5 µL of each well were transferred into buffer

(0.05 M MOPSO, pH 6.5) to yield 50 µL of the 12 desired concentrations (between 0 and 1 mM). Before starting the experiment, the Delta-8 instrument (Kibron Inc., Espoo, Finland) used for the CMC determination was calibrated with water. Then, the surface tension of each of the 12 dilutions was measured and the results were analyzed with the Vector software (Kibron, version 4.02). The assay used for CMC determination was performed at F. Hoffmann-La Roche Ltd. (Basel).

Isothermal Titration Calorimetry. ITC experiments were performed using a VP-ITC instrument from MicroCal, Inc. (GE Healthcare, Northampton). The measurements were performed at 25 °C. Injections of 10 µL ligand solutions were added from a computer controlled 300 µL microsyringe at an interval of 5 min into the sample cell solution of MAG_{d1-3}-Fc (cell volume 1.4523 mL) with stirring at 307 rpm. A control experiment was performed, where the identical ligand solutions were injected into buffer without protein. The enthalpogram showed negligible heat development, resulting from dilution effects. The assay buffer was HBS-E (10 mM HEPES, 150 mM NaCl, 3 mM EDTA, *pH* 7.4). The concentration of MAG was between 5 and 9 µM (determined by HPLC[32]) and 100 µM antagonist solution was injected. The experimental data were fitted to a theoretical titration curve (one site binding model) using *Origin version 7* software (MicroCal, Northampton), with $\Delta H°$ (enthalpy change), K_A (association constant), and N (number of binding sites) as adjustable parameters. The quantity $c = Mt(0)\ K_D^{-1}$, where Mt(0) is the initial macromolecule concentration, is of importance in titration microcalorimetry. The experiments were performed with c values of 8-30. Thermodynamic parameters were calculated from equation (1),

$$\Delta G° = \Delta H° - T\Delta S° = RT\ln K_D = -RT\ln K_A \qquad (1)$$

where $\Delta G°$, $\Delta H°$, and $\Delta S°$ are the changes in free energy, enthalpy, and entropy of binding, respectively, T is the absolute temperature, and R is the universal gas constant (8.314 J mol^{-1} K^{-1}).[33]

Molecular Modeling. Molecular-dynamic simulations (MD) using *Desmond*,[28] were performed to check the stability of the proposed binding modes along with the kinetic aspects of the binding. The complexes were simulated during 4.0 ns at 300 K using explicit solvent (TIP3P water) and sampled at 1.2 ps intervals. Those frames were then analyzed for hydrogen-bond contribution, π stacking and the **1** $-NO_2\cdots$Lys 67 interactions to complex stabilization.

Hapten binding assay. Hapten inhibiton assays were performed with wild type and mutant MAG Fc-chimeras using immobilized fetuin as target as previously described.[24b] Essentially, Fc-chimeras complexed with alkaline phosphatase coupled anti-Fc antbodies were allows to bind to fetuin immobilized in microtitre plates in the presence of increasing

concentration of inhibitors and IC50 values determined from the resulting inhibition curves. At least three independent titrations were performed with triplicate each.

Expression & purification of mutant. MAG_{d1-3}-Fc mutant K67A was generated by site directed mutagenesis with the QuikChange Kit (Stratagene, La Jolla, CA, USA) according to the manufacture's instructions using the plasmid encoding Siglec-4_{d1-3}-Fc wt as a template and the following primer pair: 5'-CAATAGTCCCTACCCCGCGAACTACCCACCGGTG-3' and 5'-CACCGGTGGGTAGTTCGCGGGGTAGGGACTATTG-3'. CHO_{Lec1} cells stably secreting MAG_{d1-3}-Fc K67A or CHOLec3.2.1.8 cells expressing MAG_{d1-3}-Fc wt proteins were maintained in chemically defined Ex-Cell® media (Sigma-Aldrich, München, Germany) supplemented with 8 mM glutamine at 8 % CO2 and 37°C and purified as described.[2]4

Acknowledgement

We are greatly indebted to Frank Senner, Severin Wendelspiess and Dr. Manfred Kansy, Roche, for giving us access to their instruments for CMC determination.

References

[1] Schwab, M. E.; Bandtlow, C. E. *Nature* **1994**, *371*, 658.
[2] Ramon y Cajal, S. *Degeneration and Regeneration of the Nervous System*; Oxford University Press: London, 1928.
[3] Filbin, M. *Nature Rev. Neurosci.* **2003**, *4*, 1019.
[4] Chaudhry, N.; Filbin, M. T. *J. Cereb. Blood Flow Metab.* **2007**, *27*, 1096.
[5] a) Quarles, R. *Neurochem. Res.* **2009**, *34*, 79. b) Vinson, M.; Strijbos, P. J. L. M.; Rowles, A.; Facci, L.; Moore, S. E.; Simmons, D. L.; Walsh, F. S. *J. Biol. Chem.* **2001**, *276*, 20280. c) Vyas, A. A.; Patel, H. V.; Fromholt, S. E.; Heffer, L.; Vyas, K. A.; Dang, J. Y.; Schachner, M.; Schnaar, R. L. *Proc. Nat. Acad. Sci. U.S.A* **2002**, *99*, 8412. d) Vyas, A. A.; Blixt, O.; Paulson, J. C.; Schnaar, R. L. *J. Biol. Chem.* **2005**, *280*, 16305. e) Strenge, K.; Schauer, R.; Kelm, S. *FEBS Letters* **1999**, *444*, 59.
[6] Filbin, M. T. *Philos. Trans. R. Soc. Lond. B Biol. Sci.* **2006**, *361*, 1565.
[7] Yang, L. J. S.; Lorenzini, I.; Vajn, K.; Mountney, A.; Schramm, L. P.; Schnaar, R. L. *Proc. Nat. Acad. Sci. U.S.A* **2006**, *103*, 11057.
[8] Ernst, B.; Magnani, J. L. *Nature Rev. Drug Discov.* **2009**, *8*, 661.
[9] Shelke, S. V.; Gao, G. P.; Mesch, S.; Gäthje, H.; Kelm, S.; Schwardt, O.; Ernst, B. *Bioorg. Med. Chem.* **2007**, *15*, 4951.
[10] Schwardt, O.; Gaethje, H.; Vedani, A.; Mesch, S.; Gao, G.; Spreafico, M.; von Orelli, J.; Kelm, S.; Ernst, B. *J. Med. Chem.* **2009**, *52*, 989.
[11] Mesch, S.; Moser, D.; Strasser, D.; Kelm, A.; Cutting, B.; Rossato, G.; Vedani, A.; Koliwer-Brandl, H.; Wittwer, M.; Rabbani, S.; Schwardt, O.; Kelm, S.; Ernst, B. *J. Med. Chem.* **2010**, *53*, 1597.
[12] Arkin, M. R.; Wells, J. A. *Nature Rev. Drug Discov.* **2004**, *3*, 301.
[13] Shelke, S. V.; Cutting, B.; Jiang, X.; Koliwer-Brandl, H.; Strasser, D. S.; Kelm, S.; Schwardt, O.; Ernst, B. *Angew. Chem. Int. Ed.* **2010**, *49*, 5721.
[14] Jahnke, W.; Perez, L. B.; Paris, C. G.; Strauss, A.; Fendrich, G.; Nalin, C. M. *J. Am. Chem. Soc.* **2000**, *122*, 7394.
[15] Jahnke, W. *ChemBioChem* **2002**, *3*, 167.
[16] a) Lewis, W. G.; Green, L. G.; Grynszpan, F.; Radic, Z.; Carlier, P. R.; Taylor, P.; Finn, M. G.; Sharpless, K. B. *Angew. Chem. Int. Ed.* **2002**, *41*, 1053. b) Manetsch, R.; Krasinski, A.; Radic, Z.; Raushel, J.; Taylor, P.; Sharpless, K. B.; Kolb, H. C. *J. Am. Chem. Soc.* **2004**, *126*, 12809. c) Mocharla, V. P.; Colasson, B.; Lee, L.; Roeper, S.; Sharpless, K. B.; Wong, C.-H.; Kolb, H.

C. *Angew. Chem. Int. Ed.* **2005**, *44*, 116. d) Krasinski, A.; Radic, Z.; Manetsch, R.; Raushel, J.; Taylor, P.; Sharpless, K. B.; Kolb, H. C. *J. Am. Chem. Soc.* **2005**, *127*, 6686. e) Whiting, M.; Muldoon, J.; Lin, Y.-C.; Silverman, S. M.; Lindstrom, W.; Olson, A. J.; Kolb, H. C.; Finn, M. G.; Sharpless, K. B.; Elder, J. H.; Fokin, V. V. *Angew. Chem. Int. Ed.* **2006**, *46*, 1435.

[17] Kelm, S.; Brossmer, R.; Isecke, R.; Gross, H. J.; Strenge, K.; Schauer, R. *Eur. J. Biochem.* **1998**, *255*, 663.

[18] a) Tornøe, C. W.; Meldal, M. in *Peptides: The Wave of the Future: Proceedings of the Second International and the Seventeenth American Peptide Symposium*, Lebl, M.; Houghten, R. A., Eds.; Springer 2001, p263. b) Tornøe, C. W.; Christensen, C.; Meldal, M. *J. Org. Chem.* **2002**, *67*, 3057. (c) Kolb, H. C.; Sharpless, K. B. *Angew. Chem. Int. Ed.* **2001**, *40*, 2004.

[19] Campos, K. R.; Woo, J. C. S.; Lee, S.; Tillyer, R. D. *Org. Lett.* **2004**, *6*, 79.

[20] Mewshaw, R. E.; Zhou, D.; Zhou, P.; Shi, X.; Hornby, G.; Spangler, T.; Scerni, R.; Smith, D.; Schechter, L. E.; Andree, T. H. *J. Med. Chem.* **2004**, *47*, 3823.

[21] Gylys, J.; Ruediger, E. H.; Smith, D. W.; Solomon, C.; Yevich, J. P.; Dextraze, P. *US Patent* 5,382,592; *US Patent* 5,382,592, **1995**.

[22] Srinivasa, A.; Mahadevan, K. M.; Sureshakumara, T. H.; Hulikal, V. *Monatsh. Chem.* **2008**, *139*, 1475.

[23] Larock, R. C.; Yum, E. K.; Refvik, M. D. *J. Org. Chem.* **1998**, *63*, 7652.

[24] a) Bock, N.; Kelm, S. in *Methods in Molecular Biology*, Vol. 347; Brockhausen, I., Ed.; Humana Press: Totowa, NJ, 2006, p 359. b) Koliwer-Brandl, H.; Siegert, N.; Umnus, K.; Kelm, A.; Tolkach, A.; Kulozik, U.; Kuballa, J.; Cartellieri, S.; Kelm, S. *Int. Dairy J.* **2011**, *21*, 413.

[25] Meanwell, N. A. *J. Med. Chem.* **2011**, *54*, 2529.

[26] a) E. J. Toone, *Curr. Opin. Struc. Biol.* **1994**, *4*, 719. b) T. K. Dam, C. F. Brewer, *Chem. Rev.* **2002**, *102*, 387. c) M. Ambrosi, N. R. Cameron, B. G. Davis, *Org. Biomol. Chem.* **2005**, *3*, 1593.

[27] a) M. S. Searle, D. H. Williams, *J. Am. Chem. Soc.* **1992**, *114*, 10690. b) D. H. Williams, E. Stephens, D. P. O'Brien, M. Zhou, *Angew. Chem. Int. Edit.* **2004**, *43*, 6596. c) V. Lafont, A. A. Armstrong, H. Ohtaka, Y. Kiso, L. Mario Amzel, E. Freire, *Chem. Biol. Drug Des.* **2007**, *69*, 413.

[28] Bowers, K. J.; Chow, E.; Xu, H.; Dror, R. O.; Eastwood, M. P.; Gregersen, B. A.; Klepeis, J. L.; Kolossvary, I.; Moraes, M. A.; Sacerdoti, F. D.; Salmon, J. K.; Shan, Y.; Shaw, D. E. in *Proceedings of the 2006 ACM/IEEE Conference on Supercomputing (SC06)*; ACM Press: New York, 2006.

[29] a) Zaccai, N. R.; Maenaka, K.; Maenaka, T.; Crocker, P. R.; Brossmer, R.; Kelm, S.; Jones, E. Y. *Structure* **2003**, *11*, 557. b) Zaccai, N. R.; May, A. P.; Robinson, R. C.; Burtnick, L. D.; Crocker, P. R.; Brossmer, R.; Kelm, S.; Jones, E. Y. *J. Mol. Biol.* **2007**, *365*, 1469.

[30] Attrill, H.; Takazawa, H.; Witt, S.; Kelm, S.; Isecke, R.; Brossmer, R.; Ando, T.; Ishida, H.; Kiso, M.; Crocker, P. R.; van Aalten, D. M. F. *Biochem. J.* **2006**, *397*, 271.

[31] McIntyre, N. A.; McInnes, C.; Griffiths, G.; Barnett, A. L.; Kontopidis, G.; Slawin, A. M. Z.; Jackson, W.; Thomas, M.; Zheleva, D. I.; Wang, S.; Blake, D. G.; Westwood, N. J.; Fischer, P. M. *J. Med. Chem.* **2010**, *53*, 2136.

[32] a) F. Bitsch, R. Aichholz, J. Kallen, S. Geisse, B. Fournier, J. M. Schlaeppi, *Anal. Biochem.* **2003**, *323*, 139. b) S. Mesch, K. Lemme, H. Koliwer-Brandl, D. S. Strasser, O. Schwardt, S. Kelm, B. Ernst, *Carbohydr. Res.* **2010**, *345*, 1348.

[33] T. Wiseman, S. Williston, J. F. Brandts, L. N. Lin, *Anal. Biochem.* **1989**, *179*, 131.

Supporting Information

Stefanie Mesch[a,#], Bea Wagner[a,#], Xiaohua Jiang[a,#], Gianluca Rossato[a], Hendrik Koliwer-Brandl[b], Katrin Lemme[a], Daniel Schwizer[a], Angelo Vedani[a], Matthias Wittwer[a], Oliver Schwardt[a], Soerge Kelm[b], Beat Ernst[a,*]

[a]*Institute of Molecular Pharmacy, Pharmacenter, University of Basel, Klingelbergstr. 50, 4056 Basel, Switzerland*

[b]*Center for Biomolecular Interactions Bremen, Glycobiochemistry, University of Bremen, P.O.B. 330440, D-28334 Bremen, Germany*

[#] *Contributed equally*

[*] *Corresponding author. Tel.: 0041 267 15 51; fax.: 0041 267 15 52; e-mail: beat.ernst@unibas.ch*

Contents:

Isothermal Titration Calorimetry.

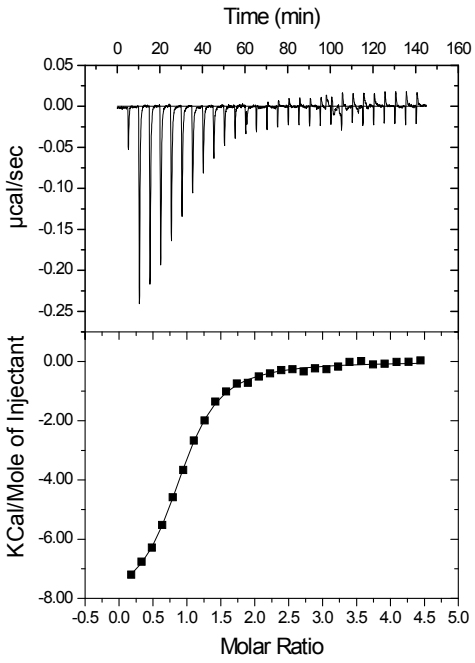

Figure S1: Enthalpogram of compound **1** with $MAG_{d1\text{-}3}$ Fc.

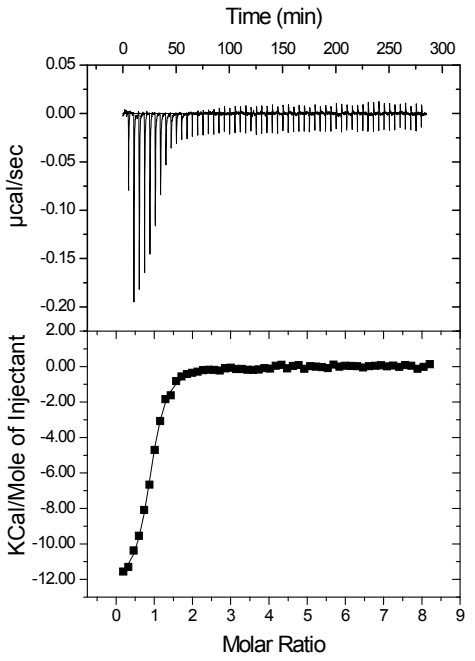

Figure S2: Enthalpogram of compound **5** with $MAG_{d1\text{-}3}$ Fc.

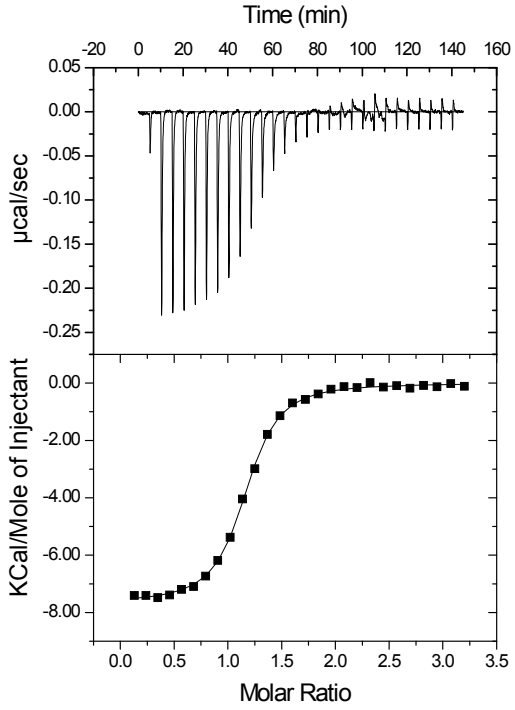

Figure S3: Enthalpogram of compound **19** with $MAG_{d1\text{-}3}$ Fc.

Compound Purity.

HPLC data for the target compounds

HPLC system: Agilent 1100 with UV detection (190-410 nm). A: Water + 0.1% formic acid; B: acetonitrile + 0.1% formic acid.

Method A: Column: Waters Atlantis dC18, 3µm, 4.6 × 75mm; gradient: 5% B → 70% B over 20 min; flow rate: 0.5 ml/min.

Method B: Column: Waters Atlantis dC18, 3µm, 4.6 × 75mm; gradient: 5% B → 95% B over 22 min; flow rate: 0.5 ml/min.

Table S1. HPLC data for the target compounds

	Formula	Method	Retention time	Purity
2	$C_{32}H_{37}N_6NaO_9$	A	12.97	97
3	$C_{33}H_{39}N_6NaO_{10}$	A	11.34	97.5
4	$C_{36}H_{41}N_6NaO_{10}$	A	13.03	97
5	$C_{39}H_{40}ClN_6NaO_{10}$	A	15.25	95
6	$C_{33}H_{36}F_3N_6NaO_9$	A	14.43	96
7	$C_{33}H_{38}N_7NaO_{11}$	A	13.70	98
8	$C_{34}H_{40}N_7NaO_{11}$	A	14.32	98
9	$C_{33}H_{37}ClN_6NaO_{10}$	A	18.98	98.5 %
10	$C_{32}H_{34}Cl_2FN_6NaO_9$	A	20.18	97.1 %
11	$C_{32}H_{34}ClF_2N_6NaO_9$	A	19.55	97.3 %
12	$C_{33}H_{37}ClFN_6NaO_9$	A	19.88	97.3 %
13	$C_{32}H_{34}Cl_2FN_6NaO_9$	A	20.00	95.7 %
14	$C_{35}H_{41}ClFN_6NaO_9$	B	14.42	95.0 %
15	$C_{35}H_{39}ClFN_6NaO_9$	A	14.13	96.8 %
16	$C_{32}H_{34}Cl_2FN_6NaO_9$	A	19.57	95.7 %
17	$C_{33}H_{34}ClN_7NaO_9$	A	18.92	98.1 %
18	$C_{33}H_{37}ClFN_6NaO_{11}S$	A	17.78	100 %
19	$C_{32}H_{35}FN_7NaO_{11}$	A	13.50	97 %
20	$C_{32}H_{34}ClFN_7NaO_{11}$	B	18.03	99.8 %

HPLC-traces of compounds 2 - 20

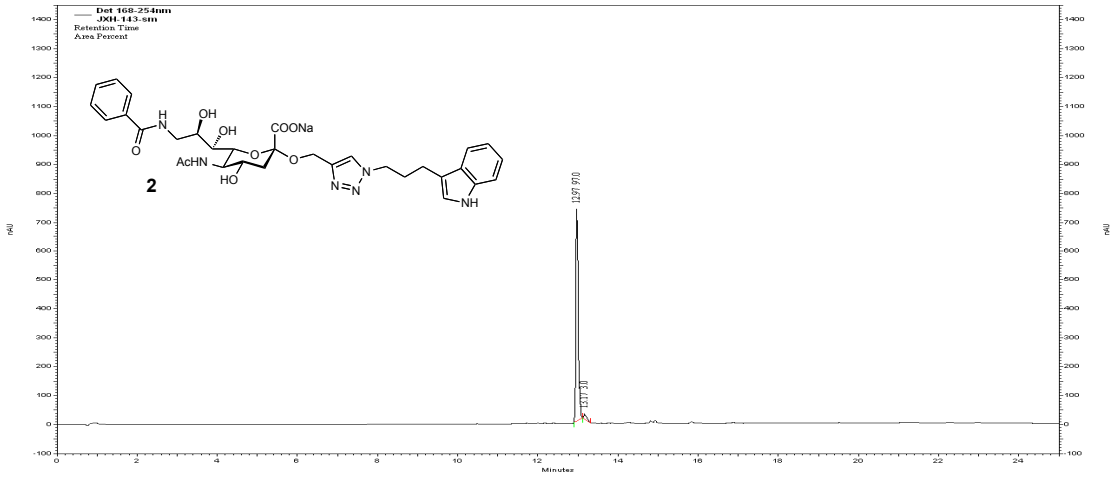

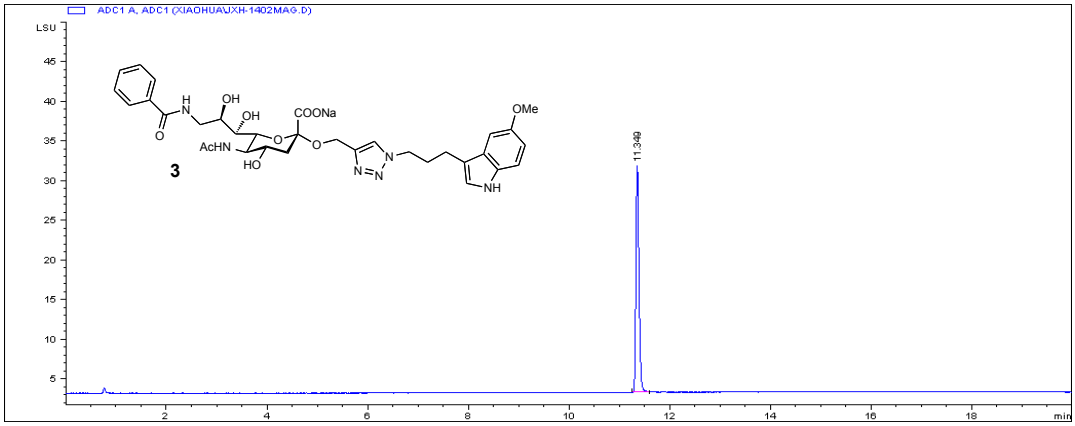

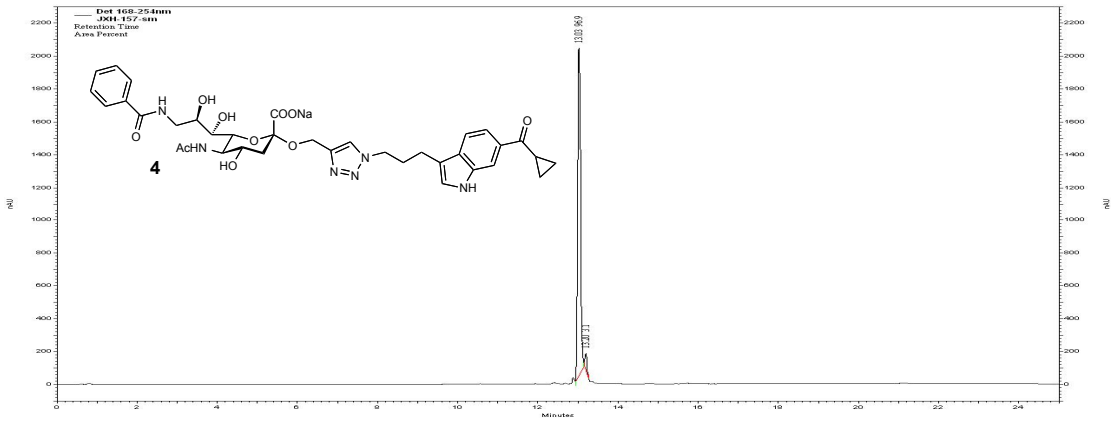

2 Results and Discussion

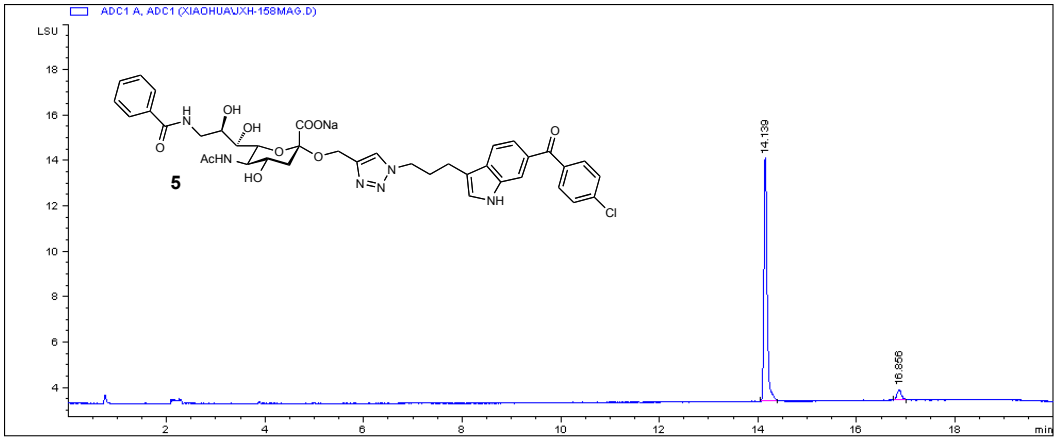

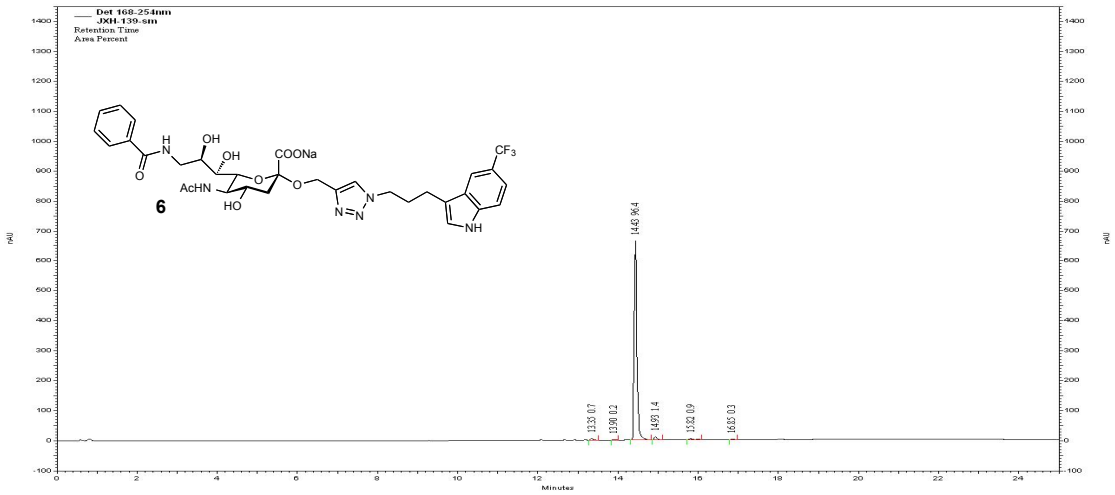

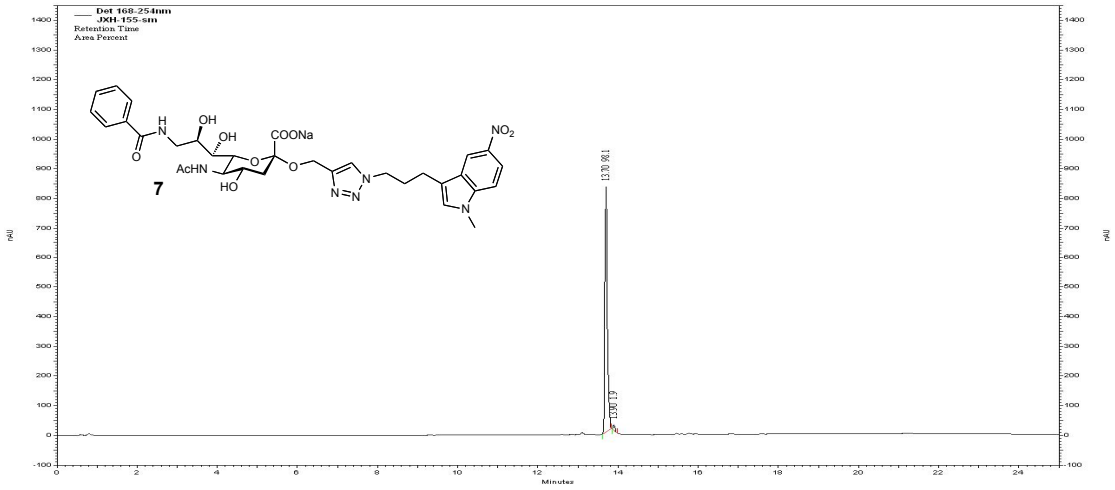

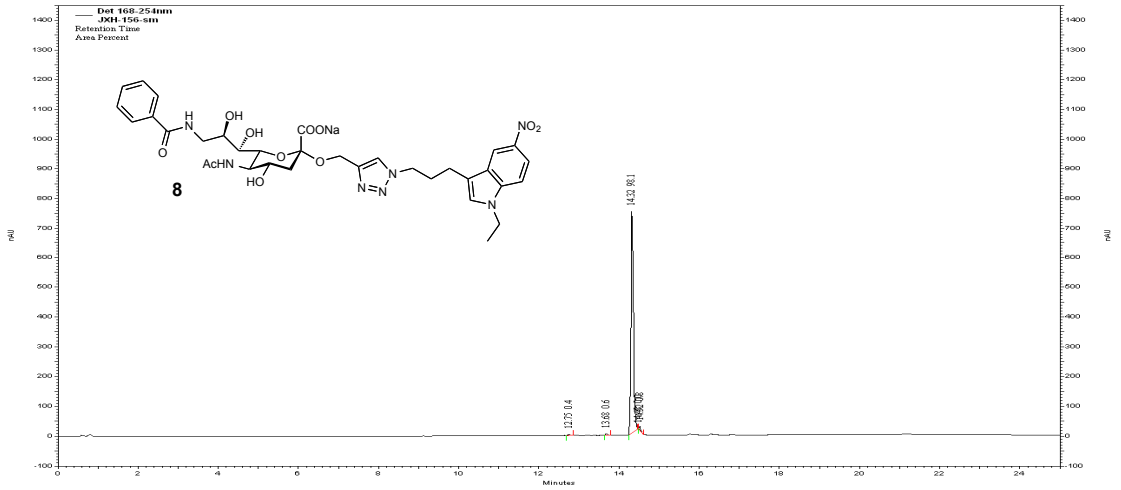
Det 168-254nm
JXH-156-sm
Retention Time
Area Percent
8
14.32 98.1
13.75 0.4
13.68 0.6
mAU
Minutes

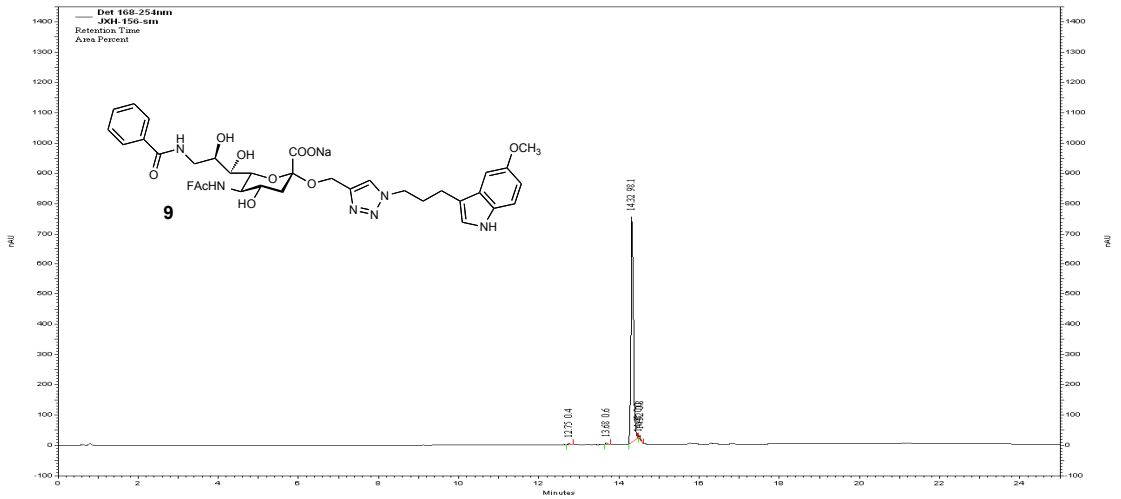
Det 168-254nm
JXH-156-sm
Retention Time
Area Percent
9
14.32 98.1
13.75 0.4
13.68 0.6
mAU
Minutes

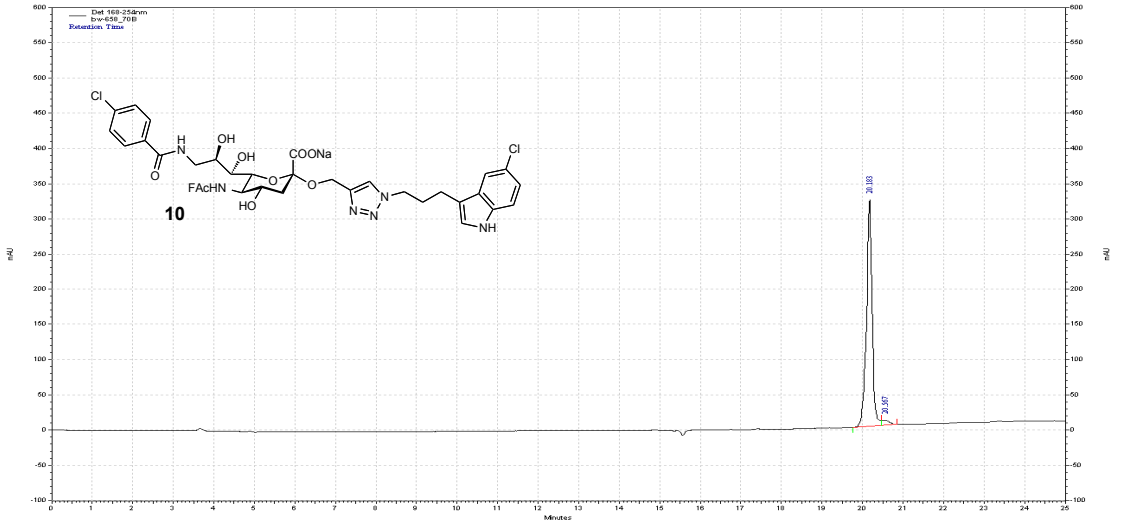
Det 168-254nm
Retention Time
10
20.183
20.387
mAU
Minutes

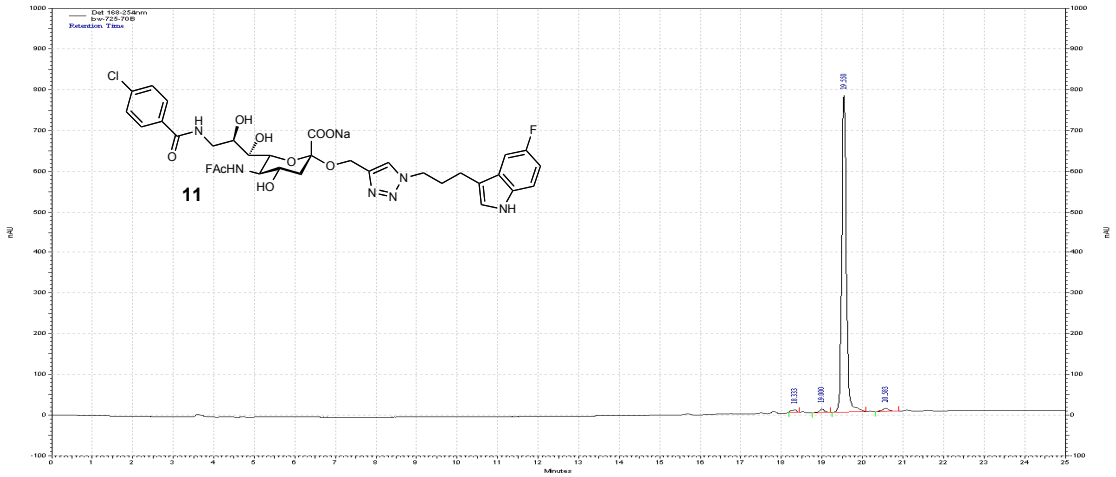
Det 168-254nm
bw-725-70B
Retention Time
Cl
H
N
O
OH
OH
COONa
O
FAcHN
HO
O
O
N
N
N
F
NH
11
19.338
18.333
19.900
20.383
nAU
Minutes

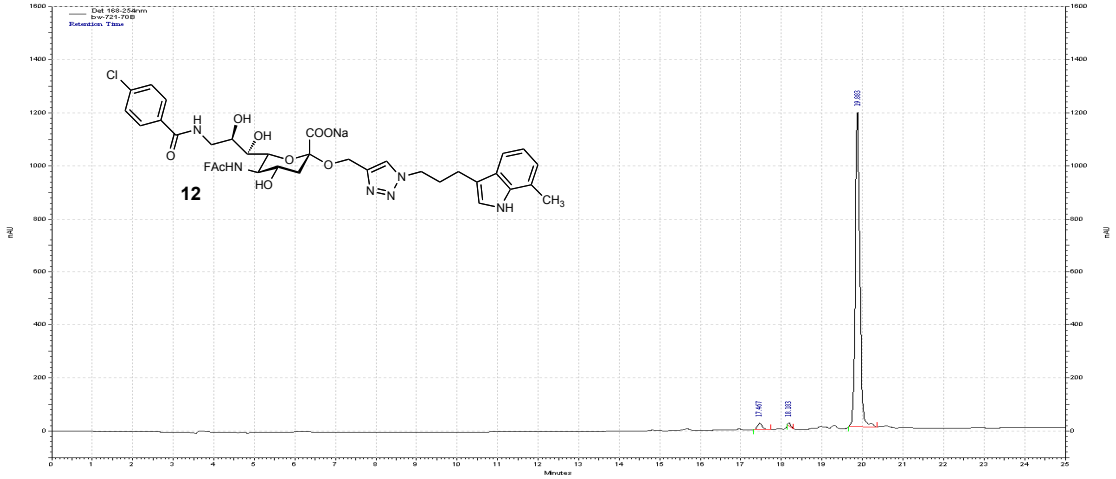
Det 168-254nm
bw-721-70B
Retention Time
Cl
H
N
O
OH
OH
COONa
O
FAcHN
HO
O
O
N
N
N
NH
CH3
12
19.883
17.467
18.383
nAU
Minutes

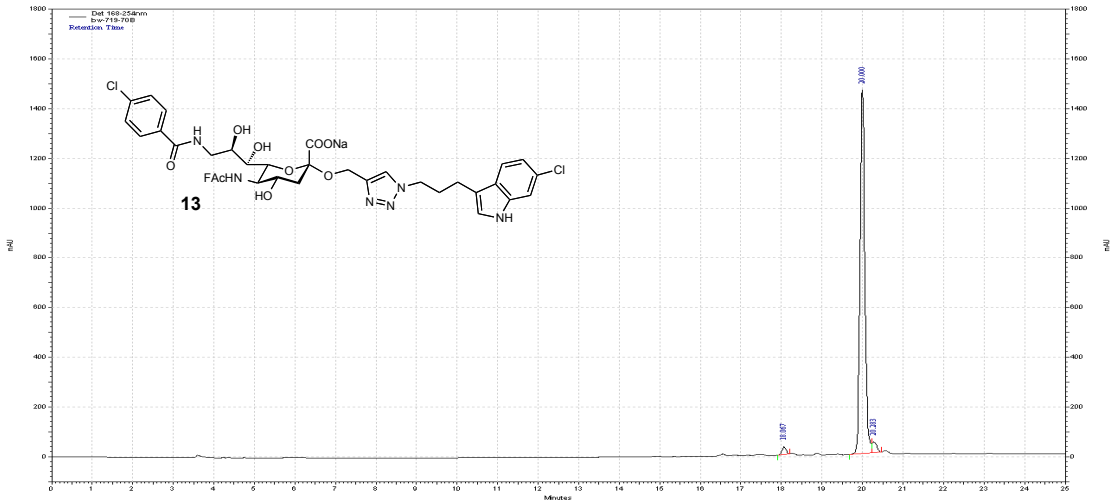
Det 168-254nm
bw-719-70B
Retention Time
Cl
H
N
O
OH
OH
COONa
O
FAcHN
HO
O
O
N
N
N
NH
Cl
13
20.000
18.967
20.283
nAU
Minutes

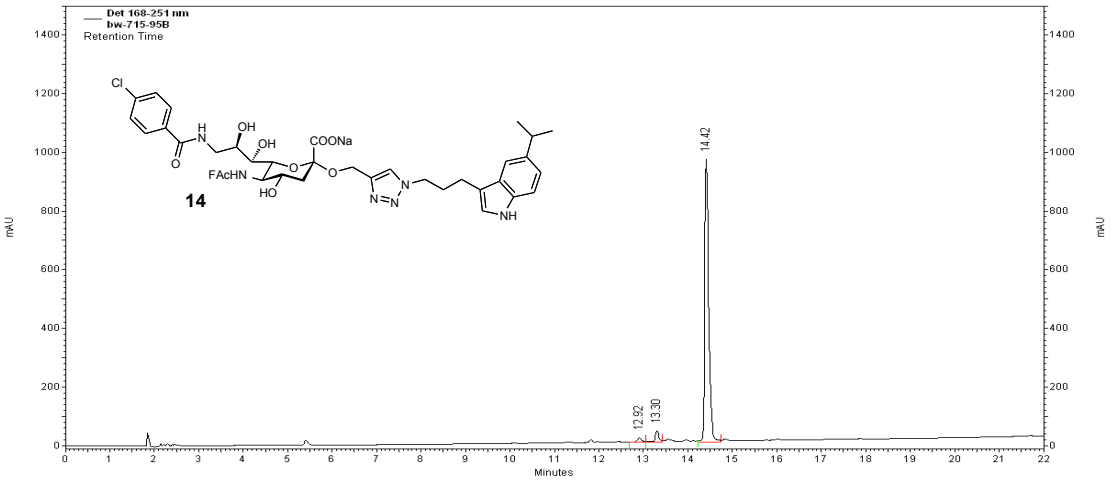
Det 168-251 nm
bw-715-95B
Retention Time
14
14.42
12.92
13.30
mAU
Minutes

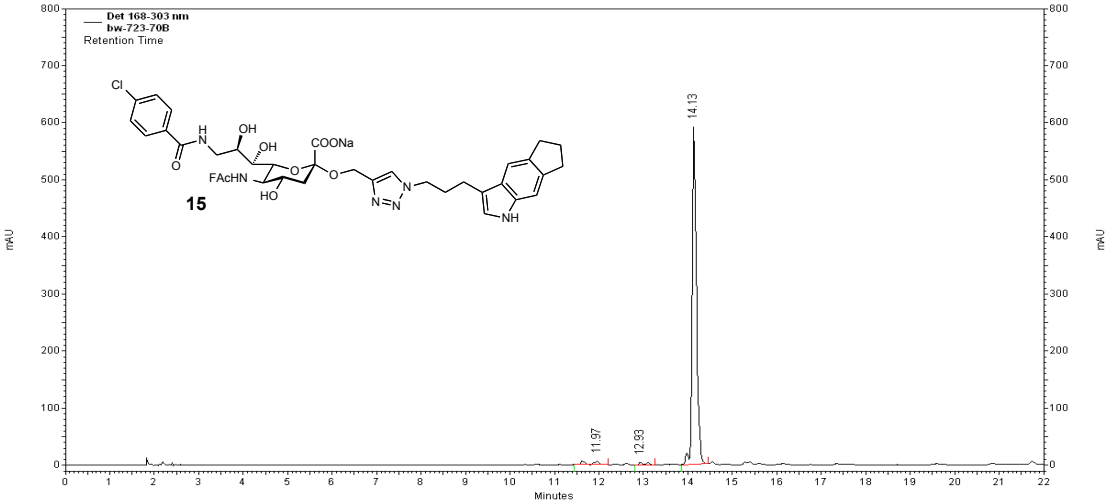
Det 168-303 nm
bw-723-70B
Retention Time
15
14.13
11.97
12.93
mAU
Minutes

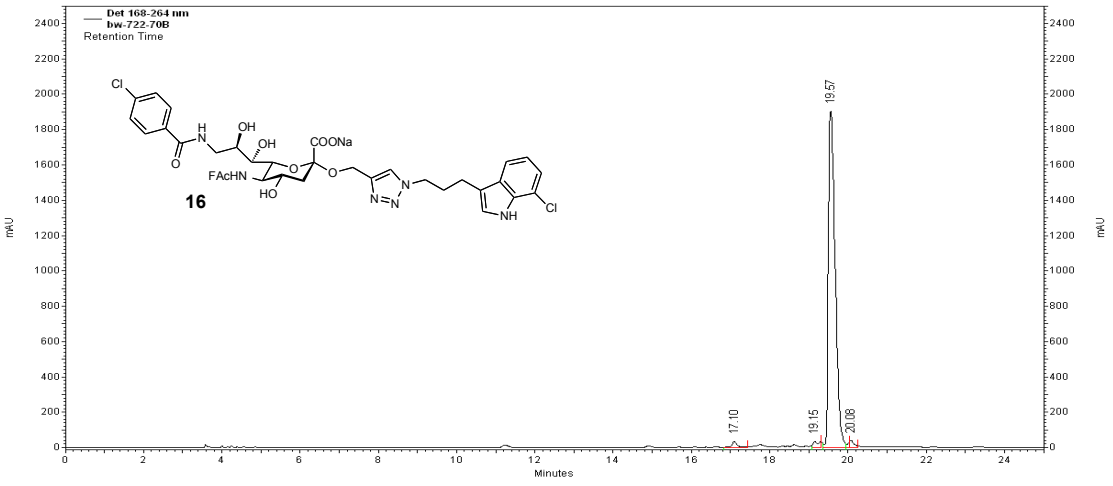
Det 168-264 nm
bw-722-70B
Retention Time
16
19.57
17.10
19.15
20.08
mAU
Minutes

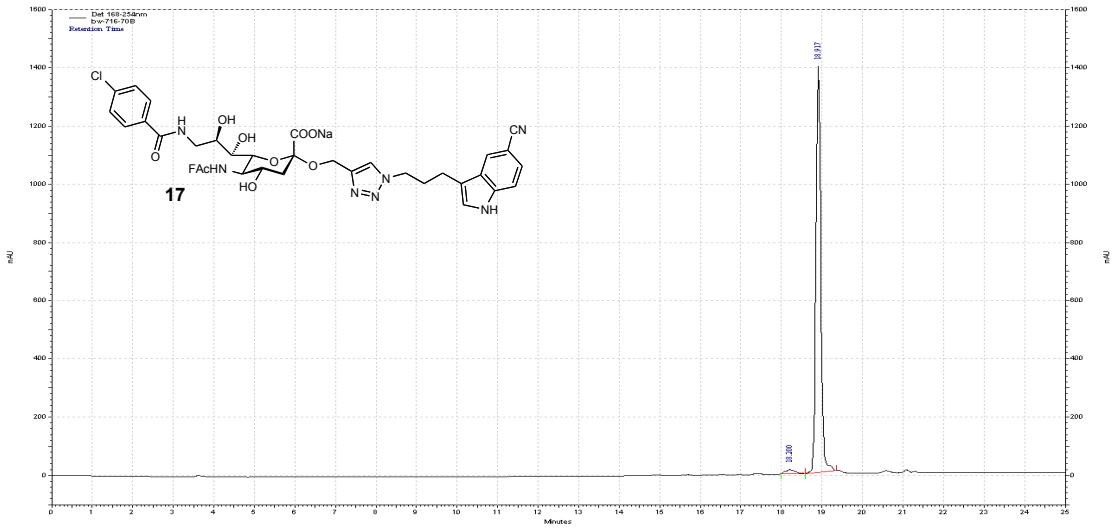
Det 168-254nm
bw-716-70B
Retention Time
mAU
Minutes
18.937
18.200
Cl
OH
COONa
CN
FAcHN
HO
17

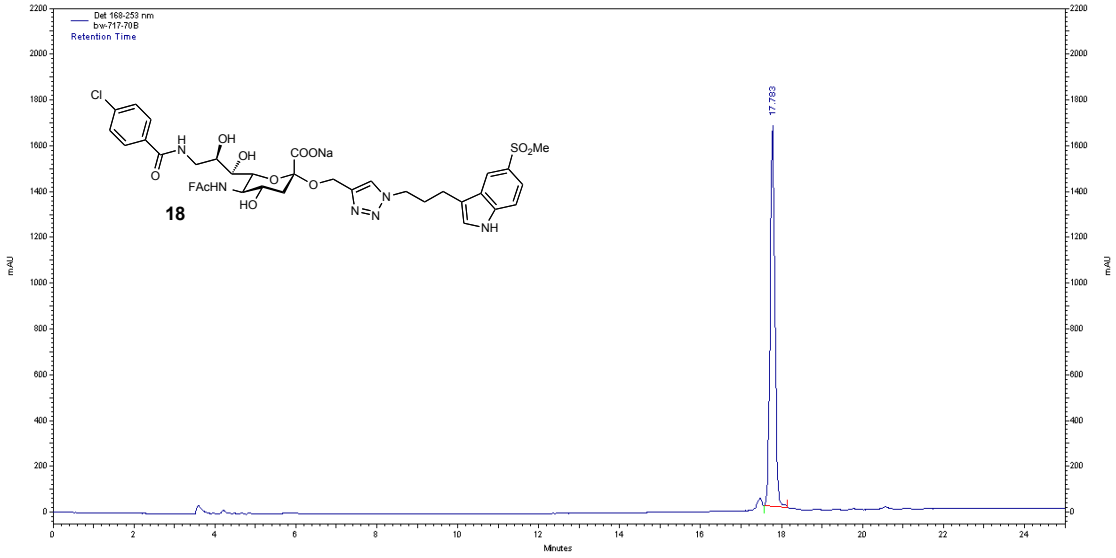
Det 168-253 nm
bw-717-70B
Retention Time
mAU
Minutes
17.783
Cl
OH
COONa
SO2Me
FAcHN
HO
18

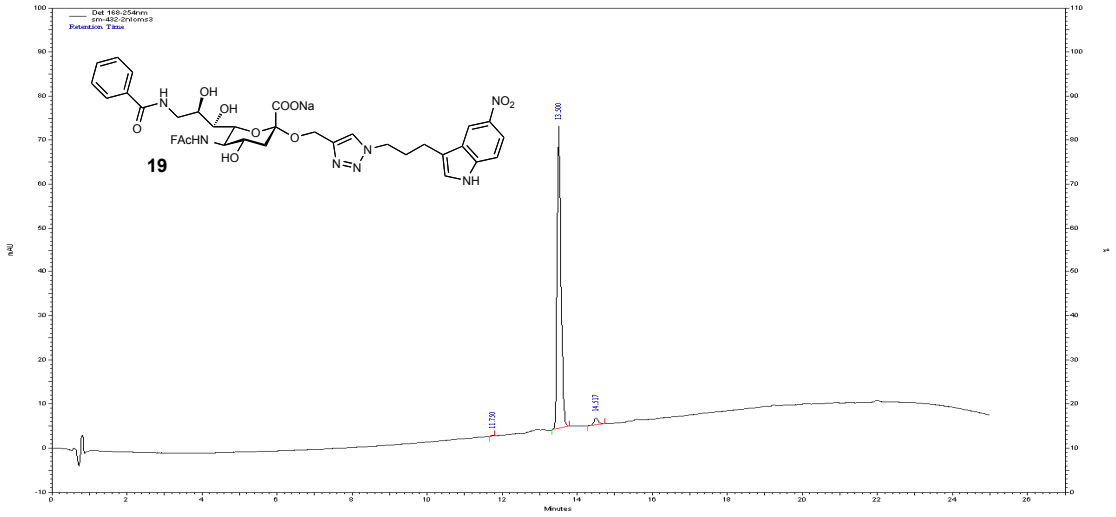
Det 168-254nm
Retention Time
mAU
Minutes
13.300
11.739
14.107
NO2
OH
COONa
FAcHN
HO
19

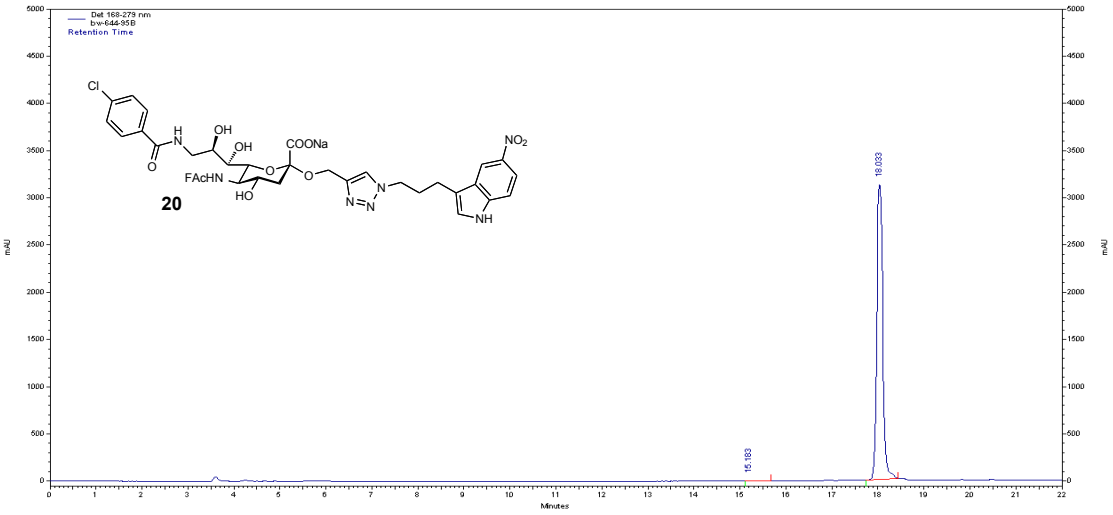
Det 168-278 nm
bw-644-95B
Retention Time
Cl
H
N
O
OH
OH
COONa
FAcHN
HO
O
O
N
N
N
NO2
NH
20
mAU
Minutes
15.183
18.033

^{1}H NMR spectra for the target compounds in CD_3OD or D_2O.

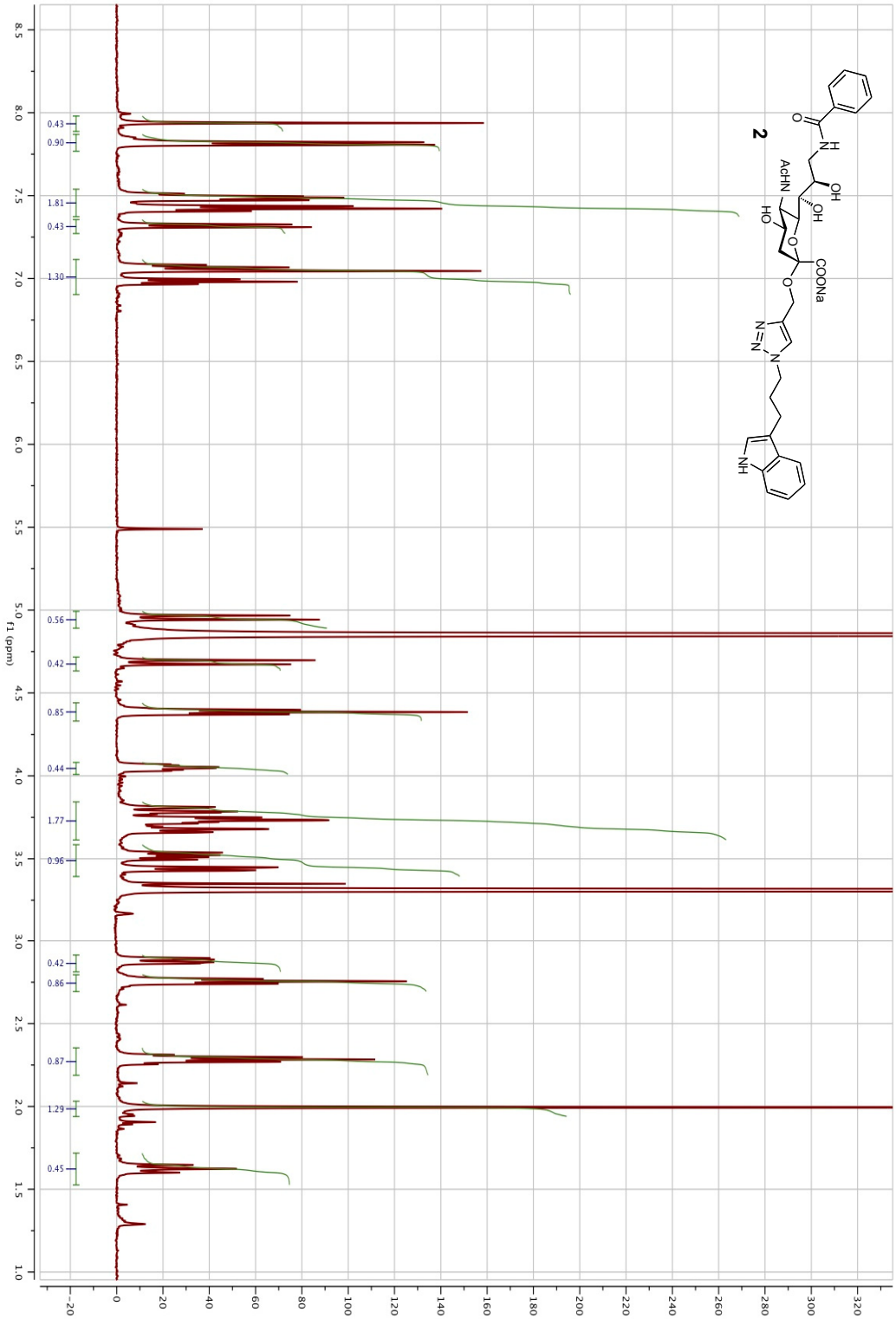

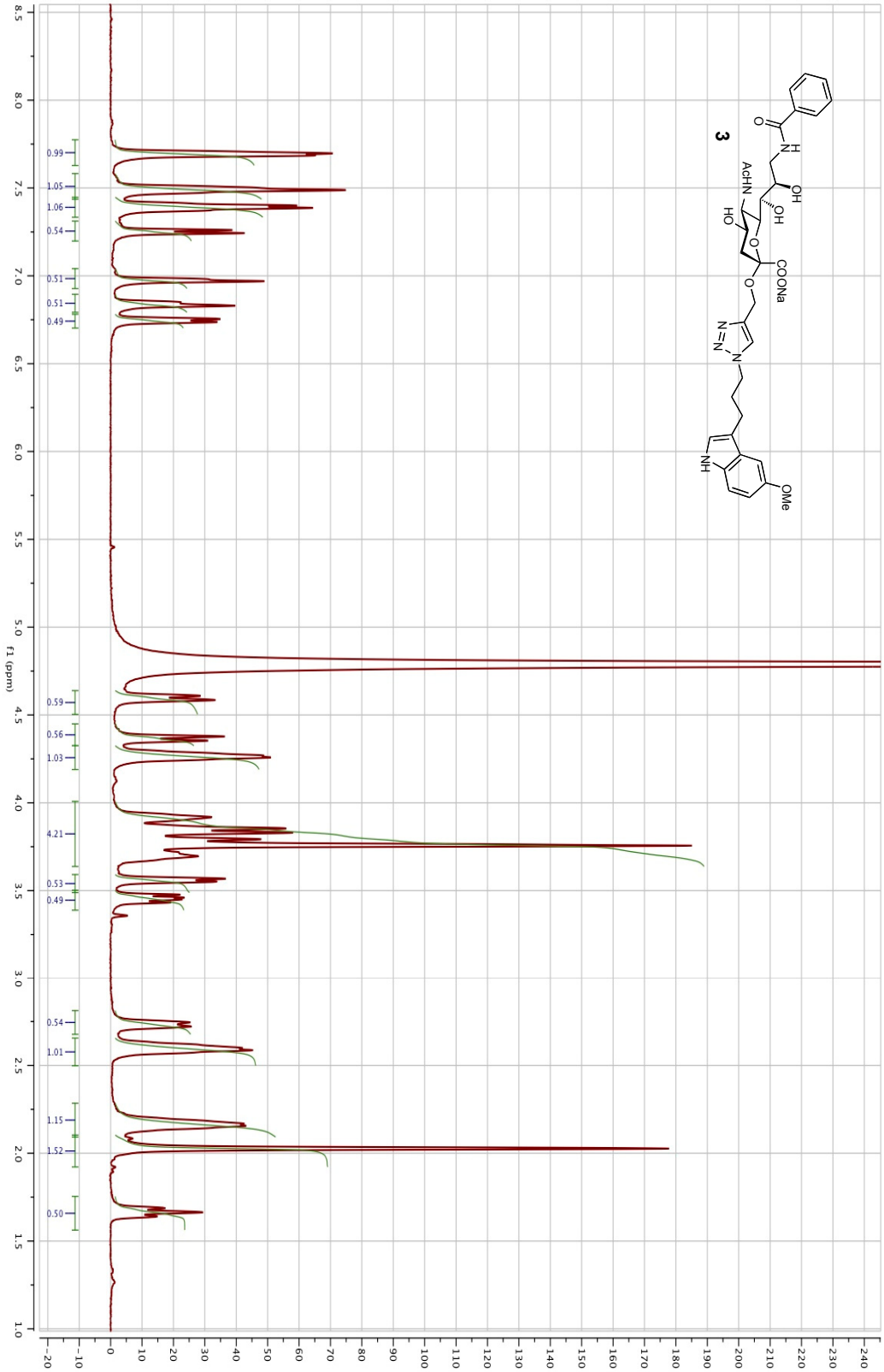
3
AcHN
HO
OH
OH
COONa
O
N
H
N
N
NH
OMe
f1 (ppm)
0.99
1.05
1.06
0.54
0.51
0.51
0.49
0.59
0.56
1.03
4.21
0.53
0.49
0.54
1.01
1.15
1.52
0.50

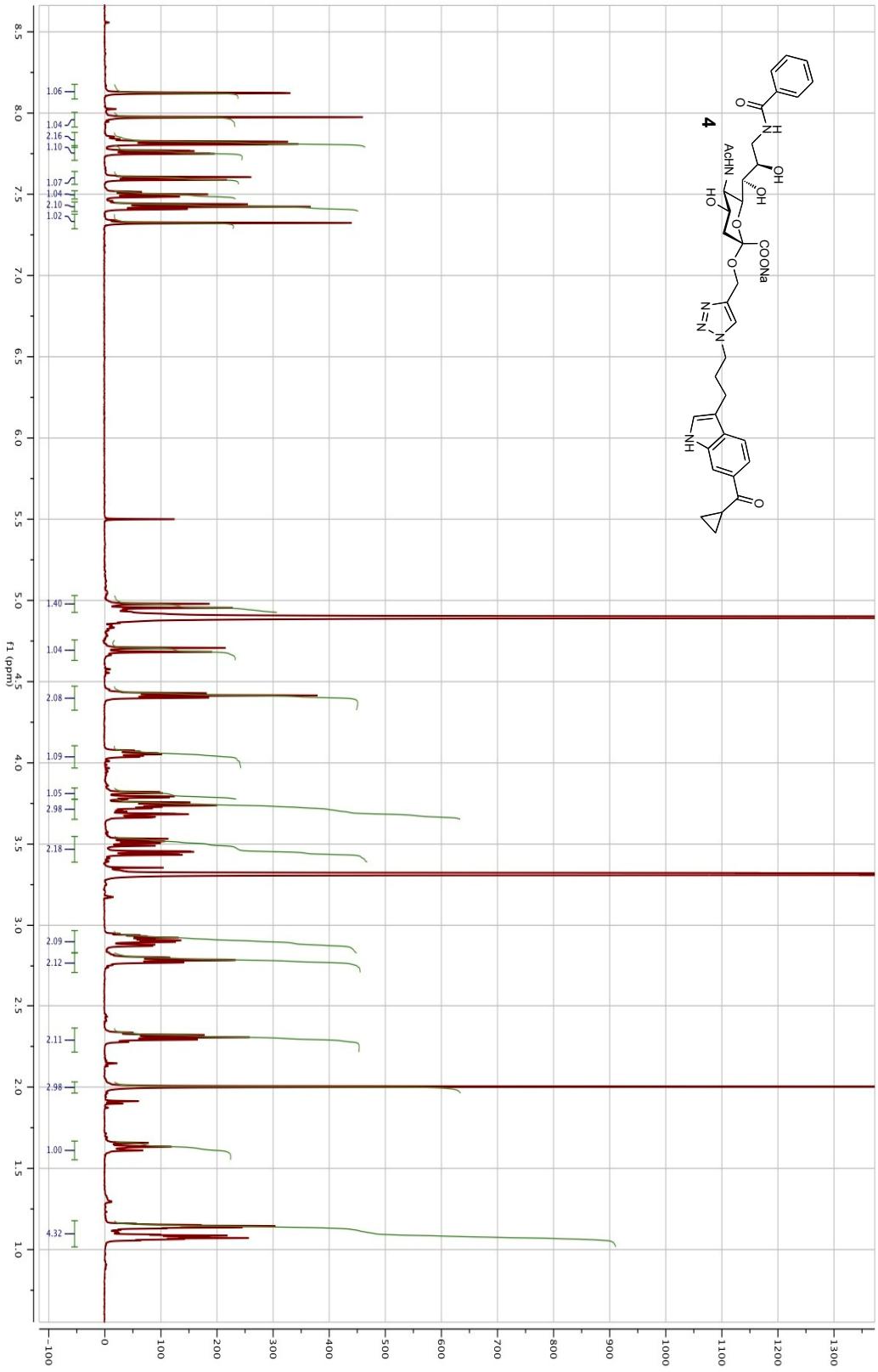
4
AcHN
HO
OH
OH
COONa
NH
O
f1 (ppm)
1.06
1.04
2.16
1.10
1.07
1.04
2.10
1.02
1.40
1.04
2.08
1.09
1.05
2.98
2.18
2.09
2.12
2.11
2.98
1.00
4.32

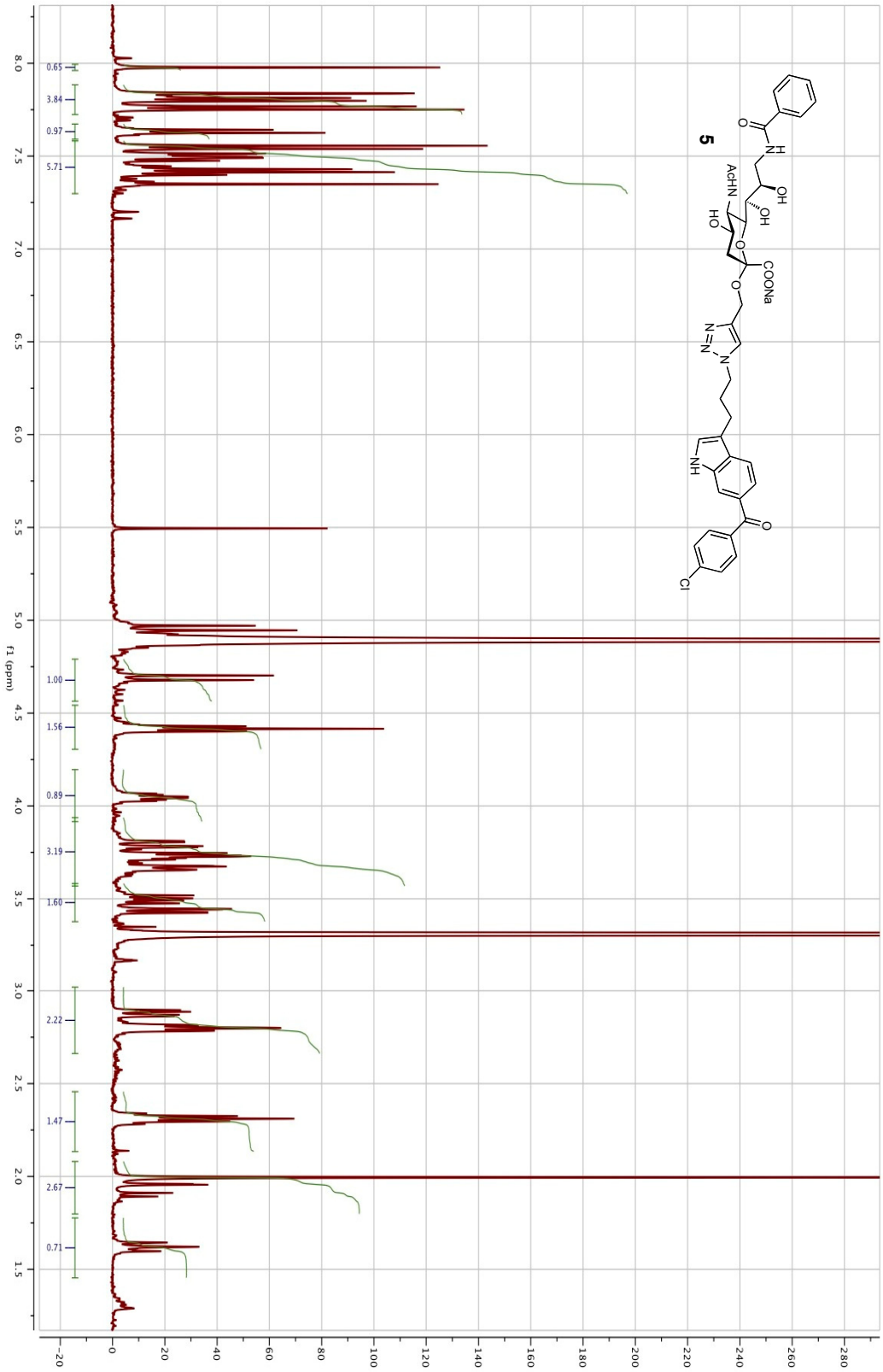
f1 (ppm)
0.65
3.84
0.97
5.71
1.00
1.56
0.89
3.19
1.60
2.22
1.47
2.67
0.71
5
AcHN
HO
OH
OH
COONa
NH
Cl

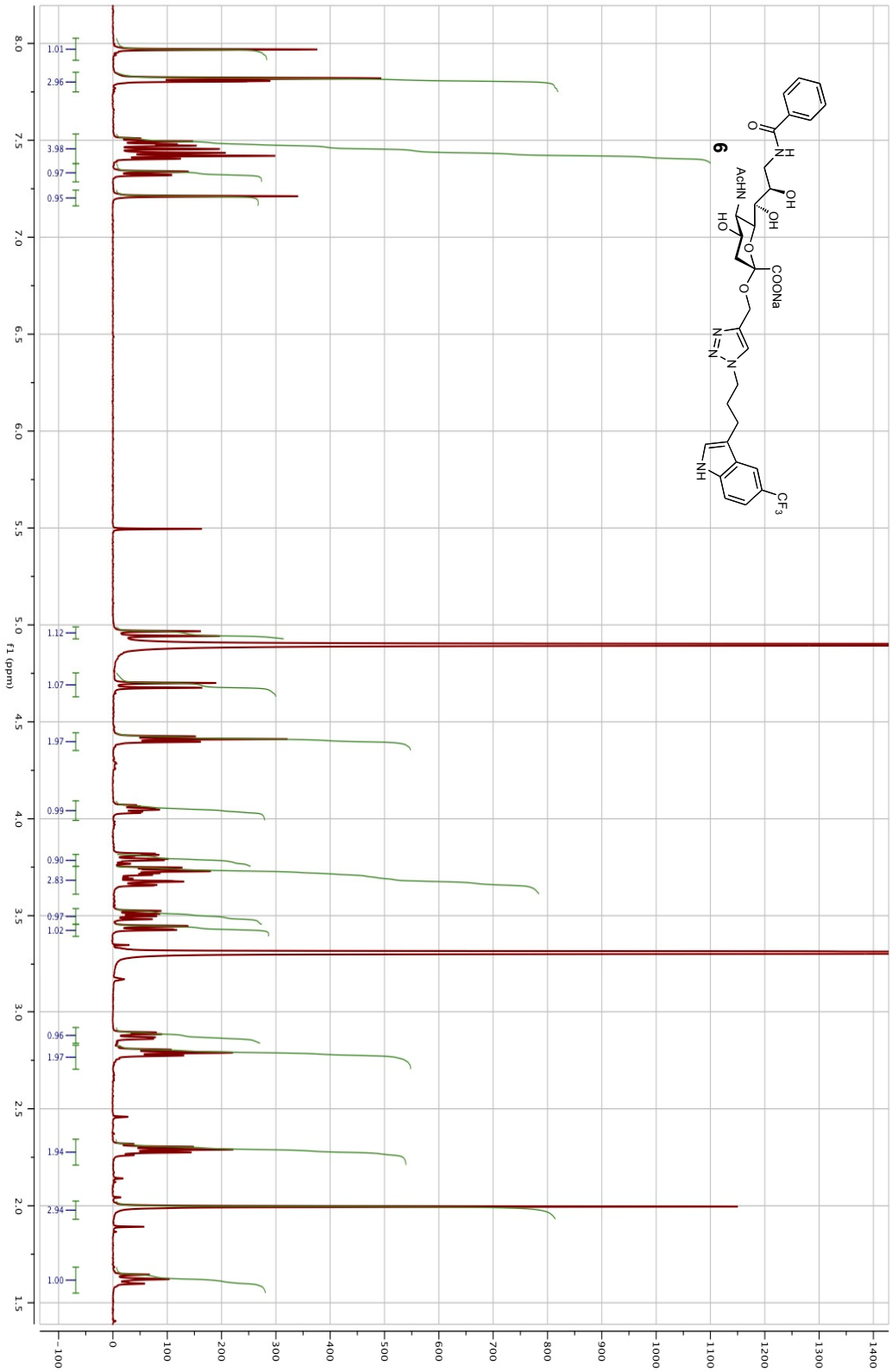
6
AcHN
HO
OH
OH
O
COONa
O
N
N
N
H
O
NH
CF3
f1 (ppm)
8.0
7.5
7.0
6.5
6.0
5.5
5.0
4.5
4.0
3.5
3.0
2.5
2.0
1.5
1.01
2.96
3.98
0.97
0.95
1.12
1.07
1.97
0.99
0.90
2.83
0.97
1.02
0.96
1.97
1.94
2.94
1.00
-100
0
100
200
300
400
500
600
700
800
900
1000
1100
1200
1300
1400

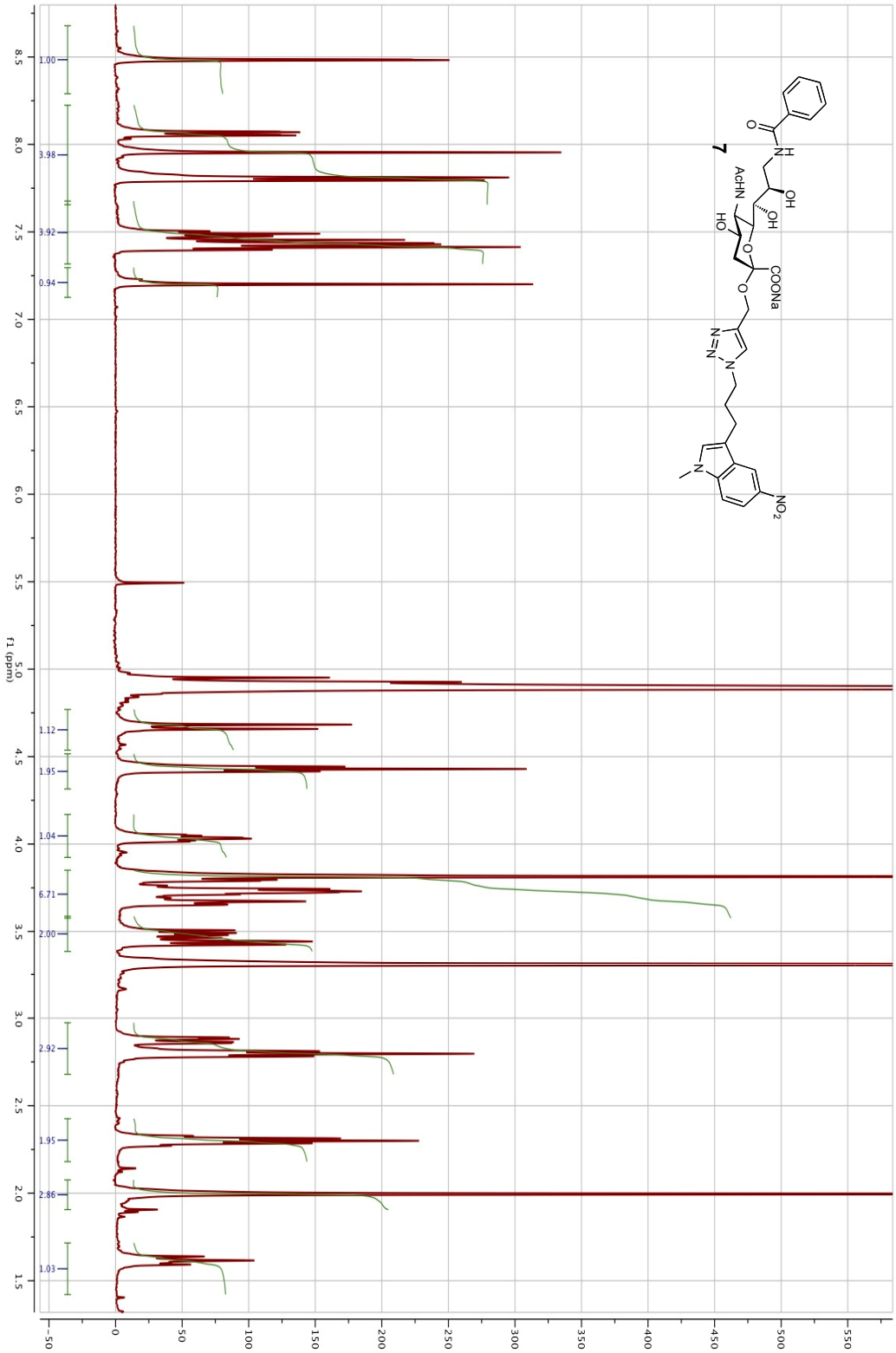
7
AcHN
HO
OH
OH
COONa
NO2
f1 (ppm)
1.00
3.98
3.92
0.94
1.12
1.95
1.04
6.71
2.00
2.92
1.95
2.86
1.03

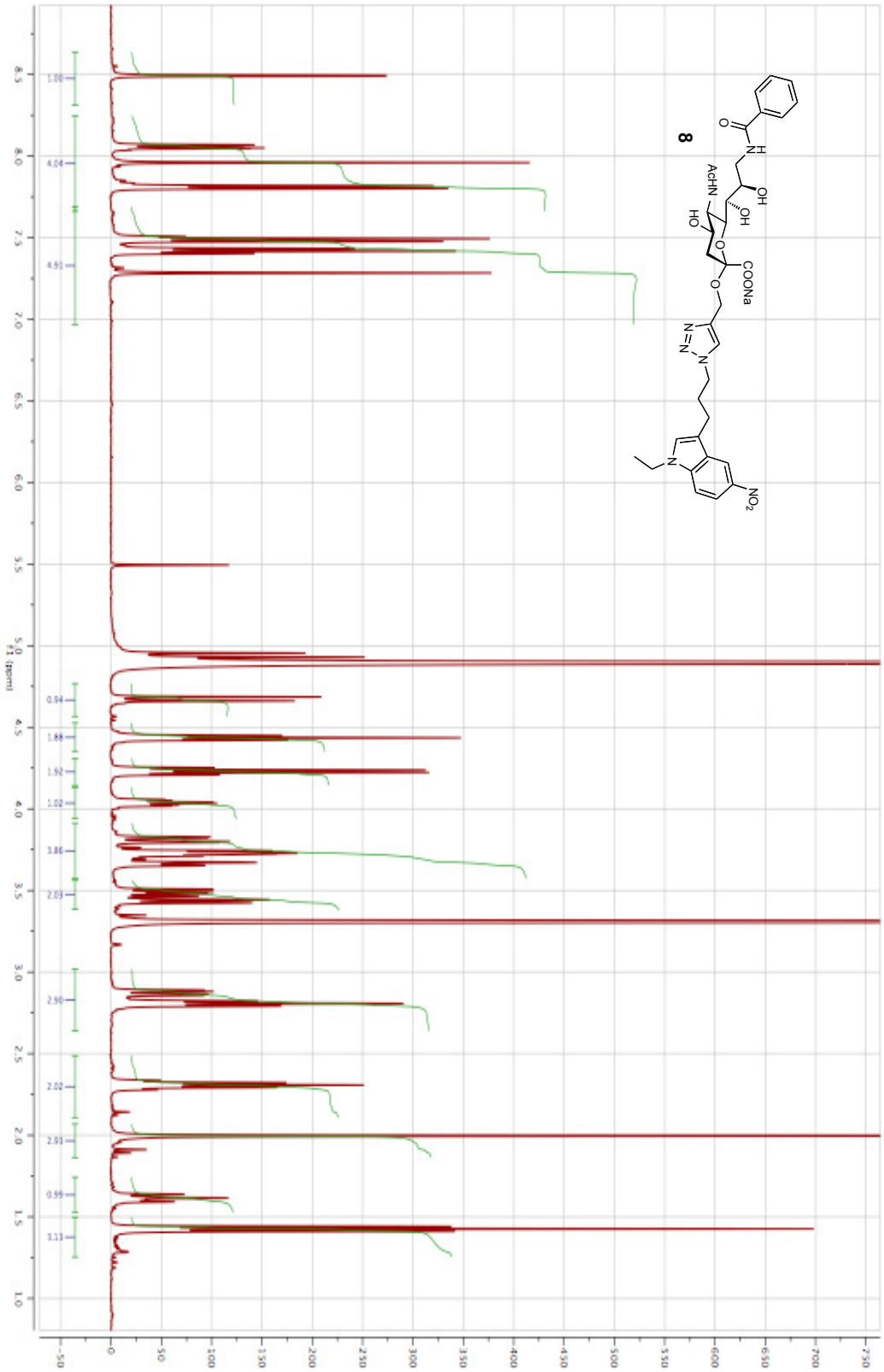
8
AcHN
HO
OH
OH
COONa
NO2
f1 (ppm)

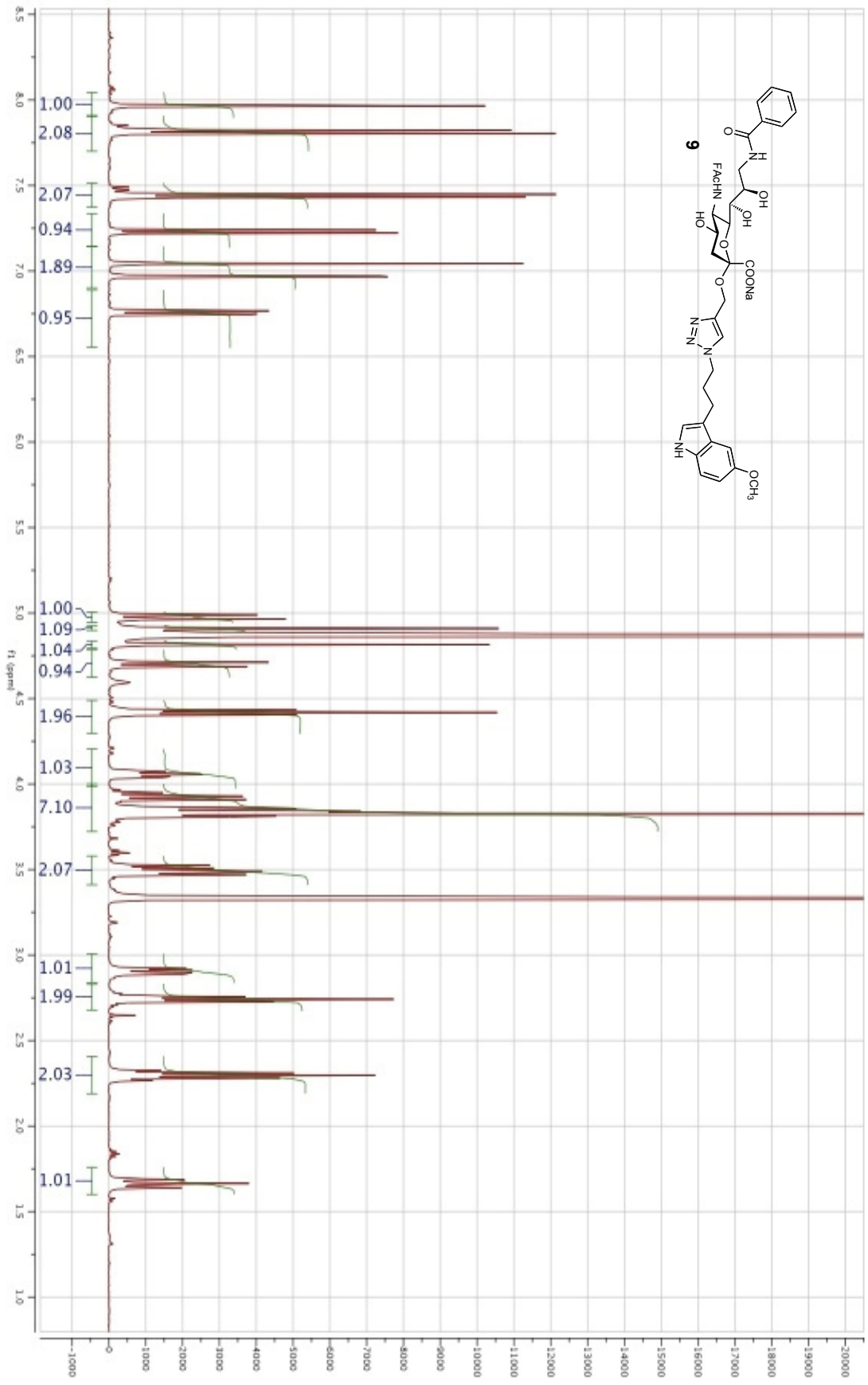
1.00
2.08
2.07
0.94
1.89
0.95
1.00
1.09
1.04
0.94
1.96
1.03
7.10
2.07
1.01
1.99
2.03
1.01
6
FAcHN
HO
OH
OH
COONa
NH
OCH3

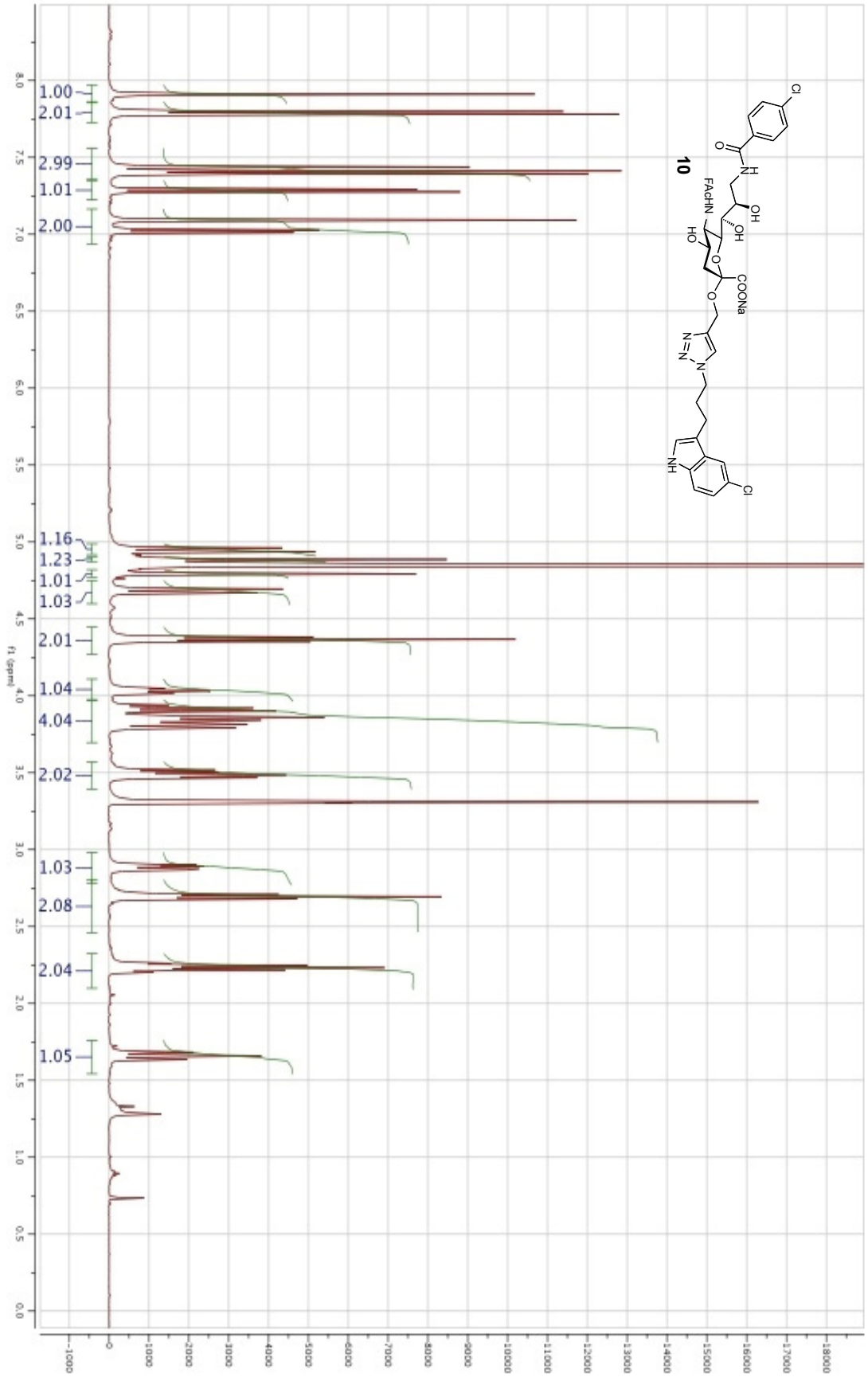
1.00
2.01
2.99
1.01
2.00
1.16
1.23
1.01
1.03
2.01
1.04
4.04
2.02
1.03
2.08
2.04
1.05
10
FAcHN
HO
OH
OH
COONa
NH
Cl
Cl

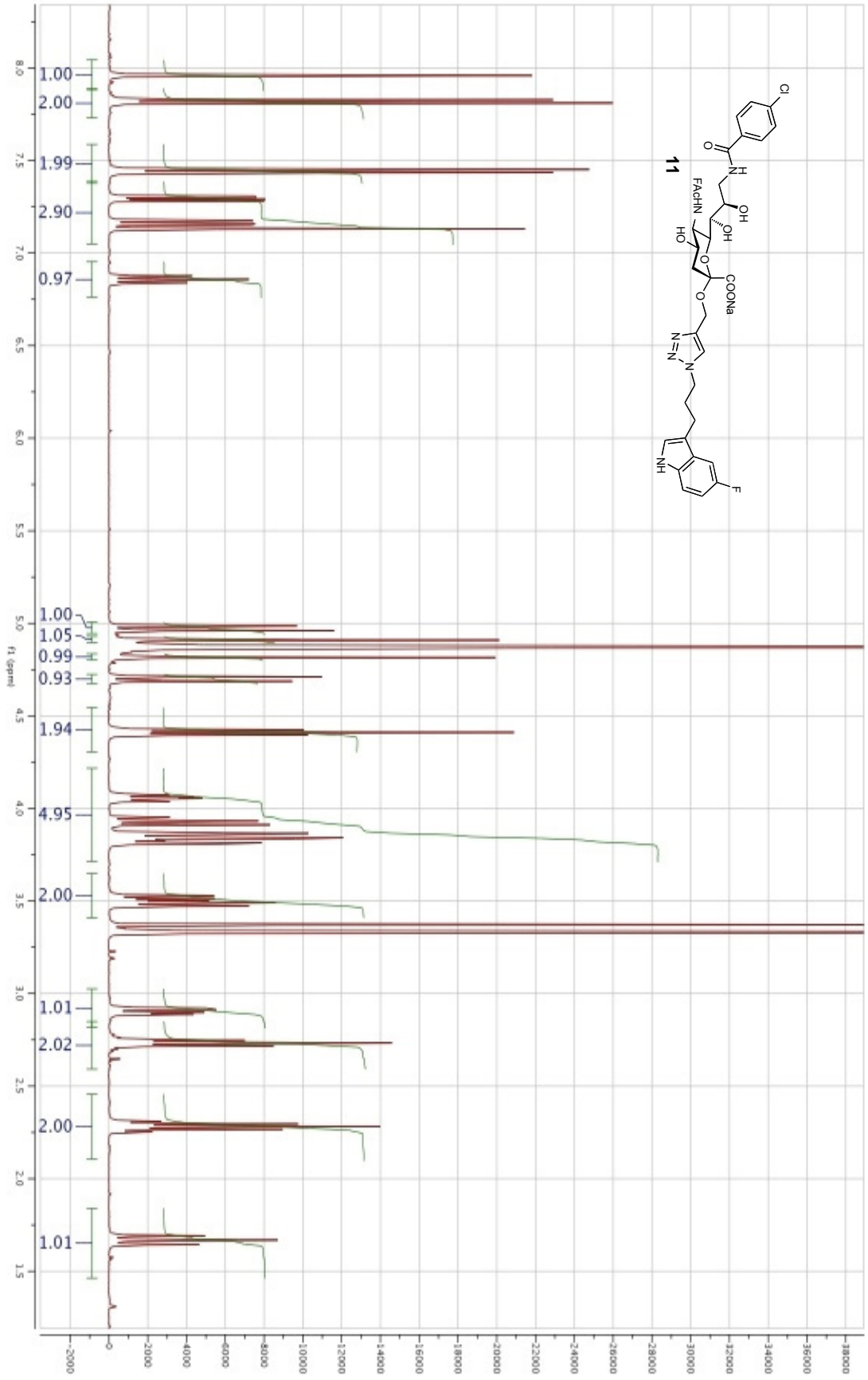
1.00
2.00
1.99
2.90
0.97
1.00
1.05
0.99
0.93
1.94
4.95
2.00
1.01
2.02
2.00
1.01
11
FAcHN
HO
OH
OH
COONa
Cl
F
NH

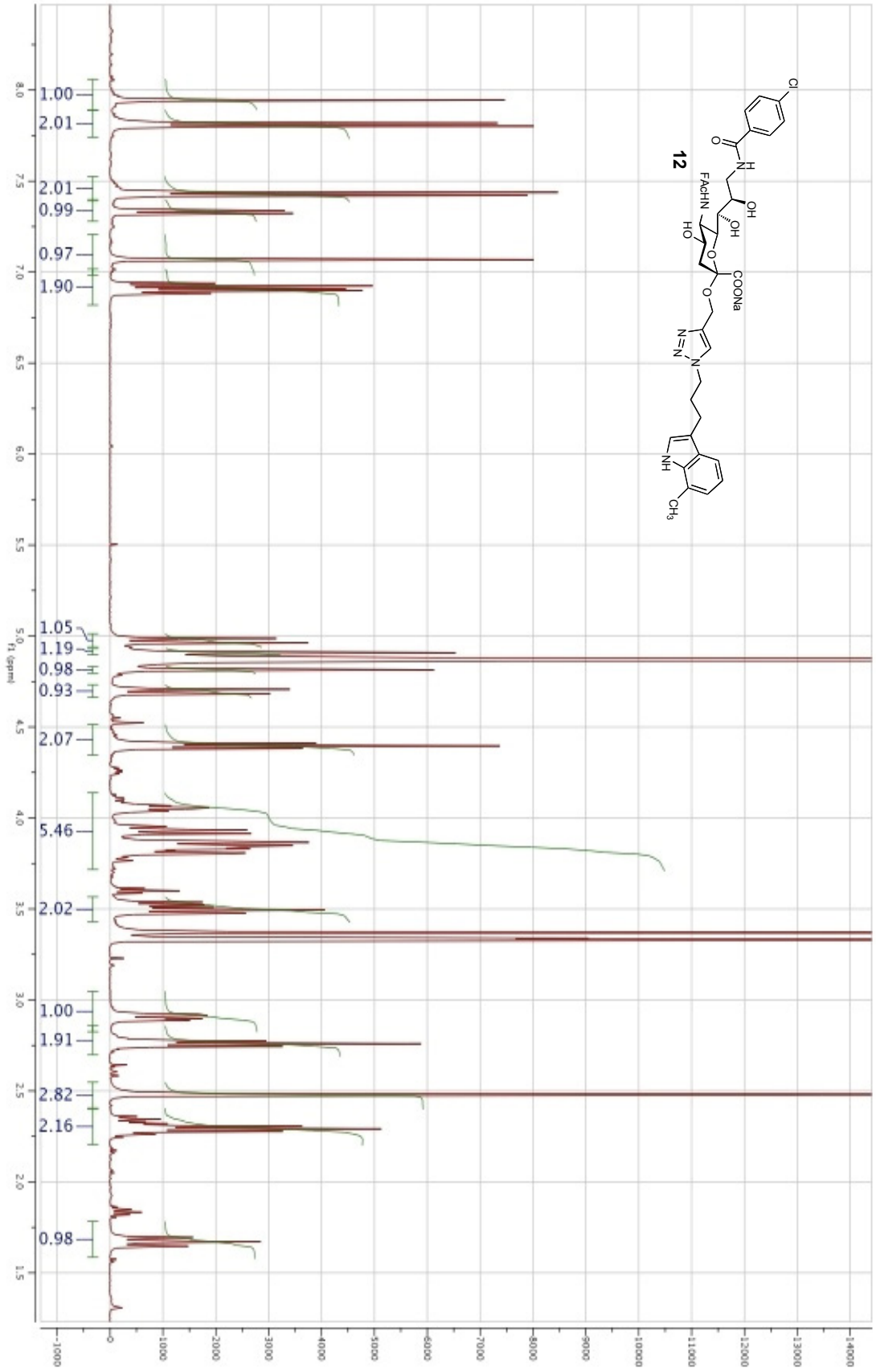
1.00
2.01
2.01
0.99
0.97
1.90
1.05
1.19
0.98
0.93
2.07
5.46
2.02
1.00
1.91
2.82
2.16
0.98
12
Cl
O
N
H
FAcHN
OH
HO
OH
O
COONa
O
N=N
N
NH
CH3

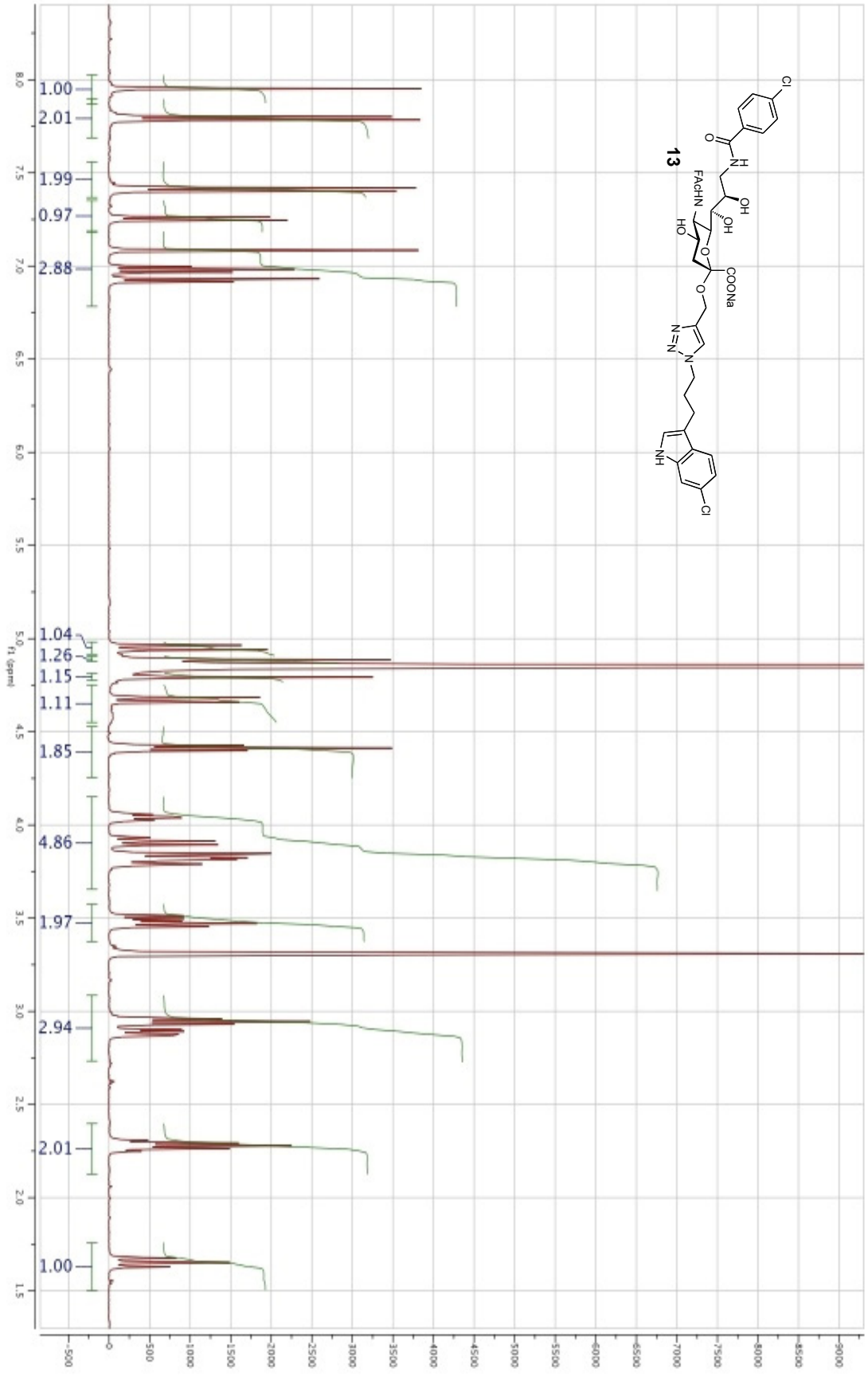
1.00
2.01
1.99
0.97
2.88
1.04
1.26
1.15
1.11
1.85
4.86
1.97
2.94
2.01
1.00
13
FAcHN
HO
OH
OH
COONa
O
N
H
Cl
NH
Cl

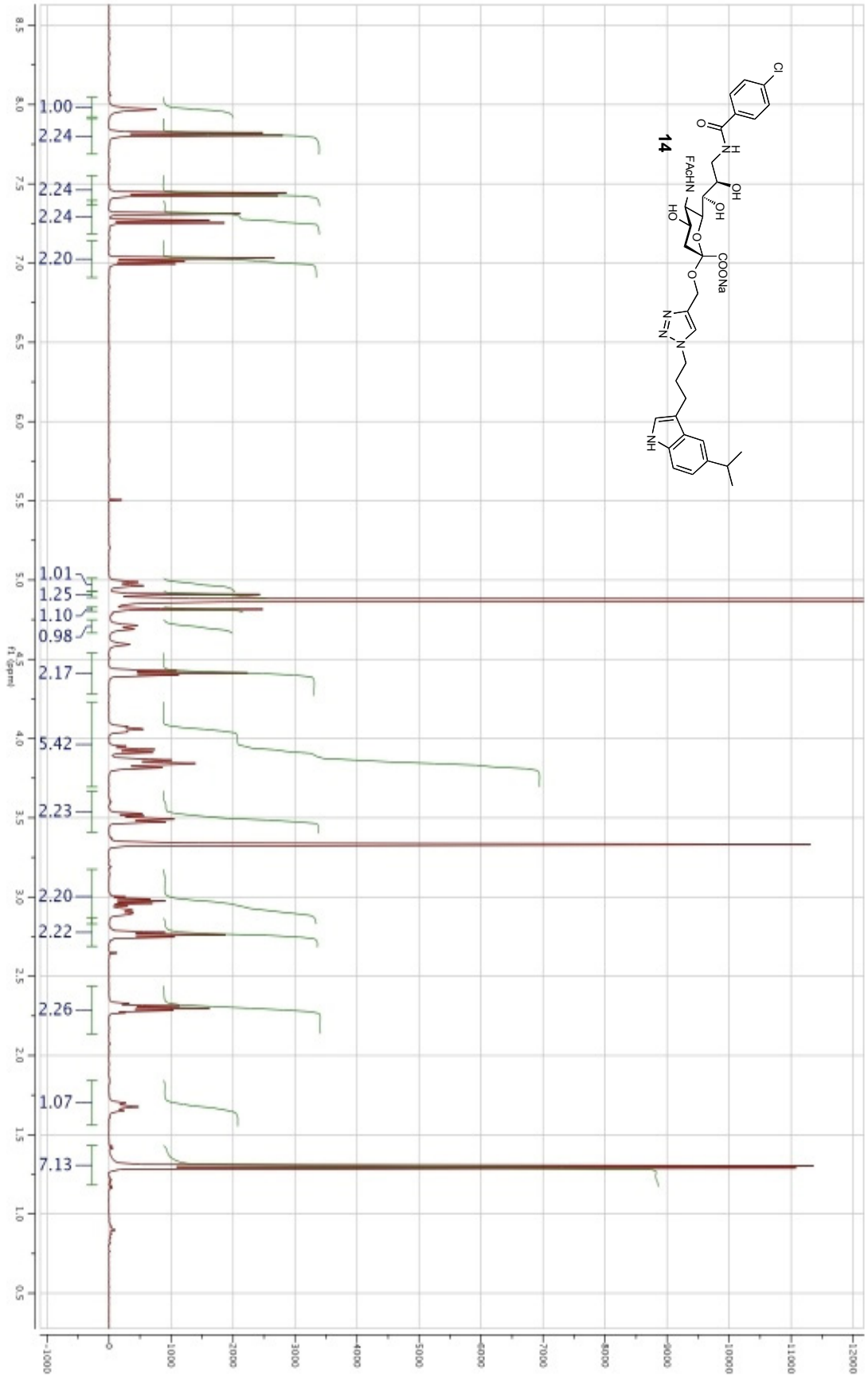
1.00
2.24
2.24
2.24
2.20
1.01
1.25
1.10
0.98
2.17
5.42
2.23
2.20
2.22
2.26
1.07
7.13
14
Cl
O
H
N
FAcHN
OH
HO
OH
O
COONa
O
N
N
N
NH

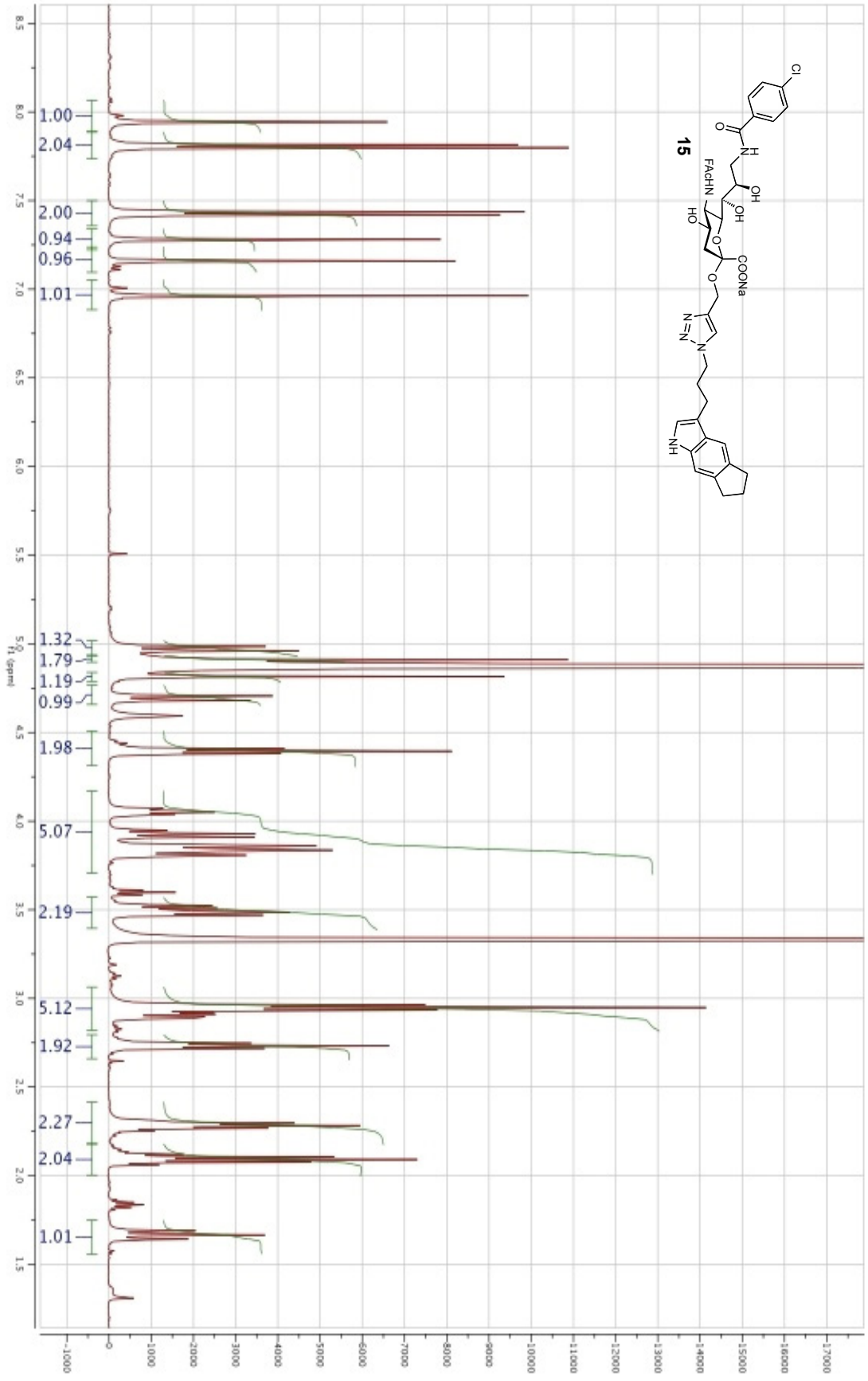
15
Cl
O
N
H
FAcHN
OH
HO
OH
O
COONa
O
N=N
N
NH
1.00
2.04
2.00
0.94
0.96
1.01
1.32
1.79
1.19
0.99
1.98
5.07
2.19
5.12
1.92
2.27
2.04
1.01

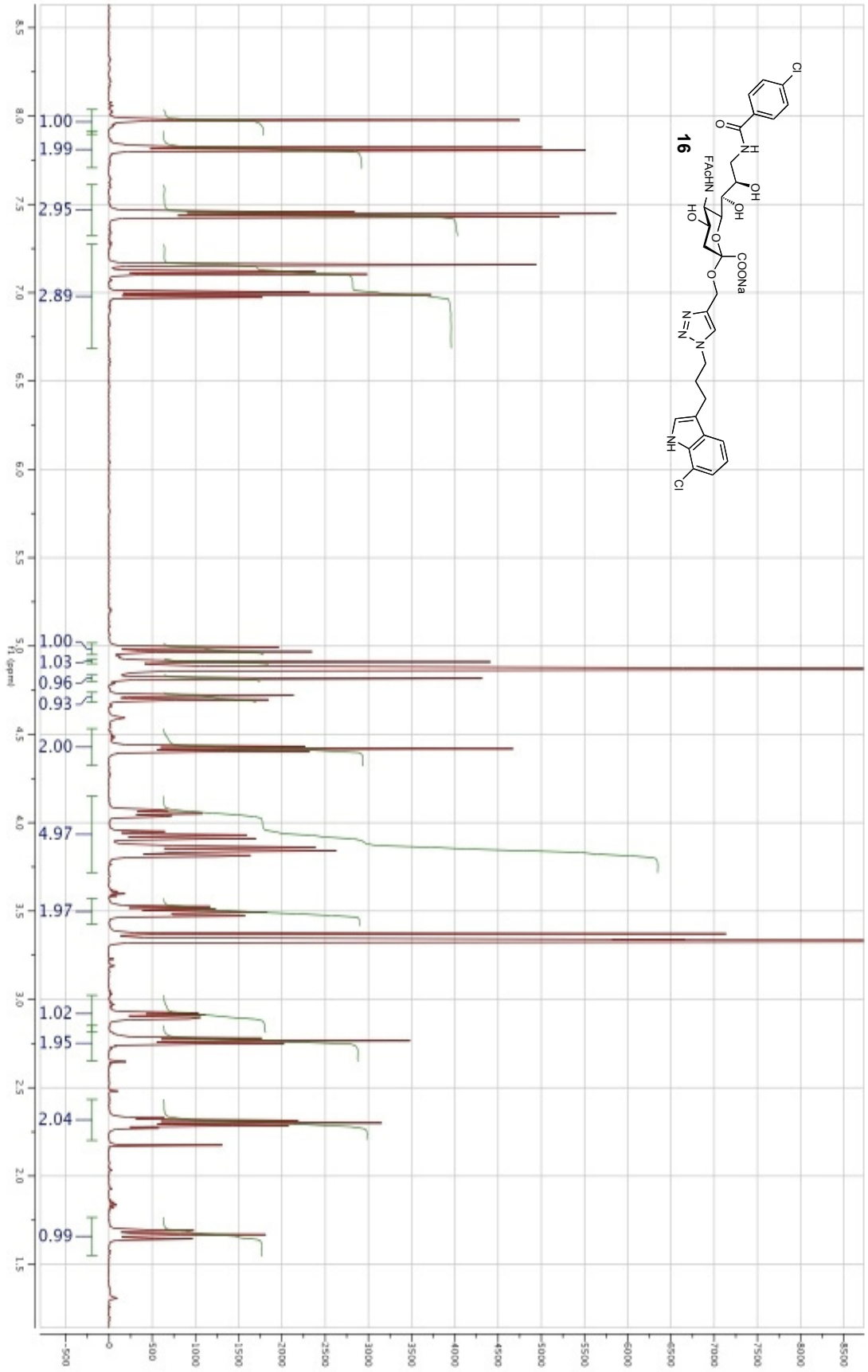
1.00
1.99
2.95
2.89
1.00
1.03
0.96
0.93
2.00
4.97
1.97
1.02
1.95
2.04
0.99
16
FAcHN
HO
OH
OH
COONa
NH
Cl
Cl

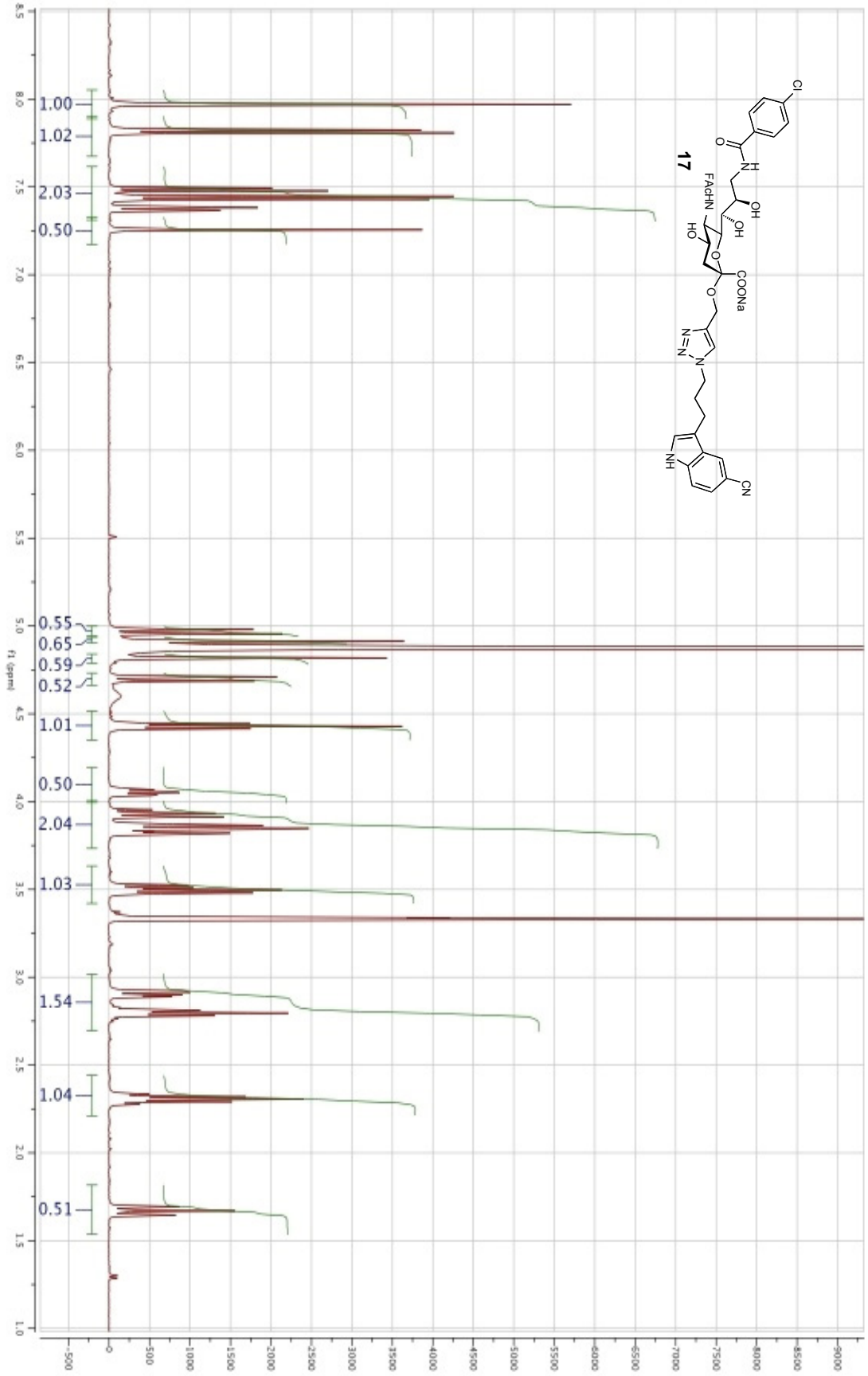
1.00
1.02
2.03
0.50
0.55
0.65
0.59
0.52
1.01
0.50
2.04
1.03
1.54
1.04
0.51
17
Cl
O
N
H
FAcHN
OH
HO
OH
O
COONa
O
N
N
N
NH
CN

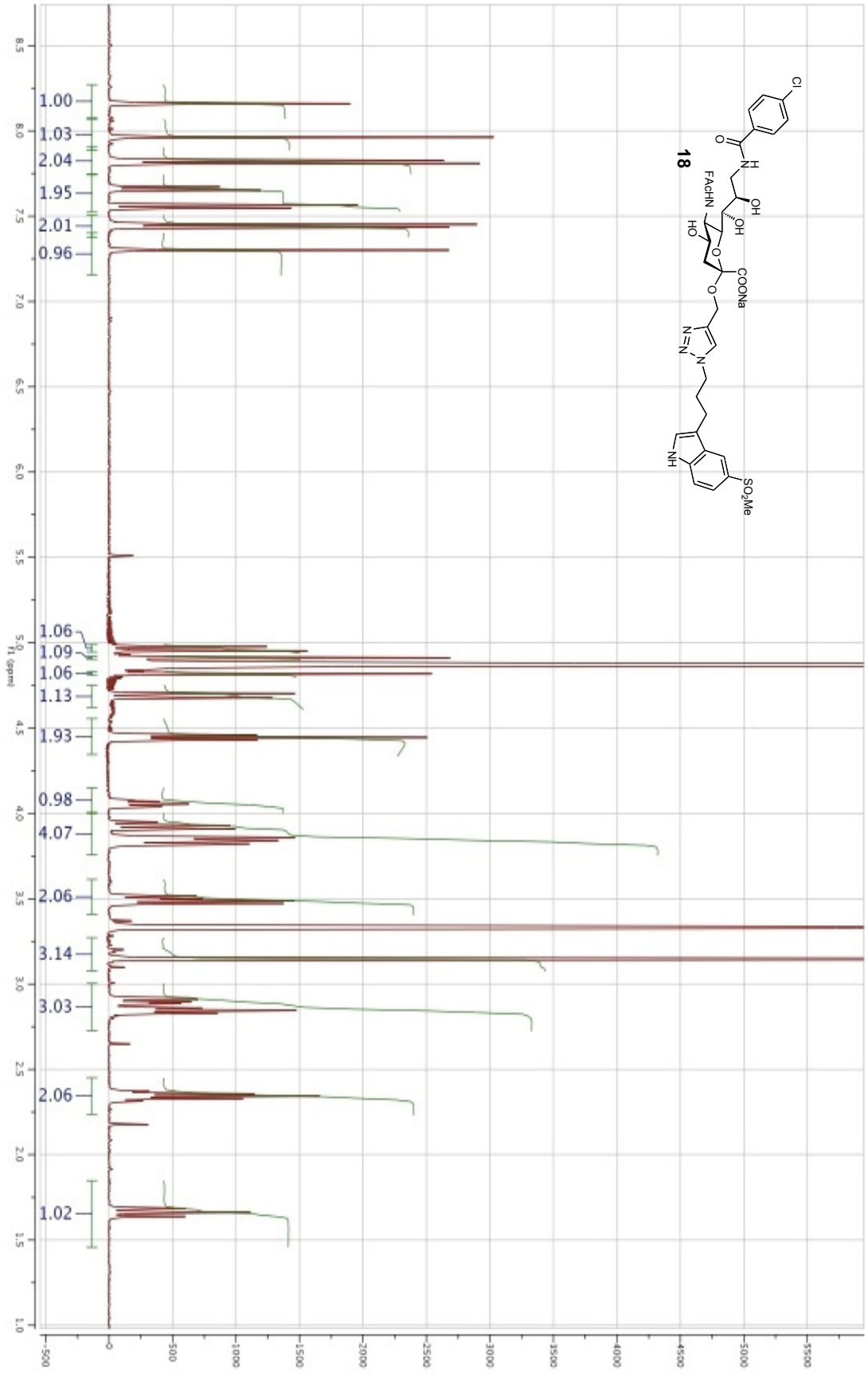
1.00
1.03
2.04
1.95
2.01
0.96
1.06
1.09
1.06
1.13
1.93
0.98
4.07
2.06
3.14
3.03
2.06
1.02
18
Cl
O
N
H
FAcHN
OH
HO
OH
O
COONa
N
N
N
NH
SO2Me

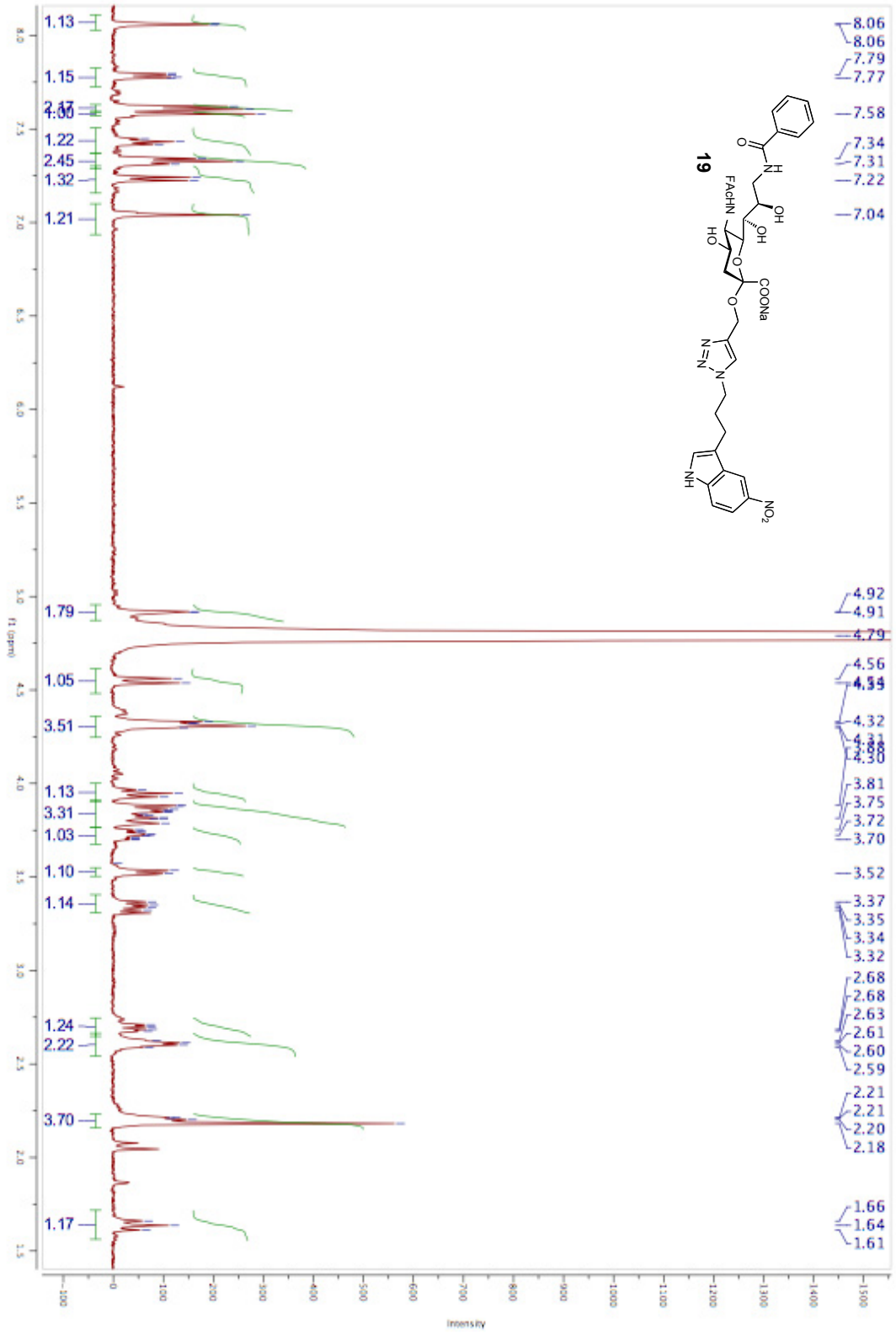
19
FAcHN
HO
OH
OH
O
COONa
NO2
HN
1.13
1.15
1.22
2.45
1.32
1.21
1.79
1.05
3.51
1.13
3.31
1.03
1.10
1.14
1.24
2.22
3.70
1.17
8.06
8.06
7.79
7.77
7.58
7.34
7.31
7.22
7.04
4.92
4.91
4.79
4.56
4.32
4.30
3.81
3.75
3.72
3.70
3.52
3.37
3.35
3.34
3.32
2.68
2.68
2.63
2.61
2.60
2.59
2.21
2.21
2.20
2.18
1.66
1.64
1.61
f1 (ppm)
Intensity

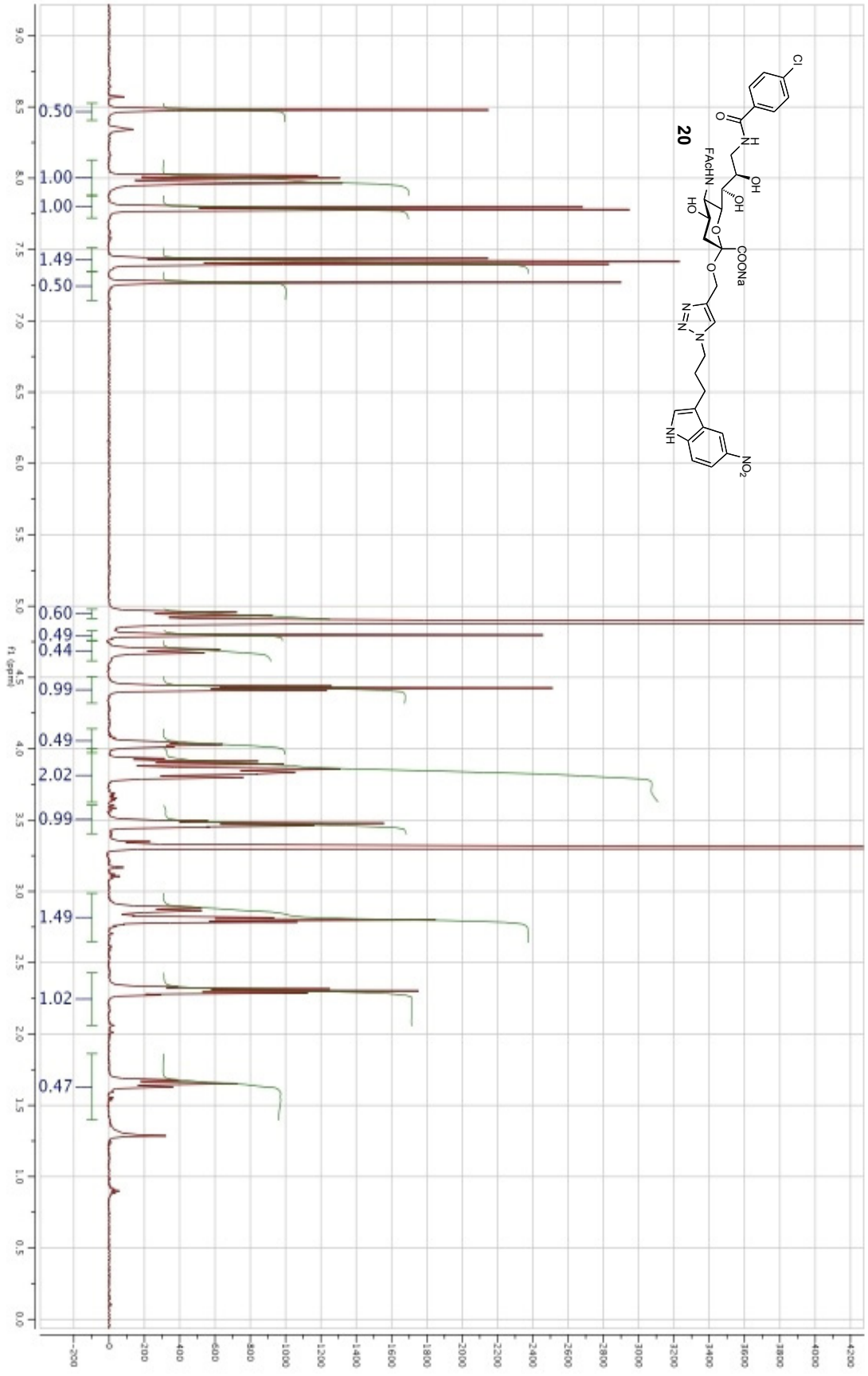
0.50
1.00
1.00
1.49
0.50
0.60
0.49
0.44
0.99
0.49
2.02
0.99
1.49
1.02
0.47
20
Cl
O
N
H
FAcHN
OH
HO
OH
O
COONa
O
N=N
N
NH
NO2

2.2.2 CD22 – Siglec-2

From a Library of MAG Antagonists to Nanomolar CD22 Ligands

Stefanie Mesch,[a] Katrin Lemme,[a] Matthias Wittwer,[a] Hendrik Koliwer-Brandl,[b] Oliver Schwardt,[a] Sørge Kelm,[b] Beat Ernst*[a]

[a]Institute of Molecular Pharmacy, University of Basel, Klingelbergstr. 50, 4056 Basel, Switzerland

[b]Center for Biomolecular Interactions Bremen, Glycobiochemistry, University of Bremen, P.O.B. 330440, D- 28334 Bremen, Germany

**Corresponding author. Tel: 0041 267 15 51; Fax: 0041 267 15 52; e-mail: beat.ernst@unibas.ch*

Published in: *ChemMedChem* ***2012****, 7,* 134-143.

Contribution of Katrin Lemme: Manuscript (not equally to first author), ITC experiments, determination of protein concentration.

CHEMMEDCHEM

DOI: 10.1002/cmdc.201100407

VIP

From a Library of MAG Antagonists to Nanomolar CD22 Ligands

Stefanie Mesch,[a] Katrin Lemme,[a] Matthias Wittwer,[a] Hendrik Koliwer-Brandl,[b] Oliver Schwardt,[a] Sørge Kelm,[b] and Beat Ernst*[a]

Siglec-2, also known as CD22, is involved in the regulation and survival of B-cells and has been successfully targeted in cell depletion therapies with antibody-based approaches. Sialic acid derivatives, already known to bind with high affinity to myelin-associated glycoprotein (MAG, Siglec-4), were screened for their binding affinity for CD22 by surface plasmon resonance. The best compound identified was further modified with various hydrophobic substituents at the 2-, 5-, and 9-positions of the sialic acid scaffold, leading to nanomolar derivatives, of which ligand **17b** shows the most promising pharmacodynamic and pharmacokinetic profiles. Isothermal titration calorimetry measurements demonstrate that the binding is enthalpy driven. Interestingly, the thermodynamic fingerprints reveal an excellent correlation between gains in enthalpy and compensation by increased entropy costs. Moreover, **17b** exhibits a residence time in the range of a few seconds, clearly prolonged relative to residence times typically observed for carbohydrate–lectin interactions. Finally, initial tests regarding drug-like properties of **17b** demonstrate the required high plasma protein binding yet a lack of oral availability, although its distribution coefficient (log *D*) is in the required range.

Introduction

Patients diagnosed with B-cell lymphomas can be effectively treated with the anti-CD20 antibody rituximab.[1] However, this therapy is not a cure, and especially for patients with indolent lymphoid malignancies novel treatments with alternative mechanisms of B-cell killing are required.[2] Numerous antibodies for B-cell depletion therapy are therefore under clinical development.[3] Two of them, the immunotoxins BL22[4] and CMC-544,[5] target CD22, a B-lymphocyte-specific receptor. CD22 (Siglec-2) is a member of the sialic acid binding immunoglobulin-like lectin (Siglec) family.[6] It is an inhibitory co-receptor for the B-cell receptor (BCR) and plays a crucial role in the regulation of activity,[7] homeostasis,[8] and survival of B-cells.[9] Upon BCR–antigen binding, tyrosine phosphorylation is induced,[10] which triggers further phosphorylation processes and finally leads to a dampening of the BCR-induced signal.[6,11] Apart from a few exceptions,[12] sialic acid binding sites of CD22 were shown to be effectively occupied by *cis* ligands, that is, ligands located on the same cell surface.[13] This interaction is important for the regulation of CD22 activity. Furthermore, it was shown that CD22 can also interact with ligands in *trans*,[14] that is, ligands located on other cells, to enable cell–cell communication. As an alternative to antibodies, sialosides that were shown to directly influence CD22 activity[15] initiated an intense search for high-affinity ligands.

The physiological ligands of Siglecs are gangliosides and sialidated glycoproteins.[16,17] CD22 recognizes sialic acid α2,6-linked to D-Gal, D-Gal*N*Ac (→**1**), or D-Glc*N*Ac. A decrease in the structural complexity yielded sialic acid derivatives **2**–**4**[15,18,19] (Figure 1), indicating that a biphenyl carboxamide moiety at the 9-position can improve affinity substantially. When this extension in the 9-position was applied to the disaccharide epitope, ligands such as **5** and **6** exhibiting sub-micromolar affinities were identified.[20] Finally, benzyl substituents at the reducing end of the disaccharide epitope led to a further improvement in affinity.[19,21]

When testing in B-cell based assays, a further aspect, the so-called density-dependent binding, must be considered.[22] In tests of monomeric sialosides (e.g., **7**[23] or **8**,[24] Figure 1) coupled to various supports such as a polyacrylamide backbone,[23] a glutamate cluster,[18] or a polymer obtained by ring-opening metathesis,[25] a substantial increase in binding affinity relative to monovalent sialosides was observed.[18,26] Interestingly, with a multivalent presentation, *cis* interactions could be abolished without precedent treatment with sialidase to remove masking by *cis* ligands.[13] Additionally, O'Reilly et al. showed that bifunctional ligands comprising a ligand of CD22 linked to an antigen can self-assemble by antibody triggering on B-cell surfaces and are able to overcome *cis* interactions as well.[24] Based on the current state of knowledge, an oligovalent presentation of glycan ligands is required for a successful competition with *cis* ligands.[27] However, further investigation is required to clarify whether an oligomeric display is mandatory to compete with *cis* ligands, or if monomeric high-affinity ligands could success-

[a] *Dr. S. Mesch, K. Lemme, Dr. M. Wittwer, Dr. O. Schwardt, Prof. Dr. B. Ernst*
Institute of Molecular Pharmacy, Pharmacenter, University of Basel
Klingelbergstr. 50, 4056 Basel (Switzerland)
E-mail: beat.ernst@unibas.ch

[b] *Dr. H. Koliwer-Brandl, Prof. Dr. S. Kelm*
Centre for Biomolecular Interactions Bremen, Glycobiochemistry
P.O. Box 330440, 28334 Bremen (Germany)

Supporting information for this article is available on the WWW under http://dx.doi.org/10.1002/cmdc.201100407.

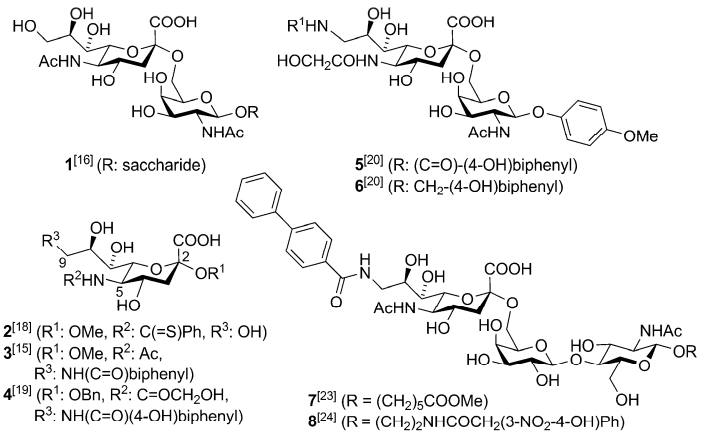

Figure 1. Overview of sialic acid based ligands of CD22: Ligands of CD22 showing affinities from the low-micromolar (**2**–**4**, **7**, and **8**) to sub-micromolar range (**5** and **6**).

fully be applied as well, as it has been shown that the monovalent ligand **3** is able to elicit a rapid modulation of B-cell signaling in the presence of fully sialylated *cis* ligands.[15]

Herein we present a series of CD22 ligands based on a screening hit identified from a small library of sialic acid derivatives, which were originally synthesized as antagonists of the myelin-associated glycoprotein (MAG, Siglec-4).[28,29] They were tested for pharmacodynamic (affinity and selectivity) and pharmacokinetic (lipophilicity, plasma protein binding, oral availability) properties.

Results and Discussion

In the intensive search for high-affinity CD22 ligands, most efforts have focused on modifications at the 9-position of sialic acid.[20] Moreover, Kiso and co-workers have reported ligands with phenyl, benzyl, and biphenylmethyl substituents at the reducing end.[21] Regarding the 5-position, van Rossenberg et al. showed that sterically demanding acyl groups, such as benzoyl and long aliphatic chains such as octanoyl, decrease affinity,[18] whereas hydroxyacetyl is well accepted.[26,30]

Screening

To further elaborate on optimal substitutions at the 2- and 5-positions, a stepwise approach was conducted, assuming that the individual contributions to binding are additive. With a small library of sialosides from our MAG project, an initial screen regarding the optimal aglycone (R^1 group) was performed (Entries 1–6, Table 1).[28,29] The affinities were determined by surface plasmon resonance (SPR, see below for details). 2,3-Dichlorobenzyl (→**9c**) led to the highest affinity and was therefore selected as aglycone for the new series of CD22 ligands. The aim of the second screen—again based on available MAG antagonists—was the identification of the optimal modification at the 5-position (R^2, Entries 7–11, Table 1).[29] As a result, *o*-nosyl (*ortho*-nitrophenylsulfonyl, →**9k**) was identified to be the superior substituent, leading to a ligand with nanomolar affinity for CD22 and a modest selectivity regarding MAG (~12-fold).

Synthesis

Based on the screening hits **9c** and **9k** as well as published data on CD22 ligands,[20] compound **13a**,[28] with biphenylcarboxamide at the 9-position and a benzyl aglycone, was considered as the starting point for our optimization campaign. Our goal was not only to elucidate the kinetic and thermodynamic profile

Table 1. Affinities of compounds **9a–k** for *h*CD22 and *m*MAG as determined by SPR experiments.

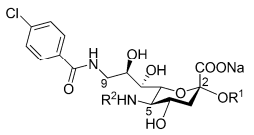

Entry	Compd	R^1	R^2	K_D [μM] CD22	MAG
1	**9a**	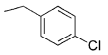	Ac	3.0	15
2	**9b**	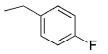	Ac	11	13
3	**9c**	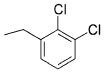	Ac	0.4	4.3
4	**9d**	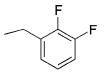	Ac	3.9	2.4
5	**9e**	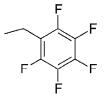	Ac	2.7	6.1
6	**9f**	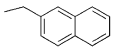	Ac	1.8	11.6
7	**9g**	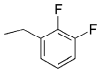		0.36	0.5
8	**9h**	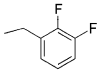		0.48	4.1
9	**9i**	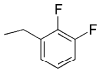		1.40	5.8
10	**9j**	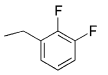		1.17	17
11	**9k**	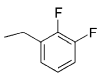		0.11	1.4

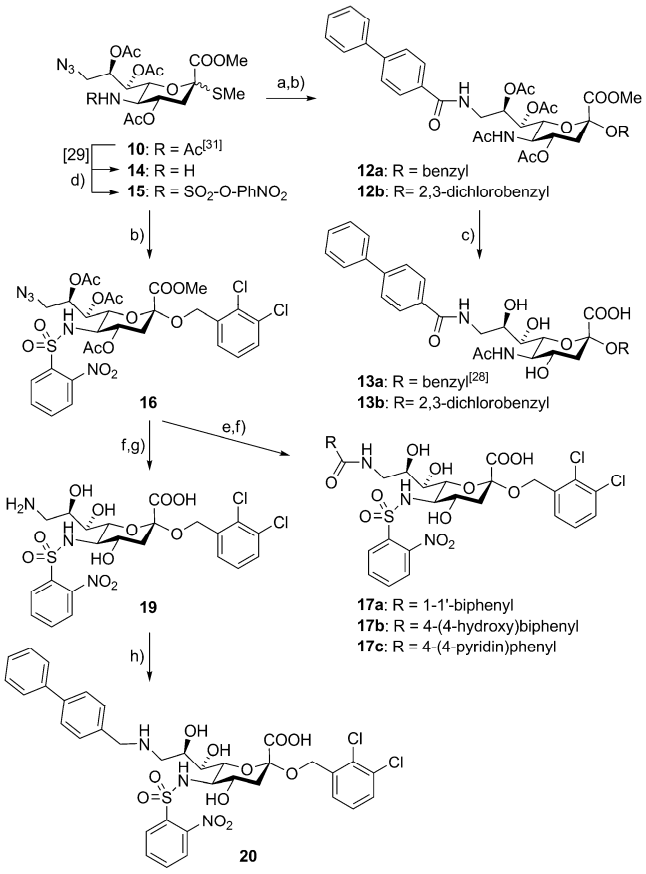

Scheme 1. *Reagents and conditions:* a) 4-phenylbenzoyl chloride, PPh_3, DCE (77%); b) ROH, NIS, TfOH, CH_3CN [**12a**: 70%, **12b**: 50%, **16**: 76%]; c) 10% aq NaOH [**13a**: 51%, **13b**: 25%]; d) *o*-nosyl-Cl, NEt_3, DMAP, CH_2Cl_2 (78%); e) RCOCl, PPh_3, DCE; f) LiOH, H_2O, THF [**17a–c**: 6–19% for two steps, →**18**: 52%]; g) PPh_3, H_2O, NEt_3, 50 °C (13%); h) 1-(bromomethyl)-4-phenylbenzene, K_2CO_3, THF (12%).

of the ligand–CD22 interaction, but also the pharmacokinetic properties of the best representatives.

Starting from sialyl donor **10**,[31] test compound **13b** was obtained according to published procedures.[28,29] The *o*-nosyl derivatives were synthesized according to a different approach (Scheme 1). After cleavage of the *N*-acetate (→**14**),[32] the amine was allowed to react with *o*-nosyl chloride (→**15**) followed by glycosylation with 2,3-dichlorobenzyl alcohol to yield intermediate **16**. Acylation by modified Staudinger conditions[33] and deprotection yielded the acyl derivatives **17a–c**. The low yields in this particular reaction can be explained by the formation of side products due to acetate migration. In addition, because of the small scale, purification, especially removal of PPh_3=O, was extremely difficult. Interestingly, lithium hydroxide in water/tetrahydrofuran had to be used for deprotection, because treatment with 10% aqueous sodium hydroxide resulted in loss of the nitro substituent. To avoid acetate migration, the 9-amino derivative **19** was obtained by deprotection of **16** (→**18**) followed by azide reduction. Upon alkylation of the amino group by reductive amination, reduction of the nitro group could not be avoided. However, alkylation of the primary amine with 1-(bromomethyl)-4-phenylbenzene in the presence of potassium carbonate furnished sialoside **20**, although only in a modest yield.

Surface plasmon resonance (SPR)

The compound library **9a–k** (Table 1) and the newly synthesized CD22 ligands **13a,b**, **17a–c**, and **20** were evaluated by SPR (Table 2). Here, $hCD22_{d1-3}$–Fc[34] was immobilized on a protein A surface, which had been covalently attached to the chip by amino coupling. In the reference cell, only protein A was immobilized to compensate for unspecific binding to the matrix. Dilution series of the compounds were prepared either in pure HBS-EP buffer (**9a–k**, **13a,b**) or in the same buffer additionally containing 5% DMSO (**17a–c**, **20**). Finally, the sensorgrams were fitted according to a 1:1 binding model.

Ligand **13a** showed a binding affinity in the submicromolar range (Entry 13). With the 2,3-dichlorobenzyl aglycone (→**13b**), a gain in affinity by a factor of eight was observed (Entry 14). Modifications at the 9-position caused a gain in affinity for 4-(4-hydroxyphenyl)benzamide **17b** (Entry 16), equal affinity for 4-(pyridin-4-yl)benzamide **17c** (Entry 17), and a loss in affinity for amine **20** (Entry 18). Surprisingly, **17a** (Entry 15) showed no affinity, neither in the SPR experiments, nor in the isothermal titration calorimetry (ITC) assay (Table 2), although the best substituents identified so far for the 2- (2,3-dichlorobenzyl) and the 5-positions (*o*-nosyl) were present. Regarding selectivity, **17b** exhibits a 50-fold higher affinity for CD22 than for MAG (K_D = 3.0 μM). This might be largely due to the biphenyl moiety at the 9-position, which has previously been shown to decrease the affinity for MAG.[20,28,35]

For the ligands **13b**, **17b**, and **17c** a clear prolongation of the residence time of the protein–ligand complex was observed (Table 3, Figure 2). Potential advantages of a prolonged

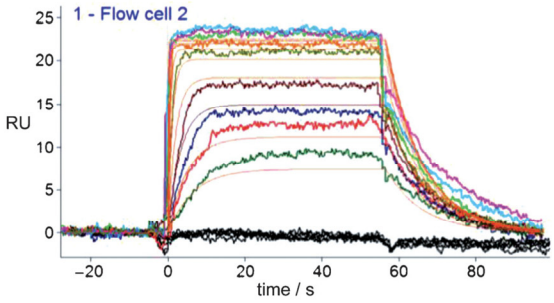

Figure 2. Sensorgram of **17b** at 25 °C measured in SPR; RU = response units.

Table 2. Affinity data for CD22 ligands as determined by SPR and ITC experiments.

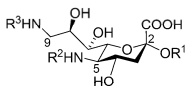

Entry	Compd	R^1	R^2	R^3	K_D [nM] SPR	K_D [nM] ITC
12	**9k**	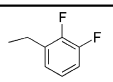		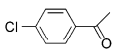	110	131
13	**13a**	Bn	Ac	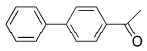	800	751 ± 224
14	**13b**	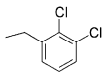	Ac	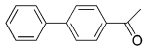	100	82 ± 19
15	**17a**	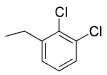		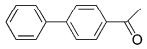	NB[a]	NB[a]
16	**17b**	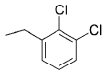		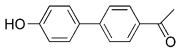	60	80 ± 9
17	**17c**	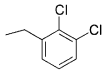		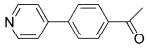	110	152 ± 43
18	**20**	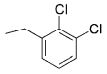		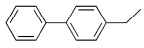	500	ND[b]

[a] No binding. [b] Not determined.

Table 3. Kinetic properties of **9k**, **13b**, and **17b,c**.

Entry	Compd	K_D [nM]	k_{on} [10^6 $M^{-1}s^{-1}$]	k_{off} [s^{-1}]	$t_{1/2}$ [s][a]
19	**9k**	130	2.1	0.27	2.6
20	**13b**	100	1.1	0.13	5.3
21	**17b**	60	1.1	0.08	8.7
22	**17c**	110	1.3	0.16	4.3

[a] $t_{1/2} = \ln 2/k_{off}$.

residence time are extended duration of the pharmacological effect and target selectivity.[36] Additionally, a therapeutic effect can be reached with a lower dose. As the half-life ($t_{1/2}$) of carbohydrate–protein complexes is typically very short (< 1 s),[37,38] this is clearly an improved property of these new CD22 ligands, although there is still a need for further improvement. The extended $t_{1/2}$ of the ligand–CD22 complex[39] might be due to the improved lipophilicity of the ligands (see log*D* values in Table 5 below).

Isothermal titration calorimetry (ITC)

The binding affinities measured by SPR and ITC experiments (Table 2) are in good agreement with each other. The thermodynamic fingerprint of a ligand describes enthalpy and entropy contributions of the interaction with its target and therefore provides characteristic insight into the binding process. ITC measurements for the ligands **9k**, **13a,b**, and **17a–c** were performed at 25 °C using *h*CD22$_{d1-3}$–Fc[34] (Table 4) and confirmed the behavior typically observed for carbohydrate–lectin interactions,[40–43] namely an enthalpy-driven binding. Less common are entropy-driven carbohydrate–lectin interactions, such as heparin binding to the agrin-G3 domain[42] or the interaction of di- and trisaccharides with calreticulin.[43]

The interaction of the parent compound **9k** is dominated by a large enthalpic contribution, which is, however, decreased by substantial entropy costs (Entry 23). The approximate sixfold drop in affinity observed for **13a** results from a large increase in entropy costs, which is only partially compensated by an improved enthalpy contribution (Entry 24). A possible explanation for the increased entropy term is a substantial conformational change caused by the spatial demands of the biphenyl substituent. Replacement of the benzyl aglycone in **13a** with the 2,3-dichlorobenzyl group (→**13b**, Entry 25) gives a further increase in enthalpy, whereas the entropy term remains stable.

Surprisingly, **17a** (Entry 26) does not bind to CD22, although the *o*-nosyl substituent does not prohibit binding of **9k**. As reported by Kiso and colleagues,[19] intramolecular attraction between benzyl at the 2-position and biphenyl at the 9-position can lead to a hydrophobic collapse. The introduction of an *o*-nosyl group at the 5-position may further support this process, abolishing the binding of **17a**. This hypothesis is also supported by the pharmacokinetic properties of **17a** because it is the only compound that was retained in an artificial membrane

Table 4. Thermodynamic parameters as determined at 25 °C by ITC.

Entry	Compd	*N*	K_D [nM]	ΔG° [kJ mol^{-1}]	ΔH° [kJ mol^{-1}]	$-T\Delta S^\circ$ [kJ mol^{-1}]
23	**9k**	0.96	131	−39.3	−54.8	+15.5
24	**13a**	0.96 ± 0.04	751 ± 224	−35.1 ± 0.8	−73.4 ± 0.8	+38.3 ± 1.6
25	**13b**	0.94 ± 0.02	82 ± 19	−40.5 ± 0.6	−80.2 ± 3.4	+39.7 ± 3.6
26	**17a**	NB[a]	NB[a]	NB[a]	NB[a]	NB[a]
27	**17b**	1.07 ± 0.01	80 ± 9	−40.6 ± 0.4	−61.6 ± 1.1	+21.0 ± 0.7
28	**17c**	0.95 ± 0.02	152 ± 43	−39.0 ± 0.7	−83.4 ± 2.8	+44.4 ± 3.5

[a] No binding.

Table 5. Pharmacokinetic properties of CD22 ligands.

Entry	Compd	log $D_{7.4}$	PAMPA log P_e	PAMPA [% Mm]	PPB [%]
29	**13a**	0.91	NP[a]	NR[b]	97
30	**13b**	2.24	−9.8	NR[b]	98
31	**17a**	3.25	−8.7	pH 5.0: 24% pH 6.2: 14% pH 7.4: NR[b]	>99
32	**17b**	3.12	NP[a]	NR[b]	>99
33	**17c**	2.08	−8.9	NR[b]	>99

[a] No permeation. [b] No retention.

(PAMPA,[44] see Table 5, Entry 31). Interestingly, compound **20**, in which the amide linker of **17a** is replaced by an amine linker, again exhibited nanomolar binding affinity in SPR (Table 2, Entry 18).

Introduction of 4-(4-hydroxyphenyl)benzamide (→**17b**, Entry 27) resulted in a ligand with an affinity similar to that of compound **13b**, although the ΔH° and $T\Delta S^\circ$ terms substantially change; they both differ by 19 kJ mol^{-1}, but with opposite signs. Introduction of a *para*-hydroxy substituent caused a favorable enthalpy change similar to an observation reported by Kiso et al.[20] Interestingly, when the terminal phenol (→**17b**) was replaced by pyridine (→**17c**, Entry 28), a substantially improved ΔH° value (−22 kJ mol^{-1}) was observed, which, however, is overcompensated by a loss of entropy leading to an overall twofold decrease in affinity. Clearly, the *o*-nosyl substituent elicits a reorientation of the ligand in the binding site, or leads to a remarkable change in desolvation energies. As a consequence, a dramatic change in the thermodynamic fingerprint results. An enthalpy–entropy plot (Figure 3) reveals a linear relationship with a high correlation coefficient ($R^2 = 0.97$), indicating enthalpy–entropy compensation, a property often reported for carbohydrate–lectin interactions.[40,45] The slope of −1 denotes that the enthalpic gain is completely compensated by an entropic penalty.

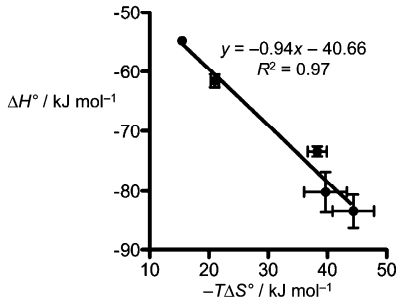

Figure 3. Enthalpy–entropy compensation plot: correlation of the change in enthalpy (ΔH°) and the change in entropy ($-T\Delta S^\circ$) of CD22 ligands interacting with hCD22$_{d1-3}$–Fc.[34]

Pharmacokinetics

As CD22 is found exclusively on B-cells, oral or intravenous applications must be considered. To elucidate the potential for oral availability, log D values were determined, as they are generally considered a rough indicator of a given compound's membrane permeation behavior,[46,47] although restrictions apply.[48] The log D values of compounds **13a**,**b** and **17a**–**c** were determined, and are in the range of 0.91–3.25 (Table 5), which indicates possible membrane permeability. However, determination of log P_e with the parallel artificial membrane permeability assay (PAMPA)[44] showed that **13a** and **17b** do not permeate at all, and **13b** and **17a**,**c** only to a very limited extent. Furthermore, retention within the membrane (PAMPA % Mm) could be excluded, except for **17a**. Here, at pH 5, 24% of the total amount of compound was retained in the membrane. The different results in the PAMPA for other ligands despite similar log D values might be caused by other molecular descriptors. For example, the log D values of **17a** and **17b** are in the same range, but their nonpolar surface areas and hydrogen bonding capacity differ. The former are generally observed to favor partition, whereas the latter seems to hinder it.[49] Due to these findings, no oral absorption based on passive diffusion can be expected for the presented CD22 ligands, as log P_e values below −6.7 indicate a very poor permeation through membranes. Therefore, if no active transport processes are involved, oral administration seems unrealistic.

Finally, plasma protein binding (PPB) of our CD22 ligands turned out to be very high. As CD22 is located on the surface of B-cells which circulate in the blood, high PPB might be beneficial, as suggested by Urien et al. for cetirizine, as an example.[50] Moreover, side effects due to distribution in various tissues of the body might be decreased as a consequence of both the high extent of PPB and the compound's inability to cross membranes. An additional positive aspect might be prolongation of plasma $t_{1/2}$, resulting from the fact that only free ligands can be metabolized and excreted. Nevertheless, the amount of unbound ligand, and consequently its distribution and clearance, depends not only on the extent of binding at equilibrium but also on the rates of association and dissociation (k_{on} and k_{off})[51] as well as tissue distribution and binding. The latter seems negligible, as PAMPA results do not indicate membrane permeation. The kinetic behavior of the ligands with respect to plasma proteins could be assessed by SPR and could provide valuable additional information.[52]

Conclusions

A series of high-affinity CD22 ligands was synthesized and investigated with regard to their biological and pharmacokinetic properties. The best ligand, sialoside **17b**, contains a dichlorobenzyl substituent at the anomeric position, an *ortho*-nitroben-

zylsulfonamide at the 5-position, and a 4′-hydroxy-4-biphenylcarboxamide at the 9-position. In addition to nanomolar affinity, ligand **17b** exhibits a prolonged residence time of the protein–ligand complex, which is atypical for carbohydrate–lectin interactions.[38] With respect to its pharmacokinetic properties, **17b** is not expected to be orally available based on PAMPA data, and therefore intravenous administration would need to be considered for an in vivo validation. However, the low permeation may be improved by a prodrug approach[47] or by replacing the carboxylate with a bioisostere.[53] Finally, **17b** shows extended plasma protein binding, which might be beneficial concerning various aspects such as pharmacological effect, plasma half-life, or side effects.

Experimental Section

Chemistry

NMR spectra were recorded on a Bruker Avance DMX-500 spectrometer (500 MHz). Assignment of ^{1}H and ^{13}C NMR spectra was performed by using 2D methods (COSY, HSQC, TOCSY). Chemical shifts are expressed in ppm using residual $CHCl_3$, CHD_2OD and HDO as references. Optical rotations were measured with PerkinElmer Polarimeters 241 and 341. MS analyses were carried out with a Waters Micromass ZQ Detector system. The spectra were recorded in positive or negative ESI mode. HPLC–HRMS analyses were carried out with an Agilent 1100 instrument equipped with a photodiode array detector and a Micromass QTOF I equipped with a 4 GHz digital time converter. All target compounds exhibited a purity of $\geq$95%. Reactions were monitored by TLC using glass plates coated with silica gel 60 F_{254} (Merck) and visualized by using UV light and/or by charring with a molybdate solution (0.02 M solution of ammonium cerium sulfate dihydrate and ammonium molybdate tetrahydrate in 10% aq H_2SO_4). Column chromatography was performed on silica gel (Uetikon, 40–60 mesh). CH_3OH was dried by holding at reflux with NaOMe and distilled immediately before use. THF was distilled over Na immediately before use. CH_2Cl_2, dichloroethane (DCE), CH_3CN, toluene, and benzene were dried by filtration over Al_2O_3 (Fluka, type 5016 A basic). Molecular sieves (3 Å) were activated under vacuum at 500 °C for 2 h immediately before use. Synthetic procedures for compounds **10**,[31] **12a**, **13a**,[28] **14**, and **15**[29] were reported earlier.

Methyl [methyl 5-acetamido-4,7,8-tri-*O*-acetyl-3,5,9-trideoxy-9-(4-phenylbenzamido)-2-thio-D-glycero-α-D-galacto-2-nonulopyranosid]onate (11): Compound **10** (250 mg, 0.50 mmol, 1.0 equiv) was dissolved in dry DCE (10 mL). 4-Phenylbenzoyl chloride (432 mg, 2.00 mmol, 4.0 equiv) and PPh_3 (290 mg, 1.10 mmol, 2.2 equiv) were added, and the reaction mixture was stirred at room temperature for 24 h. After dilution with CH_2Cl_2 (10 mL), the organic layer was washed with satd aq $NaHCO_3$ (3×5 mL) and H_2O (5 mL), dried over Na_2SO_4 and filtered. Afterward, the solvents were removed under reduced pressure and the crude product was purified by chromatography on silica gel (0.5% gradient of CH_3OH in CH_2Cl_2) to yield **11** (251 mg, 77%) as an oil. ^{1}H NMR (500 MHz, $CDCl_3$): δ=1.90 (s, 3H, OAc), 1.97 (s, 3H, SMe), 2.03, 2.07 (2 s, 6H, 2 OAc), 2.20 (dd, J=11.8, 13.8 Hz, 1H, H-3a), 2.24 (s, 3H, NHAc), 2.56 (dd, J=4.9, 13.8 Hz, 1H, H-3b), 3.05 (ddd, J=0.5, 3.5, 15.3 Hz, 1H, H-9a), 3.82 (s, 3H, OMe), 4.16 (q, J=10.3 Hz, 1H, H-5), 4.28 (dd, J=1.9, 10.6 Hz, 1H, H-6), 4.50 (ddd, J=3.9, 8.6, 15.0 Hz, 1H, H-9b), 5.16 (dt, J=3.5, 7.3 Hz, 1H, H-8), 5.20–5.33 (m, 2H, H-4, H-7), 5.43 (d, J=10.1 Hz, 1H, 5-NH), 7.22 (dd, J=4.3, 8.5 Hz, 1H, 9-NH), 7.36–7.43 (m, 1H, CH_{ar}), 7.47 (dd, J=4.8, 10.3 Hz, 2H, CH_{ar}), 7.54–7.63 (m, 2H, CH_{ar}), 7.64–7.72 (m, 2H, CH_{ar}), 7.90 ppm (d, J=8.5 Hz, 2H, CH_{ar}); ^{13}C NMR (125 MHz, $CDCl_3$): δ=11.4 (SMe), 21.0, 21.3 (3C, 3 OAc), 23.3 (NHAc), 37.3 (C3), 38.1 (C9), 49.9 (C5), 53.1 (OMe), 68.4 (C7), 69.4 (C4), 70.7 (C8), 71.0 (C6), 84.9 (C2), 127.3, 127.4, 127.7, 128.2, 129.1, 133.0, 140.1, 144.5 (12C, C_{ar}), 167.3, 168.2, 170.4, 170.5, 171.2, 172.2 ppm (6 CO); MS (ESI) m/z calcd for $C_{32}H_{38}N_2O_{11}S$ $[M+Na]^+$: 681.20, found: 681.28.

Methyl [2,3-dichlorobenzyl 5-acetamido-4,7,8-tri-*O*-acetyl-3,5,9-trideoxy-9-(4-phenylbenzamido)-D-glycero-α-D-galacto-2-nonulopyranosid]onate (12b): Compound **11** (50 mg, 7.5 μmol, 1.0 equiv) was dissolved in dry CH_3CN (2.0 mL). 2,3-Dichlorobenzyl alcohol (40 mg, 23 μmol, 3.0 equiv) and powdered MS (3 Å) were added. The mixture was stirred at room temperature for 1.5 h. The suspension was then cooled to −40 °C and subsequently treated with *N*-iodosuccinimide (NIS; 27 mg, 12 μmol, 1.6 equiv) and triflic acid (5.3 μL, 6 μmol in 0.2 mL CH_3CN, 0.8 equiv). After 30 min, the reaction mixture was warmed to −30 °C and stirring was continued for 16 h. The mixture was allowed to warm to room temperature, stirred for another 2 h and filtered through a pad of Celite. The Celite was washed with CH_2Cl_2 (5 mL) and the filtrate was subsequently washed with 20% aq $Na_2S_2O_3$ (1 mL) and satd aq $NaHCO_3$ (3×2 mL). The organic phase was dried over Na_2SO_4, filtered and concentrated under reduced pressure. The crude product was purified by chromatography on silica gel (0.5% gradient of *i*PrOH in petroleum ether (PE)/CH_2Cl_2 8:4) to yield **12b** (30 mg, 50%) as an oil. ^{1}H NMR (500 MHz, $CDCl_3$): δ=1.89 (s, 6H, NHAc, OAc), 2.01–2.06 (m, 4H, H-3a, OAc), 2.15 (s, 3H, OAc), 2.57 (dd, J=4.1, 13.4 Hz, 1H, H-3b), 3.49 (dd, J=5.6, 12.2 Hz, 1H, H-9a), 3.79 (s, 3H, OMe), 3.83 (d, J=12.4 Hz, 1H, H-9b), 4.09 (t, J=10.5 Hz, 1H, H-5), 4.15 (m, 1H, H-6), 4.58 (A of AB, J=13.7 Hz, 1H, CH_2Ar), 4.83–4.98 (m, 2H, H-4, CH_2Ar), 5.33–5.40 (m, 2H, H-7, H-8), 7.21 (t, J=7.5 Hz, 1H, CH_{ar}), 7.23–7.31 (m, 4H, CH_{ar}), 7.34–7.50 (m, 6H, CH_{ar}), 7.56–7.69 ppm (m, 1H, CH_{ar}); ^{13}C NMR (125 MHz, $CDCl_3$): δ=20.8, 20.9, 21.1 (3 OAc), 23.3 (NHAc), 37.8 (C3), 43.2 (C9), 49.5 (C5), 53.0 (OMe), 64.3 (CH_2Ar), 68.3 (C7), 68.9 (C4), 70.7 (C8), 73.0 (C6), 98.8 (C2), 126.2, 127.2, 127.3, 127.5, 129.4, 129.6, 137.3 (18C, C_{ar}), 168.1, 170.2, 170.4, 170.7, 171.0, 171.2 ppm (6 CO); MS (ESI) m/z calcd for $C_{38}H_{40}Cl_2N_2O_{12}$ $[M+Na]^+$: 809.18, found: 809.28.

Sodium [2,3-dichlorobenzyl 5-acetamido-3,5,9-trideoxy-9-(4-phenylbenzamido)-D-glycero-α-D-galacto-2-nonulopyranosid]onate (13b): Compound **12b** (30 mg, 38 μmol) was treated with 10% aq NaOH (0.4 mL) in CH_3OH (2 mL). The crude product was purified by LC–MS to yield **13b** as a white solid (6.3 mg, 25%). $[\alpha]_D^{20}$ −21.8 (c=0.33, CH_3OH); ^{1}H NMR (500 MHz, CD_3OD): δ=1.73 (t, J=11.0 Hz, 1H, H-3a), 2.00 (s, 3H, NHAc), 2.93 (d, J=11.4 Hz, 1H, H-3b), 3.46 (d, J=9.0 Hz, 1H, H-7), 3.53 (m, 1H, H-9a), 3.68 (d, J=9.0 Hz, 1H, H-6), 3.71–3.85 (m, 3H, H-4, H-5, H-9b), 4.04 (t, J=7.7 Hz, 1H, H-8), 4.73 (A, B of AB, J=13.4 Hz, 2H, CH_2Ar), 7.26 (t, J=7.9 Hz, 1H, CH_{ar}), 7.39 (t, J=6.6 Hz, 2H, CH_{ar}), 7.46 (t, J=7.4 Hz, 2H, CH_{ar}), 7.57 (d, J=7.7 Hz, 1H, CH_{ar}), 7.67 (d, J=7.4 Hz, 2H, CH_{ar}), 7.72 (d, J=7.8 Hz, 2H, CH_{ar}), 7.91 (d, J=7.9 Hz, 2H, CH_{ar}), 8.22 (d, J=6.5 Hz, 1H, 5-NH), 8.30 ppm (s, 1H, 9-NH); ^{13}C NMR (125 MHz, CD_3OD): δ=22.6 (NHAc), 42.5 (C3), 44.5 (C9), 54.1 (C5), 64.6 (CH_2Ar), 69.6 (C4), 71.2 (C8), 72.5 (C7), 74.5 (C6), 101.4 (C2), 127.9, 128.0, 128.2, 128.5, 128.6, 129.0, 129.1, 130.0, 130.1, 140.3, 145.6 (18C, C_{ar}), 175.5 ppm (3C, 3 CO); HRMS (ESI) m/z calcd for $C_{31}H_{32}Cl_2N_2O_9$ $[M+Na]^+$: 669.1384, found: 669.1384.

Methyl [methyl 4,7,8-tri-*O*-acetyl-9-azido-3,5,9-trideoxy-5-(2-nitrophenylsulfonamido)-2-thio-D-glycero-α-D-galacto-2-nonulopyranosid]onate (15): Nosyl chloride (105 mg, 0.47 mmol), NEt_3 (34.0 μL, 48.0 mg, 0.47 mmol), and DMAP (10.0 mg, 0.08 mmol)

were added successively to a solution of **14** (73.0 mg, 0.16 mmol) in dry CH_2Cl_2 (3 mL) at 0 °C. The reaction mixture was stirred at room temperature overnight and then washed with satd aq $NaHCO_3$ (2×5 mL) and H_2O (5 mL). The organic phase was dried over Na_2SO_4, filtered and concentrated under reduced pressure. The residue was purified by chromatography on silica gel (PE/EtOAc 1:1→1:2) to yield **15** (81 mg, 78%) as an oil. ^{1}H NMR (500 MHz, $CDCl_3$): δ = 1.85 (m, 1H, H-3a), 2.02 (s, 3H, SMe), 2.10, 2.13, 2.21 (3 s, 9H, 3 OAc), 2.80 (m, 1H, H-3b), 3.32 (dd, J = 6.2, 13.4 Hz, 1H, H-9a), 3.57 (dd, J = 3.2, 13.4 Hz, 1H, H-9b), 3.80 (m, 1H, H-5), 3.82 (s, 3H, OMe), 3.91 (d, J = 10.5 Hz, 1H, H-6), 4.97 (td, J = 4.7, 11.4 Hz, 1H, H-4), 5.30 (m, 2H, H-7, H-8), 5.75 (d, J = 9.4 Hz, 1H, NH), 7.70 (m, 2H, CH_{ar}), 7.90 (d, J = 7.9, 1H, CH_{ar}), 8.10 ppm (d, J = 6.5, 1H, CH_{ar}); ^{13}C NMR (125 MHz, $CDCl_3$): δ = 12.1 (SMe), 20.5, 21.1, 21.1 (3 OAc), 38.1 (C3), 50.8 (C9), 53.2, 53.5 (C5, OMe), 68.8 (C7), 69.7 (C4), 70.4 (C8), 74.7 (C6), 82.8 (C2), 125.5, 130.4, 133.5, 135.5, 147.5 (6C, C_{ar}), 167.8, 170.4 ppm (4C, 4 CO); MS (ESI) *m/z* calcd for $C_{23}H_{29}N_5O_{13}S_2$ $[M-H]^-$: 646.12, found: 646.56.

Methyl [2,3-dichlorobenzyl 4,7,8-tri-*O*-acetyl-9-azido-3,5,9-trideoxy-5-(2-nitrophenylsulfonamido)-D-glycero-α-D-galacto-2-nonulopyranosid]onate (16): Compound **15** (370 mg, 0.57 mmol, 1.0 equiv) was dissolved in dry CH_3CN (10 mL). Then, 2,3-dichlorobenzyl alcohol (302 mg, 1.71 mmol, 3.0 equiv) and powdered MS (3 Å) were added. The mixture was stirred at room temperature for 1.5 h. Afterward, the suspension was cooled to −40 °C and subsequently treated with NIS (205 mg, 0.92 mmol, 1.6 equiv) and triflic acid (40 µL, 0.4 mmol, 0.8 equiv). After 30 min, the reaction mixture was warmed to −30 °C, and stirring was continued for 16 h. The mixture was then warmed to room temperature, stirred for another 2 h and filtered through a pad of Celite. The Celite was washed with CH_2Cl_2 (15 mL), and the filtrate was subsequently washed with 20% aq $Na_2S_2O_3$ (5 mL), satd aq $NaHCO_3$ (3×5 mL), and H_2O (5 mL). The organic phase was dried over Na_2SO_4, filtered and concentrated under reduced pressure. The crude product was purified by chromatography on silica gel (0.5% gradient of *i*PrOH in PE/CH_2Cl_2 2:1) to yield **16** as a yellow solid (337 mg, 76%). $[\alpha]_D^{20}$ −43.7 (c = 0.46, CH_3OH); ^{1}H NMR (500 MHz, $CDCl_3$): δ = 1.96 (m, 1H, H-3a), 2.02, 2.14, 2.22 (3 s, 9H, 3 OAc), 2.75 (m, 1H, H-3b), 3.31 (m, 1H, H-9a), 3.50 (m, 1H, H-9b), 3.78 (s, 3H, OMe), 3.88 (m, 1H, H-5), 4.15 (d, J = 10.6 Hz, 1H, H-6), 4.58, 4.66 (A, B of AB, J = 12.7, 2H, CH_2Ar), 4.96 (m, 1H, H-4), 5.24–5.32 (m, 2H, H-7, H-8), 5.60 (d, J = 9.3 Hz, 1H, 5-NH), 7.25 (m, 1H, CH_{ar}), 7.35–7.48 (m, 2H, CH_{ar}), 7.74 (dd, J = 4.5, 10.7 Hz, 1H, CH_{ar}), 7.77–7.86 (m, 2H, CH_{ar}), 8.19 ppm (m, 1H, CH_{ar}); ^{13}C NMR (125 MHz, $CDCl_3$): δ = 20.5, 20.7, 21.0 (3 OAc), 38.2 (C3), 50.5 (C9), 51.0 (OMe), 52.9 (C5), 64.4 (CH_2Ar), 68.6 (C4), 69.7 (C7), 71.1 (C8), 76.7 (C6), 98.1 (C2), 123.7, 125.4, 126.4, 127.5, 127.7, 129.4, 132.4, 132.7, 134.1, 135.4, 149.5 (12C, C_{ar}), 168.6, 170.7, 170.9 ppm (4C, 4 CO); MS (ESI) *m/z* calcd for $C_{29}H_{31}Cl_2N_5O_{14}S$ $[M+Na]^+$: 798.08, found: 797.95.

General procedure A for the preparation of acid chlorides: The acid (0.15 mmol) was suspended in dry CH_2Cl_2 (1–2 mL) and cooled to 0 °C. Chloroenamine (0.17 mmol) was added dropwise, and the reaction was allowed to warm to room temperature. After 2 h, the initial precipitate was dissolved, and the acid chlorides were directly used without work-up and purification.

General procedure B for the synthesis of compounds 17a–c: Compound **16** (75 µmol) was added to the corresponding acid chloride (0.15 mmol), dissolved in dry CH_2Cl_2 (1 mL). PPh_3 (0.18 mmol) in dry CH_2Cl_2 (1.5 mL) was added after 5 min, and the solution was stirred at room temperature for 24 h. Then, the reaction mixture was diluted with CH_2Cl_2 (5 mL) and washed with satd aq $NaHCO_3$ (3×3 mL) and H_2O (3 mL). The organic phase was dried over Na_2SO_4, filtered, and concentrated under reduced pressure. The residue was purified by chromatography on silica gel. Afterward, the acetylated intermediate was dissolved in THF/H_2O (2.5 mL, 4:1) and treated with LiOH (0.28 mmol) at room temperature for 4 h. After completion of the reaction, the crude product was purified by LC–MS to yield the final compound.

Sodium [2,3-dichlorobenzyl 3,5,9-trideoxy-5-(2-nitrophenylsulfonamido)-9-(4-phenylbenzamido)-D-glycero-α-D-galacto-2-nonulopyranosid]onate (17a): Prepared from **16** (50 mg, 0.06 mmol) and 4-phenyl benzoic acid according to general procedures A and B. Yield: 10 mg (19%) as a white solid. $[\alpha]_D^{20}$ −1.8 (c = 0.04, CH_3OH); ^{1}H NMR (500 MHz, CD_3OD): δ = 1.64 (t, J = 12.1 Hz, 1H, H-3a), 2.40 (dd, J = 3.7, 13.0 Hz, 1H, H-3b), 3.51 (m, 1H, H-9a), 3.59 (t, J = 10.0 Hz, 1H, H-5), 3.69–3.80 (m, 2H, H-7, H-9b), 3.98 (m, 1H, H-8), 4.05 (m, 1H, H-4), 4.12 (d, J = 10.5 Hz, 1H, H-6), 4.53, 4.85 (A, B of AB, J = 12.3 Hz, 2H, CH_2Ar), 7.29 (t, J = 8.3 Hz, 1H, CH_{ar}), 7.38 (t, J = 7.2 Hz, 1H, CH_{ar}), 7.42–7.49 (m, 3H, CH_{ar}), 7.64 (d, J = 7.7 Hz, 1H, CH_{ar}), 7.68 (d, J = 7.1 Hz, 3H, CH_{ar}), 7.73 (d, J = 7.6 Hz, 4H, CH_{ar}), 7.91 (d, J = 7.6 Hz, 2H, CH_{ar}), 8.18 (d, J = 7.6 Hz, 1H, CH_{ar}), 8.35 ppm (s, 1H, NH); ^{13}C NMR (125 MHz, CD_3OD): δ = 42.3 (C3), 45.7 (C9), 58.1 (C5), 63.9 (CH_2Ar), 68.4 (C4), 71.0 (C7), 71.2 (C8), 72.6 (C6), 99.3 (C2), 125.6, 125.9, 128.1, 128.2, 128.7, 129.0, 129.1, 129.2, 130.0, 130.3, 132.4, 133.5, 134.3, 136.5, 139.6, 141.3, 145.7, 149.0 (24C, C_{ar}), 171.0 ppm (2C, 2 CO); HRMS (ESI) *m/z* calcd for $C_{35}H_{32}Cl_2N_3NaO_{12}S$ $[M+Na]^+$: 834.0880, found: 834.0893.

Sodium [2,3-dichlorobenzyl 3,5,9-trideoxy-9-[4-(4-hydroxyphenyl)benzamido]-5-(2-nitrophenylsulfonamido)-D-glycero-α-D-galacto-2-nonulopyranosid]onate (17b): Prepared from **16** (30 mg, 40 µmol) and 4-(4-hydroxyphenyl)benzoic acid according to general procedures A and B. Yield: 2.0 mg (6%) as a pale-yellow solid. $[\alpha]_D^{20}$ −88.0 (c = 0.01, CH_3OH); ^{1}H NMR (500 MHz, CD_3OD): δ = 1.65 (t, J = 12.0 Hz, 1H, H-3a), 2.78 (dd, J = 3.6, 12.0 Hz, 1H, H-3b), 3.41–3.58 (m, 2H, H-5, H-9a), 3.67 (m, 1H, H-4), 3.70–3.79 (m, 2H, H-7, H-9b), 3.88 (d, J = 10.3 Hz, 1H, H-6), 3.97 (m, 1H, H-8), 4.64, 4.87 (A, B of AB, J = 12.6 Hz, 2H, CH_2Ar), 6.91 (d, J = 7.8 Hz, 2H, CH_{ar}), 7.26 (t, J = 7.7 Hz, 1H, CH_{ar}), 7.39 (d, J = 8.0 Hz, 1H, CH_{ar}), 7.47–7.60 (m, 3H, CH_{ar}), 7.67 (d, J = 7.8 Hz, 2H, CH_{ar}), 7.70–7.80 (m, 4H, CH_{ar}), 7.85 (d, J = 7.8 Hz, 2H, CH_{ar}), 8.16 (d, J = 7.3 Hz, 1H, NH), 8.23 ppm (m, 1H, NH); ^{13}C NMR (125 MHz, CD_3OD): δ = 42.6 (C3), 43.8 (C9), 49.5 (C5), 64.7 (CH_2Ar), 70.2, 71.2, 71.9 (C4, C7, C8), 74.0 (C6), 116.8, 125.8, 127.3, 128.6, 128.7, 128.9, 129.2, 130.1, 132.1, 132.5, 133.3, 133.7, 134.6, 135.8 (24C, C_{ar}), 170.5 ppm (2C, 2 CO); HRMS (ESI) *m/z* calcd for $C_{35}H_{33}Cl_2N_3O_{13}S$ $[M+Na]^+$: 828.1009, found: 828.1009.

Sodium [2,3-dichlorobenzyl 3,5,9-trideoxy-5-(2-nitrophenylsulfonamido)-9-[4-(pyridin-4-yl)benzamido]-D-glycero-α-D-galacto-2-nonulopyranosid]onate (17c): Prepared from **16** (58 mg, 70 µmol) and 4-(pyridin-4-yl)benzoic acid according to general procedures A and B. Yield: 8.0 mg (13%) as a pale-yellow solid. $[\alpha]_D^{20}$ −45.0 (c = 0.32, CH_3OH); ^{1}H NMR (500 MHz, CD_3OD): δ = 1.71 (t, J = 12.1 Hz, 1H, H-3a), 2.72 (dd, J = 4.3, 12.3 Hz, 1H, H-3b), 3.51 (t, J = 10.0 Hz, 1H, H-5), 3.57 (dd, J = 6.3, 13.7 Hz, 1H, H-9a), 3.69 (td, J = 4.3, 11.3 Hz, 1H, H-4), 3.76–3.86 (m, 2H, H-7, H-9b), 3.91 (d, J = 10.3 Hz, 1H, H-6), 4.02 (t, J = 7.4 Hz, 1H, H-8), 4.69, 4.92 (A, B of AB, J = 13.2 Hz, 2H, CH_2Ar), 7.26 (t, J = 7.8 Hz, 1H, CH_{ar}), 7.40 (d, J = 8.0 Hz, 1H, CH_{ar}), 7.49 (d, J = 7.7 Hz, 1H, CH_{ar}), 7.76 (t, J = 6.2 Hz, 2H, CH_{ar}), 7.81 (m, 1H, CH_{ar}), 7.86–7.93 (m, 5H, CH_{ar}), 7.99 (d, J = 7.8 Hz, 2H, CH_{ar}), 8.17 (d, J = 7.0 Hz, 1H, NH), 8.67 ppm (d, J = 5.1 Hz, 2H, CH_{ar}); ^{13}C NMR (125 MHz, CD_3OD): δ = 42.3 (C3), 44.4 (C9), 57.9 (C5), 64.7 (CH_2Ar), 69.8 (C4), 71.2 (C7), 71.7 (C8), 74.5 (C6), 100.9 (C2), 123.9, 125.9, 128.5, 128.6, 128.7, 129.5, 130.4, 132.3, 133.5, 133.7, 134.6, 136.2, 136.9, 139.6, 141.2, 148.9, 151.4 (23C, C_{ar}), 170.0, 172.6 ppm

(2 CO); HRMS (ESI) *m/z* calcd for $C_{34}H_{32}Cl_2N_4O_{12}S$ $[M+H]^+$: 791.1193, found: 791.1194.

Sodium [2,3-dichlorobenzyl 9-azido-3,5,9-trideoxy-5-(2-nitrophenylsulfonamido)-D-glycero-α-D-galacto-2-nonulopyranosid]onate (18): A solution of **16** (310 mg, 0.4 mmol) in THF/H_2O (6 mL:2.5 mL) was allowed to react with LiOH (78 mg, 3.2 mmol) at room temperature for 4 h. The crude product was purified by LC–MS to yield **18** (107 mg, 52%) as an oil. ^{1}H NMR (500 MHz, CD_3OD): δ=1.68 (t, J=12.2 Hz, 1H, H-3a), 2.71 (dd, J=4.8, 12.5 Hz, 1H, H-3b), 3.31 (m, 1H, H-9a), 3.45 (m, 1H, H-5), 3.53 (dd, J=2.4, 12.8 Hz, 1H, H-9b), 3.67 (ddd, J=4.8, 9.9, 11.8 Hz, 1H, H-4), 3.81 (dd, J=1.5, 8.9 Hz, 1H, H-7), 3.86 (dd, J=1.5, 10.5 Hz, 1H, H-6), 3.95 (ddd, J=2.4, 6.6, 8.9 Hz, 1H, H-8), 4.70, 4.92 (A, B of AB, J=13.3 Hz, 2H, CH_2Ar), 7.27 (t, J=7.9 Hz, 1H, CH_{ar}), 7.44 (dd, J=1.4, 8.0 Hz, 1H, CH_{ar}), 7.50 (d, J=7.7 Hz, 1H, CH_{ar}), 7.70–7.81 (m, 2H, CH_{ar}), 7.88 (m, 1H, CH_{ar}), 8.16 ppm (dd, J=3.3, 6.0 Hz, 1H, CH_{ar}); ^{13}C NMR (125 MHz, CD_3OD): δ=42.4 (C3), 55.0 (C9), 57.9 (C5), 64.6 (CH_2Ar), 69.6 (C4), 70.5 (C7), 72.4 (C8), 74.5 (C6), 125.8, 128.5, 128.7, 130.3, 132.3, 133.5, 134.4 (12C, C_{ar}), 172.5 ppm (CO); MS (ESI) *m/z* calcd for $C_{22}H_{23}Cl_2N_5O_{11}S$ $[M-H]^-$: 634.04, found: 634.16.

Sodium [2,3-dichlorobenzyl 9-amino-3,5,9-trideoxy-5-(2-nitrophenylsulfonamido)-D-glycero-α-D-galacto-2-nonulopyranosid]onate (19): PPh_3 (33 mg, 0.13 mmol, 1.6 equiv) and NEt_3 (1.2 μL, 12 μmol, 1.5 equiv) were successively added to a solution of **18** (50 mg, 8.0 μmol, 1.0 equiv) in dry THF (5 mL) at 0 °C. After 1 h, PPh_3 (66 mg, 0.26 mmol, 3.2 equiv) and H_2O (1.5 mL) were added, and stirring was continued at 50 °C for 4 h. After cooling to room temperature, the solvent was removed under reduced pressure, and the residue was purified by LC–MS to yield **19** (6.3 mg, 13%) as an oil. $[\alpha]_D^{20}$ −43.7 (c=0.46, CH_3OH); ^{1}H NMR (500 MHz, CD_3OD): δ=1.60 (t, J=12.0 Hz, 1H, H-3a), 2.79 (dd, J=4.9, 12.3 Hz, 1H, H-3b), 2.93 (dd, J=9.3, 12.7 Hz, 1H, H-9a), 3.34 (m, 1H, H-9b), 3.38 (t, J=10.1 Hz, 1H, H-5), 3.66 (m, 1H, H-4), 3.80–3.89 (m, 2H, H-6, H-7), 4.05 (m, 1H, H-8), 4.69, 4.91 (A, B of AB, J=13.6 Hz, 2H, CH_2Ar), 7.27 (t, J=7.9 Hz, 1H, CH_{ar}), 7.42 (d, J=8.0 Hz, 1H, CH_{ar}), 7.54 (d, J=7.8 Hz, 1H, CH_{ar}), 7.71–7.81 (m, 2H, CH_{ar}), 7.89 (dd, J=3.3, 6.0 Hz, 1H, CH_{ar}), 8.17 ppm (dt, J=3.7, 7.5 Hz, 1H, CH_{ar}); ^{13}C NMR (125 MHz, CD_3OD): δ=43.0 (C3), 43.9 (C9), 57.9 (C5), 64.5 (CH_2Ar), 69.5 (C8), 70.0 (C4), 72.0 (C7), 74.1 (C6), 125.9, 128.3, 128.6, 130.0, 132.3, 133.4, 133.6, 134.5, 136.0, 140.2, 149.1 (12C, C*ar*), 173.9 ppm (CO); MS (ESI) *m/z* calcd for $C_{22}H_{25}Cl_2N_3O_{11}S$ $[M+H]^+$: 610.07, found: 610.12.

Sodium [2,3-dichlorobenzyl 3,5,9-trideoxy-5-(2-nitrophenylsulfonamido)-9-(4-phenylbenzylamine)-D-glycero-α-D-galacto-2-nonulopyranosid]onate (20): Compound **19** (2.0 mg, 3.3 μmol, 1.0 equiv) was dissolved in THF (0.6 mL). 1-(Bromomethyl)-4-phenylbenzene (1.1 mg, 6.6 μmol, 2.0 equiv) and K_2CO_3 (1.1 mg, 8.0 μmol, 2.4 equiv) were added in portions. The reaction mixture was stirred at room temperature for 4 days. The crude product was purified by LC–MS to yield **20** as an oil (0.3 mg, 12%). $[\alpha]_D^{20}$ −102.3 (c=0.01, CH_3OH); ^{1}H NMR (500 MHz, CD_3OD): δ=1.60 (t, J=11.8 Hz, 1H, H-3a), 2.77 (m, 1H, H-3b), 2.98 (t, J=10.9 Hz, 1H, H-9a), 3.39–3.41 (m, 2H, H-5, H-9b), 3.66 (m, 1H, H-4), 3.76–3.90 (m, 2H, H-6, H-7), 4.10 (t, J=8.7 Hz, 1H, H-8), 4.19 (s, 2H, NCH_2), 4.72, 4.95 (A, B of AB, 2H, CH_2Ar), 7.26 (t, J=7.5 Hz, 1H, CH_{ar}), 7.36 (m, 1H, CH_{ar}), 7.38–7.48 (m, 3H, CH_{ar}), 7.54 (d, J=7.4 Hz, 2H, CH_{ar}), 7.63 (d, J=7.3 Hz, 2H, CH_{ar}), 7.69 (d, J=7.3 Hz, 2H, CH_{ar}), 7.76 (s, 2H, CH_{ar}), 7.87 (s, 1H, CH_{ar}), 8.17 (s, 1H, CH_{ar}), 8.55 ppm (s, 1H, CH_{ar}); ^{13}C NMR (125 MHz, CD_3OD): δ=41.6 (C3), 47.3 (C9), 51.2 (NCH_2), 57.0 (C5), 63.6 (CH_2Ar), 68.5 (C8), 69.1 (C4), 70.5 (C7), 72.3 (C6), 123.9, 126.6, 126.7, 127.1, 127.5, 127.6, 128.3, 128.4, 129.7, 130.6, 132.3 ppm (24C, C_{ar}); HRMS (ESI) *m/z* calcd for $C_{35}H_{35}Cl_2N_3O_{11}S$ $[M+Na]^+$: 798.1267, found: 798.1262.

Biological assays

Siglec–Fc proteins: Human $CD22_{d1-3}$–Fc from CHO-Lec1 and murine MAG_{d1-3}–Fc from CHO-Lec3.2.8.1 cell culture supernatants were affinity purified as described previously,[34] dialyzed against 10 mM phosphate buffer (pH 7.4), sterile filtered, and stored at 4 °C. The proteins were analyzed by an ELISA and binding assay with immobilized fetuin.[34]

Surface plasmon resonance (SPR): The SPR measurements were performed on a Biacore 3000 SPR-based optical biosensor (Biacore, GE Healthcare, Uppsala, Sweden). Sensor chips (CM5), immobilization kits, maintenance supply, and HBS-EP buffer (10 mM HEPES pH 7.4, 150 mM NaCl, 3 mM EDTA, 0.005% *v/v* surfactant P20) were purchased from GE Healthcare. The carboxy groups on the CM5 chip were activated for 10 min with a 1:1 mixture of 0.1 M *N*-hydroxysuccinimide (NHS) and 0.1 M 3-(*N*,*N*-dimethylamino)propyl-*N*-ethylcarbodiimide (EDC) at a flow rate of 10 μL min^{-1}. For immobilizing protein A (P6031, Sigma), a solution of 30 μg mL^{-1} in acetate buffer was injected over the activated surface for 10 min at a flow rate of 10 μL min^{-1}. Protein A densities of ~4000 RU were achieved. Flow cells were blocked with a 10 min injection of 1 M ethanolamine, pH 8.0. For capturing, hCD22$_{d1-3}$–Fc or mMAG$_{d1-3}$–Fc solutions of 30–40 μg mL^{-1} concentration in NaOAc (pH 5.0) were injected at a flow rate of 5 μL min^{-1} for 3 min. The surface was equilibrated with HBS-EP buffer overnight at a flow rate of 5 μL min^{-1}, achieving densities of ~3000–4000 RU. Tenfold dilution series of antagonists were freshly prepared in HBS-EP. All binding experiments were conducted at 25 °C at a flow rate of 20 μL min^{-1}. The samples were injected for 1 min followed by 1 min dissociation. Each sample concentration was measured in duplicate. Double referencing was applied to correct for bulk effects and other systematic artifacts (subtraction of reference surface and blank injections). Data processing and equilibrium binding constant determinations were accomplished with Scrubber (BioLogic Software, Version 1.1g or 2.0c). Kinetic data were simultaneously fit using Scrubber 2.0c. For compounds with low solubility (→**17a–c**, **20**), 5% DMSO (for molecular biology, >99.9%, Fluka) was used in the buffer. The running buffer was 5% DMSO in HBS-EP. The surface was equilibrated at a flow of 5 μL min^{-1} until the baseline was stable. To eliminate the influence of DMSO on the signals, a calibration curve was recorded with DMSO concentrations of 4.7–5.1%. The DMSO calibration was accomplished directly in Scrubber 2.0c.

Isothermal titration calorimetry (ITC): ITC experiments were performed using a VP-ITC instrument from MicroCal Inc. (GE Healthcare, Northampton, UK). The measurements were performed at 25 °C. Injections of 5–10 μL ligand solutions were added from a computer-controlled syringe at an interval of 5 min into the sample cell solution containing hCD22$_{d1-3}$–Fc[34] (cell volume: 1.4523 mL) with stirring (307 rpm). For control experiments, identical ligand solutions were injected into buffer without protein. The heat released in this control experiment was subtracted from the experimental data. The assay buffer was HBS-E (10 mM HEPES pH 7.4, 150 mM NaCl, 3 mM EDTA, 5% DMSO). The concentration of hCD22$_{d1-3}$–Fc was 1.8–11.1 μM, calculated in terms of monomer, determined by HPLC–UV,[54] and the ligand concentration was 60–200 μM. The experimental data were fitted to a theoretical titration curve (one-site binding model) using Origin version 7 (GE Healthcare, Northampton, UK), with ΔH° (enthalpy change in kJ mol^{-1}), K_A (association constant in M^{-1}), and N (number of binding sites). The

quantity $c = K_A \cdot Mt_0$, where Mt_0 is the initial macromolecule concentration, is important in titration microcalorimetry. The experiment was performed at c values between 2 and 85. Thermodynamic parameters were calculated from Equation (1):

$$\Delta G^\circ = \Delta H^\circ - T\Delta S^\circ = RT \ln K_A = -RT \ln K_D \quad (1)$$

for which ΔG°, ΔH°, and ΔS° are the changes in free energy, enthalpy, and entropy of binding, respectively. T is the absolute temperature, and $R = 8.314\ J\,mol^{-1}\,K^{-1}$.[55]

log $D_{7.4}$ determination: Triplicate measurements were performed for every compound at two ratios of octanol to buffer according to the expected log $D_{7.4}$ value. Equal amounts of phosphate buffer (0.1 M, pH 7.4) and octanol were mixed and shaken vigorously for 5 min. Upon separation of the two phases, the buffer phase was withdrawn and analytes were dissolved therein (10^{-5} M). Predefined volumes of octanol and analyte solutions were transferred to a PCR plate, which was thermo-sealed with aluminum foil and shaken (2 h, 1350 rpm, 25 °C on a Heidolph Titramax 100 plate shaker (Heidolph, Schwabach, Germany). The plate was then centrifuged at 2000 rpm (657 *g*) and 25 °C for 5 min, and buffer samples were withdrawn from each well. The analyte concentrations were determined by LC–MS, and log $D_{7.4}$ values were calculated. Values were accepted if the mean values of the two ratios did not differ by >0.1 units.

Parallel artificial membrane permeation assay (PAMPA): log P_e was determined in a 96-well format. For each compound, measurements were performed in quadruplicate at three pH values: 5.0, 6.2, and 7.4. Each well of a deep-well plate was filled with 650 μL System Solution (pIon, Woburn MA, USA, P/N 110151) at the according pH value. Samples (150 μL) were withdrawn from each well to determine the blank spectra by UV/Vis spectroscopy. Analyte was then added to the remaining System Solution to yield 50 μM solutions. To exclude precipitation, the optical density was measured at λ 650 nm, with 0.01 being the threshold value. Again, samples of 150 μL were withdrawn to determine the reference spectra. A further 200 μL were transferred to each well of the donor plate of the PAMPA sandwich. The filter membranes at the bottom of the acceptor plate were impregnated with 5 μL GIT-0 Lipid Solution (pIon, P/N 110669), and 200 μL Acceptor Sink Buffer (pIon, P/N 110139) were filled into each acceptor well. The sandwich was assembled, then placed in the GutBox, left undisturbed for 16 h, and then disassembled again followed by the transfer of 150 μL from each donor and acceptor well to UV plates. Quantification was performed by both UV/Vis spectroscopy (SpectraMax 190, Molecular Devices, Sunnyvale, CA, USA) and LC–MS; log P_e values were calculated based on the LC–MS results and with the aid of the PAMPA Explorer Software (pIon, version 3.5).

Plasma protein binding (PPB): The dialysis membranes (HTDialysis LCC, Gales Ferry, USA; MWCO 12–14 kDa) were prepared according to the manufacturer's instructions. Human plasma (Biopredic, Rennes, France) was centrifuged (5800 rpm (4325 *g*), 25 °C, 10 min), the centrifugate (without floating plasma lipids) was adjusted to pH 7.5, and analyte was added to yield 10 μM solutions. Equal volumes (150 μL each) of phosphate buffer (0.1 M, pH 7.5) and analyte-containing plasma were transferred to the separated compartments of the assembled 96-well high-throughput dialysis block (HTDialysis). Measurements were performed in triplicate. The plate was covered with a sealing film and incubated (5 h, 37 °C). Buffer and plasma compartment were processed separately: 90 μL were withdrawn from the buffer compartment and 10 μL blank plasma were added, while 10 μL were withdrawn from the plasma compartment and 90 μL of blank buffer were added. After protein precipitation with 300 μL CH_3CN (4 °C) the solutions were mixed, centrifuged (3600 rpm (1666 *g*), 4 °C, 11 min) and 50 μL of the supernatant were withdrawn. Analyte concentrations were determined by LC–MS. The fraction unbound was calculated by dividing the concentration in the buffer compartment by the concentration in the plasma compartment (both concentrations adjusted for dilutions prior to analysis). The fraction bound was calculated by subtracting the fraction bound from 1. Values were accepted if the recovery of analyte was between 80 and 120%.

LC–MS measurements: Separation was performed on an Agilent 1100 Series HPLC instrument with a 1200 series autosampler, connected to an Agilent 6400 Series Triple Quadrupole mass spectrometer for quantification (Agilent Technologies, Santa Clara, CA, USA). Double-distilled H_2O with 0.1% formic acid (A) and CH_3CN with 0.1% formic acid (B) were used as solvents. The gradient was a follows: 0.1 min 95% A to 5% B; 1 min 5% A to 95% B; 1.2 min 95% A to 5% B. The total method duration was 4 min. For the separation, a Waters Atlantis T3 column (3 μm, 2.1×50 mm) was used (Waters, Milford, MA, USA). The column was heated at 60 °C, and the flow rate was set to 0.6 mL min^{-1}; 5 μL of analyte were injected per run. Quantification was performed with the MassHunter software (Agilent Technologies, Version B.01.04).

Acknowledgements

We thank the Swiss National Science Foundation (project 200020-120628) for their support of this project.

Keywords: carbohydrate–lectin interactions · CD22 · MAG · pharmacokinetics · surface plasmon resonance · thermodynamic fingerprint

[1] A. Molina, *Annu. Rev. Med.* **2008**, *59*, 237–250.
[2] a) C. Bello, E. M. Sotomayor, *Hematology Am. Soc. Hematol. Educ. Program* **2007**, 233–242; b) J. Castillo, E. Winer, P. Quesenberry, *Exp. Hematol.* **2008**, *36*, 755–768.
[3] M. K. O'Reilly, J. C. Paulson, *Trends Pharmacol. Sci.* **2009**, *30*, 240–248.
[4] R. J. Kreitman, I. Margulies, M. Stetler-Stevenson, Q. C. Wang, D. J. FitzGerald, I. Pastan, *Clin. Cancer Res.* **2000**, *6*, 1476–1487.
[5] J. F. DiJoseph, M. M. Dougher, D. C. Armellino, D. Y. Evans, N. K. Damle, *Leukemia* **2007**, *21*, 2240–2245.
[6] L. Nitschke, *Immunol. Rev.* **2009**, *230*, 128–143.
[7] P. R. Crocker, A. Varki, *Immunology* **2001**, *103*, 137–145.
[8] P. R. Crocker, *Curr. Opin. Pharmacol.* **2005**, *5*, 431–437.
[9] T. F. Tedder, J. C. Poe, K. M. Haas, *Adv. Immunol.* **2005**, *88*, 1–50.
[10] K. G. Smith, D. M. Tarlinton, G. M. Doody, M. L. Hibbs, D. T. Fearon, *J. Exp. Med.* **1998**, *187*, 807–811.
[11] G. M. Doody, L. B. Justement, C. C. Delibrias, R. J. Matthews, J. Lin, M. L. Thomas, D. T. Fearon, *Science* **1995**, *269*, 242–244.
[12] H. Floyd, L. Nitschke, P. R. Crocker, *Immunology* **2000**, *101*, 342–347.
[13] N. Razi, A. Varki, *Proc. Natl. Acad. Sci. USA* **1998**, *95*, 7469–7474.
[14] B. E. Collins, O. Blixt, A. R. DeSieno, N. Bovin, J. D. Marth, J. C. Paulson, *Proc. Natl. Acad. Sci. USA* **2004**, *101*, 6104–6109.
[15] S. Kelm, J. Gerlach, R. Brossmer, C. P. Danzer, L. Nitschke, *J. Exp. Med.* **2002**, *195*, 1207–1213.
[16] L. D. Powell, D. Sgroi, E. R. Sjoberg, I. Stamenkovic, A. Varki, *J. Biol. Chem.* **1993**, *268*, 7019–7027.
[17] a) S. Kelm, A. Pelz, R. Schauer, M. T. Filbin, S. Tang, M. E. de Bellard, R. L. Schnaar, J. A. Mahoney, A. Hartnell, P. Bradfield, *Curr. Biol.* **1994**, *4*, 965–972; b) S. Kelm, R. Schauer, J. C. Manuguerra, H. J. Gross, P. R. Crocker, *Glycoconjugate J.* **1994**, *11*, 576–585.

[18] S. M. van Rossenberg, L. A. Sliedregt, R. Autar, C. Piperi, A. P. van der Merwe, T. J. van Berkel, J. Kuiper, E. A. Biessen, *J. Biol. Chem.* **2001**, *276*, 12967–12973.
[19] H. H. Abdu-Allah, K. Watanabe, G. C. Completo, M. Sadagopan, K. Hayashizaki, C. Takaku, T. Tamanaka, H. Takematsu, Y. Kozutsumi, J. C. Paulson, T. Tsubata, H. Ando, H. Ishida, M. Kiso, *Bioorg. Med. Chem.* **2011**, *19*, 1966–1971.
[20] H. H. Abdu-Allah, T. Tamanaka, J. Yu, L. Zhuoyuan, M. Sadagopan, T. Adachi, T. Tsubata, S. Kelm, H. Ishida, M. Kiso, *J. Med. Chem.* **2008**, *51*, 6665–6681.
[21] H. H. Abdu-Allah, K. Watanabe, K. Hayashizaki, C. Takaku, T. Tamanaka, H. Takematsu, Y. Kozutsumi, T. Tsubata, H. Ishida, M. Kiso, *Bioorg. Med. Chem. Lett.* **2009**, *19*, 5573–5575.
[22] T. K. Dam, C. F. Brewer, *Glycobiology* **2010**, *20*, 270–279.
[23] B. E. Collins, O. Blixt, S. Han, B. Duong, H. Li, J. K. Nathan, N. Bovin, J. C. Paulson, *J. Immunol.* **2006**, *177*, 2994–3003.
[24] M. K. O'Reilly, B. E. Collins, S. Han, L. Liao, C. Rillahan, P. I. Kitov, D. R. Bundle, J. C. Paulson, *J. Am. Chem. Soc.* **2008**, *130*, 7736–7745.
[25] Z. Q. Yang, E. B. Puffer, J. K. Pontrello, L. L. Kiessling, *Carbohydr. Res.* **2002**, *337*, 1605–1613.
[26] S. Kelm, R. Brossmer, R. Isecke, H. J. Gross, K. Strenge, R. Schauer, *Eur. J. Biochem.* **1998**, *255*, 663–672.
[27] W. C. Chen, G. C. Completo, D. S. Sigal, P. R. Crocker, A. Saven, J. C. Paulson, *Blood* **2010**, *115*, 4778–4786.
[28] S. V. Shelke, G. P. Gao, S. Mesch, H. Gäthje, S. Kelm, O. Schwardt, B. Ernst, *Bioorg. Med. Chem.* **2007**, *15*, 4951–4965.
[29] S. Mesch, D. Moser, D. S. Strasser, A. Kelm, B. Cutting, G. Rossato, A. Vedani, H. Koliwer-Brandl, M. Wittwer, S. Rabbani, O. Schwardt, S. Kelm, B. Ernst, *J. Med. Chem.* **2010**, *53*, 1597–1615.
[30] E. R. Sjoberg, L. D. Powell, A. Klein, A. Varki, *J. Cell. Biol.* **1994**, *126*, 549–562.
[31] A. Hasegawa, H. Ohki, T. Nagahama, H. Ishida, M. Kiso, *Carbohydr. Res.* **1991**, *212*, 277–281.
[32] E. Kaiser, J. P. Tam, T. M. Kubiak, R. B. Merrifield, *Tetrahedron Lett.* **1988**, *29*, 303–306.
[33] P. Boullanger, V. Maunier, D. Lafont, *Carbohydr. Res.* **2000**, *324*, 97–106.
[34] H. Koliwer-Brandl, N. Siegert, K. Umnus, A. Kelm, A. Tolkach, U. Kulozik, J. Kuballa, S. Cartellieri, S. Kelm, *Int. Dairy J.* **2011**, *21*, 413–420.
[35] N. R. Zaccai, K. Maenaka, T. Maenaka, P. R. Crocker, R. Brossmer, S. Kelm, E. Y. Jones, *Structure* **2003**, *11*, 557–567.
[36] R. A. Copeland, D. L. Pompliano, T. D. Meek, *Nat. Rev. Drug Discovery* **2006**, *5*, 730–739; D. C. Swinney, *J. Pharm. Med.* **2008**, *22*, 23–34.
[37] a) M. K. Wild, M. C. Huang, U. Schulze-Horsel, P. A. van der Merwe, D. Vestweber, *J. Biol. Chem.* **2001**, *276*, 31602–31612; b) O. Schwardt, H. Gäthje, A. Vedani, S. Mesch, G. P. Gao, M. Spreafico, J. von Orelli, S. Kelm, B. Ernst, *J. Med. Chem.* **2009**, *52*, 989–1004.
[38] T. R. Bakker, C. Piperi, E. A. Davies, P. A. Merwe, *Eur. J. Immunol.* **2002**, *32*, 1924–1932.
[39] a) P. O. Markgren, M. Hämäläinen, U. H. Danielson, *Anal. Biochem.* **2000**, *279*, 71–78; b) P. O. Markgren, M. T. Lindgren, K. Gertow, R. Karlsson, M. Hämäläinen, U. H. Danielson, *Anal. Biochem.* **2001**, *291*, 207–218.
[40] a) B. A. Williams, M. C. Chervenak, E. J. Toone, *J. Biol. Chem.* **1992**, *267*, 22907–22911; b) E. J. Toone, *Curr. Opin. Struc. Biol.* **1994**, *4*, 719–728; c) T. K. Dam, C. F. Brewer, *Chem. Rev.* **2002**, *102*, 387–429; d) M. Ambrosi, N. R. Cameron, B. G. Davis, *Org. Biomol. Chem.* **2005**, *3*, 1593–1608.
[41] a) N. Ahmad, H. J. Gabius, S. Sabesan, S. Oscarson, C. F. Brewer, *Glycobiology* **2004**, *14*, 817–825; b) Y. Ito, S. Hagihara, M. A. Arai, I. Matsuo, M. Takatani, *Glycoconjugate J.* **2004**, *21*, 257–266; c) M. A. Arai, I. Matsuo, S. Hagihara, K. Totani, J. Maruyama, K. Kitamoto, Y. Ito, *ChemBioChem* **2005**, *6*, 2281–2289; d) T. K. Dam, H. J. Gabius, S. André, H. Kaltner, M. Lensch, C. F. Brewer, *Biochemistry* **2005**, *44*, 12564–12571; e) C. F. Brewer, *Glycoconjugate J.* **2004**, *19*, 459–465; f) M. S. Quesenberry, R. T. Lee, Y. C. Lee, *Biochemistry* **1997**, *36*, 2724–2732; g) P. Sörme, P. Arnoux, B. Kahl-Knutsson, H. Leffler, J. M. Rini, U. J. Nilsson, *J. Am. Chem. Soc.* **2005**, *127*, 1737–1743; h) K. Bachhawat-Sikder, C. J. Thomas, A. Surolia, *FEBS Lett.* **2001**, *500*, 75–79; i) P. Szabo, T. K. Dam, K. Smetana, B. Dvoránková, D. Kübler, C. F. Brewer, H. J. Gabius, *Anat. Histol. Embryol.* **2009**, *38*, 68–75.
[42] C. O. Sallum, R. A. Kammerer, A. T. Alexandrescu, *Biochemistry* **2007**, *46*, 9541–9550.
[43] M. Kapoor, H. Srinivas, E. Kandiah, E. Gemma, L. Ellgaard, S. Oscarson, A. Helenius, A. Surolia, *J. Biol. Chem.* **2003**, *278*, 6194–6200.
[44] M. Kansy, F. Senner, K. Gubernator, *J. Med. Chem.* **1998**, *41*, 1007–1010.
[45] E. Garcia-Hernandez, R. A. Zubillaga, E. A. Chavelas-Adame, E. Vazquez-Contreras, A. Rojo-Dominguez, M. Costas, *Protein Sci.* **2003**, *12*, 135–142.
[46] a) C. Hansch, A. Leo, *Substituent Constant for Correlation Analysis in Chemistry and Biology*, Wiley, New York, **1979**; b) M. J. Waring, *Exp. Opin. Drug Discov.* **2010**, *5*, 235–248.
[47] E. H. Kerns, L. Di, *Drug-like Properties: Concepts, Structure Design and Methods*, Academic Press, Amsterdam, **2008**.
[48] G. Corti, F. Maestrelli, M. Cirri, N. Zerrouk, P. Mura, *Eur. J. Pharm. Sci.* **2006**, *27*, 354–362.
[49] a) P. S. Burton, J. T. Goodwin, T. J. Vidmar, B. M. Amore, *J. Pharmacol. Exp. Ther.* **2002**, *303*, 889–895; b) W. J. Egan, G. Lauri, *Adv. Drug Delivery Rev.* **2002**, *54*, 273–289.
[50] S. Urien, J.-P. Tillement, J. Barre in *Pharmacokinetic Optimization in Drug Research: Biological, Physicochemical, and Computational Strategies* (Eds.: B. Testa, H. van de Waterbeemed, G. Folkers, R. Guy), Helvetica Chimica Acta, Zürich, **2001**, pp. 189–197.
[51] A. M. Talbert, G. E. Tranter, E. Holmes, P. L. Francis, *Anal. Chem.* **2002**, *74*, 446–452.
[52] R. L. Rich, Y. S. Day, T. A. Morton, D. G. Myszka, *Anal. Biochem.* **2001**, *296*, 197–207.
[53] N. A. Meanwell, *J. Med. Chem.* **2011**, *54*, 2529–2591.
[54] a) S. Mesch, K. Lemme, H. Koliwer-Brandl, D. S. Strasser, O. Schwardt, S. Kelm, B. Ernst, *Carbohydr. Res.* **2010**, *345*, 1348–1359; b) F. Bitsch, R. Aichholz, J. Kallen, S. Geisse, B. Fournier, J. M. Schlaeppi, *Anal. Biochem.* **2003**, *323*, 139–149.
[55] T. Wiseman, S. Williston, J. F. Brandts, L. N. Lin, *Anal. Biochem.* **1989**, *179*, 131–137.

Received: August 25, 2011
Published online on October 11, 2011

CHEMMEDCHEM
Chemistry & Drug Discovery

Supporting Information

From a Library of MAG Antagonists to Nanomolar CD22 Ligands

Stefanie Mesch,[a] Katrin Lemme,[a] Matthias Wittwer,[a] Hendrik Koliwer-Brandl,[b] Oliver Schwardt,[a] Sørge Kelm,[b] and Beat Ernst*[a]

cmdc_201100407_sm_miscellaneous_information.pdf

Supporting Information

Contents:

Isothermal Titration Calorimetry

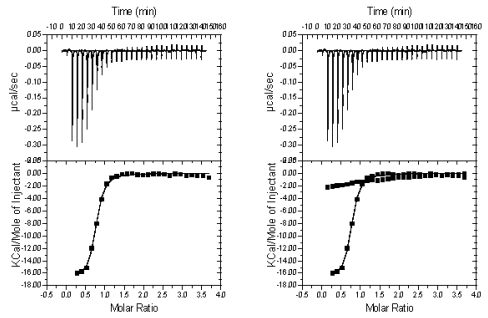

Figure S1. Exemplary enthalpogram of **13b** (left) with the corresponding reference titration (right).

Compound purity

The final compounds (**13b**, **17a-c**, **20**) were purified by preparative LCMS prior to HPLC, HRMS, NMR and activity testing.

Table S1. HRMS data for the target compounds

Compound	Formula	HRMS [*m/z*]	
		calcd	found
13b	$C_{31}H_{32}Cl_2N_2O_9$	669.1384 $[M+Na]^+$	669.1384 $[M+Na]^+$
17a	$C_{35}H_{32}Cl_2N_3NaO_{12}S$	834.0880 $[M+Na]^+$	834.0893 $[M+Na]^+$
17b	$C_{35}H_{33}Cl_2N_3O_{13}S$	828.1009 $[M+Na]^+$	828.1009 $[M+Na]^+$
17c	$C_{34}H_{32}Cl_2N_4O_{12}S$	791.1193 $[M+H]^+$	791.1194 $[M+H]^+$
20	$C_{35}H_{35}Cl_2N_3O_{11}S$	798.1267 $[M+Na]^+$	798.1262 $[M+Na]^+$

HPLC data for the target compounds

HPLC system: Agilent 1100 with UV detection (190-410 nm). A: Water + 0.1% formic acid; B: acetonitrile + 0.1% formic acid.

Method: Column: Waters Atlantis dC18, 3 μm, 4.6 × 75 mm; gradient: 5% B → 65% B over 20 min; flow rate: 1.0 mL min^{-1}.

Table S2. HPLC data for the target compounds

Compound	Formula	Retention time [min]	Purity [%]
13b	$C_{31}H_{32}Cl_2N_2O_9$	16.150	99%
17a	$C_{35}H_{33}Cl_2N_3O_{12}S$	17.683	95%
17b	$C_{35}H_{33}Cl_2N_3O_{13}S$	16.483	96%
17c	$C_{34}H_{32}Cl_2N_4O_{12}S$	11.917	98%
20	$C_{35}H_{35}Cl_2N_3O_{11}S$	15.450	93%

HPLC traces for the target compounds

Compound **13b**:

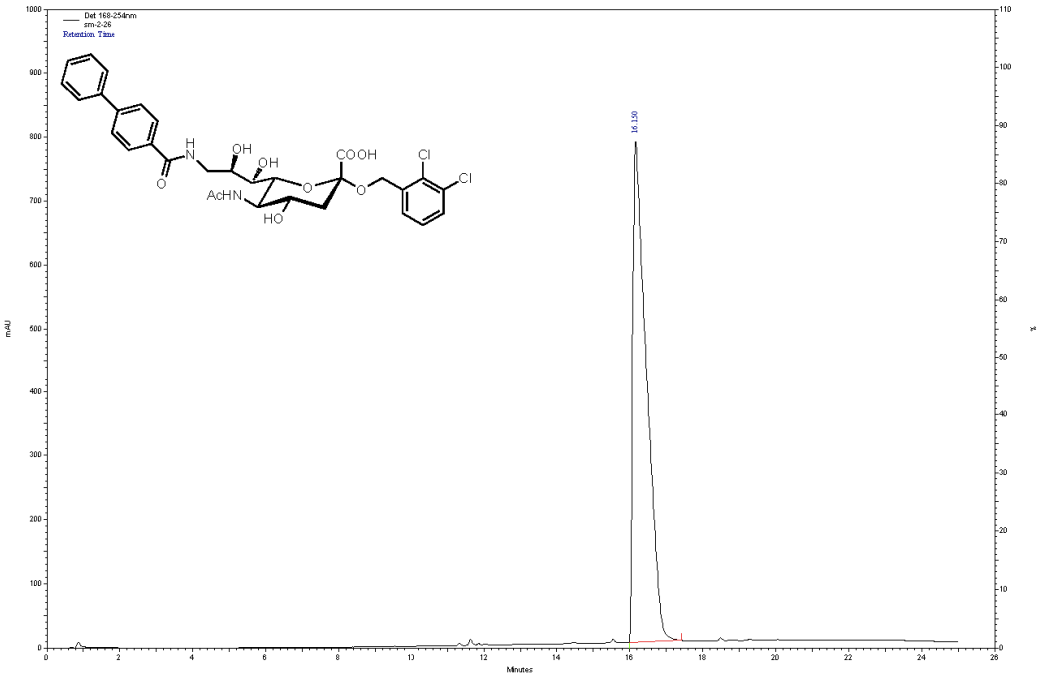

Compound **17a**:

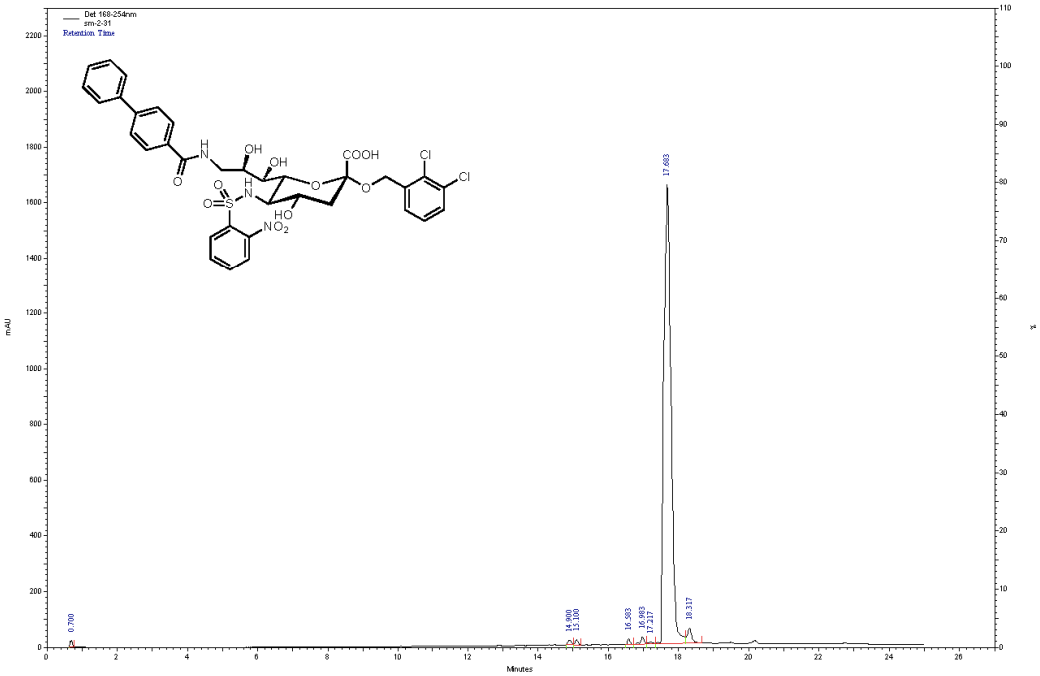

Compound **17b**:

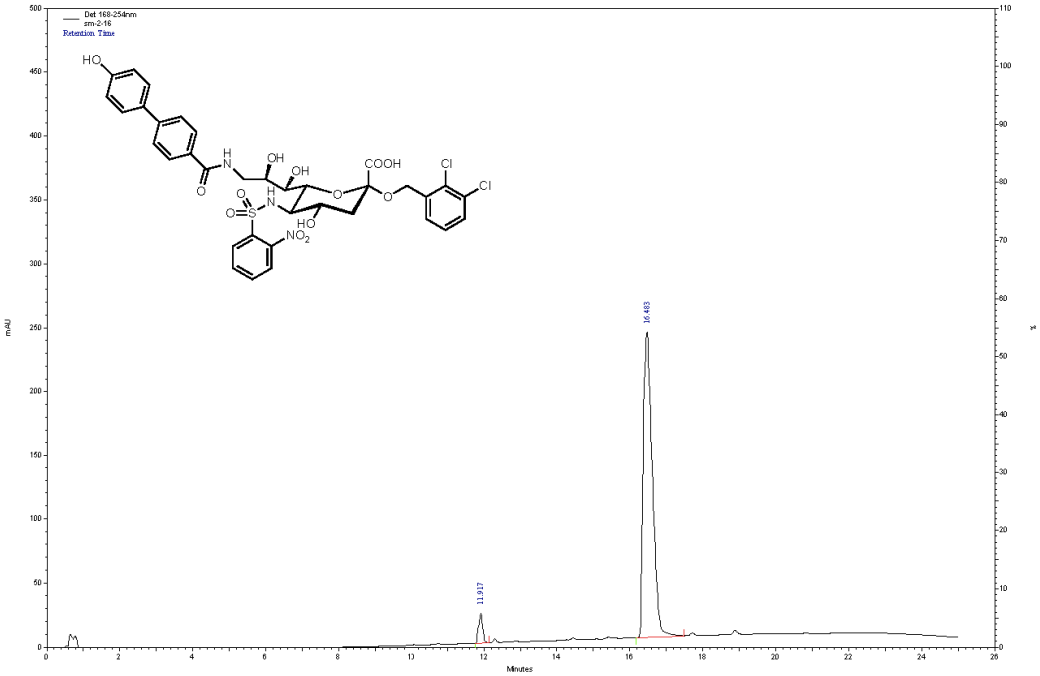

Compound **17c**:

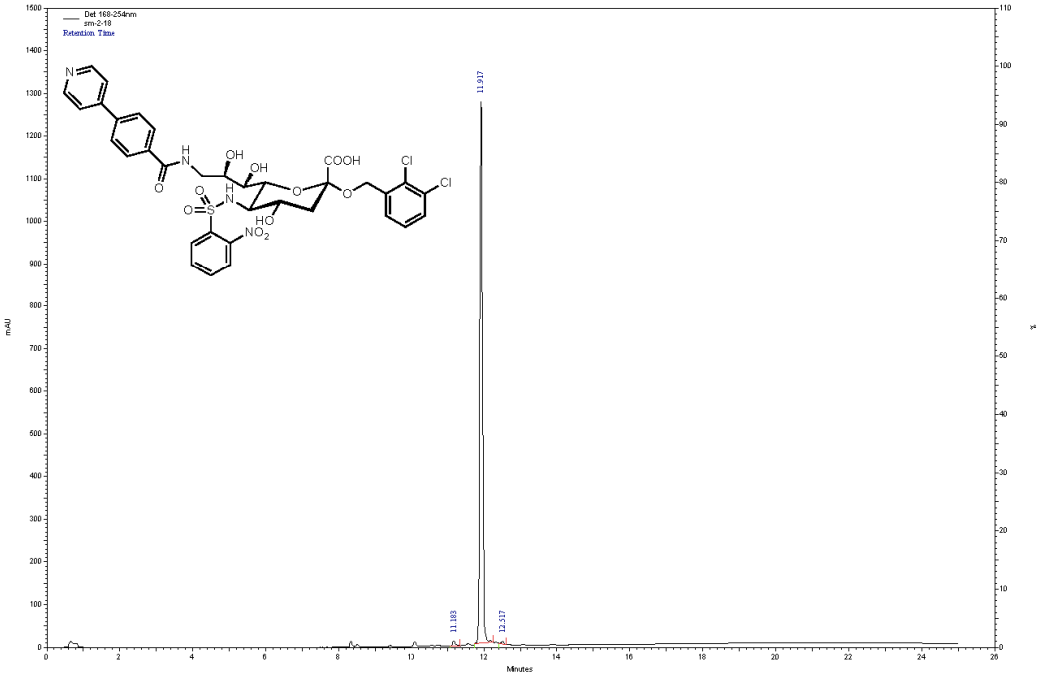

Compound **20**:

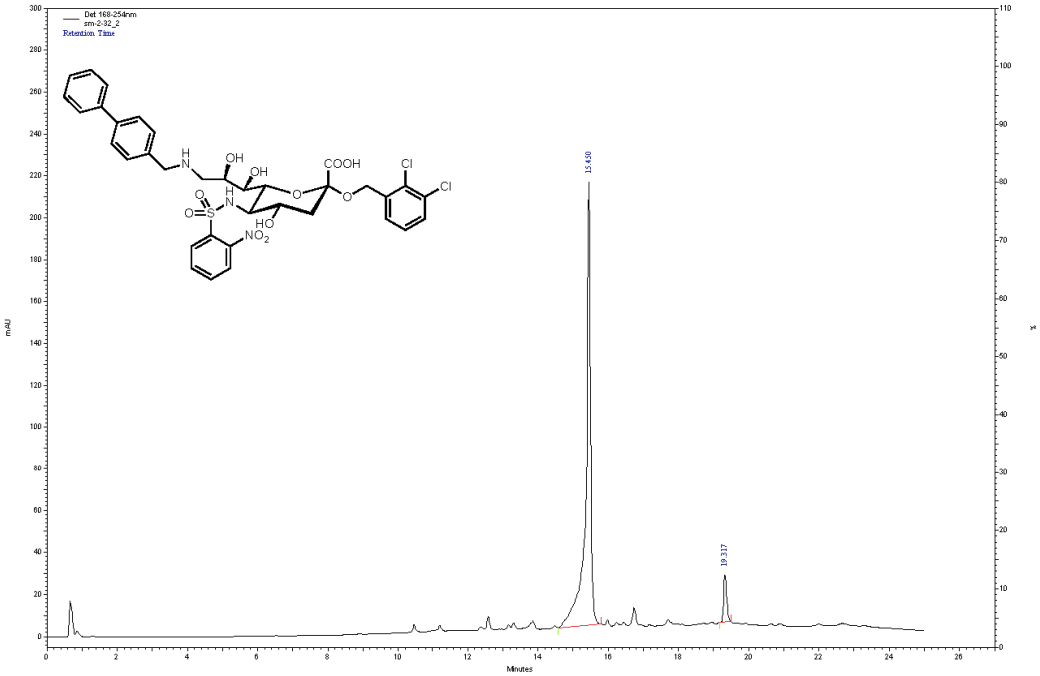

^{1}H NMR spectra for the target compounds in CD_3OD (13b, 17a-c, 20)

Compound **13b**:

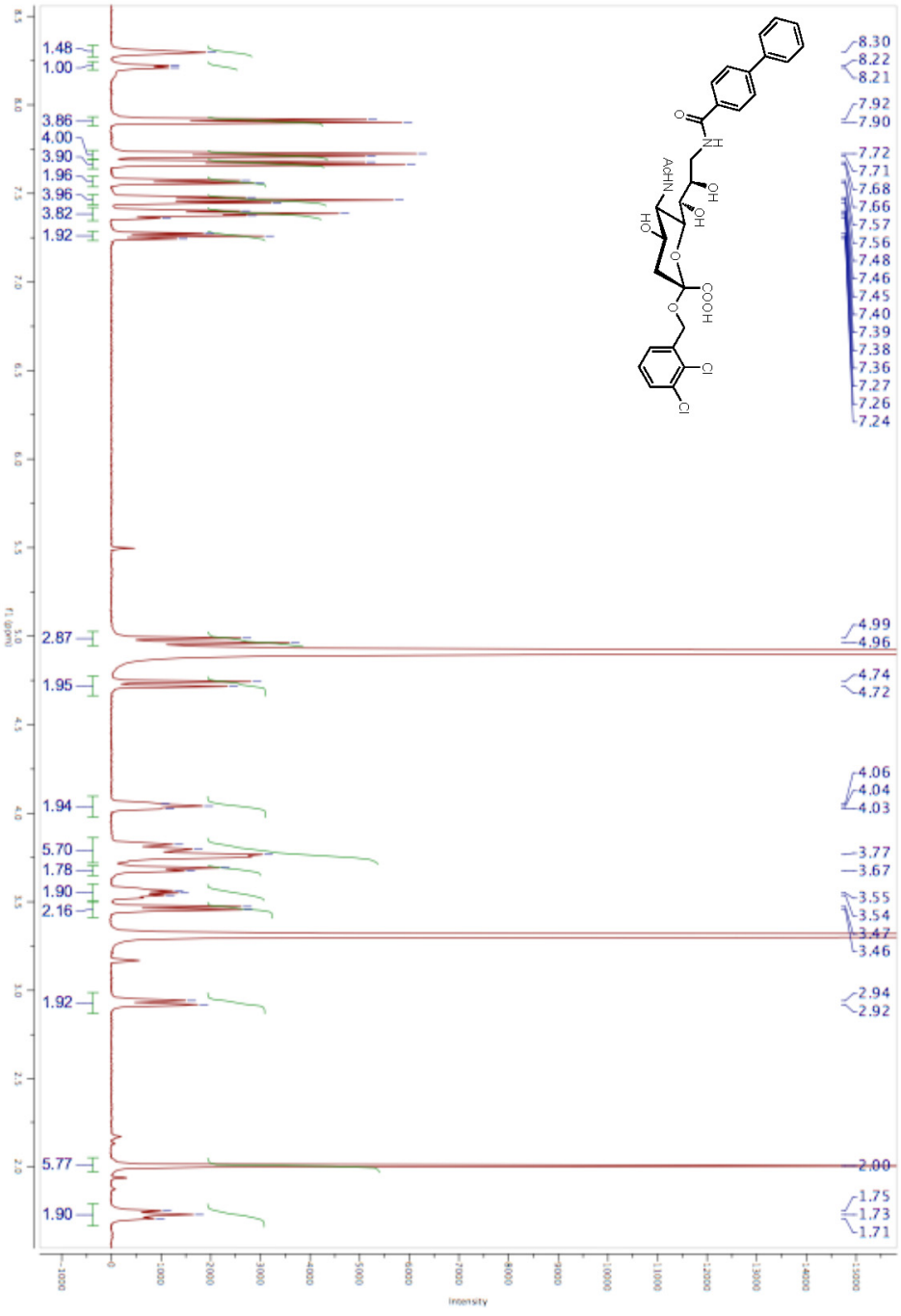

Compound **17a**:

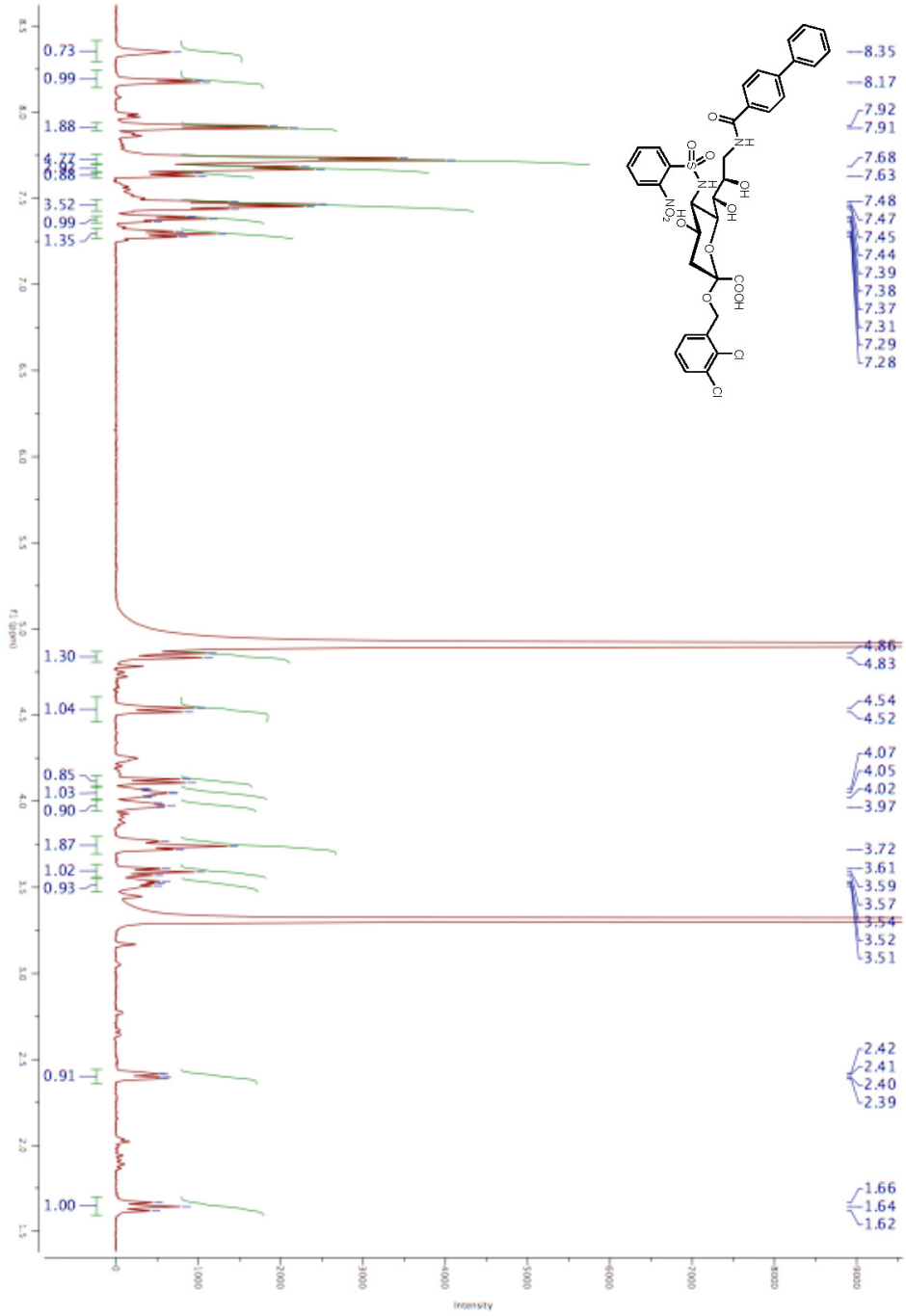

Compound **17b**.

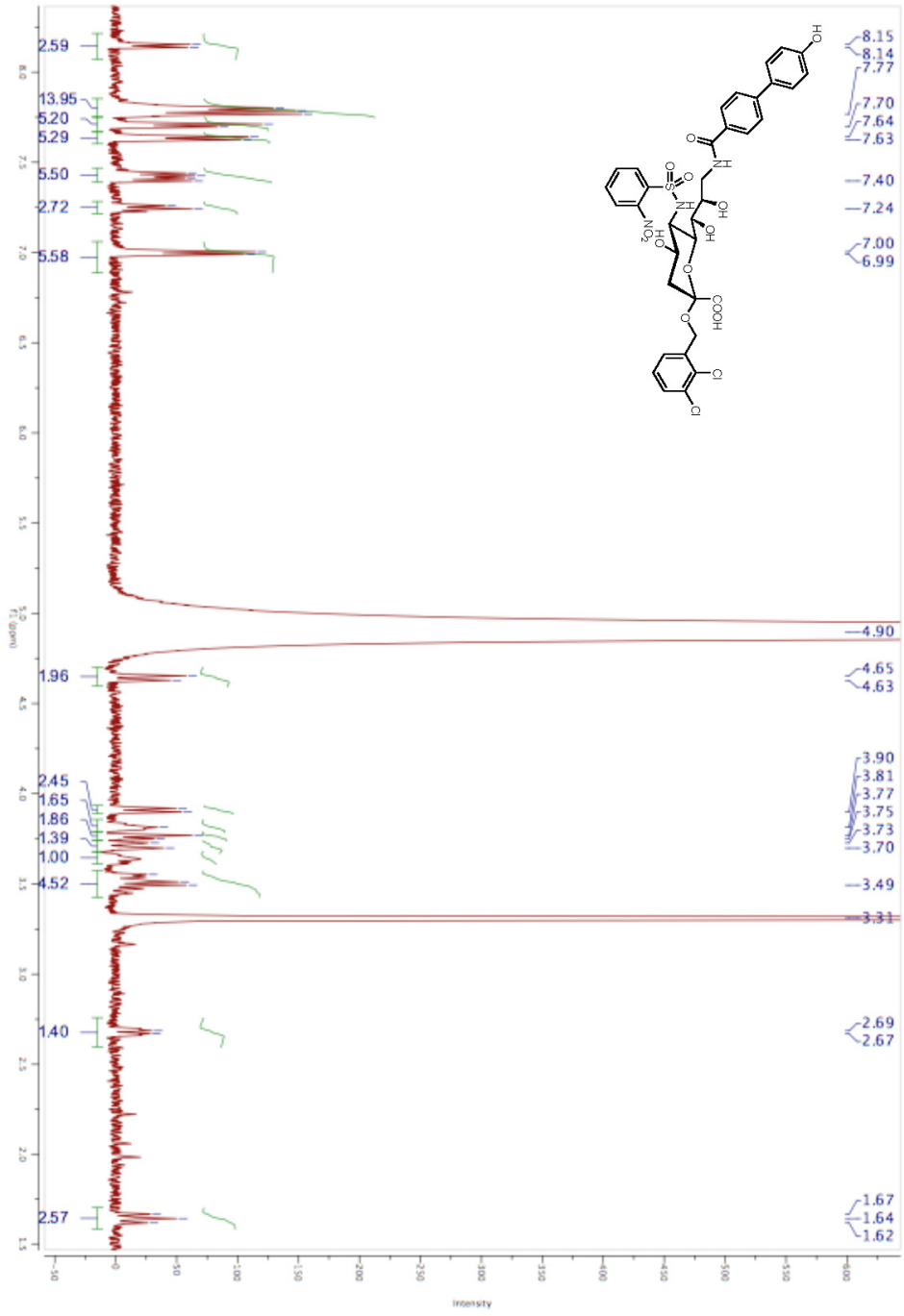

Compound **17c**.

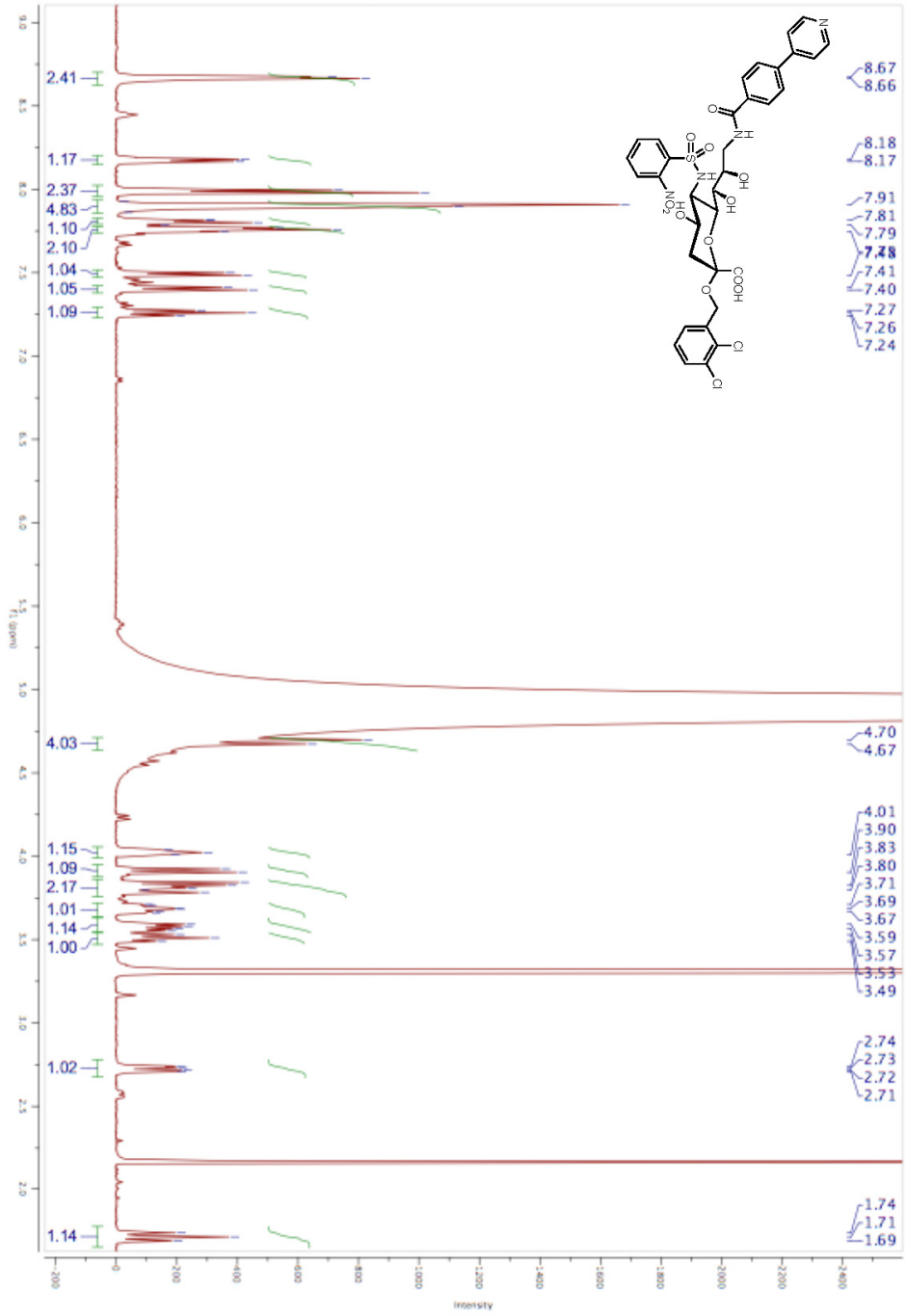

Compound **20**:

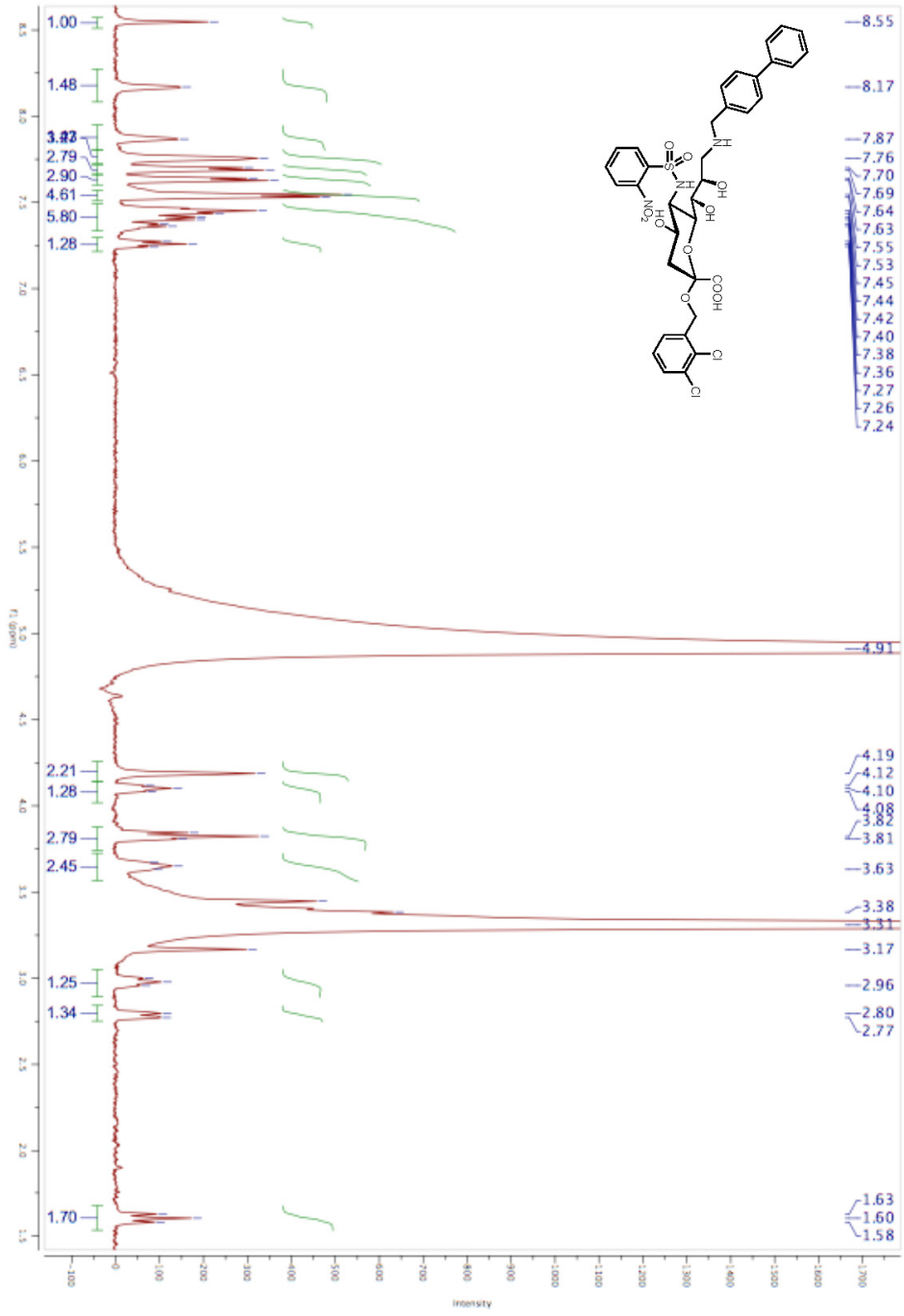
1.00
1.48
3.87
2.79
2.90
4.61
5.80
1.28
2.21
1.28
2.79
2.45
1.25
1.34
1.70
8.55
8.17
7.87
7.76
7.70
7.69
7.64
7.63
7.55
7.53
7.45
7.44
7.42
7.40
7.38
7.36
7.27
7.26
7.24
4.91
4.19
4.12
4.10
4.08
3.82
3.81
3.63
3.38
3.31
3.17
2.96
2.80
2.77
1.63
1.60
1.58
Intensity

2.3 Thermodynamics of Glycomimetics Binding to Bacterial Lectins

2.3.1 FimH

2.3.1.1 Flexibility of Mannosidic Aglycones Favors Binding

Does Flexibility Necessarily Induce Entropy Costs upon Binding?

Katrin Lemme,[#] Adam Zalewski, [#] Roland Preston, Said Rabbani, Lijuan Pang, and Beat Ernst*

Institute of Molecular Pharmacy, University of Basel, Klingelbergstr. 50, 4056 Basel, Switzerland

[#]Authors contributed equally

**Corresponding author. Tel: 0041 267 15 51; Fax: 0041 267 15 52; e-mail: beat.ernst@unibas.ch*

Keywords: Urinary tract infection, FimH, isothermal titration calorimetry, flexibility, entropy.

Contribution of Katrin Lemme: Manuscript, ITC experiments, determination of protein concentration.

Draft version.

Introduction

Urinary tract infections (UTI) are among the most common infections, affecting each year millions of people, particularly women.[1,2] The main cause of UTI are uropathogenic strains of *E. coli* (UPEC) which adhere to urothelial cells by the interaction of receptors, the so-called FimH lectins, located on the top of their pili.[3] Their host cells, the urothelial cells, form the superficial cell layer of the bladder and contain oligomannosides as part of the glycoprotein uroplakin A.[4,5] These oligomannosides are potent ligands of FimH and therefore establish the first contact between bacteria and urothelial cells, which is a prerequisite for the infectious cascade to take place.

Various FimH ligands consisting of an α–D-mannopyranoside linked to a hydrophobic aglycone have been reported.[6,7] The mannose moiety establishes a firm network of H-bonds with FimH, whereas the aglycone takes advantage of the hydrophobic interactions offered by the side chain of three amino acids lining the entrance to the mannose binding pocket. [8] According to two tyrosines (Tyr48 & 137) and one isoleucine (Ile52) this entrance is called *tyrosine gate*.[9] Among the reported ligands, *n*-butyl- and *n*-heptyl α-D-mannopyranoside (**1** and **2**) exhibit nanomolar affinities,[10] although their aglycones contain 4 and 7 rotatable bonds, respectively. Since these aglycones form hydrophobic contacts with the tyrosine gate leading to at least a partial loss of conformational flexibility, substantial entropy costs upon binding are expected.[11-14] Nevertheless, when the *n*-heptyl chain in **2** was replaced by a less flexible aglycone, e.g. a biphenyl (→**3**) affinity surprisingly remained unchanged.[15] To rationalize this unexpected result, we present in this communication the thermodynamic binding properties of the FimH ligands **1** – **3** as well as molecular dynamics simulations of their complex with the carbohydrate recognition domain of FimH.

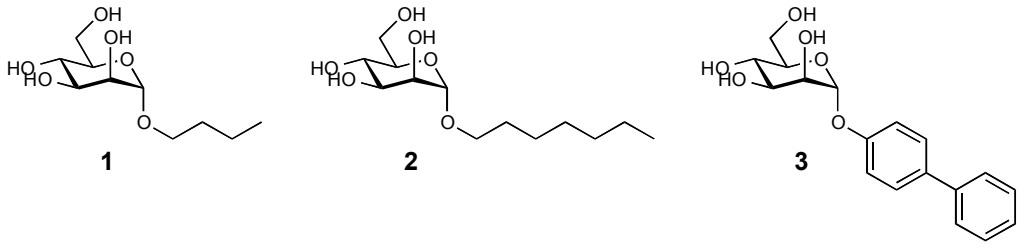

Figure 1. *n*-Butyl- (**1**) and *n*-heptyl α-D-mannopyranoside (**2**) reported to exhibit nanomolar affinities[10] and biphenyl α-D-mannopyranoside (**3**)[15] surprisingly with a binding affinity similar to **2**.

Results and Discussion

A series of mannosidic FimH antagonists with aglycones of different flexibility were synthesized (Figure 1). The binding affinities were determined by isothermal titration calorimetry (ITC) and the competitive binding assay.[16] The results are shown in Table 1. A typical ITC experiment is summarized in Figure 2.

Table 1. rIC_{50} values were determined with the competitive binding assay,[16] calculated relative to *n*-heptyl α-D-mannopyranoside (**2**), and compared to rK_D values obtained from the ITC experiments. Confidence interval (95%)[17] of the fit for ITC experiments revealed 12 to 22% deviations for K_D and below 1% deviations for N and $\Delta H°$.

FimH Antagonist	rIC_{50}	rK_D	N	K_D [nM]	$\Delta G°$ [kJ mol^{-1}]	$\Delta H°$ [kJ mol^{-1}]	$-T\Delta S°$ [kJ mol^{-1}]	ΔC_p [kJ mol^{-1} K^{-1}]
1	4.0	4.6	1.02	121	–39.5	–36.6	–2.9	–0.94
2	1.0	1.0	1.04 ± 0.04	26.2 ± 5.0	–43.3 ± 0.5	–42.3 ± 1.4	–1.1 ± 1.5	–0.90
3	1.4	0.9	1.06 ± 0.01	23.8 ± 1.7	–43.5 ± 0.1	–43.4 ± 1.4	–0.1 ± 1.6	–0.97

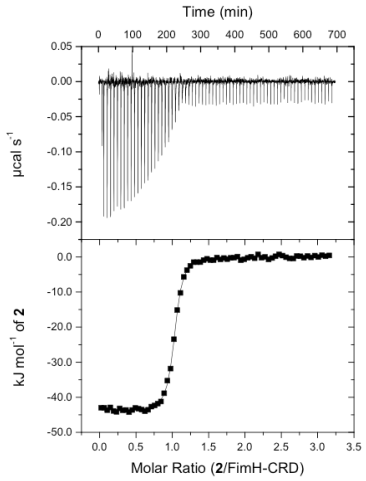

Figure 2. A typical result of ITC titration with *n*-heptyl α-D-mannopyranoside (**2**) and FimH-CRD. The top panel shows the recorded change in heat in units of µcal s^{-1} as a function of time for successive injections of ligand (raw data). The bottom panel shows the integrals of the peaks (black squares) from the top panel plotted against the molar ratio of the binding process together with a line of best fit, used to estimate $\Delta H°$, K_D, and N.

For both methods low nanomolar binding affinities were found. Three additional rotatable bonds are introduced at the aglycone going from butyl to heptyl (**1**→**2**). Since these are usually at least partially restrained upon binding, increased entropic costs are expected. [11-14] The binding affinity towards FimH increased when the alkyl chain was lengthened (**1**→**2**) as also shown in previously published affinity data.[10]

Surprisingly, a closer look into the thermodynamics revealed that only the enthalpic contribution got more favorable with little changes in the entropic term. Additionally, the term itself was almost negligible for both compounds. A possible explanation is that the heptyl aglycone (**2**) remains flexible upon binding but experience increased van-der-Waals contact with the *tyrosine gate*. In addition, solvent reorganization compensates for the entropy penalty arising for the loss of flexibility. In fact, it is known that flexible inhibitors can bind with high affinities because of reduced entropic penalties.[11,18-20]

To gain further insight, we synthesized compound **3** with a constrained biphenylic aglycone. Surprisingly, the binding affinity and their thermodynamics of interaction were comparable to the compound with the flexible heptyl aglycone. Moreover, the change in heat capacity (ΔC_p) was almost identical for all three compounds, indicating small differences in solvent restructuring and surface areas buried upon binding.[21,22] A crystal structure of a biphenyl α-D-mannopyranoside with a carboxylic ester in the 3'-position of the biphenyl moiety suggests that the biphenyl aglycone does not bind within the *tyrosine gate* (in-docking mode, Figure 3a) but favors π-π-stacking with Tyr48 (out-docking mode, Figure 3b).[15] Taken together, this indicates that compensation phenomena could allow compounds **2** and **3** to exhibit near-identical thermodynamic properties while binding in different modes.

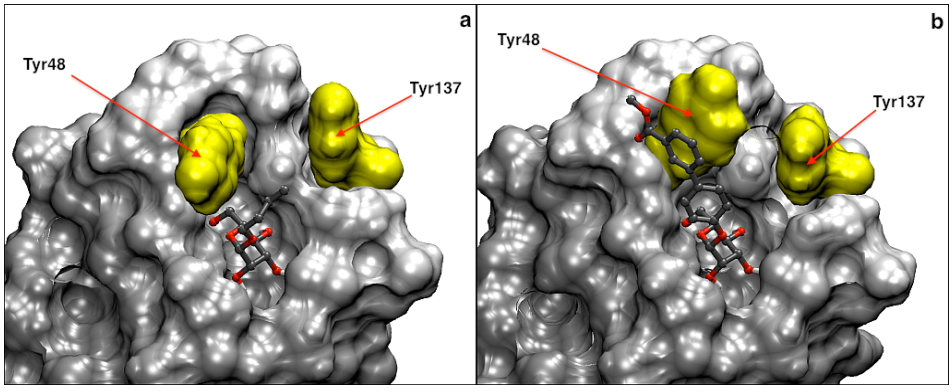

Figure 3. Surface representation of FimH crystal structures (a) co-crystallized butyl α-D-mannopyranoside (**1**)[10] and (b) co-crystallized methyl 4'-(α-D-mannopyranosyloxy)-biphenyl-3-carboxylate[15] (comparable to **3**).

To verify the stated hypotheses, a series of 10 ns molecular-dynamics (MD) simulations were performed, revealing that a substantial part of ligand/*tyrosine gate* mobility could be retained upon binding (Figure 4). For further insight, relative

binding free energy changes (averaged over ensembles of MD snapshots) were calculated using the MM-GBSA (molecular-mechanics generalized Born surface area) approach (as implemented in Prime[23]). This method is reported to achieve good accuracy for various molecular systems at a fraction of the computational expense required by more sophisticated approaches.[24] An additional advantage was the possibility of decomposing the obtained values into specific energy contributions (Table 2).

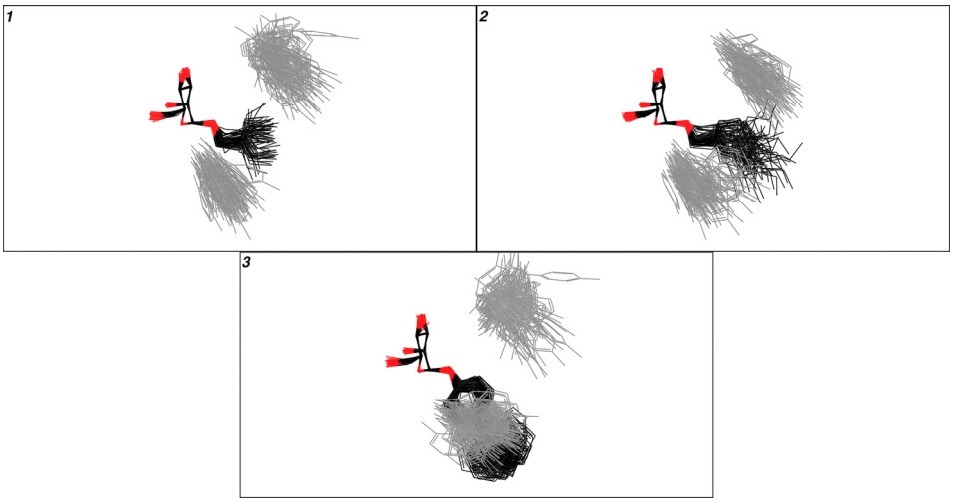

Figure 4. Distributions of aglycone and tyrosine conformers for superimposed (mannose heavy atoms) MD frames of respective simulations.

Table 2. Selected data (average MM-GBSA values) obtained from ensembles of MD snapshots for respective FimH antagonists.

FimH Antagonist	ΔG [kcal mol^{-1}]	$\Delta G_{Solv.}$ [kcal mol^{-1}]	$\Delta G_{Ele.}$ [kcal mol^{-1}]	ΔG_{vdW} [kcal mol^{-1}]
1	–64.5 ± 5.8	19.6 ± 2.4	–41.9 ± 7.5	–19.1 ± 2.8
2	–76.3 ± 6.1	20.7 ± 2.5	–41.1 ± 6.9	–23.4 ± 2.9
3	–73.0 ± 5.7	18.7 ± 2.6	–36.9 ± 6.8	–25.3 ± 2.7

These results provide valuable context to both the ITC data and the driving forces behind the binding modes. Specifically, when moving from compound **1** to **2**, we can observe a more unfavorable solvent contribution (likely related to the higher desolvation penalty of the latter), overcompensated by van der Waals interactions originating from a larger hydrophobic interface between aglycone and protein. Moving on to compound **3** reveals a less favorable electrostatic contribution – possibly due to the rigidity of the compound influencing the H-bond network quality –

balanced out by a smaller desolvation penalty and further improved interactions of the aglycone.

Though the computational approach reports total changes in free energy, it does not fully account for conformational entropy shifts occurring upon binding of highly flexible compounds. This limitation along with lack of polarization effects, are reported[24] as the main reasons for the overly large values and ranges of the calculated energies. To compensate for this, changes in the mobility of ligand aglycones and *tyrosine gate* residues (expected to vary the most between respective systems) were quantified based on MD-conformer distributions (see methods section). The obtained absolute $-T\Delta S$ data (1.7, 2.6 and 1.6 kcal mol^{-1} for compounds **1**, **2**, and **3**, respectively) supports initial assumptions about *n*-heptyl α-D-mannopyranoside (**2**) paying the biggest penalty due to its number of rotatable bonds. Nevertheless these costs are much smaller than one would expect from fully constraining a ligand and two flexible side chains, again confirming that a substantial part of their mobility is being preserved. With respect to the experimental data, this could also mean that the solvation entropy gain, originating from displacing water from the mannose-binding pocket, overcompensates the cost of only partially restraining ligand and protein.

Summary and Conclusion

The present thermodynamic study reveals that flexibility is not always accompanied with an entropic penalty. A series of mannopyranosides with aglycones of different flexibility have been investigated. The *n*-heptyl aglycone (**2**) bound with higher affinity compared to the *n*-butyl aglycone (**1**) because of an increased enthalpic contribution without any entropic penalty. Interestingly, compound **3** with the constrained biphenylic aglycone exhibited an identical thermodynamic signature compared to compound **2** with the flexible heptyl chain although the binding geometry is different. In some cases, flexibility is not a disadvantage.

Experimental Procedure

Cloning of FimH-CRD. The plasmid pfimHs-trc, encoding FimH lectin domain (FimH-CRD, 1-156 amino acids[25]), was kindly provided by R. Glockshuber (ETH Zürich, Switzerland). For the periplasmic expression of FimH-CRD the plasmid pfimHs-trc was transformed into the protease-deficient *E. coli* strain HM 125.[26]

Protein Expression and Purification. *E. coli* HM 125 expressing FimH-CRD were grown at 30 °C with vigorous shaking (300 rpm) in M9 minimal medium[27] supplemented with 2 mM $MgSO_4$, 0.1 mM $CaCl_2$, 0.4% glycerin, and 100 µg.mL^{-1} ampicillin. When an OD_{600} of 0.8 was reached, the cells were induced with 1 mM IPTG (isopropyl β-D-1-thiogalactopyranoside) and further cultivated for 16 h at 30 °C and 300 rpm. Then the cells were cooled on ice for 5 min and harvested by centrifugation at 5´000 rpm for 20 min at 4 °C. The pellet was suspended in a cold solution of 50 mM TrisHCl, pH 7.5, 150 mM NaCl, 5 mM EDTA, 1 mg mL^{-1} polymyxin B sulfate and stirred for 2 h at 4 °C. After centrifugation at 11´000 rpm for 20 min at 4 °C, the supernatant (periplasmic extract) was acidified by the addition of 0.11 volumes of 1 M acetic acid solution pH 4.5 and dialyzed at 4 °C against a 10 mM acetic acid solution pH 4.5. The acidified extract was applied to a UNO-S® column attached to a BioLogic FPLC system (BioRad, Reinach BL, Switzerland) that was pre-equilibrated with a 10 mM acetic acid solution pH 4.5. The flow through was collected and adjusted to pH 8 with a 2 M TrisHCl solution and applied to a UNO-Q® column attached to a BioLogic FPLC system (BioRad, Reinach BL, Switzerland). The column was pre-equilibrated with a 40 mM TrisHCl solution pH 8. The flow through containing FimH-CRD was dialyzed against 20 mM HEPES, 150 mM NaCl, and 1 mM $CaCl_2$, pH 7.4 overnight at 4 °C. The protein solution was concentrated by ultrafiltration (5 kDa cut off) and gelfiltrated on a Bio-Prep SE-100/17 column attached to a BioLogic FPLC system (BioRad, Reinach BL, Switzerland). The protein purity was verified by SDS–PAGE. At 4 °C, aliquots of the protein could be stored for up to 3 months. For long-term storage, the protein was frozen at −80 °C.

Competitive Binding Assay. The competitive binding assay was carried out as previously described by Rabbani *et al*.[16]

Isothermal Titration Calorimetry. ITC experiments were performed using a VP-ITC instrument from MicroCal, Inc. (GE Healthcare, Northampton) after vacuum degassing of the samples. The measurements were performed at 25 °C and for ΔC_p determination additionally at 10 and 37 °C. Injections of 3 to 14 µL ligand solutions (150 µM) were added at an interval of 10 min into the sample cell solution containing FimH-CRD (8 to 23 µM, sample cell volume 1.4523 mL) with stirring at 307 rpm. Protein concentration was determined by HPLC-UV against a BSA standard.[28,29] The quantity $c = Mt(0)\ K_D^{-1}$ where *Mt(0)* is the initial macromolecule concentration, is of importance in titration microcalorimetry. The *c*-values were between 90 and 1050. Because the smallest reliable volumes were injected, sigmoidal shaped curves were detected. Control experiments injecting ligand solution into buffer without protein showed that the heats of dilution were small and constant. The assay buffer was: 10 mM HEPES, 150 mM NaCl, and 1 mM $CaCl_2$, pH 7.4 (HBS-Ca). For compound **3**, a final concentration 2.5% DMSO was necessary to dissolve the ligand. In this case, the protein solution was adjusted to 2.5% DMSO final concentration. Control experiments with

compound **2** in presence of 2.5% DMSO revealed identical results when compared to 0% DMSO. Baseline correction and peak integration were accomplished using the software Origin 7 as described by the manufacturer (OriginLab, Northampton). The first injection was always excluded from data analysis because it usually suffers from sample loss during the mounting of the syringe and the equilibration preceding the actual titration. A three-parameter (N, K_D and $\Delta H°$, stoichiometry, dissociation constant, and change in enthalpy) nonlinear least-square data fitting was performed in an Excel (Microsoft) spreadsheet using the Solver add-in (Frontline System)[17,30] according to binding isotherms published by Ziegler and Seelig.[31]

Thermodynamic parameters were calculated from the equation (1) and (2),

$$\Delta G° = \Delta H° - T\Delta S° = RT\ln K_D = -RT\ln K_A \qquad (1)$$

$$\Delta C_p = \frac{\Delta H°_{T2} - \Delta H°_{T1}}{(T_2 - T_1)} \qquad (2)$$

where $\Delta G°$, $\Delta H°$, $\Delta S°$, and ΔC_p are the changes in free energy, enthalpy, entropy, and heat capacity of binding, respectively, T is the absolute temperature, and R is the universal gas constant (8.314 J mol^{-1} K^{-1}).

Molecular Modeling. For all simulations a 1.69 Å resolution crystal structure (PDB code 1UWF) of the FimH-CRD was used. Flexible docking was performed using Glide.[32] Poses were selected based on docking scores and protein–ligand interaction energies calculated with the OPLS 2005 force field.[33] Molecular dynamics simulations were carried out with Desmond.[34] Each MD (preceded by executing a built–in relaxation protocol) was run for 10 ns in 300 K with 1.2 ps intervals for writing energy and trajectory data. All simulations were evaluated using the Simulation Quality Analysis script. Corresponding images were generated using Maestro[35,36] and VMD.[37] MM-GBSA calculations were performed on ensembles of minimized MD snapshots (834 per simulation). *ΔGs* were obtained as average values, taking into account the local internal strains of the ligand and residues within 6.0 Å. Conformational entropies for chosen system components were obtained through RMSD-based MD (free and in-complex simulations) snapshot clustering (Desmond Trajectory Clustering). A cutoff of 1.0 Å between clusters was used. The results, corresponding to the population of unique conformational states, were used to calculate corresponding entropies similar to the approach of D'Aquino *et al*.[38] by using the standard formula:

$$S = \sum_i p_i \ln p_i$$

where p_i is the probability of state i and R is the universal gas constant. Resulting values were normalized to 45 states for each component.

References

[1] Fihn, S. D. Clinical practice. *N. Engl. J. Med.* **2003,** 349, 259-66.
[2] Hooton, T. M. *Int. J. Antimicrob. Agents* **2001,** 17, 259-68.
[3] Wiles, T. J.; Kulesus, R. R.; Mulvey, M. A. *Exp. Mol. Pathol.* **2008,** 85, 11-9.
[4] Zhou, G.; Mo, W. J.; Sebbel, P.; Min, G.; Neubert, T. A.; Glockshuber, R.; Wu, X. R.; Sun, T. T.; Kong, X. P. *J. Cell. Sci.* **2001,** 114, 4095-103.
[5] Xie, B.; Zhou, G.; Chan, S. Y.; Shapiro, E.; Kong, X. P.; Wu, X. R.; Sun, T. T.; Costello, C. E. *J. Biol. Chem.* **2006,** 281, 14644-53.
[6] Rockendorf, N.; Sperling, O.; Lindhorst, T. K. *Aust. J. Chem.* **2002,** 55, 87-93.
[7] Sperling, O.; Fuchs, A.; Lindhorst, T. K. *Org. Biomol. Chem.* **2006,** 4, 3913-22.
[8] Choudhury, D.; Thompson, A.; Stojanoff, V.; Langermann, S.; Pinkner, J.; Hultgren, S. J.; Knight, S. D. *Science* **1999,** 285, 1061-6.
[9] Hung, C. S.; Bouckaert, J.; Hung, D.; Pinkner, J.; Widberg, C.; DeFusco, A.; Auguste, C. G.; Strouse, R.; Langermann, S.; Waksman, G.; Hultgren, S. J. *Mol. Microbiol.* **2002,** 44, 903-15.
[10] Bouckaert, J.; Berglund, J.; Schembri, M.; De Genst, E.; Cools, L.; Wuhrer, M.; Hung, C. S.; Pinkner, J.; Slättegård, R.; Zavialov, A.; Choudhury, D.; Langermann, S.; Hultgren, S. J.; Wyns, L.; Klemm, P.; Oscarson, S.; Knight, S. D.; De Greve, H. *Mol. Microbiol.* **2005,** 55, 441-55.
[11] Klebe, G.; Böhm, H. J. *J. Recept. Signal Transduct. Res.* **1997,** 17, 459-73.
[12] Sigurskjold, B. W.; Berland, C. R.; Svensson, B. *Biochemistry* **1994,** 33, 10191-9.
[13] Navarre, N.; Amiot, N.; van Oijen, A.; Imberty, A.; Poveda, A.; Jimenez-Barbero, J.; Cooper, A.; Nutley, M. A.; Boons, G. J. A. *Chem-Eur. J.* **1999,** 5, 2281-2294.
[14] Udugamasooriya, D. G.; Spaller, M. R. *Biopolymers* **2008,** 89, 653-67.
[15] Han, Z.; Pinkner, J. S.; Ford, B.; Obermann, R.; Nolan, W.; Wildman, S. A.; Hobbs, D.; Ellenberger, T.; Cusumano, C. K.; Hultgren, S. J.; Janetka, J. W. *J. Med. Chem.* **2010,** 53, 4779-92.
[16] Rabbani, S.; Jiang, X.; Schwardt, O.; Ernst, B. *Anal. Biochem.* **2010,** 407, 188-95.
[17] Kemmer, G.; Keller, S. *Nat. Protoc.* **2010,** 5, 267-81.
[18] DeLorbe, J. E.; Clements, J. H.; Teresk, M. G.; Benfield, A. P.; Plake, H. R.; Millspaugh, L. E.; Martin, S. F. *J. Am. Chem. Soc.* **2009,** 131, 16758-70.
[19] Ladbury, J. E.; Klebe, G.; Freire, E. *Nat. Rev. Drug Discov.* **2010,** 9, 23-7.
[20] Edwards, A. A.; Mason, J. M.; Clinch, K.; Tyler, P. C.; Evans, G. B.; Schramm, V. L. *Biochemistry* **2009,** 48, 5226-38.
[21] Connelly, P. R. *The Cost of Releasing Site-Specific, Bound Water Molecules from Proteins: Toward a Quantitative Guide for Structure-Based Drug Design*. Springer-Verlag: 1997.
[22] Gomez, J.; Freire, E. *A Structure-Based Thermodynamic Approach to Molecular Design*. Springer Verlag: 1997.
[23] *Prime*, 3.0; Schrödinger LLC: New York, NY, 2011.
[24] Guimaraes, C. R. W. A. *J. Chem. Theory Comput.* **2011,** 7, 2296-2306.
[25] Vetsch, M.; Sebbel, P.; Glockshuber, R. *J. Mol. Biol.* **2002,** 322, 827-40.
[26] Meerman, H. J.; Georgiou, G. *Nat. Biotechnol.* **1994,** 12, 1107-10.
[27] Sambrook, J.; Fritsch, E. F.; Maniatis, T. *Molecular Cloning: Laboratory Manual*. Cold Spring Harbor Laboratory Press: Cold Spring Harbor, NY, 1994.
[28] Bitsch, F.; Aichholz, R.; Kallen, J.; Geisse, S.; Fournier, B.; Schlaeppi, J. M. *Anal. Biochem.* **2003,** 323, 139-49.
[29] Mesch, S.; Lemme, K.; Koliwer-Brandl, H.; Strasser, D. S.; Schwardt, O.; Kelm, S.; Ernst, B. *Carbohydr. Res.* **2010,** 345, 1348-59.
[30] Krylova, O. O.; Jahnke, N.; Keller, S. *Biophys. Chem.* **2010,** 150, 105-11.
[31] Ziegler, A.; Seelig, J. *Biophys. J.* **2004,** 86, 254-63.
[32] *Glide*, 5.6; Schrödinger LLC: New York, NY, **2010.**
[33] Kaminski, G. A.; Friesner, R. A.; Tirado-Rives, J.; Jorgensen, W. L. *J. Phys. Chem. B* **2001,** 105, 6474-6487.
[34] *Desmond Molecular Dynamics System*, 2.4; D. E. Shaw Research: New York, NY, 2010.
[35] Maestro. 9.1; Schrödinger, LLC: New York, NY, 2010.
[36] Tools, M.-D. I. 2.4; Schrödinger, LLC: New York, NY, 2010.
[37] Humphrey, W.; Dalke, A.; Schulten, K. *J. Mol. Graph.* **1996,** 14, 33-8.
[38] D'Aquino, J. A.; Freire, E.; Amzel, L. M. *Proteins* **2000,** 41, 93-107.

2.3.1.2 *Ortho*-Substituted Biphenyl Aglycones

FimH Antagonists: Structure–Activity and Structure–Property Relationships for Biphenyl α-D-Mannopyranosides

Lijuan Pang,* Simon Kleeb,* Katrin Lemme,* Said Rabbani,* Meike Scharenberg, Adam Zalewski, Florentina Schädler, Oliver Schwardt, and Beat Ernst**

Institute of Molecular Pharmacy, University of Basel, Klingelbergstr. 50, 4056 Basel, Switzerland

**Authors contributed equally*

***Corresponding author. Tel: 0041 267 15 51; Fax: 0041 267 15 52; e-mail: beat.ernst@unibas.ch*

Published in: *Angew. ChemMedChem* **2012**, *7*, 1404-1422.

Keywords: Carbohydrate, glycomimetics, isothermal titration calorimetry, lectin, selectin.

Contribution of Katrin Lemme: Contributed to the manuscript, determination of protein concentration, and ITC experiments.

CHEMMEDCHEM

ChemPubSoc Europe

DOI: 10.1002/cmdc.201200125

VIP

FimH Antagonists: Structure–Activity and Structure–Property Relationships for Biphenyl α-D-Mannopyranosides

Lijuan Pang, Simon Kleeb, Katrin Lemme, Said Rabbani, Meike Scharenberg, Adam Zalewski, Florentina Schädler, Oliver Schwardt, and Beat Ernst*[a]

Urinary tract infections (UTIs) are caused primarily by uropathogenic *Escherichia coli* (UPEC), which encode filamentous surface-adhesive organelles called type 1 pili. FimH is located at the tips of these pili. The initial attachment of UPEC to host cells is mediated by the interaction of the carbohydrate recognition domain (CRD) of FimH with oligomannosides on urothelial cells. Blocking these lectins with carbohydrates or analogues thereof prevents bacterial adhesion to host cells and therefore offers a potential therapeutic approach for prevention and/or treatment of UTIs. Although numerous FimH antagonists have been developed so far, few of them meet the requirement for clinical application due to poor pharmacokinetics. Additionally, the binding mode of an antagonist to the CRD of FimH can switch from an in-docking mode to an out-docking mode, depending on the structure of the antagonist. In this communication, biphenyl α-D-mannosides were modified to improve their binding affinity, to explore their binding mode, and to optimize their pharmacokinetic properties. The inhibitory potential of the FimH antagonists was measured in a cell-free competitive binding assay, a cell-based flow cytometry assay, and by isothermal titration calorimetry. Furthermore, pharmacokinetic properties such as log *D*, solubility, and membrane permeation were analyzed. As a result, a structure–activity and structure–property relationships were established for a series of biphenyl α-D-mannosides.

Introduction

Urinary tract infections (UTIs), the most prevalent series of infectious diseases worldwide, affect millions of people and account for significant morbidity as well as high medical costs.[1] The primary cause of UTIs are strains of uropathogenic *Escherichia coli* (UPEC), which make up 70–95% of reported cases.[1a,2] UTIs are treated with antibiotics; however, recurrent infections by UPEC with subsequent antibiotic exposure can lead to the emergence of antimicrobial resistance.[3]

Adhesion to host cells is the initial step of microbial infection. To gain an initial foothold within the bladder, UPEC strains encode filamentous surface-adhesive organelles called type 1 pili (fimbriae).[4] They mediate bacterial attachment to uroplakin Ia, a glycoprotein located on urothelial cells. This initial step prevents the clearance of *E. coli* by the bulk flow of urine and facilitates the invasion of host cells.[1b,5] A bacterial lectin known as FimH is located at the tips of type 1 pili. The carbohydrate recognition domain (CRD) of this lectin is responsible for binding to the complementary carbohydrate epitope of the host tissue. Blocking this lectin by a carbohydrate or a glycomimetic thereof offers a potential therapeutic approach for prevention and/or treatment of UTIs.[6]

More than two decades ago, Sharon and co-workers explored various mannosides and oligomannosides as potential antagonists for type 1 pili-mediated bacterial adhesion and observed interactions in the micro- to millimolar range.[7] The first crystal structure of FimH was solved in 1999,[8] and since then, numerous crystallographic studies have been reported, greatly facilitating the design of high-affinity ligands.[9] In summary, the reported affinities can be rationalized on the basis of the structure of FimH: First, the binding pocket accommodates the mannose with the hydroxy groups forming an extended hydrogen bond network. Second, the entrance to the binding site, referred to as the "tyrosine gate", is formed by three hydrophobic amino acids (Tyr48, Tyr137, and Ile52)[9a] and can host aliphatic and aromatic aglycones.

As a consequence of hydrophobic contacts of the alkyl aglycone, *n*-heptyl α-D-mannopyranoside (**1**) exhibits nanomolar affinity.[9b] With aromatic aglycones such as **2**–**5** (Figure 1), further improvements in affinity were observed.[10] To explore the binding mode and to improve affinity as well as ADME properties, a series of biphenyl FimH antagonists were synthesized.

Results and Discussion

An unexpected docking mode was discovered upon co-crystallization of biphenyl mannoside **3** with the FimH CRD.[10d] Whereas the alkyl aglycone of *n*-butyl α-D-mannopyranoside[9b]

[a] *L. Pang,[+] S. Kleeb,[+] Dr. K. Lemme,[+] Dr. S. Rabbani,[+] Dr. M. Scharenberg, A. Zalewski, F. Schädler, Dr. O. Schwardt, Prof. Dr. B. Ernst*
Institute of Molecular Pharmacy, Pharmacenter, University of Basel
Klingelbergstrasse 50, 4056 Basel (Switzerland)
E-mail: beat.ernst@unibas.ch

[+] *These authors contributed equally to this work.*

Supporting information for this article is available on the WWW under http://dx.doi.org/10.1002/cmdc.201200125.

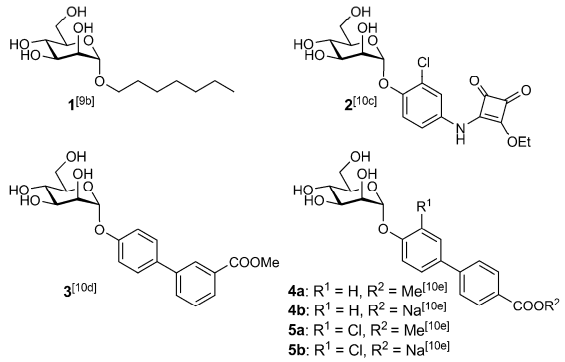

Figure 1. FimH antagonists: *n*-heptyl α-D-mannopyranoside (**1**) is used as reference compound; the squaric acid derivative **2** and biphenyl derivatives **3**–**5** exhibit nanomolar affinities.

interacts with both Tyr48 and Tyr137 of the tyrosine gate (in-docking mode),[10f] the biphenyl aglycone adopts the out-docking mode; that is, it interacts only with Tyr48 (Figure 2A), probably due to insufficient flexibility; π–π stacking of the outer aromatic ring of the biphenyl aglycone (ring B) with Tyr48 is effected by induced fit: a substantial move of Tyr48. Moreover, further stabilization of the protein–ligand complex by polar interaction between the ester in the *meta* position of **3** and the side chain of Arg98 was proposed.[10d]

In silico docking studies with biphenyl derivative **4a**[10e] suggested a similar out-docking mode (Figure 2B). A close inspection revealed empty space between the *ortho* position of the aromatic ring adjacent to the anomeric center (ring A) and the protein surface. Indeed, with an *ortho*-chloro substituent (→ **5a**, Figure 1), affinity was substantially improved. Further studies with FimH antagonists that exhibit enhanced flexibility (e.g., compound **6;** Figure 2C and Figure 3) indicated a switch from the out-docking mode to the in-docking mode. However, whether an optimal π–π stacking within the tyrosine gate can be realized remains to be determined. Finally, docking studies also indicated that elongation of the carboxylate-bearing *para* substituent enables a polar interaction between the carboxylate and Arg98 (e.g., compound **7**; Figure 2D and Figure 3).

Starting from antagonist **4**, we explored three types of modifications (Figure 3):

1) For optimizing the van der Waals contact between the *ortho* position of ring A and the binding pocket, a series of substituents — F, CH_3, CF_3, OCH_3, cyclopropyl, and CN — were introduced as depicted in Scheme 1.
2) To determine whether the out-docking mode reported for **3**[10d] results from insufficient flexibility, we increased the aglycone flexibility by introducing a methylene spacer between the anomeric oxygen and ring A of the biphenyl moiety (Scheme 2). This should decrease the conformational constraints to allow an optimized spatial arrangement of the aglycone in the tyrosine gate (→**6**, Figure 2C); at the same time, water solubility should be improved as a result of the decreased stacking tendency derived from disruption of the symmetry of the aglycone.[15]
3) To enable a polar interaction between the carboxylate substituent on ring B with Arg98 of FimH, we extended the *para* substituent of **4**, that is, we replaced it with either a flexible methyl ethanolate or a rigid methyl cyclopropanecarboxylate (Scheme 3). Biphenyl α-D-mannoside **24**[10d] shows a three- to eightfold lower affinity for FimH than its counterparts with a methoxycarbonyl substituent at the *meta* (→**3**)[10d] or *para* positions (→**4**)[10e] of ring B (Table 1). Han et al. assigned the increased affinity of compound **3** to a polar interaction of the ester with Arg98 of FimH.[10d] Because for spatial reasons the ester in the

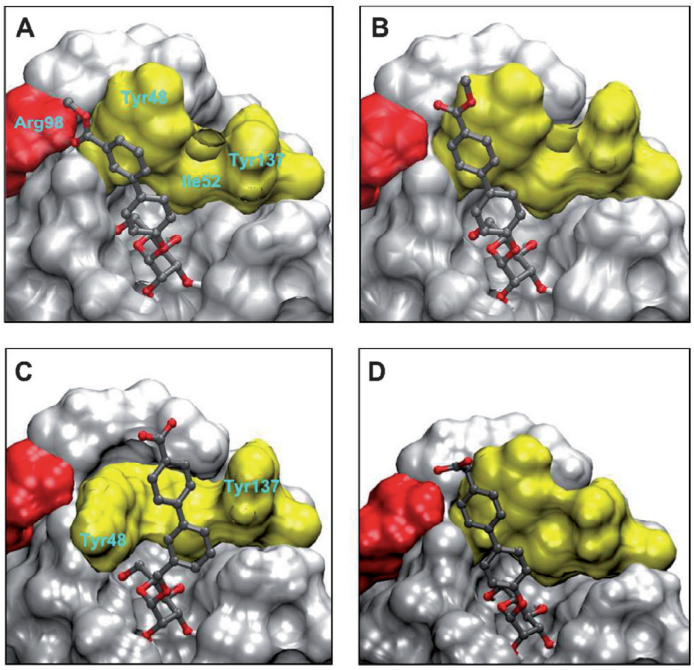

Figure 2. A) Crystal structure of biphenyl **3** (PDB ID: 3MCY)[10d] bound to the FimH CRD. B–D) In silico docking studies obtained with flexible docking (Glide software package)[11] to the same FimH CRD structure; top-scored binding mode of B) **4a**, C) **6**, and D) **7**.

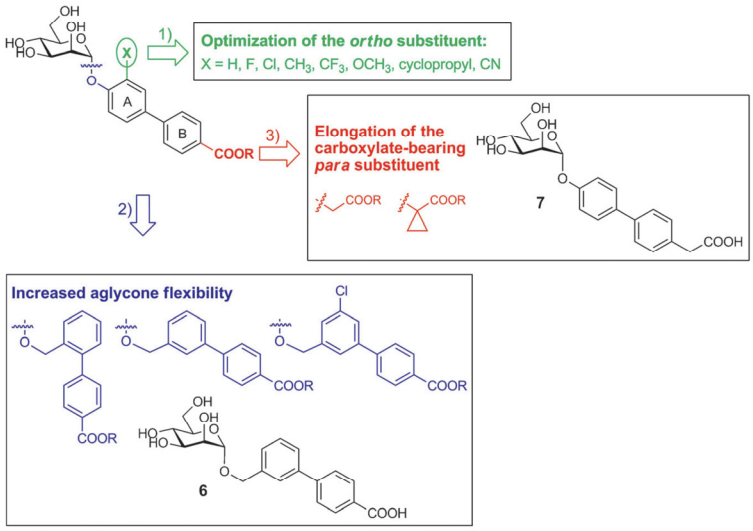

Figure 3. Modifications to the aglycone of FimH antagonists by 1) optimization of the *ortho* substituent, 2) an increase in the flexibility of the aglycone, and 3) elongation of the carboxylate-bearing *para* substituent.

para-substituted derivative **4** cannot establish a similar interaction with Arg98, the substantial improvement in affinity may result from solvation effects.

Synthesis

Optimization of ortho *substituents (Scheme 1)*

Mannosylation of phenols **9a–f** with mannosyl fluoride **8** and BF_3·OEt_2 as promoter yielded α-mannosides **10a–f** stereospecifically.[12] Whereas the phenols **9a–d** and **9f** are commercially available, the cyclopropyl derivative **9e** was prepared via tandem carbolithiation/1,3-elimination according to Ocasio and Scanlan.[13] In a palladium-catalyzed Miyaura–Suzuki coupling[14] of **10a–f** with 4-methoxycarbonylphenylboronic acid (**11**), biphenyls **12a–f** were obtained in good to excellent yields. Deacetylation using Zemplén conditions (→**13a–f**) followed by saponification of the methyl esters gave the test compounds **14a–e**. Owing to the instability of the cyano group under aqueous basic conditions, **14f** was synthesized by coupling **10f** with 4-carboxyphenylboronic acid pinacol ester (**15**) followed by transesterification under Zemplén conditions to avoid the final saponification with aqueous sodium hydroxide.

Increase in aglycone flexibility (Scheme 2)

Benzyl alcohols **16a–c** were first mannosylated with donor **8**[12] to yield the benzyl mannosides **17a–c**. Subsequent cross-coupling with 4-methoxycarbonylphenylboronic acid (**11**) afforded acetates **18a,b** and **21**. Deacetylation of the mannose moiety (→**19a,b** and **22**) followed by saponification of the methyl esters gave compounds **6**, **20**, and **23**.

Elongation of the carboxylate-bearing para *substituent (Scheme 3)*

Peracetylated mannose **25** was treated with 4-iodophenol in the presence of BF_3·Et_2O. The resulting iodide **26** was transformed into boronic acid pinacol ester **27**, which was coupled with 4-bromophenylacetic acid methyl ester (**28**) and 4-bromophenylcyclopropylcarboxylic acid methyl ester (**32**) under Miyaura–Suzuki coupling conditions[14] to yield biphenyls **29** and **33**. Deacetylation with sodium methoxide (→**30** and **34**) followed by saponification of the methyl ester yielded the sodium salts **31** and **35**.

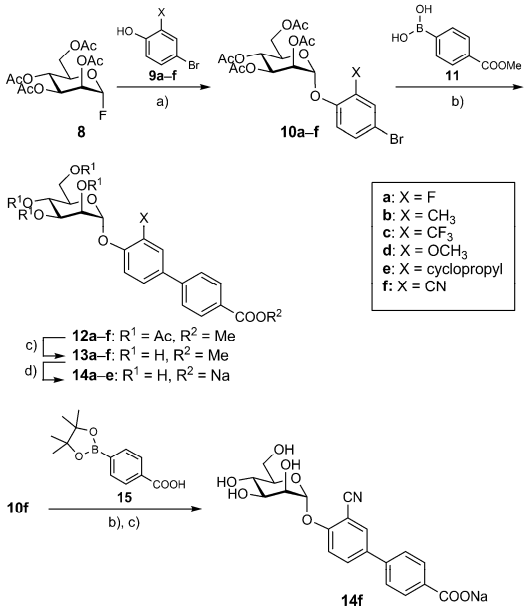

Scheme 1. *Reagents and conditions:* a) BF_3·Et_2O, CH_2Cl_2, 0 °C, 3 h (**10a–f**, 73–86%); b) $Pd(Cl_2)$dppf·CH_2Cl_2, K_3PO_4, DMF, 80 °C, overnight (**12a–f**, 55–91%); c) NaOMe, MeOH, RT, 4 h (**13a–e**, **14f**, 52–73%); d) 1. 0.2 N $NaOH_{(aq)}$, MeOH, RT, overnight; 2. Dowex (Na^+), size-exclusion chromatography (P-2 gel) (**14a–e**, 15–74%).

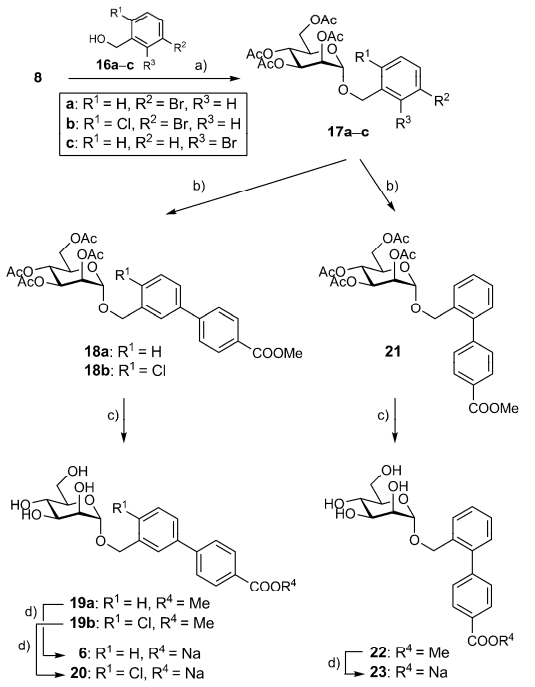

Scheme 2. *Reagents and conditions:* a) $BF_3{\cdot}Et_2O$, CH_2Cl_2, 0 °C, 3 h (**17a–c**, 34–48%); b) 4-methoxycarbonylphenylboronic acid (**11**), $Pd(Cl_2)dppf{\cdot}CH_2Cl_2$, K_3PO_4, DMF, 80 °C, overnight (**18a,b** and **21**, 73–94%); c) NaOMe, MeOH, RT, 4 h (**19a,b** and **22**, 47–90%); d) 1. 0.2 N $NaOH_{(aq)}$, MeOH, RT, overnight; 2. Dowex (Na^+), size-exclusion chromatography (P-2 gel) (**6**, **20** and **23**, 10–96%).

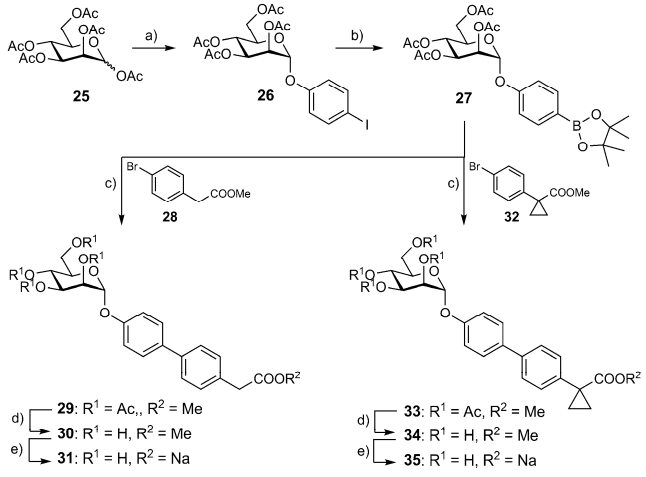

Scheme 3. *Reagents and conditions:* a) 4-iodophenol, $BF_3{\cdot}Et_2O$, CH_2Cl_2, 40 °C, overnight (70%); b) bis(pinacolato)diborone, $Pd(Cl_2)dppf{\cdot}CH_2Cl_2$, KOAc, DMF, MW 120 °C, 2 h (50%); c) $Pd(Cl_2)dppf{\cdot}CH_2Cl_2$, K_3PO_4, DMF, 80 °C, overnight (34–56%); d) NaOMe, MeOH, RT, 4 h (33–95%); e) 1. 0.2 N $NaOH_{(aq)}$, MeOH, RT, overnight; 2. Dowex (Na^+), size-exclusion chromatography (P-2 gel) (**31**: 40%; **35**: 23%).

Binding affinity and activity

The biphenyl α-D-mannosides with varying *ortho* substituents (**5a–b**, **13a–f**, **14a–f**), increased aglycone flexibility (**6**, **19**, **20**, **22**, **23**), and elongated carboxylate-bearing *para* substituents (**30**, **31**, **34**, **35**) were evaluated in vitro by two competitive assay formats (Table 1). All antagonists were tested in a cell-free competitive binding assay.[16] Subsequently, the best candidates were investigated in a cell-based flow cytometry assay.[17]

The cell-free competitive binding assay is based on the interaction of a biotinylated polyacrylamide glycopolymer as competitor with the isolated CRD of FimH. In contrast, the cell-based flow cytometry assay involves the infection of human urinary bladder epithelial carcinoma cells with GFP-labeled UPECs expressing the complete type 1 pili (see the Experimental Section below for details). The competitors in the former assay are thus polymer-bound trimannosides, whereas in the latter the antagonists compete with more potent high-mannose oligosaccharides present on uroplakin Ia, which is located on the surface of human urinary bladder cells.[18,19] The interaction is further affected by the presence of high- and low-affinity states of the CRD of FimH. Aprikian et al. experimentally demonstrated that in full-length fimbriae, the pilin domain stabilizes the CRD domain in the low-affinity state, whereas the CRD domain alone adopts the high-affinity state.[20] Furthermore, it was recently shown that shear stress can induce a conformational switch (twist in the β-sandwich fold of the CRD domain), resulting in improved affinity.[21] Therefore, differing affinities were expected in the cell-based flow cytometry assay, in which full-length fimbriae are present, relative to the cell-free competitive binding assay.

***Cell-free competitive binding assays*[16]**

These assays were performed twice for every compound with each concentration in duplicate. To ensure comparability between various antagonists, the reference compound *n*-heptyl α-D-mannopyranoside **1**[22] was tested each time in parallel. The affinities are reported relative to **1** as rIC_{50} in Table 1. A comparison of the affinities of compounds **4a** and **4b** with the *ortho*-substituted analogues **5a**, **13a–f** and **5b**, **14a–f** clearly demonstrates that *ortho* substituents on ring A indeed improve binding. However, the differences between the various substituted FimH antagonists are small. For a better understanding of these results, a more detailed analysis of the thermodynamic profile by isothermal titration calorimetry (ITC) was performed (see below). By increasing the flexibility of the aglycone, we expected a switch from the out-docking mode as present for antagonists **3** and **4** (Figure 2A,B) to the in-docking mode (represented by antagonist **6** in Figure 2C).[10f] However, affinities for all six representatives with increased spacer length between carbohydrate and aglycone (Table 1: **6**—, **19**, **20**, **22**, and **23**) were dramatically decreased. A similar tendency was observed

Table 1. Pharmacodynamic parameters of FimH antagonists.

Compd	R	Binding assay IC_{50} [nM][a]	Binding assay rIC_{50}[b]	Flow cytometry IC_{50} [μM][a,c]
1[10e]	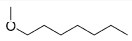	73 ± 7.9	1	3.9 ± 1.6
24[10d]	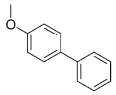	84.9	1.47	n.d.
3[10d]	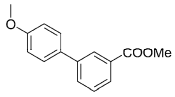	28.6	0.55	n.d.
4a[10e]	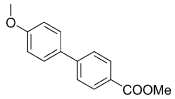	10.4 ± 1.2	0.14	n.d.
4b[10e]	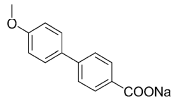	17.1 ± 2.2	0.15	n.d.
5a	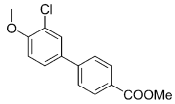	4.8 ± 1.2	0.06	n.d.
5b	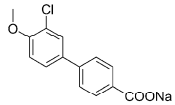	6.7 ± 2.1	0.09	0.33 ± 0.05
13a	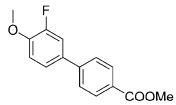	8.0	0.14	n.d.
14a	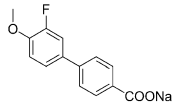	33.5	0.58	1.54 ± 0.31
13b	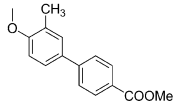	23.3	0.40	n.d.
14b	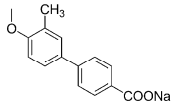	9.2	0.16	1.83 ± 0.14
13c	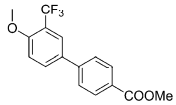	2.6	0.04	n.d.
14c	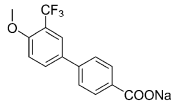	8.9	0.15	0.89 ± 0.10

Table 1. (Continued)

Compd	R	Binding assay IC_{50} [nM][a]	Binding assay rIC_{50}[b]	Flow cytometry IC_{50} [μM][a,c]
13d	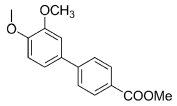	3.5	0.06	n.d.
14d	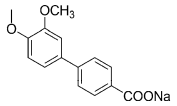	4.8	0.08	1.95 ± 0.36
13e	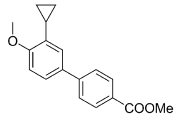	31.7	0.55	n.d.
14e	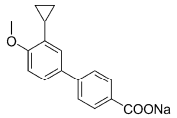	63.0	1.09	4.85 ± 0.79
13f	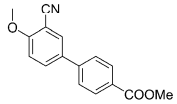	22.5	0.39	n.d.
14f	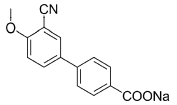	33.9	0.58	n.d.
19a	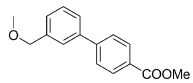	56.1	0.97	n.d.
6	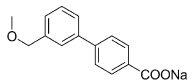	107.9	1.87	n.d.
19b	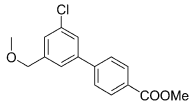	98.9	1.7	n.d.
20	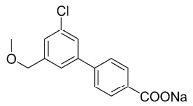	142.2	2.44	n.d.
22	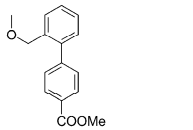	85.8	1.49	n.d.
23	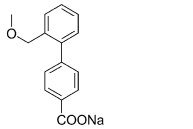	642.0	11.14	n.d.

Table 1. (Continued)

Compd	R	Binding assay IC_{50} [nM][a]	Binding assay rIC_{50}[b]	Flow cytometry IC_{50} [μM][a,c]
30	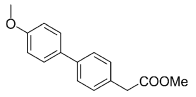	63.2	1.09	n.d.
31	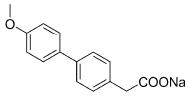	70.5	1.21	n.d.
34	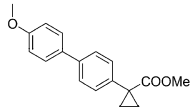	49.5	0.85	n.d.
35	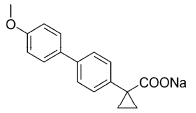	62.5	1.07	n.d.

[a] IC_{50} values were determined in a cell-free competitive binding assay.[16] [b] The rIC_{50} values were calculated by dividing the IC_{50} of the compound of interest by that of reference compound **1**; this leads to rIC_{50} values <1 for derivatives that bind better than reference **1**, and rIC_{50} values >1 for compounds with lower affinity than **1**. [c] The anti-adhesion potential to human epithelial bladder cells was determined in the flow cytometry assay;[17] n.d. = not determined.

for the biphenyls with an elongated carboxylate-bearing *para* substituent (Table 1: **30**, **31**, **34**, and **35**). It was previously described that the ester of **3** is placed within hydrogen bonding distance to form a polar interaction with Arg98 and Glu50.[10d] However, an improvement of affinity provided by a similar polar interaction between Arg98 and the antagonists **31** and **35** could not be achieved, probably due to the high desolvation penalty of Arg98. Finally, it is important to note that the free acids (sodium salt) of the antagonists in general showed slightly lower affinities than their methyl ester counterparts, with the only exceptions of **13b** and **14b** (Table 1). However, because the esters are thought to act as prodrugs and to be rapidly cleaved after oral application,[10e] the affinities of the carboxylates are relevant with regard to the therapeutic potential of the present FimH antagonists.

Cell-based flow cytometry assay[17]

These assays were performed in duplicate/triplicate, and *n*-heptyl α-D-mannopyranoside **1** was used as reference compound with an IC_{50} value of 3.9±1.6 μM. The most potent antagonists **5b** and **14c** (Table 1) showed respective IC_{50} values of 0.33±0.05 and 0.89±0.10 μM. In general, the activities obtained from the flow cytometry assay were ~50-fold lower than the affinities determined in the target-based competitive assay (see above).

Isothermal titration calorimetry

Because the biological in vitro evaluation only revealed small differences between affinities, ITC experiments were carried out to study the thermodynamic profile of the variously *ortho*-substituted biphenyl compounds **5b** and **14a–f** in binding to FimH. ITC directly measures the heat of interaction (change in enthalpy, ΔH) at a constant temperature on titrating two compounds of known concentration that form an equilibrium complex.[23] It includes contributions from all equilibria that occur as the interacting molecules go from the free to the bound state, including those associated with solvent interactions and macromolecular conformational changes. The noncovalent interaction between a protein and a ligand can be quantified by the change in free energy (ΔG), consisting of the change in enthalpy (ΔH) and change in entropy (ΔS) [Eq. (1)].[24] The binding energy under standard conditions (ΔG°), in which all reactants and products are at a concentration of 1 M, can be calculated from the dissociation constant, K_D [Eq. (2)]. With ITC, K_D and ΔH can be measured directly, whereas ΔG and the entropy term $T\Delta S$ are calculated according to Equations (1) and (2).

$$\Delta G = \Delta H - T\Delta S \quad (1)$$

$$\Delta G = RT \ln K_D \quad (2)$$

A favorable enthalpy term ΔH is associated with hydrogen bond formation, electrostatic, and dipole–dipole interactions at the overcompensation of the desolvation penalty.[25] The entropy term ΔS reflects the overall change in the degrees of freedom of a system. It can be dissected into translational and rigid body rotational entropy,[26] solvation entropy,[27] and entropy costs related to conformational changes of protein and ligand [Eq. (3)].[28] Whereas the formation of a protein–ligand complex is always associated with a decrease in translational and rotational freedom and therefore with entropy costs, the entropic contribution involving changes in solvation (ΔS_{solv}) and changes in rotational and vibrational entropy due to the loss of conformational flexibility (ΔS_{conf}) can differ both in sign and magnitude.[29]

$$\Delta S = \Delta S_{solv} + \Delta S_{trans/rot} + \Delta S_{conf} \quad (3)$$

The FimH CRD was used for the ITC experiments. It was prepared from FimH-CRD-Th-His_6 (see *Competitive binding assay*, Experimental Section below) by incubation with thrombin, as described earlier.[16]

The thermodynamic fingerprints of the various biphenyl derivatives (Table 2, Figure 4) reveal a significant improvement in the enthalpic term ($\Delta\Delta H$ −4.3 to −11.2 kJ mol^{-1}) for all substituted biphenyls (**5b**, **14a–f**) in comparison with the unsubstituted derivative **4b**. The largest enthalpy improvement was observed for the trifluoromethyl group (**14c**; Table 2). Interestingly, these largely improved enthalpic contributions are mostly compensated by entropic penalties ($-T\Delta\Delta S$ +3.2 to +7.5 kJ mol^{-1}), resulting in only marginally improved K_D values. In the best case, the trifluoromethyl derivative **14c**, a fourfold improvement in K_D was measured. Similar, but less pronounced

Table 2. Binding thermodynamics of FimH antagonists determined by ITC.

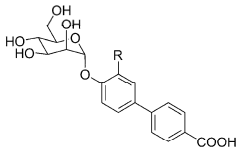

Compd	R	K_D [nM]	ΔG° [kJ mol^{-1}]	ΔH° [kJ mol^{-1}]	$-T\Delta S^\circ$ [kJ mol^{-1}]	N[a]	V_{vdW} [Å^3][b]
4b	H	14.1	−44.8	−47.3	+2.5	1.00	7.2
5b	Cl	3.7	−48.1	−55.5	+7.4	1.01	22.4
14a	F	9.2	−45.9	−51.6	+5.7	1.00	13.3
14b	Me	4.8	−47.5	−56.2	+8.7	1.01	26.7
14c	CF_3	3.2	−48.5	−58.5	+10.0	1.02	41.4
14d	OMe	7.7	−46.3	−52.5	+6.2	1.02	34.8
14e	*c*Pr	6.9	−46.6	−46.7	+0.1	1.01	52.5
14f	CN	7.4	−46.4	−55.0	+8.6	1.01	29.7

[a] Molar ratio of protein/ligand. [b] van der Waals volumes (V_{vdW}) of the *ortho* substituent were calculated with the Phase volCalc utility.[30]

effects were observed for most other *ortho* substituents. This trend was broken only by the cyclopropyl derivative **14e** ($\Delta\Delta H$ +0.7 kJ mol^{-1}, $-T\Delta\Delta S$ −2.4 kJ mol^{-1}; Table 2).

The influence of the *ortho* substituent on binding can be attributed to three factors. First, *ortho* substituents of appropriate volume establish an improved shape complementarity within the binding pocket, leading to a better van der Waals (vdW) contact and therefore an improvement in the enthalpy term ΔH. The improvement in enthalpy ($\Delta\Delta H$) correlates well with increasing vdW volumes of spherical *ortho* substituents (**5b**, **14a–c**; Figure 5). For non-spherical substituents (OMe, **14d**; cyclopropyl, **14e**; and CN, **14f**), the shape complementarity is not optimal, leading to only a decreased enthalpy contribution. However, better vdW contacts also lead to decreased conformational flexibility and therefore an entropic compensation by a less favorable ΔS_{conf} value. A second parameter is the desolvation enthalpy, which depends on the polarity of a specific *ortho* substituent and varies between −2.39 kJ mol^{-1} for CH_3 and 19.31 kJ mol^{-1} for CN.[25] Finally, depending on the surface area of the *ortho* substituent, the entropy of solvation may change. In summary, the various effects are superimposed and of opposing contributions to the free binding energy ΔG.

Physicochemical and in vitro pharmacokinetic characterization

To estimate the oral bioavailability and renal elimination of acids **4b**, **5b**, **6**, **14a–f**, **20**, **23**, **31**, **35**, and the methyl esters **4a**, **5a**, **13a–f**, **19a–b**, **22**, **30** and **34**, several physicochemical parameters (lipophilicity, solubility) as well as permeability through an artificial membrane and a cell monolayer were determined (Table 3). The free acids of the antagonists assessed in this study (**4b**, **5b**, **6**, **14a–f**, **20**, **23**, **31**, and **35**) are generally hydrophilic and soluble at pH values >5. All acids showed log $D_{7.4}$ values below zero and are therefore thought to undergo considerable renal clearance,[32] a prerequisite for FimH antagonists to reach their target in the urinary bladder. Permeation studies through an artificial membrane (PAMPA[33]) indicated for all acids except **14a** effective permeation values (log P_e) below −6.7, suggesting low absorption in the small intestine by passive permeation.[34] However, the high absorption potential of the fluoro-substituted biphenyl **14a** predicted by

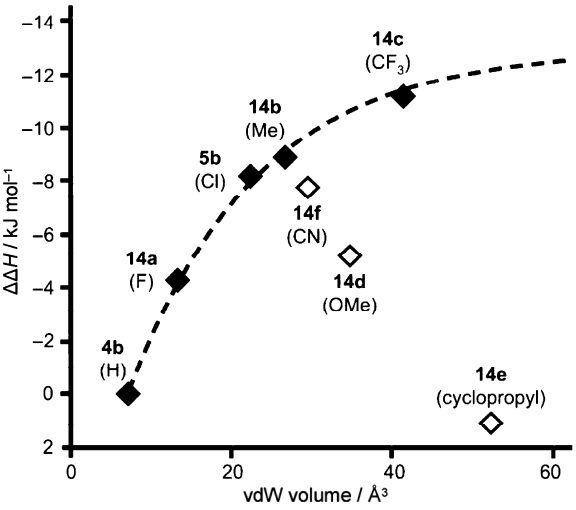

Figure 5. Correlation of $\Delta\Delta H$ (relative to antagonist **4b**) with the van der Waals volumes[30] of *ortho* substituents.

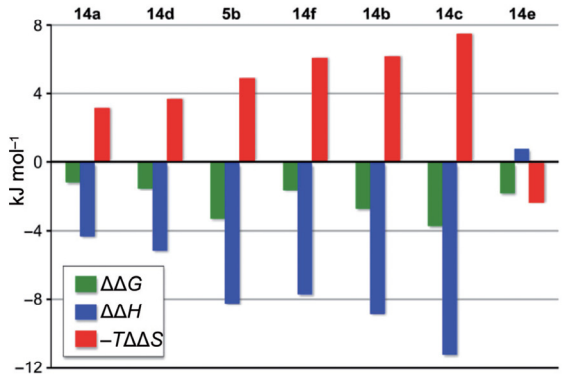

Figure 4. Enthalpy–entropy compensation, a property often reported for carbohydrate–lectin interactions,[31] for *ortho*-substituted biphenyl α-D-mannopyranosides; $\Delta\Delta G$, $\Delta\Delta H$, and $T\Delta\Delta S$ values for **5b** and **14a–f** are plotted relative to the unsubstituted derivative **4b**.

Table 3. Physicochemical and in vitro pharmacokinetic parameters of FimH antagonists.

Compd	PAMPA log P_e [log10 ^{6}cm s ^{1}]/pH[a]	Caco-2 P_{app} [10 ^{6}cm s ^{1}][b]			log $D_{7.4}$[c]	Solubility [μg mL ^{1}]/pH[d]
		a→b	b→a	(b→a)/(a→b)		
1	−4.9	7.0±0.6	9.4±0.2	1.3	1.7	>3000/6.5
24	−5.0±0.1/5.0	10.0±0.9	19.0±1.2	1.9	2.1±0.1	22±0/3.0
	−4.9±0.1/6.2					22±1/5.0
	−4.7±0.1/7.4					21±1/7.4
3	−4.9±0.0/5.0	2.2±0.2	17.6±0.4	8.0	2.0±0.0	>150/3.0
	−4.9±0.0/6.2					>150/5.0
	−4.9±0.0/7.4					>150/7.4
4a	−4.7	1.5±0.0	6.4±0.4	4.3	2.1	14±1/3.0
						13±1/5.0
						12±1/7.4
4b	n.p.	n.d.	n.d.	n.d.	<−1.5	>3000/6.6
5a	−4.6	5.3±0.6	17.5±1.3	3.3	2.3	16±2/3.0
						15±0/5.0
						17±2/7.4
5b	n.p.	0.2±0.0	0.4±0.0	1.6	−0.8	>3000/6.5
13a	−4.8±0.0/5.0	5.6±0.7	22.0±0.6	4.0	2.7±0.1	22±1/3.0
	−4.8±0.0/6.2					24±3/5.0
	−4.8±0.0/7.4					17±6/7.4
14a	−5.8±0.1/5.0	0.2±0.1	0.2±0.0	0.8	<−1.5	30±3/3.0
	−6.3±0.1/6.2					>100/5.0
	−7.4±0.1/7.4					>100/7.4
13b	−4.5±0.1/5.0	6.2±1.3	22.7±1.2	3.6	2.4±0.2	7±0/3.0
	−4.5±0.0/6.2					7±0/5.0
	−4.6±0.1/7.4					7±0/7.4
14b	−8.6±1.7/5.0	n.d.	n.d.	n.d.	−0.6±0.1	34±3/3.0
	−8.8±1.4/6.2					>200/5.0
	−8.7±1.5/7.4					>200/7.4
13c	−4.4±0.0/5.0	9.2±0.1	16.9±1.5	1.8	2.8±0.1	17±1/3.0
	−4.4±0.0/6.2					15±1/5.0
	−4.5±0.1/7.4					16±1/7.4
14c	−8.4±1.3/5.0	n.d.	n.d.	n.d.	−0.8±0.1	15±1/3.0
	−9.3±1.4/6.2					140±6/5.0
	−8.6±1.6/7.4					>200/7.4
13d	−5.4±0.0/5.0	4.2±0.7	16.4±1.2	3.9	1.8±0.1	24±0/3.0
	−5.4±0.0/6.2					24±1/5.0
	−5.4±0.0/7.4					26±1/7.4
14d	−8.5±0.6/5.0	n.d.	n.d.	n.d.	<−1.5	127±4/3.0
	−9.1±0.2/6.2					>200/5.0
	−9.2±0.4/7.4					>200/7.4
13e	−4.5±0.2/5.0	6.1±0.6	17.9±1.2	3.0	2.9±0.1	14±2/3.0
	−4.4±0.0/6.2					13±0/5.0
	−4.4±0.1/7.4					14±1/7.4
14e	−9.3±1.3/5.0	n.d.	n.d.	n.d.	−0.8±0.1	31±2/3.0
	−8.7±1.5/6.2					>200/5.0
	−8.7±1.5/7.4					>200/7.4
13f	−6.5±0.0/5.0	0.9±0.7	18.1±0.6	19.7	1.7±0.0	22±2/3.0
	−6.5±0.1/6.2					24±1/5.0
	−6.3±0.1/7.4					23±1/7.4
14f	−8.5±1.7/5.0	n.d.	n.d.	n.d.	<−1.5	35±11/3.0
	−7.3±0.3/6.2					>200/5.0
	−7.8±1.5/7.4					>200/7.4
19a	−4.9±0.0/5.0	4.4±0.1	18.8±1.7	4.3	1.9±0.1	103±8/3.0
	−4.9±0.0/6.2					100±6/5.0
	−4.9±0.1/7.4					95±5/7.4
6	−8.6±1.6/5.0	n.d.	n.d.	n.d.	<−1.5	>130/3.0
	−9.3±1.4/6.2					>130/5.0
	−8.7±1.5/7.4					>130/7.4
19b	−5.3±0.1/5.0	n.d.	n.d.	n.d.	2.4±0.1	30±0/3.0
	−5.6±0.1/6.2					29±1/5.0
	−5.1±0.2/7.4					31±1/7.4
20	−8.6±1.6/5.0	n.d.	n.d.	n.d.	−1.2±0.2	>130/3.0
	−9.3±1.4/6.2					>130/5.0
	−10/7.4					>130/7.4

Table 3. (Continued)

Compd	PAMPA log P_e [log 10 $^{-6}$ cm s $^{-1}$]/pH[a]	Caco-2 P_{app} [10 $^{-6}$ cm s $^{-1}$][b]			log $D_{7.4}$[c]	Solubility [μg mL $^{-1}$]/pH[d]
		a→b	b→a	(b→a)/(a→b)		
22	−5.1 ± 0.0/5.0	n.d.	n.d.	n.d.	1.7 ± 0.1	> 130/3.0
	−5.1 ± 0.0/6.2					> 130/5.0
	−5.1 ± 0.0/7.4					> 130/7.4
23	−7.3 ± 1.8/5.0	n.d.	n.d.	n.d.	< −1.5	> 130/3.0
	−8.1 ± 2.2/6.2					> 130/5.0
	−10/7.4					> 130/7.4
30	−5.5 ± 0.0/5.0	n.d.	n.d.	n.d.	1.6 ± 0.1	> 130/3.0
	−5.5 ± 0.0/6.2					> 130/5.0
	−5.4 ± 0.1/7.4					> 130/7.4
31	−7.7 ± 1.6/5.0	n.d.	n.d.	n.d.	< −1.5	> 130/3.0
	−8.1 ± 1.3/6.2					> 130/5.0
	−10/7.4					> 130/7.4
34	−5.3 ± 0.1/5.0	n.d.	n.d.	n.d.	2.2 ± 0.1	> 130/3.0
	−5.6 ± 0.0/6.2					> 130/5.0
	−5.3 ± 0.2/7.4					> 130/7.4
35	−8.0 ± 1.3/5.0	n.d.	n.d.	n.d.	n.d.	63 ± 8/3.0
	−8.6 ± 1.6/6.2					> 130/5.0
	−10/7.4					> 130/7.4

[a] P_e = effective permeation: passive permeation through an artificial membrane was determined by parallel artificial membrane permeation assay (PAMPA); values represent the mean ± SD of quadruplicate measurements taken at three pH values (pH 5.0, 6.2, and 7.4).[33] [b] P_{app} = apparent permeability: permeation through cell monolayers was assessed by a Caco-2 assay in the absorptive (a→b) and secretory (b→a) directions in triplicate;[42] n.p. = no permeation, n.d. = not determined. [c] Distribution coefficients (log *D*) were measured by a miniaturized shake-flask procedure at pH 7.4. [d] Kinetic solubility was measured in a 96-well format using the μSOL Explorer solubility analyzer at three pH values (pH 3.0, 5.0, and 7.4) in triplicate.

PAMPA could not be confirmed by the colorectal adenocarcinoma (Caco-2) cell permeation assay. In contrast, the methyl esters (**3**, **4a**, **5a**, **13a–f**, **19a–b**, **22**, **30**, and **34**) showed log $D_{7.4}$ values > 1.5, that is, they are more lipophilic and hence more permeable than the corresponding acids, as shown by the PAMPA and Caco-2 permeation assay. Despite this high absorption potential, the ratios between the apparent permeability coefficients (P_{app}) in the basolateral-to-apical (b→a, secretory) and apical-to-basolateral (a→b, absorptive) directions revealed active efflux processes as an additional issue of all the assessed compounds. Moreover, the methyl esters must be readily hydrolyzed after absorption to become more polar and to be renally eliminated. Rapid metabolic turnover by the enzyme carboxylesterase was previously shown for the methyl esters **4a** and **5a**.[10e]

The different substituents at the *ortho* position of ring A (**5a**, **5b**, **13a–f**, **14a–f**; Table 3) only have a minor influence on the physicochemical properties. The addition of chloro, fluoro, methyl, trifluoromethyl, or cyclopropyl substituents slightly increases the lipophilicity of the respective acids and methyl esters, whereas methoxy and cyano substituents render the compounds more hydrophilic and less permeable. Moreover, the substituents at the *ortho* position have negligible effects on the low aqueous solubility, which is a major drawback of all methyl esters.[35] In contrast, the modifications with increased spacer length between carbohydrate and aglycone (**6**, **19a–b**, **20**, **22**, and **23**; Table 3) show higher aqueous solubility. Extending the spacer and linking it at the *ortho* or *meta* positions of the biaryl moiety disrupts the symmetry of the molecular structure, leading to increased solubility.[15,36] However, an additional chloro substituent at the 4-position (**19b**, **20**; Table 3) restores the symmetrical character of the structure, which in turn lowers the solubility of the compound. Disrupted structural symmetry might also hold true for the enhanced solubility of the biphenyls with an elongated carboxylate-bearing *para* substituent (**30**, **31**, **34**, and **35**; Table 3). The introduction of a methylene or cyclopropylene group between the biphenyl and the carboxylate moiety markedly improved the aqueous solubility of the methyl esters, whereas the absorption potential was only slightly decreased.

Summary and Conclusions

In this study, we investigated the structure–affinity relationship for *ortho* substituents on ring A of the biphenyl aglycone of the FimH antagonists **13** and **14**. The correlation between vdW volumes of these substituents and the enthalpy term clearly indicates the importance of shape complementary. This interpretation is further supported by the fact that the electronic character of the substituent [Cl in **5a** (Table 2), CF_3 in **14c** versus CH_3 in **14b**] is less important. The correlation of enthalpic improvements ($\Delta\Delta H$) with vdW volumes offers a potent tool for guiding further structural optimization.

The successful oral application using a prodrug approach was recently demonstrated with the ester **5a**.[10e] A major drawback of the biphenyl methyl esters is their insufficient solubility, which is mostly in the range of 15–35 μg mL $^{-1}$. As expected,[15] solubility could be substantially improved when the symmetry of the aglycone was disrupted. Thus, the solubility of **3** (> 150 μg mL $^{-1}$; Table 3), **19a** (100 μg mL $^{-1}$), and **22** (> 130 μg mL $^{-1}$) was improved by a factor of ~10. However, for these more flexible derivatives, the expected optimized fit leading to improved affinities in the in-docking mode could not be observed. In fact, the affinities for the members of this

family of compounds are drastically decreased, for example, compounds **20** or **23** (Table 1).

Finally, the elongation of the ester-bearing *para* substituent (Table 1; compounds **31** and **35**) did not lead to the expected additional polar interaction with Arg98. Instead, a five- to sevenfold decrease in affinity was observed. Clearly, the desolvation penalty for the guanidinium group could not be matched by the geometrically possible salt bridge with the carboxylate of the antagonists **31** and **35**.

In summary, our study confirms the earlier selection of the FimH antagonists **5a** for oral and **5b** for intravenous application. However, the methoxy derivative **13d** (Table 1) shows slightly improved pharmacokinetic properties and therefore represents an additional candidate for future in vivo studies.

Experimental Section

General methods: NMR spectra were recorded on a Bruker Avance DMX-500 (500.1 MHz) spectrometer. Assignment of ^{1}H and ^{13}C NMR spectra was achieved using 2D methods (COSY, HSQC, HMBC). Chemical shifts are expressed in ppm using residual $CHCl_3$, CHD_2OD, or HDO as references. Optical rotations were measured with a PerkinElmer Polarimeter 341. Electrospray ionization mass spectrometry (ESI-MS) data were obtained on a Waters Micromass ZQ instrument. LC–HRMS analyses were carried out using an Agilent 1100 LC equipped with a photodiode array detector and a Micromass QTOF I equipped with a 4 GHz digital time converter. Microwave-assisted reactions were carried out with a CEM Discover and Explorer. Reactions were monitored by TLC using glass plates coated with silica gel 60 F_{254} (Merck) and visualized by UV light and/or by charring with a molybdate solution (0.02 M solution of ammonium cerium sulfate dihydrate and ammonium molybdate tetrahydrate in aqueous 10% H_2SO_4). MPLC separations were carried out on a CombiFlash Companion or R_f from Teledyne Isco equipped with RediSep normal-phase or RP-18 reversed-phase flash columns. LC–MS separations were carried out on a Waters system equipped with sample manager 2767, pump 2525, PDA 2525, and Micromass ZQ. Size-exclusion chromatography was performed on Bio-Gel P-2 Gel (45–90 mm) from Bio-Rad (Reinach, Switzerland). All compounds used for biological assays are at least of 98% purity based on analytical HPLC results. Commercially available reagents were purchased from Fluka, Aldrich, Alfa Aesar or Iris Biotech (Germany). Solvents were purchased from Sigma–Aldrich (Buchs, Switzerland) or Acros Organics (Geel, Belgium) and were dried prior to use where indicated. MeOH was dried by reflux with sodium methoxide and distilled immediately before use. CH_2Cl_2 was dried by filtration over Al_2O_3 (Fluka, type 5016 A basic). Molecular sieves (4 Å) were activated in vacuo at 500 °C for 1 h immediately before use.

General procedure A for the synthesis of mannosides 10a–f and 17a–c: To an ice-cold suspension of **8**[12] (200 mg, 0.57 mmol, 1.1 equiv), phenol **9a–f** or benzyl alcohol **16a–c** (0.52 mmol, 1.0 equiv), and molecular sieves (4 Å, 600 mg) in dry CH_2Cl_2 (5 mL), $BF_3{\cdot}Et_2O$ (0.3 mL, 2.44 mmol, 4.7 equiv) was added dropwise under argon. The mixture was stirred at 0 °C for 3 h, and then at RT overnight. The reaction mixture was filtered over Celite, and the filtrate was diluted with CH_2Cl_2 (50 mL), extracted with 0.5 N $NaOH_{(aq)}$ (50 mL), H_2O (50 mL), and brine (50 mL). The organic layer was dried over Na_2SO_4 and concentrated in vacuo. The residue was purified by MPLC on silica gel (petroleum ether (PE)/EtOAc) to yield **10a–f** or **17a–c**.

General procedure B for the synthesis of mannosylated biphenyls: A Schlenk tube was charged with aryl bromide (1.0 equiv), boronic acid or boronate (1.1 equiv), $Pd(dppf)Cl_2{\cdot}CH_2Cl_2$ (0.03 equiv), K_3PO_4 (1.5 equiv) and a stirring bar. The tube was closed with a rubber septum and was evacuated and flushed with argon. This procedure was repeated once, then anhydrous DMF (2 mL) was added under a stream of argon. The mixture was degassed in an ultrasonic bath and flushed with argon for 5 min, and then stirred at 80 °C overnight. The reaction mixture was cooled to RT, diluted with EtOAc (50 mL), and washed with H_2O (50 mL) and brine (50 mL). The organic layer was dried over Na_2SO_4 and concentrated in vacuo. The residue was purified by MPLC on silica gel (PE/EtOAc) to afford biphenyls **12a–f**, **18a,b**, **21**, **29** or **33**.

General procedure C for deacetylation: To a solution of **12a–f**, **18a,b**, **21**, **29** or **33** (1.0 equiv) in dry MeOH (5 mL) was added freshly prepared 1 M NaOMe/MeOH (0.1 equiv) under argon. The mixture was stirred at RT until the reaction was complete (monitored by TLC), then neutralized with Amberlyst-15 (H^+) ion-exchange resin, filtered and concentrated in vacuo. The residue was purified by MPLC on silica gel (CH_2Cl_2/MeOH, 10:1–8:1) to afford **13a–f**, **19a,b**, **22**, **30** or **34** as white solids.

General procedure D for saponification: To a solution of **12a–e**, **18a,b**, **21**, **29** or **33** (1.0 equiv) in MeOH (5 mL) was added 1 M NaOMe/MeOH (0.1 equiv) at RT. The reaction mixture was stirred at RT for 4 h and concentrated. The residue was treated with 0.5 M $NaOH_{(aq)}$ (1 mL) for 24 h at RT. The solution was then adjusted to pH 3–4 with Amberlyst-15 (H^+), and the mixture was filtered and concentrated. The crude product was transformed into the sodium salt by passing through a small column of Dowex 50X8 (Na^+ form) ion-exchange resin. After concentration, the residue was purified by MPLC (RP-18, H_2O/MeOH, 1:0–2:1) followed by size-exclusion chromatography (P-2 gel, H_2O) to give **14a–e**, **6**, **20**, **23**, **31** or **35** as white solids after final lyophilization from H_2O.

4-Bromo-2-fluorophenyl 2,3,4,6-tetra-*O*-acetyl-α-D-mannopyranoside (10a): Prepared according to general procedure A from **8**[12] and 4-bromo-2-fluorophenol (**9a**). Yield: 220 mg (74%) as white solid. R_f = 0.48 (PE/EtOAc, 2:1); $[\alpha]_D^{20}$ +83.0 (c = 0.70, EtOAc); ^{1}H NMR (500 MHz, $CDCl_3$): δ = 7.30 (dd, J = 2.3, 10.1 Hz, 1H, Ar-H), 7.21 (dt, J = 1.7, 8.8 Hz, 1H, Ar-H), 7.08 (t, J = 8.6 Hz, 1H, Ar-H), 5.54 (dd, J = 3.5, 10.0 Hz, 1H, H-3), 5.50 (dd, J = 1.8, 3.4 Hz, 1H, H-2), 5.46 (d, J = 1.5 Hz, 1H, H-1), 5.36 (t, J = 10.0 Hz, 1H, H-4), 4.26 (dd, J = 5.5, 12.2 Hz, 1H, H-6a), 4.17 (ddd, J = 2.1, 5.5, 10.0 Hz, 1H, H-5), 4.10 (dd, J = 2.2, 12.2 Hz, 1H, H-6b), 2.20, 2.07, 2.05, 2.04 ppm (4 s, 12H, 4 OAc); ^{13}C NMR (125 MHz, $CDCl_3$): δ = 170.51, 169.95, 169.82, 169.76 (4 CO), 153.28 (d, J = 251.4 Hz, Ar-C), 142.64 (d, J = 11.1 Hz, Ar-C), 127.58 (d, J = 4.0 Hz, Ar-C), 120.4 (d, J = 21.5 Hz, Ar-C), 120.28 (d, J = 0.9 Hz, Ar-C), 115.73 (d, J = 8.1 Hz, Ar-C), 97.49 (C-1), 69.76 (C-5), 69.15 (C-2), 68.60 (C-3), 65.76 (C-4), 62.09 (C-6), 20.87, 20.71, 20.69, 20.67 ppm (4 $COCH_3$); elemental analysis calcd (%) for $C_{20}H_{22}BrFO_{10}$: C 46.08, H 4.25, found: C 46.11, H 4.26.

4-Bromo-2-methylphenyl 2,3,4,6-tetra-*O*-acetyl-α-D-mannopyranoside (10b): Prepared according to general procedure A from **8**[12] and 4-bromo-2-methylphenol (**9b**). Yield: 254 mg (86%) as white solid. R_f = 0.60 (PE/EtOAc, 2:1); $[\alpha]_D^{20}$ +61.8 (c = 1.00, EtOAc); ^{1}H NMR (500 MHz, $CDCl_3$): δ = 7.31 (d, J = 1.9 Hz, 1H, Ar-H), 7.24 (dd, J = 2.3, 8.7 Hz, 1H, Ar-H), 6.97 (d, J = 8.8 Hz, 1H, Ar-H), 5.53 (dd, J = 3.4, 10.0 Hz, 1H, H-3), 5.47 (d, J = 1.7 Hz, 1H, H-1), 5.45 (dd, J = 2.0, 3.4 Hz, 1H, H-2), 5.37 (t, J = 10.0 Hz, 1H, H-4), 4.28 (dd, J = 5.6, 12.3 Hz, 1H, H-6a), 4.10–4.03 (m, 2H, H-5, H-6b), 2.27 (s, 3H, CH_3), 2.20, 2.06, 2.05, 2.04 ppm (4 s, 12H, 4 OAc); ^{13}C NMR (125 MHz, $CDCl_3$): δ = 170.53, 170.04, 169.96, 169.73 (4 CO), 152.96, 133.78,

129.88, 129.61, 115.81, 115.23 (Ar-C), 95.91 (C-1), 69.39 (C-5), 69.38 (C-2), 68.88 (C-3), 65.76 (C-4), 62.12 (C-6), 20.88, 20.70, 20.68 (4C, 4 $COCH_3$), 16.07 ppm (CH_3); elemental analysis calcd (%) for $C_{21}H_{25}BrO_{10}$: C 48.76, H 4.87, found: C 48.84, H 4.91.

4-Bromo-2-trifluoromethyl-phenyl 2,3,4,6-tetra-*O*-acetyl-α-D-mannopyranoside (10c): Prepared according to general procedure A from **8**[12] and 4-bromo-2-trifluoromethylphenol (**9c**). Yield: 260 mg (80%) as white solid. R_f=0.50 (PE/EtOAc, 2:1); $[\alpha]_D^{20}$ +64.6 (c=1.00, EtOAc); ^{1}H NMR (500 MHz, $CDCl_3$): δ=7.74 (d, J=2.3 Hz, 1H, Ar-H), 7.61 (dd, J=2.4, 8.9 Hz, 1H, Ar-H), 7.15 (d, J=8.9 Hz, 1H, Ar-H), 5.60 (d, J=1.6 Hz, 1H, H-1), 5.51 (dd, J=3.5, 10.1 Hz, 1H, H-3), 5.45 (dd, J=2.0, 3.3 Hz, 1H, H-2), 5.39 (t, J=10.1 Hz, 1H, H-4), 4.27 (dd, J=5.3, 12.4 Hz, 1H, H-6a), 4.08–4.00 (m, 2H, H-5, H-6b), 2.21, 2.06, 2.05, 2.04 ppm (4 s, 12H, 4 OAc); ^{13}C NMR (125 MHz, $CDCl_3$): δ=170.41, 169.91, 169.74, 169.62 (4 CO), 152.16 (d, J=1.7 Hz, Ar-C), 136.07 (Ar-C), 130.35 (t, J=5.3 Hz, Ar-C), 122.30 (d, J=271.4 Hz, CF_3), 121.72 (d, J=31.7 Hz, Ar-C), 117.08, 114.88 (Ar-C), 95.75 (C-1), 69.96 (C-5), 69.02 (C-2), 68.45 (C-3), 65.44 (C-4), 61.95 (C-6), 20.84, 20.70, 20.67, 20.63 ppm (4 $COCH_3$); elemental analysis calcd (%) for $C_{21}H_{22}BrF_3O_{10}$: C 44.15, H 3.88, found: C 44.10, H 3.88.

4-Bromo-2-methoxyphenyl 2,3,4,6-tetra-*O*-acetyl-α-D-mannopyranoside (10d): Prepared according to general procedure A from **8**[12] and 4-bromo-2-methoxyphenol (**9d**). Yield: 234 mg (77%) as white solid. R_f=0.32 (PE/acetone, 4:1); $[\alpha]_D^{20}$ +70.3 (c=0.70, EtOAc); ^{1}H NMR (500 MHz, $CDCl_3$): δ=7.03–6.95 (m, 3H, Ar-H), 5.58 (dd, J=3.5, 10.0 Hz, 1H, H-3), 5.52 (dd, J=1.8, 3.4 Hz, 1H, H-2), 5.42 (d, J=1.8 Hz, 1H, H-1), 5.34 (t, J=10.0 Hz, 1H, H-4), 4.28–4.24 (m, 2H, H-5, H-6a), 4.10 (m, 1H, H-6b), 3.84 (s, 3H, OCH_3), 2.19, 2.07, 2.05, 2.04 ppm (4 s, 12H, 4 OAc); ^{13}C NMR (125 MHz, $CDCl_3$): δ=170.58, 169.98, 169.89, 169.80 (4 CO), 151.52, 143.91, 123.49, 120.37, 116.69, 115.94 (Ar-C), 97.52 (C-1), 69.45 (C-5), 69.36 (C-2), 68.80 (C-3), 66.06 (C-4), 62.27 (C-6), 56.04 (OCH_3), 20.91, 20.73, 20.71, 20.69 ppm (4 $COCH_3$); elemental analysis calcd (%) for $C_{21}H_{25}BrO_{11}$: C 47.29, H 4.72, found: C 47.20, H 4.70.

4-Bromo-2-cyclopropylphenyl 2,3,4,6-tetra-*O*-acetyl-α-D-mannopyranoside (10e): Prepared according to general procedure A from **8**[12] and 4-bromo-2-cyclopropylphenol (**9e**). Yield: 235 mg (76%) as white solid. R_f=0.30 (PE/EtOAc, 3:1); $[\alpha]_D^{20}$ +64.7 (c=0.40, EtOAc); ^{1}H NMR (500 MHz, $CDCl_3$): δ=7.20 (d, J=8.7 Hz, 1H, Ar-H), 7.00–6.69 (m, 2H, Ar-H), 5.58 (d, J=10.1 Hz, 1H, H-3), 5.50 (s, 2H, H-1, H-2), 5.39 (t, J=10.1 Hz, 1H, H-4), 4.28 (dd, J=5.4, 12.2 Hz, 1H, H-6a), 4.14–4.08 (m, 2H, H-5, H-6b), 2.21, 2.09, 2.04 (3 s, 12H, 4 OAc), 1.02 (d, J=8.1 Hz, 2H, CH_2-*c*Pr), 0.65 ppm (d, J=4.6 Hz, 2H, CH_2-*c*Pr); ^{13}C NMR (125 MHz, $CDCl_3$): δ=170.54, 170.03, 170.15, 169.75 (4 CO), 153.64, 135.64, 129.11, 128.94, 116.29, 115.79 (Ar-C), 96.15 (C-1), 69.46 (C-5), 69.39 (C-2), 68.93 (C-3), 65.78 (C-4), 62.16 (C-6), 21.07, 20.89, 20.70 (4C, 4 $COCH_3$), 9.73, 7.88, 7.82 ppm (*c*Pr); elemental analysis calcd (%) for $C_{23}H_{27}BrFO_{10}$: C 50.84, H 5.01, found: C 50.82, H 5.00.

4-Bromo-2-cyanophenyl 2,3,4,6-tetra-*O*-acetyl-α-D-mannopyranoside (10f): Prepared according to general procedure A from **8**[12] and 4-bromo-2-cyanophenol (**9f**). Yield: 220 mg (73%) as white solid. R_f=0.51 (PE/EtOAc, 2:3); $[\alpha]_D^{20}$ +54.3 (c=0.60, EtOAc); IR (KBr): $\tilde{\nu}$=2232 (s, C≡N), 1749 cm^{-1} (vs, C=O); ^{1}H NMR (500 MHz, $CDCl_3$): δ=7.73 (d, J=2.5 Hz, 1H, Ar-H), 7.66 (dd, J=2.5, 9.0 Hz, 1H, Ar-H), 7.15 (d, J=9.0 Hz, 1H, Ar-H), 5.62 (d, J=1.7 Hz, 1H, H-1), 5.56 (dd, J=3.5, 10.0 Hz, 1H, H-3), 5.51 (dd, J=2.0, 3.4 Hz, 1H, H-2), 5.41 (t, J=10.0 Hz, 1H, H-4), 4.28 (dd, J=4.9, 12.1 Hz, 1H, H-6a), 4.13–4.08 (m, 2H, H-5, H-6b), 2.21, 2.07, 2.05, 2.04 ppm (4 s, 12H, 4 OAc); ^{13}C NMR (125 MHz, $CDCl_3$): δ=169.37, 168.93, 168.71, 168.48 (4 CO), 155.18, 136.28, 135.00, 116.12, 114.41, 112.97, 104.62 (Ar-C, CN), 95.68 (C-1), 69.26 (C-5), 68.02 (C-2), 67.35 (C-3), 64.38 (C-4), 60.85 (C-6), 19.81, 19.67, 19.64, 19.58 ppm (4 $COCH_3$); elemental analysis calcd (%) for $C_{21}H_{22}BrNO_{10}$: C 47.74, H 4.02, N 2.65, found: C 47.78, H 4.29, N 2.67.

Methyl 4′-(2,3,4,6-tetra-*O*-acetyl-α-D-mannopyranosyloxy)-3′-fluorobiphenyl-4-carboxylate (12a): Prepared according to general procedure B from **10a** (100 mg, 0.192 mmol), 4-methoxycarbonylphenylboronic acid (**11**, 38.0 mg, 0.211 mmol), $Pd(dppf)Cl_2{\cdot}CH_2Cl_2$ (4.7 mg, 5.8 μmol) and K_3PO_4 (61.1 mg, 0.288 mmol). Yield: 83 mg (75%) as white solid. R_f=0.26 (PE/EtOAc, 2:1); $[\alpha]_D^{20}$ +93.0 (c=0.60, EtOAc); ^{1}H NMR (500 MHz, $CDCl_3$): δ=8.03–8.02 (m, 2H, Ar-H), 7.53–7.52 (m, 2H, Ar-H), 7.33 (dd, J=2.1, 11.8 Hz, 1H, Ar-H), 7.27 (dd, J=1.5, 8.9 Hz, 1H, Ar-H), 7.20 (t, J=8.3 Hz, 1H, Ar-H), 5.53 (dd, J=3.4, 10.0 Hz, 1H, H-3), 5.49–5.47 (m, 2H, H-1, H-2), 5.32 (t, J=10.0 Hz, 1H, H-4), 4.22 (dd, J=5.4, 12.1 Hz, 1H, H-6a), 4.17 (m, 1H, H-5), 4.05 (dd, J=1.8, 12.1 Hz, 1H, H-6b), 3.87 (s, 3H, OCH_3), 2.15, 2.01, 1.98, 1.97 ppm (4 s, 12H, 4 OAc); ^{13}C NMR (125 MHz, $CDCl_3$): δ=170.54, 170.00, 169.86, 169.79, 166.82 (5 CO), 153.50 (d, J=247.0 Hz, Ar-C), 143.56 (d, J=1.8 Hz, Ar-C), 143.22 (d, J=11.2 Hz, Ar-C), 136.48 (d, J=6.7 Hz, Ar-C), 130.27, 129.29, 126.75 (5C, Ar-C), 123.16 (d, J=3.4 Hz, Ar-C), 119.32 (Ar-C), 115.64 (d, J=19.4 Hz, Ar-C), 97.42 (C-1), 69.71 (C-5), 69.26 (C-2), 68.70 (C-3), 65.83 (C-4), 62.10 (C-6), 52.24 (OMe), 20.91, 20.74, 20.72, 20.70 ppm (4 $COCH_3$); HRMS: *m/z*: calcd for $C_{28}H_{29}FNaO_{12}$ $[M+Na]^+$: 599.1535, found: 599.1536.

Methyl 4′-(2,3,4,6-tetra-*O*-acetyl-α-D-mannopyranosyloxy)-3′-methylbiphenyl-4-carboxylate (12b): Prepared according to general procedure B from **10b** (100 mg, 0.193 mmol), **11** (38.2 mg, 0.212 mmol), $Pd(dppf)Cl_2{\cdot}CH_2Cl_2$ (4.7 mg, 5.8 μmol) and K_3PO_4 (61.5 mg, 0.290 mmol). Yield: 87 mg (79%) as white solid. R_f=0.41 (PE/EtOAc, 1:0.9); $[\alpha]_D^{20}$ +85.4 (c=0.80, EtOAc); ^{1}H NMR (500 MHz, $CDCl_3$): δ=8.09–8.07 (m, 2H, Ar-H), 7.61 (m, 2H, Ar-H), 7.46 (d, J=1.8 Hz, 1H, Ar-H), 7.40 (dd, J=2.3, 8.5 Hz, 1H, Ar-H), 7.18 (d, J=8.5 Hz, 1H, Ar-H), 5.61–5.58 (m, 2H, H-1, H-3), 5.50 (dd, J=2.0, 3.5 Hz, 1H, H-2), 5.41 (t, J=10.0 Hz, 1H, H-4), 4.31 (dd, J=5.9, 12.8 Hz, 1H, H-6a), 4.14–4.09 (m, 2H, H-5, H-6b), 3.94 (s, 3H, OCH_3), 2.37 (s, 3H, CH_3), 2.22, 2.08, 2.05, 2.04 ppm (4 s, 12H, 4 OAc); ^{13}C NMR (125 MHz, $CDCl_3$): δ=170.55, 170.06, 169.98, 169.75, 167.00 (5 CO), 154.05, 144.94, 134.54, 130.10, 130.02, 128.54, 128.05, 126.66, 125.76, 114.46 (12C, Ar-C), 95.84 (C-1), 69.48 (C-5), 69.37 (C-2), 68.98 (C-3), 65.81 (C-4), 62.13 (C-6), 52.12 (OCH_3), 21.06, 20.91, 20.72, 20.70 (4 $COCH_3$), 16.40 ppm (CH_3); HRMS: *m/z*: calcd for $C_{29}H_{32}NaO_{12}$ $[M+Na]^+$: 595.1786, found: 595.1786; elemental analysis calcd (%) for $C_{29}H_{32}O_{12}$: C 60.84, H 5.63, found: C 60.76, H 5.80.

Methyl 4′-(2,3,4,6-tetra-*O*-acetyl-α-D-mannopyranosyloxy)-3′-trifluoromethylbiphenyl-4-carboxylate (12c): Prepared according to general procedure B from **10c** (100 mg, 0.175 mmol), **11** (34.6 mg, 0.193 mmol), $Pd(dppf)Cl_2{\cdot}CH_2Cl_2$ (4.3 mg, 5.3 μmol) and K_3PO_4 (55.7 mg, 0.263 mmol). Yield: 100 mg (91%) as white solid. R_f=0.25 (PE/EtOAc, 2:1); $[\alpha]_D^{20}$ +43.3 (c=1.00, EtOAc); ^{1}H NMR (500 MHz, $CDCl_3$): δ=8.13–8.11 (m, 2H, Ar-H), 7.87 (d, J=2.1 Hz, 1H, Ar-H), 7.75 (dd, J=2.2, 8.7 Hz, 1H, Ar-H), 7.63–7.61 (m, 2H, Ar-H), 7.35 (d, J=8.7 Hz, 1H, Ar-H), 5.70 (d, J=1.7 Hz, 1H, H-1), 5.57 (dd, J=3.5, 10.1 Hz, 1H, H-3), 5.50 (dd, J=2.0, 3.4 Hz, 1H, H-2), 5.43 (t, J=10.0 Hz, 1H, H-4), 4.30 (dd, J=5.6, 12.8 Hz, 1H, H-6a), 4.11–4.08 (m, 2H, H-5, H-6b), 3.95 (s, 3H, OCH_3), 2.24, 2.07, 2.06, 2.05 ppm (4 s, 12H, 4 OAc); ^{13}C NMR (125 MHz, $CDCl_3$): δ=170.45, 169.96, 169.78, 169.65, 166.76 (5 CO), 152.94, 143.37, 134.59, 130.34, 129.40, 126.79, 126.14, 115.79 (12C, Ar-C), 95.67 (C-1), 69.91 (C-5), 69.15 (C-2), 68.56 (C-3), 65.50 (C-4), 61.97 (C-6), 52.25 (OCH_3), 20.88, 20.71,

20.66 ppm (4C, 4 $COCH_3$); HRMS: *m/z*: calcd for $C_{29}H_{29}F_3NaO_{12}$ $[M+Na]^+$: 649.1503, found: 649.1503.

Methyl 4′-(2,3,4,6-tetra-*O*-acetyl-α-D-mannopyranosyloxy)-3′-methoxybiphenyl-4-carboxylate (12d): Prepared according to general procedure B from **10d** (100 mg, 0.188 mmol), **11** (37.1 mg, 0.206 mmol), $Pd(dppf)Cl_2{\cdot}CH_2Cl_2$ (4.6 mg, 5.6 μmol) and K_3PO_4 (59.9 mg, 0.282 mmol). Yield: 91 mg (83%) as white solid. R_f=0.25 (PE/EtOAc, 1:0.9); $[\alpha]_D^{20}$ +50.7 (*c*=1.40, EtOAc); ^{1}H NMR (500 MHz, $CDCl_3$): δ=8.10–8.08 (m, 2H, Ar-H), 7.62–7.60 (m, 2H, Ar-H), 7.19–7.13 (m, 3H, Ar-H), 5.64 (dd, *J*=3.5, 10.0 Hz, 1H, H-3), 5.58 (dd, *J*=1.8, 3.5 Hz, 1H, H-2), 5.53 (d, *J*=1.7 Hz, 1H, H-1), 5.38 (t, *J*=10.0 Hz, 1H, H-4), 4.34–4.28 (m, 2H, H-5, H-6a), 4.12 (m, 1H, H-6b), 3.94 (2 s, 6H, 2 OCH_3), 2.21, 2.08, 2.05, 2.04 ppm (4 s, 12H, 4 OAc); ^{13}C NMR (125 MHz, $CDCl_3$): δ=170.61, 170.02, 169.92, 169.83, 166.94 (5 CO), 151.01, 145.06, 144.92, 136.51, 130.13, 128.86, 126.87, 119.72, 119.32, 111.60 (12C, Ar-C), 97.50 (C-1), 69.48 (C-5), 69.43 (C-2), 68.91 (C-3), 66.12 (C-4), 62.29 (C-6), 56.01 (OCH_3), 52.18 (CO_2CH_3), 20.95, 20.76, 20.74, 20.72 ppm (4 $COCH_3$); HRMS: *m/z*: calcd for $C_{29}H_{32}NaO_{13}$ $[M+Na]^+$: 611.1735, found: 611.1736.

Methyl 4′-(2,3,4,6-tetra-*O*-acetyl-α-D-mannopyranosyloxy)-3′-cyclopropylbiphenyl-4-carboxylate (12e): Prepared according to general procedure B from **10e** (100 mg, 0.184 mmol), **11** (36.4 mg, 0.202 mmol), $Pd(dppf)Cl_2{\cdot}CH_2Cl_2$ (4.5 mg, 5.5 μmol) and K_3PO_4 (58.6 mg, 0.276 mmol). Yield: 60 mg (55%) as white solid. R_f=0.48 (PE/EtOAc, 2:1); $[\alpha]_D^{20}$ +53.0 (*c*=0.70, EtOAc); ^{1}H NMR (500 MHz, $CDCl_3$): δ=8.08–8.07 (m, 2H, Ar-H), 7.59–7.57 (m, 2H, Ar-H), 7.37 (dd, *J*=2.4, 8.5 Hz, 1H, Ar-H), 7.19–7.17 (m, 2H, Ar-H), 5.64 (dd, *J*=3.5, 10.1 Hz, 1H, H-3), 5.61 (d, *J*=1.6 Hz, 1H, H-1), 5.54 (dd, *J*=1.9, 3.4 Hz, 1H, H-2), 5.42 (t, *J*=10.1 Hz, 1H, H-4), 4.31 (dd, *J*=5.3, 12.2 Hz, 1H, H-6a), 4.19–4.10 (m, 2H, H-5, H-6b), 3.94 (s, 3H, OCH_3), 2.22 (s, 3H, OAc), 2.17 (m, 1H, H-*c*Pr), 2.08–2.05 (m, 9H, 3 OAc), 1.06–1.05 (m, 2H, CH_2-*c*Pr), 0.74–0.73 ppm (m, 2H, CH_2-*c*Pr); ^{13}C NMR (125 MHz, $CDCl_3$): δ=170.55, 170.06, 170.02, 169.75, 166.98 (5 CO), 154.76, 145.12, 134.83, 133.56, 130.08, 128.58, 126.71, 125.33, 125.06, 114.84 (12C, Ar-C), 96.04 (C-1), 69.49 (C-5), 69.42 (C-2), 69.02 (C-3), 65.81 (C-4), 62.15 (C-6), 52.12 (OCH_3), 20.91, 20.71 (4C, 4 $COCH_3$), 9.78, 7.58 ppm (3C, *c*Pr); elemental analysis calcd (%) for $C_{29}H_{32}O_{12}$: C 62.20, H 5.72, found: C 62.00, H 5.86.

Methyl 4′-(2,3,4,6-tetra-*O*-acetyl-α-D-mannopyranosyloxy)-3′-cyanobiphenyl-4-carboxylate (12f): Prepared according to general procedure B from **10f** (100 mg, 0.189 mmol), **11** (37.5 mg, 0.208 mmol), $Pd(dppf)Cl_2{\cdot}CH_2Cl_2$ (4.6 mg, 5.7 μmol) and K_3PO_4 (60.2 mg, 0.284 mmol). Yield: 92 mg (84%) as white solid. R_f=0.18 (PE/EtOAc, 2:1); $[\alpha]_D^{20}$ +61.4 (*c*=0.80, EtOAc); ^{1}H NMR (500 MHz, $CDCl_3$): δ=8.06–8.05 (m, 2H, Ar-H), 7.80 (d, *J*=2.3 Hz, 1H, Ar-H), 7.72 (dd, *J*=2.3, 8.8 Hz, 1H, Ar-H), 7.53–7.51 (m, 2H, Ar-H), 7.28 (d, *J*=8.8 Hz, 1H, Ar-H), 5.64 (d, *J*=1.7 Hz, 1H, H-1), 5.55 (dd, *J*=3.5, 10.0 Hz, 1H, H-3), 5.49 (dd, *J*=1.9, 3.4 Hz, 1H, H-2), 5.37 (t, *J*=10.0 Hz, 1H, H-4), 4.24 (dd, *J*=5.0, 12.4 Hz, 1H, H-6a), 4.12 (ddd, *J*=2.2, 4.9, 10.0 Hz, 1H, H-5), 4.05 (dd, *J*=2.2, 12.4 Hz, 1H, H-6b), 3.88 (s, 3H, OCH_3), 2.16, 2.01, 1.99, 1.98 ppm (4 s, 12H, 4 OAc); ^{13}C NMR (125 MHz, $CDCl_3$): δ=170.45, 170.01, 169.78, 169.54, 166.65 (5 CO), 156.84, 142.44, 135.67, 132.36, 129.77, 126.76, 115.99, 115.18, 104.47 (13C, Ar-C, CN), 96.63 (C-1), 70.24 (C-5), 69.17 (C-2), 68.49 (C-3), 65.48 (C-4), 60.85 (C-6), 20.88, 20.73, 20.71, 20.64 ppm (4 $COCH_3$); HRMS: *m/z*: calcd for $C_{29}H_{29}NNaO_{12}$ $[M+Na]^+$: 606.1582, found: 606.1583.

Methyl 3′-fluoro-4′-(α-D-mannopyranosyloxy)biphenyl-4-carboxylate (13a): Prepared according to general procedure C from **12a** (33 mg, 0.057 mmol). Yield: 15 mg (65%). $[\alpha]_D^{20}$ +114.3 (*c*=0.30, MeOH); ^{1}H NMR (500 MHz, CD_3OD): δ=7.98–7.97 (m, 2H, Ar-H), 7.63–7.61 (m, 2H, Ar-H), 7.42–7.36 (m, 3H, Ar-H), 5.45 (d, *J*=1.7 Hz, 1H, H-1), 3.99 (dd, *J*=1.9, 3.4 Hz, 1H, H-2), 3.82–3.84 (m, 4H, H-3, OCH_3), 3.71–3.56 ppm (m, 4H, H-4, H-5, H-6); ^{13}C NMR (125 MHz, CD_3OD): δ=168.34 (CO), 154.75 (d, *J*=243.8 Hz, Ar-C), 145.6 (2C, Ar-C), 136.37 (d, *J*=6.9 Hz, Ar-C), 130.20, 129.20, 127.80, 124.33, 120.33 (7C, Ar-C), 116.00 (d, *J*=20.0 Hz, Ar-C), 101.40 (C-1), 75.97 (C-5), 72.31 (C-3), 71.82 (C-2), 68.18 (C-4), 62.65 (C-6), 52.65 ppm (OCH_3); HRMS: *m/z*: calcd for $C_{20}H_{21}FNaO_8$ $[M+Na]^+$: 431.1113, found: 431.1112.

Methyl 4′-(α-D-mannopyranosyloxy)-3′-methylbiphenyl-4-carboxylate (13b): Prepared according to general procedure C from **12b** (31 mg, 0.054 mmol). Yield: 16 mg (73%). $[\alpha]_D^{20}$ +110.5 (*c*=0.35, MeOH); ^{1}H NMR (500 MHz, CD_3OD): δ=7.96–7.94 (m, 2H, Ar-H), 7.60–7.58 (m, 2H, Ar-H), 7.40–7.37 (m, 2H, Ar-H), 7.22 (d, *J*=8.5 Hz, 1H, Ar-H), 5.47 (d, *J*=1.6 Hz, 1H, H-1), 3.97 (dd, *J*=1.9, 3.4 Hz, 1H, H-2), 3.87 (dd, *J*=3.4, 9.5 Hz, 1H, H-3), 3.82 (s, 3H, OMe), 3.67–3.52 (m, 3H, H-4, H-6), 3.46 (m, 1H, H-5), 2.21 ppm (s, 3H, Me); ^{13}C NMR (125 MHz, CD_3OD): δ=168.56 (CO), 156.20, 146.86, 134.70, 131.07, 130.07, 130.54, 129.45, 128.92, 127.63, 126.85, 115.83 (12C, Ar-C), 99.76 (C-1), 75.55 (C-5), 72.64 (C-3), 72.11 (C-2), 68.31 (C-4), 62.68 (C-6), 52.59 ppm (OCH_3), 16.54 (CH_3); HRMS: *m/z*: calcd for $C_{21}H_{24}NaO_8$ $[M+Na]^+$: 427.1363, found: 427.1370.

Methyl 3′-trifluoromethyl-4′-(α-D-mannopyranosyloxy)biphenyl-4-carboxylate (13c): Prepared according to general procedure C from **12c** (30 mg, 0.048 mmol). Yield: 14 mg (64%). $[\alpha]_D^{20}$ +113.1 (*c*=0.40, MeOH); ^{1}H NMR (500 MHz, CD_3OD): δ=8.11–8.10 (m, 2H, Ar-H), 7.92–7.90 (m, 2H, Ar-H), 7.75–7.73 (m, 2H, Ar-H), 7.63 (d, *J*=8.4 Hz, 1H, Ar-H), 5.69 (d, *J*=1.5 Hz, 1H, H-1), 4.09 (dd, *J*=1.8, 3.3 Hz, 1H, H-2), 3.98–3.94 (m, 4H, H-3, OMe), 3.79–3.73 (m, 3H, H-4, H-6), 3.61 ppm (ddd, *J*=2.3, 5.7, 9.6 Hz, 1H, H-5); ^{13}C NMR (125 MHz, CD_3OD): δ=168.29 (CO), 155.54, 145.13, 134.74, 133.45, 131.36, 131.29, 130.32, 127.91, 127.85, 126.44, 117.80 (Ar-C), 100.27 (C-1), 76.13 (C-5), 72.24 (C-3), 71.74 (C-2), 68.09 (C-4), 62.67 ppm (C-6), 52.69 (OMe); HRMS: *m/z*: calcd for $C_{21}H_{21}F_3NaO_8$ $[M+Na]^+$: 481.1081, found: 481.1082.

Methyl 4′-(α-D-mannopyranosyloxy)-3′-methoxybiphenyl-4-carboxylate (13d): Prepared according to general procedure C from **12d** (32 mg, 0.055 mmol). Yield: 12 mg (52%). $[\alpha]_D^{20}$ +133.1 (*c*=0.20, MeOH); ^{1}H NMR (500 MHz, CD_3OD): δ=7.97–7.96 (m, 2H, Ar-H), 7.63–7.61 (m, 2H, Ar-H), 7.21–7.11 (m, 3H, Ar-H), 5.37 (d, *J*=1.7 Hz, 1H, H-1), 4.00 (dd, *J*=1.8, 3.4 Hz, 1H, H-2), 3.86 (dd, *J*=3.5, 8.8 Hz, 1H, H-3), 3.82 (s, 6H, 2 CH_3), 3.70–3.63 ppm (m, 4H, H-4, H-5, H-6); ^{13}C NMR (125 MHz, CD_3OD): δ=168.50 (CO), 152.33, 147.40, 146.83, 136.56, 131.08, 129.76, 127.87, 120.86, 120.10, 112.54 (Ar-C), 101.51 (C-1), 75.66 (C-5), 72.40 (C-2), 72.00 (C-3), 68.34 (C-4), 62.70 (C-6), 56.61 (OMe), 52.63 ppm (OMe); HRMS: *m/z*: calcd for $C_{21}H_{24}NaO_9$ $[M+Na]^+$: 443.1313, found: 443.1315.

Methyl 3′-cyclopropyl-4′-(α-D-mannopyranosyloxy)biphenyl-4-carboxylate (13e): Prepared according to general procedure C from **12e** (21 mg, 0.035 mmol). Yield: 10 mg (67%). $[\alpha]_D^{20}$ +101.6 (*c*=0.24, MeOH); ^{1}H NMR (500 MHz, CD_3OD): δ=8.07–8.05 (m, 2H, Ar-H), 7.68–7.67 (m, 2H, Ar-H), 7.46 (dd, *J*=2.4, 8.5 Hz, 1H, Ar-H), 7.33 (d, *J*=8.5 Hz, 1H, Ar-H), 7.21 (d, *J*=2.4 Hz, 1H, Ar-H), 5.60 (d, *J*=1.7 Hz, 1H, H-1), 4.13 (dd, *J*=1.9, 3.3 Hz, 1H, H-2), 4.02 (dd, *J*=3.4, 9.5 Hz, 1H, H-3), 3.93 (s, 3H, OMe), 3.81–3.74 (m, 3H, H-4, H-6), 3.69 (m, 1H, H-5), 2.19 (m, 1H, H-*c*Pr), 1.01–0.99 (m, 2H, CH_2-*c*Pr), 0.76–0.74 ppm (m, 2H, CH_2-*c*Pr); ^{13}C NMR (125 MHz, CD_3OD): δ=168.54 (CO), 156.92, 146.98, 135.00, 134.59, 131.07, 127.34, 127.67, 126.39, 125.34, 116.29 (12C, Ar-C), 100.14 (C-1), 75.61 (C-5), 72.64 (C-3), 72.14 (C-2), 68.33 (C-4), 62.71 (C-6), 52.60 (OCH_3), 10.93,

8.06 ppm (3C, *c*Pr); HRMS: *m/z*: calcd for $C_{23}H_{26}NaO_8$ $[M+Na]^+$: 453.1520, found: 453.1519.

Methyl 3′-cyano-4′-(α-D-mannopyranosyloxy)biphenyl-4-carboxylate (13 f): Prepared according to general procedure C from **12 f** (37 mg, 0.063 mmol). Yield: 19 mg (73%). $[\alpha]_D^{20}$ +101.1 (*c*=0.30, MeOH); ^{1}H NMR (500 MHz, CD_3OD): δ=8.00–7.99 (m, 2H, Ar-H), 7.90–7.85 (m, 2H, Ar-H), 7.65–7.63 (m, 2H, Ar-H), 7.50 (d, *J*=8.8 Hz, 1H, Ar-H), 5.63 (s, 1H, H-1), 4.03 (m, 1H, H-2), 3.91 (dd, *J*=2.8, 9.4 Hz, 1H, H-3), 3.83 (s, 3H, OMe), 3.69–3.60 (m, 3H, H-4, H-6), 3.50 ppm (m, 1H, H-5); ^{13}C NMR (125 MHz, CD_3OD): δ=168.22 (CO), 159.29, 144.38, 135.61, 134.50, 133.08, 131.31, 130.56, 127.87, 117.36, 116.75, 104.35 (13C, Ar-C, CN), 100.62 (C-1), 76.39 (C-5), 72.27 (C-2), 71.62 (C-3), 68.07 (C-4), 62.64 (C-6), 52.71 ppm (OMe); HRMS: *m/z*: calcd for $C_{21}H_{21}NNaO_8$ $[M+Na]^+$: 438.1159, found: 438.1162.

Sodium 3′-fluoro-4′-(α-D-mannopyranosyloxy)biphenyl-4-carboxylate (14 a): Prepared according to general procedure D from **12 a** (50 mg, 0.087 mmol). Yield: 21 mg (58%). $[\alpha]_D^{20}$ +112.7 (*c*=0.40, MeOH); ^{1}H NMR (500 MHz, D_2O): δ=7.78–7.77 (m, 2H, Ar-H), 7.46–7.45 (m, 2H, Ar-H), 7.30–7.15 (m, 3H, Ar-H), 5.43 (s, 1H, H-1), 4.07 (s, 1H, H-2), 3.93 (d, *J*=3.3 Hz, 1H, H-3), 3.68–3.62 ppm (m, 4H, H-4, H-5, H-6); ^{13}C NMR (125 MHz, D_2O): δ=175.19 (CO), 153.02 (d, *J*=242.6 Hz, Ar-C), 142.52 (d, *J*=10.8 Hz, Ar-C), 141.23 (Ar-C), 135.53 (d, *J*=6.4 Hz, Ar-C), 135.07, 129.43, 126.25, 126.01, 122.96, 119.13 (Ar-C), 114.83 (d, *J*=19.4 Hz, Ar-C), 99.32 (C-1), 73.65 (C-5), 70.23 (C-3), 69.67 (C-2), 66.35 (C-4), 60.52 ppm (C-6); HRMS: *m/z*: calcd for $C_{19}H_{19}FNaO_8$ $[M+Na]^+$: 417.0956, found: 417.0957.

Sodium 4′-(α-D-mannopyranosyloxy)-3′-methylbiphenyl-4-carboxylate (14 b): Prepared according to general procedure D from **12 b** (46 mg, 0.081 mmol). Yield: 5 mg (15%). $[\alpha]_D^{20}$ +85.7 (*c*=0.20, MeOH); ^{1}H NMR (500 MHz, D_2O): δ=7.78–7.76 (m, 2H, Ar-H), 7.53–7.52 (m, 2H, Ar-H), 7.43–7.37 (m, 2H, Ar-H), 7.10 (d, *J*=8.6 Hz, 1H, Ar-H), 5.52 (d, *J*=1.6 Hz, 1H, H-1), 4.07 (dd, *J*=1.9, 3.4 Hz, 1H, H-2), 3.95 (dd, *J*=3.5, 9.6 Hz, 1H, H-3), 3.63–3.50 (m, 4H, H-4, H-5, H-6), 2.14 ppm (s, 3H, CH_3); ^{13}C NMR (125 MHz, D_2O): δ=153.33, 142.57, 134.59, 133.97, 129.47, 128.42, 126.25, 125.43, 114.99 (12C, Ar-C), 97.46 (C-1), 73.39 (C-5), 70.54 (C-3), 69.88 (C-2), 66.53 (C-4), 60.60 (C-6), 15.31 ppm (CH_3); HRMS: *m/z*: calcd for $C_{20}H_{22}NaO_8$ $[M+Na]^+$: 413.1207, found: 413.1209.

Sodium 3′-trifluoromethyl-4′-(α-D-mannopyranosyloxy)biphenyl-4-carboxylate (14 c): Prepared according to general procedure D from **12 c** (45 mg, 0.072 mmol). Yield: 25 mg (74%). $[\alpha]_D^{20}$ +94.2 (*c*=0.30, MeOH); ^{1}H NMR (500 MHz, D_2O): δ=7.83–7.81(m, 3H, Ar-H), 7.75 (d, *J*=8.7 Hz, 1H, Ar-H), 7.57–7.55 (m, 2H, Ar-H), 7.31 (d, *J*=8.8 Hz, 1H, Ar-H), 5.64 (s, 1H, H-1), 4.09 (d, *J*=1.5 Hz, 1H, H-2), 3.94 (dd, *J*=3.4, 9.7 Hz, 1H, H-3), 3.67–3.60 (m, 3H, H-4, H-6), 3.54 ppm (m, 1H, H-5); ^{13}C NMR (125 MHz, D_2O): δ=175.25 (CO), 152.40, 141.31, 135.09, 133.53, 131.93, 129.46, 126.34, 125.59, 115.86 (12C, Ar-C), 97.20 (C-1), 73.68 (C-5), 70.19 (C-3), 69.58 (C-2), 66.36 (C-4), 60.55 ppm (C-6); HRMS: *m/z*: calcd for $C_{20}H_{19}F_3NaO_8$ $[M+Na]^+$: 467.0924, found: 467.0923.

Sodium 4′-(α-D-mannopyranosyloxy)-3′-methoxybiphenyl-4-carboxylate (14 d): Prepared according to general procedure D from **12 d** (47 mg, 0.080 mmol). Yield: 10 mg (29%). $[\alpha]_D^{20}$ +115.1 (*c*=0.30, MeOH); ^{1}H NMR (500 MHz, D_2O): δ=7.81–7.79 (m, 2H, Ar-H), 7.54–7.53 (m, 2H, Ar-H), 7.19–7.11 (m, 3H, Ar-H), 5.43 (d, *J*=1.6 Hz, 1H, H-1), 4.10 (dd, *J*=1.8, 3.5 Hz, 1H, H-2), 3.96 (dd, *J*=3.5, 9.0 Hz, 1H, H-3), 3.78 (s, 3H, OCH_3), 3.70–3.62 ppm (m, 4H, H-4, H-5, H-6); ^{13}C NMR (125 MHz, D_2O): δ=175.24 (CO), 149.53, 144.24, 142.42, 135.59, 134.75, 129.40, 126.41, 119.86, 118.03, 111.44 (12C, Ar-C), 99.23 (C-1), 73.53 (C-5), 70.32 (C-3), 69.78 (C-2), 66.40 (C-4), 60.54 (C-6), 55.81 ppm (OCH_3); HRMS: *m/z*: calcd for $C_{20}H_{22}NaO_9$ $[M+Na]^+$: 429.1156, found: 429.1154.

Sodium 3′-cyclopropyl-4′-(α-D-mannopyranosyloxy)biphenyl-4-carboxylate (14 e): Prepared according to general procedure D from **12 e** (28 mg, 0.047 mmol). Yield: 6 mg (26%). $[\alpha]_D^{20}$ +149.8 (*c*=0.20, MeOH); ^{1}H NMR (500 MHz, D_2O): δ=7.79–7.77 (m, 2H, Ar-H), 7.48–7.46 (m, 2H, Ar-H), 7.30 (d, *J*=7.8 Hz, 1H, Ar-H), 7.07–7.05 (m, 2H, Ar-H), 5.52 (s, 1H, H-1), 4.10 (m, 1H, H-2), 3.98 (dd, *J*=3.4, 9.5 Hz, 1H, H-3), 3.69–3.62 (m, 4H, H-4, H-5, H-6), 1.99 (m, 1H, H-*c*Pr), 0.86–0.84 (m, 2H, CH_2-*c*Pr), 0.58–0.56 ppm (m, 2H, CH_2-*c*Pr); ^{13}C NMR (125 MHz, D_2O): δ=175.34 (CO), 153.82, 142.58, 134.57, 134.34, 133.74, 129.38, 126.26, 125.01, 124.01, 115.47 (12C, Ar-C), 97.88 (C-1), 73.47 (C-5), 70.55 (C-3), 69.93 (C-2), 66.46 (C-4), 60.57 (C-6), 9.16, 7.26, 7.06 ppm (*c*Pr); HRMS: *m/z*: calcd for $C_{22}H_{24}ONaO_8$ $[M+Na]^+$: 439.1363, found: 439.1363.

Sodium 3′-cyano-4′-(α-D-mannopyranosyloxy)biphenyl-4-carboxylate (14 f): A two-neck flask was charged with **10 f** (150 mg, 0.28 mmol), 4-carboxybenzene boronic acid pinacol ester (**15**) (77 mg, 0.31 mmol), Pd(dppf)Cl_2·CH_2Cl_2 (7 mg, 0.008 mmol), K_3PO_4 (89 mg, 0.42 mmol) and a stirring bar. The flask was evacuated and flushed with argon, then anhydrous DMF (2 mL) was added under a stream of argon. The mixture was degassed in an ultrasonic bath and flushed with argon for 5 min, and then stirred at 80 °C overnight. The reaction mixture was cooled to RT, diluted with EtOAc (50 mL), and washed with H_2O (50 mL) and brine (50 mL). The organic layer was dried over Na_2SO_4 and concentrated in vacuo. The residue was purified by MPLC on silica gel (CH_2Cl_2/MeOH, 10:1–8:1) to afford the biphenyl intermediate (162 mg). The intermediate was dissolved in dry MeOH (4 mL) and treated with freshly prepared 1 M NaOMe/MeOH (28 μL) for 4 h at RT. The reaction mixture was neutralized with Amberlyst-15 (H^+), filtered and concentrated. The crude product was transformed into the sodium salt by passing through a small column of Dowex 50X8 (Na^+ form) ion-exchange resin. After concentration the residue was purified by MPLC (RP-18, H_2O) followed by size-exclusion chromatography (P-2 gel, H_2O) to give **14 f** (19 mg, 17%) as a white solid after final lyophilization from H_2O. $[\alpha]_D^{20}$ +75.3 (*c*=0.20, MeOH); ^{1}H NMR (500 MHz, D_2O): δ=7.86–7.79 (m, 4H, Ar-H), 7.53–7.52 (m, 2H, Ar-H), 7.31 (d, *J*=8.9 Hz, 1H, Ar-H), 5.64 (d, *J*=1.9 Hz, 1H, H-1), 4.11 (dd, *J*=1.9, 3.4 Hz, 1H, H-2), 4.00 (dd, *J*=3.5, 9.7 Hz, 1H, H-3), 3.73–3.65 (m, 3H, H-4, H-6), 3.58 ppm (ddd, *J*=2.4, 5.5, 9.9 Hz, 1H, H-5); ^{13}C NMR (125 MHz, D_2O): δ=175.12 (CO), 156.82, 140.37, 134.39, 133.56, 131.83, 129.58, 126.25, 116.82, 115.78, 102.08 (13C, Ar-C, CN), 98.09 (C-1), 73.97 (C-5), 70.29 (C-3), 69.54 (C-2), 66.36 (C-4), 60.56 ppm (C-6); HRMS: *m/z*: calcd for $C_{21}H_{21}NNaO_8$ $[M+Na]^+$: 424.1003, found: 424.1003.

3-Bromobenzyl 2,3,4,6-tetra-*O*-acetyl-α-D-mannopyranoside (17 a): Prepared according to general procedure A from **8**[12] and 3-bromobenzyl alcohol (**16 a**). Yield: 100 mg (34%) as colorless oil. R_f=0.43 (PE/EtOAc, 2:1); $[\alpha]_D^{20}$ +42.0 (*c*=1.40, EtOAc); ^{1}H NMR (500 MHz, $CDCl_3$): δ=7.48–7.46, 7.30–7.24 (m, 4H, Ar-H), 5.37 (dd, 1H, *J*=3.4, 10.1 Hz, H-3), 5.33–5.29 (m, 2H, H-2, H-4), 4.88 (d, 1H, *J*=1.3 Hz, H-1), 4.68, 4.54 (A, B of AB, *J*=12.1 Hz, 2H, CH_2Ar), 4.29 (dd, 1H, *J*=5.2, 12.3 Hz, H-6a), 4.07 (dd, 1H, *J*=2.3, 12.3 Hz, H-6b), 3.99 (ddd, 1H, *J*=2.4, 5.2, 9.9 Hz, H-5), 2.15, 2.13, 2.05, 2.00 ppm (4 s, 12H, 4 OAc); ^{13}C NMR (125 MHz, $CDCl_3$): δ=170.59, 169.98, 169.87, 169.69 (4 CO), 138.49, 131.34, 131.09, 130.24, 126.66, 122.57 (Ar-C), 96.83 (C-1), 69.43, 69.02, 68.90, 68.78 (C-2, C-3, C-5, CH_2Ar), 66.03 (C-4), 62.36 (C-6), 20.86, 20.76, 20.68 ppm (4C, $COCH_3$); ESI-MS: *m/z*: calcd for $C_{21}H_{25}BrNaO_{10}$ $[M+Na]^+$: 539.05, found: 539.14.

5-Bromo-2-chlorobenzyl 2,3,4,6-tetra-*O*-acetyl-α-D-mannopyranoside (17b): Prepared according to general procedure A from **8**[12] and 5-bromo-2-chlorobenzyl alcohol (**16b**). Yield: 152 mg (48%) as a white solid. R_f=0.56 (PE/EtOAc, 2:1); $[\alpha]_D^{20}$ +48.0 (*c*=1.50, EtOAc); ^{1}H NMR (500 MHz, $CDCl_3$): δ=7.48 (t, *J*=1.8 Hz, 1H, Ar-H), 7.38 (s, 1H, Ar-H), 7.35 (d, *J*=1.8 Hz, 1H, Ar), 5.33 (m, 3H, H-2, H-3, H-4), 4.88 (d, *J*=1.5 Hz, 1H, H-1), 4.65, 4.51 (A, B of AB, *J*=12.3 Hz, 2H, CH_2Ar), 4.30 (dd, *J*=5.3, 12.3 Hz, 1H, H-6a), 4.09 (dd, *J*=2.4, 12.3 Hz, 1H, H-6b), 3.98 (ddd, *J*=2.4, 5.2, 9.7 Hz, 1H, H-5), 2.16, 2.13, 2.05, 2.01 ppm (4s, 12H, 4 OAc); ^{13}C NMR (125 MHz, $CDCl_3$): δ=170.58, 169.98, 169.89, 169.69 (4 CO), 139.77, 135.35, 129.25, 126.85, 122.91 (6C, Ar-C), 96.96 (C-1), 69.33, 68.93, 68.24 (4C, C-2, C-3, C-5, CH_2Ar), 65.98 (C-4), 62.38 (C-6), 20.86, 20.77, 20.68 ppm (4C, 4$COCH_3$); ESI-MS: *m/z*: calcd for $C_{21}H_{24}BrClNaO_{10}$ $[M+Na]^+$: 573.01, found: 573.06.

2-Bromobenzyl 2,3,4,6-tetra-*O*-acetyl-α-D-mannopyranoside (17c): Prepared according to general procedure A from **8**[12] and 2-bromobenzyl alcohol (**16c**). Yield: 140 mg (47%) as a white solid. R_f=0.55 (petrol ether/EtOAc, 2:1); $[\alpha]_D^{20}$ +44.6 (*c*=2.10, EtOAc); ^{1}H NMR (500 MHz, $CDCl_3$): δ=7.57 (dd, *J*=1.0, 8.0 Hz, 1H, Ar-H), 7.47 (dd, *J*=1.4, 7.6 Hz, 1H, Ar-H), 7.35 (td, *J*=1.1, 7.5 Hz, 1H, Ar-H), 7.20 (td, *J*=1.7, 7.9 Hz, 1H, Ar-H), 5.41 (dd, *J*=3.5, 10.0 Hz, 1H, H-3), 5.35 (dd, *J*=1.8, 3.5 Hz, 1H, H-2), 5.31 (t, *J*=9.9 Hz, 1H, H-4), 4.98 (d, *J*=1.6 Hz, 1H, H-1), 4.83, 4.61 (A, B of AB, *J*=12.7 Hz, 2H, CH_2Ar), 4.29 (dd, *J*=5.8, 12.6 Hz, 1H, H-6a), 4.10–4.06 (m, 2H, H-6b, H-5), 2.17, 2.12, 2.04, 2.00 ppm (4s, 12H, 4 OAc); ^{13}C NMR (125 MHz, $CDCl_3$): δ=170.64, 170.02, 169.88, 169.72 (4 CO), 135.77, 132.69, 129.58, 129.49, 127.64, 122.96 (Ar-C), 97.33 (C-1), 69.48, 69.30, 69.10, 68.84 (C-2, C-3, C-5, CH_2Ar), 66.05 (C-4), 62.35 (C-6), 20.88, 20.76, 20.69 ppm (4C, 4$COCH_3$); ESI-MS: *m/z*: calcd for $C_{21}H_{25}BrNaO_{10}$ $[M+Na]^+$: 539.05, found: 539.14.

Methyl 3′-[(2,3,4,6-tetra-*O*-acetyl-α-D-mannopyranosyloxy)methyl]biphenyl-4-carboxylate (18a): Prepared according to general procedure B from **17a** (87.0 mg, 0.167 mmol), **11** (33.1 mg, 0.184 mmol), Pd(dppf)Cl_2·CH_2Cl_2 (4.1 mg, 5.0 μmol) and K_3PO_4 (53.2 mg, 0.251 mmol). Yield: 70 mg (73%) as colorless oil. R_f=0.30 (PE/EtOAc, 2:1); $[\alpha]_D^{20}$ +41.2 (*c*=1.00, EtOAc); ^{1}H NMR (500 MHz, $CDCl_3$): δ=8.13–8.11 (m, 2H, Ar-H), 7.68–7.67 (m, 2H, Ar-H), 7.60–7.58 (m, 2H, Ar-H), 7.48 (t, *J*=4.7 Hz, 1H, Ar-H), 7.39 (d, *J*=7.7 Hz, 1H, Ar-H), 5.41 (dd, *J*=3.4, 10.0 Hz, 1H, H-3), 5.33–5.30 (m, 2H, H-2, H-4), 4.94 (d, *J*=1.5 Hz, 1H, H-1), 4.79, 4.64 (A, B of AB, *J*=12.0 Hz, 2H, CH_2Ar), 4.30 (dd, *J*=5.0, 12.1 Hz, 1H, H-6a), 4.09–4.03 (m, 2H, H-6b, H-5), 3.94 (s, 3H, OMe), 2.15, 2.11, 2.04, 2.00 ppm (4s, 12H, 4 OAc); ^{13}C NMR (125 MHz, $CDCl_3$): δ=170.64, 170.03, 169.91, 169.73, 166.94 (5 CO), 145.11, 140.41, 136.97, 130.15, 129.27, 129.09, 127.94, 127.22, 127.11 (12C, Ar-C), 96.76 (C-1), 69.57, 69.09, 68.94, 66.12 (C-2, C-3, C-5, CH_2Ar), 62.40 (C-4), 60.38 (C-6), 52.15 (OMe), 20.89, 20.77, 20.69 ppm (4C, 4$COCH_3$); ESI-MS: *m/z*: calcd for $C_{29}H_{32}NaO_{12}$ $[M+Na]^+$: 595.18, found: 595.21.

Methyl 3′-[(2,3,4,6-tetra-*O*-acetyl-α-D-mannopyranosyloxy)methyl]-4′-chlorobiphenyl-4-carboxylate (18b): Prepared according to general procedure B from **17b** (143 mg, 0.260 mmol), **11** (51.5 mg, 0.286 mmol), Pd(dppf)Cl_2·CH_2Cl_2 (6.4 mg, 7.8 μmol) and K_3PO_4 (82.8 mg, 0.390 mmol). Yield: 133 mg (84%) as colorless oil. R_f=0.30 (PE/EtOAc, 2:1); $[\alpha]_D^{20}$ +45.9 (*c*=1.20, EtOAc); ^{1}H NMR (500 MHz, $CDCl_3$): δ=8.13–8.11 (m, 2H, Ar-H), 7.65–7.64 (m, 2H, Ar-H), 7.57 (t, *J*=1.8 Hz, 1H, Ar-H), 7.47 (s, 1H, Ar-H), 7.37 (s, 1H, Ar-H), 5.40 (dd, *J*=3.4, 10.1 Hz, 1H, H-3), 5.33–5.29 (m, 2H, H-2, H-4), 4.93 (d, *J*=1.4 Hz, 1H, H-1), 4.76, 4.61 (A, B of AB, *J*=12.1 Hz, 2H, CH_2Ar), 4.31 (dd, *J*=5.2, 12.3 Hz, 1H, H-6a), 4.11 (dd, *J*=2.3, 12.3 Hz, 1H, H-6b), 4.03 (ddd, *J*=2.4, 5.2, 9.9 Hz, 1H, H-5), 3.95 (s, 3H, OMe), 2.16, 2.12, 2.05, 2.00 ppm (4s, 12H, 4OAc); ^{13}C NMR (125 MHz, $CDCl_3$): δ=170.61, 170.02, 169.90, 169.72, 166.75 (5 CO), 143.68, 142.16, 138.79, 135.11, 130.26, 129.68, 127.14, 125.14 (12C, Ar-C), 96.85 (C-1), 68.99, 68.89, 68.85, 66.07 (C-2, C-3, C-5, CH_2Ar), 62.42 (C-4), 60.39 (C-6), 52.23 (OMe), 20.89, 20.78, 20.71, 20.69 ppm (4$COCH_3$); ESI-MS: *m/z*: calcd for $C_{29}H_{31}ClNaO_{12}$ $[M+Na]^+$: 629.14, found: 629.10.

Methyl 2′-[(2,3,4,6-tetra-*O*-acetyl-α-D-mannopyranosyloxy)methyl]biphenyl-4-carboxylate (21): Prepared according to general procedure B from **17c** (115 mg, 0.223 mmol), **11** (44.1 mg, 0.245 mmol), Pd(dppf)Cl_2·CH_2Cl_2 (5.5 mg, 6.7 μmol) and K_3PO_4 (71.0 mg, 0.335 mmol). Yield: 120 mg (94%) as colorless oil. R_f=0.41 (PE/EtOAc, 2:1); $[\alpha]_D^{20}$ +38.3 (*c*=2.00, EtOAc); ^{1}H NMR (500 MHz, $CDCl_3$): δ=8.11–8.10 (m, 2H, Ar-H), 7.51–7.48 (m, 1H, Ar-H), 7.45–7.41 (m, 4H, Ar-H), 7.29 (m, 1H, Ar-H), 5.27–5.21 (m, 2H, H-3, H-4), 5.19 (dd, *J*=1.9, 3.3 Hz, 1H, H-2), 4.77 (d, *J*=1.4 Hz, 1H, H-1), 4.67, 4.34 (A, B of AB, *J*=11.3 Hz, 2H, CH_2Ar), 4.13 (dd, *J*=5.2, 12.5 Hz, 1H, H-6a), 3.94 (s, 3H, OMe), 3.90 (dd, *J*=2.2, 12.3 Hz, 1H, H-6a), 3.52 (ddd, *J*=2.2, 5.1, 9.3 Hz, 1H, H-5), 2.13, 2.05, 2.04, 1.99 ppm (4s, 12H, 4 OAc); ^{13}C NMR (125 MHz, $CDCl_3$): δ=170.52, 169.95, 169.82, 169.74, 166.77 (5 CO), 145.48, 141.44, 133.46, 129.99, 129.91, 129.58, 129.22, 128.52, 128.21 (12C, Ar-C), 97.20 (C-1), 69.47 (C-2), 68.98 (C-3), 68.48 (C-5), 68.13 (CH_2Ar), 65.88 (C-4), 62.15 (C-6), 52.18 (OMe), 20.85, 20.66, 20.62 ppm (4C, 4$COCH_3$); ESI-MS: *m/z*: calcd for $C_{29}H_{32}NaO_{12}$ $[M+Na]^+$: 595.18, found: 595.21.

Methyl 3′-[(α-D-mannopyranosyloxy)methyl]biphenyl-4-carboxylate (19a): Prepared according to general procedure C from **18a** (24 mg, 0.042 mmol). Yield: 11 mg (65%). R_f=0.40 (CH_2Cl_2/MeOH, 8:1); $[\alpha]_D^{20}$ +68.0 (*c*=0.34, MeOH); ^{1}H NMR (500 MHz, CD_3OD): δ=8.11–8.09 (m, 2H, Ar-H), 7.77–7.75 (m, 2H, Ar-H), 7.70 (s, 1H, Ar-H), 7.63 (d, *J*=7.6 Hz, 1H, Ar-H), 7.49 (t, *J*=7.6 Hz, 1H, Ar-H), 7.45 (d, *J*=7.6 Hz, 1H, Ar-H), 4.90 (d, *J*=1.8 Hz, 1H, H-1), 4.86, 4.63 (A, B of AB, *J*=12.0 Hz, 2H, CH_2Ar), 3.94 (s, 3H, OMe), 3.89–3.87 (m, 2H, H-2, H-3), 3.79–3.73 (m, 2H, H-4, H-6a), 3.68–3.64 ppm (m, 2H, H-5, H-6b); ^{13}C NMR (125 MHz, CD_3OD): δ=168.42 (CO), 146.91, 141.31, 139.97, 131.13, 130.20, 129.07, 128.17, 127.91, 127.67 (12C, Ar-C), 100.76 (C-1), 75.02 (C-5), 72.65 (C-3), 72.22 (C-2), 69.73 (CH_2Ar), 68.65 (C-4), 62.98 (C-6), 52.66 ppm (OMe); HRMS: *m/z*: calcd for $C_{21}H_{24}NaO_8$ $[M+Na]^+$: 427.1363, found: 427.1361.

Methyl 4′-chloro-3′-[(α-D-mannopyranosyloxy)methyl]biphenyl-4-carboxylate (19b): Prepared according to general procedure C from **18b** (40 mg, 0.066 mmol). Yield: 26 mg (90%). R_f=0.19 (CH_2Cl_2/MeOH, 8:1); $[\alpha]_D^{20}$ +101.8 (*c*=0.50, MeOH); ^{1}H NMR (500 MHz, CD_3OD): δ=8.06 (d, *J*=8.4 Hz, 2H, Ar-H), 7.69 (d, *J*=8.4 Hz, 2H, Ar-H), 7.57–7.56 (m, 2H, Ar-H), 7.41 (s, 1H, Ar-H), 4.87 (s, 1H, H-1), 4.80, 4.58 (A, B of AB, *J*=12.3 Hz, 2H, CH_2Ar), 3.91 (s, 3H, OMe), 3.87–3.83 (m, 2H, H-2, H-3), 3.74–3.57 ppm (m, 4H, H-4, H-5, H-6); ^{13}C NMR (125 MHz, CD_3OD): δ=168.74 (CO), 145.78, 143.68, 142.71, 136.55, 131.75, 131.31, 129.02, 128.77, 127.95, 126.63 (12C, Ar-C), 101.47 (C-1), 75.65 (C-5), 73.16 (C-3), 72.65 (C-2), 69.49 (CH_2Ar), 69.13 (C-4), 63.49 (C-6), 53.26 ppm (OMe); HRMS: *m/z*: calcd for $C_{21}H_{23}ClNaO_8$ $[M+Na]^+$: 461.0974, found: 461.0975.

Methyl 2′-[(α-D-mannopyranosyloxy)methyl]biphenyl-4-carboxylate (22): Prepared according to general procedure C from **21** (48 mg, 0.084 mmol). Yield: 16 mg (47%). R_f=0.42 (CH_2Cl_2/MeOH, 8:1); $[\alpha]_D^{20}$ +61.9 (*c*=0.90, MeOH); ^{1}H NMR (500 MHz, CD_3OD): δ=8.11–8.09 (m, 2H, Ar-H), 7.57 (m, 1H, Ar-H), 7.51–7.49 (m, 2H, Ar-H), 7.43–7.40 (m, 2H, Ar-H), 7.31 (m, 1H, Ar-H), 4.71 (A of AB, *J*=11.4 Hz, 1H, CH_2Ar), 4.70 (d, *J*=1.5 Hz, 1H, H-1), 4.38 (B of AB, *J*=11.4 Hz, 1H, CH_2Ar), 3.75–3.60 (m, 5H, H-2, H-3, H-4, H-6), 3.95 (s, 3H, OMe), 3.40 ppm (ddd, *J*=3.0, 5.6, 6.8 Hz, 1H, H-5); ^{13}C NMR

(125 MHz, CD_3OD): δ=168.42 (CO), 147.33, 142.66, 136.03, 130.83, 130.53, 130.47, 129.26, 129.15 (12C, Ar-C), 101.14 (C-1), 74.78 (C-5), 72.60 (C-3), 72.18 (C-2), 68.37 (2C, C-4, CH_2Ar), 62.71 ppm (C-6), 52.69 (OMe); HRMS: *m/z*: calcd for $C_{21}H_{24}NaO_8Na$ $[M+Na]^+$: 427.1363, found: 427.1367.

Sodium 3′-[(α-D-mannopyranosyloxy)methyl]biphenyl-4-carboxylate (6): Prepared according to general procedure D from **18a** (35 mg, 0.061 mmol). Yield: 24 mg (96%). $[\alpha]_D^{20}$ +64.5 (*c*=0.30, MeOH/H_2O 1:1); ^1H NMR (500 MHz, D_2O): δ=7.80–7.78 (m, 2H, Ar-H), 7.50–7.43 (m, 4H, Ar-H), 7.31–7.24 (m, 2H, Ar-H), 4.82 (s, 1H, H-1), 4.58, 4.40 (A, B of AB, *J*=11.5 Hz, 2H, CH_2Ar), 3.82 (m, 1H, H-2), 3.75–3.50 ppm (m, 5H, H-3, H-4, H-5, H-6); ^{13}C NMR (125 MHz, D_2O): δ=175.14 (CO), 142.69, 140.05, 137.34, 135.01, 129.46, 129.28, 127.92, 126.87, 126.64 (12C, Ar-C), 99.40 (C-1), 72.84 (C-5), 70.51 (C-3), 70.01 (C-2), 69.29 (CH_2Ar), 66.61 (C-4), 60.71 ppm (C-6); HRMS: *m/z*: calcd for $C_{20}H_{22}NaO_8$ $[M+Na]^+$: 413.1207, found: 413.1211.

Sodium 4′-chloro-3′-[(α-D-mannopyranosyloxy)methyl]biphenyl-4-carboxylate (20): Prepared according to general procedure D from **18b** (54 mg, 0.089 mmol). Yield: 4 mg (10%). $[\alpha]_D^{20}$ +44.7 (*c*=0.30, MeOH); ^1H NMR (500 MHz, D_2O): δ=7.86 (d, *J*=7.8 Hz, 2H, Ar-H), 7.58–7.56 (m, 3H, Ar-H), 7.46, 7.34 (2 s, 2H, Ar-H), 4.90 (s, 1H, H-1), 4.58, 4.50 (A, B of AB, *J*=12.3 Hz, 2H, CH_2Ar), 3.91 (s, 1H, H-2), 3.78–3.75 (m, 2H, H-3, H-4), 3.71–3.59 ppm (m, 3H, H-5, H-6); ^{13}C NMR (125 MHz, D_2O): δ=174.76 (CO), 141.82, 141.55, 139.40, 134.37, 129.56, 127.34, 126.74, 126.62, 125.15 (12C, Ar-C), 99.99 (C-1), 72.96 (C-5), 70.55 (C-3), 70.04 (C-2), 68.72 (CH_2Ar), 66.66 (C-4), 60.77 ppm (C-6); HRMS: *m/z*: calcd for $C_{20}H_{21}ClNaO_8$ $[M+Na]^+$: 447.0817, found: 447.0816.

Sodium 2′-[(α-D-mannopyranosyloxy)methyl]biphenyl-4-carboxylate (23): Prepared according to general procedure D from **21** (78 mg, 0.137 mmol). Yield: 26 mg (46%). $[\alpha]_D^{20}$ +53.2 (*c*=0.40, MeOH); ^1H NMR (500 MHz, D_2O): δ=7.91–7.89 (m, 2H, Ar-H), 7.43–7.34 (m, 5H, Ar-H), 7.26 (m, 1H, Ar-H), 4.68 (s, 1H, H-1), 4.57, 4.31 (A, B of AB, *J*=10.8 Hz, 2H, CH_2Ar), 3.57 (m, 1H, H-2), 3.46–3.39 (m, 4H, H-3, H-4, H-6), 2.83 ppm (m, 1H, H-5); ^{13}C NMR (125 MHz, D_2O): δ=173.20 (CO), 144.48, 141.80, 133.47, 132.43, 130.69, 129.95, 129.27, 128.96, 128.32 (12C, Ar-C), 99.90 (C-1), 72.44 (C-5), 70.33 (C-3), 69.82 (C-2), 68.14 (CH_2Ar), 65.99 (C-4), 60.25 ppm (C-6); HRMS: *m/z*: calcd for $C_{20}H_{22}NaO_8$ $[M+Na]^+$: 413.1207, found: 413.1208.

4-(4,4,5,5-Tetramethyl)-1,3,2-dioxaborolan-2-yl)phenyl 2,3,4,6-tetra-*O*-acetyl-α-D-mannopyranoside (27): A microwave tube was charged with **26**[37] (240 mg, 0.55 mmol), KOAc (161 mg, 1.65 mmol), bis(pinacolato)diborone (152 mg, 0.60 mmol) and Pd(dppf)Cl_2·CH_2Cl_2 (13 mg, 0.017 mmol). The tube was closed, evacuated and flushed with argon. Then anhydrous DMF (1 mL) was added under a stream of argon. The mixture was degassed in an ultrasonic bath and flushed with argon for 5 min, and then heated by microwave irradiation at 120 °C for 2 h. The reaction mixture was cooled to RT and diluted with CH_2Cl_2/H_2O (100 mL, 1:1). The organic layer was washed with H_2O (50 mL) and brine (50 mL), dried over Na_2SO_4 and concentrated. The residue was purified by MPLC (toluene/EtOAc, 4:1) to afford **27** (120 mg, 50%) as colorless oil. $[\alpha]_D^{20}$ +58.1 (*c*=0.60, EtOAc); ^1H NMR (500 MHz, $CDCl_3$): δ=7.76 (d, *J*=8.6 Hz, 2H, Ar-H), 7.08 (d, *J*=8.6 Hz, 2H, Ar-H), 5.58–5.55 (m, 2H, H-1, H-3), 5.45 (dd, *J*=1.9, 3.4 Hz, 1H, H-2), 5.37 (t, *J*=10.0 Hz, 1H, H-4), 4.28 (dd, *J*=5.0, 12.0 Hz, 1H. H-6a), 4.05–4.02 (m, 2H, H-6b, H-5), 2.20, 2.05, 2.03 (3 s, 12H, 4 OAc), 1.33 ppm (s, 12H, 4 CH_3); ^{13}C NMR (125 MHz, $CDCl_3$): δ=170.55, 169.91, 169.74 (4C, 4 CO), 157.98, 136.62, 136.58, 115.67 (5C, Ar-C), 95.44 (C-1), 83.77 (Ar-C), 69.37 (C-2), 69.21 (C-5), 68.87 (C-3), 65.92 (C-4), 62.06 (C-6), 24.86, 24.58 (4C, 4 CH_3), 20.87, 20.69 ppm (4C, 4$COCH_3$); ESI-MS: *m/z*: calcd for $C_{26}H_{35}BNaO_{12}$ $[M+Na]^+$: 573.21, found: 573.32.

Methyl 2-[4′-(2,3,4,6-tetra-*O*-acetyl-α-D-mannopyranosyloxy)biphenyl-4-yl]acetate (29): Prepared according to general procedure B from methyl 2-(4-bromophenyl)acetate (**28**, 41.2 mg, 0.180 mmol), **27** (109 mg, 0.198 mmol), Pd(dppf)Cl_2·CH_2Cl_2 (4.4 mg, 5.4 μmol) and K_3PO_4 (57.3 mg, 0.270 mmol). Yield: 35 mg (34%) as yellow oil. R_f=0.25 (petrol ether/EtOAc 2:1); $[\alpha]_D^{20}$ +75.09 (*c*=0.8, EtOAc); ^1H NMR (500 MHz, $CDCl_3$): δ=7.52–7.49 (m, 4H, Ar-H), 7.35–7.33 (m, 2H, Ar-H), 7.17–7.14 (m, 2H, Ar-H), 5.60–5.56 (m, 2H, H-1, H-3), 5.47 (dd, *J*=1.8, 3.5 Hz, 1H, H-2), 5.38 (t, *J*=10.0 Hz, 1H, H-4), 4.29 (dd, *J*=5.0, 11.9 Hz, 1H, H-6a), 4.15–4.08 (m, 2H, H-6b, H-5), 3.71 (s, 3H, OMe), 3.66 (s, 2H, $ArCH_2$), 2.21, 2.06, 2.05, 2.03 ppm (4 s, 12H, 4 OAc); ^{13}C NMR (125 MHz, $CDCl_3$): δ=171.99, 170.53, 169.99, 169.95, 169.76 (5 CO), 155.09, 139.26, 135.72, 132.83, 129.73, 128.21, 127.03, 116.82 (12C, Ar-C), 95.87 (C-1), 69.43 (C-2), 69.23 (C-5), 68.91 (C-3), 65.99 (C-4), 62.15 (C-6), 52.11 (OMe), 40.78 ($ArCH_2$), 20.88, 20.71, 20.70, 20.67 ppm (4$COCH_3$); ESI-MS: *m/z*: calcd for $C_{29}H_{32}NaO_{12}$ $[M+Na]^+$: 595.18, found: 595.21.

Methyl 2-[4′-(2,3,4,6-tetra-*O*-acetyl-α-D-mannopyranosyloxy)biphenyl-4-yl]cyclopropanecarboxylate (33): Prepared according to general procedure B from methyl 1-(4-bromophenyl)cyclopropanecarboxylate (**32**, 42.6 mg, 0.167 mmol), **27** (101 mg, 0.184 mmol), Pd(dppf)Cl_2·CH_2Cl_2 (4.1 mg, 5.0 μmol) and K_3PO_4 (53.2 mg, 0.251 mmol). Yield: 60 mg (56%) as colorless oil. R_f=0.31 (PE/EtOAc, 2:1); $[\alpha]_D^{20}$ +70.2 (*c*=1.00, EtOAc); ^1H NMR (500 MHz, $CDCl_3$): δ=7.54–7.48 (m, 4H, Ar-H), 7.40–7.39 (m, 2H, Ar-H), 7.17–7.14 (m, 2H, Ar-H), 5.59 (dd, *J*=3.55, 10.1 Hz, 1H, H-3), 5.56 (d, *J*=1.6 Hz, 1H, H-1), 5.46 (dd, *J*=1.9, 3.5 Hz, 1H, H-2), 5.38 (t, *J*=10.0 Hz, 1H, H-4), 4.29 (dd, *J*=5.1, 12.0 Hz, 1H, H-6a), 4.15–4.09 (m, 2H, H-6b, H-5), 3.65 (s, 3H, OMe), 2.21, 2.06, 2.05, 2.03 (4 s, 12H, 4 OAc), 1.64–1.62 (m, 2H, *c*Pr), 1.27–1.16 ppm (m, 2H, *c*Pr); ^{13}C NMR (125 MHz, $CDCl_3$): δ=175.04, 170.53, 169.98, 169.95, 169.75 (5 CO), 155.10, 139.25, 138.43, 135.76, 130.94, 128.24, 126.61, 116.80 (12C, Ar-C), 95.89 (C-1), 69.44 (C-5), 69.23 (C-2), 68.90 (C-3), 66.00 (C-4), 62.15 (C-6), 52.42 (OMe), 28.67 (*c*Pr), 20.71, 20.68 (4C, 4$COCH_3$), 16.75 ppm (*c*Pr); ESI-MS: *m/z*: calcd for $C_{31}H_{34}NaO_{12}$ $[M+Na]^+$: 621.19, found: 621.26.

Methyl 2-[4′-(α-D-mannopyranosyloxy)biphenyl-4-yl]acetate (30): Prepared according to general procedure C from **29** (30 mg, 0.052 mmol). Yield: 20 mg (95%). R_f=0.25 (CH_2Cl_2/MeOH, 8:1); $[\alpha]_D^{20}$ +116.0 (*c*=0.50, MeOH); ^1H NMR (500 MHz, CD_3OD): δ=7.57–7.53 (m, 4H, Ar-H), 7.34–7.33 (m, 2H, Ar-H), 7.22–7.20 (m, 2H, Ar-H), 5.54 (d, *J*=1.5 Hz, 1H, H-1), 4.05 (dd, *J*=1.8, 3.3 Hz, 1H, H-2), 3.95 (dd, *J*=3.4, 9.5 Hz, 1H, H-3), 3.82–3.74 (m, 3H, H-4, H-6), 3.71 (s, 3H, OMe), 3.66 (s, 2H, $ArCH_2$), 3.65 ppm (ddd, *J*=2.5, 5.2, 9.7 Hz, 1H, H-5); ^{13}C NMR (125 MHz, CD_3OD): δ=174.02 (CO), 157.50, 140.77, 136.22, 134.29, 130.81, 129.00, 127.77, 118.13 (12C, Ar-C), 100.23 (C-1), 75.42 (C-5), 72.45 (C-3), 72.03 (C-2), 68.38 (C-4), 62.70 (C-6), 52.49 (OMe), 41.34 ppm ($ArCH_2$); HRMS: *m/z*: calcd for $C_{21}H_{24}NaO_8$ $[M+Na]^+$: 427.1363, found: 427.1363.

Methyl 2-[4′-(α-D-mannopyranosyloxy)biphenyl-4-yl]cyclopropanecarboxylate (34): Prepared according to general procedure C from **33** (38 mg, 0.063 mmol). Yield: 9 mg (33%). R_f=0.33 (CH_2Cl_2/MeOH, 8:1); $[\alpha]_D^{20}$ +108.0 (*c*=0.30, MeOH); ^1H NMR (500 MHz, CD_3OD): δ=7.46–7.39 (m, 4H, Ar-H), 7.28–7.26 (m, 2H, Ar-H), 7.10–7.07 (m, 2H, Ar-H), 5.42 (d, *J*=1.7 Hz, 1H, H-1), 3.93 (dd, *J*=1.9, 3.4 Hz, 1H, H-2), 3.82 (dd, *J*=3.4, 9.4 Hz, 1H, H-3), 3.69–3.61 (m, 3H, H-4, H-6), 3.53 (m, 4H, OMe, H-5), 1.49–1.47 (m, 2H, *c*Pr), 1.14–1.11 ppm (m, 2H, *c*Pr); ^{13}C NMR (125 MHz, CD_3OD): δ=157.50, 140.87, 139.51, 136.26, 132.03, 129.04, 127.43, 118.11 (12C, Ar-C),

100.20 (C-1), 75.43 (C-5), 72.42 (C-3), 72.02 (C-2), 68.34 (C-4), 62.68 (C-6), 52.81 (OMe), 17.20 ppm (2C, *c*Pr); HRMS: *m/z*: calcd for $C_{23}H_{26}NaO_8$ $[M+Na]^+$: 453.1520, found: 453.1523.

Sodium 2-[4′-(α-D-mannopyranosyloxy)biphenyl-4-yl]acetate (31): Prepared according to general procedure D from **29** (59 mg, 0.103 mmol). Yield: 17 mg (40%). $[\alpha]_D^{20}$ +94.0 (*c*=0.20, MeOH/H_2O 1:1); ^1H NMR (500 MHz, D_2O): δ=7.61 (d, *J*=8.6 Hz, 2H, Ar-H), 7.55 (d, *J*=8.0 Hz, 2H, Ar-H), 7.31 (d, *J*=8.0 Hz, 2H, Ar-H), 7.19 (d, *J*=8.6 Hz, 2H, Ar-H), 5.60 (s, 1H, H-1), 4.13 (m, 1H, H-2), 4.00 (dd, *J*=3.2, 8.5 Hz, 1H, H-3), 3.75–3.67 (m, 4H, H-4, H-5, H-6), 3.51 ppm (s, 2H, $ArCH_2$); ^{13}C NMR (125 MHz, D_2O): δ=154.94, 137.93, 136.29, 135.08, 129.76, 128.07, 126.72, 117.49 (12C, Ar-C), 98.20 (C-1), 73.37 (C-5), 70.40 (C-3), 69.89 (C-2), 66.58 (C-4), 60.65 (C-6), 43.89 ppm ($ArCH_2$); HRMS: *m/z*: calcd for $C_{20}H_{22}NaO_8$ $[M+Na]^+$: 413.1207, found: 413.1208.

Sodium 2-[4′-(α-D-mannopyranosyloxy)biphenyl-4-yl]cyclopropanecarboxylate (35): Prepared according to general procedure D from **33** (59 mg, 0.099 mmol). Yield: 10 mg (23%). $[\alpha]_D^{20}$ +95.0 (*c*=0.20, dioxane/H_2O 1:1); ^1H NMR (500 MHz, D_2O): δ=7.62–7.60 (m, 2H, Ar-H), 7.54–7.53 (m, 2H, Ar-H), 7.38–7.19 (m, 4H, Ar-H), 5.60 (s, 1H, H-1), 4.13 (m, 1H, H-2), 4.00 (m, 1H, H-3), 3.75–3.67 (4H, H-4, H-5, H-6), 1.33 (s, 2H, *c*Pr), 1.01 ppm (s, 2H, *c*Pr); ^{13}C NMR (125 MHz, D_2O): δ=128.67, 126.10, 124.37, 115.47 (12C, Ar-C), 96.18 (C-1), 71.35 (C-5), 68.38 (C-3), 67.87 (C-2), 64.56 (C-4), 58.62 (C-6), 12.66 ppm (2C, *c*Pr); HRMS: *m/z*: calcd for $C_{22}H_{24}NaO_8$ $[M+Na]^+$: 439.1363, found: 439.1363.

Competitive binding assay

A recombinant protein consisting of the CRD of FimH linked with a thrombin cleavage site (Th) to a His_6-tag (FimH-CRD-Th-His_6) was expressed in *E. coli* strain HM125 and purified by affinity chromatography.[16] To determine the affinity of the various FimH antagonists, a competitive binding assay described previously[16] was applied. Microtiter plates (F96 MaxiSorp, Nunc) were coated with a 10 μg mL^{-1} solution of FimH-CRD-Th-His_6 in 20 mM HEPES, 150 mM NaCl, and 1 mM $CaCl_2$, pH 7.4 (assay buffer), 100 μL per well, overnight at 4 °C. The coating solution was discarded, and the wells were blocked with 3% BSA in assay buffer (150 μL per well) for 2 h at 4 °C. After three washing steps with assay buffer (150 μL per well), a fourfold serial dilution of the test compound (50 μL per well) in assay buffer containing 5% DMSO and streptavidin-peroxidase coupled Man-α(1–3)[Man-α(1–6)]-Man-β(1–4)-Glc*N*Ac-β(1–4)-Glc*N*Acβ polyacrylamide (TM-PAA) polymer (50 μL per well of a 0.5 μg mL^{-1} solution) were added. On each individual microtiter plate, *n*-heptyl α-D-mannopyranoside (**1**) was tested in parallel. The plates were incubated for 3 h at 25 °C and 350 rpm and then carefully washed four times with 150 μL per well assay buffer. After the addition of 100 μL per well of 2,2′-azino-di-(3-ethylbenzthiazoline-6-sulfonic acid) (ABTS) substrate, the colorimetric reaction was allowed to develop for 4 min and then was stopped by the addition of 2% aqueous oxalic acid before the optical density (OD) was measured at 415 nm on a microplate reader (Spectramax 190, Molecular Devices, CA, USA). The IC_{50} values of the compounds tested in duplicate were calculated with Prism software (GraphPad Software Inc., La Jolla, CA, USA). The IC_{50} defines the molar concentration of the test compound that decreases the maximal specific binding of TM-PAA polymer to FimH-CRD by 50%. The relative IC_{50} (rIC_{50}) is the ratio of the IC_{50} of the test compound to the IC_{50} of *n*-heptyl α-D-mannopyranoside (**1**).

Cell-based flow cytometry assay

The assay was performed as described previously.[17] Briefly, 5637 cells (DSMZ, Braunschweig, Germany) were grown to confluence in 24-well plates. Before infection, a serial dilution of test compound in 5% DMSO, PBS (Sigma–Aldrich) was prepared. GFP-labeled UTI89 bacteria (200 μL) in RPMI 1640 medium (Invitrogen, Basel, Switzerland) were pre-incubated with test compound (25 μL) for 10 min at RT. The bacteria–antagonist mixtures were then added to the monolayers of 5637 cells. The multiplicity of infection (MOI) was 1:50 (cell/bacteria). To homogenize the infection, plates were centrifuged at RT for 3 min at 600 *g*. After an incubation time of 1.5 h at 37 °C, infected cells were washed four times with RPMI 1640 medium and suspended in ice-cold PBS for 5–20 min (treatment with ice-cold PBS results in the detachment of the infected cells). Cells were then kept in the dark until analysis. Samples were measured with a CyAn ADP flow cytometer (Beckman–Coulter, Brea, CA, USA) and analyzed by gating on the eukaryotic cells based on forward (FSC) and side scatter (SSC), which excludes unbound labeled bacteria and debris from analysis. A total of 10^4 cells were measured per sample. Data were acquired in a linear mode for the SSC and logarithmic mode for FSC and the green fluorescent channel FL1-H (GFP). The mean fluorescence intensity (MFI) of GFP was counted as a surrogate marker for the adherence of bacteria. Quantification of adhesion was evaluated with the FlowJo software 9.0.1 (Tree Star Inc., Ashland, OR, USA). IC_{50} values were determined by plotting the concentration of the antagonist in a logarithmic mode versus the MFI and by fitting the curve with Prism software (GraphPad, inhibition curve, variable slope), (n=2–3, in duplicate/triplicate).

Isothermal titration calorimetry (ITC)

For the ITC experiments, the His tag in FimH-CRD-Th-His_6 was cleaved.[16] Briefly, the protein (1 mg) was incubated with 10 U thrombin (T-6884, Sigma–Aldrich) in 20 mM Tris·HCl, pH 8.4, 150 mM NaCl and 2.5 mM $CaCl_2$ (cleavage buffer) at 20 °C for 16 h. The mixture was then applied to a gel filtration column (Bio-Prep SE100/17, Bio-Rad) attached to an FPLC system. The chromatography was run with assay buffer and analyzed by SDS-PAGE. The fractions containing FimH-CRD were pooled and concentrated by ultrafiltration (MWCO10, Sartorius AG, Tagelswangen, Switzerland).

The ITC experiments were performed using a VP-ITC instrument from MicroCal Inc. (GE Healthcare, Northampton, MA, USA). The measurements were performed at 25 °C. Prior to measurements, the protein was dialyzed in assay buffer (10 mM HEPES, 150 mM NaCl, 1 mM $CaCl_2$, pH 7.4 (HBS-Ca). Injections of 3–5 μL ligand solutions (150 μM) were added at an interval of 10 min into the sample cell solution containing FimH-CRD (8–22 μM, sample cell volume 1.4523 mL) with stirring at 307 rpm. Protein concentration was determined by HPLC-UV against a BSA standard.[38] The quantity $c = Mt(0)\ K_D^{-1}$, where $Mt(0)$ is the initial macromolecule concentration, is of importance in titration microcalorimetry. The c values ranged between 300 and 3200. Because the smallest reliable volumes were injected, sigmoidal curves were obtained. Control experiments injecting ligand solution into buffer without protein showed that the heat of dilution was small and constant. Baseline correction and peak integration were accomplished using Origin 7 as described by the manufacturer (OriginLab, Northampton, MA, USA). The first injection was always excluded from data analysis because it usually suffers from sample loss during the mounting of the syringe and the equilibration preceding the actual titration. A three-parameter (N (stoichiometry), K_D (dissociation constant) and ΔH° (change in enthalpy) nonlinear least-square data fitting was per-

formed in a Microsoft Excel spreadsheet using the Solver add-in (Frontline System)[39,40] according to binding isotherms published by Ziegler and Seelig.[41]

Thermodynamics parameters were calculated from Equation (4).

$$\Delta G = \Delta H - T\Delta S = RT \ln K_D = -RT \ln K_A \quad (4)$$

where ΔG, ΔH, and ΔS are the changes in free energy, enthalpy, and entropy of binding, respectively, T is the absolute temperature, and R is the universal gas constant (8.314 J mol^{-1}K^{-1}).

Determination of pharmacokinetic parameters

Materials: Dimethyl sulfoxide (DMSO), 1-octanol, Dulbecco's modified Eagle's medium (DMEM) high glucose, L-glutamine solution, penicillin–streptomycin solution, Dulbecco's phosphate-buffered saline (DPBS), and trypsin–EDTA solution were purchased from Sigma–Aldrich. MEM nonessential amino acid (MEM-NEAA) solution, fetal bovine serum (FBS), and DMEM without sodium pyruvate and phenol red were bought from Invitrogen. PAMPA System Solution, GIT-0 Lipid Solution, and Acceptor Sink Buffer were ordered from pion (Woburn, MA, USA). Acetonitrile (MeCN) was bought from Acros Organics. The Caco-2 cells were kindly provided by Prof. G. Imanidis, FHNW, Muttenz, Switzerland and originated from the American Type Culture Collection (Rockville, MD, USA).

Parallel artificial membrane permeation assay (PAMPA)

Values of logP_e were determined in a 96-well format with the PAMPA[33] permeation assay. For each compound, measurements were performed at three pH values (5.0, 6.2, 7.4) in quadruplicate. For this purpose, 12 wells of a deep-well plate, i.e., four wells per pH value, were filled with 650 μL System Solution. Samples (150 μL) were withdrawn from each well to determine the blank spectra by UV spectroscopy (SpectraMax 190). Then, analyte dissolved in DMSO was added to the remaining System Solution to yield 50 μM solutions. To exclude precipitation, the optical density was measured at 650 nm, with 0.01 being the threshold value. Solutions exceeding this threshold were filtered. Afterward, samples (150 μL) were withdrawn to determine the reference spectra. Further 200 μL were transferred to each well of the donor plate of the PAMPA sandwich P/N 110 163 (pion, Woburn MA, USA). The filter membranes at the bottom of the acceptor plate were impregnated with 5 μL of GIT-0 Lipid Solution, and 200 μL of Acceptor Sink Buffer were filled into each acceptor well. The sandwich was assembled, placed in the GutBox, and left undisturbed for 16 h. It was then disassembled, and samples (150 μL) were transferred from each donor and acceptor well to UV plates. Quantification was performed by both UV spectroscopy and LC–MS; logP_e values were calculated with the aid of the PAMPA Explorer Software (pion, version 3.5).

Colorectal adenocarcinoma (Caco-2) cell permeation assay

Caco-2 cells were cultivated in tissue culture flasks (BD Biosciences, Franklin Lakes, NJ, USA) with DMEM high-glucose medium containing L-glutamine (2 mM), nonessential amino acids (0.1 mM), penicillin (100 U mL^{-1}), streptomycin (100 μg mL^{-1}), and FBS (10%). The cells were kept at 37 °C in humidified air containing 5% CO_2, and the medium was changed every second day. When ~90% confluence was reached, the cells were split in a 1:10 ratio and distributed to new tissue culture flasks. At passage numbers between 60 and 65, they were seeded at a density of 5.3×10^5 cells per well to Transwell 6-well plates (Corning Inc., Corning, NY, USA) with 2.5 mL culture medium in the basolateral and 1.8 mL in the apical compartment. The medium was renewed on alternate days. Permeation experiments were performed between days 19 and 21 post-seeding. Prior to the experiment, the integrity of the Caco-2 monolayers was evaluated by measuring the transepithelial electrical resistance (TEER) with an Endohm tissue resistance instrument (World Precision Instruments Inc., Sarasota, FL, USA). Only wells with TEER values >300 Ω c m^2 were used. Experiments were performed in the apical-to-basolateral (absorptive) and basolateral-to-apical (secretory) directions in triplicate. Transport medium (DMEM without sodium pyruvate and phenol red) was withdrawn from the donor compartments of three wells and replaced by the same volume of compound stock solutions to reach an initial sample concentration of 62.5 μM. The Transwell plate was then shaken (250 rpm) in the incubator. Samples (40 μL) were withdrawn after 15, 30, and 60 min from the donor and acceptor compartments, and their concentrations were determined by LC–MS. Apparent permeability coefficients (P_{app}) were calculated according to the equation

$$P_{app} = \frac{dQ}{dt} \times \frac{1}{A \times c_0} \quad (5)$$

where dQ/dt is the permeability rate, A the surface area of the monolayer, and c_0 the initial concentration in the donor compartment.[42] After the experiment, TEER values were assessed again for each well and results from wells with values <300 Ω c m^2 were discarded.

log D$_{7.4}$ determination

The in silico prediction tool ALOGPS[43] was used to estimate the log$P$ values of the compounds. Depending on these values, the compounds were classified into three categories: hydrophilic compounds (log$P<0$), moderately lipophilic compounds ($0\leq$ log$P\leq1$) and lipophilic compounds (log$P>1$). For each category, two different ratios (volume of 1-octanol to volume of buffer) were defined as experimental parameters (Table 4).

Table 4. Compound classification based on estimated log$P$ values.[43]

Compound type	log$P$	Ratio (1-octanol)/(buffer)
hydrophilic	<0	30:140, 40:130
moderately lipophilic	0–1	70:110, 110:70
lipophilic	>1	3:180, 4:180

Equal amounts of phosphate buffer (0.1 M, pH 7.4) and 1-octanol were mixed and shaken vigorously for 5 min to saturate the phases. The mixture was left until separation of the two phases occurred, and the buffer was retrieved. Stock solutions of the test compounds were diluted with buffer to a concentration of 1 μM. For each compound, six determinations, i.e., three determinations per 1-octanol/buffer ratio, were performed in different wells of a 96-well plate. The respective volumes of buffer containing analyte (1 μM) were pipetted to the wells and covered by saturated 1-octanol according to the chosen volume ratio. The plate was sealed with aluminum foil, shaken (1350 rpm, 25 °C, 2 h) on a Heidoph Titramax 1000 plate shaker (Heidolph Instruments GmbH & Co. KG, Schwabach, Germany) and centrifuged (2000 rpm, 25 °C,

5 min, 5804 R Eppendorf centrifuge, Hamburg, Germany). The aqueous phase was transferred to a 96-well plate for analysis by LC–MS.

$\log D_{7.4}$ was calculated from the 1-octanol/buffer ratio (o/b), the initial concentration of the analyte in buffer (1 μM), and the concentration of the analyte in the aqueous phase (c_B) with equation:

$$\log D_{7.4} = \log\left(\frac{1\mu M - c_B}{c_B} \times \frac{1}{o:b}\right) \quad (6)$$

Solubility

Solubility was determined in a 96-well format using the μSOL Explorer solubility analyzer (plon, version 3.4.0.5). For each compound, measurements were performed at three pH values (3.0, 5.0, 7.4) in triplicates. For this purpose, nine wells of a deep-well plate, that is, three wells per pH value, were filled with 300 μL of an aqueous universal buffer solution. Aliquots (3 μL) of a compound stock solution (10–50 mM in DMSO) were added and thoroughly mixed. The final sample concentration was 0.1–0.5 mM, the residual DMSO concentration was 1.0% (*v*/*v*) in the buffer solutions. After 15 h, the solutions were filtered (0.2 μm 96-well filter plates) using a vacuum to collect manifold (Whatman Ltd., Maidstone, UK) to remove any precipitates. Equal amounts of filtrate and *n*-propanol were mixed and transferred to a 96-well plate for UV detection (190–500 nm). The amount of material dissolved was calculated by comparison with UV spectra obtained from reference samples, which were prepared by dissolving compound stock solution in a 1:1 mixture of buffer and *n*-propanol (final concentrations 0.017–0.083 mM).

LC–MS measurements

Analyses were performed using an 1100/1200 Series HPLC System coupled to a 6410 Triple Quadrupole mass detector (Agilent Technologies, Inc., Santa Clara, CA, USA) equipped with electrospray ionization. The system was controlled with the Agilent MassHunter Workstation Data Acquisition software (version B.01.04). The column used was an Atlantis T3 C_{18} column (2.1×50 mm) with a 3 μm particle size (Waters Corp., Milford, MA, USA). The mobile phase consisted of two eluents: solvent A (H_2O, containing 0.1% formic acid, *v*/*v*) and solvent B (MeCN, containing 0.1% formic acid, *v*/*v*), both delivered at 0.6 mL min^{-1}. The gradient was ramped from 95% A/5% B to 5% A/95% B over 1 min, and then held at 5% A/95% B for 0.1 min. The system was then brought back to 95% A/5% B, resulting in a total duration of 4 min. MS parameters such as fragmentor voltage, collision energy, and polarity were optimized individually for each analyte, and the molecular ion was followed for each compound in the multiple reaction monitoring mode. The concentrations of the analytes were quantified by the Agilent Mass Hunter Quantitative Analysis software (version B.01.04).

Abbreviations

Caco-2 cells, colorectal adenocarcinoma cells; CRD, carbohydrate recognition domain; *D*, distribution coefficient octanol/H_2O; GFP, green fluorescent protein; HPLC, high-performance liquid chromatography; IC_{50}, half-maximal inhibitory concentration; ITC, isothermal titration calorimetry; MFI, mean fluorescence intensity; PAMPA, parallel artificial membrane permeability assay; P_{app}, apparent permeability coefficient; P_e, effective permeation value; SAR, structure–activity relationship; SPR, structure–property relationship; UPEC, uropathogenic *E. coli*; UTI, urinary tract infection.

Acknowledgement

Financial support from the Swiss National Science Foundation (SNF interdisciplinary grant K-32K1-120904) is gratefully acknowledged.

Keywords: bacterial adhesin · FimH antagonists · flow cytometry · isothermal titration calorimetry · urinary tract infections

[1] a) T. M. Hooton, W. E. Stamm, *Infect. Dis. Clin. North Am.* **1997**, *11*, 551–581; b) T. J. Wiles, R. R. Kulesus, M. A. Mulvey, *Exp. Mol. Pathol.* **2008**, *85*, 11–19; c) S. D. Fihn, *N. Engl. J. Med.* **2003**, *349*, 259–266.

[2] C. Svanborg, G. Godaly, *Infect. Dis. Clin. North Am.* **1997**, *11*, 513–529.

[3] a) J. D. Schilling, S. J. Hultgren, *Int. J. Antimicro. Ag.* **2002**, *19*, 457–460; b) M. G. Blango, M. A. Mulvey, *Antimicrob. Agents Chemother.* **2010**, *54*, 1855–1863.

[4] G. Capitani, O. Eidam, R. Glockshuber, M. G. Grutter, *Microbes Infect.* **2006**, *8*, 2284–2290.

[5] a) M. A. Mulvey, *Cell Microbiol.* **2002**, *4*, 257–271; b) S. G. Gouin, A. Wellens, J. Bouckaert, J. Kovensky, *ChemMedChem* **2009**, *4*, 749–755.

[6] N. Sharon, *Biochim. Biophys. Acta.* **2006**, *1760*, 527–537.

[7] a) N. Firon, I. Ofek, N. Sharon, *Biochem. Biophys. Res. Commun.* **1982**, *105*, 1426–1432; b) N. Firon, I. Ofek, N. Sharon, *Carbohydr. Res.* **1983**, *120*, 235–249; c) N. Sharon, *FEBS Lett.* **1987**, *217*, 145–157.

[8] D. Choudhury, A. Thompson, V. Stojanoff, S. Langermann, J. Pinkner, S. J. Hultgren, S. D. Knight, *Science* **1999**, *285*, 1061–1066.

[9] a) C. S. Hung, J. Bouckaert, D. Hung, J. Pinkner, C. Widberg, A. DeFusco, C. G. Auguste, R. Strouse, S. Langermann, G. Waksman, S. J. Hultgren, *Mol. Microbiol.* **2002**, *44*, 903–915; b) J. Bouckaert, J. Berglund, M. Schembri, E. D. Genst, L. Cools, M. Wuhrer, C. S. Hung, J. Pinkner, R. Slättergard, A. Zavialov, D. Choudhury, S. Langermann, S. J. Hultgren, L. Wyns, P. Klemm, S. Oscarson, S. D. Knight, H. De Greve, *Mol. Microbiol.* **2005**, *55*, 441–455; c) A. Wellens, C. Garofalo, H. Nguyen, N. Van Gerven, R. Slättergard, J.-P. Hernalsteens, L. Wyns, S. Oscarson, H. De Greve, S. Hultgren, J. Bouckaert, *PLoS ONE* **2008**, *3*, e2040.

[10] a) N. Firon, S. Ashkenazi, D. Mirelman, I. Ofek, N. Sharon, *Infect. Immun.* **1987**, *55*, 472–476; b) T. K. Lindhorst, S. Kötter, J. Kubisch, U. Krallmann-Wenzel, S. Ehlers, V. Kren, *Eur. J. Org. Chem.* **1998**, 1669–1674; c) O. Sperling, A. Fuchs, T. K. Lindhorst, *Org. Biomol. Chem.* **2006**, *4*, 3913–3922; d) Z. Han, J. S. Pinker, B. Ford, R. Obermann, W. Nolan, S. A. Wildman, D. Hobbs, T. Ellenberger, C. K. Cusumano, S. J. Hultgren, J. W. Janetka, *J. Med. Chem.* **2010**, *53*, 4779–4792; e) T. Klein, D. Abgottspon, M. Wittwer, S. Rabbani, J. Herold, X. Jiang, S. Kleeb, C. Lüthi, M. Scharenberg, J. Bezençon, E. Gubler, L. Pang, M. Smieško, B. Cutting, O. Schwardt, B. Ernst, *J. Med. Chem.* **2010**, *53*, 8627–8641; f) O. Schwardt, S. Rabbani, M. Hartmann, D. Abgottspon, M. Wittwer, S. Kleeb, A. Zalewski, M. Smieško, B. Cutting, B. Ernst, *Bioorg. Med. Chem.* **2011**, *19*, 6454–6473; g) C. K. Cusumano, J. S. Pinkner, Z. Han, S. E. Greene, B. A. Ford, J. R. Crowley, J. P. Henderson, J. W. Janetka, S. J. Hultgren, *Sci. Transl. Med.* **2011**, *3*, 109ra115; h) J. Berglund, J. Bouckaert, H. De Greve, S. Knight, *Anti-Adhesive Compounds to Prevent and Treat Bacterial Infections*, Intl. Pat. PCT/US 2005/089733, **2005**.

[11] Glide, version 5.7, Schrödinger, LLC, New York, NY (USA), **2011**.

[12] I. L. Scott, R. V. Market, R. J. DeOrazio, H. Meckler, T. P. Kogan, *Carbohydr. Res.* **1999**, *317*, 210–216.

[13] C. A. Ocasio, T. S. Scanlan, *Bioorg. Med. Chem.* **2008**, *16*, 762–770.

[14] M. Prieto, E. Zurita, E. Rosa, L. Muñoz, P. Lloyd-Williams, E. Giralt, *J. Org. Chem.* **2004**, *69*, 6812–6820.

[15] M. Ishikawa, Y. Hashimoto, *J. Med. Chem.* **2011**, *54*, 1539–1554.

[16] S. Rabbani, X. Jiang, O. Schwardt, B. Ernst, *Anal. Biochem.* **2010**, *407*, 188–195.

[17] M. Scharenberg, D. Abgottspon, E. Cicek, X. Jiang, O. Schwardt, S. Rabbani, B. Ernst, *Assay Drug Dev. Technol.* **2011**, *9*, 455–464.
[18] J. Bouckaert, J. Mackenzie, J. L. de Paz, B. Chipwaza, D. Choudhury, A. Zavialov, K. Mannerstedt, J. Anderson, D. Pierard, L. Wyns, P. H. Seeberger, S. Oscarson, H. De Greve, S. D. Knight, *Mol. Microbiol.* **2006**, *61*, 1556–1568.
[19] G. Zhou, W. J. Mo, P. Sebbel, G. W. Min, T. A. Neubert, R. Glockshuber, *J. Cell Sci.* **2001**, *114*, 4095–4103.
[20] P. Aprikian, V. Tchesnokova, B. Kidd, O. Yakovenko, V. Yarov-Yarovoy, E. Trinchina, V. Vogel, W. Thomas, E. Sokurenko, *J. Biol. Chem.* **2007**, *282*, 23437–23446.
[21] I. Le Trong, P. Aprikian, B. A. Kidd, M. Forero-Shelton, V. Tchesnokova, P. Rajagopal, V. Rodriguez, G. Interlandi, R. Klevit, V. Vogel, R. E. Stenkamp, E. V. Sokurenko, W. E. Thomas, *Cell* **2010**, *141*, 645–655.
[22] D. Abgottspon, G. Rölli, L. Hosch, A. Steinhuber, X. Jiang, O. Schwardt, B. Cutting, M. Smieško, U. Jenal, B. Ernst, A. Trampuz, *J. Microbiol. Methods* **2010**, *82*, 249–255.
[23] a) J. E. Ladbury, *Biochem. Soc. Trans.* **2010**, *38*, 888–893; b) G. A. Holdgate, W. H. Ward, *Drug Discovery Today* **2005**, *10*, 1543–1550; c) R. Perozzo, G. Folkers, L. Scapozza, *J. Recept. Signal Transduction Res.* **2004**, *24*, 1–52; d) J. E. Ladbury, G. Klebe, E. Freire, *Nat. Rev. Drug Discovery* **2010**, *9*, 23–27; e) K. P. Murphy, D. Xie, K. S. Thompson, L. M. Amzel, E. Freire, *Proteins* **1994**, *18*, 63–67.
[24] a) B. Baum, L. Muley, M. Smolinski, A. Heine, D. Hangauer, G. Klebe, *J. Mol. Biol.* **2010**, *397*, 1042–1054; b) M. C. Chervenak, E. J. Toone, *J. Am. Chem. Soc.* **1994**, *116*, 10533–10539; c) J. E. DeLorbe, J. H. Clements, M. G. Teresk, A. P. Benfield, H. R. Plake, L. E. Millspaugh, S. F. Martin, *J. Am. Chem. Soc.* **2009**, *131*, 16758–16770.
[25] S. Cabani, P. Gianni, V. Mollica, L. Lepori, *J. Solution Chem.* **1981**, *10*, 563–595.
[26] A. V. Finkelstein, J. Janin, *Protein Eng.* **1989**, *3*, 1–3.
[27] K. P. Murphy, *Biophys. Chem.* **1994**, *51*, 311–326.
[28] E. Freire, *Drug Discovery Today* **2008**, *13*, 869–874.
[29] a) T. S. G. Olsson, M. A. Williams, W. R. Pitt, J. E. Ladbury, *J. Mol. Biol.* **2008**, *384*, 1002–1017; b) C. Diehl, O. Engstrom, T. Delaine, M. Hakansson, S. Genheden, K. Modig, H. Leffler, U. Ryde, U. J. Nilsson, M. Akke, *J. Am. Chem. Soc.* **2010**, *132*, 14577–14589.
[30] Phase, version 3.3, Schrödinger, LLC, New York, NY (USA), **2011**.
[31] a) B. A. Williams, M. C. Chervenak, E. J. Toone, *J. Biol. Chem.* **1992**, *267*, 22907–22911; b) E. J. Toone, *Curr. Opin. Struc. Biol.* **1994**, *4*, 719–728; c) T. K. Dam, C. F. Brewer, *Chem. Rev.* **2002**, *102*, 387–429; d) M. Ambrosi, N. R. Cameron, B. G. Davis, *Org. Biomol. Chem.* **2005**, *3*, 1593–1608; e) E. Garcia-Hernandez, R. A. Zubillaga, E. A. Chavelas-Adame, E. Vazquez-Contreras, A. Rojo-Dominguez, M. Costas, *Protein Sci.* **2003**, *12*, 135–142.
[32] H. Van de Waterbeemd, D. A. Smith, K. Beaumont, D. K. Walker, *J. Med. Chem.* **2001**, *44*, 1313–1333.
[33] M. Kansy, F. Senner, K. Gubernator, *J. Med. Chem.* **1998**, *41*, 1007–1010.
[34] A. Avdeef, S. Bendels, L. Di, B. Faller, M. Kansy, K. Sugano, Y. Yamauchi, *J. Pharm. Sci.* **2007**, *96*, 2893–2909.
[35] C. A. Lipinski, *J. Pharmacol. Toxicol. Methods* **2000**, *44*, 235–249.
[36] J. Kasuga, M. Ishikawa, M. Yonehara, M. Makishima, Y. Hashimoto, H. Miyachi, *Bioorg. Med. Chem.* **2010**, *18*, 7164–7173.
[37] R. Roy, S. K. Das, F. Santoyo-González, F. Hernández-Mateo, T. K. Dam, C. F. Brewer, *Chem. Eur. J.* **2000**, *6*, 1757–1762.
[38] a) F. Bitsch, R. Aichholz, J. Kallen, S. Geisse, B. Fournier, J. M. Schlaeppi, *Anal. Biochem.* **2003**, *323*, 139–149; b) S. Mesch, K. Lemme, H. Koliwer-Brandl, D. S. Strasser, O. Schwardt, S. Kelm, B. Ernst, *Carbohydr. Res.* **2010**, *345*, 1348–1359.
[39] G. Kemmer, S. Keller, *Nat. Protoc.* **2010**, *5*, 267–281.
[40] O. O. Krylova, N. Jahnke, S. Keller, *Biophys. Chem.* **2010**, *150*, 105–111.
[41] A. Ziegler, J. Seelig, *Biophys. J.* **2004**, *86*, 254–263.
[42] P. Artursson, J. Karlsson, *Biochem. Biophys. Res. Commun.* **1991**, *175*, 880–885.
[43] a) VCCLAB, Virtual Computational Chemistry Laboratory, 2005, http://www.vcclab.org (accessed May 3, 2012); b) I. V. Tetko, J. Gasteiger, R. Todeschini, A. Mauri, D. Livingstone, P. Ertl, V. A. Palyulin, E. V. Radchenko, N. S. Zefirov, A. S. Makarenko, V. Y. Tanchuk, V. V. Prokopenko, *J. Comput. Aid. Mol. Des.* **2005**, *19*, 453–463.

Received: March 6, 2012
Revised: April 27, 2012
Published online on May 29, 2012

3 Summary

Most of the lectins are characterized calorimetrically for the first time except FimH[1] and an indirect thermodynamic determination of E-selectin binding to ESL-1.[2] All these interactions enrich the dataset with variable thermodynamic fingerprints. A typical carbohydrate-lectin interaction was found for physiological ligands and mimics interacting with DC-SIGN that are enthalpically favorable interaction largely compensated by an entropic penalty that result in a micromolar binding affinity. In contrast, carbohydrates binding to E-selectin are entropically favored and as well in the micromolar range. The other carbohydrate-lectin interactions that were investigated exhibit nanomolar binding affinities. All these interactions are enthalpically driven with variable entropic contribution ranging from unfavorable for CD22 ligands, over negligible to unfavorable contributions for MAG and FimH antagonists. Overall, the thermodynamics among the investigated lectins are very divers and gave insights into the driving force of interactions.

References

[1] M. Durka, K. Buffet, J. Iehl, M. Holler, J. F. Nierengarten, J. Taganna, J. Bouckaert, S. P. Vincent, *Chem. Commun.* **2011**, *47*, 1321-1323; M. Almant, V. Moreau, J. Kovensky, J. Bouckaert, S. G. Gouin, *Chem. Eur. J.* **2011**, *17*, 10029-10038.

[2] M. K. Wild, M. C. Huang, U. Schulze-Horsel, P. A. van der Merwe, D. Vestweber, *J. Biol. Chem.* **2001**, *276*, 31602-31612.

Table 1. Experiment index for chapter 2.1.1.1 and 2. Binding thermodynamics of E-selectin antagonists determined by ITC at 25 °C (HBS-Ca buffer) compared to rIC_{50}/IC_{50} values from competitive binding assay where **BW69669** was used as reference compound.

Structure	Ligand	IC_{50} [µM]	rIC_{50})	K_D [µM]	rK_D [µM]	$\Delta G°$ [kJ mol^{-1}]	$\Delta H°$ [kJ mol^{-1}]	$-T\Delta S°$ [kJ mol^{-1}]	N	c-value
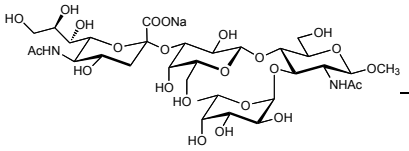	Methyl sLe^x			943.4		–17.3	+5.9	–23.2	1	0.2
	2.1.1.1 **1**									
	2.1.1.2 **1**			811.7		–17.6	+4.9	–22.5	1	0.1
	Mean ± SD	875.4 ± 138.5	12.9 ± 3.7	877.5 ± 93.1	14.9	–17.5 ± 0.2	+5.4 ± 0.7	–22.9 ± 1.1	1	
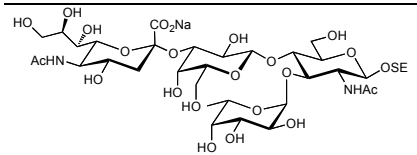	**FB119**	822.8 ± 162.3	12.4 ± 2.4	885	15	–17.4	+5.9	–23.3	1	0.2
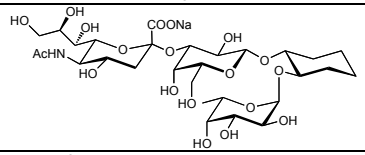	**FB89** 2.1.1.1 **3**	312.5 ± 479.1	4.4 ± 2.4	316.5	5.4	–20.0	–0.5	–19.5	1	0.6
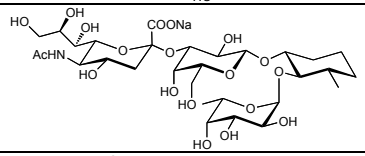	**FB87** 2.1.1.1 **4**	60.3 ± 15.2	0.59 ± 0.28	37.6	0.64	–25.3	+0.9	–26.2	0.94	3.0
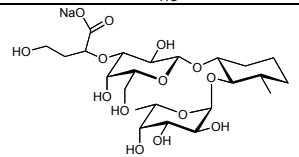	**FB321**	43.0 ± 16.8	0.66 ± 0.05	62.9	1.1	–24.0	–5.9	–18.1	0.98	1.8
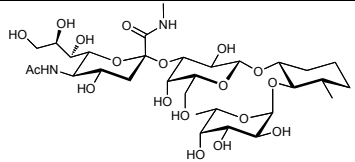	**FB109**	311.8 ± 107.8	3.6 ± 0.3	414.9	7.0	–19.3	+5.2	–24.5	1	1.0

Structure	Ligand	IC_{50} [µM]	rIC_{50})	K_D [µM]	rK_D [µM]	$\Delta G°$ [kJ mol^{-1}]	$\Delta H°$ [kJ mol^{-1}]	$-T\Delta S°$ [kJ mol^{-1}]	N	c-value
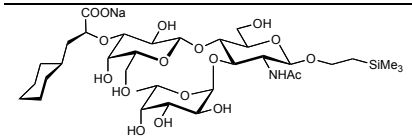	**FB289**	344.5 ± 154.5	4.4 ± 0.9	107.3	1.8	–22.7	–0.8	–21.9	1	1.0
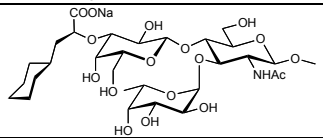	**FB329** 2.1.1.1 **5**	233.4 ± 69.2	3.5 ± 0.3	259.7	4.4	–20.5	–2.2	–18.3	1	0.9
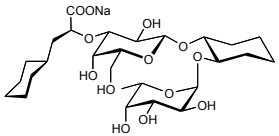	**BW69669** 2.1.1.1 **6**			62.1		–24.0	–5.0	–19.0	0.99	1.5
	2.1.1.2 **2**			55.9		–24.3	–5.5	–18.8	0.87	1.2
	Mean ± SD	61.4 ± 13.6	1	59.0 ± 4.4	1	–24.2 ± 0.2	–5.3 ± 0.4	–18.9 ± 0.6	0.93 ± 0.08	
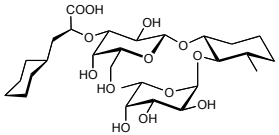	**DS4115** 2.1.1.1 **2**			17.2		–27.2	–5.7	–21.5	0.97	4.8
	2.1.1.2 **3**			19.7		–26.9	–5.9	–21.0	0.97	4.2
	Mean ± SD	13.7 ± 3.3	0.18 ± 0.02	18.5 ± 1.8	0.31	–27.1 ± 0.2	–5.8 ± 0.1	–21.3 ± 0.4	0.97 ± 0.01	
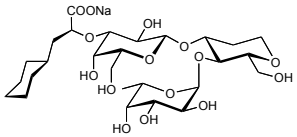	**CGP77175 A**			30.3		–25.7	–7.8	–17.9	1.13	4.4
				29.6		–25.8	–7.4	–18.4	1.17	2.9
	Mean ± SD	17.5 ± 6.9	0.29 ± 0.07	30.0 ± 0.5	0.51	–25.8 ± 0.1	–7.6 ± 0.3	–18.2 ± 0.4	1.15 ± 0.03	
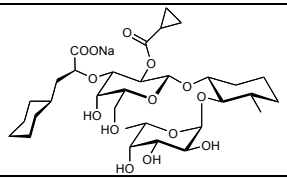	**BW534** 2.1.1.2 **4**	8.7 ± 0.1	0.09 ± 0.01	4.8		–30.3	–7.2	–23.1	1.17	4.6
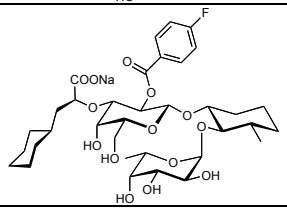	**BW510** 2.1.1.2 **6**	7.4 ± 1.5	0.08 ± 0.01	3.6	0.06	–31.1	–11.3	–19.8	1.08	11

Structure	Ligand	IC_{50} [µM]	rIC_{50})	K_D [µM]	rK_D [µM]	$\Delta G°$ [kJ mol^{-1}]	$\Delta H°$ [kJ mol^{-1}]	$-T\Delta S°$ [kJ mol^{-1}]	N	c-value
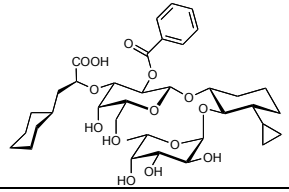	**DS0565** 2.1.1.2 **7**	5.2 ± 1.0	0.05 ± 0.01	8.6	0.15	–28.9	–11.6	–17.3	1.04	8.7
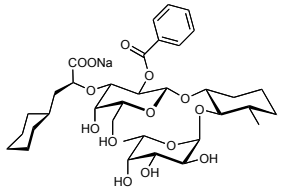	**GMI1077** 2.1.1.2 **5**			4.3		–30.6	–13.0	–17.6	0.95	10.5
				4.0		–30.8	–12.1	–18.7	0.97	10.1
				3.8		–31.0	–12.0	–19.0	1.08	8.0
	Mean ± SD	6.7 ± 2.0	0.07 ± 0.01	4.0 ± 0.3	0.07	–30.8 ± 0.2	–12.4 ± 0.6	–18.4 ± 0.7	1.00 ± 0.07	
	E-selectin monomer					–31.2	–11.8	–19.4	1.14	19.7
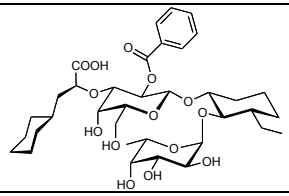	**DS0567** 2.1.1.2 **8**	6.1 ± 1.7	0.06 ± 0.02	2.1	0.04	–32.5	–12.7	–19.8	1.11	35.7

Table 2. Experiment index for chapter 2.1.1.1 and 2. rIC_{50}/IC_{50} values from competitive binding assay for E-selectin antagonists (HBS-Ca buffer) whith **BW69669** was used as reference compound.

Structure	Ligand	IC_{50} [µM]	rIC_{50}
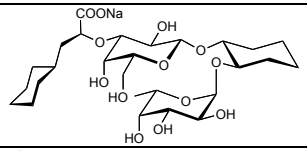	**BW69669**	61.4 ± 13.6	1.0
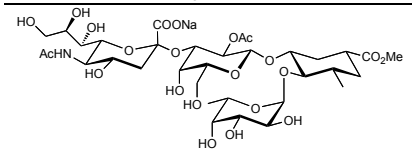	**FB124**	57.9	1.0
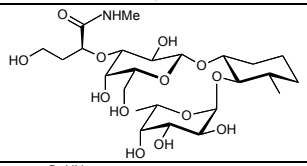	**FB298**	336.2 ± 170	3.5 ± 2.7
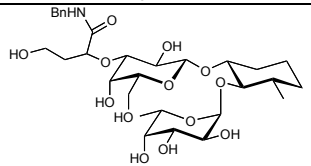	**FB320**	146.8	2.7
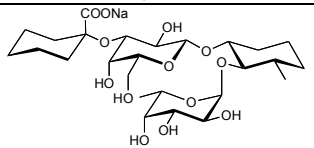	**FB333**	1423	22.0
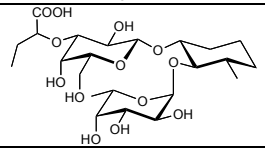	**FB341**	77.5 ± 22.4	1.5 ± 0.3

Structure	Ligand	IC_{50} [µM]	rIC_{50}
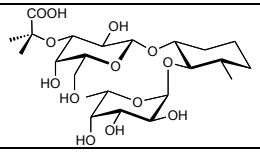	**FB344**	629.3	14.7
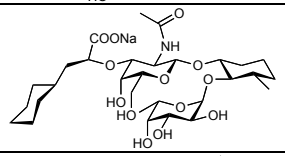	**BW570**	7.8 ± 0.6	0.08 ± 0.01
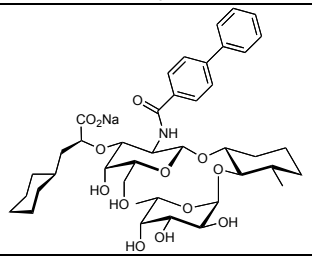	**BW585**	11.0 ± 0.6	0.15 ± 0.05
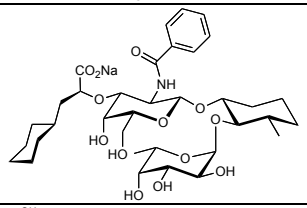	**BW588**	7.3 ± 0.6	0.10 ± 0.03
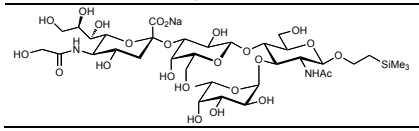	**GG-2-109**	497.5 ± 62.4	7.1 ± 1.7

Table 3. Experiment index for chapter 2.1.2. Binding thermodynamics of DC-SIGN antagonists determined by ITC at 25 °C (HBS-Ca buffer) compared to rIC_{50}/IC_{50} values from competitive binding assay (determined by Meike Scharenberg) where phenyl Le[a] was used as reference compound.

Structure	Ligand	rIC_{50}	K_D [nM]	rK_D	$\Delta G°$ [kJ mol^{-1}]	$\Delta H°$ [kJ mol^{-1}]	$-T\Delta S°$ [kJ mol^{-1}]	*N*	*c*-value
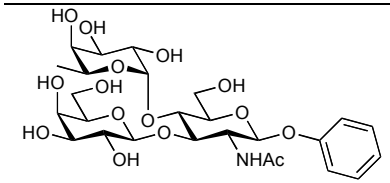	Phenyl Le[a] 2.1.2 **1**		553	KL	–18.6	–29.4	+10.8	1	0.14
			610	KL	–18.4	–26.6	+8.3	1	0.08
	Mean ± SD	1	**582 ± 40**	1	**–18.5 ± 0.1**	**–28.0 ± 2.0**	**+9.5 ± 2.1**	**1**	
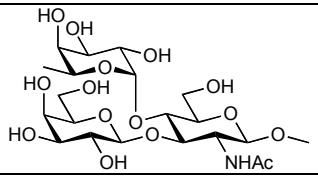	methyl Le[a] 2.1.2 **2**	2.9 ± 0.5	735	1.3	–17.9	–27.9	+10.0	1	0.12
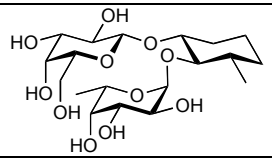	**KM65** 2.1.2 **4**	1.8 ± 0.5	645	1.1	–18.2	–31.4	+13.2	1	0.09
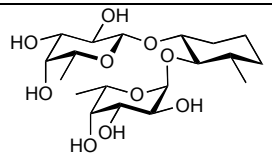	**KM153** 2.1.2 **5**	4.7 ± 1.0	1277	2.2	–16.5	–29.7	+13.2	1	0.04
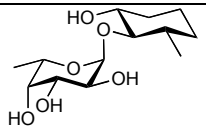	**KM151** 2.1.2 **6**		1073	1.8	–16.9	–34.4	+17.5	1	0.03

Table 4. Experiment index for chapter 2.2.1.1 and 2. Binding thermodynamics of MAG_{d1-3}-Fc antagonists determined by ITC at 25 °C (HBS-E buffer) compared to K_D values from SPR (determined by Stefanie Mesch).

Structure	Ligand	K_D [nM] SPR	K_D [nM] ITC	$\Delta G°$ [kJ mol^{-1}]	$\Delta H°$ [kJ mol^{-1}]	$-T\Delta S°$ [kJ mol^{-1}]	*N*	*c*-value
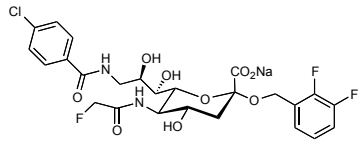	**SM5FAc** 2.2.1.1 **5**	500	142	–39.1	–39.2	+0.1	1.02	151.8
			106.3	–39.8	–43.3	+3.5	0.91	33.9
	Mean ± SD		124.2 ± 25.2	–39.5 ± 0.5	–41.3 ± 2.9	+1.8 ± 2.4	0.97 ± 0.08	
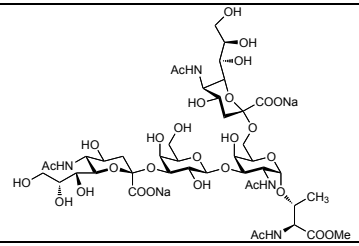	2.2.1.1 **13a**		2900	–31.6	–22.5	+9.1	0.77	5.9
			1200	–33.8	–24.9	+8.9	0.89	12.3
	Mean ± SD		2100 ± 1200	–32.7 ± 1.6	–23.7 ± 1.7	+9.0 ± 0.1	0.83 ± 0.08	
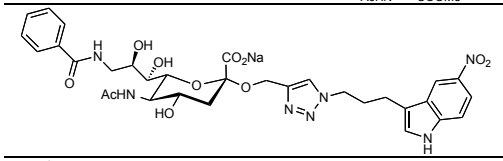	**SH281/ JXH144** 2.2.1.2 **1**	190	610	–35.5	–33.4	–2.1	1.01	14.8
			568	–35.7	–34.6	–1.1	0.91	10.9
	Mean ± SD		582.3 ± 18.7	–35.6 ± 0.1	–34.0 ± 0.9	–1.6 ± 0.7	0.96 ± 0.07	
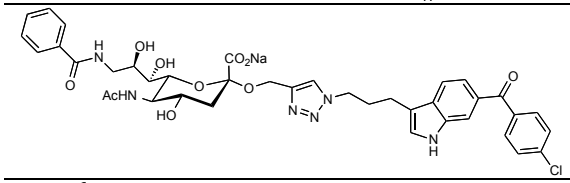	**JXH158** 2.2.1.2 **5**	75	118.0	–39.6	–52.0	+12.4	0.93	19.2
			146.2	–39.1	–51.8	+12.7	0.88	23.7
	Mean ± SD		132.1 ± 19.9	–39.3 ± 0.4	–51.9 ± 0.1	+12.6 ± 0.2	0.91 ± 0.04	
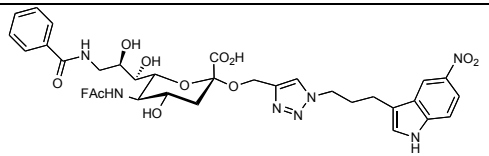	**SM432** 2.2.1.2 **19**	50	207	–38.2	–32.9	–5.3	0.97	30.4
			136	–39.2	–32.1	–7.1	1.13	47.8
	Mean ± SD		171.5 ± 50.2	–38.7 ± 0.7	–32.5 ± 0.6	–6.2 ± 1.3	1.05 ± 0.11	

Table 5. Experiment index for chapter 2.2.2. Binding thermodynamics of $CD22_{d1-3}$-Fc antagonists determined by ITC at 25 °C (HBS-E buffer) compared to K_D values from SPR (determined by Stefanie Mesch).

Structure	Ligand	K_D [nM] SPR	K_D [nM] ITC	$\Delta G°$ [kJ mol^{-1}]	$\Delta H°$ [kJ mol^{-1}]	$-T\Delta S°$ [kJ mol^{-1}]	*N*	*c*-value
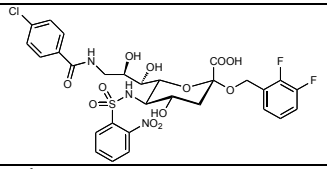	**DM-N3** 2.2.2 **9k**	110	131.4	–39.3	–54.8	+15.5	0.96	85
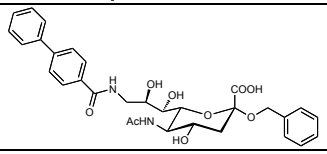	**SMC-9-4** 2.2.2 **13a**	800	592	–35.6	–72.8	+37.2	0.93	3.0
			909	–34.5	–73.9	+39.4	0.98	3.1
	Mean ± SD		750.5 ± 224.2	–35.1 ± 0.8	–73.4 ± 0.8	+38.3 ± 1.6	0.96 ± 0.04	
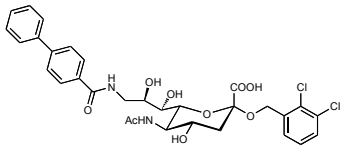	**SM-2-26-2** 2.2.2 **13b**	100	64.1	–41.1	–81.1	+40.0	0.93	64.8
			81.3	–40.4	–76.5	+36.1	0.95	34.4
			101.5	–39.9	–83.1	+43.2	0.92	15.3
	Mean ± SD		82.3 ± 18.7	–40.5 ± 0.6	–80.2 ± 3.4	+39.7 ± 3.6	0.94 ± 0.02	
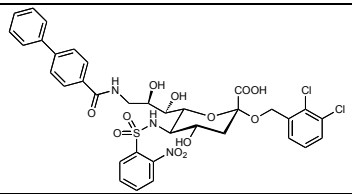	**SM-2-31** 2.2.2 **17a**				n.b.			
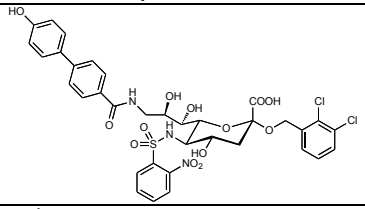	**SM-2-16** 2.2.2 **17b**	60	86.1	–40.3	–60.8	+20.5	1.08	32.5
			73.0	–40.8	–62.3	+21.5	1.06	19.2
	Mean ± SD		79.6 ± 9.3	–40.6 ± 0.4	–61.6 ± 1.1	+21.0 ± 0.7	1.07 ± 0.01	
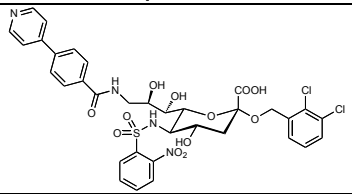	**SM-2-18** 2.2.2 **17c**	110	122.0	–39.5	–81.4	+41.9	0.96	14.8
			182.8	–38.5	–85.3	+46.8	0.93	13.1
	Mean ± SD		152.4 ± 43.0	–39.0 ± 0.7	–83.4 ± 2.8	+44.4 ± 3.5	0.95 ± 0.02	

Table 6. Experiment index for chapter 2.3.1.1 and 2. Binding thermodynamics of FimH-CRD antagonists determined by ITC at 25 °C (HBS-Ca buffer) compared to rIC_{50}/IC_{50} values from competitive binding assay (determined by Said Rabbani) where *n*-Heptyl α-D-mannopyranoside was used as reference compound.

Structure	Ligand	rIC_{50}	K_D [nM]	rK_D	$\Delta G°$ [kJ mol^{-1}]	$\Delta H°$ [kJ mol^{-1}]	$-T\Delta S°$ [kJ mol^{-1}]	*N*	*c*-value	
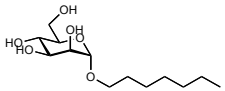	*n*-Heptyl α-D-manno-pyranoside (HM) 2.3.1.1 **2** 2.3.1.2 **1**	1	22.4		–43.7	–42.6	–1.1	1.06	1052	KL
			16.9		–44.4	–42.6	–1.8	1.05	519	KL
			19.8		–44.0	–42.4	–1.6	1.09	520	KL
			22.7		–43.6	–43.1	–0.5	1.08	454	KL
			25.9		–43.3	–41.5	–1.8	1.09	375	KL
			26.1		–43.4	–39.1	–4.3	1.01	458	KL
			28.3		–43.1	–42.4	–0.7	1.01	399	KL
			31.8		–42.8	–43.9	+1.1	1.01	314	KL
			29.8		–43.0	–42.4	–0.6	1.04	342	KL
			30.2		–42.9	–43.5	+0.6	1.02	348	RP
			27.4		–43.2	–40.4	–2.8	1.02	365	KL
			33.5		–42.7	–43.1	+0.4	0.98	412	KL
	Mean ± SD		**26.2 ± 5.0**	1	**–43.4 ± 0.5**	**–42.3 ± 1.4**	**–1.1 ± 1.5**	**1.04 ± 0.04**		
	1,5–Anhydro mannitol	39	705		–35.1	–38.0	+2.9	1.08	33	RP
			892		–34.5	–39.9	+5.4	1.05	26	RP
	Mean ± SD		**798 ± 132**	30	**–34.8 ± 0.4**	**–39.0 ± 1.3**	**+4.2 ± 1.8**	**1.05 ± 0.03**		
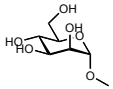	MM	34	1123		–34.0	–30.7	–3.3	1.12	19	KL
			1298		–33.6	–31.5	–2.1	1.00	18	RP
	Mean ± SD		**1211±124**	46	**–33.8 ± 0.3**	**–31.1 ± 0.6**	**–2.7 ± 0.8**	**1.06 ± 0.08**		
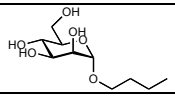	**PLJ01234A** 2.3.1.1 **1**	4.0	121	4.6	–39.5	–36.6	–2.9	1.02	93.6	KL
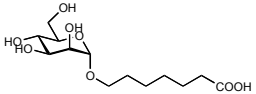	**AV277**	1.2	40.2		–42.2	–42.7	+0.5	1.02	281	KL
			50.6		–41.6	–41.4	–0.2	1.03	216	KL
	Mean ± SD		**45.4 ± 7.4**	1.7	**–41.9 ± 0.4**	**–42.1 ± 0.9**	**0.2 ± 0.5**	**1.03 ± 0.01**		

Structure	Ligand	rIC_{50}	K_D [nM]	rK_D	$\Delta G°$ [kJ mol^{-1}]	$\Delta H°$ [kJ mol^{-1}]	$-T\Delta S°$ [kJ mol^{-1}]	*N*	*c*-value	
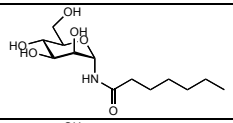	**OS429**	3.6	59.1	2.3	–41.3	–43.0	+1.7	1.02	191	KL
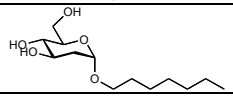	**JXH@031** (2–deoxy HM)	147	4953	189	–30.3	–12.5	–17.8	1.02	7.1	KL
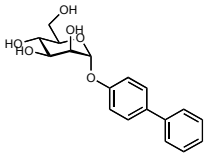	**PLJ01192A** (2.5% DMSO) 2.3.1.1 **3**	1.4	22.6		–43.6	–42.4	–1.2	1.05	449	KL
			25.0		–43.4	–44.4	+1.0	1.06	420	RP
	Mean ± SD		**23.8 ± 1.7**	0.91	**–43.5 ± 0.1**	**–43.4 ± 1.4**	**–0.1 ± 1.6**	**1.06 ± 0.01**		
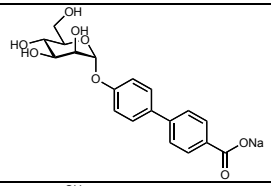	**PLJ01238A** 2.3.1.2 **4b**	0.20	14.1	0.54	–44.8	–47.3	+2.5	1.00	688	KL
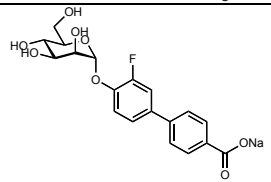	**PLJ01175B** 2.3.1.2 **14a**	0.58	9.2		–45.9	–51.6	+5.7	1.01	1120	KL
			11.7		–45.3	–49.9	+4.6	1.00	829	KL
	Mean ± SD		**10.5 ± 1.8**	0.40	**–45.6 ± 0.4**	**–50.8 ± 1.2**	**+5.2 ± 0.8**	**1.00 ± 0.01**		
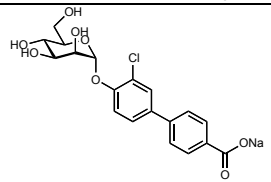	**TK05** 2.3.1.2 **5b**	0.09	3.7		–48.1	–55.5	+7.4	1.01	2784	KL
			4.6		–47.6	–54.3	+6.7	1.01	2109	KL
	Mean ± SD		**4.2 ± 0.6**	0.16	**–47.9 ± 0.4**	**–54.9 ± 0.9**	**+7.0 ± 0.5**	**1.01**		
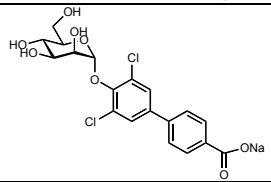	**TK23** (0.6% DMSO)		12.9		–45.0	–53.2	+8.2	1.02	713	KL
			22.7		–43.6	–56.0	+12.4	1.03	604	KL
	Mean ± SD		**17.8 ± 6.9**	0.49	**–44.3 ± 1.0**	**–54.6 ± 2.0**	**+10.3 ± 3.0**	**1.03 ± 0.01**		

Structure	Ligand	rIC_{50}	K_D [nM]	rK_D	$\Delta G°$ [kJ mol^{-1}]	$\Delta H°$ [kJ mol^{-1}]	$-T\Delta S°$ [kJ mol^{-1}]	*N*	*c*-value	
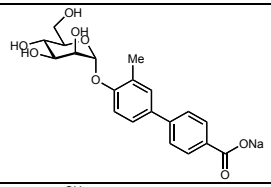	**PLJ01179B** 2.3.1.2 **14b**	0.16	4.8		–47.5	–56.2	+8.7	0.99	2146	KL
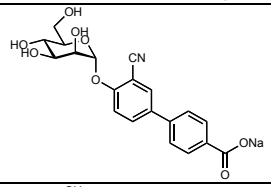	**PLJ01224A** 2.3.1.2 **14f**	0.58	7.4	0.28	–46.4	–55.0	+8.6	1.01	1311	KL
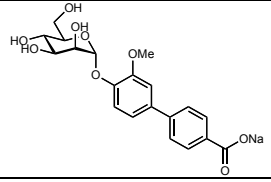	**PLJ01178B** 2.3.1.2 **14d**	0.08	7.7		–46.3	–52.5	+6.2	1.02	1338	KL
			10.9		–45.4	–51.0	+5.6	1.02	890	KL
	Mean ± SD		**9.3 ± 2.3**	0.35	**–45.9 ± 0.6**	**–51.8 ± 1.1**	**+5.9 ± 0.4**	**1.02**		
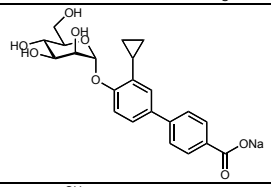	**PLJ01181B** 2.3.1.2 **14e**	1.09	6.9	0.26	–46.6	–46.7	+0.1	1.01	1493	KL
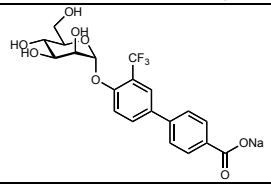	**PLJ01194B** 2.3.1.2 **14c**	0.15	3.2	0.12	–48.5	–58.5	+10.0	1.00	3219	KL
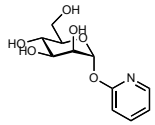	**PLJ01005A**	2.0	249		–38.0	–36.8	–1.2	0.98	44	KL
			651		–35.3	–34.5	–0.8	1.09	19	KL
	Mean ± SD		**450 ± 284**	17	**–36.7 ± 1.9**	**–35.7 ± 1.6**	**–1.0 ± 0.3**	**1.04 ± 0.08**		

Structure	Ligand	rIC_{50}	K_D [nM]	rK_D	$\Delta G°$ [kJ mol^{-1}]	$\Delta H°$ [kJ mol^{-1}]	$-T\Delta S°$ [kJ mol^{-1}]	*N*	*c*-value	
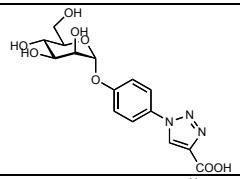	**PLJ01066A**	0.29	5.4		–47.2	–57.1	+9.9	0.92	1733	KL
			1.5		–50.3	–51.7	+1.4	1.03	6333	KL
	Mean ± SD		**3.5 ± 2.8**	0.13	**–48.8 ± 2.2**	**–54.4 ± 3.8**	**+5.6 ± 6.0**	**0.98 ± 0.08**		
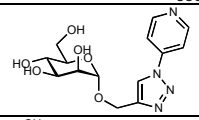	**MHa31**	1.1	189	7.2	–38.4	–37.2	–1.2	1.02	61	KL
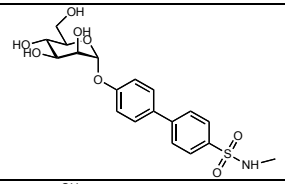	**PLJ01089A**	12.8	2.4		–49.2	–52.6	+3.4	0.98	3704	KL
			4.6		–47.6	–49.4	+1.8	0.91	1641	KL
	Mean ± SD		**3.5 ± 1.6**	0.14	**–48.4 ± 1.1**	**–51.0 ± 2.2**	**+2.6 ± 1.1**	**0.95 ± 0.05**		
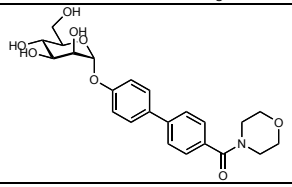	**PLJ01076A**	0.22	6.4		–46.8	–53.3	+6.5	1.13	1320	KL
			3.4		–48.3	–53.6	+5.3	1.05	1903	KL
	Mean ± SD		**4.9 ± 2.1**	0.19	**–47.6 ± 1.1**	**–53.5 ± 0.2**	**+5.9 ± 0.8**	**1.09 ± 0.06**		
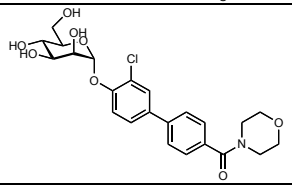	**PLJ01128A**	0.70	1.1		–51.1	–56.5	+5.4	1.00	8355	KL
			1.8		–50.1	–52.0	+1.9	1.01	3839	KL
	Mean ± SD		**1.5 ± 0.5**	0.06	**–50.6 ± 0.8**	**–54.3 ± 3.2**	**+3.7 ± 2.4**	**1.01 ± 0.01**		